WORLD METEOROLOGICAL ORGANIZATION

INSTRUMENTS AND OBSERVING METHODS

REPORT No. 70

7. April 1998

BIBLIOTHÈQUE OMM WMO LIBRARY

PAPERS PRESENTED at the WMO TECHNICAL CONFERENCE ON METEOROLOGICAL AND ENVIRONMENTAL INSTRUMENTS AND METHODS OF OBSERVATION

(TECO-98)

Casablanca, Morocco, 13 - 15 May 1998

WMO/TD - No. 877

1998

01-457L

BIBLIOTHÈQUE OMM WMO LIBRARY

NOTE

The designations employed and the presentation of material in this publication do not imply the expression of any opinion whatsoever on the part of the Secretariat of the World Meteorological Organization concerning the legal status of any country, territory, city or area, or of its authorities, or concerning the delimitation of its frontiers or boundaries.

This report has been produced without editorial revision by the WMO Secretariat. It is not an official WMO publication and its distribution in this form does not imply endorsement by the Organization of the ideas expressed.

IOM 70
TD 877
c. 3

FOREWORD

The forty-sixth session of the WMO Executive Council approved in 1994 the proposal of the eleventh session of the Commission for Instruments and Methods of Observation (CIMO-XI) to organize a *WMO Technical Conference on Meteorological and Environmental Instruments and Methods of Observation* (TECO-98). The Direction de la Meteorology Nationals of Morocco kindly offered to host the Conference in Casablanca from 13 to 15 May 1998.

TECO-98 which occurred immediately following the twelfth session of CIMO provided a good opportunity for CIMO delegates to participate in this Conference. An *Exhibition on Meteorological Instruments, Equipment and Services*(METEOREX-98) was also organized on this occasion.

The *Programme Committee* for TECO-98, composed of Messrs A. Van Gysegem (Scientific Director of TECO-98), J. Kruus (Canada), M. Rochas (France), A. Belhouji (Morocco), and E. Ekuwem (Nigeria), has been responsible for specifying the themes and contents of sessions as well as for selecting the papers.

The Conference reflects the diversity of the main areas of CIMO activities, as stated in the WMO Instruments and Methods of Observation Programme (IMOP), in the fields of intercomparisons, calibrations, new developments, automation and quality management of surface, upper-air and remote sensing meteorological measuring technologies. Papers shown the great concern to improve quality and homogeneity of observations and compatibility of measuring techniques in order to better meet observational needs and requirements of WMO Programmes and of National Meteorological and Hydrological Services.

This report contains the papers to be presented at the Conference and will place them on permanent record, making them available to a much wider audience than the participants at the Conference. I hope that all readers of this report will find the contents useful and informative and that the Conference will provide opportunities to exchange experience and to learn from others.

I wish to express my deep gratitude to the Government and the Direction de la Météorologie Nationale of Morocco, to all authors of papers, to members of the Programme Committee, to the Local Organizing Committee and to the Secretary-General of WMO for all efforts and resources devoted to planning and holding TECO-98.

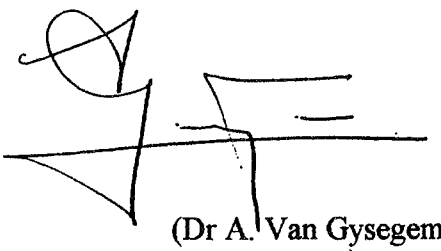

(Dr A. Van Gysegem)
Vice-president of CIMO
Scientific Director of TECO-98

TABLE OF CONTENTS

O. KEYNOTE PAPERS

I. INTERCOMPARISONS OF INSTRUMENTS FOR SURFACE OBSERVATIONS

II. CALIBRATION OF INSTRUMENTS

POSTER PRESENTATION

III. WIND PROFILERS

IV. REMOTE SENSING

POSTER PRESENTATIONS

V. QUALITY MANAGEMENT

POSTER PRESENTATIONS

VI. INTERCOMPARISONS FOR UPPER-AIR INSTRUMENTS

Session A

VII. RADIOSONDE TECHNOLOGY

POSTER PRESENTATIONS

VIII. PRESENT WEATHER OBSERVATIONS

IX. AUTOMATION OF SURFACE OBSERVATIONS

X. VISIBILITY AND TEMPERATURE OBSERVATIONS

XI. PRECIPITATION AND RADIATION OBSERVATIONS

POSTER PRESENTATIONS

APPENDICES

- List of members of the International Organizing Committee for the preparation of TECO-98

- List of publications in the Instruments and Observing Methods Report series

****

KEYNOTE PAPERS

OBSERVING URBAN WEATHER AND CLIMATE

T. R. Oke
Department of Geography, University of British Columbia,
Vancouver, B.C. Canada V6T 1Z2

INTRODUCTION

No environment offers more challenges to the meteorological observer than the city (Van Gysegem, 1978; Oke, 1984). Quite simply the normal protocols governing observing practice break down. Given the necessary instruments to establish a modern weather or climate station even a seasoned meteorologist does not know where to put them to generate useful data, because almost no site conforms with the WMO rules for exposure (WMO, 1983a,b) and in any case it's not clear what the observations are meant to characterise. At sites in most other environments the person installing the station is clear that the aim is to observe the state of the atmosphere without undue influences from the surface microclimate. This paper is about what the meteorological community should do to build a similar clarity of aims and rules for exposure when siting instruments in cities, where microclimates are everywhere. It argues for a serious attempt to develop new protocols and guidelines for those charged with installing and operating urban stations and networks.

On the whole the present state of meteorological measuring systems in cities is at best inadequate and in many cases an embarrassment. Stations are sited in bizarre locations, over widely differing surfaces, at various heights and the exposure of individual instruments commonly violates WMO rules of observing practice. When faced with these facts, those involved with installing and maintaining meteorological systems commonly shrug their shoulders and point out that it is very difficult to do better given the real diversity and constraints provided by cities and the guidelines they are given to work with. They are correct, but I argue here that it doesn't have to be this way. Establishing and running a station can be an expensive undertaking, it is therefore an enormous waste when, because of poor siting and exposure, the system underperforms or produces nonsensical information.

As I see it obvious problems arise from at least four sources:

- *confusion over the purpose of observation* – most meteorological stations are established either to:
  (a) observe the local climate, and its trends, free of microclimatic influences
  (b) observe the weather free of local climatic effects in support of operational services; such as air mass state used as input to the synoptic forecast system, or specialised storm warning or air pollution management systems
  (c) observe special atmospheric features as part of research studies.

  The spatial and temporal scales and focus of these objectives are very different so it may be that the observations required should not be combined at a single site.
- *human settlements are dynamic* – land uses change over time. Consider a site, which may have been established in the park-like grounds of a town hall a century ago, but subsequently has been moved from one spot to another as new buildings take precedence. The station is now lucky to have a place next to a parking lot and a tall building. Later it may be moved to the top of the building. Hence its original conformity with WMO guidelines for exposure have been eroded.

- *avoidance* – the complexity of the urban system and the complications associated with working within an array of tall buildings and trees causes many meteorologists to ignore cities or to turn to modelling rather than measurement (Van Gysegem, 1978)
- *lack of understanding of micro- and urban climates* – many meteorologists are trained to focus on synoptic or regional scale objectives, relatively few appreciate the large differences that occur at smaller scales or the structure of city climates.

SCALES AND PATTERNS OF URBAN CLIMATE

It cannot be over-stressed that understanding urban climates (and observing them) is critically tied to notions of scale and boundary layer development, as illustrated in Figure 1. At the smallest scale, that of individual elements, each building, tree, road, etc. creates its own microclimate. Because the city usually possesses repetitive structures, such as building lots and streets, these elements are recombined into larger microscale climate units such as *street canyons* which generate their own features, e.g. cross-canyon vortex flow (Figure 1c). These are features which exist beneath roof-level, so in analogy with plant stands this layer is called the *urban canopy layer (UCL)*. A larger neighbourhood comprising several similar street canyons plus their intervening buildings, gardens and courtyards creates a local scale climate which extends horizontally, but is restricted to the UCL (Figure 1b). The influences of each element also extend above roof-level as a jumbled set of plumes and wakes in the *roughness sublayer*. Due to the mixing of turbulence these eventually merge to form a more horizontally homogeneous *surface layer* in which micrometeorological theory for extensive homogeneous surfaces applies (Figure 1b,c). If there are distinct urban terrain zones (i.e. areas of different physical character, such as the type and density of buildings) in the city, new internal boundary layers will form at each zone border. These are mixed together to form the *urban boundary layer (UBL)* of the whole city. This is a mesoscale phenomenon within which the air shows the integrated presence of the city.

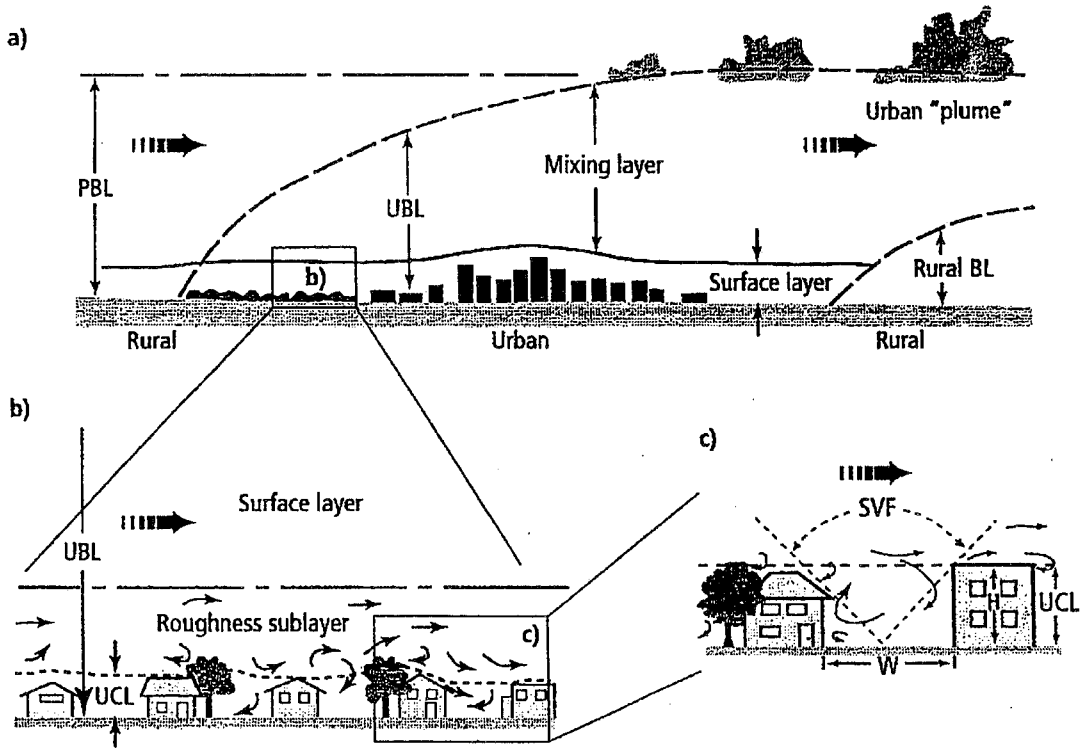

Figure 1: Idealised vertical structure of the urban atmosphere over (a) a whole city (mesoscale), (b) a single urban terrain zone (local scale), and (c) a single street canyon (microscale). Source: Oke (1997).

The structure illustrated by Figure 1 looks complicated, but it reveals three essential scales of importance to most climate station networks:

- *the micro- and local scale of the UCL* - within this layer there are many subclasses of climates, each determined by the physical character of the surface and its immediate surroundings. The climate of a single building or single street may be identifiable. This is the source of the nightmare for the person who has the responsibility to locate a single station. Every surface component (hot road, sheltering tree, shading building) threatens to swamp the readings. However, if particularly anomalous elements can be avoided, it is often possible to find areas of sufficiently similar character (say within one type of urban terrain zone (UTZ); Ellefsen, 1985), and of sufficient horizontal dimensions (a circle of about 0.5 km around the site), that a representative UCL climate station can be established. 'Anomalous' in this context means an element which is sufficiently close and generates a strong climatic effect so that it skews the results relative to the local mean. This would be a local scale climate in the UCL.
- *the local scale of the surface layer* – in addition to observing local climate in the UCL, as above (which is still fraught with microclimatic difficulties) a more stable local climate response can be observed in the surface layer. Only a restricted range of measurement heights exists (see below), but if these limitations are met, data representative of the local scale zone can be gathered. However, a concern may be that the results apply to a non-standard height. Achieving a more stable spatial average comes at the price of muting the surface effects seen in the UCL.
- *the mesoscale of the UBL* – if characteristics of the mixing layer in the UBL can be monitored the integrated effects of the whole city can be expressed in their contribution to the downwind mesoscale urban plume (Figure 1a).

The spatial patterns of these climates are distinct. For example, the well known modification of air temperature at screen-level in the UCL, known as the urban heat island (UHI), has a steep gradient at the edge of the city, but the distribution is much flatter over most of the rest of the urban area except for relatively 'hot' and 'cool' spots in particularly densely built-up (high rise, narrow canyons) or open and/or vegetated (parks, vacant land) areas, respectively. Again, one must remember that the nature of UCL climates is dominated by the immediate surroundings, not distance from the edge or the centre. Knowledge of these patterns is essential if we wish to sample appropriately with a station network. Presumably if only a single urban station can be installed the choice is between an urban core location, where the 'maximum' urban effect occurs, or a site in the thermal plateau region, well away from edge or 'hot' or 'cool' spot effects. If multiple stations are available it must be decided if the aim is to sample all urban terrain zones or to faithfully represent the spatial pattern. If it is the latter this will require stations in all zones, but also at sites positioned to show the gradients across the city. Since the patterns in small settlements are miniature versions of those in large cities Munn (1973) notes that it may take almost as many stations to portray the pattern of the UCL climates in a small city as for a large one. Similar patterns are found for humidity. It seems arguable that wind and precipitation measurements in the UCL are sufficiently open to micro-variability that it may be better to sample them only above roof-level. In this case distance from the urban-rural border, and transitions in UTZ, are more relevant because of changes in surface roughness. For radiation measurements anticipated patterns of air pollution and cloud may be significant.

GUIDANCE FOR LOCAL MEASUREMENTS

Let's look at considerations which face establishment of a standard climatological station at a site within a city. That is, we are looking at the advice provided to someone installing a station to measure air temperature, humidity, wind speed and direction, precipitation and perhaps radiation, soil temperature and evaporation.

1. Choosing the site

In terms of where to locate within the city limits, and in which UTZ, the central question relates to the purpose of the station. Therefore decisions should be based on recognition of the patterns outlined at the end of the preceding section, and whether the station is solitary or part of a network. Once the UTZ and part of the city are chosen the next criterion is homogeneity; i.e. to locate in a part of the zone, that is reasonably representative of its surroundings. At this stage is helpful to draw up first order descriptive statistics of the area, such as the mean height of the up-standing elements (buildings and trees), and the dimensions of the spaces between them (gardens, courtyards, streets). From these measures a simple list of typical characteristics of the zone can be drawn up, perhaps in terms of normalised measures such as mean height, height to width ratio, and the ratio of built:greenspace area. This helps to develop a notion of typical exposure in the zone and provides objective scales so that potential sites can be ranked. Recognising that in the end you can only site where the opportunity/permission exists, at least you gain some idea of how fair the representation might be. What is different about this thinking, compared to that normally required, is that the essential notions of an "open" or unobstructed site are abandoned in favour of representativity. This concept is already recognised, for example in the Canadian Guidelines for Autostations which note that the site should be consistent with the purpose of the data to be collected – if the station is to obtain synoptic air mass observations, small scale or human features should not exert an influence, but if it is to represent smaller climates the site should reflect them (AES, 1992). Failure to exercise this judgement leads to some nonsensical stations. The most common being the lovely grassed park site in the core of a large city – such a site is an anomaly for the city, in fact it doesn't take a very large vegetated park to come up with a climate which is thermally quite similar to that of the city's rural environs (Spronken-Smith and Oke, 1998).

2. Site layout and instrument exposure

Once the site is chosen, the layout of the station, and the placement of the instruments, should be governed by existing WMO and/or national Guides where possible, but again some bounded flexibility is useful. For example, the standard short grass surface may be appropriate if the UTZ is one of open-set houses with gardens and roadside verges, but this tenet should be relaxed to accommodate artificial surfaces as the built:greenspace ratio increases. Similarly the size of the plot, and the rules regarding how many multiples of obstruction height a given instrument must be away from an obstruction, should be relaxed for certain measures. For example, if the local climate of a city core is wanted, and the typical height of buildings and trees (z_H) is say 20 m, it may be difficult to find a site which allows for $2z_H$ in all directions for temperature and humidity, more so for the $4z_H$ required for precipitation and almost impossible to get $10z_H$ for wind. What is far more important in siting the instruments is to reflect the typical dimensions of the spaces within the UCL, so preserving some notion of the local ratio of element height to inter-element spacing (W) – often called the aspect ratio (z_H/W) – may be a more sensible approach. After that the station should be centred within the space, i.e. at approximately W/2. This may be acceptable for temperature and humidity, but almost certainly not for wind or precipitation (see below). On the other hand, whilst the rules for surface type and distance from obstruction may have to be relaxed, or at least re-specified, those regarding micro-scale influences to be avoided (e.g. "excessive human traffic", "vehicle parking areas" and "where heat is exhausted by vehicles and buildings") may have to be specified much more carefully.

3. Developing guidelines for individual climatological elements

If new guidelines are to be formulated at the local scale the following may be relevant to individual climatological elements:

- *temperature and humidity* – normal screen-level exposure seems appropriate, with modifications along the lines mentioned above (i.e. regarding relaxation of surface character and distance from obstruction guidelines for non-urban sites). Some relaxation in the recommended height may also be necessary to avoid vandalism and human or vehicular traffic. Since the height variation of these properties in urban canyons is relatively slight (Nakamura and Oke, 1988) this may be acceptable. Sensor shields may need to include protection from sources of infrared as well as solar radiation.
- *soil temperature* – few climate stations include this quantity. Urban sites certainly present sampling difficulties for shallow depths because of the wide variability of surface covers, but deep soil temperatures should not be over-looked. At depths of say 0.5 m and greater the accumulated heat storage change of the city can be seen. Long-term trends in soil temperatures may in fact provide better insight into urban thermal modification than the more sensitive air temperature record.
- In the same vein few stations gather grass-minimum temperature in cities. Given that grass may be irrelevant to some parts of the city this is understandable, but the less commonly gathered concrete minimum temperature has interesting applications in highway meteorology and building climatology.
- *wind speed and direction* – UCL wind climate in the vicinity of trees, and especially buildings and streets, is far too complex and erratic (Hosker, 1985) to be usefully monitored as part of a standard network. Except in areas of small z_H (say < 4 m) using the international standard height of 10 m for measurement will not give acceptable results in cities. However, variability of wind components decreases upwards through the roughness sublayer, and returns to values typical of adjusted boundary layers in the surface layer (Rotach, 1995; Figure 1a,b). Guidelines should therefore indicate that the minimum height for wind measurements is the top of the roughness sublayer, and give methods to predict its height. In very crude terms it is about 2½ to 4 times z_H, but it is also thought to depend on the spacing of the roughness elements (see Grimmond and Oke, 1998). The maximum height of measurement is limited by the distance from the nearest upwind UTZ boundary. Therefore this distance is also relevant to the choice of location within the city. Appropriate methods to calculate distance of fetch are given by Schmid (1994). Given the inherent differences of z_H and building density between cities, and between different parts of the same city, wind observations will have to be conducted at different heights. Nevertheless standardisation to a single height, say 30 m, is a simple calculation via wind profile theory.

  The nature of the supporting structure is also critical to wind measurements. Even open lattice towers distort the flow in their vicinity, so use of solid masts, chimney stacks and booms on buildings raises serious concerns which must be addressed in urban guidelines. We are all aware of anemometers mounted on masts atop tall buildings; they are open to serious errors. Measures of gustiness and the standard deviation of speed and direction may be especially important to air quality and wind engineering applications in cities.
- *precipitation* – except in the most open of UTZ, observations of precipitation in the UCL are open to many of the concerns noted for wind, because they are subject to the chaotic airflow. In order to reduce spatial variability in catch, consideration may have to be given to exposing rain and snow gauges near the ground at an open space which meets or approximates the standard exposure guidelines, even if it is not co-located with the screen. Exposure at a similar height to the anemometer, might be contemplated but: (a) this means the speed of catch is greater than near the ground and gauge efficiencies are sensitive to this, (b) interception by the

sides of buildings and trees is not accounted for, and (c) even automated elevated gauges present difficulties of maintenance. Due to drifting, snow accumulation on the ground presents a knotty sampling problem, at least as difficult as that in forests.
The measurement of rate of precipitation, in addition to total accumulation, is valuable especially for urban hydrologic applications.

- *radiation and bright sunshine* – measurement of incoming fluxes of radiative energy in the city present little problem. Exposure requirements are met by mounting on the roof of a tall building as long as the horizon is free of obstruction. On the other hand, measurement of upwelling and net fluxes, which require that the sensor 'see' a representative sample of the reflecting or emitting surface, must be made from a tall tower. Height above ground is important as a determinant of the radiative source area. If an appropriate observation platform is available good estimates of the radiation balance and its components can be made. Soiling of the sensor windows by pollution necessitates more frequent maintenance than cleaner sites.
- *evaporation* - it is doubtful if meaningful observations of evaporation can be made using the pan approach in cities. Firstly, the variability of winds again arises, secondly, microscale advection of heat from built surfaces is likely to boost evaporation well beyond potential rates, and thirdly, it seems unlikely that sensible pan coefficients can be devised to cover the range of possible urban surroundings.

4. Accommodating changing urban form

To be flexible the long-term observation scheme for an urban site must recognise the dynamic nature of a city's structure over history. Initial site selection should presumably take care to avoid a site where massive change is already slated. But by the same token it may not necessarily be a good idea to be certain it will not keep pace with changes around it. If, some time after establishment, clearly unacceptable change renders the site either unable to gather sensible data or makes it anomalous for its urban terrain zone (UTZ), relocation should be considered a reasonable solution, not something to be fought without thought. Naturally potential sites for relocation should be in the same UTZ, and not subject to different local or mesoclimate controls because of different relief, proximity to water bodies, etc.).

The key to this must be a strictly-adhered to protocol concerning the documentation of metadata. The metadata archive must be kept up-to-date on a reasonable schedule (say annually), and should include: exact co-ordinates, elevation, dimensions, maps and photographs of the surroundings, the form of the local horizon, surface materials, tree species, human activities and heat sources, etc. as well as the descriptions of the instruments their calibrations, height above ground, exposure, recorders and software. Such simple and inexpensive documentation is invaluable to all who subsequently wish to make use of the data.

ON THE PRESSING NEED FOR URBAN STATION GUIDELINES

Very soon, more people will live in cities than anywhere else. For that reason alone meteorological services have a major responsibility to focus more on the needs of city dwellers, especially those in the rapidly urbanising tropical world. At the 12th World Meteorological Congress in Geneva, and subsequently at Habitat II in Istanbul, WMO committed itself to give high priority to the delivery of better services to cities.

If that is to be meaningful, more and better urban observing stations will be required. But before National Meteorological Services invest in this infrastructure it seems imperative that the poor state of measurement practice regarding the stations we already have be addressed, and that we develop guidelines for what might be called the representative urban climatological station.

This suggestion is not without precedent. As long ago as 1975 WMO circulated a questionnaire to discover the state of the art of urban observation and the need for guidelines. At the conclusion of his report Van Gysegem (1978) stated: "before definite guidelines can be given more research is necessary". He suggested that topics needing more investigation included: errors of exposure, representativity of data in specific land-use areas, measurement errors due to sensor response in the turbulent urban atmosphere, and the development of new low cost instruments and data processing systems.

In the 20 years since that review and recommendation the field of urban meteorology/climatology has made tremendous strides. One only has to consult reviews of the field to know that significant advances in the base of physical understanding and model development have been made (e.g. Oke, 1988; Arnfield *et al.*, 1991; Hanna and Chang, 1992; Cermak *et al.*, 1995). Together with the improvement and automation of commercial instrumentation in general there seems no doubt that Van Gysegem's concerns have been met. The need for guidelines has been restated. In 1982 an Expert Group recommended "there is need for WMO to define and urban climatological station as well as [to] specify [the] type and programme of observations, instrumentation, exposure and observational practice" (WMO, 1982). Further, in 1997 the Taskforce on TRUCE recommended the preparation of an "Urban Climate Study Guide" (WMO, 1997).

In some respects the measurement of air pollutants poses a greater array of difficulties than for meteorological elements, but because they are concentrated in cities the need to devise urban guidelines for networks and sites has been greater. The meteorological community should be able to draw upon this work (e.g. Ludwig and Kealoha, 1975; Munn, 1981).

In my view the fields of urban meteorology, climatology and hydrology now contain sufficient knowledge about the physical basis of urban atmospheres, and the technical requirements for measurement, to attempt to formulate useful and much needed addenda to the existing Guides to observing practice in their respective fields. If such a recommendation is acted upon, a significant challenge in the process of formulating guidelines will be merging the bedrock concept of standardisation, with the physical reality of the ever-changing physical nature of cities. But as Van Gysegem (1978) pointed out "there is no obvious reason why there [has to] be a unique solution". Maintenance of rigorous principles of measurement is not incompatible with recognition that the system being observed changes over time.

REFERENCES

AES, 1992: *AES Guidelines for Co-operative Climatological Autostations, Version 2.0*, Canadian Climate Centre, Environment Canada, Guide 92-1, Downsview, 84 p.

Arnfield, J., A.J. Brazel, D.E. Greenland and C.J. Willmott, 1991: Physical and boundary-layer climatology, *Physical Geography*, **12**, 189-206.

Cermak, J.E., A.J. Davenport, E.J. Plate and D.X. Domingos (eds.), 1995: *Wind Climate in Cities*, Kluwer Academic Publishers, Dordrecht, 772 p.

Ellefsen, R., 1985: *Urban Terrain Zone Characteristics*, Technical Monograph 18-87, US Army Human Engineering Laboratory, Aberdeen Proving Ground, Maryland.

Grimmond, C.S.B. and T.R. Oke, 1998: Aerodynamic properties of urban areas derived by analysis of urban form, *Journal of Applied Meteorology*, in review.

Hanna, S.R. and J.C. Chang, 1992: Boundary-layer parameterizations for applied dispersion modelling over urban areas, *Boundary-Layer Meteorology*, **58**, 229-259.

Hosker, R.P. Jr., 1985: Flow around isolated structures and building clusters: A review, *ASHRAE Transactions*, **91 (2B)**, 1671-1692.

Ludwig, F.L. and J.H.S. Kealoha, 1975: Selecting sites for carbon monoxide monitoring, EPA Report 450/3-75-077, Research Triangle Park, NC, 149p.

Munn, R.E., 1973: Urban meteorology: some selected topics, *Bulletin American Meteorological Society*, **54**, 90-93.

Munn, R.E., 1981: *The Design of Air Quality Networks*, Macmillan Publishers, London, 130p.

Nakamura, Y. and T.R. Oke, 1988: Wind, temperature and stability conditions in an east-west oriented urban canyon, *Atmospheric Environment*, **22**, 2691-2700.

Oke, T.R., 1984: Methods in urban climatology, in *Applied Climatology*, Zürcher Geographische Schriften, **14**, 19-29.

Oke, T.R., 1988: The urban energy balance, *Physical Geography*, **12**, 471-508.

Oke, T.R., 1997: Urban environments, in *The Surface Climates of Canada*, Bailey, W.G., T.R. Oke, and W.R. Rouse (eds.), McGill-Queen's University Press, Montreal, 303-327.

Rotach, M., 1995: Profiles of turbulence statistics in and above an urban street canyon, , *Atmospheric Environment*, **29**, 1473-1486.

Schmid, H.P., :1994. Source areas for scalars and scalar fluxes. *Boundary-Layer Meteorology*, **67**, 293-318.

Spronken-Smith, R. and T.R. Oke, 1998: Survey of the thermal regime of urban parks in two cities with different summer climates, *International Journal of Remote Sensing*, (in press).

Van Gysegem, A., 1978: Meteorological observations in urban environment, Institut Royal Météorologique de Belgique, Bruxelles, Publications Série B, No. 93, 19 p.

WMO, 1982: Report of the Meeting of Experts on Urban and Building Climatology, WCP – 37, World Meteorological Organization, Geneva, 38 p.

WMO, 1983a: Guide to Meteorological Instruments and Methods of Observation, 5th edn., WMO-No.8, World Meteorological Organization, Geneva.

WMO, 1983b: Guide to Climatological Practices, 2nd edn., WMO-No. 100, World Meteorological Organization, Geneva.

WMO, 1997: Report of the Meeting of the Taskforce on TRUCE, WCASP – 40, World Meteorological Organization, Geneva, 9 p.

****

WIND PROFILER RADAR:
Operational Remote Sensing of upper-air winds

Wim A. Monna, Russell B. Chadwick, Jochen Dibbern
John Nash and Hans Richner

1. Introduction

Information on upper-air wind is of vital importance for weather forecasting. Schreiber already realised this (1886), when he followed the flight of a balloon with two theodolites. It was only with the invention of radiosondes, that from the 1930's onwards, operational measurements of upper-air wind became feasable. In modern weather forecasting there is an increasing demand for high time resolution data, measured with systems that can operate nearly unattended. In this respect, modern remote sensing techniques now offer alternatives. With wind data from a combined network of radiosonde stations and wind profilers, the quality of numerical and local weather forecasting can be improved.

Woodman and Gullien (1974) were among the first to demonstrate the feasibility of wind and turbulence measurements in the upper atmosphere with a wind profiler. Much of the early work regarding radar remote sensing of the clear atmosphere and possible applications was reviewed by Chadwick and Gossard (1983). Other review papers on wind profilers with extensive references are given by e.g. Crochet (1989), May (1991) and Monna (1994).

The first step towards operational use of wind profilers was made in the United States in 1986, when NOAA started the development and deployment of a network of 31 wind profilers in the central part of the USA (Chadwick, 1986). Experiments with simulated wind profiler data (Kuo and Guo, 1989) indicated that a profiler network would improve numerical forecasts. This was shown in practise after the completion of the NOAA Profiler Network (NPN) in 1992 (Schlatter and Zbar, 1994).

In Europe the development and use of wind profilers was from 1987 till 1993 co-ordinated by the CEC-sponsored COST-74 project[1] (COST 74, 1994), and thereafter by the follow-up project COST-76, which will end in 1999. In 1997 COST-76 carried out an experiment in parallel with FASTEX, to demonstrate the operational exchange of wind profiler data, and to create a database for further usefulness studies (Oakley at al., 1997).

Also in Japan, the usefulness of wind profilers for weather forecasting was shown, using a 404 MHz system for weather forecasting research and rawindsonde comparisons (MRI, 1995).

In Australia, substantial research into radar probing of the atmosphere has been done (Vincent et al., 1987). The development and operational use of a wind profiler network was part of this research. The preliminary plan is to use a system near 50 MHz for wind measurements in the upper atmosphere and one near 1000 MHz for wind and rain measurements in the boundary layer.

On several fronts important progress is being made. In the fall of 1997 the World Radiocommunication Conference of the ITU allocated frequency bands for wind profilers (see section 5). A BUFR code for wind profiler data exchange has been developed, which will soon be submitted to WMO for acceptance. The monitoring of wind profiler data by NWP centers has been started. The development of data assimilation techniques that can handle the high (hourly) time resolution wind data is in progress. With all these developments, wind profilers are becoming mature remote sensing systems that are now entering operational use. However, it is important to realize that wind profilers are not a complete replacement for radiosondes, because they do not measure temperture and humidity. This paper provides background information on the characteristics of wind profilers, and on their use and drawbacks. Moreover, some information on RASS (Radio Acoustic Sounding System) is also presented, since RASS is a proven technique nowadays which is often used as an extension of a wind profiler to measure (virtual) temperature profiles.

---

[1] COST: European co-operation in the field of scientific and technical research. COST programmes are concerted actions of European countries, and are supported by the Commission of the European Communities.

2. What is a wind profiler

A wind profiler is an ultra-sensitive, upward-looking Dopplerradar. Half wavelength fluctuations of the radio refractive index, caused by atmospheric turbulence, provide (back)scatter (Tatarskii, 1961). The usual frequencies for operation are in the range 40 and 1400 MHz. The Doppler frequency shift of the return signal for a given delay is proportional to the radial wind velocity at a height determined by that delay.

Measurement of vertical profiles of horizontal wind speed and direction requires at least three different beam directions: generally one vertical and two orthogonal beams at elevation angles of about 75 degrees. This geometry also gives vertical profiles of vertical wind. It is important to realize that the separation distance between the air parcels that are sensed by the individual beams increases with altitude, so combining the measurements is only possible when the wind field is horizontally homogeneous. This is almost always the case for hourly integrated measurements. Shorter averaging times are also widely used and usually yield good results. However, times much shorter than 6 minutes can sometimes yield inconsistent horizontal winds.

The design of the antenna is important both for overall performance and for cost. With larger antennas, winds can be measured to higher altitudes. Usually wind profiler antennas are stationary arrays of radiating elements. The desired beams are generated sequentially by changing the relative electrical phasing of the signals to each element.

An advantage of a large arrays is that the formed beam is narrow, thus reducing the risk of signals from unwanted targets. Moreover, large arrays can have low antenna side lobes at ground level, reducing ground clutter and ground-based interference. Low side lobes close to the main beam can reduce returns from nearby rain storms or aircraft. The antenna size depends on the frequency, varying from 2mx2m for 1000 MHz to 13mx13m for 400 MHz and 100mx100m for 50 MHz. Wind profilers are commercially available at prices ranging from USD 200,000 to over USD 1 million.

3. System performance

Wind profiler clear air backscatter is caused by half wavelength turbulent eddys. In the upper atmosphere the small eddys are more rapidly converted into heat by viscous action than in the lower atmosphere. Hence, the clear air scattering in the upper atmosphere is weaker for shorter wavelengths. So, in general an increase in frequency (shorter wavelengths) decreases the height coverage.

Height coverage also depends on the transmitter and antenna. At the same frequency, wind profilers with larger power and antenna apertures will see to higher altitudes. A figure of merit is the power aperture product, which is the transmitted average power in Watts times the antenna physical area in square meters.

Another important parameter is the height resolution which is determined by the pulse length of the transmitted RF signal. The shorter pulse lengths give better (smaller) resolutions. Unfortunately the bandwith of the transmitted RF signal fundamentaly increases for shorter pulse lengths. This is a serious complication with respect to frequency allocations (section 5).

In practise, wind profilers are built for three frequency bands, i.e. around 50 MHz, 400 MHz and 1 GHz. Corresponding characteristic values for height coverage are 3 - 30 km, 1 - 16 km and 0.3 - 2 km respectively, with 300, 250 and 75 m vertical resolution. It is important to realize that the characteristics for these three frequency bands are complementary, since in meteorology we need data with better resolution at lower altitudes. Height coverage statistics and system performance for several wind profilers are given by Martner et al. (1993).

For example, 30 of the profilers of the NOAA Profiler Network (NPN) operate at 404 MHz with 6 kW peak power and an antenna aperture of 169 m^2. In the high mode the duty cycle is 13%, so the average power is 780 W and the power aperture product is about 132,000 $W.m^2$. This gives height coverage up to about 14 km 90% of the time in the central USA averaged over the year. The transmitted pulse is a coded sequence of three 6.67 microsecond elements, which gives resolution of about 900 m, and a total pulse length of 20 microseconds. In the low mode the pulse is a coded sequence of two 1.67 microsecond elements, which gives resolution of 320 m, and a total pulse length of 3.33 microseconds. In the high mode the -20 dB bandwith is about 0.25 MHz and in the low mode it is about 0.8 MHz.

Rain affects the performance of wind profilers operating
around 1 GHz. At this frequency the echo from raindrops is much stronger than the clear-air echos. As a consequence, the measurement of the radial winds is easier in stratiform precipitation. As long as there is a radial velocity measurement from a vertical beam, it is relatively easy to correct for the fall velocity on the oblique beams.

Wind profilers can operate at severe weather conditions, though lightning strikes can cause dammage. Apart from changing atmospheric conditions, performance is affected by equipment faults, and communications and hub problems. Performance statistics of the NOAA profiler network are routinely monitored, and are posted on the World Wide Webb (*www-dd.fsl.noaa.gov*). Data from European wind profilers can for the moment be found on the CWINDE web page: *http://www.meto.gov.uk/sec5/sec5pg5.html.*

The accuracy of wind profiler measurements is usually assessed by comparison with rawinsonde data, or against numerical weather prediction fields for the profiler location. In evaluating comparisons between rawinsonde and wind profiler measurements, it is necessary to take account of the differences in the temporal resolution and location of the two sets of measurements. Comparisons reported by Weber and Wuertz (1990), May (1993), Martner et al., (1993), Nash, (1994), MRI (1995) and Riddle et al. (1996) show that the accuracy of wind profiler and rawinsonde measurements is comparable. The COST 74 report (1974) indicates the information that can be derived from comparison of profiler observations with numerical forecast fields.

4. Data processing

The main steps of wind profiler data processing are:

-conversion to meteorological data
-quality control
-encoding for data transmission

4.1 Conversion of radar output to meteorological data

At the receiver output of a wind profiler the signal power from the atmosphere can be much smaller than the noise power, i.e. less than a hundredth. After the signal plus noise analog voltage has been converted to digital form, time averaging is used to increase the signal to noise ratio for each of the range gates. Next, each of the averaged time data streams (from each range gate) are transformed to the frequency domain using a conventional Fast Fourier Transform (FFT). The output of the FFT is converted to a power spectrum. Then the power spectra for each range gate are averaged to further reduce the fluctuations caused by noise. This power spectrum is interpreted as a Doppler velocity spectrum so that the mean (or first moment) of the spectrum is the radial wind velocity for that range gate. The zeroth moment (area under the curve) is proportional to the structure coefficient of the radio refractive index at that range. The second moment (width of the spectrum) can be interpreted as the turbulent dissipation rate or the rate at which turbulent energy is being converted into heat through atmospheric viscosity.

4.2 Quality control of the data

The radar signal processing and the data processing are necessarily sensitive to many different types of signals. Examples of erroneous signals are reflections from stationary objects like buildings, metal towers, even the ground. These returns will show up near zero velocity and can in principle be eliminated. Moving objects, like automobiles, airplanes, swinging power lines, and leaves on trees appear at other than zero velocity which requires special approaches. Biological targets like migrating birds and large insects can also affect the output.

Some of these unwanted signals can be identified (and eliminated) by recognizing the fingerprint of the spectrum. One can also compare the spectrum from a range gate with that from the adjacent range gates and use consistency arguments to find and eliminate unwanted features in adjacent spectra. A widely used approach is to consider the time-height display and find features which form continuous two-dimensional regions known to be representative of atmospheric signals (Weber and Wuertz, 1991).

Processing of the velocity spectra also can be used to identify regions of rain and change the processing so that incorrect information is not distributed. In straitiform rain, the vertical profiles of horizontal wind are still easily obtained, but zeroth and second moments now have different interpretations from the clear air case.

Research to improve quality control procedures is ongoing, especially regarding the detection of rain and migrating birds. There are indications that wavelet transformation is more powerful than FFT (Jordan et al., 1997), especially in the prescense of large clutter signals. This research could well lead to better wind profiler performance at poor conditions.

4.3 Encoding for data transmission

Operational use of wind profiler radar data is only possible when data can be transmitted rapidly to users and readily understood. This requires suitable pre-arranged codes and formats. The Rawinsonde code cannot be used, because a wind profiler produces much more information, so a special code, called the Profiler Data Exchange Format was developed by NOAA (Forberg and Barth,1985), and is presently used for data transmissions between the NOAA profilers and the central hub. In Europe, COST-76 co-ordinated the development of a BUFR code for wind profilers. This code is now being commented upon in the USA, and will finally be submitted to WMO.

5. Frequency allocation for operational use

For many years the operation of wind profilers was possible only with a frequency assignment for a limited time and on non-interference basis. It is obvious that for operational use frequencies must be allocated in an internationally co-ordinated way, to allow long-term operation of wind profilers.

In 1989 WMO requested the allocation of frequencies for the operational use of wind profilers. ITU Task Group 8/2 was installed to prepare input documents. It was argued that allocations were needed in the frequency bands around 50, 400 and 1000 MHz, because of the complementary characteristics of systems at these three frequencies. It was made clear that the large bandwiths of wind profilers was unavoidable, given the need for specific vertical resolutions. After many years of preparatory work, especially in Europe (COST-76) and the USA, and various full-size tests and experiments, the ITU World Radiocommunication Conference (WRC-97), held in Geneva in the fall of 1997, issued Resolution COM5-5 which provides the appropriate guidance to any country regarding wind profiler frequency allocation.

Four important points are made by Resolution COM5-5.

a. To conduct measurements up to a height of 30 km with appropriate resolutions, it is necessary to allocate frequency bands for wind profilers in the vicinity of 50 MHz (3 to 30 km), 400 MHz (0.5 to about 10 km) and 1000 MHz (0.1 to 3 km).

b. Wind profilers operating in the meteorological aids service in the band 400.15 - 406.0 MHz interfere with satellite emergency position-indicating radio beacons operating in the mobile-satellite service in the band 406.0 - 406.1 MHz. Therefore any emission capable of causing harmful interference to the authorized uses of the band 406 - 406.1 MHz is prohibited.

c. Countries should not implement wind profilers in the 400.15 - 406.0 MHz band, and those currently operating wind profilers in this band should discontinue operations as soon as possible.

d. Countries should implement wind profilers as radiolocation service systems in the following bands, having due regard to the potential for incompatibility with other services and assignments to stations in these services:

46 - 68 MHz
440 - 450 MHz
470 - 494 MHz
904 - 928 MHz (North and South America only)
1270 - 1295 MHz
1300 - 1375 MHz
420 - 435 MHz or 438 - 440 MHz (if compatibility between wind profilers and other radio applications operating in the band 440 - 450 MHz or 470 - 494 MHz cannot be achieved)

Resolution COM5-5 of WRC-97 gives advice and assistance to countries of the world regarding the identification of appropriate frequencies to accommodate allocations and assignments for wind profilers. Given the participation of so many countries at the WRC, it is expected that this resolution will be a sound basis for the operational use of wind profiler technology.

In France, a permanent license has been issued for a 48.62 MHz system in 1997. In the United States, an operational frequency allocation for government wind profilers has recently been granted for the 448 - 450 MHz band.

6. RASS temperature profiling

The use of a combination of acoustic and radar signals to remotely measure vertical profiles of virtual temperature was first demonstrated in the early 1970's (Marshall et al., 1972; North et al., 1973). The acoustic waves and the radar waves are both directed upward and interact to cause a backscattered radar signal which has information on the virtual temperature. Oftentimes it is said that the backscattered signal tells the speed of the acoustic wave. However, the more precise way of saying this is that the radar wave Bragg-matches a component of the acoustic signal determined by the local virtual temperature.

Acoustic energy causes density fluctuations resulting in radio refractive index fluctuations which scatter wind profiler signals, just as naturally occurring turbulence. However, these fluctuations are traveling with the local acoustic velocity plus the mean vertical wind rather than just the mean wind as in the case of the naturally occurring fluctuations. The RASS temperature measurement is made by determining the local acoustic wavelength through Bragg matching, i.e the acoustic wavelength is one half of the wind profiler wavelength. This acoustic wavelength is proportional to the acoustic velocity which is proportional to the square root of the virtual temperature. For a detailed description of the technique, see May et al. 1990 and May, 1991.

The requirements on the acoustic energy are that it be directed upward as much as possible and that it cover a band of acoustic frequencies within the proper range for Bragg matching, which changes with virtual temperature. Note that a single CW acoustic tone will not suffice. Note also that a very wide band acoustic source (like music) will be inefficient since most of the acoustic energy will not affect the backscattered signal.

One type of acoustic signal that has been used is a tone with linear FM-CW imposed. This works well, but it sounds very much like a police siren. A better approach is to modulate the tone with a random signal, sometimes referred to as "pink noise", which is more acceptable for people living nearby, while transmitting the same amount of power. The acoustic energy is generated by a electro-mechanical transducer directed toward a parabolic reflector to project the sound upward. Usually the parabola is surrounded with acoustic absorber so the sound is attenuated in all directions except vertical.

There are generally two things which limit the height to which temperatures can be measured under most circumstances. The first is the acoustic attenuation. Wind profiler radars operating at 50 MHz use acoustic signals at about 100 Hz where the attenuation is quite small, about 0.3 dB/km. With 400 MHz profilers the acoustic signal is about 900 Hz and the acoustic attenuation is about 10 dB/km. With a 915 MHz profiler the acoustic signal is at about 2000 Hz and the attenuation is up to 40 dB/km for a dry atmosphere.

The other thing limiting the measurement height is the horizontal wind. The stronger the lower tropospheric wind, the greater the likelihood that the acoustic signal will be carried out of the radar beam. Results from the 404 MHz NPN in the United States indicate that usually the measurement height is 3-5 km under normal wind conditions. However, when there are strong winds in the lowest few km, the RASS measurement height may only be 1 km. In this respect upwind placement of the acoustic transducer is more effective than increasing the acoustic output.

Experience with RASS temperature profiling with the NPN shows that accuracies of less than 1 degree C up to 3 to 5 km with routine operation in rural areas within 400 m of people is feasible. The performance can be degraded by strong low level horizontal winds. Long term comparisons of RASS with radiosonde measurements in Germany showed a systematic underestimation of the virtual temparature in the lower levels. Based on comprehensive investigations on paramaters affecting the accuracy of RASS, corrections were developed that reduces the bias for the measurements in 1997 from 1.1 K to 0.2 K.

7. Towards operational use

For numerical weather forecasting and for the local meteorologist, information on upper-air winds is of crucial importance. For many decades, radiosondes have been the standard equipment for these measurements. However, more than four flights a day are practically impossible because of the cost of the radiosonde and the manpower involved. With the increasing demand for high time resolution data, and the need for systems that can operate nearly unattended, wind profilers are now starting to play a role in operational upper-air wind measurements.

An important step toward operational use of wind profilers has been the experience with the NOAA Profiler Network (NPN) in the USA. It was designed from the start to acquire, process and distribute data to operational users in real time. The network and its components were procured from commercial sources using standard government procedures with specified reliability and maintainability requirements. Modular construction made most maintanance functions easily performed by National Weather Service (NWS) operational field personnel. The logistics and depot maintenance are also handled by operational branches of the NWS. Complete data availability and performance statistics have been recorded since the NPN was deployed, and have been used to make improvements and correct problems. The wind measurement capability has been complemented with colocated Radio Acoustic Sounding System (RASS) temperature profiling (May et al, 1990; May, 1991) and GPS Integrated Precipitable Water Vapor measurements (Businger et al., 1996).

In Europe the development and use of wind profilers has been co-ordinated by COST since 1987. The first action, COST-74, was started to support the development and implementation of wind profiler networks in Europe. The main objectives were the assessment of user requirements, the development of standard specifications for wind profiler systems and data exchange, and the realization of frequency allocations. Having organized two workshops (Versailles, France, 1989 and at the XVIIIth EGS meeting at Wiesbaden, Germany, 1993), COST-74 ended in 1993, after having produced a final report (COST 74, 1994).

Because not all goals were reached, it was decided to start a follow-up project to finalize the work. COST-76 started in March 1995 and has a mandate for five years. The original objectives are more or less unchanged. In short, all preparations for the future deployment of a European wind profiler network must be made, and the feasability of such a network must be demonstrated. In the first four years substantial progress has been made. In May 1997 a workshop with global participation was organized at Engelberg (Switzerland). The realization of frequency allocations at the ITU WRC 97 was supported by e.g. the demonstration that profilers can be operated without causing harmful interference on TV reception and GPS systems. The CWINDE (COST Wind Initiative for a Network Demonstration in Europe) experiment (Oakley et al., 1997) was organized in the fall of 1997. This experiment was carried out in parallel with FASTEX (Fronts and Atlantic Storm Track EXperiment), with the intention to demonstrate the operational exchange of wind profiler data with the recently developed BUFR code, and to create a database for further usefulness studies. The CWINDE profiler network is still in operation. The usefulness studies are in progress. The network will also be used during MAP. It is intended to organize a final workshop in mid 1999. The future operational deployment of a wind profiler network in Europe may be co-ordinated by EUMETNET.

7.1 Single systems

In modern weather forecasting, information is needed in data sparse areas. Moreover, the development of high time resolution assimilation techniques (Rabier et al., 1992) leads to a demand for high time resolution data i.e. hourly wind profiles. In this case, wind profilers can play an important role. In data sparse areas, wind profilers have a positive impact on the quality of the numerical weather forecasts. This was shown clearly for the Pacific by Gage et al. (1988). At remote locations it may be expensive to operate a rawinsonde station. For example in the Canadian High Arctic, seven people are required to operate a remote rawinsonde station, while a wind profiler can be operated unattended and give hourly wind profiles, probably for lower operational costs. In these situations the 50 MHz system, or eventually a 400 MHz one are best suitable to realise the desired height coverage.

7.2 Networks
Wind profilers can also be used to improve the spatial and temporal resolution of existing radiosonde networks. Experiments with a simulated network some ten years ago showed an improvement of the short term forecast (Kuo and Guo, 1989). This result was confirmed when the NOAA Profiler Network in the USA became operational (Smith and Benjamin, 1993). Ciesielski et al. (1997) also report an improvement of the analyses when rawinsonde and profiler data are merged.

7.3 Local forecasting
In addition to the use of wind profiler data in numerical models, the real time information from nearby profilers is also useful to keep local meteorologists informed about development and displacement of features like fronts and mesoscale circulations. This has a positive impact on short-term forecasts (Steranka, 1990). Moreover, this local information can also be used to evaluate the analyses of numerical models (Beckman, 1990). Next to 400 MHz profilers, 1 GHz systems with their high vertical resolution are well suited here.

7.4 Aviation
A special version of local weather forecasting is needed on airports, where the meteorologist needs wind and wind shear information with high temporal and spatial resolution, especially for severe weather warnings. Here, a 1 GHz system, with its lowest measuring level close to the ground, can play an important role to support flight operations (Malherbe et al, 1989; Strauch et al., 1989). Unfortunately, the wind shear related to convective storms, which is particularly dangerous for aircraft during take-off and landing, is so local in time and space, that it cannot be detected by a single wind profiler (Strauch et al, 1989).

7.5 Air pollution
Another operational application of 1 GHz profilers is the forecasting of the atmospheric dispersion of pollutants with air pollution transport models, that need high resolution 10 minute wind information in the boundary layer (Van Dop, 1986). Since these systems can also detect the boundary layer height, they are very useful in air pollution monitoring systems (Connolly and Dagle, 1991).

8. Conclusions
Wind profiler technology can be deployed and function well in the operational arena of weather services. The field personnel of any national weather service organization can, with training, maintain wind profilers for continuous operation in most regions of the world. The data produced by these profilers, if used correctly, will improve weather forecasts. However, at this time, wind profilers should not be thought of as a complete replacement for radiosondes because they do not measure temperature and humidity. Rather wind profilers complement conventional radiosondes by providing wind profiles with much greater time resolution. In this respect, current thinking stresses the concept of an integrated observing system, employing different components (Cogan et al, 1997). As for upper air winds one can think of the integration of wind reports from wind profilers, raiosondes and aircraft measurements. While wind profilers have been used in the atmospheric research world for the past two decades, only recently this technology has started to move into weather service operations. This trend is expected to continue into the next century.

9. Acknowledgements
The authors thank Margot Ackley and Henk Klein Baltink for carefully reading the manuscript.

10. References
Beckman, S.K., 1990: Operational use of profiler data and satellite imagery to evaluate the NMC numerical models in predicting heavy snow. Wea. Forecasting, 5, 259-277.

Businger, S., S.R. Chiswell, M. Bevis, J. Duan, R.A. Anthes, C. Rocken, R.H. Ware, M. Exner, T. VanHove and F.S. Solheim, 1996: The promise of GPS in atmospheric monitoring. Bull. Amer. Meteor. Soc., 77, 5-19.

Chadwick, R.B., 1986: Wind Profiler Demonstration Network. MAP Handbook, vol.20, S.A. Bowhill and B. Edwards, Eds., Urbana, IL, Univ of Illinois Press, 336-337.

Chadwick, R.B. and E.E. Gossard, 1983: Radar Remote Sensing of the Clear Atmosphere - Review and Applications. Proc. IEEE, 71, 738-753.

Ciesielski, P.E., L.M. Hartten and R.H. Johnson, 1997: Impacts of merging profiler and rawinsonde winds on TOGA COARE analyses. J. Atmos. Oceanic. Technol., 14, 1264-1279.

Cogan, J., E. Measure and D. Wolfe, 1997: Atmospheric soundings in near-real time from combined satellite and ground-based remotely sensed data. J. Atmos. Oceanic. Technol., 14, 1127-1138.

Connolly, S.T. and W.R. Dagle, 1991: A radar profiler for monitoring of winds and boundary layer height. Lower tropospheric profiling: Needs and technologies, Boulder, CO, USA, Sept 10-13, 141-142.

COST 74, 1994: COST 74 final report: Utilization of UHF/VHF radar wind profiler networks for improving weather forecasting in Europe. C. Lafaysse, Ed., European Commission, Directorate-General Science, Research and Development, Luxembourg, EUR
15450 EN.

Crochet, M., 1989: The atmospheric profiler radar; developments and outstanding questions. Proc. First European Wind Profiler Workshop, Versailles, France, March 6-8, C3-C32.

Forberg, J. and M. Barth, 1985: Profiler standard format for data exchange: Profiler site to hub computer. NOAA Technical Memorandum, ERL-WPL-126.

Gage, K.S., J.R. McAfee, W.G. Collins, D. Söderman, H. Böttger, A. Radford and B. Balsley, 1988: A comparison of winds observed at Christmas Island using a wind-profiling Doppler radar with NMC and ECMWF analyses. Bull. Amer. Meteor. Soc., 69, 1041-1046.

Jordan, J.R., R.J. Lataitis and D.A. Carter, 1997: Removing ground clutter and intermittent clutter contamination from wind profiler signals using wavelet transforms. J. Atmos. Oceanic Technol., 14, 1280-1297.

Kuo, Y.-H. and Y.-R. Guo, 1989: Dynamic initialisation using observations from a hypothetical network of profilers. Mon. Weath. Rev., 117, 1975-1998.

Marshall, J.M., A.M. Petersen and A.A. Barnes Jr., 1972: Combined radar-acoustic sounding system. Appl. Optics, 11, 108-112.

Martner, B.E., D.B. Wuertz, B.B. Stankov, R.G. Strauch, E.R. Westwater, K.S. Gage, W.L. Ecklund, C.L. Martin and W.F. Dabberdt, 1993: An evaluation of wind profiler, RASS, and microwave radiometer performance. Bull. Amer. Meteor. Soc., 74, 599-613.

May, P.T., 1991: Recent developments and performance of radar wind profilers and RASS. Aust. Meteor. Mag., 39, 237-245.

May, P.T., 1993: Comparison of wind-profiler and radiosonde measurements in the tropics. J. Atmos. Oceanic Technol., 10, 122-127.

May, P.T., R.G. Strauch, K.P. Moran and W.L. Ecklund, 1990: Temperature sounding by RASS with wind profiler radars: A preliminary study. IEEE Transact. Geosci. Rem. Sens., 28, 19-28.

Monna, W.A.A., 1994: On the use of wind profilers in meteorology. Ann. Geophysicae, 12, 482-486.

MRI (Meteorological Research Institute, Japan), 1995: Studies on wind profiler techniques for the measurements of winds. MRI Technical Report No. 35.

Nash, J., 1994: Upper wind observing systems used for meteorological operations. Ann. Geophysicae, 12, 691-710.

North, E.M., A.M. Peterson and H.D. Parry, 1973: RASS, a remote sensing system for measuring low-level temperature profiles. Bull. Amer. Meteor Soc., 54, 912-919.

Oakley, T.J., A. Glennie and D. Jerrett, 1997: CWINDE 97 - Report from project office. COST-76 Profiler Workshop 1977, Engelberg, Switzerland, May 12-16, 23-26.

Rabier, F., P. Courtier, J. Pailleux, O. Talagrand, J.-N. Thépaut and D. Vasiljevic, 1992: Comparison of four-dimensional variational assimilation with simplified sequential assimilation. Workshop on variational assimilation, with special emphasis on three-dimensional aspects, ECMWF, Reading, UK, Nov. 9-12, 271-325.

Riddle, A.C., W.M. Angevine, W.L. Ecklund, E.R. Miller, D.B. Parsons, D.A. Carter and K.S. Gage, 1996: In siru and remotely sensed horizontal winds and temperature intercomparisons obtained using integrated sounding systems during TOGA COARE. Beitr. Phys. Atmos., 69, 49-61.

Schlatter, T.W. and F.S. Zbar, 1994: Wind profiler assessment report and recommendations for further use. NOAA Forcast Systems Laboratory R/E/FS3, 325 Broadway, Boulder, CO 80303-3328.

Schreiber, P., 1886: Bestimmung der Bewegung eines Luftballons durch trigonometrische Messungen von zwei Standpunkten. Meteorologische Zeitschrift, 3, 341-345.

Smith, T.L. and S.G. Benjamin, 1993: Impact of network wind profiler data on a 3-h data assimilation system. Bull. Amer. Meteor. Soc., 74, 801-807.

Steranka, J., 1990: Meteorological and aviation applications of radar wind profiler measurements. Weather, 45, 426-430.

Strauch, R.G., D.A. Merrit, K.P. Moran, B.L. Weber, D.B. Wuertz and P.T. May, 1989: Wind profilers for support of flight operations. J. Aircraft, 26, 1009-1015.

Tatarskii, V., 1961: Wave propagation in a turbulent medium. Mc GrawHill Book, New York.

Van Dop, H., 1986: The CCMS air pollution model intercomparison study. Atmos. Environment, 20, 1261-1271.

Vincent, R.A., P.T. May, W.K. Hocking, W.G. Elford, B.H. Candy and B.H. Briggs, 1987: First results with the Adelaide VHF radar: spaced antenna studies of tropospheric winds. J. Atmos. Terr. Phys., 49, 353-366.

Weber, B.L. and D.B. Wuertz, 1990: Comparison of rawinsonde and wind profiler radar measurements. J. Atmos. Oceanic Technol., 7, 157-174.

Weber, B.L. and D.B. Wuertz, 1991: Quality control algoritm for profiler measurements of wind and temperatures. NOAA Technical Memorandum ERL-WPL-212.

Woodman, R.F, and A. Gullien, 1974: Radar observations of winds and turbulence in the stratosphere and mesosphere. J. Atmos. Sci., 31, 493-505.

Author affiliation:

-W.A. Monna, Royal Netherlands Meteorological Institute KNMI,
De Bilt, the Netherlands; Chairman COST-76; monna@knmi.nl
-R.B. Chadwick, NOAA/FSL, Boulder, USA; chadwick@fsl.noaa.gov
-J. Dibbern, German Meteorological Service DWD, Offenbach (M)
Germany; jdibbern@dwd.d400.de
-J. Nash, UK Met. Office/RSS, Bracknell, UK; jnash@meto.gov.uk
-H. Richner, ETH Zürich/LAPETH, Zürich, Switzerland;
richner@atmos.umnw.ethz.ch

Session I

INTERCOMPARISONS OF INSTRUMENTS FOR SURFACE OBSERVATIONS

PREWIC, THE WMO INTERCOMPARISON FOR PRESENT WEATHER SENSORS

Michel Leroy (France)

Météo-France, BP202, 78195 Trappes, France
e_mail : michel.leroy@meteo.fr

1. INTRODUCTION

The first WMO Intercomparison for Present Weather sensors (PREWIC) was held in St. John's, Newfoundland Canada by the Atmospheric Environment Service (AES) of Canada and in Trappes, France by Météo-France from December 1993 to June 1995. Twenty instruments of 10 different designs were entered by six members of WMO. The final report will be edited by WMO in the next few months. The paper presented here will give only an overview of PREWIC.
The intercomparison was conducted in two phases :

- Phase I started in December 93 and stopped in June 94 in St. John's. Then some sensors were transferred from St. John's to Trappes and a new phase was held in St. John's from July 94 to June 95.
- Phase II started in October 94 and stopped in June 95 in Trappes

The organizing committee (OC) agreed that only sensors/systems allowing the detection and determination of the type of precipitation should be considered for participation in the comparison. The OC considered that WMO Code 4680 gave the greatest flexibility for evaluating the sensors under different weather classes, but agreed to restrict the intercomparison to classes 00 and 40-98.

2. DESCRIPTION OF INSTRUMENTS, SITE AND FACILITIES

An announcement letter for the intercomparison was distributed by WMO to state members. It was intended to have two samples of each of the participating instruments available during both phases to ensure intercomparability. Individual sensors were also accepted. When 2 sensors were available, they both participated to Phase I. Then one sensor of each type was allowed to be checked by the manufacturer before being sent to Trappes for Phase II. Additional sensors were sent to St. John's to reconstruct a pair for Phase II.

The following instruments participated to the intercomparison.

- **FD12P**, Vaisala submitted by **Finland** : optical sensors, combining a forward scattermeter and a grid detector.
- **PW402B**, HSS Inc. submitted by **USA** : optical sensors, double scattermeter (forward and back), analyzing the size and speed distribution of particles.
- **LEDWI** (OWI-240), ScTi submitted by **USA** : optical sensors, analyzing the fluctuations (scintillometry) of an infrared beam.
- **POSS**, Andrew Canada Inc. submitted by **Canada** : bistatic radar, using the Doppler shift related to the falling speed of particles.
- **SCHUBERT**, prototype submitted by **France** : bistatic radar, same principle as the POSS.
- **OPVD**, prototype submitted by **Sweden** :optical sensor, back scattermeter, counting particles.
- **IRSS88**, Eigenbrodt submitted by **Germany** : optical detectors, counting the number of particles occulting infrared beams.
- **RS85**, Eigenbrodt submitted by **Germany** : heated grid detectors.
- **CAPMON**, submitted by **Canada** : heated grid detectors.
- **R872E1**, Rosemount submitted by **USA** : ice accretion detectors, detecting icing by the frequency change if a vibrating pod.

The FD12P, PW402B, LEDWI, POSS and SCHUBERT sensors output precipitation type and intensity. These four first sensors have also a temperature measurement to help the discrimination between solid and liquid precipitation. The IRSS88, RS85 and CAPMON are only precipitation detectors.

The St. John's site offers unique severe conditions. A large number of storms track through the area each year, bringing a variety of wind driven liquid, freezing and frozen precipitation. A special concern is the high level of wind speed, leading to frequent blowing and drifting snow events.
The Trappes' site is located near Paris and is representative of quite temperate climatic countries.
On both sites, additional classic meteorological variables were recorded. The data acquisition system was developed by AES. A copy of this system was installed in Trappes, thus greatly minimizing the efforts. One minute data were recorded for the whole intercomparison.

3. REFERENCE OBSERVATIONS

It was agreed that the selection of the comparison reference was one of the most important tasks for the success of the intercomparison. It was stated that it will be very difficult to design special instrumentation to be used as comparison reference because there is no reliable equipment available for this purpose. Therefore, it was agreed that the human observer should be given preference to deliver the reference data for the distinction of the present weather code figures of the WMO Code 4680. In addition to the regular observations available from each of the comparison sites both host countries provided other observers to deliver detailed high frequency reports during periods of interest. These observations were called « clinic observations ». These high frequency

reports were thought to be the best reference to be compared to the direct minute output of the sensor. But these observations are very costly and were limited in time.

At Trappes, « Clinic » observations were made on a true one minute basis. An original method was used to detect and classify precipitation. The observer was inside a car, activating the windscreen wipers every minute. He then estimated the number of droplets on the windscreen. This method gives a very low detection threshold, as just one droplet per minute may be detected on the windscreen. The observer made the distinction between drizzle and rain from the droplet size and estimated the intensity from the number of droplets. The precipitation intensity was noted as heavy, moderate, light or very light.

4. DATA ANALYSIS

A huge amount of data is available. 3 different phases have been documented. For each phase, it is possible to use 2 different references : the clinic observer and the routine observation. Each of them has its own advantages : accuracy or whole period covered. Each data analysis may be applied to 6 different sets of data. The results may also be presented sensor by sensor or for the whole set of sensors.
The OC recommended to use the 4680 table code for the data analysis. Contingency tables have been constructed using this code for each sensor, each phase and each reference. These tables are the more detailed results of the intercomparison. Nevertheless, they may be laborious to read. They do not allow a clear comparison of the relative performances of the sensors.
Another approach has been also followed. For each phase and for each reference, 3 levels of analysis have been conducted on the whole set of sensors available. These analysis have been applied to periods when all the sensors where working, to get comparable results.

4.1 Precipitation detection

The precipitation detection has been analyzed when the reference observation detected a precipitation. It was felt useful to detail the detection according to the type and intensity of the precipitation observed by the reference. Very quickly appeared the necessity to make a distinction between very light and light intensity. A specific analysis on false alarms has been conducted.

4.2 Precipitation identification

To improve the readability of the results, separate tables for each type of precipitation observed by the reference were constructed. This approach allowed to display the results for all the sensors in the same table.

4.3 Precipitation intensity

An indirect evaluation of the intensity has been conducted by integrating the intensity with time. This integration of the minute intensity output from a sensor gives an amount of precipitation, which has been compared with an usual rain gauge. This procedure gives an indirect evaluation of the validity of the intensity output by the sensors. Nevertheless it applies mainly for intensities leading to measurable amount of precipitation. This method is not well suited for the very low intensities.

5. RESULTS

5.1 Evaluation of detection threshold

From the Trappes' phase, an analysis has been conducted to identify the dependence of detection capacity with the precipitation intensity. The percentage of detection of the sensors has been computed for different classes of intensity, when the clinic observer detected a precipitation. This analysis covers only liquid precipitation.

The disdrometer, CAPMON, RS85, POSS, FD12P, IRSS88, LEDWI and HSS appear to be quite sensitive with a detection threshold as low as 0.025 mm/h in 80% of cases.

5.2 Precipitation detection

A large difference in detection exist between very light and light intensity. As the threshold above which a sensor (or a human observer) should detect a precipitation is not well defined (today), it is very important to make the distinction between very light and light intensity. Otherwise the apparent performance of a sensor may be greatly dependent on the distribution of precipitation intensities.

The detection of very light intensity of drizzle and rain may be quite low for many sensors.

5.3 False alarms

A detection analysis must be completed by a specific false alarm analysis. A very sensitive sensor may indicate a high rate of false alarm. Some sensors have some delay to begin and end a precipitation detection. They can also have a different detection threshold. Therefore the beginning and the end of a precipitation event may be documented differently by the sensors and a human observer. Such differences cannot be considered as false alarms.
The method used has been the analysis of the duration of precipitation, deduced from the one minute detection of each sensor. This minute indicator of precipitation has been summed with time and compared with the routine observations, covering the whole periods of PREWIC.
Some sensors had several real false alarm periods during some of the phases. Several sensors didn't exhibit any special false alarm periods during the tests.

5.4 Precipitation identification

The constructed tables were slightly different from phase to phase and from the clinic and the regular human observations.

6. CONCLUSIONS

These conclusions are based on the events observed during observations of the intercomparison and thus do not intend to give a definitive judgment on the sensors. Some significant differences have been found between the different phases and sites and between the 2 sensors of the same model. Nevertheless the majority of sensors had a quite good behavior and it is thought that several sensors are able to give very

valuable information. It is difficult to objectively check the performance of the sensors against the user needs, as these needs are not objectively defined. Considering meteorology, there is no international or WMO definition of intensity. The WMO SYNOP code doesn't make a distinction between very light and light intensities. There is also no real objective definition of a precipitation occurrence : when should a precipitation be detected ? Therefore, the performance of a present weather sensor is strongly dependent on such definitions.
Despite these restrictions, a range of present weather sensors are now available commercially that can detect precipitation when operating continuously over extended period of time (at least 6 months). Some sensors are also able to identify certain types of precipitation, and measure the intensity and cumulative amount. (There were no present weather sensors tested that were capable of detecting the state of ground, state of the sky or obscuration phenomena.)

- For many present weather sensors, the identification of rain and snow may be correct in more than 90% of cases. A correct identification is strongly intensity dependent. Well established rain or snow events may be very adequately identified by several sensors.
  Few sensors are able to identify drizzle ; drizzle was well identified in hardly 50% of cases.
  Hail was not identified by any of the present weather sensors (though some were supposed to do so).
  Mixed precipitation are seen as a single hydrometer, with a preference for snow. Only one sensor is able to report mixed precipitation (drizzle/rain or rain/snow).
- Incorrect precipitation typing mainly occur during very light intensities. The sensors having a lower sensitivity or choosing an unknown precipitation for very light events, thus tend to exhibit less false identification. Therefore, there is a compromise, perhaps a choice, between no detection, unknown precipitation and an identified hydrometeor. Some sensors are affected by heavy wind, which may induce false alarms and false identifications.
- Icing detectors exist which are able to detect a large amount of icing conditions, while giving an information on the phenomena intensity.
- Several present weather sensors indicate cumulative amounts of precipitation which are comparable to gauge measurements.
- Many sensors are able to detect precipitation above very low intensity. Detection of precipitation is improved significantly when intensity is above 0.05 mm/h. Well established precipitation events are very adequately detected by several sensors.

It is not possible to give a definitive judgment on the technology, but from this intercomparison it seems that :

- Heated grid detectors have a good detection of liquid precipitation and a limitation in detection of snow.
- The optical detector has a good detection of any precipitation. It is subject to a quite high false alarm rate.
- Radar present weather instruments have a good detection of rain, a medium detection of snow. Detection of drizzle was depending on the phase and was good or poor.
- Optical present weather instruments have a good detection of rain and snow, but have problems in detecting drizzle.
- Some sensors have a significant amount of false alarm during days without any precipitation.
- Significant differences in detection, false alarm and identification have been found from 2 sensors of the same model or from phase to phase. One explanation may be differences in calibration or in internal parameters used by the sensor software. The more sensitive sensors also indicate a higher false alarm rate.

7. ACKNOWLEDGEMENTS

The author and Météo-France would like to express their gratitude to the many members of staff of the Atmospheric Environment Service (AES) of Canada, who contributed to the successful management of the Intercomparison, and to the members of the International Organizing Committee for the invaluable expert guidance given both in the planning of the Intercomparison and the preparation of the final Report.
We want to particularly mention the excellent collaboration between AES and Météo-France.

The intercomparison and associated reports are dedicated to the memory of Roger Van Cauwenberghe, AES.

	Reliability	Drizzle detection	Rain detection	Snow detection	False alarm
FD1P	+	+/=	+	+	+
HSS	+/-	-	+	+	-/+
LEDWI	+	-	+	+	-
POSS	+/-	-/=	+	=/+	+/-
SHUBERT	+	-	-	-/=	+
OPVD	-	-	-	-	-
IRSS	-	=/+	+	=/+	-
RS85	-	=/+	+	-/+	-
CAPMON	-	=/+	+	-	-

This table summarizes the results in terms of reliability and detection. Two levels are indicated when the results are significantly different from phase to phase. (+ is for good, = is for medium, - is for indicating problems).

	Drizzle identification	Rain identification	Snow identification
FD1P	=/-	+	+
HSS	-	+	+
LEDWI	-	+/=	+
POSS	-	+	+
SHUBERT	-	+	-
OPVD	-	-	-

This table summarizes the results in terms of identification. Differences, not appearing in this table, exist between the different sensors. All the sensors have not the same identification capabilities.

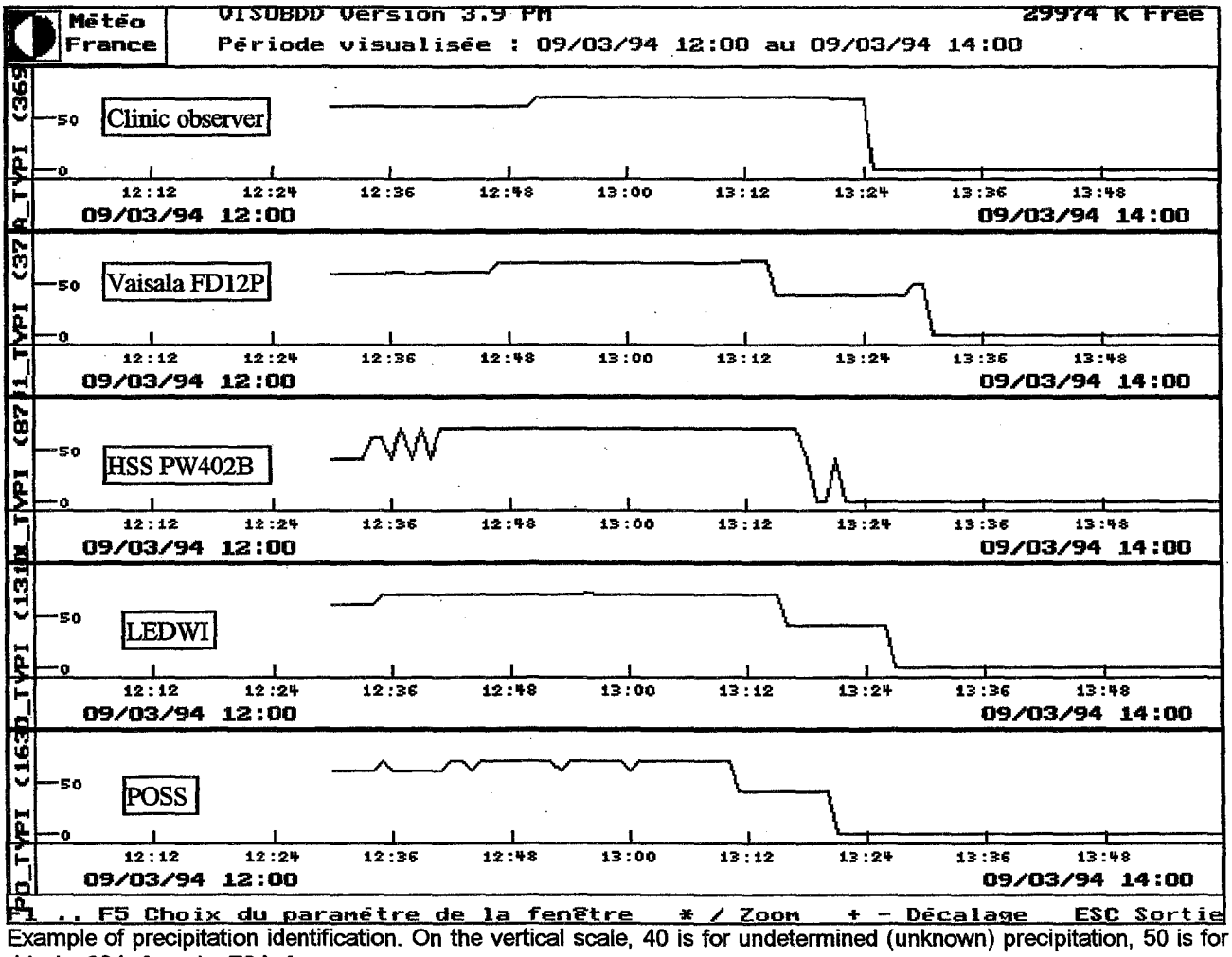

Example of precipitation identification. On the vertical scale, 40 is for undetermined (unknown) precipitation, 50 is for drizzle, 60 is for rain, 70 is for snow.

The clinic observer documented mixed rain and snow, followed by snow.

The FD12P detected rain, followed by snow, followed by unknown precipitation.

The HSS detected unknown, rain (short period) followed by snow.

The LEDWI started by rain, followed by snow and ended by unknown precipitation.

The POSS started by rain, followed by snow and ended by unknown precipitation.

WMO Solid Precipitation Measurement Intercomparison: Results and Challenges for the Future

B.E. Goodison[1], P.Y.T. Louie[1], and D. Yang[2]
([1]Atmospheric Environment Service, Toronto, Ontario, Canada;
[2]on leave from the Lanzhou Inst. of Glaciology and Geocryology, P.R. China)

Introduction

The WMO Solid Precipitation Measurement Intercomparison was initiated after approval by CIMO-IX in 1985. Its goal was to assess national methods of measuring solid precipitation against methods whose accuracy and reliability were known, including past and current procedures, automated systems and new methods of observation. The Intercomparison was especially designed to:

1) determine wind related errors in national methods of measuring solid precipitation, including consideration of wetting and evaporative losses;
2) derive standard methods for adjusting solid precipitation measurements; and
3) introduce a reference method of solid precipitation measurement for general use to calibrate any type of precipitation gauge.

This study would also complement the WMO Pit Gauge Intercomparison for liquid precipitation (Sevruk and Hamon, 1984). Field studies for the WMO Solid Precipitation Measurement Intercomparison were started by some countries during the 1986/87 winter and the last official field season was 1992/93, allowing most countries to collect data during five winter seasons. Some sites have continued to operate with reduced programs. Table 1 provides a summary of the participating countries and the sites operated. Experimental results were obtained from 26 sites in 13 countries.

Table 1 Summary of Participating Countries

Country	No. of Sites	Years of Data	National Gauge(s)	DFIR	Country Report(s)
Canada	6	6	Canadian Nipher shielded gauge	Yes	Yes
Croatia	1	3	Hellmann	Yes	No
China	1	6	Chinese Standard	Yes	Yes
Denmark, Finland, Norway, Sweden	1	6	Hellmann (Denmark) Wild (Finland) Tretyakov (Finland) H&H 90 (Finland) Norwegian Standard Swedish Standard	Yes	Yes (Denmark & Finland)
Germany	1	7	Hellmann	Yes	Yes
India	4	2	Indian Standard	No	No
Japan	2	3	RT-1, RT-3, RT-4	Yes	Yes
Slovakia	1	7	METRA 886	No	Yes
Switzerland	1	2	tested Belfort gauge	Yes	Yes
Romania	1	3	Romanian IMC	Yes	No
Russian Federation	1	14	Tretyakov	Yes	Yes
United Kingdom	2	3	UK Met Office Standard Mk 2	No	No
United States	4	6	NWS 8 inch Belfort Universal	Yes	Yes

Reference standard for this Intercomparison

For this Intercomparison, determination of the reference standard designed to measure snowfall precipitation was critical. The International Organizing Committee for this Intercomparison designated the octagonal vertical double fence shield (with manual Tretyakov gauge) as the Double Fence Intercomparison Reference (DFIR) (Figure 1). It is acknowledged that a gauge situated in a natural bush shelter would provide the best estimate of "ground true" precipitation; however, since natural bush sheltering was not available in all climatic regions which were to be studied, an artificial shield was selected. The DFIR is a practical secondary standard and its ongoing assessment as a reference is recommended.

The hydrological station at Valdai (Russian Federation) was the only site where the DFIR was assessed against gauges situated in bushes kept at gauge height. Precipitation totals, as summarized in Table 2 for November 1991 to March 1992, show the average differences between the DFIR, the bush gauge, and some of the other gauges operated at Valdai. The measurements show the need to adjust the DFIR to the value of the bush gauge to account for the effect of wind and other environmental factors (e.g. temperature). Errors in measurement using the DFIR and adjustment procedures are given in Golubev (1986), WMO/CMIO (1993) and Yang et al. (1993).

Figure 1 Cross section of WMO Double Fence Intercomparison Reference (DFIR)

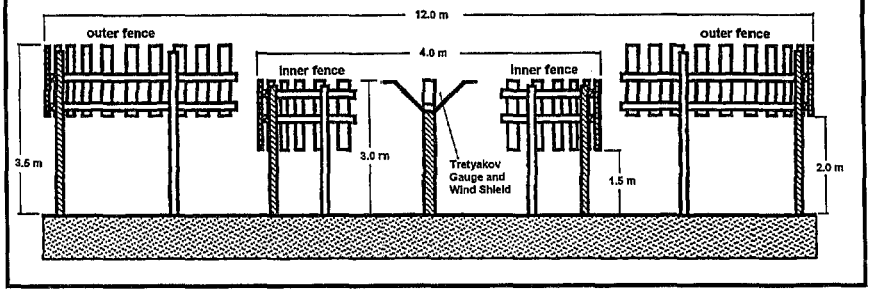

Intercomparison results

The systematic errors in the measurement of solid precipitation were determined in the Intercomparison quantitatively for over 20 different precipitation gauge and shield combinations. Experimental results reported in the Intercomparsion Final Report (Goodison, *et al.*, 1998) confirmed that solid precipitation measurements must be adjusted for wetting loss (for volumetric measurements), evaporation loss and for wind induced gauge undercatch before the actual precipitation at ground level can be estimated. Studies in precipitation physics have shown that the falling velocity of snowflakes depends on their shape which is a temperature phenomenon. Since the total wind effect depends on the shape of snowflakes, air temperature at screen or upper air levels can also be used as a variable in adjusting precipitation gauge measurements. Systematic losses varied by type of precipitation (snow, mixed snow and rain, and rain).

Table 2 Precipitation totals (rain and snow) measured by different gauges at Valdai, Russia, November 1991-March 1992 (WMO/CIMO, 1992)

Gauge type	Total Precip (mm)	% of bush total
Tretyakov in bushes	367	100
DFIR (Tretyakov)	339	92
DFIR (Canadian Nipher)	342	93
Canadian Nipher shielded	314	86
Tretyakov	258	70
8" USA Alter shielded	273	75
8" USA unshielded	208	57

Evaporation from manual gauges can significantly contribute to the systematic undermeasurement of precipitation. Aaltonen *et al.* (1993) reported on the comprehensive assessment by Finland on evaporation loss. Average daily losses varied by gauge type and time of year. Cumulative evaporative losses from the gauge in April of over 0.8 mm/day were measured. Losses during winter were much less than that recorded during comparable spring and summer comparisons, and ranged from 0.1-0.2 mm/day.

Wetting loss is another cumulative systematic loss from manual gauges which varies with precipitation type, gauge type, and the number of times the gauge is emptied. Average wetting loss for some gauges can be up to 0.3 mm per observation. At synoptic stations where precipitation is frequent and measured every six hours, this can become a very significant amount. At some Canadian stations, for example, wetting loss was calculated to be 15-20 per cent of the measured winter precipitation.

Data from all Intercomparison sites confirmed that solid precipitation measurements must be adjusted to account for errors and biases. The results confirmed that wind speed was the most important environmental factor contributing to the systematic under-measurement of solid precipitation. Countries operating a reference gauge (DFIR) with corresponding wind data were able to develop adjustment equations for their National gauges. Deviations from the DFIR measurement varied according to gauge type and precipitation type (snow, mixed snow and rain, and rain). The derived catch ratio equations for the four most widely used non recording gauges for solid precipitation measurement in the world (the Russian Tretyakov Gauge, the Hellmann Gauge, the Canadian Nipher Gauge, and the US NWS 8" standard gauge) are presented in Table 3. This analysis was based on the combined international data set collected by the WMO Solid Precipitation Measurement Intercomparison project. For all gauges and at all sites, it was confirmed that wind was the most dominant environmental variable affecting the gauge catch efficiency. Temperature had a much smaller overall effect on the catch ratio, and was found to be more important for mixed precipitation than for snow. A graphical comparison of the catch ratio equations for snow is shown in Figure 2. These results show that the catch efficiency for snow of these gauges can vary greatly, for example, from ~20% up to ~70% at 6 m/s wind speed. As expected, shielded gauges generally performed better than unshielded gauges. Goodison, *et al.* (1998) provides a detailed discussion of individual country analyses of National gauge data and includes examples of applying the results to archive data.

Table 3 Regression equations for catch ratio versus wind and temperature for Nipher, Tretyakov, US NWS8" and Hellmann gauges

Gauge	Catch Ratio versus Wind and Temperature	n	r^2	SE
	Snow			
Nipher	$CR_{NIPHER} = 100.00 - 0.44*W_s^2 - 1.98*W_s$	241	0.40	11.05
Tretyakov	$CR_{Tretyakov} = 103.11 - 8.67 * W_s + 0.30 * T_{max}$	381	0.66	10.84
US NWS 8"_Sh	$CR_{NWS\ 8\text{-}Alter\ Shield} = \exp(4.61 - 0.04*W_s^{1.75})$	107	0.72	9.77
US NWS 8"_Unsh	$CR_{NWS8\text{-}unshield} = \exp(4.61 - 0.16*W_s^{1.28})$	55	0.77	9.41
Hellmann	$CR_{Hellmann,\ unsh.} = 100.00 + 1.13*W_s^2 - 19.45*W_s$	172	0.75	11.97
	Mixed			
Nipher	$CR_{NIPHER} = 97.29 - 3.18*W_s + 0.58* T_{max} - 0.67*T_{min}$	177	0.38	8.02
Tretyakov	$CR_{Tretyakov} = 96.99 - 4.46 *W_s + 0.88 * T_{max} + 0.22*T_{min}$	433	0.46	9.15
US NWS 8"_Sh	$CR_{Alter\ Shield} = 101.04 - 5.62*W_s$	75	0.59	7.56
US NWS 8"_Unsh	$CR_{Unshield} = 100.77 - 8.34*W_s$	59	0.37	13.66
Hellmann	$CR_{Hellmann,\ unsh.} = 96.63 + 0.41*W_s^2 - 9.84*W_s + 5.95 * T_{mean}$	285	0.48	15.14

W_s = Wind Speed (m/s) at Gauge Height T = Air Temperature (°C) n = Number of obs.
r^2 = Coefficient of Determination SE = Standard Error or Estimate

Other issues and challenges

The Intercomparison study and the subsequent development of adjustment procedures for gauge measurements of solid precipitation also identified other issues which must be addressed. Using the results of the experiment, procedures are proposed to adjust precipitation measurements for many different gauges for wind induced errors and losses due to wetting and evaporation. Wind speed at gauge height is one of the required variables in the adjustment procedure; it can be measured or derived using a mean wind speed reduction procedure. This is a very site dependent value and estimation will require a good knowledge of the station and gauge location, hence a good metadata record. At new automatic stations, the measurement of wind speed at gauge height is encouraged.

Figure 2 Plot of Catch Ratios versus Wind based on best fit regression equations shown in Table 3 for snow; the Tretyakov curve was plotted for T_{max} = -2.0 °C.

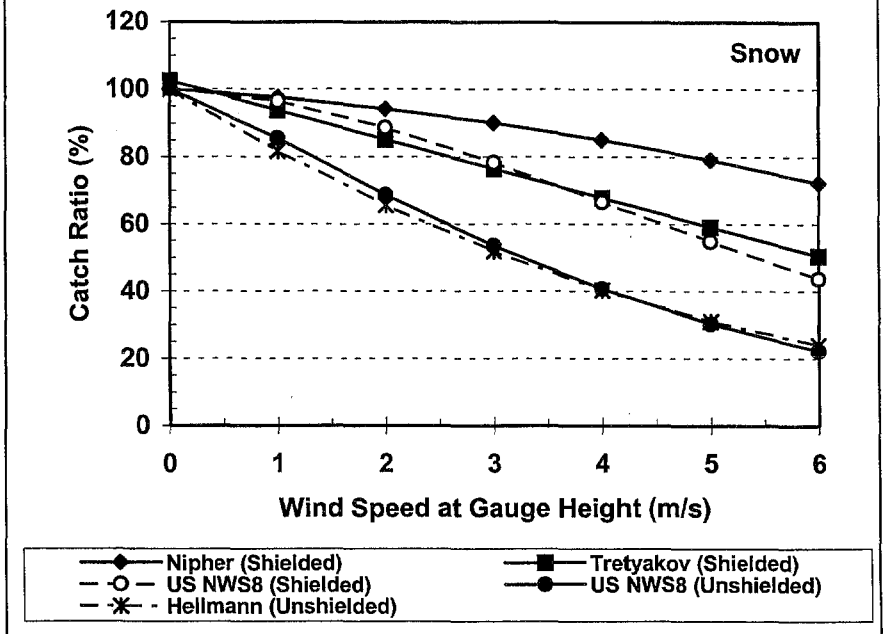

Wetting loss associated with manual guage measurements is cumulative and depends on the number of times the gauge is emptied; it can become a very large value for the year. The adjustment of data on a daily basis seems logical, but precipitation measurements may be made every six hours, twice per day or only once per day, depending on the type of station. Each country archives its data differently and the exact number of times the gauge was emptied may not be retrievable from the historical digital archives. Wetting loss is an average value which could be added to the measurement at the time of observation. Use of a digital balance to weigh the contents of simple manual gauges, hence eliminating the need for adjusting for wetting loss, is a reliable alternative, but for most National Services it would be too expensive to implement. The adjustment for wetting loss at the time of observation is feasible, but would require a change in observing and reporting procedures by Member countries, and could lead to confusion later during analyses.

In testing adjustment procedures on its digital archive, Canada identified the additional challenge of quantifying trace precipitation. Currently, trace precipitation is recorded and archived as a "trace", but is assigned a zero value in the computation of daily, monthly or annual precipitation totals. Some Canadian Arctic stations have reported over 80 per cent of all precipitation observations as trace amounts (over 1000 observations per year). Recognizing that there are losses for wetting, trace amounts can be a measurable amount, ranging from 0.0 to 0.15 mm or more, per observation. Trace precipitation must be considered as a non-zero value when adjusting precipitation data, with the assigned value varying according to the method of observation and climatic conditions. It is not a problem with recording gauges. Distinguishing between whether an event is "measurable" or just a "few flurries" is important; the use of two categories in the reporting of trace precipitation should be considered. Review of this issue by countries where trace precipitation is frequently recorded is warranted.

The WMO Solid Precipitation Measurement Intercomparison included some of the automatic gauges currently in use in some countries. Experiences of countries testing precipitation gauges suitable for measuring solid precipitation at automatic stations are given in Goodsion, *et al.* (1998). Although wind-induced errors negatively affect gauge catch, as for National non-recording gauges, there are several other problems which contribute to the serious undermeasurement of solid precipitation. Problems with both weighing and heated devices were identified. Heated gauges, including heated tipping bucket gauges, have been used in many countries. Finland and Germany reported a large undercatch by unshielded heated gauges, caused by the wind and the evaporation of melting snow. In Finland, the performance of heated tipping buckets was found to be very poor. Heated gauges are not recommended for use in measuring solid precipitation in regions were temperatures fall below 0^{o}C for prolonged periods of time.

Automatic weighing gauges are another alternative and were assessed in Canada, Finland and the United States. One serious operational problem with recording weighing gauges is that wet snow or freezing rain can stick to the inside of the orifice of the gauge and does not fall into the bucket to be weighed until some time later, often after an increase in ambient air temperature. There can be other complications, such as gauges catching blowing snow, differentiation of the type of precipitation and wind-induced oscillation of the weighing mechanism (wind pumping). These problems affect real-time interpretation and use of the data as well as the application of an appropriate procedure to adjust the measurement for systematic errors. The adjustment of weighing gauge data on an hourly or daily basis may be more difficult than on longer time periods, such as with monthly climatological summaries. Ancillary data from the automatic weather station, such as air

temperature, wind at gauge height, present weather, or snow depth will be useful in accurately interpreting and adjusting the precipitation measurements from automatic gauges. A comprehensive assessment of automatic gauges for measuring solid precipitation (not just wind-induced undercatch) is warranted.

Conclusions and recommendations

The goal and objectives of the experiment were achieved. A quality controlled digital database of all intercomparison data submitted by participants for the period up to April 1993 has been prepared. The database is currently maintained by Canada and will be made available to interested Members and other researchers in accordance to WMO policy on the access to research data sets from Intercomparison projects. It is clear that in order to achieve data compatibility when using different gauge types and shielding during all weather conditions, adjustments to the actual measurements will be necessary. Since shielded gauges catch more than their unshielded counterparts, gauges should be shielded either naturally (e.g. forest clearing) or artificially (e.g. Alter, Canadian Nipher type, Tretyakov wind shield) to minimize the adverse effect of wind. However, even when using shielded gauges, adjustment of the measurements will still be necessary.

At this time, the International Organizing Committee for this Intercomparison is not recommending that a single precipitation gauge be adopted by all Members for the measurement of solid precipitation. Instead, Members should review the results of the Intercomparison for their National gauge and decide on the most appropriate action to address the errors in precipitation measurement within their country.

Specific recommendations on the measurement and adjustment of solid precipitation prepared by the International Organizing Committee and participants in the Intercomparison include:

1) Accept the Double Fence Intercomparison Reference (DFIR) as a secondary reference for the measurement of solid precipitation;

2) Review and test the application of procedures developed in the Intercomparison on precipitation measurements and further develop these procedures; implement the creation of an adjusted precipitation archive of historical data which should then be kept separate from the original archive of observations; and

3) Establish National Precipitation Centres to facilitate necessary ongoing studies on precipitation measurement such as: new gauges and observational procedures, assessment of gauges for use at automatic stations, quantification of trace precipitation, assessment of blowing snow on measurements, further development and validation of adjustment models under more extreme wind and lower temperature conditions, etc.

The accuracy of methods of precipitation measurements currently used by the Members does not meet - in any way - the WMO requirements. The application of adjustments for precipitation data sets for systematic errors due to the adverse effect of wind, wetting and evaporation will improve significantly the quality of precipitation time series. Adjustment procedures and reference measurements have been developed and evaluated by several Intercomparison participants. The application of these procedures for different types of precipitation gauges tested during the WMO Intercomparison has been assessed in various countries, as summarized in the Final Report. Members are urged to test the application of these procedures on their precipitation observations and to continue to further develop them.

References

Aaltonen, A., E. Elomaa, A. Tuominen, and P. Valkovuori, 1993: Measurement of precipitation. *Proc. Symp. on Precipitation and Evaporation (ed. B. Sevruk and M. Lapin)*, Vol.1, Bratislava, Slovakia, Sept. 20-24, 1993, Slovak Hydrometeorlogical Institute, Slovakia and Swiss Federal Institute of Technology, Zurich, Switzerland, 42-46.

Golubev, V.S., 1986: *On the problem of standard condition for precipitation gauge installation.* Proc. International Workshop on the Correction of Precipitation Measurements, WMO/TD No.104, Geneva, 57-59.

Goodison, B.E., P.Y.T. Louie and D. Yang, 1998: *WMO Solid Precipitation Measurement Intercomparison Final Report,* WMO Instrument and Observing Methods Report No. 67, WMO/TD No. 872, WMO, Geneva, 88 p.

Sevruk, B., and W.R. Hamon, 1984: *International comparison of national precipitation gauges with a reference pit gauge.* WMO Instrument and Observing Methods Report No.17, WMO, Geneva, 111p.

WMO/CIMO, 1993: *International Organizing Committee for the WMO Solid Precipitation Measurement Intercomparison, Final Report of the Sixth Session*, Toronto, Canada. WMO, Geneva, 15 p.

Yang, D., J. R. Metcalfe, B. E. Goodison E. and Mekis, 1993: *An Evaluation of double fence intercomparison reference (DFIR) gauge.* Proc. Eastern Snow Conference), 50th Meeting, Quebec City, 105-111.

NEW RESULTS ON MEASUREMENT OF ATMOSPHERIC THERMAL RADIATION

K. Dehne, K. Behrens
Deutscher Wetterdienst, Meteorologisches Observatorium Potsdam

1. Introduction

The improvement of the methods to measure meteorological relevant longwave radiation belongs to the terms of reference of the work on radiation since a lot of CIMO periods. This reflects both, the increasing requirements of accuracy (in the last decade first of all for climate research), as well as the severe problems in the precise radiometric measurement of hemispheric longwave radiation because of the necessary elimination of the shortwave solar radiation below 3 μm from the totally incident radiation fluxes in the field, for instance. With regard to the separation of the shortwave radiation there are generally only two methods commercially realized:

- the pyrgeometric method by using a silicon dome coated with an edge interference filter (at 3-4 μm) above the black painted sensor plane of the pyrgeometer
- the pyrradiometric method which determines the longwave hemispherical radiation as difference between the total radiation measured by a pyrradiometer (mostly covered by a polyethene dome) and the shortwave radiation measured by a pyranometer.

The measurement accuracy of the methods depends not only on the quality of the used radiometers but also on the quality of the evaluation formula and the choice of an appropriate calibration procedure. An important improvement in that sense concerning the method of the Eppley pyrgeometer PIR was performed by the World Radiation Center (WRC). It improved the radiometer by a three-fold representative measurement of the dome temperature, and the calibration procedure by a new blackbody radiator with separately variable heating and cooling of the body and the dome of the radiometer to determine the 4 constants needed in an improved evaluation formula. The recommendation of shading the so equipped pyrgeometer dome against direct solar radiation remains valid, if required a more precise separation of the shortwave range.

For the pyrradiometric method the shading of the direct solar beam from both radiometers means the only important step recommended in the last decade to improve the accuracy of the data.

Up to now it exists no absolute method for measuring longwave hemispherical radiation in the field. To get some suggestions about the possible deviation from ideal values as well as to investigate what precision is operationally realizable field intercomparisons of different methods have to be performed from time to time.

Respective field intercomparisons in the last decade were performed 1989 in Uppsala, 1989/90 in Hamburg (IEA-SHCP) and 1991 in Coffeyville (FIRE II-BSRN).

In 1996 (May till October) at Met.Obs. Potsdam (MOP) a national relative intercomparison of different methods to measure the longwave atmospheric radiation (also called: "atmospheric heat rad.") was performed and since Mai 1997 continued with modified instrumentation. The main aim was to study the deviation of measurement values of different methods (especially of a pyrradiometric method improved by MOP) from reference values measured by the above mentioned WRC-advanced PIR method.

2. Facts of the Longwave Intercomparisons at Met.Obs. Potsdam (1996/97)

The comparison site is the garden area between forest and the institution building of the Radiation Center of the Met.Obs. Potsdam (φ 52,35°; λ = 13,07°). Since the horizon is disturbed up to about 10° seven places for shaded radiometers are concentrated on a measurement table (0,8 m x 4,7 m) with a distance between the radiometers of about 0,8 m. The data are taken every 1 s and archived every minute by the datalogger system COMBILOG 1020.

All radiometers are equipped with a sidely flanged ventilation device (air flow around the body to the dome) and a shade disk-device (driven by a synchronous motor, shaded angle 9,6°). The exposed instruments were changed sometimes. But in any case the PIR 30475 (equipped with 3 dome thermistors and well calibrated by WRC) as reference and a shaded pyranometer type CM21 (No. 910009), and mostly also two of new developed "CM 21-pyrradiometer" Lup (see section 3) were exposed. Furthermore, special interest exists to compare a Foot-modified PIR (UK/MRF No. 15086F3) as well as PIR's with only one or no dome thermistor. In the comparison period of 1997 (since May 1997) the PIR 30477 (modified and calibrated by WRC as PIR 30475) was included as well as the Foot-pyrgeometer equipped now with a

WRC-dome thermistor. The calibration of the participating radiometers was performed, with exception of PIR 30475 and 30477, by the two-blackbody-procedure of the MOP-laboratory. According to the reproduction of the longwave responsivity (in the "short evaluation formula") of the above mentioned two PIR's within 1 % the responsivities determined by MOP for the PIR's equipped by only 1 dome-thermistor should be in a comparable precision.

3. Description of the "CM 21-Pyrradiometer"

The CM 21-pyrradiometer was designed as an approach to improve the pyrradiometric method of measuring hemispherical longwave radiation by the combination of the output of an original Kipp & Zonen high quality pyranometer CM 21 with a second one (+ Pt-100-thermometer) which is equipped by a polyethene dome instead of the double glass dome. The polyethene dome is made by MOP from a 20 μm thick film having the same diameter as the outer glass dome. It has to be inflated by dry air (ca. 25 hPa). The improvement is achieved by using for both needed radiometers the same high quality sensor type with approximately the same properties (time constant, temperature coefficient, cosine error, excess temperature) as well as by the extremely thin dome which absorption in three bands is strongly reduced and approximates better the desired ideal flat and high spectral transmittance than other pyrradiometers in use. The dome temperature cannot be measured. But because of the small mass of the dome (< 0,5 g) a small wind stream is able to temperate the dome. This was verified with low speed ventilation during the calibration routine. Comparing the performances of this method and those of the advanced pyrgeometers, an advantage of the latter is generally only given on the operational side (use of 2 radiometers, regularly replacement of the dome, careful dome cleaning etc.) as already known in advance; the CM 21-pyrradiometer was designed first of all for special studies.

4. Preliminary Results of the Longwave Intercomparison

The reporting is restricted to compiled preliminary facts concerning the deviations of the atmospheric heat irradiances A from those of the reference method Aref at special weather situations. The strong requirements on the quality of methods are given in the case of clear sky (and low humidity), the lowest at overcast sky with thick and low clouds or foggy conditions. For most of the comparison days diagrammes of the daily courses of the absolute and relative A-values are prepared. Here only one example of the diagrammes is shown in Fig. 1 representing a nearby clear summer day with a typical course of ambient air temperatures. To be able to follow the curves in this black/white diagramme the number of curves are reduced and the A-values are integrated to 10 min. means. The PIR 30475 R data, which are derived by use of the high advanced formula represent the references; the PIR 30475 data are based on a simpler formula without the temperature term. In the case of strong fog the A-values of all methods deviate from the reference by less than 0.5% corresponding to the measuring accuracy of the body temperature of the respective radiometers.

The results of the different methods could be preliminarily summarized as follows:

a) From the PMOD calibrated PIR-Pyrgeometers (equipped by 3 dome thermistors) the PIR 30475 shows the lowest "noise" in the 1 min. display of the daily courses. Its relatively high temperature dependency is detectable in the daily courses of the relative A-values derived by means of the shortened evaluation formula: The deviations during a summer day are generally within 0,5%, during the seasons between $\pm$ 1%. For the second PIR in this group the deviations of the "shortened curve" are smaller, while the data evaluated by the full formula deviate at clear sky conditions by about 0,5 % with a relative maximum around summer noons of about 1 %, as expected.

b) PIR-Pyrgeometers with only one special dome thermistor (30474 and 30476) participated in 1996 for several months. The deviations from the reference are very stable between about + 0,5% and - 0,5% (at clear nights) with a relative maximum around sunny summer noons of about + 0,5% (see Fig. 1), as expected since only the short version of the evaluation formula was used.

c) The MRF-PIR as used 1996 in the original Foot-version without a thermistor at the dome showed frequently, at least in the summer months, a daily course similar to that of the CM 21-pyrradiometer Lup 275, with a clear night deviation of about 2% and an daily increase of sometimes more than 1%. However the "1 min noise" is lower than that of Lup 275, but is remarkable higher than those of the PIR's. For the use of this radiometer in 1997 its dome was equipped with a thermistor. The application of the correction term for temperature differences between dome and body in the evaluation formula results for clear sky conditions in about 1 % lower values; but since in winter the devation are down to -2 % the correction causes worse data deviating by -3 %.

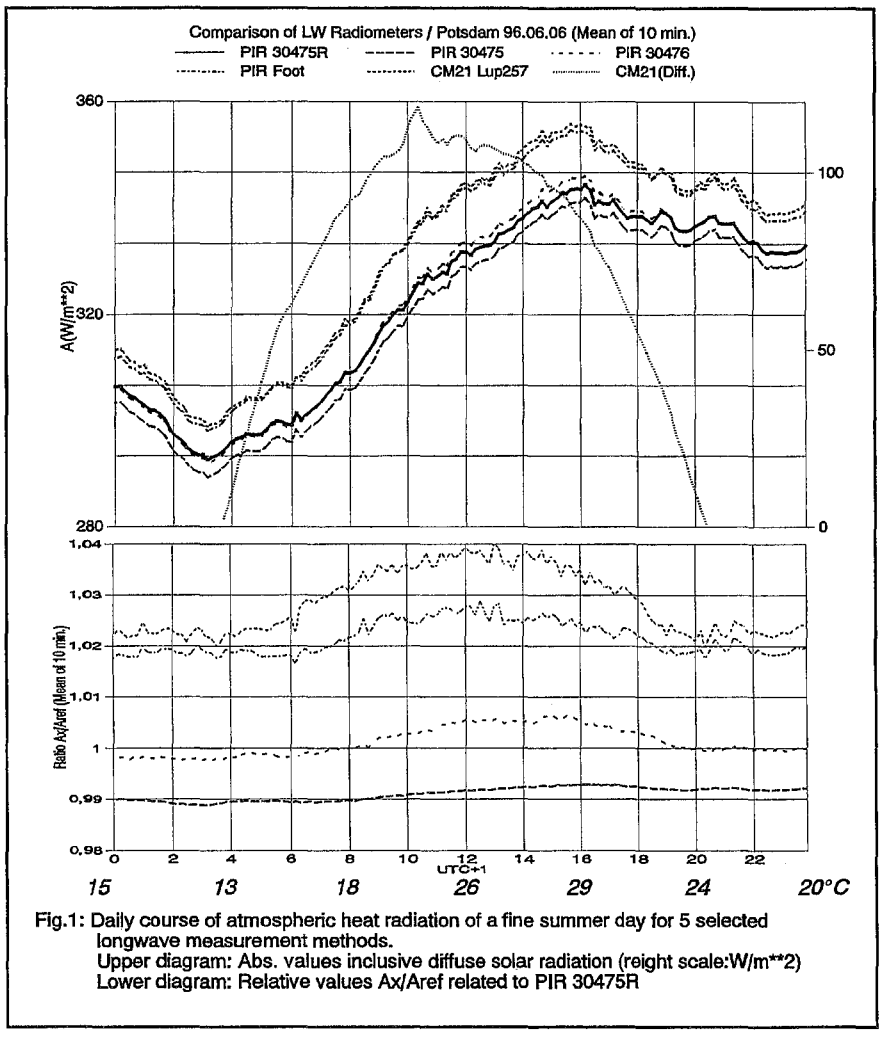

Fig.1: Daily course of atmospheric heat radiation of a fine summer day for 5 selected longwave measurement methods.
Upper diagram: Abs. values inclusive diffuse solar radiation (reight scale:W/m**2)
Lower diagram: Relative values Ax/Aref related to PIR 30475R

d) The A-curves of CM 21-pyrradiometer Lup 275 (only 1996) and Lup 092 can be typically identified by their strong "1 min-noise" in the daily curves, especially in summer around noon upto about 0,5% and 1,0%, respectively. The typical clear night deviations are about 2% and 3%, with summerly relative A-maxima of about up to 2% around noon. At a clear cold winter day (-10 °C) the Lup 092-data deviate permanently by +3%.

e) Rain and wind effects are observed especially for the pyrradiometers because of their thin dome cover. Effect of severe precipitation are also seen in pyrgeometer data, because of their bigger mass and heat conductivity of the domes as well as the dome temperature correction. The strong "noise" of the pyrradiometer curves should be interpreted as a micrometeorological phenomenon of the speed and the changing temperature of air parcels in that environment of the comparison site; a clear correlation with the speed alone was not found.

5. Improvement of Data Accuracy by Fitting the Longwave Responsivity during Field Measurements

This fitting procedure is based only on the comparison of clear night- A-values (mostly the mean of 1 hour) of the reference and a respective method. The result is a corrected value of the longwave responsivity which value is the most sensitive parameter of the evaluation formula. The improvement of the daily means of A-values (in the sense of reduced deviations from the reference values) are shown in Table 1 for 7 fitting days within the months June to December, compiling the absolute and relative deviations under A): of the daily means without fitting (use of lab-calibration data) as worst case; under B): of the daily means if fitting is performed at all 7 days, generally best case; and under C): of the daily means if the fitting of 6 June is applied till September and the fitting of 17 December is applied backwards till October.

Looking trough the percentage values to detect the desired fitting effect the results for the high advanced PIR-methods are not uniform, but all deviations are below 1% (mostly below 0,5%). In the case of higher deviations as for daily means of the PIR-Foot and Lup 092, the fitting affects generally a remarkable improvement, if the field-recalibration by fitting is repeated about every half year (the values of Lup 092 for July till September are related only to night hours).

6. Conclusions

a) Concerning the state-of-the-art

From the results of the intercomparison studies the following can be concluded:

Assuming that the WRC advanced and calibrated PIR pyrgeometers represent the best method at the time beeing to measure longwave radiation for meteorological purposes the deviation of the results of two of this radiometers suggests a measurement precision of atmospheric heat radiation of 0,5 % in clear nights and 1 % (around clear summer noons).

Table 1: Fitting of longwave responsivity using clear night values of atmospheric heat radiation of 7 selected days by using the corresponding reference values (absol. values in Wm^{-2}, rel. values in percentage).

Date		06.06.97		13.07.97		10.08.97		01.09.97		28.10.97		04.11.97		17.12.97	
Method		abs	rel	abs	rel	abs	rel	abs	rel	abs	rel	abs	rel	abs	rel
daily mean of reference		321		314		348		337		228		233		192	
PIR 30475	A)	1,33	0,41	1,23	0,39	1,39	0,40	1,08	0,32	0,59	0,26	0,60	0,26	1,25	0,65
(short formula)	B)	0,66	0,21			0,67	0,19	0,65	0,19	0,31	0,14	0,22	0,09	0,13	0,07
	C)	0,66	0,21	0,62	0,20	0,77	0,22	0,59	0,18	0,99	0,43	0,83	0,36	0,13	0,07
PIR 30477	A)	2,73	0,85	2,85	0,91	2,11	0,61	1,17	0,35	1,24	0,54	0,83	0,36	0,41	0,21
	B)	0,80	0,25			0,57	0,16	0,31	0,09	0,36	0,16	0,29	0,12	0,19	0,10
	C)	0,80	0,25	0,87	0,28	0,47	0,13	0,31	0,09	0,98	0,43	0,59	0,25	0,19	0,10
PIR 30477	A)	2,44	0,76	2,55	0,81	2,14	0,61	1,16	0,34	0,34	0,15	0,19	0,08	0,57	0,30
(short formula)	B)	0,80	0,25			0,50	0,14	0,27	0,08	0,35	0,15	0,21	0,09	0,27	0,14
	C)	0,80	0,25	0,84	0,27	0,64	0,18	0,39	0,12	1,26	0,55	0,93	0,40	0,27	0,14
PIR-Foot	A)	7,76	2,42	8,17	2,60	7,38	2,12	6,14	1,82	2,51	1,10	1,52	0,65	2,57	1,34
15086	B)	1,44	0,45			1,80	0,52	1,44	0,43	2,36	1,04	1,00	0,43	1,56	0,81
(orginal form)	C)	1,44	0,45	1,88	0,60	1,80	0,52	1,34	0,40	3,84	1,68	3,12	1,34	1,56	0,81
PIR-Foot	A)	6,19	1,93	7,04	2,24	6,45	1,85	5,52	1,64	3,46	1,52	3,33	1,43	4,79	2,50
15086	B)	1,01	0,32			1,31	0,38	1,13	0,34	2,76	1,21	0,74	0,32	1,36	0,71
(enlarged form)	C)	1,01	0,32	1,59	0,51	1,66	0,48	1,13	0,34	4,35	1,91	3,30	1,42	1,36	0,71
CM21-Pyrrad.	A)			11,20	3,57	11,35	3,26	8,78	2,60	7,02	3,08	6,04	2,59	5,26	2,74
Lup 092	B)					3,53	1,01	1,32	0,39	1,02	0,45	1,19	0,51	1,05	0,55
	C)			11,20	3,57	11,35	3,26	1,32	0,39	2,13	0,93	1,81	0,78	1,05	0,55

The use of a shortened evaluation formula, that means no correction term for the temperature dependency is available, provides additional deviations of $\pm 0{,}5$ %.

The seasonal dependent deviation of the MRF-modified PIR (Food design for the use in aircrafts) from the reference values at clear sky conditions (summer $\leq$ 2%, winter $\geq$ -2%) could be probably reduced by use of a temperature depending evaluation formula. Without this measure the correction method (as used successfully for the PIR's) concerning the dome temperature difference between dome and body reduces by up to 1 % the deviation from the reference only in the summer halfyear; in cold winter days the deviations are amplificied to - 3%.

The deviation of the results of the pyrradiometric method (using CM21-radiometers) from the reference of about 2-3 % at clear nights (and about 1% and more around sunny summer noons) seems to be independent from the seasons. This deviation should be considered for estimating the achieved accuracy of longwave measurement. Since the pyrradiometric method is completely different from the pyrgeometric one which should be, for instance, only effective for longwave radiation < 50 μm.

The field calibration of longwave radiometric methods is possible by a short comparison with the atmosperic heat radiation value of an advanced PIR-reference at a clear night hour to "adjust" the longwave responsivity. For the pyrradiometric method and partly also for the PIR-Foot the recalibration has to be repeated only in a period of several months, if daily mean values are required with a precision of lower than 1,5 %.

b) Concerning the necessary future work

There are activities running to improve the existing methods stepwise by better domes and evaluation formula as well as better performances for special applications. A lot of work is initiated by accuracy targets of BSRN of WCRP corresponding to requirements of the climate research. The most important step should be done probably this year by WRC Davos designing an absolute radiometer to provide a reference for determine the accuracy of the existing methods. Two methods are now in the test phase, the one is based on the classical cavity radiometry and the other is a more operational approach using pyroelectric detectors.

COMPARACIONES ENTRE INSTRUMENTAL CONVENCIONAL Y AUTOMÁTICO EN LAS ESTACIONES SINÓPTICAS DEL SERVICIO METEOROLOGICO NACIONAL EN MÉXICO

Leticia Gómez Mendoza

Servicio Meteorológico Nacional
Av. Observatorio 192
C.P. 11860, México, D.F.

ABSTRACT

At the ending of 1992, the Mexican National Weather Service began the automation of the observation network with the instalation of the first automatic weather station in the Central Observatory in Mexico City. In 1994, there were 65 synoptic observatories with automatic equipment. Taking into account the experiences in other countries , we began a comparison program between conventional and automatic stations in the temperature, pressure, rain and relative humidity values. The first probes were carring out in the central observatory en 1994. Differences for temperature were of 0.7°C and 1.5°C in maximum and minimum temperatures. These values were higher than other others reported by weather services that had been made this kind of comparisons at the begining of this decade. In 1996 and 1997 twenty-one more stations of the network were compared. It was found that in the hourly averange temperature differences were arroud 0.5°C and relative humidity of 1%. In atmospheric pressure the value was of 0.9 hPa, and 5 mm of difference in total amount rain higher than 10 mm/24 hr. Results show differences in diurnal and nocturnal values as well. Now a days, we had found that the different instalation place of conventional and automatic instruments has a decisive roll in our results. That is why a re-instalation of some sensors has been made in order to get the more near values between sensors so these new statios could be commissioned for national and international usage.

1. INTRODUCCIÓN

En la actualidad es inminente la necesidad de automatizar las redes mundiales de observación para ahorrar costos de operación de las estaciones convencionales y para expandir sus redes en aquellas áreas de interés y poco accesibles y aumentar la exactitud en la toma de los datos. Sin embargo, la aceptación de las estaciones automáticas ha tomado tiempo, básicamente porque la transición de un tipo de instrumental en otro y los cambio en los registros climatológicos de largo periodo, aún no ha sido estudiado con profundidad. Por otra parte el cambio de instrumental supone un cambio en la recepción y proceso de la información que implica a su vez el cambio de equipo de cómputo que se suma a los costos de modernización de las redes.

Tal como menciona Nadolsky (1995) el éxito de una red automática depende de la aceptación de las diferencias tanto en el funcionamiento como en los valores con respecto a las estaciones convencionales. Para lograr dicha aceptación la Organización Meteorológica Mundial recomienda que cuando los servicios meteorológicos instalan equipos nuevos en sus redes, deben realizar pruebas de compatibilidad de los equipos en el terreno. La pruebas deben realizarse durante un periodo suficientemente largo, cuando menos en un número seleccionado de estaciones automáticas. (OMM, 1995).

A partir de 1992 el Servicio Meteorológico Nacional (SMN) inició un programa de modernización de sus redes de observación de superficie. Esta modernización consistió en la instalación de 65 estaciones meteorológicas automáticas (EMAS) marca Ericsson en 65 de los 78 observatorios de la red. Siguiendo las recomendaciones de la OMM, el SMN en 1995 inicio un proceso de validación de 21 EMAS (fig. 1). La oficialización de los datos de estas depende de la verificación y validación tanto de los valores en si, como de las características de transmisión y del buen estado y funcionamiento de los sensores.

Las estaciones envían los datos generados al satélite meteorológico GOES cada tres horas con bloques de información de cada 10 minutos correspondientes a los parámetros de dirección e intensidad del viento, temperatura ambiente, temperatura del suelo, humedad relativa, presión atmosférica, precipitación pluvial y radiación solar. Las EMAS instaladas en los sitios, recolectan la información meteorológica, la almacenan en memoria y en disco. Una vez en el SMN, la información es procesada para obtener datos que puedan ser consultados por los meteorólogos como auxiliar en la elaboración de sus boletines. A mediano plazo se pretende que el instrumental automático sea la base de las mediciones en los observatorios y mantener una plantilla mínima de observadores que supervisen la estación y eventualmente transmitan datos del equipo convencional y complementar los informes sinópticos con las observaciones sensoriales.

2. METODOLOGÍA Y DATOS

A principios de 1995 los observatorios realizaron intercomparaciones cada dos meses durante los primeros 15 días de cada mes, anotando las diferencias horarias observadas para las variables de temperatura, humedad , presión y precipitación. Las observaciones realizadas en sitio y de manera simultánea con el instrumental convencional, nos garantizaban la eliminación de errores por transmisión a satélite.

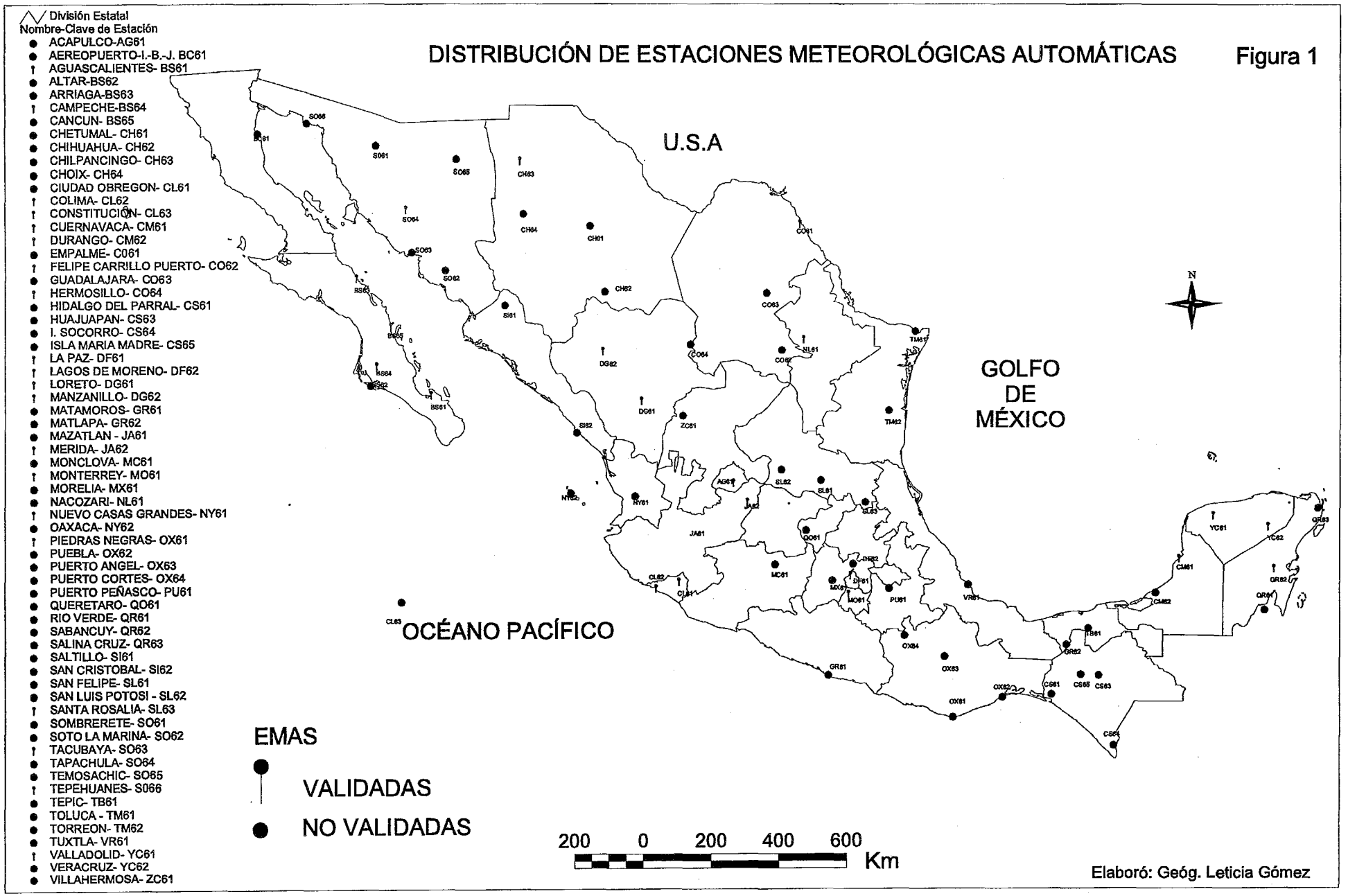
División Estatal
Nombre-Clave de Estación
ACAPULCO-AG61
AEREOPUERTO-I.-B.-J. BC61
AGUASCALIENTES- BS61
ALTAR-BS62
ARRIAGA-BS63
CAMPECHE-BS64
CANCUN- BS65
CHETUMAL- CH61
CHIHUAHUA- CH62
CHILPANCINGO- CH63
CHOIX- CH64
CIUDAD OBREGON- CL61
COLIMA- CL62
CONSTITUCIÓN- CL63
CUERNAVACA- CM61
DURANGO- CM62
EMPALME- C061
FELIPE CARRILLO PUERTO- CO62
GUADALAJARA- CO63
HERMOSILLO- CO64
HIDALGO DEL PARRAL- CS61
HUAJUAPAN- CS63
I. SOCORRO- CS64
ISLA MARIA MADRE- CS65
LA PAZ- DF61
LAGOS DE MORENO- DF62
LORETO- DG61
MANZANILLO- DG62
MATAMOROS- GR61
MATLAPA- GR62
MAZATLAN - JA61
MERIDA- JA62
MONCLOVA- MC61
MONTERREY- MO61
MORELIA- MX61
NACOZARI- NL61
NUEVO CASAS GRANDES- NY61
OAXACA- NY62
PIEDRAS NEGRAS- OX61
PUEBLA- OX62
PUERTO ANGEL- OX63
PUERTO CORTES- OX64
PUERTO PEÑASCO- PU61
QUERETARO- QO61
RIO VERDE- QR61
SABANCUY- QR62
SALINA CRUZ- QR63
SALTILLO- SI61
SAN CRISTOBAL- SI62
SAN FELIPE- SL61
SAN LUIS POTOSI - SL62
SANTA ROSALIA- SL63
SOMBRERETE- SO61
SOTO LA MARINA- SO62
TACUBAYA- SO63
TAPACHULA- SO64
TEMOSACHIC- SO65
TEPEHUANES- SO66
TEPIC- TB61
TOLUCA - TM61
TORREON- TM62
TUXTLA- VR61
VALLADOLID- YC61
VERACRUZ- YC62
VILLAHERMOSA- ZC61
DISTRIBUCIÓN DE ESTACIONES METEOROLÓGICAS AUTOMÁTICAS
Figura 1
U.S.A
GOLFO DE MÉXICO
OCÉANO PACÍFICO
N
EMAS
VALIDADAS
NO VALIDADAS
200 0 200 400 600
Km
Elaboró: Geóg. Leticia Gómez

3. RESULTADOS

Las comparaciones piloto se realizaron en el Observatorio Central de Tacubaya de 1992 a 1994. En las cuales se encontró que las diferencias de temperatura promedio eran de 0.2 a 0.5 °C, las diferencias de humedad oscilaban entre 1 y 5% mientras que las de presión entre 0.3 a 1.9 hpa . No obstante, las máximas diferencias registradas fueron aumentando a medida que pasaba el tiempo. Las diferencias de temperatura máximas pasaron de 0.6°C en 1992 a 1.8°C en 1994. Las diferencias de humedad pasaron de 3.5% a 10% y las de presión se mantuvieron en 1.9 hpa. Para el caso de la precipitación las diferencias encontradas para la temporada de mayo a octubre de 1995 indicaron que para precipitaciones menores a 5 mm en 24 horas las diferencias son de 1 mm como máximo y del 1.7% para precipitaciones mayores a 5 mm en 24 horas.

En la bibliografía internacional de las década de los 70, se encontró que las diferencias entre instrumental convencional y automático eran cercanas a las obtenidas en México.

Rozdestvenskii (1975) obtuvo las siguientes diferencias: temperatura: +/- 0.8°C, presión atmosférica: +/- 1 hPa, precipitación: +/- 5%. Debe hacerse notar que se utilizo un sistema automático más antiguo que el utilizado en México. Klemm (1980) al comparar dos estaciones automáticas se tuvieron los siguientes resultados: temperatura del aire: +/- 1°C y presión atmosférica/- 1hPa. Para la década de los 90 Németh, P. (1995) en Hungría los resultados que se obtuvieron fueron: las diferencias de presión fueron de 0.5 hPa, existió inconsistencia en los datos de humedad, la temperatura presentó diferencias de 0.2°C. Como se puede observar, los resultados en México fueron mayores a las reportados por otros autores durante la presente década.

El promedio nacional de las diferencias de temperatura para México, fue de 0.5 °C, las diferencias extremas fueron las de Nuevo Casas Grandes con 4.0°C y la menor, Manzanillo con 0.0°C. Se presentó una diferencia máxima extrema de 12.4°C para la estación de Colima seguido de Aguascalientes con 8.1°C y la menor diferencia máxima fue de 0.8 en Monterrey. Comparaciones independientes a las calibraciones nacionales, realizadas en el Observatorio de Tacubaya con relación a las temperaturas máximas y mínimas diarias registradas en el periodo de 1993 a 1995 mostraron que las diferencias más grandes se encontraron en los meses de enero a junio (época de secas) en dicho periodo, con diferencias de -1.0 °C a -2.2°C. En los tres años, las temperaturas máximas registradas por la estación automática siempre estuvo por abajo de la convencional. En el caso de las temperaturas mínimas automáticas, éstas fueron más altas que las convencionales de enero a octubre y en los meses de noviembre y diciembre las diferencias fueron de 1.8°C, más altas que las convencionales.

El promedio de las diferencias fue de 0.9 hPa en donde la mayor diferencia promedio fue de -0.1°C en Cuernavaca y el mayor Santa Rosalia con 3.7 hPa. La diferencia máxima fue de 11.0 hPa en Piedras Negras y la mínima fue de -1.1 hPa en Felipe Carrillo Puerto.

Las diferencias promedio de humedad ralativa fueron de -1% donde las diferencias extremas fueron de -41% como máxima en Felipe Carrillo Puerto y la mínima de Tepehuanes con 0 %, Campeche y Piedras Negras con 1 y -1%. La diferencia máxima fue de 78% en Nuevo Casas Grandes se debió a una descompostura del sensor.

3.1 Comportamiento de las diferencias a lo largo del periodo de comparación

Las diferencias de temperatura, parecen comportarse de manera similar a lo largo de las validaciones bimestrales. La humedad se mantuvo constante durante el primer año, pero para el segundo año fue necesario realizar un ajuste a los sensores ya que las diferencias comenzaban a aumentar. Este sensor ha presentado diferencias muy altas con respecto a las normas establecidas por OMM. (Ver cuadro 1)

Con respecto a la presión esta mantiene diferencias arriba de 1hPa pero comienzan a aumentar a partir de mediados de 1995, por ello, para finales de 1995 y principios de 1996 se inició una calibración de los sensores de presión, con lo que se obtuvo una disminución notable de las diferencias.

No es posible diferenciar cambios estaciones en las diferencias de las variables estudiadas, sin embargo por experiencia en algunas estaciones se ha determinado que las diferencias de temperatura se hacen más grandes conforme se acerca la temporada de calor entre los meses de marzo y abril. Las diferencias de humedad se vuelven más marcadas en los sitios desérticos durante el verano cuando la humedad llega a ser menor de 10% y la mayoría de los sensores no registran datos menores a 12%.

Por otra parte de acuerdo a nuestra experiencia, todas las estaciones parecen tener un comportamiento

diurno que se caracteriza por presentar menores diferencias de todas las variables estudiadas en las horas nocturnas (de 20:00 a 7:00 horas locales) y las mayores diferencias se presentan en las horas del día. Por ejemplo la máxima diferencia de temperatura suele presentarse entre las 10:00 y 15:00 hrs al igual que la mayor diferencia de humedad.

A mediados de 1996 se logró determinar que algunas de las diferencias que se presentaron se debían a: a) La altura del sensor de temperatura así como su exposición a la intemperie no era la misma que los termómetros convencionales dentro de las garitas meteorológicas. En algunos casos los sensores tenían sombras que originaban b)Las diferencias en los principios de operación de los sensores de humedad, mientras que el sensor automático es un arpa de cabellos, el sensor convencional es un psicrómetro

De acuerdo a los resultados obtenidos se decidió comparar las normas de tolerancia recomendadas por la OMM con las máximas precisiones observadas en las estaciones Ericsson a lo largo de las comparaciones La máxima precisión encontrada en los equipos Ericsson está dentro de las normas de OMM, sin embargo son pocos los casos en los que se obtiene en la práctica con las estaciones instaladas. Por ello, para fines prácticos y considerando el equipo que se utiliza para comparar, se ha determinado que cada estación no sobrepase los límites del cuadro siguiente:

Cuadro 1

VARIABLE	PRECISION REQUERIDA (OMM)	PRECISION REQUERIDA EN MEXICO
Temperatura del aire	± 0.1 °C	± 0.5 °C
Temperaturas extremas (máxima y mínima)	± 0.5 °C	± 0.5 °C
Presión Atmosférica	± 0.1 hPa	± 1.0 hPa
Precipitación	± 0.1 mm para ≤5 mm ± 2% para ≥ 5 mm	± 0.1 mm para ≤ 5mm ± 1.7% para ≥ 5 mm
Humedad Relativa	± 3%	± 5%

Sin embargo, sólo 11 estaciones presentan diferencias aceptables en todas las variables: Campeche, Cuernavaca, Durango, Hermosillo, Lagos de Moreno, La Paz, Manzanillo, Mérida, Piedras Negras, Tepehuanes y Tacubaya.

4. CONCLUSIONES

Las diferencias obtenidas en la red de estaciones automáticas en México se encuentran alejadas de las que recomienda la OMM y con los resultados en otros países. Sin embargo se ha comprobado en la práctica que ni aún en la estación Tacubaya que, por encontrarse en las oficinas centrales del Servicio Meteorológico Nacional, cuenta con mantenimiento y calibración constante de sus sensores; alcanza estos valores de precisión. Todos los esfuerzos de calibración de los equipos deber ser realizados en sitio y encaminados a evitar la deriva de los valores en el tiempo, principalmente los relativos a la humedad y a la presión.

Durante el presente año, el Servicio Meteorológico Nacional tiene contemplado la reparación y remplazo de sensores automáticos de las EMAS, con ello un programa continuo de calibración que conlleve a la oficialización de estas estaciones y utilizarlas como una herramienta de consulta nacional para aquellos observatorios que no cuenten con personal observador las 24 horas del día.

5. REFERENCIAS

Nadolski, V. 1995. Operational experiences with the automated surface observing system - ASOS International Workshop on experience with automatic weather stations on operational use within national weather services Vienna , 1995.s/p

OMM 1995 Organización Meteorológica Mundial, (OMM), 1995. Guía del Sistema Mundial de Observación. Publicación núm.488.

Rozdetvenski Rozdestvenskii, B. G. y V.A. Yurmanov., 1975. Some technique problems of meteorological measurements and development of automated observational systems. *WMO Technical Conference on Automated Meteorological Systems , Washington D.C. February 1975. WMO 420.*p 19-21

Klemm Klemm, S. 1975. Meteorological and Technical Problems in Operating Automatic Weather Stations (AFMS) in the Meterological Service of the German Democratic Republic. Automated Meteorological Systems . *WMO Technical Conference on Automated Meteorological Systems , Washington D.C. February 1975. WMO 420.* p. 254-259

Nemeth Németh, P. 1995. First experiences with the intercomparison of meteorological data measured by traditional instruments and sensors of AWS in Hungary. International Workshop on experience with automatic weather stations on operational use within national weather services Vienna , 1995.s/p

Session II

CALIBRATION OF INSTRUMENTS

2.1

THE METEO-FRANCE METROLOGY LABORATORY : EQUIPMENT AND EXPERIENCE
LE LABORATOIRE DE METROLOGIE DE METEO-FRANCE : EQUIPEMENTS ET EXPERIENCE

Jérôme DUVERNOY, FRANCE
Météo-France SETIM/QMR/LM
B.P. 202 78195 TRAPPES Cedex, FRANCE
email : jerome.duvernoy@meteo.fr

1. Introduction

The SETIM, which is the Regional Instrument Centre (RIC) for RA VI, has set its own Metrology Laboratory 8 years ago. It is equipped with international level calibration references for the measurement of pressure, temperature and humidity. These systems are used for the calibration of surface network sensors but also for the calibration of some French industrial sensors and of some foreign meteorological service sensors. An air conditioned room guarantees a temperature and humidity stable environment (23°C ± 1°C; 50% ± 10%).

2. Laboratory equipment

2.1 Pressure

The pressure reference is a Degranges et Huot dead weight standard. The pressure is generated in laboratory with a Degranges et Huot generator from 20 to 1100 hPa. The accuracy (2σ) achieved in this range is lower than 0.1 hPa. The temperature calibration of barometers is achieved with a Weiss climatic chamber (possible range is -70°C to 60°C).

For network barometers and field calibration, two Desgranges and Huot quartz barometers are used as working and transfer standard. The laboratory is also equipped with a portable generator for field calibration from 500 to 1100 hPa.
About 200 calibration certificates were issued last year.

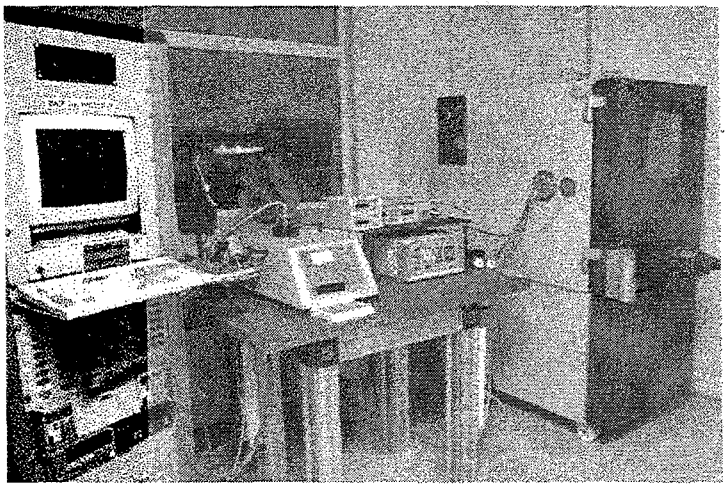

Figure 1 : Pressure calibration bench

2.2 Temperature

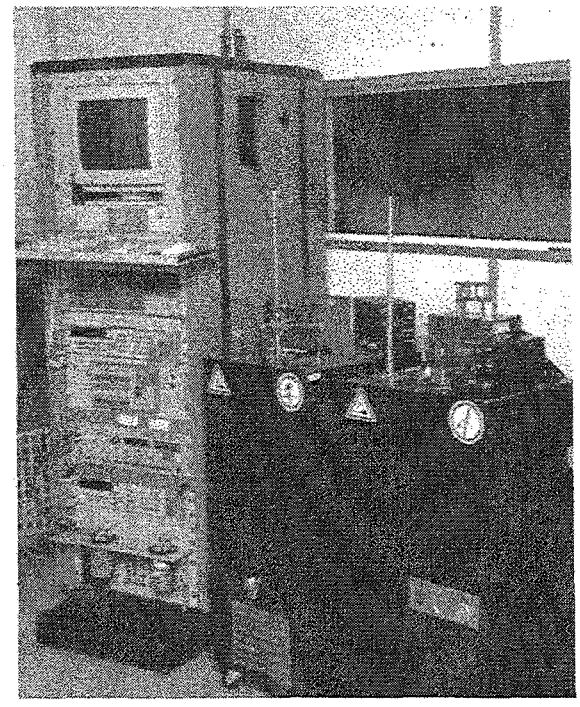

Figure 2 : Temperature calibration bench

The temperature reference is a Tinsley platinum resistance. The ratio of the standard thermometer's resistance to a reference resistance is measured with an ASL F17 resistor bridge. The resistance of the calibrated thermometer is measured with a HP3458 multimeter. A Heto stirred liquid bath is used to produce a stable temperature from -75°C to +60°C. A Gallium Isotech cell is used to control the calibration in one point (around 29°C). Best measurements capabilities are 0.15°C.
On average, 200 calibration certificates are edited every year.

2.3 *Humidity*

In 1996, the metrology laboratory was equipped with a humid air generator. This bench is not only a generator but also a calibration reference (Accuracy (2σ) is better than 1.5%).

A saturator in a stirred liquid bath generates humid air which is pumped into the testing chamber. The chamber temperature is regulated by a Weiss climatic chamber. When the equilibrium state is reached, air temperature is measured by the testing chamber thermometer and dew point temperature is given by the saturator temperature.

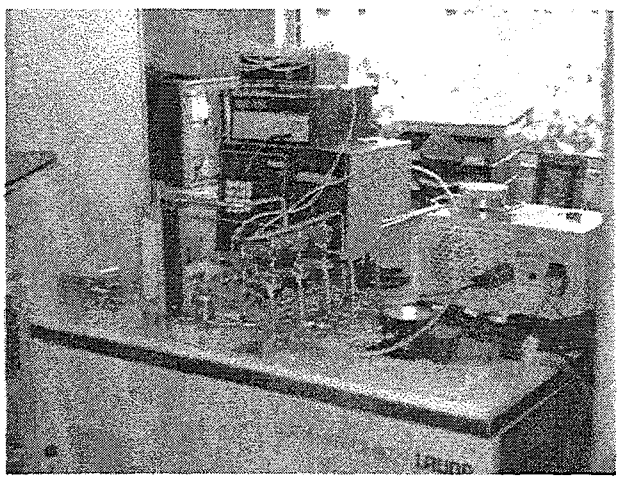

Figure 3 : Humid air generator bench

3. Calibration experience

3.1 *Pressure*

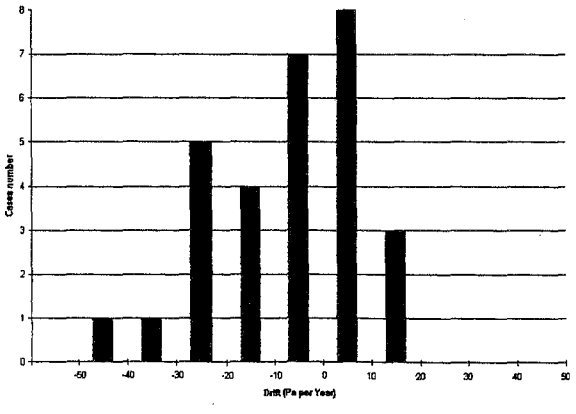

Figure 4 : Histogram of pressure drift

Météo-France is using about 150 Vaisala PTB 220 numeric barometers in its network. They are controlled every year by the metrology laboratory. In 1997, 78 barometers were calibrated. 15 of them were new barometers. 63 were at least one year old barometers. 29 have been adjusted because the correction was more than 15 Pa.

The manufacturer claims a ±10 Pa per year drift. The drift of 15 barometers was lower than this threshold. 14 sensors had a higher drift, but no drift was above 50 hPa per year (see fig. 4).

3.2 *Temperature*

The return rate of temperature sensors is very low. A special study has been done to control sensor drift. 17 platinum air thermometers have been calibrated for a second time. All were still in A class (±0.15 K). Just two of them were a little bit over Météo-France limits (0.1 K). This study confirms that platinum probes are very reliable. Because of technical problems, the annual drift can not be calculated. Sensors were at least 4 years old (12 years old max).

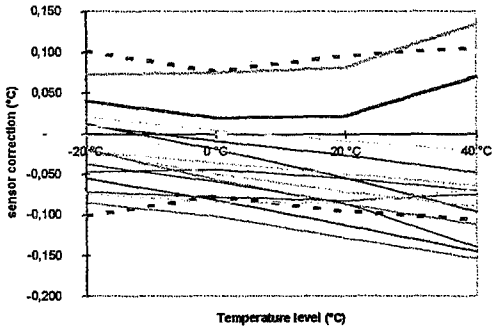

Figure 5 : Temperature correction (°C)

3.3 *Humidity*

More than 550 Vaisala hygrometers HMP 35 DE are used in the French observation network. All of them are calibrated every year. The usual hygrometer calibration is done with saturated salt solutions. This system is an easy, practical and cheap bench for numerous calibrations. Care must be taken to avoid any temperature gradient. So it is done in the air conditioned laboratory.

Sensors drift is less than 2% at 11% level. But The drift is some times up to 5% for 75 and 95% level. The drift seams to be independent with the time between two calibrations. But it confirms the need of a regular calibration.

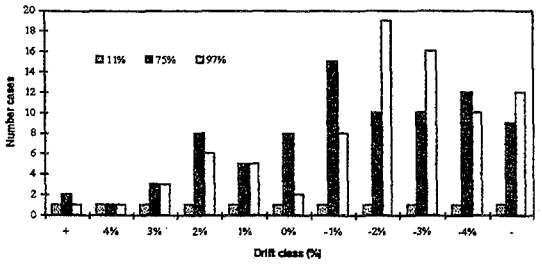

Figure 6 : Histogram of humidity sensor drift

4. Conclusion

The metrology laboratory is ready to continue is international calibration work for pressure, temperature and humidity. This is a guarantee of quality for international network observations.

The metrology laboratory is also organizing training courses. It develops every kind of exchange in term of pressure, temperature or hygrometry.

Today, our laboratory is not officially recognized by the national metrology authority. Efforts are made to comply the laboratory quality systems with the ISO 9002 model and to obtain a calibration accreditation.

SENSORS CALIBRATION TECHNOLOGY

by
SAID M.ELSAYED
DIRECTOR OF WORKSHOP
METEOROLOGICAL AUTHORITY
CAIRO/EGYPT

The old Method to Calibrate Pressure Sensors

In this method we change the different Barometers , cleaning the mercury from dust and impurities and making the mercury tube free from air then we make a comparison between these Barometers and the semi-standard one in room pressure for several days . Of course this method is not accurate because we calibrate only within 2 or 3 Hpa variation during this period but we need to calibrate the whole scale. for this reason we intend to have a new chamber for this purpose.

New Method To Calibrate The pressure Sensors

Pressure Chamber:

Pressure/Vacuum chamber is used for testing several aneroids, barotrasmitters , barographs and mercury barometers . Test chamber consists of cylindrical steel body coated with flange and covered by steel plate ; one large inspection pane in the door made of 40 m.m acrylic glass ; installed vibrating table with rung stand ,actuated by push-button from outside ; on the right 8 electrical ducts , on the left 2 air ducts for connection to Hg-test barometer or an external units on the front operating taps.

The chamber can calibrate several mercury barometers and aneroid barometers in the same time and we can change the pressure inside the room on request in addition to the possibility of keeping the pressure constant in the room as long as we need. By this way we can save time and human effort to calibrate a lot of instruments in short time beside the good quality of calibration, also we can use this chamber to calibrate the pressure sensor of the automatic stations.

Calibration of Temperature Sensors (Thermometers)

1- An old method to calibrate temperature sensors

In this method we put the thermometers in a tank as shown in Fig(1) and we put the reference thermometers beside the thermometers to be tested and we put hot water in the tank and take the reading , then we add cold water and take the reading again and so on. By this way we cant not control the temperature inside the tank ,so this method is not accurate. Therefore we look for a new device for calibrating thermometers.

2- New Equipment to Calibrate Temperature sensors (Thermometers)

Thermometer Test Equipment:

It consists of a thermometer testing bath, continuous cooler, an electrical temperature control device , special lamp and a set of standard thermometers. Thermometer Test bath with fault - free double safety glass; very easy reading of the testing and controlling thermometer ; adjustable frame for installation of different thermometer diameters ; pares

in contact with the liquid are made of stainless steel; flow regulation by means of a circulating pump; cooling spiral for external connection e.g. of a Cryomat.
The continuous cooler : is an air cooled refrigerator engine which works in continuous run basing on the principle of counterflow heat exchange (evaporator) ; connection to the circulating pump of the test bath , giving an intensive and constant cooling.
The electronic Temperature Controller is a platinum Resistance Thermometer Pt100 . An accuracy of + 0.01 C is obtained. The special lamp is suitable for lighting the test bath ;it produces a light similar to daylight and free of heat radiation. By this equipment we can change the temperature as we want for the whole scale.

An old method for humidity sensor calibration

The old method is composed of a room with two parts as shown in fig (2) ,the upper part is for the instrument to be calibrated and the lower part is for putting silca-gel or boiling water , a fan to distribute the air inside the chamber . By this method we have two readings only, one greatest and the other is smallest and of course is not an accurate method because we need to have reading in all the scale of the instrument and for this reason we get a new chamber for humidity calibration.

New Chamber for humidity Sensor
Humidity Test Cabinet

It is used for graduating and calibrating hygographs, thermohygro-graphs; it consists of moistening and demoistening unit; air circulator , membrane air pumps ; as well as the entire measuring and controlling equipment ; light gray coated metal sheethousing ; the total test chamber is insulated, door with insulator glass panes; on the left it is equipped with 6 electrical ducts ; on the right there is a device for measuring air humidity using psychrometric principle ; installed ventilator in the test in the test chamber , producing air circulation and constant temperature ; for moistening the sucked - out air is conducted through a water bath in a great number of small air bubbles which during the process are saturated with water . The water bath is tempered by an electrical heating element . For demoistening the sucked - out air is blown through a dryer. The relative humidity is indicted by a hygrostat with two limiting contacts (max./min.) for humidity control, an indication for operation by means of red control lamps. by this chamber we can control the humidity as we want from 15% up to 96% and we can calibrate the sensors of humidity for the automatic station in this chamber.

An old method to calibrate wind speed

It is a machine composed of *a gear box as shown in fig (3) which changes the value of the* reading of the wind transmitter to revolution /minute and there is a connection between this reading and the reading of speed indicator in knots. We can change the speed as we want and of course this method is not accurate.

New equipment to calibrate wind
Wind Tunnel

The wind tunnel is basically designed as test equipment for meteorological sensors . Typical application would be the test and calibration of wind speed , wind run and wind direction sensors . Its open construction with the measuring section in the suction part enables compact dimensions and therefore operation in relatively small rooms. An SCR-Controlled

DC motor drive enables a wide operation range and stable rotational speed . We can use the wind tunnel to calibrate the wind sensors of the automatic stations

An old method to calibrate mercury in steel recording thermohygrograph

It is a tank as shown in fig (4). We put the instrument on the stand and its arms in the tank, then warm water in the tank and we take the reading of the reference thermometer which immersed in the water of the tank and the reading on the chart of the instrument . The way is not accurate because it is difficult to have a constant temperature to a certain time, so the need to have a room to Calibrate the instrument is very important.

New cabinet to calibrate recording temperature sensors

Temperature test cabinet

It is Special design for calibration of meteorological instruments ,especially thermographs and thermohygro-graphs;. The maximum capacity is suitable for 4 thermographs respectively , 2 thermohygro-graphs . Temperature selection by preset switch ; indication of actual value by means of an LED. Adjustable excess temperature protection. Connector of remote program feed respectively connection of a printer .Opening at the top suitable for electrical feed- through. we can calibrate The sensors of temperature for the automatic station in this chamber.

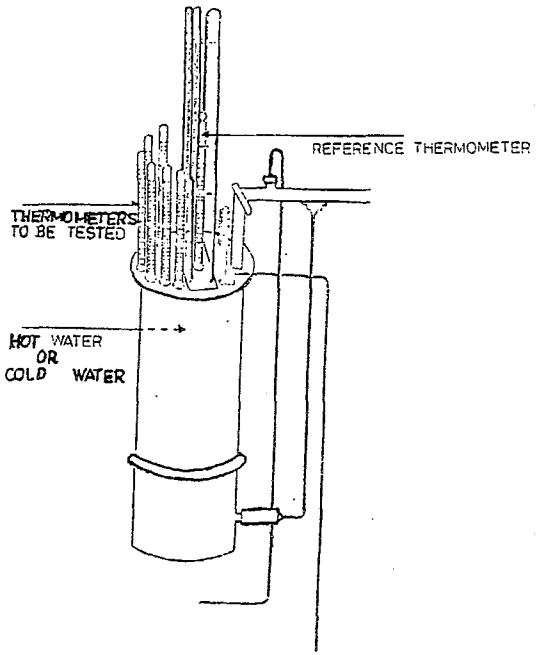

OLD CHAMBER FOR THERMOMETER CALIBRATION (FIG1)

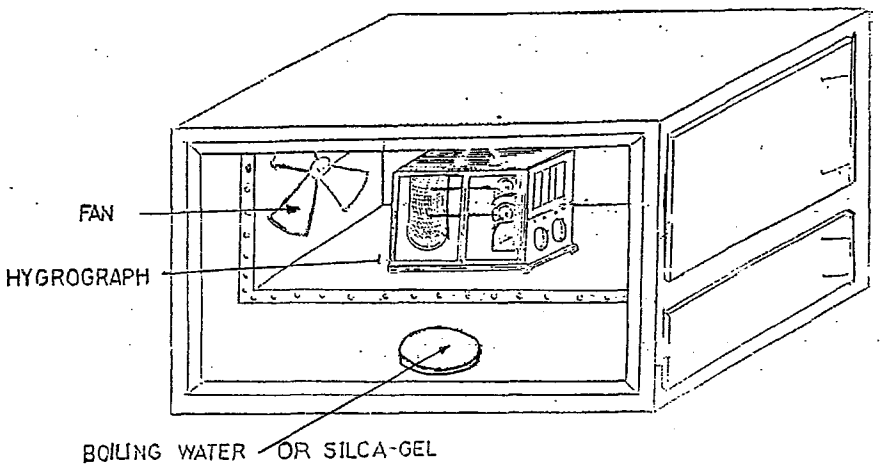

OLD CHAMBER FOR HYGROGRAPHS CALIBRATION (FIG 2)

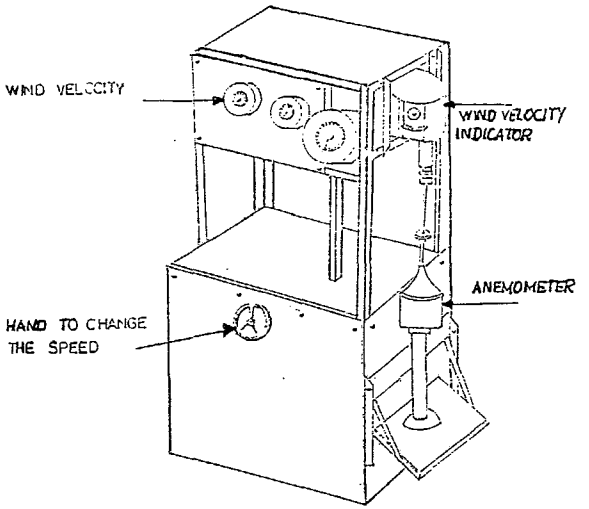

OLD MACHINE FOR WIND SPEED COMPARISON (FIG3)

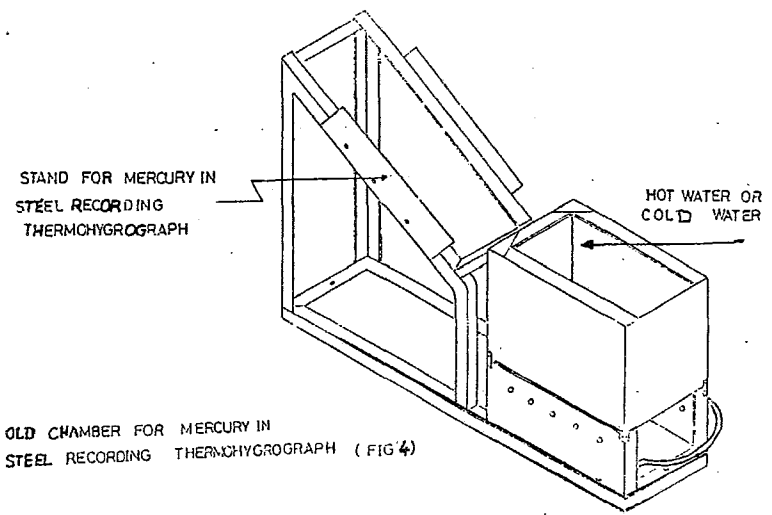

OLD CHAMBER FOR MERCURY IN STEEL RECORDING THERMOHYGROGRAPH (FIG 4)

Wind Sensor Calibration with the Help of Laser Doppler Technology

Olbrück, G.

Deutscher Wetterdienst
Abteilung Meßnetze und Daten, Meßsysteme
Frahmredder 95, D-22361 Hamburg 65

1.0 Introduction

The increasing use of electrical sensors in automatic meteorological weather stations brings about that the calibration procedures are carried out with an electronic equipment which has to allow for the connection of different types of sensors with different kinds of signals and data formats. The Deutscher Wetterdienst DWD set up reference systems for the calibration of secondary references to be used in the maintenance branche of the service. Reference systems for temperature, pressure and humidity are operated with high accuracies up to: T = 0,01 ^{0}C +/- 0,0001 K, P = +/-0,02 hpa and U ≈ +/-0,1 % RH.

The calibration of wind sensors is carried out in the wind channel using hot wire anemometer and doppler laser technic which today are very common as measuring methods in the fluid mechanics. To capture instantaneously the flow velocity in a wind channel with flow fields of pronounced spatial structures and temporal or spatial changes - transition from laminar to turbulent flow - new experimental technics, such as particle image velocity, are required.

2.0 LDA-technic for air velocity measurements

The LDA-System includes a laser, transmitter and receiver optics, a signal processor and a computer system with LDV (Laser Doppler Velocitimeter) software. The LDA offers an optical procedure which detects the frequency shift of mono-chromatic light scattered from particles transported in the air stream of the DWD wind channel, that means, using the Doppler effect for velocity measurements.

The Laser Doppler Velocimeter of the Deutscher Wetterdienst is used for highly accurate measurements of fluid velocity in the gaseous flow of the wind channel. Scattered light from generated water particles passing through the probe volume produce a Doppler frequency proportional to the particle velocity. In order not to infer the fluid velocity from the introduced particles, they must be small enough to follow the flow field accelerations and yet large enough to scatter sufficient light

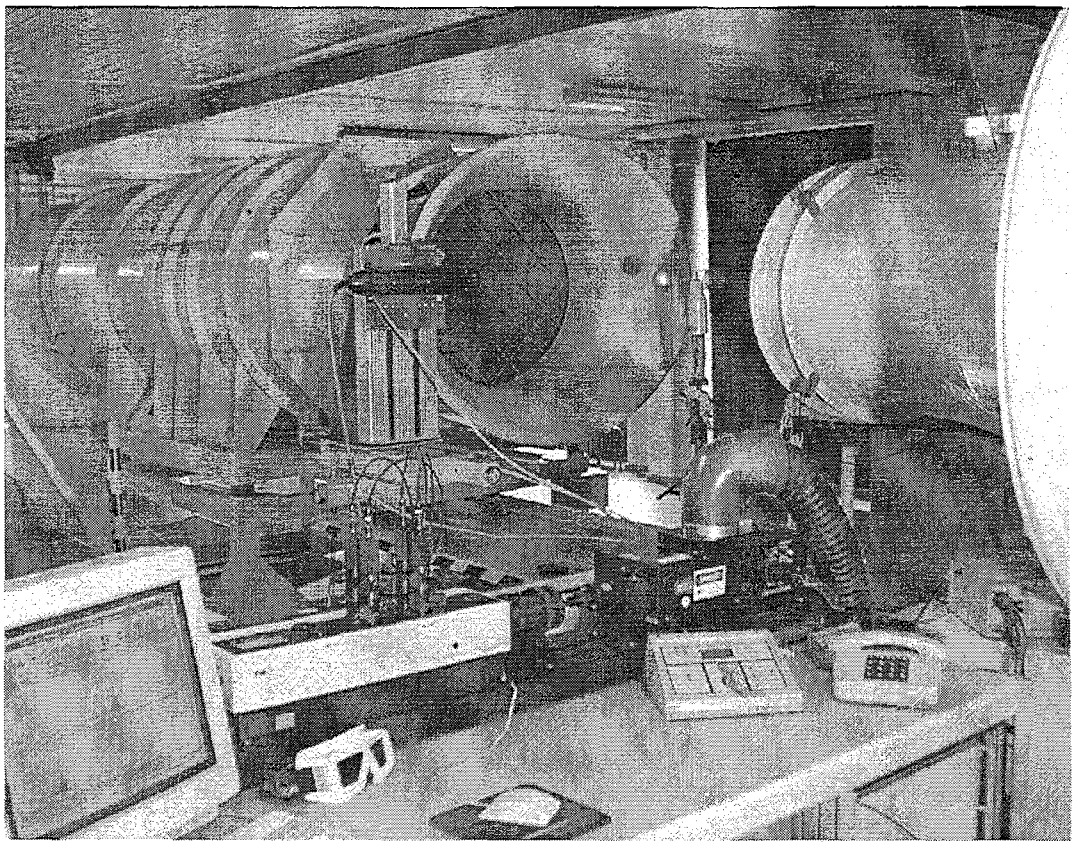

Fig. 1

intensity.Optimum particle size is generally between 0,5 and 2 micrometers. DWD operates a particle size generator which insures that only particles of a desired size are included during a series of measurements.

The advantages of using LDA measurements for wind sensor calibration are:

- no flow disturbance by in-situ reference sensors, LDA is a remote sensing technic by transmitting information on an optical path applicable to open and closed air streams when using glas windows
- no corrections of the data with regard to temperature and humidity are necessary
- velocity independent of ambient conditions
- measures two directional components
- dynamic measuring range extending from < 1 cm/s to 200 m/s
- high accuracy of measurement (0,002 m/s), the components of the velocity vector v, the optical constant d (m) and the detected Doppler frequency F (s^{-1}) are represented in the following formula:

$$v = d * F \text{ (m/s)}$$

- excellent spatial resolution
- no calibration

Observing the laser light before the scattering process shows that when the wave fronts from the two laser beams cross, they create an interference pattern. This "fringe" pattern is composed of planar layers of high and low intensity light.

Air velocity measurements in DWD are made with two wavelenght (green λ_1, blue λ_2) - see fig. 2 - while the water particles in the flow scatter light passing through the laser beam crossing region. The angles of each beam pair relative to particle motion produce a pair of two different Doppler-shifted signals. The beat frequency, commonly referred to as DOPPLER-frequency, is actually the difference between two doppler-shifted signals, and it is proportional to the particle velocity. If, for Gaussian beams, the e^{-2} intensity points are used to define cylindrical beam surfaces, the beam crossing region (fringe pattern) will have an ellipsoidal shape.

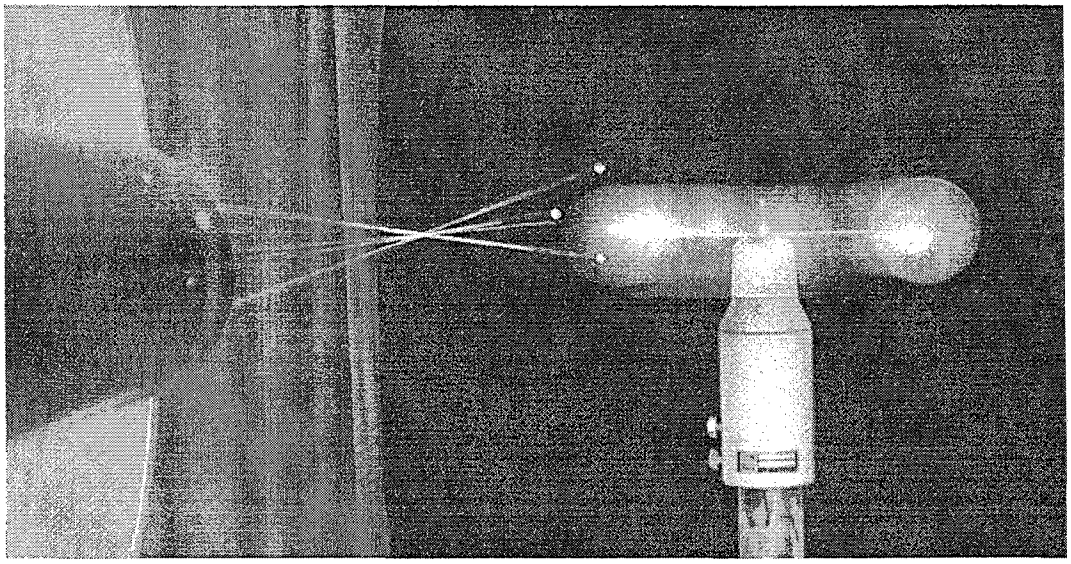

Fig. 3

One component of the velocity stream vector is detected by one beam pair. Additional components will be detected by additional beam pairs and different frequencies; it is always the component in the plaine mounted between the partial laser beams. Particles moving through the fringe pattern create a scattered light signal with sinusoidally varying intensity. A signal's burst envelop is caused by the Gaussian intensity distribution across the measurement volume. Since the fringe spacing (d_f) is known, the velocity normal to the fringes can be easily calculated by measuring the signal frequency:

$$Particle\ velocity = \frac{d_f}{t} = d_f * F$$

d_f = fringe spacing
F = Doppler shift frequency of the scattered light
t = time taken for the particle to cross a pair of fringes

A receiving optic delivers the scattered light (in figure 2 represented as a central beam) to a photodetector where the signal is filtered and fed to the signal processor. When the flow velocity is changed, particles with changed velocities give Doppler bursts with differing frequencies. With these results, a detailed information of the flow can be obtained and the remote sensed air velocity in the immediate environment of the calibrated wind sensor is detected with an accuracy of 0,002 m/s.

A measuring value is always an average over a distinct number of measurements from a single particle. The individual values are normal distributed as the fig. 4 demonstrates in the example with an air stream velocity of 5 m/s

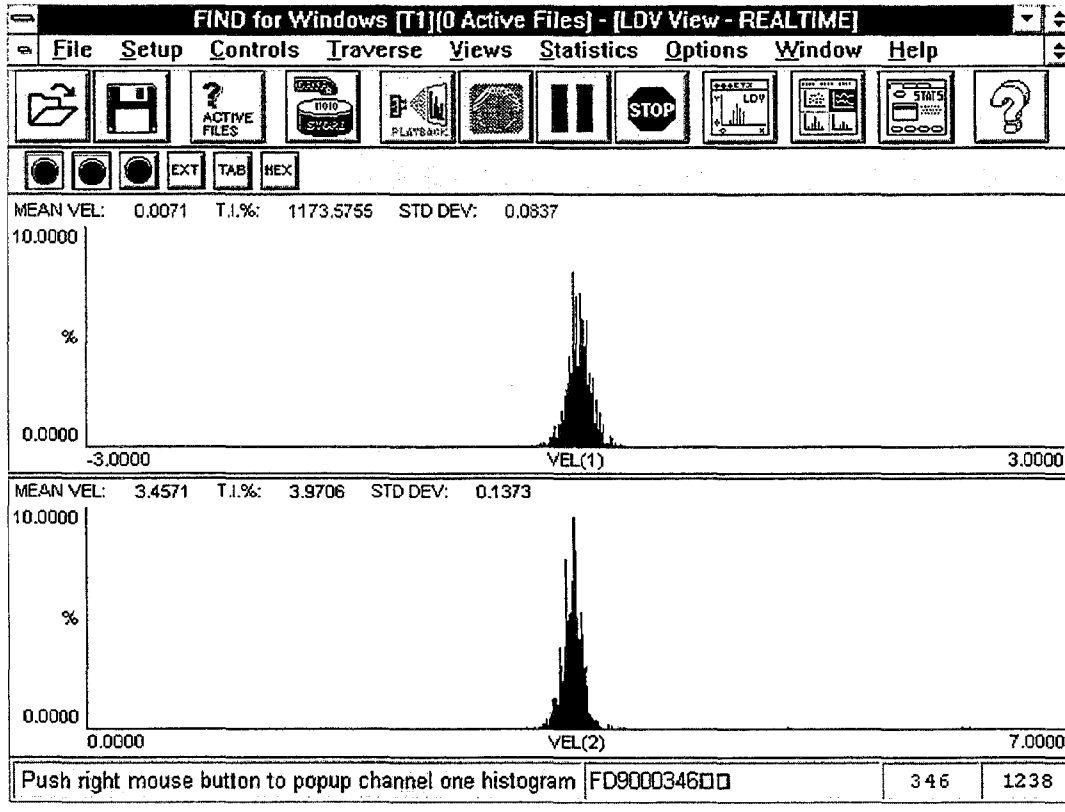

Fig. 4

Particularities of the procedure:

- high capital expenditure
- high technical expenditure (knowledge in systems and proceedings, training in the operating instructions for a programme steered measuring course)
- adjustment controll of some optical components in fixed time intervals
- due to the laser output the appertaining security requests have to be followed
- the chemical compounds of the injected tracer particles have to be non-toxic, nevertheless, the natur of the chemicals is very important with regard to the loss of particles by evaporation and separation;

3.0 LDA-activities

The LDA-System is used to certificate wind sensors of different manufacturers by confirming that the properties of the test sensors are in agreement with the recommendations of CIMO-IX which are published in the CIMO-report discussing the results of the Ottawa-session from 15. - 26. July 1985 - Annex to Recommendation 3.

In the specification of the DWD test performance the following requests have been layed down:

Accuracy requests:

-	wind direction:	+/- 5 degrees for the scale 0-360 degrees
-	wind speed:	0,5 m/s in the velocity range 0,5 m/s to 5 m/s 10% in the velocity range 5 m/s to 75 m/s (wind channel tests up to 45 m/s)

Operational qualifications:

-	wind direction:	time constant: 1 s distance constant: 2 m to 5 m linearity: +/- 2 to +/- 5 degrees decay relation: 0,3 to 0,7
-	wind speed:	time constant: 1 s distance constant: 2 m to 5 m linearity: +/- 0,5 m/s starting threshold: 0,5 m/s

Remarcs: The distance constant is the air distance by which an anemometer has to be passed in order to represent 63% of the change from the starting to the end value; this is analog to the time constant.

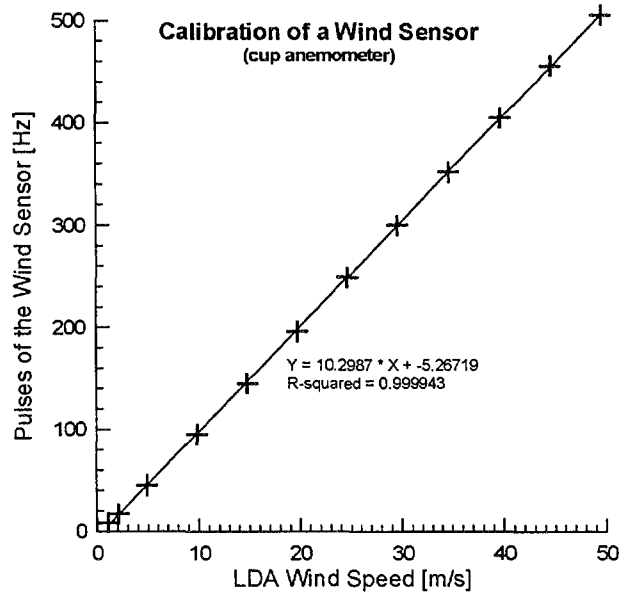

Fig. 5

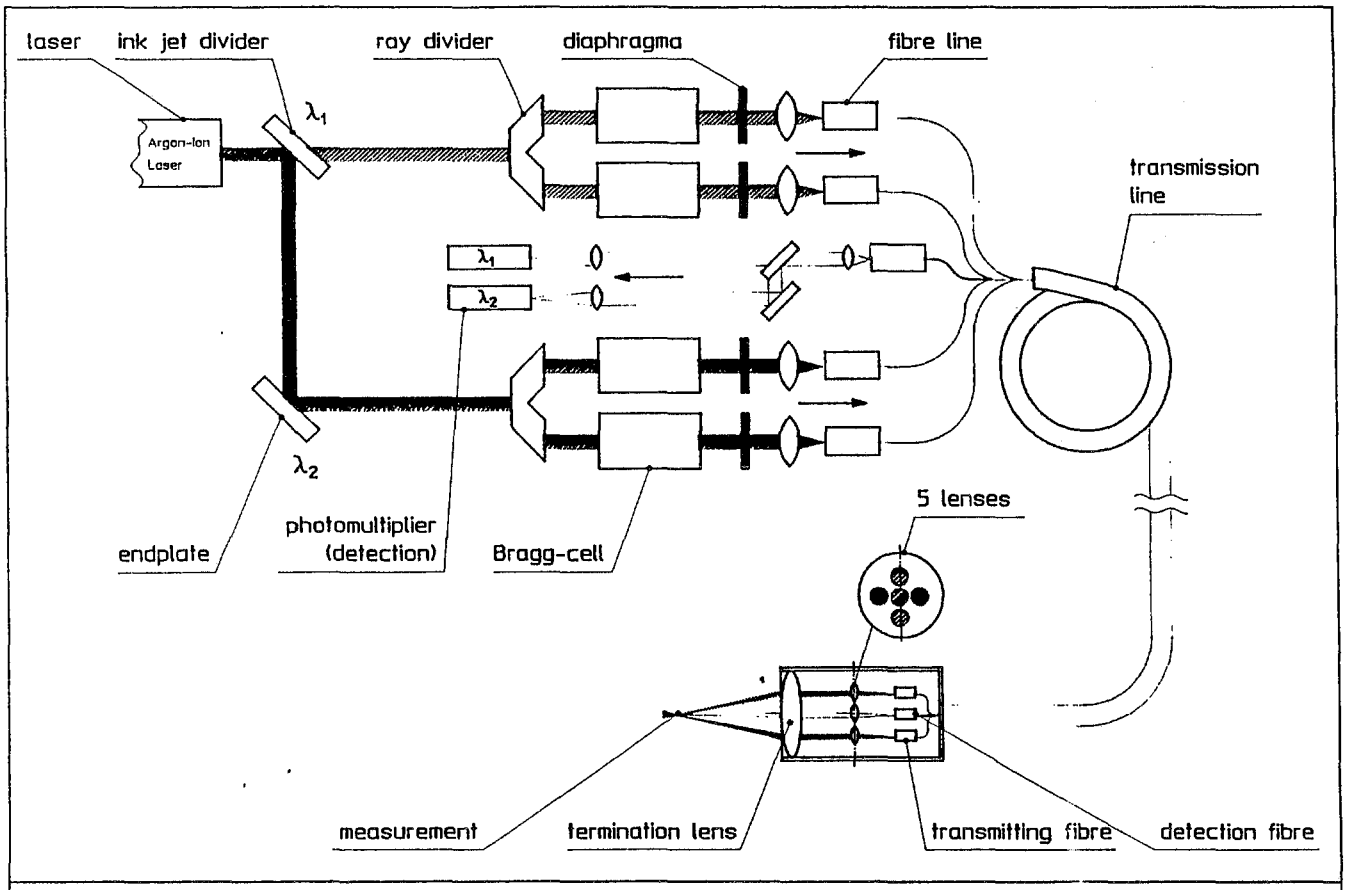

Fig. 2 two-dimensional LDA-Sondesystem Wind-Channel-DWD/TI 23

/Szabo/WINDKANAL/ 'Schau_englisch'

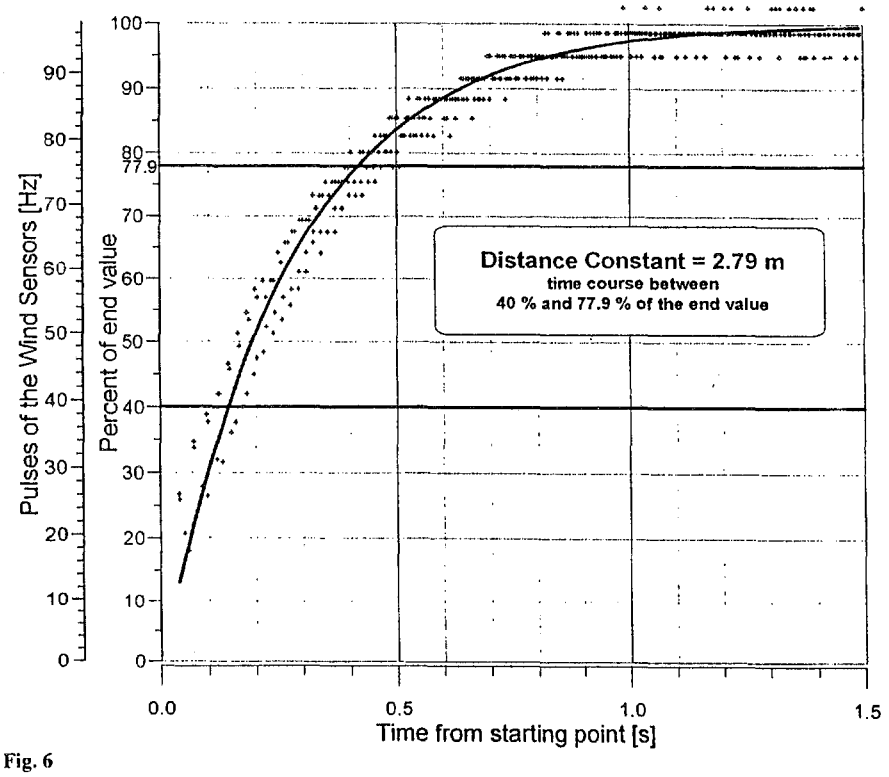

Fig. 6

INTERCOMPARISONS IN THE FREE ATMOSPHERE AND IN THE WIND TUNNEL TO ESTIMATE ANEMOMETER CALIBRATION UNCERTAINTY

Thomas J. Lockhart, CCM, CMet
Meteorological Standards Institute, Box 26, Fox Island, WA 98333, USA

1. INTRODUCTION

Calibration of an anemometer is usually based on a series of average measurements of the output of the test instrument as compared to a known wind speed. The averaging time is usually equal at each speed and is sufficient for the resolution of the instrument outputs and the turbulence or speed variability of the controlled environment. The averaging time is usually in the range of 30 to 100 seconds. The number of speeds is selected to adequately describe performance using some statistical model. Usually 5 to 15 speeds are selected within the range of the calibration facility and application needs. Often duplicate measurements are made to estimate precision. Sometimes the duplicates are taken during increasing speed and during decreasing speed to challenge possible hysteresis of the test facility. Consideration should be given to applying a constant distance of air past the sensor at each speed rather than a constant time.

2. STATISTICAL MODEL CONSIDERATIONS

Test data from a calibration by the U.S. National Institute of Standards and Technology (NIST) are used as an example. The test instrument is a cup anemometer with a frequency output. The first test for the series of pairs of values is a standard least squares or regression analysis. The independent or controlled variable is the wind speed provided by NIST. The dependent variable or predictand is the output of the test instrument (Hz). The regression equation shown in Figure 1 permits the calculation of Hz from each NIST wind speed to define the best fit straight line. The figure shows all of the points at 11 speeds and the linear regression line. The analysis also provides a measure of correlation. The test method described in NEL 1995 [1] requires a linear correlation coefficient R to be 0.99995 or greater ($R^2 \geq 0.9999$) for an acceptable test. The data in Figure 1 has an unacceptable correlation coefficient of 0.99985.

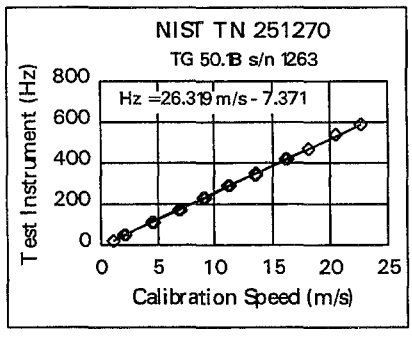

Figure 1

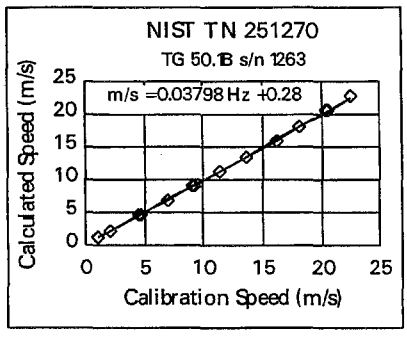

Figure 2

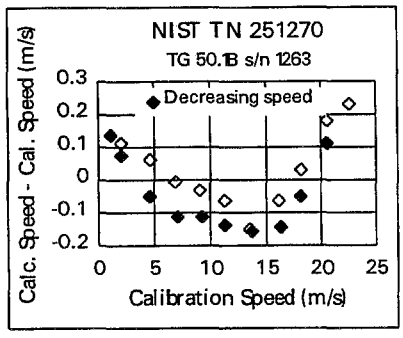

Figure 3

It is hard to see much detail in Figure 1. When the independent variable is the output (Hz) and the dependent variable is the NIST speed, the regression equation can be used to convert Hz to wind speed. Figure 2 shows this construction. Now the speed difference at each pair of points can be calculated, assuming the calibration facility speed to be correct. A third regression analysis, using the speed differences as the predictand, will provide more detailed information. Figure 3 shows this analysis. Now details can be seen. This figure shows that the duplicate tests were taken during increasing speeds (open diamonds) and decreasing speeds (filled diamonds). There is clearly a hysteresis from some source. There is also a clear pattern to the differences as a function of speed. Does this non-linearity describe the sensor performance or the wind tunnel performance?

Once a transfer function is calculated as shown in Figure 2, a strategy is required for its application. If the non-linearity is ascribed to the calibration facility and not the sensor, the calibration test data should be represented with the best fit straight line. If two or more calibrations are being compared, the multiplier (slope) and constant (offset) from each calibration should be used. Pick a frequency which represents an important speed and calculate the speed using all the transfer functions. If different interests require a broader analysis, an average from a series of frequencies can be used. Wind speed distribution models can be used to calculate statistical differences resulting from the use of the different transfer functions.

3. CALIBRATION FACILITY UNCERTAINTY

The Round-Robin experiment was designed to estimate the relative uncertainty of calibration facilities. The latest data in Lockhart, 1998 [2], describes the results from Round-Robin 2, (RR2). An estimated true pitch (ETP) of 0.2985 meters per revolution with zero offset was deduced from 22 selected tests representing 20 facilities in Europe and the United States. A rate of rotation of 30 rps, representing about 9 m/s, was used to compare all the transfer functions from the linear regression analyses of the RR2 tests. Only two of the 22 tests failed the correlation coefficient test. These resulted from calibration facility problems. Figure 4 shows the results of RR2-17 at NEL in Glasgow. A straight line cannot properly represent these test data. Figure 5 shows the results of RR2-19 at CIEMAT in Madrid. This facility showed considerable scatter and hysteresis between increasing speed and decreasing speed.

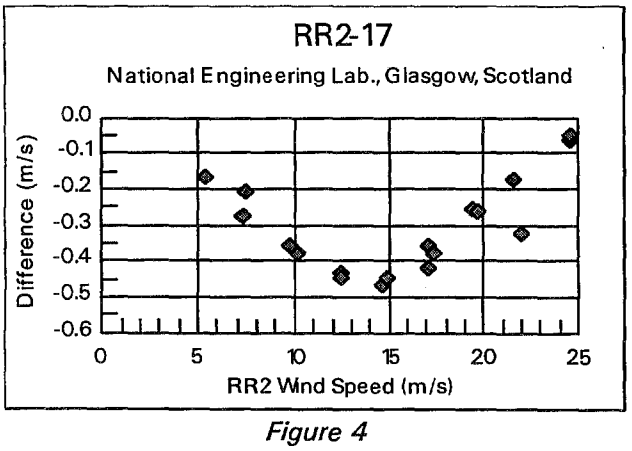

Figure 4

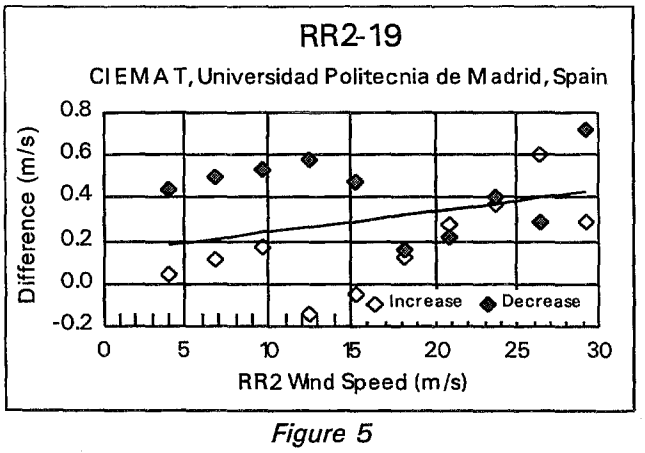

Figure 5

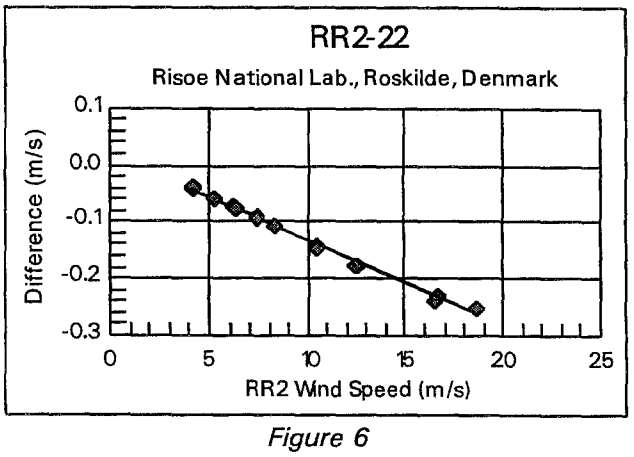

Figure 6

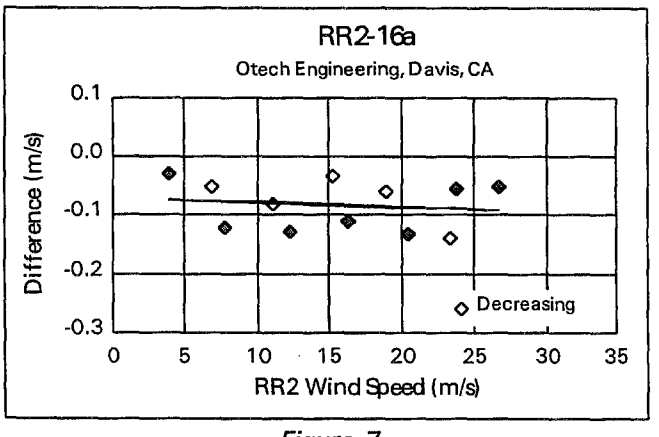

Figure 7

The majority of facilities (59%) found the speed at 30 rps to within ±0.5% of the ETP value. Three facilities (13%) were between ±0.5% and ±1.0%. Figure 6 shows the results of the RR2-22 test at Risoe National Laboratory in Denmark in order to verify that the helicoid propeller is really a linear instrument. The duplicates were taken during increasing and decreasing speeds demonstrating that hysteresis is not a result of the sensor memory. The standard error of the Y estimate from the linear regression analysis, a measure of scatter about the best fit straight line, was 0.006 m/s, the lowest of all the tests.

The moving vehicle facility used by Otech Engineering in Davis, California, was a member of the ±0.5% majority. Figure 7 shows the RR2-16a test with a scatter (standard error of the Y estimate) of 0.043 m/s. This demonstrates that one can control the flow reasonably by moving through the air at different speeds, given careful selection of test periods and comprehensive flow measurement instrumentation.

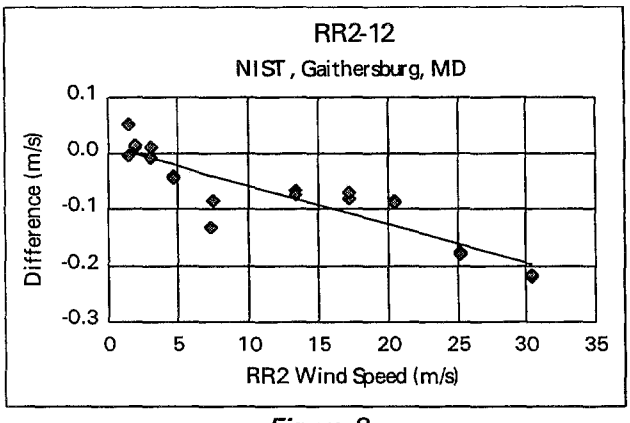

Figure 8

The RR2-12 test at NIST is shown in Figure 8. While it is not as non-linear as the cup calibration shown in Figure 3, it does have some of those characteristics. It clearly does not describe the helicoid propeller as the linear sensor that Figure 6 shows it to be. The scatter or standard error of the Y estimate is 0.035 m/s but the transfer function, when applied to 30 rps, finds a speed that is within ±0.05% of the ETP value.

4. UNCERTAINTY IN COLLOCATED COMPARISONS IN THE FREE ATMOSPHERE

4.1 USEPA Boulder Atmospheric Observatory Tests

Some measure of comparison will result from careful tests in the free atmosphere. There is a standard method of designing such tests. ASTM [3] has published the standard used in many such tests. Lockhart, 1989, [4] showed that the best likely agreement (standard deviation of the differences) in wind speed is ±0.2 m/s and wind direction is ±2°, with orientation bias removed. This conclusion was based on a month of field data in Boulder, CO, where 15-minute average values were collected from a small cup and vane and a vane oriented propeller. The standard deviation of the differences has all the calibration and mounting bias errors removed and addresses the simple question of data coming from slightly different locations being measured with different technologies.

The siting guidance in the ASTM standard states that the two sensors must be within a cylinder with a diameter of 10 m and a height which is the lesser of 1 m or one-tenth *H*, where *H* is the height above the earth's surface of the base of the volume. Operational comparability of the two instruments is the root mean square of the differences between simultaneous readings. The averaging time must be long enough to minimize the influence of the response distance or frequency response of the sensors. It should be short enough to provide a large sample size in a reasonable period of time. Five to 15-minute averages are common.

4.2 Lawrence Livermore National Laboratory Tests

In 1997 a series of data were collected from collocated sensors at 10 meters. A new 2-dimensional sonic anemometer (Handar 425) was mounted near a Met One Model 010C cup and 020C vane. This central California site has a high occurrence of light winds. There is a considerable difference in performance between a sonic anemometer and a cup and vane at threshold speeds. For this test (Gouveia and Lockhart, 1998) [5] a subset of data with speeds ≥2 m/s was used (3,208 15-minute pairs of averages).

The wind speed comparability was 0.11 m/s with a bias or systematic difference of -0.03 m/s. There was no significant calibration bias. The peak 1-second samples in each 15-minute sample did show a systematic difference of 0.3 m/s. The sonic was higher than the cup because of the cup's inertial response. The operational comparability of the peak 1-second speed was 0.5 m/s.

The wind direction had a -4° bias or systematic difference. This is likely an alignment difference. When the bias is removed, the operational comparability was 1.6°. Both speed and direction differences were smaller than the minimum differences found in Boulder.

5. DISCUSSION

There is an uncertainty in wind tunnel calibrations caused by inhomogeneity of the test section. Some wind tunnels test for this and find variations on the order of 0.5% to 1%. The pattern usually changes with wind speed to add to the confusion. This may be considered similar to the small differences in collocated sensor exposure caused by local bias.

There is another cause of uncertainty in wind tunnels depending on how they are used. When an object is installed in a test section the flow will be modified because of the presence of the object. The size of this blockage effect is dependent on the shape of the object and the relative sizes of the object and the wind tunnel test section. If mounting structures are aerodynamically shaped such that no turbulence is generated, the blockage effect can be nearly zero as compared to the projected area used. If the active element of the anemometer is a helicoid propeller, as it is with RR2, blockage is nearly zero because the propeller creates nearly zero turbulence. If the active element is a cup wheel, there will be some blockage since the active cup wheel creates a large turbulent wake. It is likely that the blockage will be smaller than the projected area of the cup wheel. Perhaps 50% of the projected area would be a good estimate.

The uncertainty of anemometer calibration is sensitive to the calibration strategy. Some wind tunnel calibrations use a transfer standard and essentially transfer the performance of a calibrated anemometer to an uncalibrated one. Either the transfer standard or the test anemometer is in the same location of the wind tunnel. Both are exactly the same design. Blockage effects are therefore effectively canceled. Other strategies use a transfer standard in the wind tunnel at the same time as the test anemometer. This may be another way to eliminate blockage effects. The most common strategy, however, uses a measure of speed at some monitoring location. The common measure is air pressure using pitot tubes and static ports. Unless the static pressure is measured in the plane of the test anemometer, the blockage of the test anemometer will not be sensed by the speed monitoring system. In this case a blockage correction is appropriate. There is a need for better information on how to estimate the blockage effect.

6. REFERENCES

[1] NEL, 1995: Recommendations on the Use and Calibration of Cup Anemometers. National Engineering Lab. National Wind Turbine Centre, 139/95, East Kilbride, Glasgow, Scotland, October, 58 pp.

[2] Lockhart, 1998: Relative Uncertainty in Wind Tunnel Calibrations. 10th Symposium on Meteorological Observations and Instrumentation. Phoenix, AZ, 11-16 January, pp 392-397.

[3] ASTM, 1996: Standard Practice for Determining the Operational Comparability of Meteorological Measurements D4430-96. American Society for Testing and Materials, 100 Barr Harbor Drive, West Conshohocken, PA 19428.

[4] Lockhart, 1989: Accuracy of the collocated transfer standard method for wind instrument auditing. *J. Atmos. Oceanic Technol.*, **6**, 715-723.

[5] Gouveia, F.J. and T.J. Lockhart, 1989: Comparison of In-situ Data from the Handar Sonic Anemometer and the Met One Cup and Vane. UCRL-JC-128469. 10th Symposium on Meteorological Observations and Instrumentation. Phoenix, AZ, 11-16 January, pp 237-242.

METEOROLOGICAL MEASUREMENT REPRESENTATIVITY, NEARBY OBSTACLES INFLUENCE

Michel Leroy (France)

Météo-France, BP202, 78195 Trappes, France
e_mail : michel.leroy@meteo.fr

1. INTRODUCTION

This document is dealing with in situ classical surface measurements (air temperature, humidity, precipitation, solar radiation, wind).
The World Meteorological Organization (WMO) has been stating guidelines for meteorological measurements for many years, in term of measurement uncertainty and exposure recommendations. All national meteorological services are issuing guidelines in accordance with these recommendations. But in real world, these rules are not systematically followed. When they are not, it is seldom said to the users and there is no real limit to the rules deviation. That is why a siting classification is proposed for documentation purpose. But first, go back to some quality matters.

2. QUALITY OF A MEASUREMENT

Quality is the ability to satisfy implicit or explicit needs. For meteorological measurements, this is often translated to a statement of operational accuracy requirements. Several factors have an influence on the « quality » of a measurement ; one can quote :

a) The intrinsic characteristics of sensors or measurement methods.
They are coming from technical specifications, emitted by technical services, users or manufacturers. These characteristics are commonly controlled, estimated from intercomparisons and are generally well known and mastered, at least for the classic measurements which we are dealing with. Météo-France has been traditionally dealing with this aspect.

b) The operations of maintenance (including calibration) needed to maintain the system in nominal conditions.
These operations are often expensive and necessitate a continuous effort. Preventive maintenance is the best guaranty to maintain a system close to its nominal performance, allowing final measurements close to the « intrinsic » performances of the sensor. Our experience shows that this maintenance is not always well mastered in case of a dense network.

c) The site representativity and therefore the measurement representativity.
This representativity is sometimes neglected, especially when the density of the network is increasing. The exposure rules are known by the people selecting a site, but numerous logistic constraints are existing. For money and availability considerations, the measurement system is often (at least in France) hosted on a site, not belonging to the owner (or the administrator) of the network. The access to the site, its supervision, the availability of telephone and power lines are important elements. These logistic aspects, and also the orography, may surpass the strict application of exposure rules, quite restricting, especially for wind measurements (10 times the height of nearby obstacles, which exclude nearby trees or buildings). A compromise is often selected. But when the rules are not applied, in lack of any gradation for these rules, there may be no limits. Who have not ever seen anemometers close to high trees, or even raingauges under a tree ! That exists !

3. SITE CLASSIFICATION

To take into account the existence of stations not respecting the WMO recommendations, a classification has been defined for each variable to document the representativity of a site. This classification ranges from 1 to 5. By convention, a class 1 site follows the WMO recommendations. A class 5 site is a site where nearby obstacles create an inappropriate environment for a meteorological measurement.
For some classes, an estimation of the associated errors or perturbations has been indicated. This estimation is coming from bibliographic studies and/or some comparative tests.
An abstract of the proposed classification is now presented.

3.1 Classification for temperature and humidity measurements

The screen (or more precisely the sensors inside the screen) should be installed at a standard height of 1.5 m (in France). The disturbing environment may consist of artificial heating sources or obstacles shading the screen. The relative importance of the perturbations associated to concrete surfaces and shading obstacles has still to be established. The following classes are therefore subject to further modifications.

Class 1

- Flat and horizontal ground, surrounded by a clearing surface with a slope below 1/3 (19°).
- Ground covered by grass or low vegetation (< 10 cm) representative of the area (and of it's albedo).
- Far from any artificial heating or reflecting source (buildings, concrete surfaces, parking, ...) which should be at a distance greater than 100 meters.
- Far from any water surface (except if representative of the area) which should be at a distance greater than 100 meters.
- No shading when the sun elevation is above 3°.

Class 2
See class 1 with the following differences
- Vegetation of height below 25 cm.
- No artificial heating source at a distance smaller than 30 m.
- No shading for a sun elevation above 5°.

Class 3 (error 1 K ?)
See class 2 with no artificial heating source at a distance smaller than 10 m.

Class 4 (error 2 K or more ?)
Artificial heating sources exist at a distance smaller than 10 m.

Class 5 (error 5 K or more ?)
The screen is located above an artificial heating source (by example, parking or concrete surface).

3.2 *Classification for precipitation measurements*

Wind is the major disturbing factor for precipitation measurements. The ideal siting conditions stated by WMO correspond to a place surrounded by uniform obstacles of regular height, such as a uniform clearing. Such a site is incompatible with the exposure constraints of the other meteorological variables. Therefore, these ideal siting conditions are commonly inapplicable. If the nearby obstacles are not uniform, they generate turbulence disturbing the measurements. That is why the more realistic exposure guidelines request to move away from perturbing obstacles.

Class 1
- Flat and horizontal ground, surrounded by a clearing surface with a slope below 1/3 (19°).
- Any obstacle must be located at a distance of at least 4 times the height of the obstacle, above the gauge.
- An obstacle is any object seen from the raingauge with an angular width of 10° or more.

Class2 (error 5% ?)
See class 1, but any obstacle must be located at a distance of at least 2 times its height.

Class 3 (error 10 to 20% ?)
- Ground with a slope below 1/2 (30°).
- Any obstacle must be located at a distance of at least its height.

Class 4 (error > 20% ?)
- Ground with a slope greater than 30°.
- Obstacles located at a distance less than their height.

Class 5 (error > 50% ?)
Obstacle overhanging the raingauge !

3.3 *Classification for wind measurements*

Wind measurements impose the more restricting conditions, with no obstacles at a distance of at least 10 times their height (WMO states that 10 times is an absolute minimum). Wind measurements are not only disturbed by nearby obstacles ; aerodynamic roughness has also an influence. For WMO, the surface wind is the wind at a standard 10 m height above an area with a roughness length of 0.03 m. This surface wind would be a reference wind with known and ideal environment conditions.
The proposed classification is therefore twofold. The first classification is dealing with surface aerodynamic roughness. The second one is dealing with the nearby environment and possible obstacles.

Roughness classification
Several authors (Davenport, Wieringa) have proposed a classification table from 1 to 8 for roughness length. A 0.03 m roughness is for an open flat terrain, with grass and few isolated obstacles. With a logarithmic profile, it is possible to estimate the relationship between winds above terrain of different roughness. So, a (common) terrain with numerous low obstacles (bushes, hurdles, ...) is a class 6, with a roughness length of about 0.5 m. The 10 m wind is then about 20% lower than the « potential » WMO wind above 0.03 m roughness terrain (class 3). More details may be found in bibliography, especially the last edition of doc. 8 WMO (known as the CIMO Guide).

Environment classification
The existence of obstacles nearly always lead to a decrease of the mean wind speed. Extreme values are generally also decreased, but not always. Obstacles increase turbulence and may lead to (random) temporary increase of instantaneous wind speed.
The following classes are considering a conventional 10 m measurement. When measurements are made at a 2 m height for agro-climatological needs, the same type of classification may be used, replacing 10 m heights by 2 m heights. This leads quite often to high rank classes and militates in favor of more representative 10 m measurements (which may be reduced to 2 m, using a logarithmic profile). When many obstacles are present, a WMO recommendation is to raise the wind sensors 10 m above these obstacles, to decrease their influence. This practice is seldom used in France.

Class 1
- The wind tower must be erected at a distance of at least 10 times the height of the nearby obstacles (therefore seen under an elevation angle below 5.7°)
- An object is considered as an obstacle if it is seen under an angular width greater than 10°.
- The obstacles must be below 5.5 m within a 100 m distance around the tower (and if possible be below 7 m within a 300 m distance).
- Obstacles with a height less than 2 meters may be neglected (but they participate to the roughness evaluation).
- The wind sensors must be located at a minimum distance of 15 times the width of thin nearby obstacles (mast, thin tree with angular width < 10°).
- A relief change within a 100 m radius is also considered as an obstacle.

Class 2 (error 10% ?)
- The wind tower must be erected at a distance of at least 10 times the height of the nearby obstacles.
- An object is considered as an obstacle if it is seen under an angular width greater than 10°.

- Obstacles with a height less than 3 meters may be neglected.
- The wind sensors must be located at a minimum distance of 15 times the width of thin nearby obstacles (mast, thin tree with angular width < 10°).
- A relief change within a 100 m radius is also considered as an obstacle.

Class 3 (error 20% ?)
- The wind tower must be erected at a distance of at least **5** times the height of the nearby obstacles (elevation angle < 11.3°)
- Obstacles with a height less than 4 meters may be neglected.
- A relief change within a 50 m radius is also considered as an obstacle.
- The wind sensors must be located at a minimum distance of 10 times the width of thin nearby obstacles.

Class 4 (error 30% ?)
- The wind tower must be erected at a distance of at least **2.5** times the height of the nearby obstacles (elevation angle < 21.8°)
- Obstacles with a height less than 6 meters may be neglected.
- There must not be obstacles with a height above 10 meters, seen with an angular width greater than 60°, within a 40 m radius.

Class 5 (error > 40% ?)
- Site non respecting the class 4 conditions.
- Obstacles with a height greater than 8 meters are existing within a 25 m radius.

4. CLASSIFICATION METHOD

The site classification is mainly based on the angular bearing of nearby obstacles. This plot may be quickly done with an optical theodolite. A high accuracy is not necessary. A 5° azimuth plot, with a 0.5° uncertainty should be acceptable. For wind classification, it is necessary to estimate the height and the distance of obstacles within 100 m (with the angular elevation, only one of these parameters is enough). Existing laser range finders allow an easy measurement. There is even laser binoculars with a magnetic compass incorporated, giving distance, elevation and azimuth within an numeric output, which may be connected to a computer.

5. EXAMPLE

A plot example is presented for the Trappes' synoptic station (WMO code 07145). This station is a class 4 site for wind measurements (with a roughness length of about 1 m), a class 2 for precipitation measurements. Nearby roads and parking lead to a class 3 for temperature measurements.

Comparisons have been done between the Trappes' station wind measurements and the wind measurements made from a class 2 10 m tower located at a 230 m distance. The mean wind speed of the class 4 Trappes' tower has been found 25% lower than the wind speed of this clearer tower.
When compared with a 100 m neighbor screen, located in an open grass field (class 2), the air temperature measured by the Trappes' station (class 3) have been found to be 0.7 K warmer, in presence of high solar radiation. The two screens are of the same model.
Both for wind and air temperature, these differences are in accordance with the above estimated errors, associated with some classes.

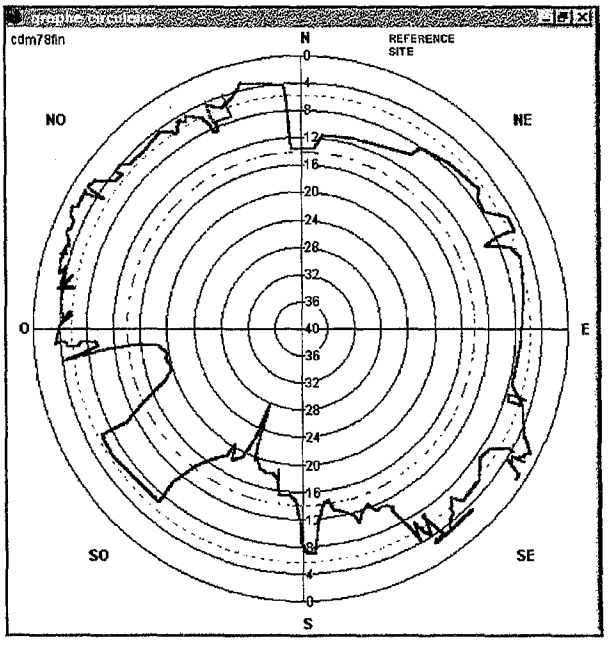

6. CONCLUSION

The measurement errors, associated to a site not respecting the usual exposure rules, are often much larger than the intrinsic uncertainty of the sensors. The site representativity is therefore the more important factor for the global quality of a measurement. The proposed classification allows to objectively document a site to inform users about the quality and how representative is a measure. This information may lead to a displacement or even a closure of a station. The classification of a potential site before a definitive choice should allow an objective choice, with a quantitative estimation of the site representativity.
To increase the quality insurance of its network, Météo-France has engaged the site documentation of its entire network (about 500 surface stations). This documentation will then be extended to all external stations (not belonging to Météo-France) from which Météo-France get and integrate data in climatological data bases.

The scientific base of this classification is not well established. Except for wind measurements (see bibliography), quite few publications were found dealing with this subject. Météo-France intend to deepen the subject, in particular for the temperature classification. Any suggestion or comment on this classification approach is welcomed and wished.
An analog classification for visual observation sites could be useful, in particular for visibility and cloud cover

This site classification approach would illustrate that some sites are not ideal, which may not be an usual official language. A WMO site classification would be interesting and would give valuable information to the users. It could be interpreted as an acceptation of non ideal siting situations, but would be, probably, a better image of the real world.

7. REFERENCES

WMO, Doc 8, 1996 : Guide des Instruments et Méthodes d'Observation.

Bowen A.J., Lindley D., 1977 : A wind-tunnel investigation of the wind speed and turbulence characteristics close to the ground over various escarpement shapes (Boundary-Layer Meteorology, 12, p. 259-271).

Ehinger J., 1993 : Siting and exposure of meteorological instruments (WMO, CIMO)

Frederick R.H., 1961 : A study of the effect of tree leaves on wind movement (Monthly Weather Review, 89, p. 39-44).

Fujita T.T., Wakimoto R.M., 1982 : Effects of miso- and mesoscale obstructions on PAM winds obtained during project NIMROD (Journal of Applied Meteorology, 21, p. 840-858).

Malet L., 1989 : Le vent dans les premières centaines de mètres (Institut Royal Météorologique de Belgique).

Rider N.E., 1952 : The effect of a hedge on the flow of air (Quarterly Journal of the Royal Meteorological Society, 78, 97-101).

Taylor P.A., Salmon J.R.,1993 : A model for the correction of surface wind data for sheltering by upwind obstacles (Journal of Applied Meteorology, 32, p. 1683-1694).

Van Eimer N J. (chairman), 1964 : Windbreaks and shelterbelts (World Meteorological Organization, Technical note n° 59, WMO n° 147).

Wieringa J., 1976 : An objective exposure correction method for average wind speeds measured at a sheltered location (Quarterly Journal of the Royal Meteorological Society, 102, p. 241-253).

Wieringa J., 1977 : Wind representativity due to an exposure correction, obtainable from past analog station wind records (World Meteorological Organization, WMO n° 480).

Wieringa J., 1983 : Description requirements for assessment of non-ideal wind stations (Journal of Wind Engineering and Industrial Aerodynamics, 11, p. 121-131).

Wieringa J, 1986 : Roughness-dependent geographical interpolation of surface wind speed averages (Quarterly Journal of the Royal Meteorological Society, 112, p. 867-889).

Wolfson M.M., Fujita T.T., 1989 : Correcting wind speed measurements for site obstructions (Journal of Atmospheric and Oceanic Technology, 6, p. 343-352).

SLTEST
A SURFACE LAYER TURBULENCE AND ENVIRONMENTAL SCIENCES TEST FACILITY

Christopher A. Biltoft
U.S. Army Dugway Proving Ground, Utah, USA

1. Introduction

The surface layer is the near-surface portion of the atmospheric boundary layer (ABL). It is characterized by high Reynolds number flows responding to the diurnal heat flux cycle and other large scale forcings that originate at the earth's surface. ABL flows feature temporal and spatial scales several orders of magnitude greater than comparable scales found in other boundary layers. The continuously varying fluxes of heat and momentum, directional shear and divergence fields, and complex surface roughness features in the surface layer make the ABL more complex than most "engineering" boundary layers found in pipes, channels, and wind tunnels. Thus, although laboratory flows can model some simple boundary layers, many important scales of motion found within the ABL are not correctly replicated in this way. Therefore, a requirement exists for a laboratory capable of producing flows over the entire range of scales found within the ABL. The Surface Layer Turbulence and Environmental Sciences Test (SLTEST) Facility is being developed at Dugway Proving Ground, Utah for this purpose.

2. Site Description

SLTEST is located on the Great Salt Lake Desert in western Utah (40° 8' N, 113° 26' W) approximately 150 km southwest of Salt Lake City. This site features a flat, undisturbed, vegetation-free surface with a slope of 1/10000 and an extended upwind fetch unobstructed by wake-generating obstacles. The lake bed surface becomes wet during the winter, and a new salt crust forms as water evaporates in the spring. This process produces a nearly uniform surface with a roughness length of less than 1 mm. Except during periods of high winds, this surface is free of micrometer-size dust particles that decalibrate hot-wire anemometer probes. When convection is not present, periods of predictable steady flow occur at SLTEST because there are few upwind terrain obstacles to induce wind meander. With a steady flow over its smooth unobstructed surface, SLTEST serves as a large open-air wind tunnel where high Reynolds number fluid dynamics experiments of geophysical interest can be conducted.

SLTEST infrastructure includes trailer platforms, electrical power service (60 Hz), and fiberoptic communications links to a centralized computer facility. When completed in 1998, these services will permit the continuous operation of on-site instrumentation and real-time display of data. SLTEST includes a staging area and equipment platform space for visiting researchers performing academic, commercial, and government-sponsored studies. Because it is located on a remote part of a secure installation, experiments can be conducted at SLTEST free of obstruction and tampering. Dugway Proving Ground is also capable of providing extensive logistical support.

3. SLTEST Facilities

SLTEST development began with a series of joint boundary layer studies that led to the establishment of a Cooperative Research and Development Agreement (CRDA) between Dugway Proving Ground (DPG), Utah State University (USU), and the University of Utah (U of U). The CRDA is designed to develop the SLTEST site and to enhance cooperative boundary layer study

programs. With the help of a National Science Foundation infrastructure grant and matching funds from USU and the U of U, SLTEST is becoming a permanent boundary layer measurement and research site.

Unlike other sites used for ABL measurements, SLTEST is designed for equipment to probe the entire ABL, ranging from the viscous sublayer to the outer regions of the convective mixed layer. To obtain measurements over such a range of scales, SLTEST includes the diverse collection of instrumentation shown in Figure 1. A radiation facility provides surface temperature and radiative balance. The Near Surface Turbulence Measurement Platform (NSTMP) enables flow visualizations and measurements to be made within the viscous sublayer and buffer layer. A 10-m tower supports sonic anemometer/ thermometers and atmospheric constituent flux probes. Remote sensing instrumentation will be used to probe the upper portions of the ABL. These include an Echosonde minisodar for detailed wind profile measurements to a height of 200 m above ground level and a 924 MHz wind profiling radar for wind profile measurements to the top of the boundary layer. The Frequency-Modulated Continuous Wave (FM-CW) radar provides vertical profiles of backscattered signal intensity that depicts ABL eddy structure with a resolution on the order of 2 meters.

4. SLTEST Studies

Data from SLTEST will contribute to improvements in our understanding of ABL processes and hence to improved micrometeorological models such as the subgrid scale parameterizations used in large eddy simulations. Although the entire SLTEST facility is not yet complete, several on-site studies have already been performed there. A consortium of university researchers have used an NSTMP prototype at SLTEST for near-surface measurements and flow visualization studies. These studies of Reynolds number and stability dependence in boundary layer flow are described by Klewicki et al., (1995); Klewicki and Metzger, (1996); and Folz, (1997). Biltoft (1997) also conducted tracer gas experiments at SLTEST to develop data sets for atmospheric dispersion model validation.

5. References

Biltoft, C.A., 1997: Phase 1 of Defense Special Weapons Agency transport and dispersion model validation. DPG-FR-97-058, U.S. Army Dugway Proving Ground, UT.

Folz, A. B., 1997: An experimental study of the near-surface turbulence in the atmospheric surface layer. Ph.D. Thesis, U. of MD, College Park, MD.

Klewicki, J.C., M. M. Metzger, E. Kelner, and E. M. Thurlow, 1995: Viscous sublayer flow visualizations at $R\theta \approx 1500000$. J. Fluid Mech., 219, 119-142.

Klewicki, J. C. and M. M. Metzger, 1996: Viscous wall region structure in high and low Reynolds number turbulent boundary layers. 27th AIAA Fluid Dynamics Conference, New Orleans, LA, American Institute of Aeronautics and Astronautics, 370 L,Enfant Promenade, S. W. Washington, D.C. 20024.

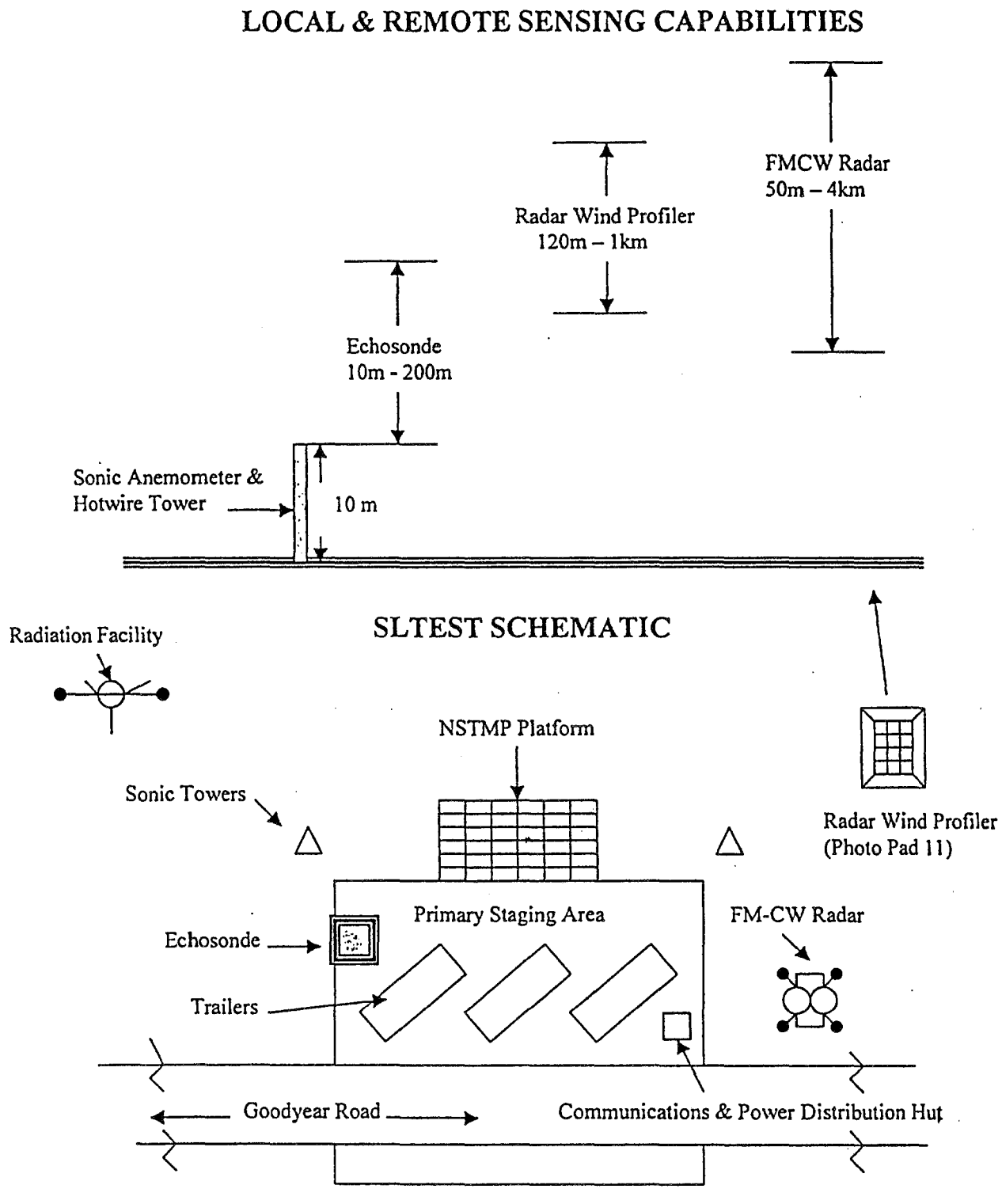

Figure 1. A schematic diagram of the SLTEST Facility (courtesy of Mr. Kam Liang, U. of Utah Department of Mechanical Engineering).

Session III

WIND PROFILERS

OPERATIONAL EXPERIENCE WITH A 1290 MHz WINDPROFILER/RASS AND COMPARISON WITH TOWER AND RADIOSONDE DATA.

Henk Klein Baltink and Wim Monna
Royal Netherlands Meteorological Institute (KNMI)
the Netherlands.

Introduction.

Since July 1994 a 1290 MHz LAP™-3000 windprofiler/RASS operates continously at a short distance from a 200 m high meteorological tower. The profiler and tower are located at the atmospheric research site of KNMI at Cabauw, the Netherlands (51°.58' N, 04°.55' E). The lowest range gates of the profiler/RASS overlap with tower measurements at 140 m and 200 m agl. respectively. Radiosondes (RS80-15N) are launched four times daily at station 'De Bilt' (06260), about 25 km north-east of Cabauw. The data from the three systems have been analysed over a long period to assess the accuracy of the profiler/RASS data. Comparisons of windprofiler data with radiosonde data have been performed numerous times. However, comparison with tower data is performed only during a few experiments and mostly only over a short period (Ye et al. 1993). The long-term tower intercomparison presented here is therefore rather unique as it extends over more than two years of continuous measurements.

One of the main applications of the KNMI's profiler/RASS is atmospheric boundary layer research i.e. to collect data for validation of parametrisations of boundary layer processes in climate models. But the profiler is also operated semi-operationally and wind and temperature data are transmitted in real-time to the weather forecast office at Schiphol Airport since October 1995. Furthermore, within the framework of the CWINDE97-project a BUFR-interface was written and since January 1997 the data are transmitted on the GTS as well and displayed on the CWINDE97-website by the UK-MetOffice. We will briefly discuss the characteristics of the 1290 MHz system and our experience with real-time operation. Thereafter we present some of the results of the intercomparison.

The 1290 MHz Windprofiler/RASS.

Fundamentally the 1290 MHz windprofiler is a pulsed Doppler radar. The system transmits sequentially in 5 different, fixed beam directions, i.e. one vertical and 4 orthogonal oblique directions 15.5° from zenith. The radar signals are backscattered by refractive index fluctuations of the atmosphere, commonly referred to as Bragg-scattering. Four different radar pulse lengths can be chosen, corresponding to a vertical range resolution of 60, 100, 200 or 400 m resp. The atmospheric return signal is sampled at equally-spaced time intervals, corresponding to equally-spaced sample heights (range gates) above the antenna. The time-series of the return echoes at each range gate are transformed to the spectral domain by a Fourier transformation. Next the strongest peak in the Doppler spectrum is determined. The mean radial velocity of each range gate is calculated from the first moment of the peak. Usually several spectra are averaged to obtain a sufficient large signal-to-noise (SNR). The typical time for a measurement in one direction (dwelltime) is about 20 sec. The total cycle time to measure one wind profile in low and high mode is a little less than 5 min. From the mean radial velocities of all 5 beams the vertical profiles of the wind speed, wind direction and vertical wind speed are calculated using a consensus averaging method (Carter et al. 1995). The averaging period used operationally at the KNMI is one hour, but shorter periods are also commonly used with similar systems.

Capability to measure the vertical profile of the virtual air temperature is easily added to the windprofiler. Four acoustic transmitters are placed around the profiler antenna, the combined system is a so-called Radio Acoustic Sounding System (RASS). The radar pulse transmitted by the profiler is reflected by the refractive index fluctuations caused by the acoustic energy, just as in naturally occurring turbulence. These fluctuations travel with the local acoustic speed plus the mean vertical wind speed. Therefore the propagation speed of the vertically transmitted acoustic waves can be measured with the profiler as well. A simple relation exits between acoustic speed and the virtual air temperature. Thus by measuring the acoustic speed a vertical profile of the virtual air temperature is obtained.

The windprofiler/RASS is an all-weather measuring system. The height coverage depends on the typical system characteristics (e.g. power-aperture product, pulse length, duty-cycle, etc.) and on the atmospheric conditions (e.g. turbulence, moisture gradients). Furthermore, clutter from either fixed (e.g.

towers) or moving (e.g. birds) objects can interfere with the measurements. Quality control of the data is needed to remove the disturbed measurements. The high temporal and spatial resolution of the data resolve many atmospheric features e.g. frontal passages,low-level jets and temperature inversions. Furthermore, during precipitation the fall-speed of the droplets can be measured. In some cases the mixing height of the convective boundary layer may be determined from the SNR-profile. In principle it is also possible to measure heat and momentum fluxes with a profiler/RASS, although sofar this was limited to some experimental studies and not performed operationally.

Operational experience.

The profiler is operated in wind mode and RASS mode alternately, i.e. each hour consists of 55 min. wind and 5 min. RASS measurements resp. The data are downloaded hourly to the KNMI main office through a modem connection. The hourly data are processed by a quality control program to remove outliers in the data.

The availability of profiler data has been fluctuating during the three years of operation. The system and data output are not monitored continuously, therefore failures can remain unnoticed for some time, also some down-time is needed for maintenance. Also we have experienced a number of interrupts due to software failures. No major hardware failures have been encountered so far. The monthly availability of hourly data is presented in fig. 1. The height coverage depends on the operating parameters selected, system characterictics and the atmospheric conditions. The monthly height coverage in 1997 for a range resolution of 400 m and 100 m is shown in fig. 2 and 3 resp. Note the low coverage in January when it was rather cold and dry in the Netherlands. The height coverage of the RASS is rather limited mainly due to the strong absorbtion of the acoustic waves at 3 kHz and to drifting of the acoustic waves out of the radar beam. Furthermore, to comply with environmental regulations the acoustic power was reduced in the evening and night from Jan. 1996 onwards. This limits the RASS coverage at night even more. Coverage for 1995 is presented in fig. 4 when the night-time acoustic power reduction had not been installed yet.

Comparison with tower data.

From Oct. 1994 up to Feb. 1997 data were collected from both the profiler/RASS and the tower. The comparison comprises two periods. The first period from Oct. 1994 up to Feb. 1996 during which the standard mean spectral averaging and a vertical resolution of 60 m was used. In the second period from Apr. 1996 up to Feb. 1997 the more advanced Intermittent Clutter Reduction (ICRA) algorithm and a 100 m vertical resolution was used. Examples of scatter plots for a subset of the data are presented in fig. 5 and 6. In general profiler wind speed and direction compare very well with the tower data, considering the differences in measuring methods. The standard deviation of wind speed difference is about 0.9 m/s and for wind direction about 10° for the first period at both 140 m and 200 m agl. For the second period we found a standard deviation of 1.2 m/s and 16° resp. However, if a small number of ground clutter contaminated data are ignored (about 2% of the dataset) the same values are found as for the first period. The RASS data also compare well (fig. 7). The RASS data show a small temperature dependence mainly due to some approximations in the retrieval algorithm (Klein Baltink 1998). The standard deviation of the difference is about 0.5° C.

Comparison with radiosonde data.

For the first period (Oct. 1994 - Jan. 1996) the results of the comparison with radiosonde data are presented in fig. 8,9 and 10. The data have been analysed for each of the four radiosonde launch times separately, but the difference was negligible. Again a good agreement is found, especially since radiosonde measurements are essentially point measurements in time, whereas the profiler measurements are hourly averaged. Furthermore the radiosonde data and profiler data are not collocated but measured at a distance apart. The windprofiler data from this period have been edited manually. Therefore contaminated data due e.g. to migrating birds have been removed. Bird contamination can be a problem in spring and autumn nights when huge number of birds migrate. The automatic quality control applied is not capable of detecting these contaminated data (Wilczak et al 1995). The increasing bias and standard deviation below 500 m agl. for the low mode of the profiler is most likely due to inaccuracy of the radiosonde data at these low heights.

The typical height dependent bias in the radiosonde-RASS temperature data was found in many other studies as well. Corrections for vertical speed, approximations in the retrieval algorithm and for range dependent backscatter

need to be applied before the accuracy of the RASS data as compared to radiosonde data can be assessed. These corrections haven't been applied yet to the data presented here.

Concluding remarks.

The 1290 MHz windprofiler/RASS has proven to be a versatile all-weather instrument. The system provides data with a high temporal and spatial resolution for wind and virtual temperature for both research and operational applications. The profiler/RASS data compare well with both tower and radiosonde data. Some improvements in data quality can be expected when new signal processing techniques will be applied. Recently some promising results have been obtained with wavelet transforms (Jordan et al. 1997), fuzzy logic and neural network type of profiler signal processing.

References.

Carter D.A., K.S. Gage, W.L. Ecklund, et al. 1995: Developments in UHF lower tropospheric wind profiling at NOAA's Aeronomy Laboratory, Radio Sci. 30, 977-1001.

Jordan J.R., R.J. Lataitis, D.A. Carter, 1997: Removing ground clutter and intermittent clutter contamination from wind profiler signals using wavelet transforms, J. Atm. Oceanic Techn. 14, 1280 - 1297.

Klein Baltink H., 1998: A long term intercomparison of windprofiler/RASS and tower measurements, accepted by: Meteorol. Zeitschr., N.F.

Wilczak J.M., R.G. Strauch, F.M. Ralph, et al. 1995: Contamination of wind profiler data by migrating birds: characteristics of corrupt bird data and potential solutions, 12, 449 - 467.

Ye J.P., D.E. Wolfe, J.E.Gaynor, D.C. Welsh, 1993: A detailed comparison between wind profiler and tower measurements, in: Preprints Eighth Symp. on Met. Obs. and Instrum., Anaheim, USA, January 17-22, 298-303.

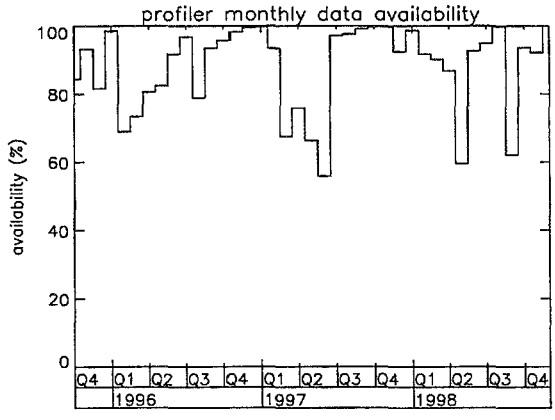

Fig. 1 Availability: Oct.94 - Dec.97

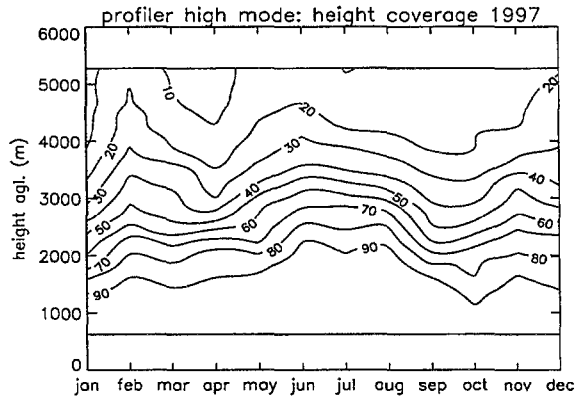

Fig. 2 Coverage (%), (400 m gate).

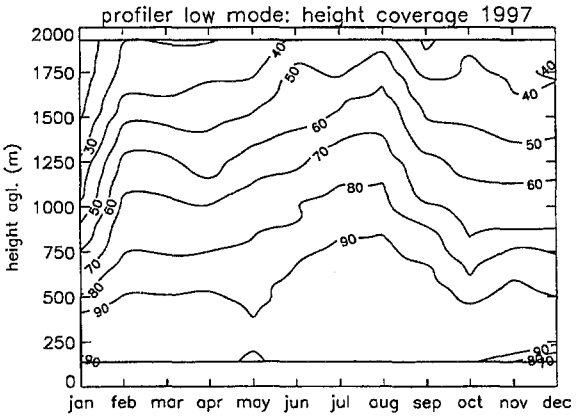

Fig. 3. Coverage (%), (100 m gate).

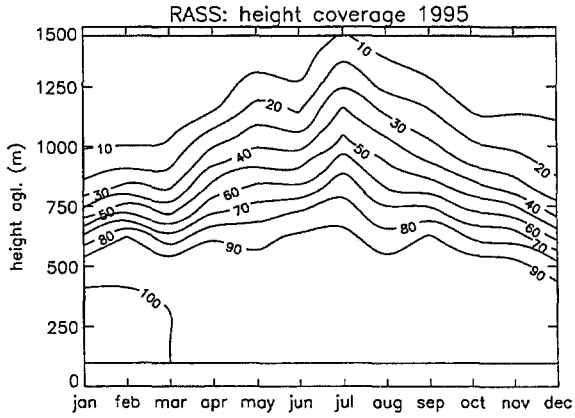

Fig. 4. Coverage (%), (100 m gate).

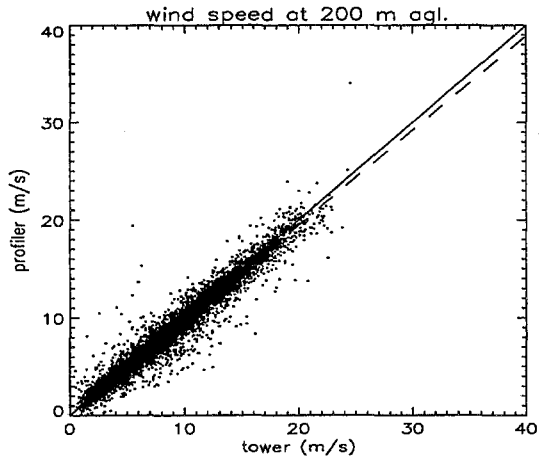

Fig. 5. Oct.94-Jan.96, (60 m gate)

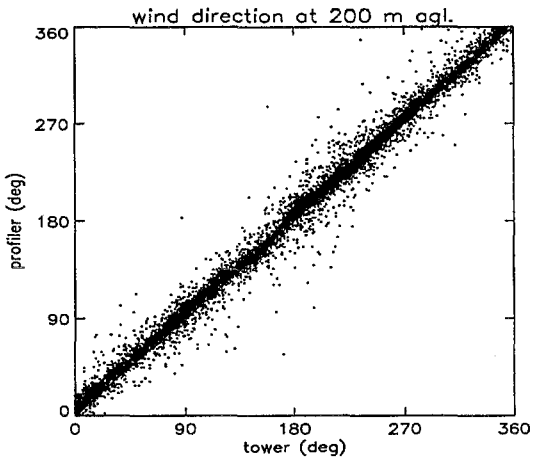

Fig. 6. Oct.94-Jan.96, (60 m gate).

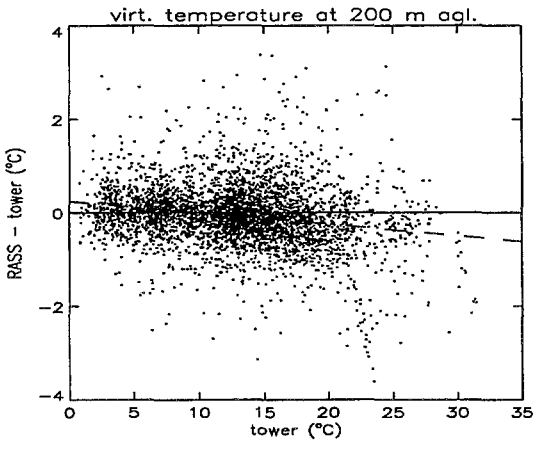

Fig. 7. Temp. difference Apr.96-Jan.97.

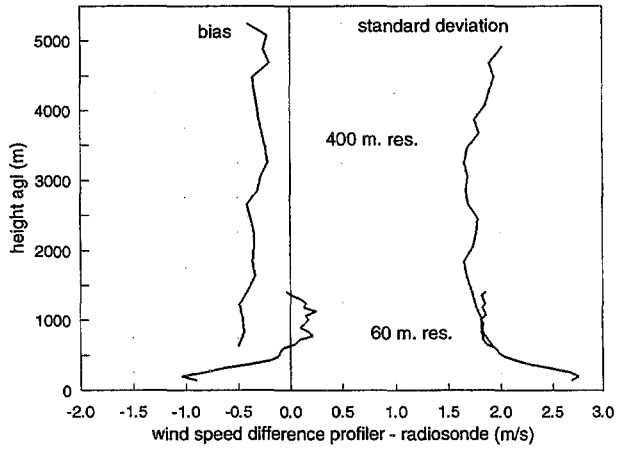

Fig. 8. Profiler-radiosonde: Oct.94-Jan.96.

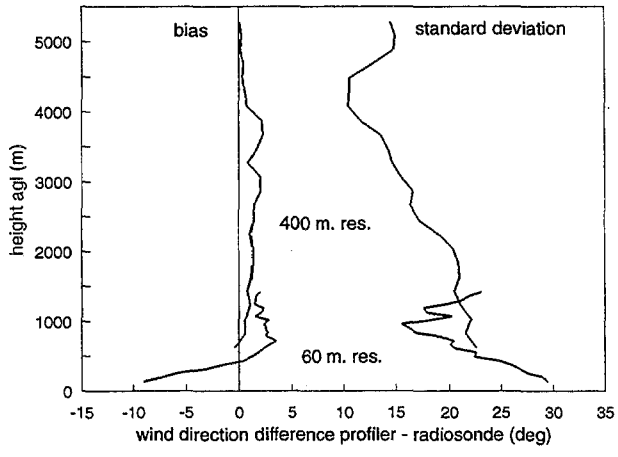

Fig. 9. Profiler-radsonde: Oct.94-Jan.96.

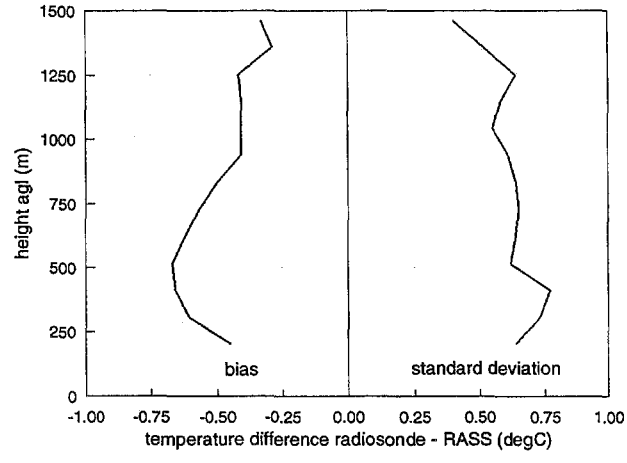

Fig. 10. Profiler-radsonde: Oct.94-Jan.96.

Experience of using a 915 MHz wind-profiler radar at Camborne, UK.

T. Oakley and J. Nash (UK Met Office.)

Introduction

The Met Office began using wind profilers in 1992 with the MST radar at Aberystwyth. The Aberystwyth radar provides essentially continuous coverage of horizontal wind speed and direction at 300m intervals from about 2.5 km up to 16 km. However, customers complained about the lack of wind measurements between the surface and about 2.5 km above the surface. The availability of aircraft wind measurements is increasing in Europe. The resolution in the horizontal of the observing network in the upper troposphere over the western parts of the British Isles has benefited, but there is little prospect of this happening in the lower troposphere given that most of the main busy airports are in central or eastern locations. The coverage of the network in the lower troposphere could be improved by the use of 1 GHz wind profilers .

A 915 MHz Radian Lower Atmosphere Wind Profiler (LAP-3000), was loaned for 3 months to the Met. Office and installed at Aberystwyth from January to March 1995. The LAP system produced reliable low level wind measurements in the stormy and wet wintertime conditions encountered in the western parts of the British Isles. During clear conditions at night with westerly winds, problems were encountered with birds migrating from Ireland to eastern Europe. A similar LAP-3000 wind-profiler radar was installed at (Camborne) in the south-west of the United Kingdom in late January 1997. This was in time to provide winds to the COST 76 CWINDE network demonstration . The main aims of this trial were:

- to monitor the long-term performance of the equipment (both hardware and software) in preparation for operational and research use in the UK.
- to evaluate the quality of the LAP measurements under a wider range of weather conditions than were encountered in the initial test at Aberystwyth.
- to provide initial information on the potential usefulness of low-level wind Profiler radar measurements in local and regional forecasts in the British Isles .
- to participate in CWINDE demonstration tests in collaboration with others in western Europe

Installation and System specification.

Setting up the LAP-3000 for operation took about 4 to 5 hours from unpacking the shipping crates and used about 4 people in total. The actual installation procedure was relatively simple, with little need for specialised tools. The LAP-3000 four panel antenna system is described as mobile. However a number of units, notably the antenna, were large and heavy when housed in their shipping crates. Therefore, although the Profiler may technically be considered mobile, allowance should be made for significant staff time and transport costs when costing short-term deployments of the radar.. The LAP profiler has been mostly operated without daily involvement of the Camborne staff. The 400 km separation from the UK Met Office HQ (Bracknell) has been used to evaluate the remote access software and simulate operating the equipment in a 'no-staff' environment

The LAP radar has a vertical beam and four off-vertical (23°) beams spaced in azimuth at a separation of 90°. The usual method of LAP operation is to use all 5 beams to calculate wind speed and direction, however the Camborne profiler was configured in a 3 beam mode. Tests in this mode during set-up provided measurements to satisfactory heights and without major failures in accuracy. The basic parameter set-up used is shown in Table 1. By operating with two modes interleaved the user obtains observations to larger heights with the larger pulse width, whilst retaining higher resolution near the surface with the shorter pulse length. However in interleaved mode, the amount of spectral data used to calculate wind measurements for each mode will be halved compared to single mode operation. This may prove a limitation , if measurements are required at high temporal resolution, 30 minutes or less, when backscattered signals are low. For real time operations it may be desirable for the mode of radar operation to be adjusted according to conditions to provide the information most critical to users.

Mode	Bandwidth	Height Resolution	Lowest Height	Highest Height	Time Resolution
Low	400ns	60 meters	198 meters	2500 meters	30 min.
High	1400ns	200 meters	198 meters	7000 meters	30 min.

Table 1 : Parameter set-up for Camborne LAP.

Data availability and height coverage.

A few days after setting up and testing the LAP , the final amplifier unit failed and had to be shipped back to the USA for repair. Table 2 gives details of the data availability of the system, once the repaired amplifier was installed on 20/02/98. The LAP was producing viable data for 73 % of the evaluation period. On some days one or two thirty minute samples were lost due to maintenance, software 'lock-ups' and reprocessing but these have not been included in the figures below. Continuous operation of the profiler was sustained for long periods, but when hardware faults have occurred substantial downtimes have resulted. It should be noted that the UPS unit providing the USA mains requirements was purchased for the Aberystwyth trial in 1994 and was not the responsibility of Radian. Radian had informed the UK Met Office of the possible failure of the phase-shifter, once a faulty batch of components had been traced to the system. Given the long repair times (4 - 6 weeks for shipping and repair), the purchase of system spares is critical if the LAP is going to be used for operational measurements. No significant operational problems were experienced with the software on the LAP system.

Description	Date	No. of days.	LAP Operating	Percentage of period.
Evaluation period	20/02/97 - 31/12/97	315	229	73 %
UPS failure.	15/05/97 - 05/06/97	22		7 %
Phase Shifter.	16/06/97 - 04/08/97	50		15 %
Final Amplifier	15/12/97 - 31/12/97	16 (Ongoing)		5 % +

Table 2 Impact of system failures on the availability of LAP measurements

Fig. 1 shows the monthly averages of the daily maximum and minimum height of the uppermost wind reports obtained in each mode. The heights appeared to improve once the phase shifter unit had been repaired. This requires further investigation, this may be related to variation in the number of significant weather events passing the site.

Time series analysis.

Fig. 2 shows a daily time-series plot of the LAP wind data used to assess the quality of the measurements. Camborne is an operational radiosonde station using Loran-C navaid radiosonde to measure winds with a Vaisala PC-CORA ground system. 4 radiosonde ascents are usually performed per day and the surface sensors provided useful reference measurements. On the day shown in Fig. 2, measurements from the radiosonde ascents were available every 3 hours. The time-series technique is useful for identifying gross errors (e.g. in the low mode data around 800 minutes). It also provides a consistency check between the high and low mode which is not always clear on the standard output from the Radian software. The radiosonde measurements show a general good agreement between the two systems although for the 400m level there are some larger differences and differences between the two LAP measurement modes that require further investigation.

Comparison with radiosonde wind measurements.

Fig. 3 shows a summary of profiler -radiosonde comparison statistics for March 97. The radiosonde data has been compared with the 30 minute profiler average centred at the same time (i.e. 0515Z R/S flight v 0500Z - 0530Z profiler). About 120 radiosonde ascents were compared with the profiler measurements, the actual number of flights used for each calculation is given at the bottom right of Fig. 3.

Figs 3 (a) and (b) show the average profiler -radiosonde difference for each wind component (u & v) and the standard deviation of the differences. Typically, bias in profiler measurements appears to be in range 0 to -1 ms^{-1} up to 5 km. Above 5 km the numbers of points used in the calculation drops significantly. Associated standard deviations are typically 1.6 ms^{-1} , suggesting an rms error in the profiler measurements slightly larger than 1 ms^{-1}. Figs 3(c) and (d) show the profiler-radiosonde differences in terms of wind direction and speed. The results are consistent with a direction bias of 1½° in the profiler measurements. This may be due to inaccurate measurements used for the beam orientation. Overall , comparisons with the radiosonde measurements for March 97 was very good with less than 1% of the profiler data being rejected due to large differences. Migrating birds did not cause a significant problem, but interference in the lowest range gates needed to be eliminated from time to time. Statistics for other months during the evaluation period will be calculated and an overall summary presented at the meeting.

Future Work.

The UK Met Office has now purchased the LAP system installed at Camborne. It is due to be upgraded to a 9-panel system and have new software (Win NT, 2000 compliant). Several case studies using the data obtained in CWINDE-97 are assessing the usefulness of profiler observations for forecasts and for forecast verification and scientific studies of severe weather. During 1998, the communications with the LAP system will be improved to provide reliable 'real-time' observations for local forecasters and for the mesoscale numerical weather prediction model.

Figure 1 : Height coverage of Camborne Wind Profiler : 1997

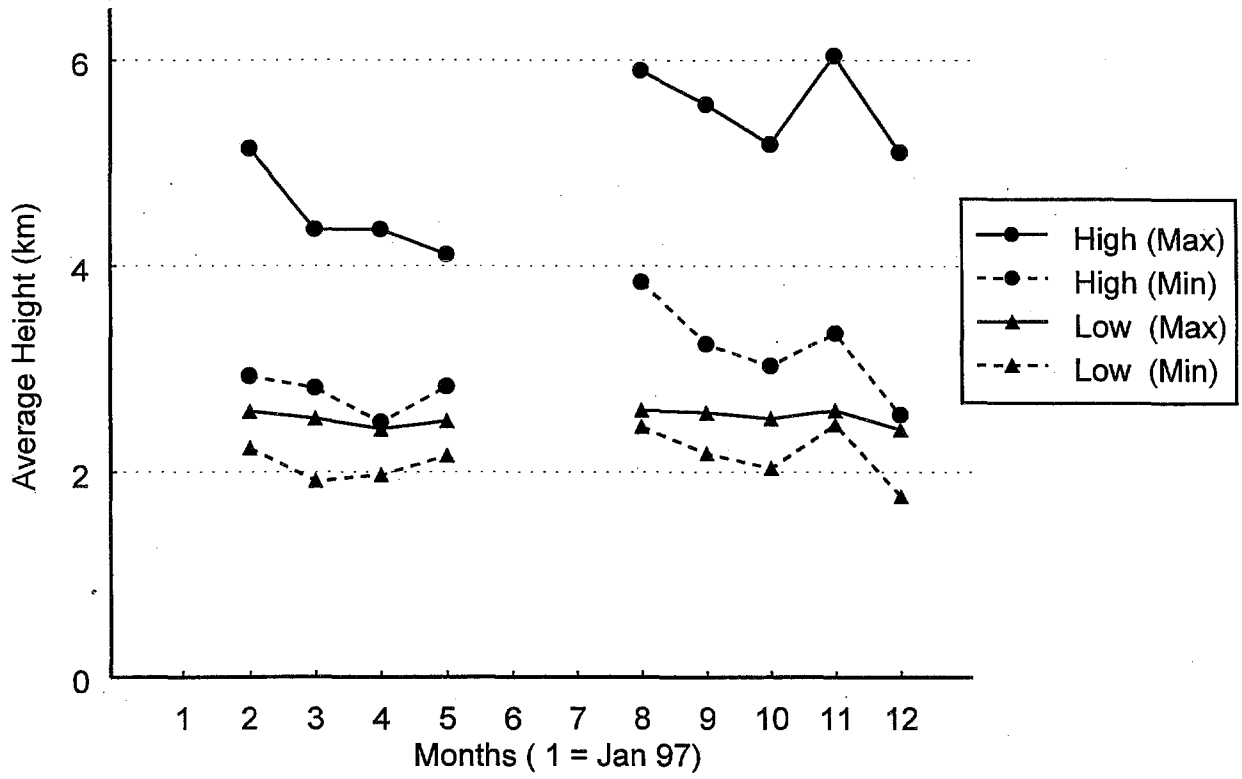

Figure 2 : Time Series Analysis Plot. : U - Component.

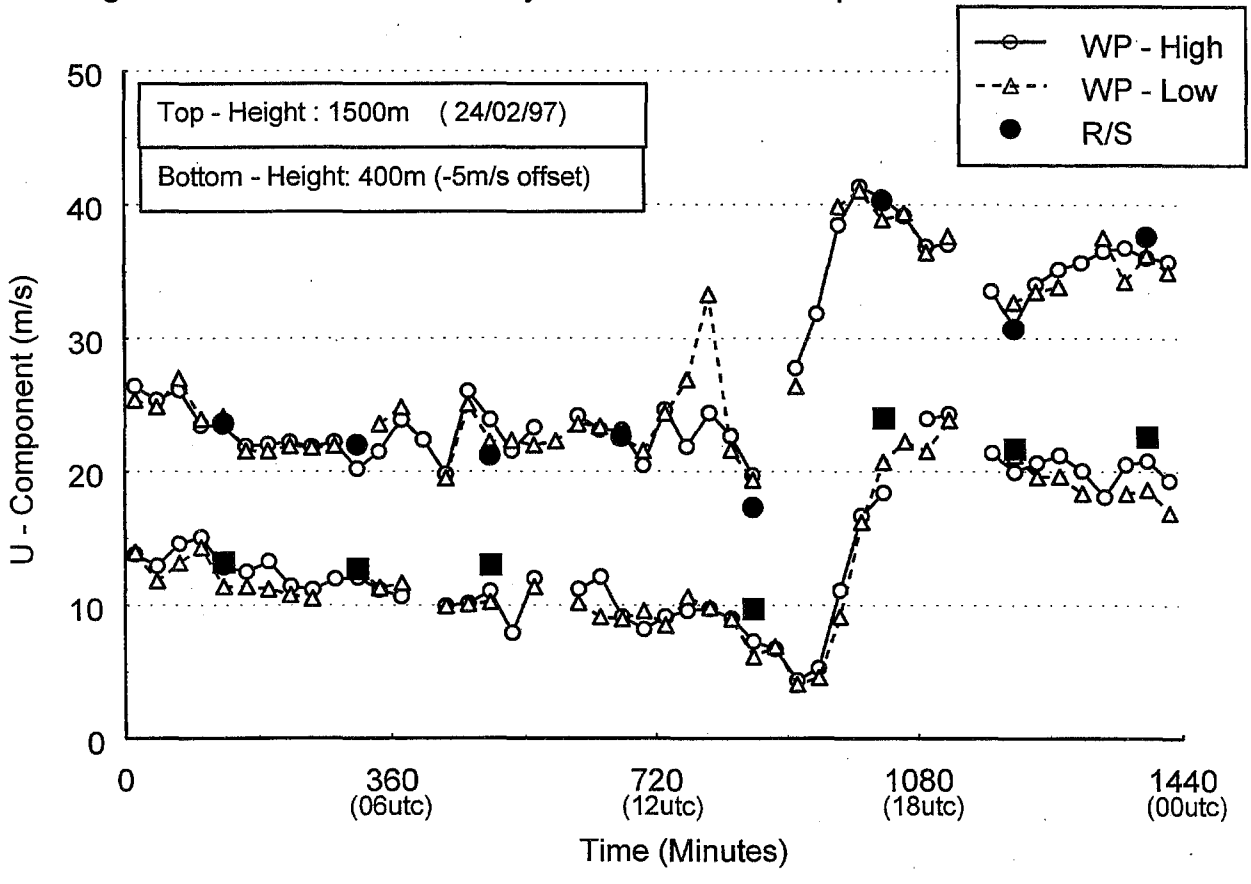

Figure 3 : Comparison of Wind-Profiler v Radiosonde Wind Measurments
Camborne, UK. March 1997

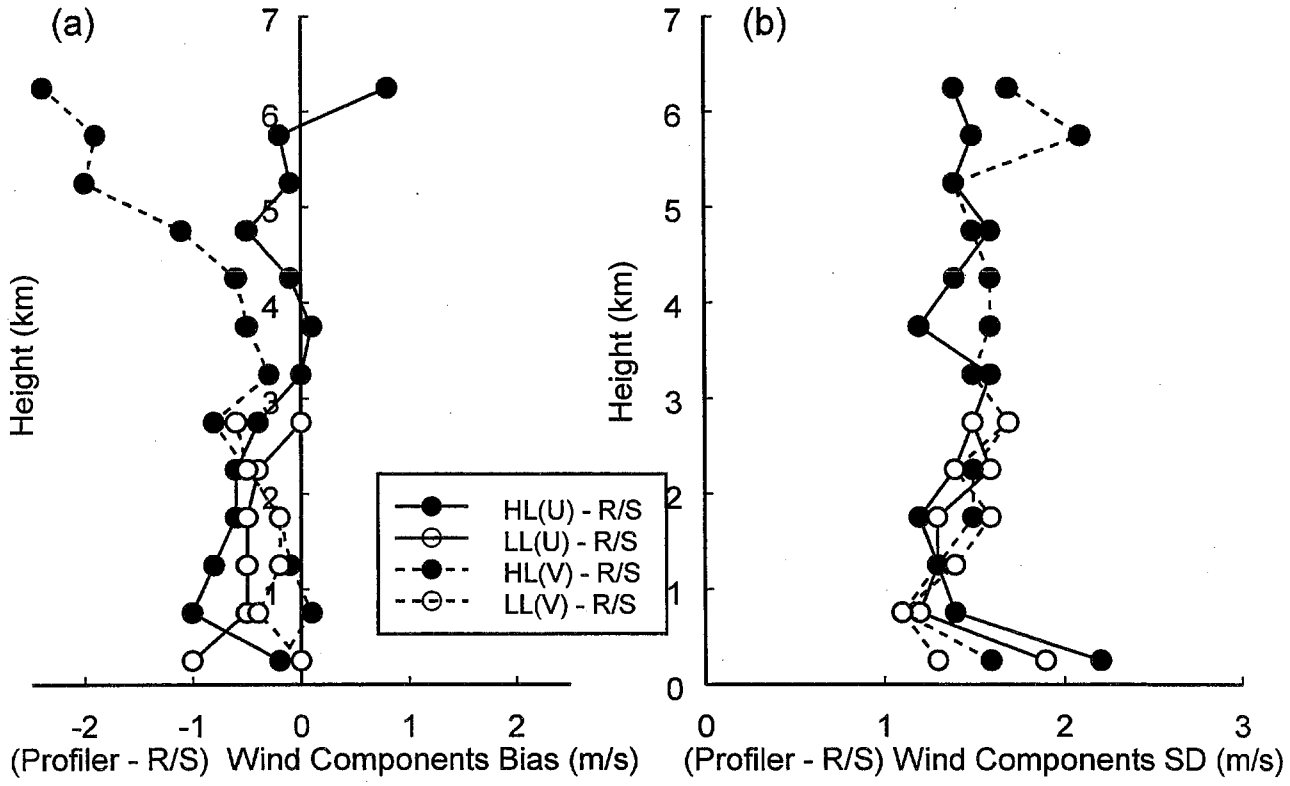

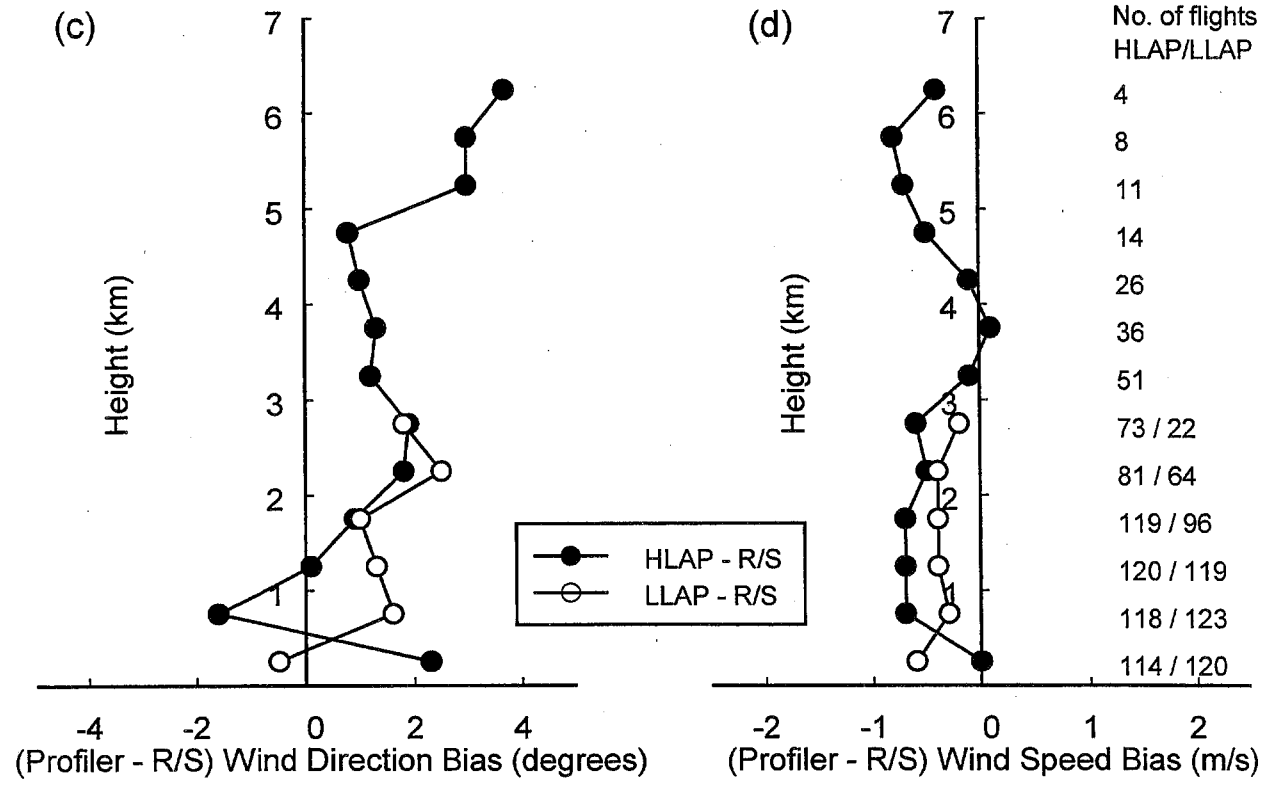

OPERATIONAL EXPERIENCES WITH THE 482 MHZ WIND PROFILER RADAR/RASS IN THE GERMAN METEOROLOGICAL SERVICE

J.Dibbern[1], H.Steinhagen[2], and U.Görsdorf[2]

[1]Deutscher Wetterdienst, Frankfurterstr.135, D-63067 Offenbach(M);Germany;
[2]DWD,Meteorologisches Observatorium Lindenberg, D-15864 Lindenberg; Germany;

0 Abstract

A 482 MHz Wind Profiler Radar (WPR) with a Radio-Acoustic Sounding System (RASS) has been operated at the Meteorological Observatory Lindenberg since July 1996. The WPR can operate with different height and time resolutions in the height range from 0.5 up to approximately 16 km. The installed WPR/RASS combination allows also the measurement of profiles of the virtual temperature with the Low Mode resolution in the height range from 500 m up to approximately 4000 m.
The objectives of this paper are investigations of availability, accuracy, and reliability of the WPR/RASS based on operational measurements during 1997. Nearly 22000 profiles of wind and temperature were used for the statistical analysis on data availability. An estimation of the accuracy can be given on the base of about 1300 comparisons between WPR/RASS and Rawinsonde data. Concerning the system reliability, the suitability for operational use could be proved.

1 Introduction

Wind Profiler Radars (WPR), operating in the frequency band near 400 MHz, are useful devices to measure vertical wind profiles from 0.5 km up to 16 km with high temporal and vertical resolution. The use of this new real-time information can improve the numerical weather predictions as well as nowcasts (NOAA, 1994) due to the ability of WPRs to provide information about the temporal and spatial wind field structure of passing weather systems ranging down to Micro-α, e.g. fronts, short-wave troughs, squall lines, wind shears, and others (Smith and Benjamin, 1993).
The application of 400 MHz WPR in Europe turned out to be a difficult problem considering this crowded frequency band (Richner,1994). To solve this problem, it has been proposed to use a television (TV) channel (22 or 21 respectively) for WPRs (Wolko,1997). So, the opportunity was given to operate a 482 MHz WPR in Germany on the base of an experimental frequency allocation to investigate the use of this new technology in the German Meteorological Service.
The comprehensive assessment of the 482 MHz WPR system in view of height availability, accuracy, and reliability under operational conditions at the Meteorological Observatory Lindenberg was planned to be a first step. Then, the rawinsonde network of the German Meteorological Service will be complemented by some WPRs in future. In this way, WPRs play an important role in the framework of a future effective composite upper-air observing network of the German Weather Service (Dibbern,1997).
The 482 MHz WPR/RASS has been operated at the Meteorological Observatory Lindenberg since July 3rd, 1996. Here, we want to present the system characteristics as well as results regarding availability, accuracy, and reliability, obtained from measurements during 1997.

2 Characteristics of the 482 MHz WPR/RASS

The 482 MHz WPR operates unattended and provides continuously real-time atmospheric wind data. The WPR generates radar pulses sequentially in up to 5 different directions (vertical and 15° tilted beams) transmitted by a phased array antenna, and evaluates the backscattered signals by determination of the Doppler shift.
The WPR operates normally in an averaging period of 50 minutes to get one complete wind profile with two complementary vertical resolutions of 250 m in the Low Mode for the height range of 0.5 -8 km and of 500 m in the High Mode for the height range of 3 - 16 km respectively.
Components of the 482 MHz WPR are a phased array antenna (aperture 140 m^2) with clutter fence, transmitter (peak power 16 kW), receiver, radar computer, gateway computer, and system components for a Radio-Acoustic-Sounding-System (RASS) to measure temperature profiles.
The WPR antenna is a coaxial-collinear phased array with 120 antenna elements and a phase shifter to tilt the electromagnetic beam into up to five linear independent directions e.g. north, south, west, and east with an elevation angle of 75° and also vertical. The antenna elements are arranged above a ground sheet of 13 m * 13 m in two planes. The one-axis antenna gain is greater than 35 dBi.

In order to avoid interferences with the TV channel and also ground clutter echos from trees or other obstacles, a special clutter fence has been arranged around the WPR antenna (Steinhagen and Frye,1997). Fieldstrength measurements around the antenna without and with clutter fence showed a decrease by about 14 dB. It could be demonstrated that WPR can be operated in a TV channel and that a TV reception of the same channel is possible even in the near field of the WPR antenna.
The transmitter is a multistage system with a pulse shaper to minimize the occupied bandwidth and a linear television amplifier. To separate the transmit and receive channel, a passive ferrite circulator is used. After down-conversion and A/D- conversion, the digital receiving signals get to the radar computer to compute the power spectrum, the noise level, and the first 3 moments (power, radial velocity, and spectral width) of the spectrum. A spectral averaging is applied to improve the detectability of the Doppler peak. The dwell time for producing one averaged spectrum for every range gate of one beam is approximately 20 - 40 seconds depending on the selected processing parameters. Mean wind values for the 50 min period are calculated by consensus averaging of the radial velocities (1. moments).
The calculated wind and temperature profile data are transmitted to the gateway computer via an optical cable for further data handlings, like quality control check (Weber and Wuertz, 1991), displaying and archiving the measured profiles of meteorological data. The hourly messages of wind and temperature profiles (the so-called BUFR format data) are sent to the computer center of the German Meteorological Service in Offenbach/Main and from there to various users, like the UK Meteorological Office in Bracknell, where the data are available on a World- Wide-Web server.
To complete the 482 MHz WPR with a Bragg RASS, four acoustic sources are arranged around the WPR antenna to generate a pattern of sound pressure waves in the atmosphere for the measurement of virtual temperature. The determination of the virtual temperature occurs on the basis of the connection between speed of sound and virtual temperature (Görsdorf,1997). The RASS measurements are carried out with a vertical resolution of 250 m and a vertical spacing of 120 m in the range of 0,5 to 4 km for an averaging period of ten minutes each hour.

3 Availability of Wind and Temperature measurements

For the future operational use of WPR data in the numerical weather prediction, the availability of wind and temperature measurements in the different height levels is an important question. Therefore, we calculated the Quality Control Pass Rate, defined as the percentage ratio of the number of valid measurements, passing the consensus averaging as well as the quality control algorithm (Weber and Wuertz,1991), to the total number of measurements for each range gate over the whole observation time, using hourly averaged measurements exclusively. Periods of hardware failures and special measurements are excluded from the statistics.
Considering the time period of 1997, we get a quality control pass rate of more than 80% up to a height range of about 9.5 km in the wind High Mode (500 m res.; Fig.1 left), 7.8 km in the wind Low Mode (250 m res.; Fig. 1, middle), and 2.3 km in the RASS mode (250 m res.; 120 m vertical spacing; Fig. 1; right).

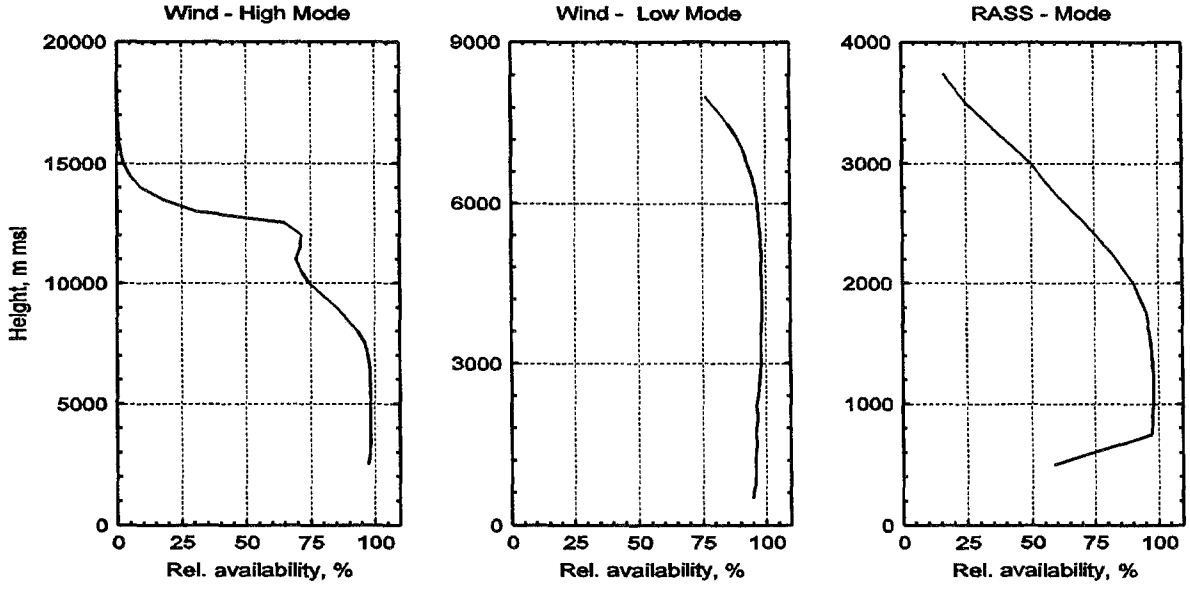

Figure 1: Relative availability of wind measurements in High and Low Mode (left and middle, respectively) and temperature measurements (right) with the 482 MHz WPR/RASS for the time period 1997;

The height coverage in the wind High Mode was higher in the first than in the second half year. So, a 80 % availability of 13.8 km has been obtained for January and February 1997. As cause for this decrease, some faulty antenna elements have been found out and must be exchanged soon. To fulfil the requirements of the operational use with a 80 % availability up to 16 km, an higher power-aperture product will be necessary.

4 Comparisons with rawinsonde measurements

Rawinsonde measurements represent the reference for newly developed sounding technologies to assess the consistency of new measurements in an operational network. The Meteorological Observatory Lindenberg is a very suitable site for comparisons of the 482 MHz WPR/RASS and rawinsonde measurements because radiosoundings with the Vaisala RS 80 and a tracking radar for wind measurements are performed routinely with 4 launches per day. Here, we present results obtained 1997.

Fig. 2 shows the bias and the standard deviation of the wind velocity in the High and Low Mode (Figure 2, left and middle, respectively). The bias of the wind measurement is less than 1.0 m/s in the whole probing range for both wind modes. Especially in the Low Mode (Fig.2, middle), we found excellent agreement with a bias of less than 0,4 m/s at the range from 0.5 to 8.0 km. The bias is slightly larger in the High Mode and changes sign near the tropopause level. So, we noticed in the High Mode an underrestimation of the wind velocity up to 0.5 m/s below 10 km and an overerestimation up to 1.0 m/s above 10 km (Fig.2, left). Therefore, the system delays, used for the different pulse lengths, have been checked. As a result, differences have been found out between the adjusted and the measured system delays which led to a range time sampling error. If we correct this range error, a smaller underestimation of about 0.2 to 0.5 m/s remains near the tropopause, where the wind speed is maximum. The remaining bias could be caused by the weighting of the wind velocity within the scattering volume with the vertical profile of reflectivity. This effect is proportional to the height resolution. Yet, a correction of this error has to be developed and checked before using this 482 MHz WPR in an operational network.

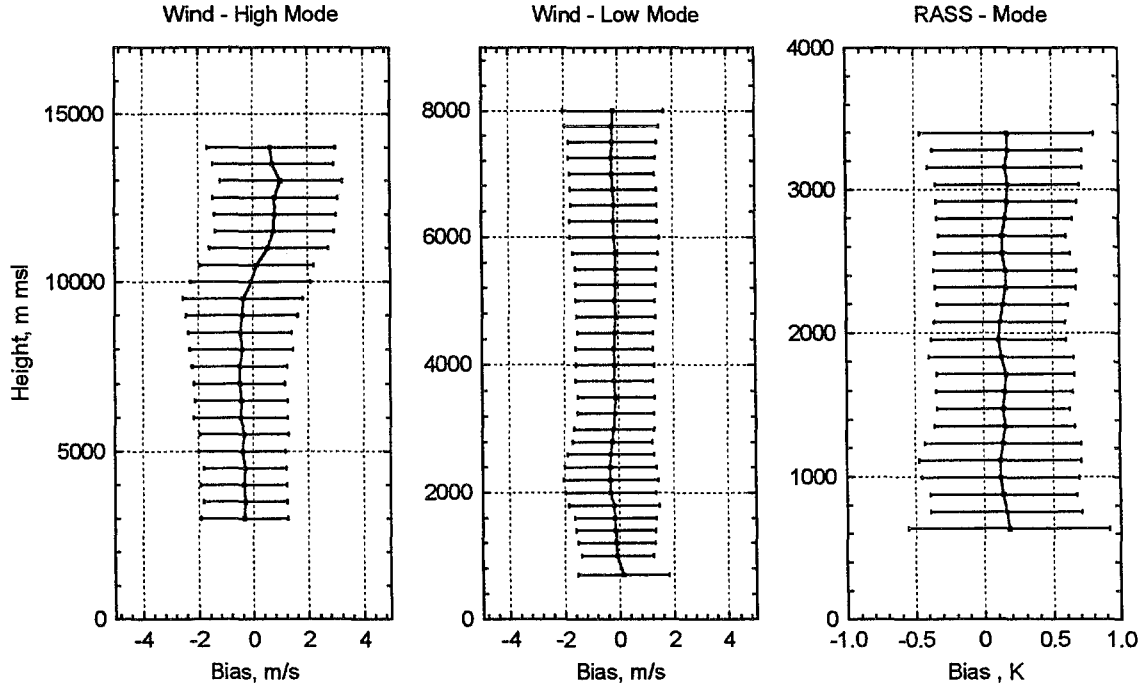

Figure 2: Mean differences (WPR/RASS-Rawinsonde) and standard deviation (horizontal bars) of the horizontal wind velocity in the High Mode with a resolution of 500 m (left), in the Low Mode with a resolution of 250 m (middle), and of the virtual temperature with a resolution of 250 m and a vertical spacing of 120 m for the time period of January to December 1997. The statistics is based on about 1300 rawinsonde measurements compared with hourly averaged wind profiler measurements during the rawinsonde ascents.

The comparison of 482 MHz WPR/RASS and rawinsonde measurements shows an overestimation of the RASS temperature to about 1 K without any corrections. A newly developed algorithm to correct influences of the vertical wind velocity, the variability of the constants in the temperature retrieval equation as well as variations of the acoustic signal intensity reduced this overestimation up to 0.2 K (Fig. 2; right), (Görsdorf,1997).

5 System reliability

Table 1 gives an overview about the system reliability of the 482 MHz WPR/RASS. The high percentage of missing BUFR messages was caused by the newly developed BUFR software which was still in a test phase as well as transmission problems. This high value isn't a special WPR problem and can be avoided by improvements of the BUFR software. The missing hourly measurements were caused by hardware (7.1%; one transmitter breakdown in the guarantee period) and software breakdowns (1%), realization of special WPR/RASS measurements (2.9%), maintenance (2%), and the necessity to switch out the WPR during the construction work of the clutter fence (0.8%). Note that these results were obtained only few month after switching on the WPR. In view of the operational use in an observing network, an essentially reduced number of missing measurements should be feasible by improvements in the automatic data communication as well as a higher reliability of all WPR components.

	Number	Percentage
Maximum possible hourly measurements (Wind High and Low Mode; RASS Mode)	**26 280**	**100 %**
Generated hourly measurements	**22 647**	**86.2 %**
Real-time transmitted hourly BUFR messages	**16 189**	**61.6 %**
Missing hourly measurements	**3 633**	**13.8 %**
Missing hourly BUFR messages	**6 458**	**23.6 %**

Table 1: Reliability statistics for the 482 MHz WPR/RASS from January 1 to December 31, 1997

6 Conclusion

The first 482 MHz WPR in Europe completed with RASS operates successfully under operational conditions at the Meteorological Observatory Lindenberg, sampling wind data in the height range of 0.5 to 16 km and temperature data from 0.5 to 4 km. During 1997, the estimated 80 % availability was 9.5 km in the wind mode and 2.3 km in the RASS mode. Comparing WPR/RASS and rawinsonde measurements the bias is lower than 0.4 m/s in the wind Low Mode, 1.0 m/s in the wind High Mode, and 0.2 K in the RASS Mode.

The 482 MHz WPR/RASS is a powerful system for operational use in European Observing Systems due to the time averaging with adjustable time resolution typically from 10 to 60 minutes, the unattended system operation, and the possibility to receive additional information like backscattered power, spectral width, and also turbulence parameters.

The effectiveness of the operational use in national weather services depends on the solution of some problems, like the increase of the height coverage, the avoidance of the influence of "fliers" (e.g. migrating birds, airplanes) as well as ground clutter on the measurement by newly developed signal processing algorithms, and the development of a real-time quality control with efficient performance adapted to the different meteorological conditions. Evaluating the results obtained by the operational system test at the Meteorological Observatory, the 482 MHz WPR/RASS will be an essential part of the future effective composite upper-air observing network of the German Meteorological Service.

7 References

Dibbern,J., 1997: Requirements on a Composite Upper-Air Observing Network of the Deutscher Wetterdienst, COST-76 Profiler Workshop, May 12-16, 1997, Engelberg, Switzerland, Extended Abstracts, vol. II, 366-368.

Görsdorf,U., 1997: About the accuracy of temperature measurements with RASS; COST-76 Profiler Workshop, May 12-16, 1997, Engelberg, Switzerland, Extended Abstracts, vol. II, 231-234.

NOAA, 1994: Wind Profiler Assessment Report and Recommendations for future use; NOAA, Silver Spring, Maryland, 141 p.

Richner,H., 1994: The struggle for frequencies for the operation of European Wind Profiler; COST 74 Final Report EUR 15450; 143-154.

Smith,T.L., and S.G.Benjamin, 1993: Impact of Network Wind Profiler Data on a 3-h Data Assimilation System; Bull. Am. Met. Soc., vol. 74, no. 5, 801-807.

Steinhagen,H., and A.Frye, 1997: Configuration and effectiveness of clutter fences for 482 MHz Wind Profiler Radar; COST-76 Profiler Workshop, May 12-16, 1997, Engelberg, Switzerland, Extended Abstracts, vol. 1, 35-38.

Weber,B.L., and D.B.Wuertz, 1991: Quality control algorithm for profiler measurements of wind and RASS temperatures. - NOAA Techn. Memo: ERL WPL, 212 p.

Wolko,B.-D., 1997: Frequency and sharing aspects of wind profiler radars; COST-76 Profiler Workshop, May 12-16, 1997, Engelberg, Switzerland, Extended Abstracts, vol. I, 43-48.

Session IV

REMOTE SENSING

MOROCCAN WEATHER RADAR NETWORK

Mohammed NBOU & Noureddine FILALI BOUBRAHMI
Centre National de Recherches Météorologiques/Direction de la Météorologie Nationale , MAROC

ABSTRACT:

Since the end of 1995, the National Meteorological Service is equipped with an operational Doppler weather radars network which meets some forecasters and hydrological needs. The goals of this network are the detection and identification , in real time, of severe storms related to convectives situations, the instantaneous evaluation of the spatial coverage of precipitation.
The goal of this paper is to give an idea about technical aspect of the radars network and some examples of operational applications.

I. INTRODUCTION

As part of its extensive modernisation program (CRAY supercomputers, Mesoscal model Al Bachir, Workstations, etc.) ; the National Meteorological Service set up at the end of 1995, a meteorological Doppler Radar network to better accomplish its mission of providing early detection and timely warnings of severe weather such as thunderstorms.
This network makes use of five new generation Doppler Radar (Doppler Weather Surveillance Radar 92C) operating in the C band (5.4cm) located in Agadir, Casablanca, Khouribga, Larache, Fez. The Radar located in Fez has the particularity of including the polarimetric technique, useful for detecting hail, which is a real menace in this area.
All of the network's observations are transmitted to the central site through dedicated line connections, where a composite picture is made every 10 minutes. The forecasters use intensively the radar image for the nowcasting and hydrological purposes. Here the most important features of the network, and some operational examples including convective cell producing flash flood and frontal situation are presented.

II.TECHNICAL FEATURES OF THE RADAR NETWORK

2.1 Spatial coverage

The Moroccan radar network is relatively dense, and provide a good quality of data at low antenna elevation angle over the most part of the north of the country. Although each radar makes measurements out to a range of 200 km, the density of radar is such (see figure 1) that is not necessary to use the data from extreme range over much of composite area. Overlapping from adjacent radar reduce certain problems linked to attenuating the wave (C band) , anomalous propagation, and to the « cone of silence » .

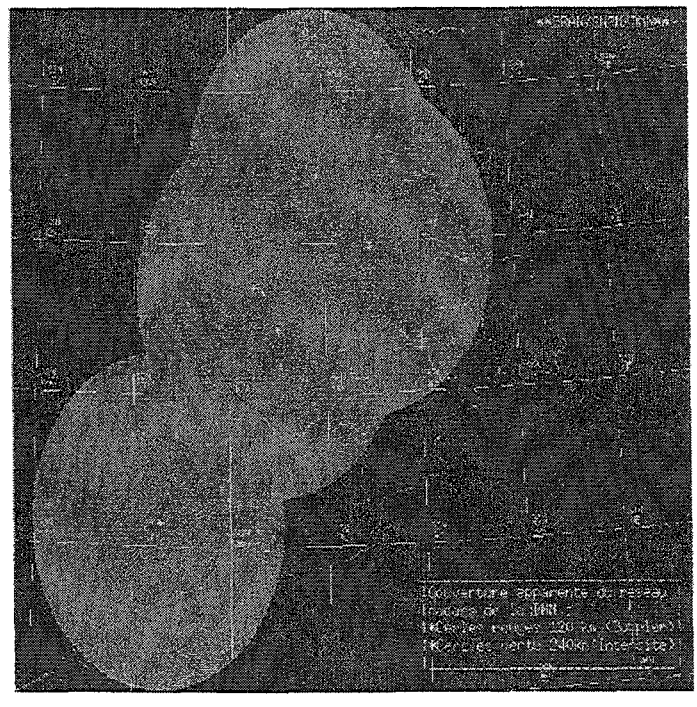

figure 1 : Spatial coverage of the radar network

2.2 Data acquisition : DWSR 92 C

2.2.1 Technical characteristics

Some of the important characteristics of the DWSR 92-C are given in table 1. Performance factors of the DWSR 92-C , i.e., sensitivity, accuracy, resolution and antenna rotation speed make it a good tool for both weather surveillance and warning ; this performance factors are also comparable to those of research radar.

Pedestal Technical Characteristics	
Azimuth movement :	
Azimuth Rate	variable from 0 to 36 °/s
Azimuth Accuracy	0.2 degrees
Elevation movement:	
Upper limit/ Lower limit	+90 / -1 degree
elevation Position accuracy	0.2 degrees
Antenna Technical Characteristics	
Type	Hornfeed into parabolic surface reflector
Diameter	4.2 meter (14 feet)
Gain	44 dB
Beamwidth	0.95 degrees at 5600 MHz measured at -3dB pints
Polarisation	linear horizontal
Sidelobes	22 dB down from the main lobe out 12 degrees on either side of the main lobe; 34 dB down beyond 12 degrees either side of the main lobe.
Transmitter Technical Characteristics	
Transmitter Frequency	tuneable over the range of 5500 to 5650 MHz
Peak Power	250 kW
Pulse Width : Intensity	2.0μ Sec
Velocity	0.8 μSec
PRF : Intensity	250 pulse/second
Velocity	1180 pulse/second
Receiver Technical Characteristics	
RF frequency	5500 to 5650 MHz
Amplifiers	logarithmic and linear
Sensitivity (MDS)	-108 dBm
Dynamic Range :Log receiver	80 dB
Linear receiver	26 dB to 80 dB

Table 1 . Technical characteristics of the DWSR 92-C

2.2.2 Signal processing

The Digital Processing of the Radar Signal is performed by the RVP5 (Radar Video Processor) that is built on a single circuit card. the processor forms the interface between the radar and the display ,sampling the received signal, deriving various parameters such as clutter corrected reflectivity, mean velocity and spectral width. To improve the accuracy of the reflectivity measurements, the RVP-5 performs range averaging of the logs data. Its ability to "unfold" mean velocity measurements, based on a dual PRF algorithm, increase the maximum unambiguous velocity from 16m/s to 48m/s.

Function	Interface between the Transmitter/Receiver and the Pre-processor. Process the log , I and Q video generating the intensity and velocity data.
Processor Type	Autocorrelation at lags R0 , R1 and Z integration, all with rectangular weighting. Five point finite impulse response (FIR) clutter filter for I and Q video.
Intensity	Calibrated, with clutter correction
Velocity	Pulse Pair with multiple PRF unfolding mode
Spectral Width	Pulse Pair gaussian width, noise correction.
Number of range bins	240 per radial
Range bin size	125 m,250m,500m,1km and 2 km selectebale
Ground clutter filters	Five point FIR filter selectebale
Numbers of filters	8 selectable
Ground Clutter	30 dB depending upon set radar parameters

Table 2. Technical Characteristics of the RVP-5

2.2.3 The Radar software and products

The radar control and data display is performed by the " Weather Windows " software under a UNIX operating environment running on a Silicon Graphics Workstation. The package controls all the radar functions (antenna rotation rate, digital signal processing parameters, and electronics calibration, etc.) necessary to produce accurate real time displays . Products available to the forecasters include PPI,RHI, and volume scan products (CAPPI, Column-Maxima and Echo Top).

2.3 Compositing

The composite site hardware is primarily focused on the central site workstation (Silicon Graphics Iris Indigo R4000) with peripherals to provide for communications to remote sites, storage capabilities, and hard copy colour archive. The central site workstation performs tasks necessary to communicate via the network with the remote radar sites and ingest the desired products. Once the products has been received , this workstation combines the individual images into the composite geographic area forming the mosaic for meteorological forecasting.
The composite software ARGUS works closely with Weather Windows (the radar site software) to ingest and combine the appropriate data files. The ARGUS system manager can use the scheduler menu to set up the desired product to receive, specific parameters to be adhered to, and the time intervals between ingested products. Once this has been accomplished , the system manager can update all of the network radar sites by sending the central site schedule to each remote radar site. At that time each radar site that has been placed into the "REMOTE" mode, will begin data gathering and product generation according to the request made by the central site .

III. OPERATIONNAL APPLICATION

3.1Strategy scanning

In the presence of frontal situation; the PPI scan is used with low elevations angle to better meet the needs of hydrological and forecasts purposes. For convectives situations; volumic scan are performed to early detect signature of dangerous convective storm.

3.2 Examples

situation of 08th of June 1996 :

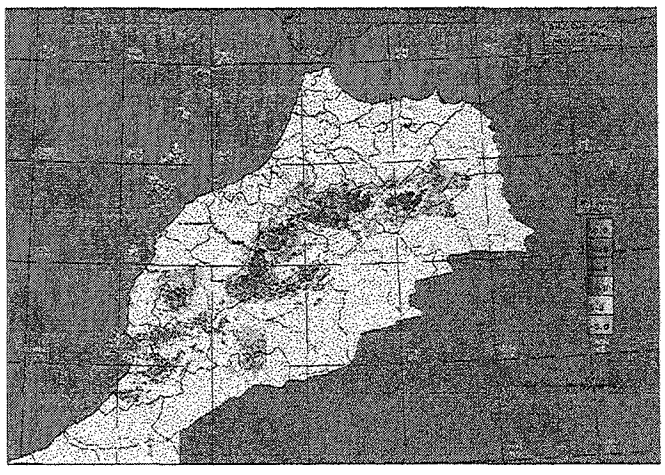

The 08th of June 1996, atmospheric conditions were favourable to convective activity , it's leads to development of thunderstorms that produced heavy rains and hail . Figure 2 represent composite radar display of the Colum-Maxima product, issued from volumic scanning at 17H43, it's shows the localisation of thunderstorms that takes place with a reflectivity higher than 45 dBZ.

figure 3 : Column Maxima product of the 08/06/96

Situation of 21th of December 1996 :

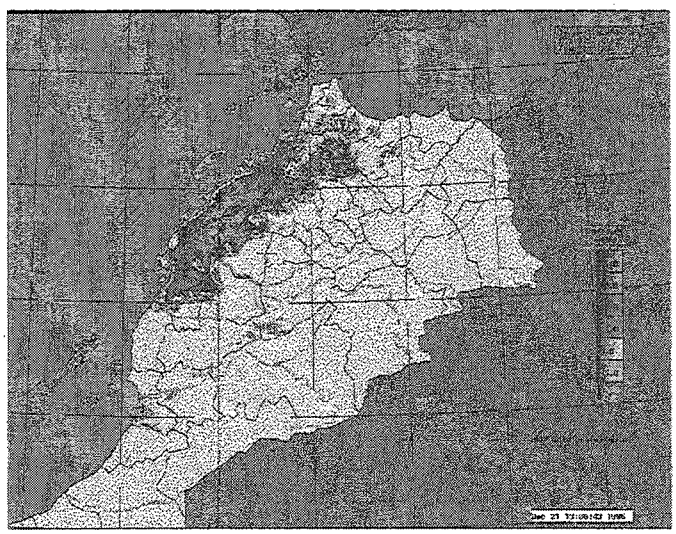

This composite radar display shows an example of frontal situation associated with large band echo organisation as seen in 21st of December 1996. Reflectivity vary from 15 dBZ to 30 dBZ with embedded convection associated with high reflectivity that reach 40 dBZ.

figure 4 : PPI image of the 21th of December 1996

Situation of 28th of September 1997 :

The 28th of September 1997 , the region covered by the radar of Fez was interested by a convective situation that lead to development of thunderstorms that produce heavy rain and hail. This image present a Range Height Indicator(RHI) radar display of thunderstorm as seen by the radar located at FES showing a descending high reflectivity core more than 45dBZ, the height is about 12km.

figure 5 :Range Height Indicator(RHI)

IV. CONCLUDING REMARKS

After two years of operational use of the radars network; forecasters have learnt how to incorporate the radar information in their forecasting process.
The effort is now focused on the development of new products and algorithms that help to eliminate some problems linked with radar measurement (bright band , attenuation, etc.).

REFERENCES

Brandes E.A. and Zrnic D.S. : The Next Generation Weather Radar (WSR-88D) as an Applied Research Tool, 25th INTERNATIONAL CONFERENCE OF METEOROLOGY. Paris,France 1991.

Cheze J.,Tardieu J. And Gilet M. : The French Weather Radar Network, 25th INTERNATIONAL CONFERENCE OF METEOROLOGY. Paris,France 1991.

Rinehart R.E. : Radar for Meteorologist, Second Edition

Entreprise Electronics Corp. : DWSR 92-C , Technical Manual vol. 2

Entreprise Electronics Corp. : ARGUS , operator's manual

MODERNISATION DE LA METEOROLOGIE NATIONALE DU MAROC

APPLICATION ET EXPLOITATION DES SYSTEMES A HAUTE TECHNOLOGIE

Abdelaziz BELHOUJI

Direction de la Météorologie Nationale -MAROC

Introduction

Toutes les activités humaines sont sensibles au temps et au climat. Cette situation place les services météorologiques dans une position clé pour aider à résoudre les problèmes de développement durable.

Les prévisions météorologiques et les études climatiques , progrès scientifiques et technologiques aidant, sont devenues des outils d'aide à la décision indispensables pour les opérateurs économiques et les planificateurs.

Au Maroc, pays à forte vocation agricole ,où les phénomènes météorologiques et climatiques extrêmes et récurrents (Sécheresses, Inondations,...) vécues ces dernières années ont montré l'enjeu que constitue une information météorologique fiable et pertinente (prévision météorologique et saisonnière) dans la planification et la gestion des ressources du pays .

A cet effet, les pouvoirs publics, suite aux directives Royales(*), ont chargé la DMN d'initier et de mettre en œuvre un programme de modernisation du secteur pour la période 1991 – 1996.L'objectif du programme vise l'adaptation des structures et le renforcement des capacités techniques pour répondre aux exigences et aux préoccupations des secteurs socio-économiques du pays. Il s'insère également au contexte international caractérisé par des progrès scientifiques et technologiques majeurs dans le domaine de la météorologie et sciences connexes.

La réalisation de ce programme dans les délais fixés a permis, à la DMN, l'application et l'exploitation des systèmes de haute technologie dans les domaines de l'observation (réseau Radars Doppler , imagerie Satellitale METEOSAT et HRPT), des télécommunications (système de commutation de messages météorologiques, MDD) et du traitement des données (Super-Calculateur Vectoriel CRAY et périphériques) et la fourniture aux utilisateurs de produits et services fiables et de qualité supérieure que par le passé.

Objectifs stratégiques du Programme

- Améliorer la qualité de la prévision en augmentant sa fiabilité et son échéance.
- Adapter le produit météorologique aux exigences des secteurs socio-économiques du pays.
- Orienter l'effort de recherche vers les préoccupations nationales.

Plan d'action

*Phase de diagnostic (Mai 90 - Décembre 90)

Cette phase est caractérisée par la constitution de Commissions de travail adhoc qui avaient pour mission de faire un inventaire de l'existant, de décrire d'une manière exhaustive les fonctions principales de la Météorologie Nationale et de définir les besoins.

* Commissions de travail

1/ - Commission réseaux météorologiques
2/ - Commission Télécommunication
3/ - Commission Climatologie
4/ - Commission Prévisions et Applications
5/ - Commission Communication
6/ - Commission Formation

La synthèse des travaux des Commissions a fixé, sur la base des objectifs stratégiques arrêtés par les pouvoirs publics, les axes de développement prioritaires, les mesures d'accompagnement et les ressources financières nécessaires.

* Phase de mise en œuvre (Janvier 91 - Juin 96)

Malgré les contraintes budgétaires imposées par une conjoncture économique défavorable les principales actions et les projets qui les sous-tendent ont été réalisés :

1/ Renforcement des moyens d'observations

- Construction de 5 stations d'observation en Surface.
- Ouverture d'une station d'observation en Altitude.
- Installation d'un réseau de 5 Radars Doppler.
- Mise en service d'une station de réception des données AVHRR (HRPT) et mise à niveau de la station PDUS.

2/ Développement et amélioration des moyens de traitement et de diffusion du produit météorologique

- Mise en service des nouveaux systèmes de réception des données par satellites (MDD et RETIM).
- Mise en service d'un système de commutation de messages météorologiques de type « TRANSMET ».
- Mise en service du Super calculateur Vectoriel Cray et ses périphériques.
- Mise en service d'un système d'intégration et de gestion des données météorologiques « SYNERGIE ».
- Mise en service d'un serveur de messagerie vocale et de fax pour les usagers.

3/ Mise en œuvre de projets de recherche à des fins opérationnels

- Mise en œuvre du modèle à domaine limité à échelle fine AL BACHIR (version marocaine du modèle ALADIN)
- Mise en œuvre des modèles de prévisions saisonnières AL MOUBARAK et EL MASSIFA.

Mesures d'accompagnement

* L'infrastructure

Les services techniques et administratifs de la DMN étaient implantés dans des locaux exigus et vétustes. La construction d'un nouveau siège avec des structures techniques modernes et conviviales était impérative pour l'accueil et l'installation de nouveaux équipements. C'est l'une des réalisations qui doit être bien dimensionnée et suivie attentivement compte tenu des répercussions négatives et souvent coûteuses qu'elle peut engendrer à court, moyen et long terme sur les autres composantes du projet.

* La formation

La mise en service de nouvelles technologies dans toute organisation introduit fatalement un risque qu'il faut évaluer et réduire. La réduction du risque passe par la capacité et les prédispositions que montrent les professionnels envers l'assimilation et la maîtrise des technologies nouvelles avant leur déploiement.

A cet effet , une politique soutenue de formation de base et continue est mise en place visant la valorisation des ressources humaines et l'amélioration de l'encadrement qui s'adapte avec le programme de modernisation. Elle est concrétisée par la création d'une filière de formation d'ingénieurs au sein d'une grande école supérieure à Casablanca. Ainsi, entre 1990 et 1995, Le nombre de cadres est passé de 72 à 125 et celui des agents de maîtrise de 630 à 751 ; Soit respectivement une croissance de l'ordre de 43 % et de 16 % .

Le durée globale des stages de formation / spécialisation, tous volets confondus , a dépassé entre 1991 et 1996 les 83 Hommes / Mois.

* Accroissement des ressources

La modernisation génère à court terme des charges supplémentaires qui ne pouvaient être supportées par le budget de l'Etat compte tenu de la politique de désengagement et de compression du budget de fonctionnement adoptée par les pouvoirs publics. Les ressources additionnelles nécessaires pour l'exploitation, la maintenance et l'entretien des nouveaux équipements devraient être dégagées en dehors du budget de l'Etat.

Cette contrainte ouvrait, à la DMN en 1993, l'accès à la commercialisation de prestations météorologiques ; L'évolution dans ce domaine fut rapide puisque la part des recettes atteint aujourd'hui presque 30%.

* La communication

La météorologie est l'une des branches d'activités publiques qui a le plus d'impact non seulement sur les citoyens mais également sur les institutions privées et publiques.
A cet effet, des réunions et des points d'informations ont lieu avec les principaux partenaires (Agriculture, Hydraulique, Média, etc.,...) pour les informer sur les nouvelles possibilités qui seront offertes et produits disponibles.

La création d'une entité « Communication » au sein de la structure de la DMN dénote l'importance accordée à ce volet.

Planning des opérations et phases de transition

Le programme mis en œuvre est un programme de grande envergure. Une exigence fondamentale est que les systèmes à haute technologie introduits devaient être opérationnels immédiatement après leur installation.

Cet enjeu important nécessite une cohérence entre les différents projets, un planning minutieux des réalisations et une transition douce entre l'exploitation des anciens et des nouveaux systèmes acquis. La défaillance d'une des ces composantes engendrerait des surcoûts, des pertes et des retards dans la réalisation des objectifs et des interruptions de services.

Conduire la formation et redéployer du personnel, construire un nouveau siège, transférer et installer de nouveaux systèmes à haute technologie tout en maintenant un service météorologique régulier, sont des opérations à grand risque si elles ne sont pas bien conduites.

Leur synchronisation est une donnée cruciale dans le planning compte tenu des liens critiques qui existent entre les tâches et les étapes et principalement entre le lancement de la commande d'acquisition des équipements d'une part et l'installation, la mise en service et l'exploitation opérationnelle sur le nouveau site d'autre part.

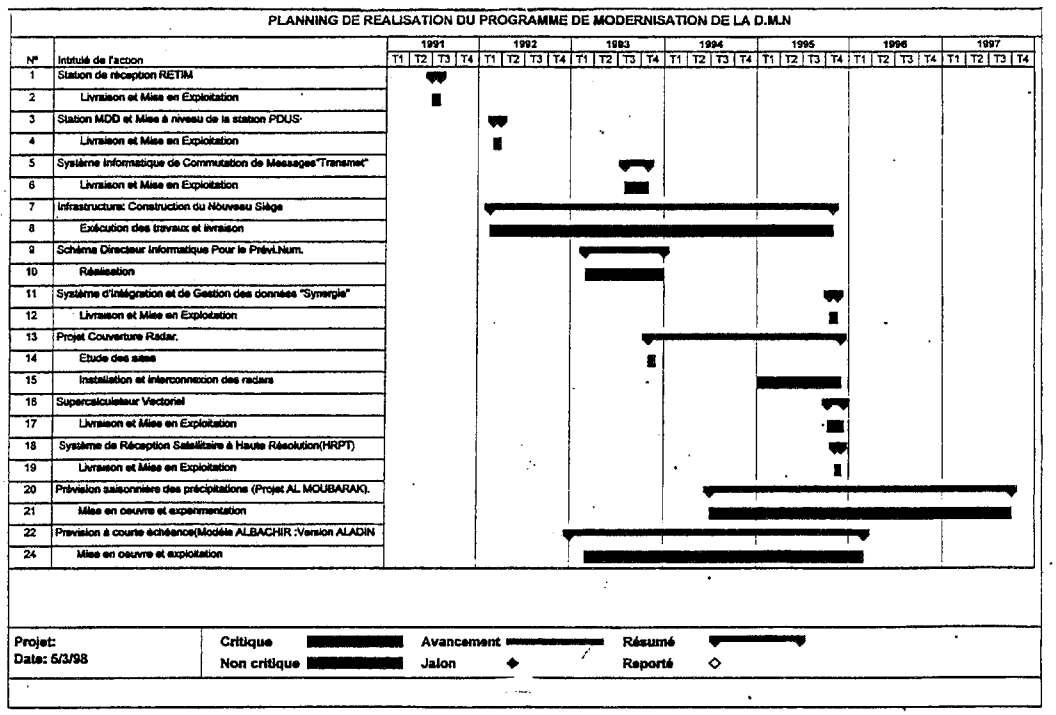

Exploitation des nouveaux systèmes et impact sur le développement

Une des attentes primordiales du programme de modernisation est de fournir des services d'un niveau de fiabilité supérieur que par le passé(voir figure 1).

La mise en service et l'exploitation des nouvelles technologies avancées a contribué fortement d'une part, à améliorer l'analyse et la prévision météorologique à différentes échéances et d'autre part à concevoir de nouveaux produits tels que les avis d'alertes des conditions météorologiques extrêmes et principalement les orages et les fortes précipitations.

Le réseau de radars Doppler permet aux météorologistes de mieux investiger les nuages d'orages, d'estimer quantitativement les précipitations et d'avoir une connaissance précoce sur l'évolution des orages. Le chevauchement des zones de couverture radars permet le suivi continue des orages en déplacement. Les informations sur la position et la quantité des précipitations sont primordiales pour la gestion rationnelle des ressources en eau, le transport Aérien et le public d'une manière générale.

Les images satellitales à haute résolution provenant des satellites géostationnaires et à défilement complètent l'information fournie par le réseau de 40 stations d'observation en surface et de quatre stations de radio– sondage.

La panoplie de produits du modèle à domaine limité et à mailles fines (≈ 16 KM) ALBACHIR (version Marocaine d'ALADIN) qui tourne actuellement, à Casablanca ,en routine sur le les calculateurs CRAY J916 et le CRAY CS 6400 permet aux météorologistes d'affiner l'analyse et d'améliorer la prévision météorologique à une échelle spatio-temporelle encore plus fine.

L'intégration de toutes ces données provenant des différentes sources d'informations, radars, satellites, supercalculateurs, observations météorologiques , dans le système «SYNERGIE » via le système de télécommunication «TRANSMET » permet aux prévisionnistes d'extraire et d'assimiler rapidement les informations les plus pertinentes pour la prévision du temps à différentes échéances, jusqu'à Six (06) jours ,et constitue actuellement pour les prévisionnistes un outil incontournable d'aide à la décision et au développement de nouveaux produits (Avis d'Alerte d'orages, de précipitations fortes, de vents forts, prévision saisonnière etc,...).

Les cas des événements de fortes précipitations des hivers passés et des orages convectifs d'été ont montré l'apport considérable et bénéfique à plusieurs niveaux d'une information météorologique de qualité dans la gestion de la problématique des ressources en eau, de la protection civile, de l'agriculture ainsi que d'autres secteurs.

EVOLUTION DE LA QUALITE DE LA PREVISION A 24H

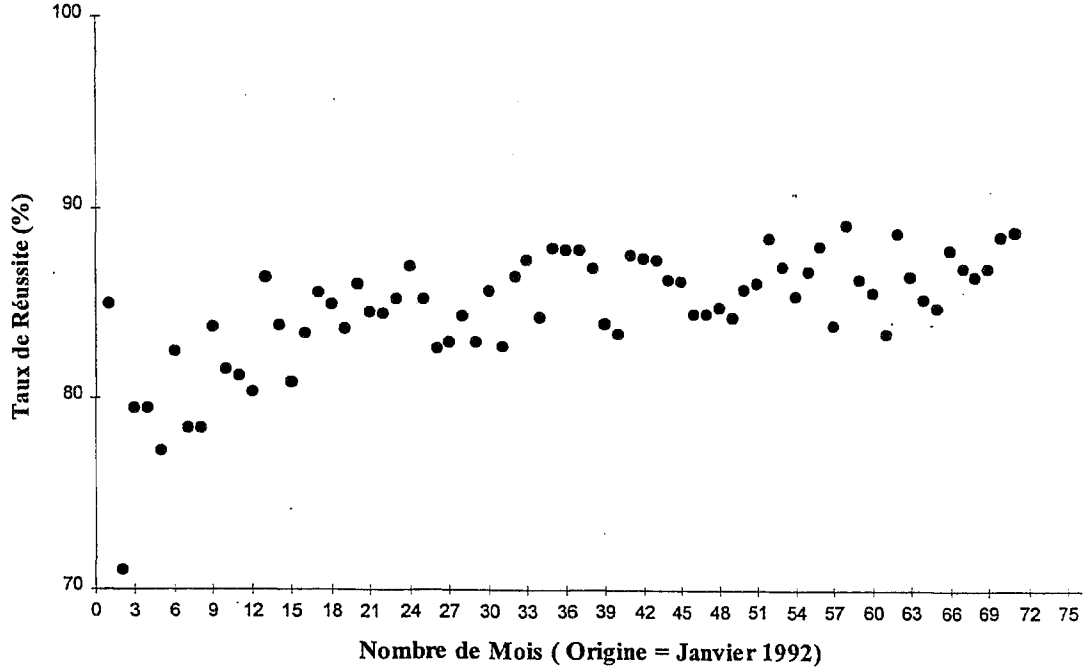

figure 1

Exploitation des nouveaux systèmes et impact sur le développement

Une des attentes primordiales du programme de modernisation est de fournir des services d'un niveau de fiabilité supérieur que par le passé(voir figure 1).

La mise en service et l'exploitation des nouvelles technologies avancées a contribué fortement d'une part, à améliorer l'analyse et la prévision météorologique à différentes échéances et d'autre part à concevoir de nouveaux produits tels que les avis d'alertes des conditions météorologiques extrêmes et principalement les orages et les fortes précipitations.

Le réseau de radars Doppler permet aux météorologistes de mieux investiger les nuages d'orages, d'estimer quantitativement les précipitations et d'avoir une connaissance précoce sur l'évolution des orages. Le chevauchement des zones de couverture radars permet le suivi continue des orages en déplacement. Les informations sur la position et la quantité des précipitations sont primordiales pour la gestion rationnelle des ressources en eau, le transport Aérien et le public d'une manière générale.

Les images satellitales à haute résolution provenant des satellites géostationnaires et à défilement complètent l'information fournie par le réseau de 40 stations d'observation en surface et de quatre stations de radio– sondage.

La panoplie de produits du modèle à domaine limité et à mailles fines ($\approx$ 16 KM) ALBACHIR (version Marocaine d'ALADIN) qui tourne actuellement, à Casablanca ,en routine sur le les calculateurs CRAY J916 et le CRAY CS 6400 permet aux météorologistes d'affiner l'analyse et d'améliorer la prévision météorologique à une échelle spatio-temporelle encore plus fine.

L'intégration de toutes ces données provenant des différentes sources d'informations, radars, satellites, supercalculateurs, observations météorologiques , dans le système «SYNERGIE » via le système de télécommunication «TRANSMET » permet aux prévisionnistes d'extraire et d'assimiler rapidement les informations les plus pertinentes pour la prévision du temps à différentes échéances, jusqu'à Six (06) jours ,et constitue actuellement pour les prévisionnistes un outil incontournable d'aide à la décision et au développement de nouveaux produits (Avis d'Alerte d'orages, de précipitations fortes, de vents forts, prévision saisonnière etc,...).

Les cas des événements de fortes précipitations des hivers passés et des orages convectifs d'été ont montré l'apport considérable et bénéfique à plusieurs niveaux d'une information météorologique de qualité dans la gestion de la problématique des ressources en eau, de la protection civile, de l'agriculture ainsi que d'autres secteurs.

Conclusion

L'aboutissement du programme de modernisation de la DMN est la traduction opérationnelle des Directives Royales confirmées dans le message adressé à la VIII ème Session du Conseil Supérieur de l'Eau et du Climat (C.S.E.C).

Sa réalisation a permis la revalorisation des prestations météorologiques et l'ancrage définitif de la DMN aux services météorologiques les plus développés tant par la mise œuvre de moyens technologiques basés sur l'état de l'art et les standards internationaux que par la mobilisation de compétences qui ont capitalisé savoir-faire et expériences qui pourraient servir aussi à de nombreux pays .

L'apport essentiel du programme se fait principalement à travers l'amélioration des produits de la prévision météorologique et par la mise en place de systèmes de prévisions et d'alerte dédiés et des programmes de recherches à des fins d'applications opérationnelles (Al Moubarak ,El Massifa, Al Ghait, projets agrométéorologiques etc,...).

Au delà des résultats positifs obtenus ; La DMN s'est attelée à renforcer son rôle dans le développement socio-économique du pays ,à consolider les investissements acquis et à asseoir la pérennité du programme de modernisation précédant par l'élaboration d'un nouveau plan stratégique(Horizon 2002) . Ce nouveau plan basé sur une évaluation du programme précédant est

centré autour de trois objectifs majeurs qui sont la régionalisation météorologique, la veille météorologique et climatologique et le développement institutionnel.

Références

- Plan intégré pour l'amélioration et le développement de l'exploitation et de la recherche météorologiques à l'appui de projets sociaux économiques –1992 (DMN)
- Météo plus : Plan de développement de la DMN-1991. (DMN)
- Structure and Technological Capabilities of National Meteorological Services in Africa-ca 1996.D.schiessl (WMO).
- Adaptation de la Structure des Services Météorologiques Nationaux au nouvel ordre economique –1996. A.Diouri (DMN).
- Meteohytec 21 -1995,WMO TD/N°672
- Horizon 2002 (Plan de développement de la DMN 1998-2002)-1997 (DMN).

CONFIGURATION DES SYSTEMES INFORMATIQUES DE TRAITEMENT DE DONNEES METEOROLOGIQUES A LA DMN

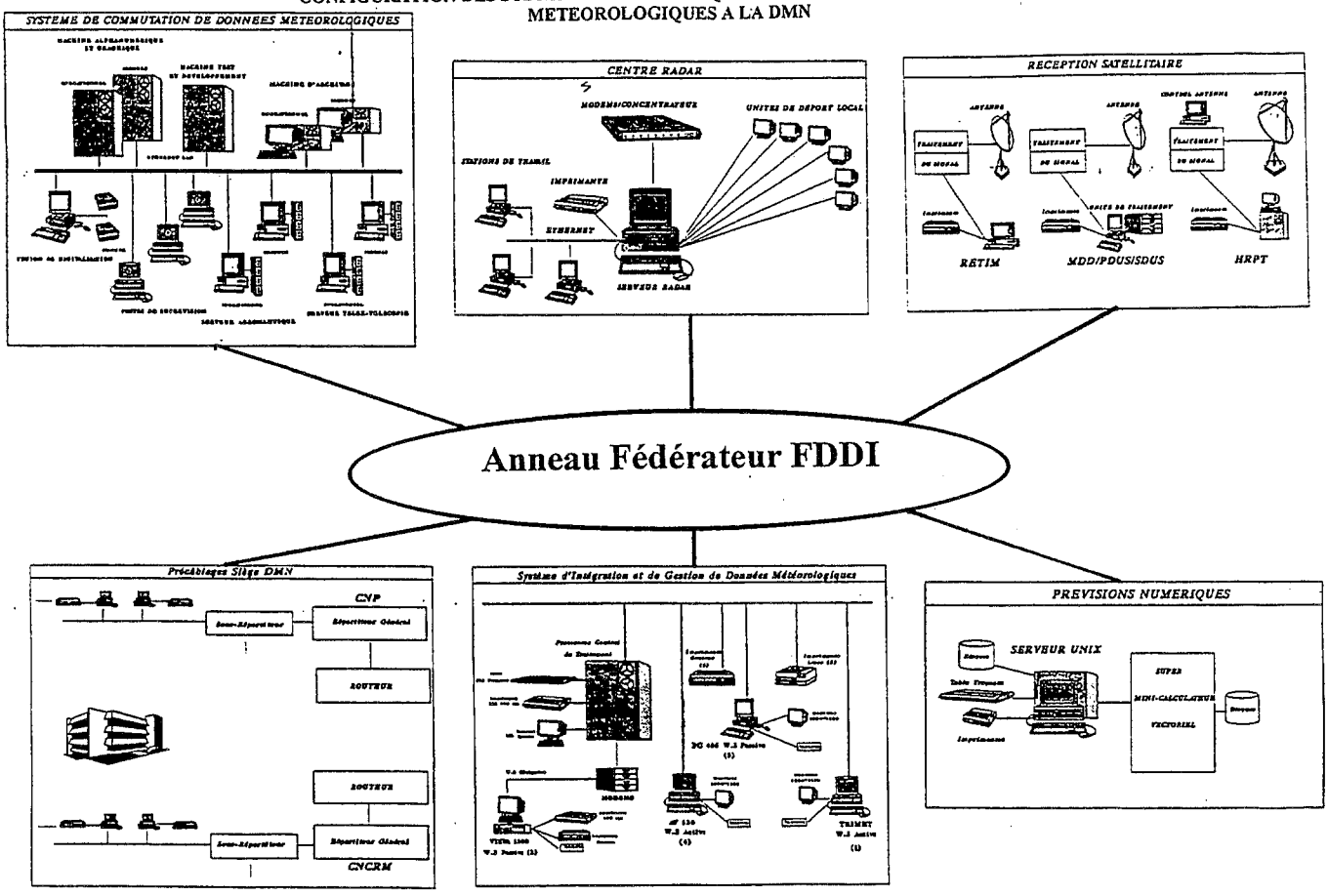

MICROWAVE TEMPERATURE PROFILER: RESULTS OF FIELD TESTING AND INTERCOMPARISONS

Ivanov A., Kadygrov E., Likov A., Miller E., Moiseev D., Viazankin A.
Central Aerological Observatory, Russia

1. INTRODUCTION

Remote - sensing of low-altitude temperature profiles is important for a variety of studies, including air pollution, air/sea interaction and short-term meteorological forecasting. The method that was used for microwave remote sensing of the atmospheric boundary layer temperature profiles is based on measuring the thermal radiation at the centre of the molecular oxygen absorption band near 60 GHz. Accuracy of the temperature profiles retrieving is about 0,2 K in the case of a simple profile and about 0,5K for profile with inversion. During 1994-1998 were successfully conducted comparisons of microwave remote sensing data with in-situ sensors at Meteorological Tower, at tethered balloon, at radiosonde, and with remote sensing data of 915 MHz Radio Acoustic Sounding System. Applications of single channel radiometer on 60 GHz for investigations of brightness temperature fluctuations are discussed also.

Angular scanning single channel radiometers with the frequency 60 GHz has been used for measurements of planetary boundary layer [1-4]. Sensing on this frequency has several advantages that connected with high absorption coefficient. The measurements are not sensitive to air humidity and fog. The temperature contrast in all directions of sensing is relatively small, about several degrees K that enhance the role of brightness temperature fluctuations.

2. METHODS AND INSTRUMENTATION

The radio brightness temperature detected by radiometer can be written as expression:

$$T_b(\nu,\theta)=1/\cos(\theta)\int_0^{\infty} T(h)k(h,T)\exp[-1/\cos(\theta)\int_0^{h} k'(h,T)dh']dh$$

were T(h) - temperature of atmosphere

k(h,T)- molecular oxygen absorption coefficient

θ - zenith angle

ν - frequency

For solution of this equation Tikhonov method in form of generalised variation have been used. Several serious changes improving the stability of the retrieval method have been done on the base of the experimental work in Russia, Canada, Japan, United Kingdom and USA lead to development of new meteoprotection. The experience of exploitation of new meteoprotection make it possible to get reliable data within much wider range of environment condition including intensive snow-fall.

3. INTERCOMPARISONS

During 1994-1998 different intercomparisons with in-situ sensors carried out.

Joint experiments with National Institute of Environmental Studies(NIES), Tsukuba, Japan on May-June 1994 have showed that errors in retrieved temperatures for night measurements equals 0,2-0,4 K and for day measurements about 0,5 K. The comparison have conducted with in-situ sensors at Meteorological Tower. Sensors had been mounted on the heights of 10,25,50,100,150,200 and 213 m. The height of radiometer installation was about 20

m and it was about 50 m apart from the Tower. It seems the sun heating of tower sensors (Fig.1-2) could explain the day-night difference in compared data [5].

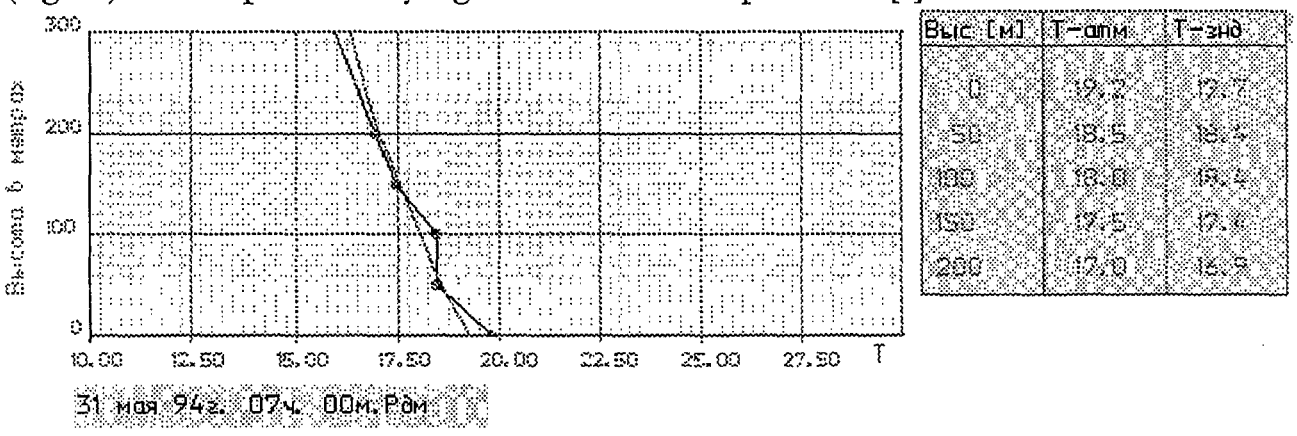

Fig. 1

On September-October 1994 at Inuvic, Canada during BASE (Beufort Arctic Storms Experiment)[6] comparison with radiosonde data gave the opportunity to note that within an average square difference of 0,6-0,7 K two measurement systems performed essentially the same.94 sets of experiment launch have been used in statistical analysis (Fig.3).

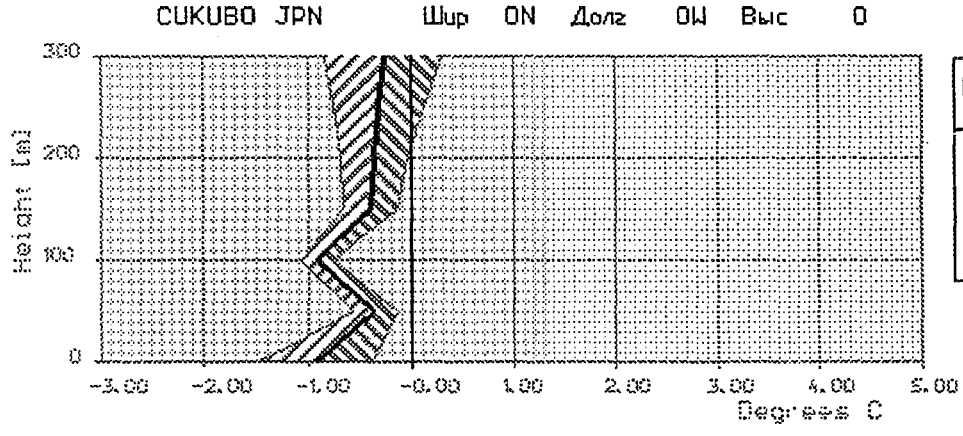

Height м	Middle difference degr. C	R.M.S degr.C.
200	-0.360	0.3
150	-0.405	0.2
100	-0.916	0.1
50	-0.355	0.2
0	-0.927	0.5

Interconparison between radiozonds temperature measurements and microwave remote temperature profiling. (195 set)

Fig. 2.

Two techniques for deriving temperature profiles were evaluated at an experiment conducted from November 1996 to January 1997 at the Boulder Atmospheric Observatory[7,8]. The first was the microwave technique discussed above. The second was a Radio Acoustic Sounding System(RASS) that operated at 915 MHz. Radiometric profiles were produced every 15 min and RASS one were available each hour. Every 5 min the temperature have been measured on 300-m height Meteorological Tower. The height of sensors was 10,50,100,200,300 m. Occasionally measurements from released radiosonde took place. Radiometer gave an excellent comparison during winter conditions at the 300-m Tower; several days of data were obtained during a snow storm, with no degradation of the quality of the data[Fig.4]. Comparisons with RASS, showed the ability of the radiometer to derive temperature profiles to about 500 m.

As a part of the U.S. Department of Energy's Atmospheric Radiation Program (ARM), Russian profiler was purchased and deployed on the North Slope of Alaska (NSA).

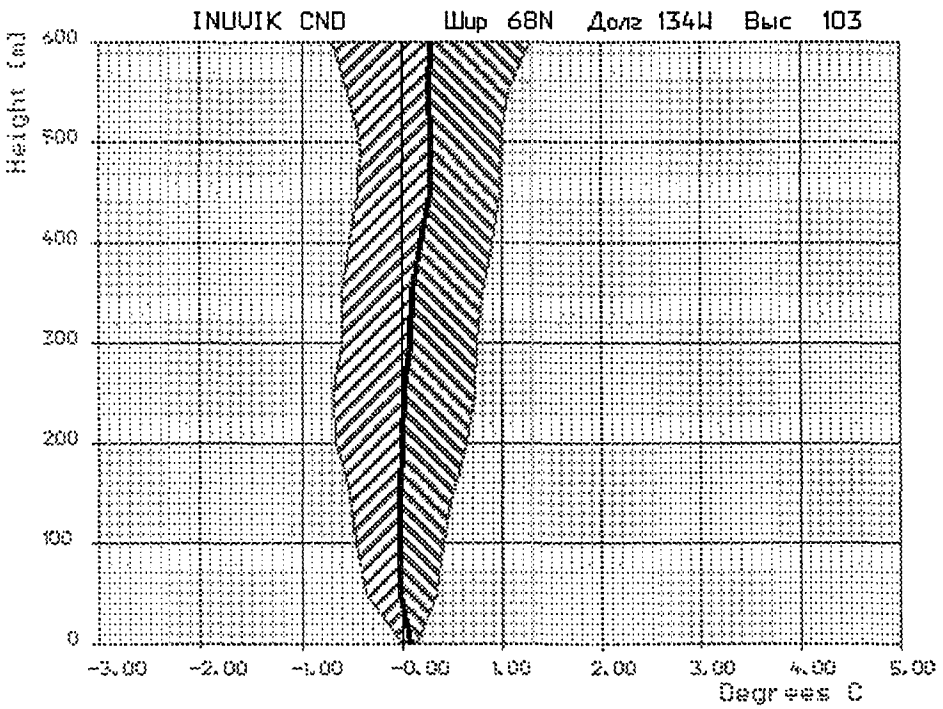

Height M	Middle difference degr. C	R.M.S degr.C.
600	0.283	0.9
550	0.258	0.8
500	0.277	0.7
450	0.274	0.7
400	0.188	0.7
350	0.093	0.7
300	0.074	0.6
250	0.021	0.7
200	-0.009	0.6
150	-0.013	0.5
100	-0.029	0.4
50	-0.016	0.3
0	0.078	0.0

Intercomparison between radiozonds temperature measurements and microwave remote temperature profiling. (94 set)

Fig. 3.

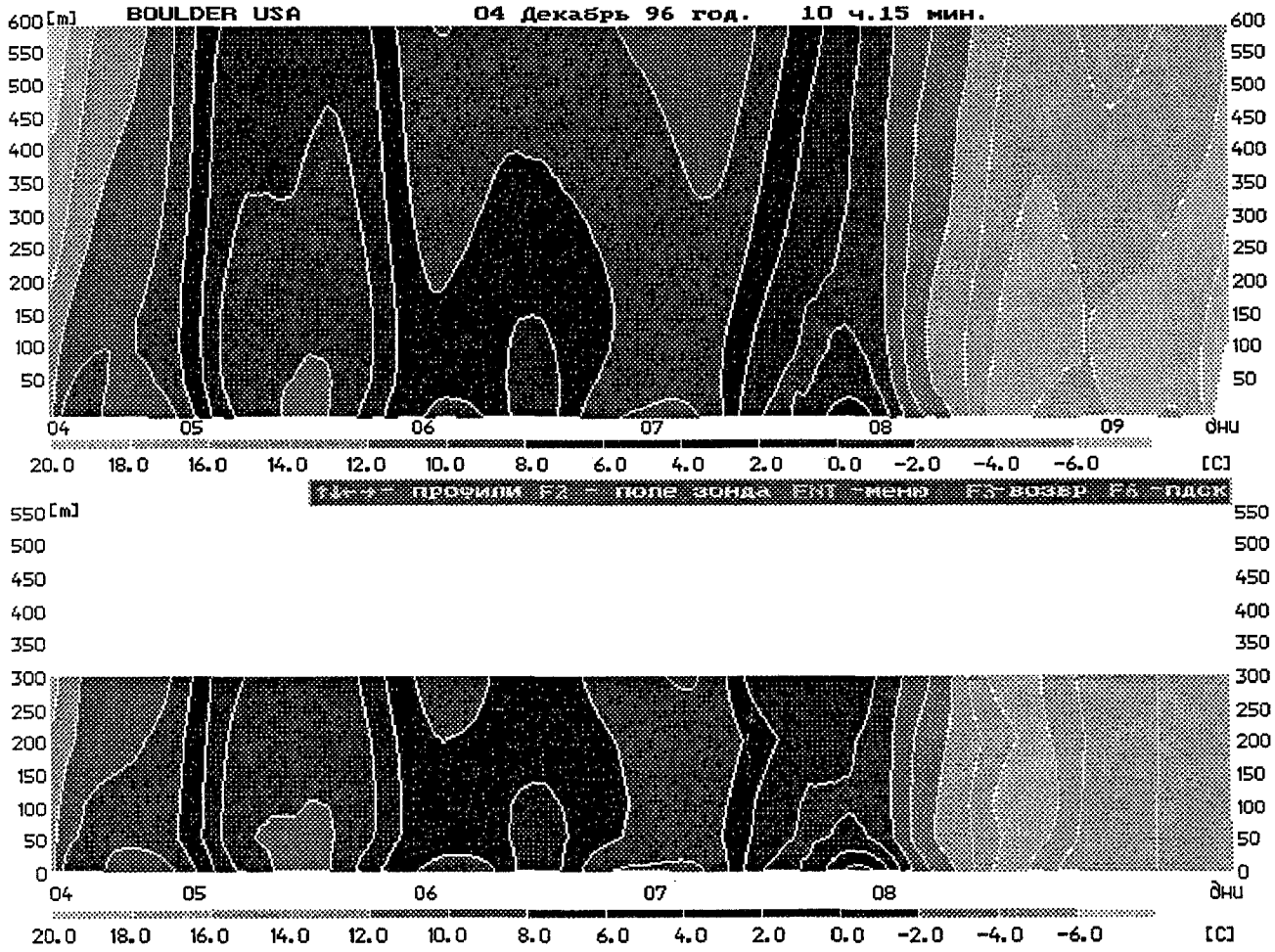

Fig. 4.

4. FLUCTUATION MEASUREMENTS

High sensitivity about 0,03 K of new radiometers made it possible to conduct investigations on atmospheric turbulence and as a result wind measurements simultaneously with the atmospheric temperature profile. The maximum in the microwave emission spectrum of the clear atmosphere with the period about 4-6 min and the amplitude about 0,18 K has been discussed earlier [9]. The fact connected with the dynamic-convection mode of air motion is that the characteristic horizontal turbulence scale of temperature variations was about 600 m if observed average wind speed was about 3-5 m/sec .

5. CONCLUSION

New meteo-protection system for microwave temperature profiler and improved retrieval method enable to provide continuos measurements. Those measurements give a new possibility for investigations of an atmospheric boundary layer dynamics, particularly in Arctic. The regular measurements allowed to create data bank for three fundamental temperature inversion characteristics: height of inversion, inversion depth and temperature. The progress in wind measurements will extend the application of the device and will make temperature profiler one of the most useful instrument for investigations of the climatogical characteristics of the low-level troposphere.

6. REFERENSES

1.E.R.Westwater. Monthly Weather Rev., vol.100,pp.12-22, 1972

2.V.D. Gromov, E.N. Kadygrov, A.S. Kosov. In: Proc.Symp. Wave propagation and remote sensing, Ravenskar, United Kingdom,8-12 June 1992, pp.3.4.1-3.4.5

3. A.V.Troitsky, K.P.Gajkovich, V.D.Gromov, E.N.Kadygrov,A.S.Kosov,. 1993, on IEEE Trans on Geosci.and Remote Sens.,vol.31, N1, pp.116-120

4.A.Ivanov, E.Kadygrov. WMO Report N57,Instruments and Observing Methods, WMO/TD N 588, pp. 407-412,Geneva, 1994

5.I.Matsui, N.Sugimoto, S.Maksyutov, G.Inoue, E.Kadygrov, S.Viazankin, Jpn.J.Appl.Phys., vol.35 (1996), pp.2168-2169, Part 1, No. 4A, April 1996.

6.B.D.Zak,E.N.Kadygrov,A.V.Koldaev,A.V.Troitsky., Abstracts of the 6-th ARM Science Team Meeting, March 4-7,1996, San Antonio, Texas, pp.38-39.

7.E.R.Westwater,Y.Han,V.Leuskiy,V.Irisov,E.N.Kadygrov,S.A.Viazankin. Proceedings of the 7-th ARM Science Team Meeting, March 3-7,1997, San Antonio, Texas (in press)

8.E.R.Westwater,Y.Han,V.Leuskiy,V.Irisov,E.N.Kadygrov,S.A.Viazankin.IGARSS'97, 03-08 August, 1997, Singapore ,vol.IV, pp.2093-2096

9.A.V.Troitsky, E.N.Kadygrov. Proc. URSI XXV-th General Assembly, Lille, France, 1996, p. 655

THE MET OFFICE'S UPGRADED LIGHTNING LOCATION SYSTEM.

G. L. Hamer
Met Office, London Road, Bracknell,
Berkshire, RG12 2SZ, UK

1 Introduction

The U.K. Met. Office has operated instruments capable of locating lightning since the 1940's. The Met. Office's original system, known as the Cathode Ray Direction Finding System (CRDF), used a VLF (~ 10kHz) magnetic direction finding lightning location technique. This was the first system to routinely submit lightning location data onto the World Meteorological Organisation's (WMO) Global Telecommunications Network. In the late 1970's the Met Office decided to move away from the magnetic direction finding technique of lightning location, because of inaccuracies at long range caused by bearing errors. A system was developed which applied the arrival time difference (ATD) location technique. This system consists of seven outstations located at Bracknell, Hemsby, Camborne, Lerwick, Stornoway, Gibraltar and Cyprus (see Figure 1) and a manned control station located at Bracknell. It became operational in 1986 and produces routine lightning reports for WMO every thirty minutes for the region 40W to 40E and 30N to 70N and a high resolution message every five minutes for the region 160W to 160E and 60S to 80N. For a detailed description of the ATD technique and details of its application to the Met Office's Thunderstorm Location System see Lee (1986a, 1986b).

Over the past ten years the ATD system has operated satisfactorily as a thunderstorm location system with meteorological users accepting a relatively low detection efficiency for individual strokes. However, advances in other meteorological observing systems and forecast applications mean that requirements for lightning location have changed. These new requirements meant that any Met Office lightning location system must have improved location accuracy (RMS 2.5km over UK) and detection efficiency (95% over UK) compared to the current system. Over the UK the system should determine stroke type, calculate stroke strength and identify multiple stroke events. The extended service area offered by the current system must also be retained. After a period of consultation with commercial providers of lightning location systems the decision was made (in 1994) to upgrade the current ATD system's hardware and enhance its software in order to meet these requirements and retain the operational and commercial advantages of the ATD system.

The hardware component of the upgrade should be completed by summer 1998. However, the software enhancements will require a period of testing and development before they can be used operationally. These enhancements should be implemented by summer 1999.

Figure 1 **Met Office's ATD Thunderstorm Location System's outstation network overlaid on a METEOSAT visible image from 11th March 97 at 1500 with ATD data from 1445 to 1515 overlaid. Each black square represents one lightning discharge.**

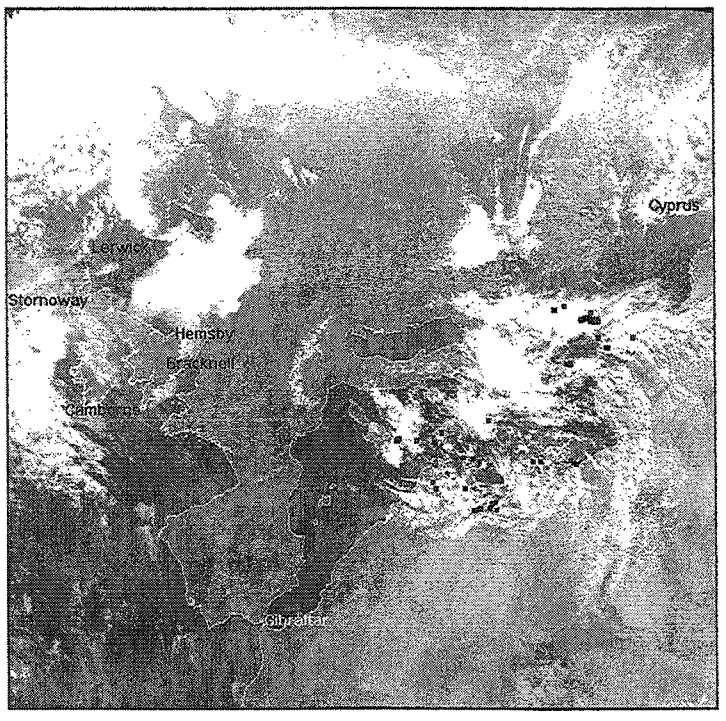

2 Upgraded system.

The Met Office's upgraded lightning location system will operate automatically on a dual processor (748/743i configuration) Hewlett Packard platform. The communications between each outstation and the control station are also being improved from their current 100 bits per second to 2400 bits per second. The combination of these improvements will allow the present location rate of 300 to 500 events per hour to be increased to 10000 to 12000 per hour. In order to achieve this increase in the number of events processed the waveform selection threshold in the upgraded system will be lowered. As a result received waveforms which are currently too weak to be considered will now be suitable for processing.

In the following subsections the methods chosen to determine flash attribute information from received waveforms are summarised.

2.1 Lightning Location

The technique for determining the source of a received waveform will remain the same (Lee, 1986). A VLF propagation model is being developed to model variations in VLF group velocity caused by changes in ionospheric height and ground surface type (following Volland, 1995) with the aim of improving the location accuracy of the system. This model will have its greatest effect when the day/night terminator lies between the system's UK and Mediterranean outstations. Under these conditions the mean velocity of the VLF waveform along each path from source to receiver is not constant. The current location algorithm does not allow for these variations. Therefore, by modelling the waveform velocity along each path and incorporating them in the location process it is hoped to minimise the location errors introduced in such circumstances.

2.2 Stroke Strength and Polarity.

To determine the peak current flowing in a return stroke, or stroke strength, the electric field change due to a discharge measured at an outstation must be quantified (in V/m) and the distance of the lightning event from the receiving site known. In quantifying the magnitude of the detected field change the polarity of the lightning may be determined. Using these parameters and assuming the radiative component of the total electric field change is dominant then the theoretical relationship shown in Equation 1, may be used to determine stroke strength;

Equation 1.

$$i = \frac{-2\pi\varepsilon_0 c^2}{v} ED$$

where i = peak current (A)
ε_0 = permittivity of free space (8.854×10^{-12} Fm^{-1})
c = speed of light (3.00986×10^{8} ms^{-1})
v = velocity of current flow in return stroke channel (ms^{-1})
E = measured peak electric field (V/m)
D = Distance or source from receiver (m)

VLF radiation propagates in the earth - ionosphere waveguide in the form of a ground wave (travels directly between source and receiver) and a series of skywaves (travels between source and receiver via reflections at the ionosphere and surface). If the receiver is located more than approximately 400km from the source then the groundwave and first and subsequent skywaves will interfere with each other. Therefore, E, may only be determined accurately (and simply) if the source of a waveform is located within approximately 400km of an outstation. Therefore, with the current outstation network configuration, E, can be determined accurately for any waveforms that originated from lightning events located in the UK.

If E can be determined accurately then the largest unknown is the velocity of current flow in the return stroke channel, v. Cooray and Orville (1990) suggests a velocity of 2.2×10^{8} ms^{-1} occurs in the first few hundred metres of the return stroke channel. However Casper and Bent (1992) suggest a velocity of 1.0×10^{8} ms^{-1} and this is suggested as the default velocity in the Lightning Positioning and Tracking System (LPATS). Work is ongoing to determine which value the Met Office's upgraded system should use.

2.3 Multiplicity.

A lightning event is generally made up of a leader process, an initial return stroke possibly followed by a series of return strokes which traverse the same path between cloud and ground as the initial return stroke. Each of these return strokes may be located by the Met Office's system and would be reported separately as unrelated events. It is proposed that if an event is separated spatially and temporally from the previous event by less than 5km and 500ms respectively then they shall be reported as a single event with a specified number of strokes.

2.4 Stroke Type.

Both cloud to ground return strokes and inter cloud activity are sources of VLF radiation. Therefore, the Met Office's ATD system is capable of detecting waveforms from both these types of lightning. However, the required breakdown potential within a cloud is less than that required for lightning to occur between cloud and ground so inter cloud events are generally weaker sources of VLF radiation than cloud to ground discharges. Vertically polarised radiation may propagate with little attenuation in the earth - ionosphere waveguide but the horizontally polarised component is strongly attenuated. Therefore, VLF radiation from inter cloud activity, which generally has a large horizontally polarised component, will be strongly attenuated compared to VLF radiation from cloud to ground lightning which tends to be vertically polarised. As a result, the magnitude of received VLF radiation from inter cloud activity is generally an order of magnitude less than that from a cloud to ground return stroke. Therefore, waveforms produced by inter cloud activity occurring at greater distances from the system are unlikely to be strong enough to be successfully located. However, in the region of the outstation network the detection of inter cloud activity is likely.

To distinguish between the type of lightning responsible for each received waveform a simplistic pattern recognition algorithm will be used. A waveform from a cloud to ground return stroke is generally of a well defined shape compared to those from inter cloud strokes which are generally more complex in shape. Work on this section of the project is still at an early stage.

3 Performance of the Current System.

The current operational ATD system was designed as a 'thunderstorm' location system rather than a system capable of detecting a high proportion of lightning events in all circumstances. The system's performance is routinely monitored in the region 40W to 40E and 30N to 70N. Reports of thunder (WMO present weather codes 17, 28, 91 to 99 inclusive) from meteorological observing stations are compared with ATD reports. If an ATD report occurred within the reporting hour within 50km of a station which reported thunder, ATD was judged to have successfully located that thunderstorm. Figure 2 shows the results of this analysis for data from 1995 to 1997 inclusive. During this period ATD detected over 70% of reported thunderstorms in the NW European region.

Figure 2Contour Plot of the percentage of synoptically reported thunderstorms with an ATD report located within 50km during the period 1995 to 1997 inclusive. Statistics calculated on the five by five degrees of latitude and longitude grid shown.

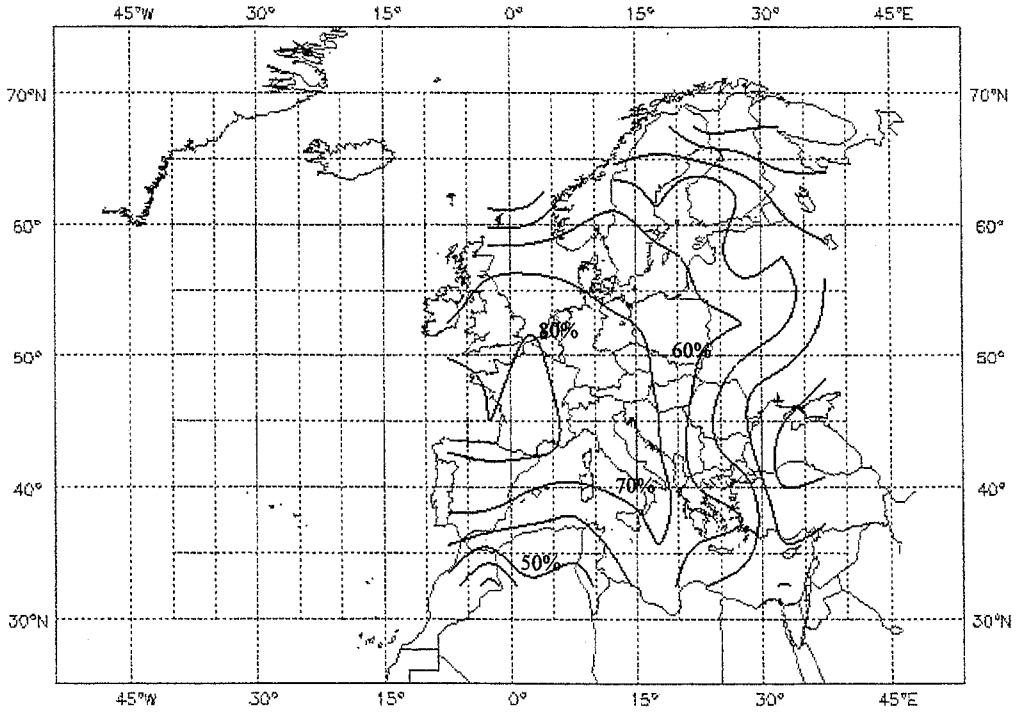

In areas south of the Mediterranean Sea the proportion of synoptically reported thunderstorms successfully reported by ATD fell sharply. In the region from 0 to 5W and 30N to 35N there were 727 synoptic reports of thunder during the period 1995 to 1997. ATD only reported these thunderstorms on 25% of occasions. However, the ATD system, reported 28984 events in this region during the same period. This suggests that a high proportion of storms reported synoptically produced lightning that was not strong enough to be detected by ATD and as a result of the sparse distribution of synoptic observing stations in this region the storms that were the source of the 28984 events reported by ATD, were generally not observed by the synoptic network.

More detailed comparison work has also been performed between the Met Office's ATD system and other European lightning location systems (SAFIR France, SAFIR Belgium, LPATS Germany, EATechnology UK). Each comparison has shown that within the limited area of mutual coverage, location reports from the Met Office's system compared well with those from other systems. However, in each comparison, ATD's relatively poor lightning event detection efficiency was identified. The Met Office's upgraded ATD system will have a twenty fold increase in processing capability which should rectify this short coming.

The area of coverage of the ATD system is much larger than that discussed above. Lightning events over the Atlantic, North and South America and the Pacific are often identified if activity in the main service area is low. The accuracy of these data may be assessed using satellite images. Figure 3 shows a GOES East image with ATD data overlaid. This image shows a cold frontal structure that had moved eastward off the eastcoast of North America and over a relatively warm Atlantic Ocean. This thermal instability triggered deep convection on the leading edge of the front. ATD located a chain of thunderstorms stretching along the front from east of Newfoundland to the Bahamas. In the same satellite image isolated cumulonimbus can be identified in the West Indies and Central America. ATD has located lightning events in many of these regions suggesting these clouds were electrically active.

Figure 3GOES East infra red image from 0930 on 200996 with ATD data overlaid from 0900 to 1000 on the same day. Each symbol represents a single ATD report.

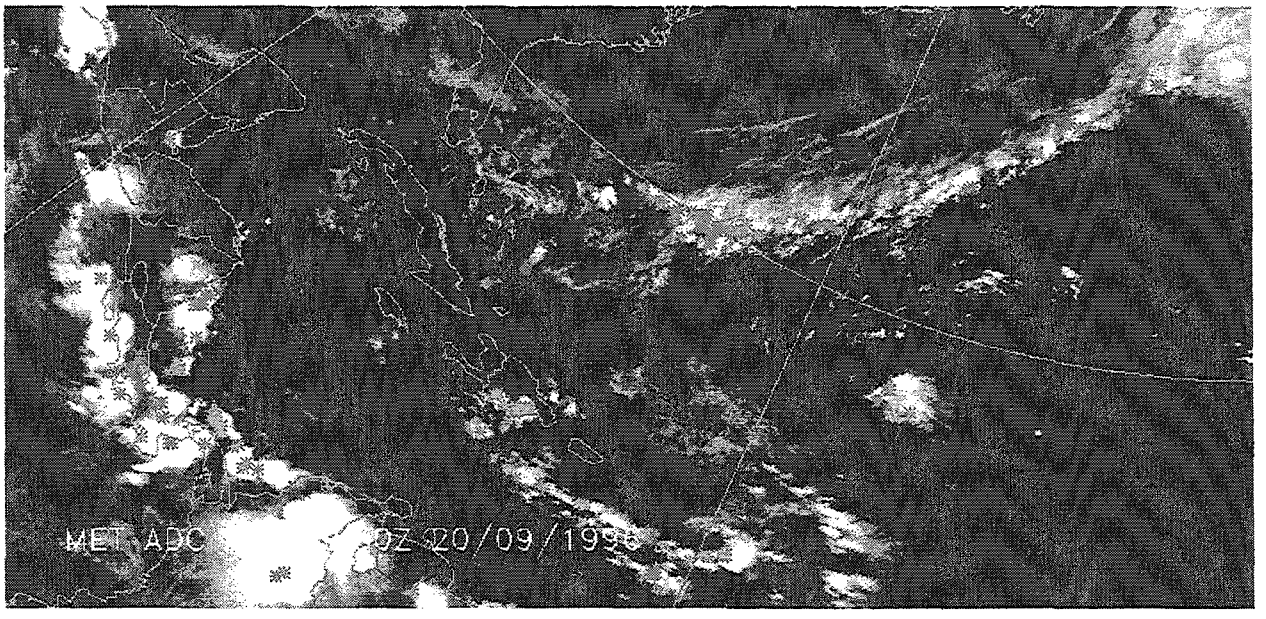

4 Conclusion

The application of developments in computing, communication and signal processing techniques will transform the Met Office's Arrival Time Difference (ATD) Thunderstorm Location System into a system that offers lightning location information over an unrivalled area aswell as flash attribute information over the UK. These enhancements are hoped to produce an upgraded system capable of providing a service that will satisfy the needs of both current and future users.

5 Acknowledgements

The author would like to thank the members of the Sferics Project Team for their efforts during the ATD Sferics System Upgrade Project.

6 References

CASPER,P.W. BENT,R.B. (1992) Results of the LPATS USA National Lightning Detection and Tracking System for the 1991 Lightning Season. 21st International Conference on Lightning Protection. Berlin. September 1992

COORAY,V. ORVILLE,R.E. (1990) The effects of Variation of Current Amplitude ,Current Risetime and Current Stroke Velocity Along the Return Stroke Channel on the Electromagnetic Fields Generated by Return Strokes. Journal of Geophysical Research Vol. 95 No D11 p18617-18630

LEE,A.C.L. (1986) An experimental study of the remote location of lightning flashes using a VLF arrival time difference technique. Quart. J. Roy Meteor. Soc. 112, 203-229

LEE,A.C.L. (1986) An Operational System for the Remote Location of Lightning Flashes using a VLF Arrival Time Difference Technique. J. of Atmos. and Ocean. Tech. 1986, Vol 3, No. 4 pp630-642

VOLLAND,H. (1995) Longwave Sferics Propagation within the Atmospheric Waveguide. Handbook of Atmospheric Electrodynamics. CRC Press.

Extended Abstract

LONG-RANGE SODAR INTERCOMPARISONS WITH METEOROLOGICAL TOWERS AND ASCENT BALLOONS TRACKED BY RADAR

by

Mr FAGE Jean-Michel
REMTECH
2/4, avenue de l'Europe
BP 101
78143 VELIZY CEDEX
FRANCE

Mr VOGT Siegfried
FORSCHUNGSZENTRUM KARLSRUHE
Institut für Meteorologie & Klimaforschung
Postfach 3640
D-76021 KARSRUHE
GERMANY

SYSTEM DESCRIPTION :

A long range Sodar (acoustic wind profiler) needs to operate at lower frequencies than usual sodars in order to reduce the sound attenuation during the signal roundtrip. But a lower frequency means higher environmental noise. Therefore as it is (at least for nuisance considerations reasons but also for practical reasons) impossible to increase the output power accordingly the only solution is improved signal coding.

Its principle is shown on the following figure :

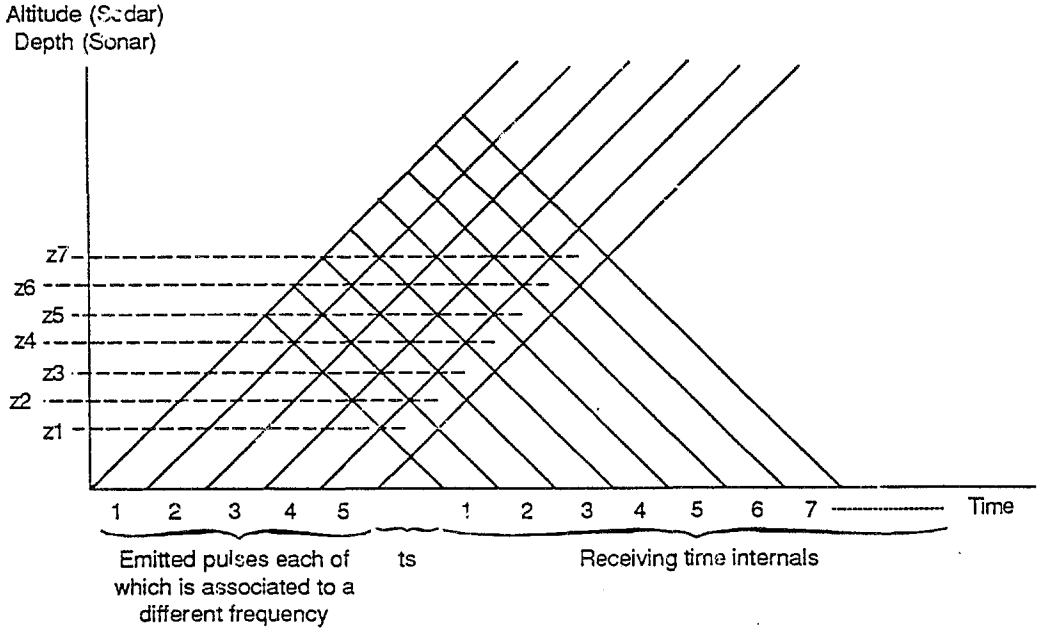

Looking at the previous figure, one can see that information on first altitude sampled z1 can be found in backscattered signal received during interval 1 like for all monofrequency sodars (in our case the single frequency corresponds to pulse N° 5).

But for z2 we have two independent pieces of information :
- in time interval 1 corresponding to pulse 4,
- in time interval 2 corresponding to pulse 5.

Similarily for z3 we have 3 independent pieces of information.
Similarily for z4 we have 4 independent pieces of information.
Similarily for z5 (and above) we have 5 independent pieces information.

Generally speaking, if the emission includes N pulses we have :

- i ...dependent pieces of information for zi with $1 \leq i \leq N$ and N independent pieces of information for zi with $i > N$.

This technique offers two main advantages :

- Firstly, it allows longer emission without degrading vertical resolution. More energy is sent, thus increasing the signal to noise ratio S/N by 10 $\log_{10}$ when compared to single frequency systems.

- Secondly, as the different emitted frequencies travel through layer zi nearly at the same time when compared to turbulence time scales we have independent measurements at altitude zi.
  We can therefore run a very efficient consensus method at this end of the averaging period as the following time series :

time mark ↓ frequency index ↓

X i j t with $1 \leq j \leq N$ (i is the altitude index)

(X being backscattered echo intensity, spectral broadening, Doppler shift...) have the same

statistical expectations $\bar{X}_i$, σX_i...

By experience, when comparing this to a single frequency system, the gain in dBs allowed by a good consensus technique is well described by the following empirical formula :

$$2 * (N - 1) \text{ (dB(s))}$$

Since we are presently using N = 9, the total gain when compared to single frequency systems is therefore :

$$10 \log_{10} 9 + 2 * (9 - 1) \cong 26 \text{ dB}$$

which is equivalent to increasing output power by a factor of **400** !

Moreover the PA1-LR operates along 5 beams with simultaneous emission on two tilted opposite beams and this is equivalent to a further doubling of the power.

EDF intercomparisons will be released officially this coming April and presented during the conference.

The same remark applies to NOAA data which are still not available officially at this time.

Finally the intercomparison in Karlsruhe is presently taking place as it started some months later than originally expected. Of course intercomparison data will be available at the conference.

Advances in Profiling Technology...A New 8-mm Doppler Cloud Radar

H.A. Winston
Radian International LLC, Boulder, Colorado, USA

K.P. Moran, B.E. Martner, M.J. Post, D.C. Welsh, D.A. Merritt, D.A. Hazen
NOAA Environmental Technology Laboratory, Boulder, Colorado, USA

R.G. Strauch
Cooperative Institute for Research in the Environmental Sciences, University of Colorado, Boulder Colorado, USA

The United States Department of Commerce (DOC) National Oceanic and Atmospheric Administration (NOAA) developed an 8-mm Doppler cloud radar for the Department of Energy's (DOE) Atmospheric Radiation Measurement (ARM) program. Also known as Millimeter-wave Cloud Radars (MMCR's), these systems provide observations of non-precipitating and weakly precipitating clouds at the ARM Cloud and Radiation Testbed (CART) Sites. The radar's unique design is intended for unattended and continuous operation for at least 10 years, and requires only minimum maintenance. These new cloud radars will help scientists understand the role of clouds in radiative aspects of climate change. The information in this article represents a condensation of a more comprehensive instrument description by Moran et. al. (1998).

NOAA and Radian International LLC entered into a Cooperative Research and Development Agreement (CRADA) in May of 1997 for the technology transfer and commercialization of the 8-mm Doppler cloud radar developed within NOAA's Environmental Technology Laboratory (ETL). The CRADA provides the mechanism under which this technology is available to international scientific, aviation, defense, and operational weather support programs.

Scientific requirements for the MMCR radars included the need for excellent sensitivity and resolution to detect weak and thin multiple layers of ice and liquid water clouds over the site, and long-term unattended operation in remote locales. In response to these requirements, the ETL design features a vertically pointing, 35-GHz (K_a-band) Doppler system which uses a low-peak-power but high-duty-cycle TWTA (Traveling Wave Tube Amplifier) transmitter for reliability, and a high-gain antenna and pulse-compressed waveforms for heightened sensitivity. The radar design philosophy emphasizes the use of commercial off-the-shelf subsystems, including its primary processor, which is the same as used in Radian's commercially available LAP® boundary layer and tropospheric wind profilers.

The primary processor has flexibility to allow operating modes to be selected or modified to match specific conditions or objectives. It routinely operates with a repetitive sequence of four modes, which, collectively, optimize sensitivity, resolution, height coverage and other factors for the wide variety of anticipated cloud conditions. The first MMCR (Fig. 1) began operations at ARM's CART site in northern Oklahoma in November 1996 and has run nearly continuously since then. This unit uses a 3-meter diameter antenna with a simple protective radome; the beam width is 0.2°. A more easily transported 2-meter antenna will be used at CART sites in the tropical

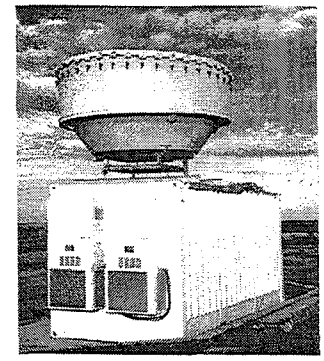

Fig. 1. MMCR at the ARM CART site in Oklahoma.

western Pacific and in Alaska. Excluding the antenna, the entire radar hardware weighs about 140 kg and occupies about 2 m^3 of space.

Fig. 2 is the block diagram depicting functional radar components. The primary processor (OS/2 computer), interface and IF modulator/receiver constitute the data system acquired from Radian's commercial wind profiler product line. The data system generates the transmitted waveforms and receives the backscattered signals, both at a nominal intermediate frequency (IF) of 60 MHz. The up-down converter transforms the transmitted frequency from IF to 34.86 GHz, and *vice versa* for the return signal. Twin circulators are used to protect the low-noise receiving pre-amplifier during pulse transmission, and to inject several known levels of RF noise into the receiver chain to calibrate the radar. The vertically-pointed antenna is covered by a tilted flat radome to protect the precisely-shaped antenna surface and to encourage rain and condensation to run off.

Two personal computers (PCs) that are connected via Ethernet are used in the design; the primary processor, which uses an OS/2 operating system, provides radar control and data acquisition. The second PC, operating under Solaris, provides data calibration and communication. A full Doppler data stream (spectra and spectral moments vs. altitude) is generated and displayed by the primary processor, together with calculated signal-to-noise ratios. It also monitors the environment surrounding the radar (temperature, humidity, power, etc.) and other critical system parameters (e.g., TWTA status, VSWR, waveguide pressure, etc.) and takes appropriate actions if problems arise. The radar can also be controlled remotely over the Internet through this computer. The Solaris PC ingests data from the primary processor, calibrates and archives these data, and communicates information (including health and status) to the outside world. A single monitor/keyboard can be switched

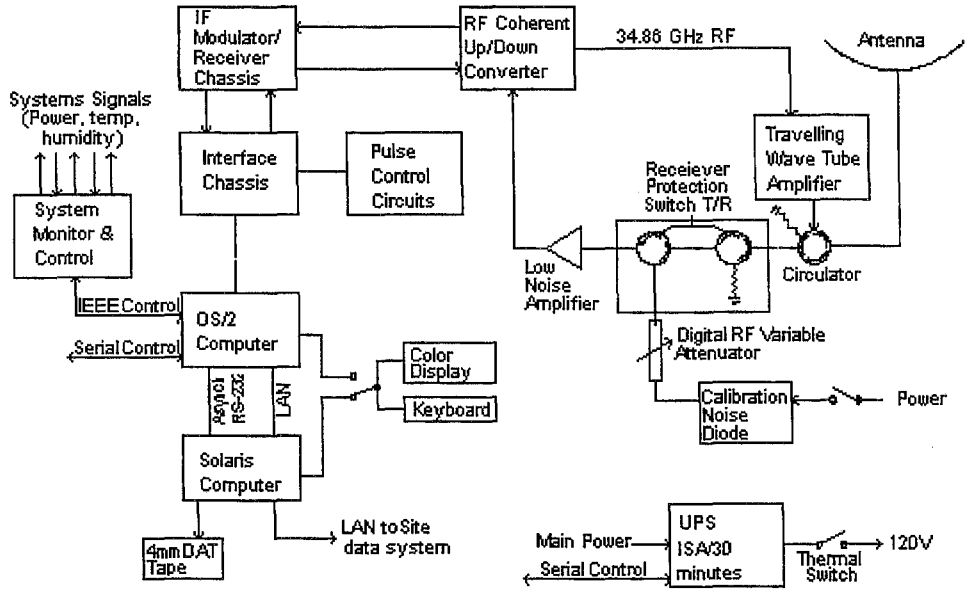

Fig. 2. Block Diagram of radar. Note provisions for receiver protection and automatic calibration via noise diode and attenuators. Computer controls, health monitoring, and data system are not indicated.

manually to function with either PC. The two computers work together when a critical system failure occurs (such as imminent loss of backup power for the UPS) to gracefully shut down the entire system in such a way that the radar can automatically restart itself when the problem is corrected.

The MMCR achieves excellent resolution and relatively high average power output (25 w) from the low peak-power (100 w) TWTA by employing pulse compression techniques, *i.e.* by transmitting long pulses (up to 20 μs) that are internally phase-coded, typically in 0.6 or 0.3 μs segments. Standard techniques (Schmidt *et al.*, 1979) are used to decode the pulses and retain the range resolution associated with the phase-coded segments (90 or 45m). The radar's excellent sensitivity is attributable to its short wavelength (8.7 mm), relatively high average power, large antenna, a low noise receiver, and long averaging (dwell) times (~1 s).

Table 1 shows important system parameters used in routine operations in Oklahoma in the spring of 1997. The system's estimated sensitivities at 5 km height vary from about –32 dBZ in the uncoded-pulse, 45-meter resolution mode to about –51 dBZ in the coded-pulse, 90-meter resolution mode. For comparison, ETL's much more sophisticated, but attended, NOAA/K scanning research 35-GHz radar (Martner and Kropfli, 1993; Kropfli and Kelly, 1996) is capable of detecting about –36 dBZ at this range. Years of experience with NOAA/K indicate that it can detect most visible clouds overhead. Side-by-side field comparisons with NOAA/K confirm that the Oklahoma MMCR has similar sensitivity with its uncoded modes and superior sensitivity with its coded modes. It has impressed ARM scientists with its ability to reveal the structure of clouds over the CART site with remarkable detail, including complicated multiple layer situations with and without precipitation, such as shown in Fig 3.

In addition to revealing the macrophysical structure of clouds (layer heights, thickness, etc.) in detail, the MMCR is expected to become the central instrument for a number of experimental techniques for estimating microphysical features of clouds (particle sizes, concentrations, mass content) when combined

Table 1. MMCR Characteristics – Oklahoma CART

Frequency: 34.86 GHz (λ mm, K_a-band)
Peak Transmitted Power: 100W
Max. Duty Cycle: 25%
Antenna Diameter: 3 m
Antenna Gain: 57.2 dB
Beam Width (full-width, half-maximum): 0.2 deg.
Cycles through 4 modes with selectable parameters.
Parameters selected for use in April 1997:

Mode →	**1**	**2**	**3**	**4**
Inter-Pulse Period (μs)	82	126	106	72
Pulse Width (μs)	0.3	0.6	0.3	0.6
Gate Spacing (μs)	0.3	0.6	0.3	0.6
Number of Gates	220	167	167	220
Coherent Averages	8	6	6	4
Spectral Averages	16	21	60	37
FFT Length	64	64	64	64
Coded Bits	32	32	no	no
Dwell Time (s)	0.7	1.0	0.6	0.7
Obsv./Processing Time (s)	9	9	9	9
Min. Det. Signal (dBm)	-129	-132	-132	-132
Height Resolution (m)	45	90	90	45
Min. Height AGL (km)	0.1	0.1	0.1	0.1
Max. Height AGL (km)	10.0	15.1	15.1	10.0
Nyquist Velocity (m/s)	3.2	2.8	3.4	7.5
Velocity Resolution (cm/s)	10	9	11	23
2^{nd} –Trip Height (km)	12.5	18.9	15.9	10.8
Estimated Sensitivity (dBZ at 5 km)	-49	-51	-36	-32

with the data of collocated radiometers or lidars, such as those available at the CART sites (eg. Mastrosov *et al.*, 1994; Frisch *et al.*, 1995; Intrieri *et al.*, 1995). It is essential to use full Doppler information from the radar in these applications. Fig. 4 displays the first three spectral moments in time-height format. Note the resolution and precision in the second moment data (lowest panel), which provide important information on turbulent processes occurring both within cloud layers and at cloud boundaries.

In addition to climate research applications, these radars have the potential to improve aviation safety by operationally monitoring detailed terminal area cloud conditions at civil and military airfields. Some of

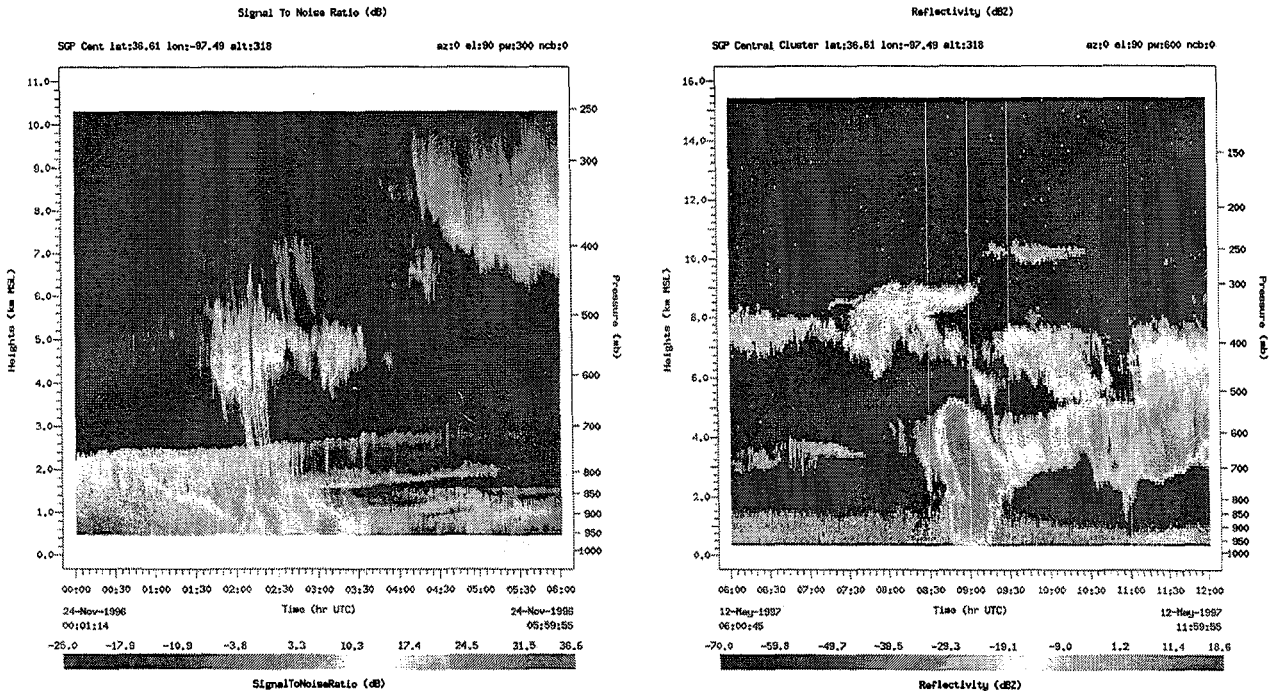

Fig. 3. Six-hour time-height histories of MMCR Signal-to-Noise Ratio (a) reflectivity (dBZ) measurements (b) at ARMS Oklahoma CART site showing multiple cloud layers, cloud types, and precipitation

the data also suggest an application for the radar to monitor cloud conditions conducive to terminal area and enroute aircraft icing programs and turbulence. An early bi-static non-Doppler K_a-band radar, AN/TPQ-11 (Paulson and Pettrocchi, 1970), was deployed by the U.S. Air Force in the early 1970s to support air operations, but it was decommissioned because of high maintenance costs. The cloud radar's innovative design eliminates the high maintenance costs experienced by the AN/TPQ-11, resulting in a cost effective, self-calibrating, operational cloud radar providing continuous and unattended operation. The Oklahoma radar has been operating the longest of the three profilers delivered to date. Its performance has been excellent, exhibiting a greater than 98% operational reliability over a fourteen-month period

ETL is constructing five of these radars in support of the ARM program and another one for the National Science Foundation's (NSF) Surface Heat Budget of the Arctic (SHEBA) program. When completed, the five ARM radars will be installed and operated at several locations worldwide. These include Barrow Alaska, USA, Lamont, Oklahoma, USA, Manus Island, Papua New Guinea, Nauru Island, and a "hot spare" in Boulder, Colorado, USA. The ARM program is considering the purchase of a sixth cloud radar to be installed on Krikiritimati (Christmas Island) in the central Pacific sometime in 1999. The SHEBA radar is currently operating on the Arctic ice sheet approximately 500 km north of Barrow, Alaska. This radar will be decommissioned and reinstalled on NOAA's newest research vessel, the R/S *Ronald H. Brown*, in the summer of 1999 where it will support various research initiatives in the Central Pacific and Indian Oceans.

To expedite the technology transfer under the CRADA, Radian will construct one (or more) of the ARM program's radars over the next several months. Radian will concurrently construct a production prototype radar incorporating design changes that address production issues as well as enhance system performance. From this production prototype, Radian will begin the manufacture of commercial systems that will become available in early 1999.

ACKNOWLEDGEMENTS

The U.S. DEPT. of Energy's Office of Health and Environmental Research sponsors development of the MMCR. The authors wish to thank Julie Poyton in the preparation of this manuscript.

REFERENCES

Frisch, A.S., and coauthors, 1995: Measurement of stratus cloud and drizzle parameters in ASTEX with Dopller radar and microwave radiometer. *J. Atmos. Sci.*, **52**, 2788-2799.

Intrieri, J.M., and coauthors, 1995: Multi-wavelength observations of a developing cloud system: the FIRE-II 26 November case study. *J. Atmos. Sci.*, **52**, 4079-4093.

Kropfli, R.A., and R.D. Kelly, 1996: Meteorological research applications of mm-wave radar. *Meteor. & Atmos. Phys.*, **59**, 105-121.

Martner, B.E., and R.A. Kropfli, 1993: Observations of multi-layered clouds using K_a-band radar. *Paper 93-394, Proc. 31st. Aerospace Sci. Mtg.*, AIAA, Washington, D.C., 8pp.

Matrosov, S.Y., and coauthors, 1994: Retrieval of vertical profiles of cirrus cloud microphysical parameters from Doppler radar and infrared radiometer measurements. *J. Appl. Meteor.*, **33**, 617-626.

Moran, K.P., and coauthors, 1998: An unattended cloud-profiling radar for use in climate research. *Bull Amer. Met. Soc.*, **79**, "in press".

Paulson, W.H. and P.J. Petrocchi, 1970: Operational utilization of the AN/TPQ-11 cloud detection radar. Air Force Cambridge Instrumentation Paper No. 166, 37pp.

Schmidt G., and coauthors, 1979: Complementary code and digital filtering for detection of weak VHF radar signals from the mesosphere. *Geosci. Electronics*, **GE-11**, 154-161.

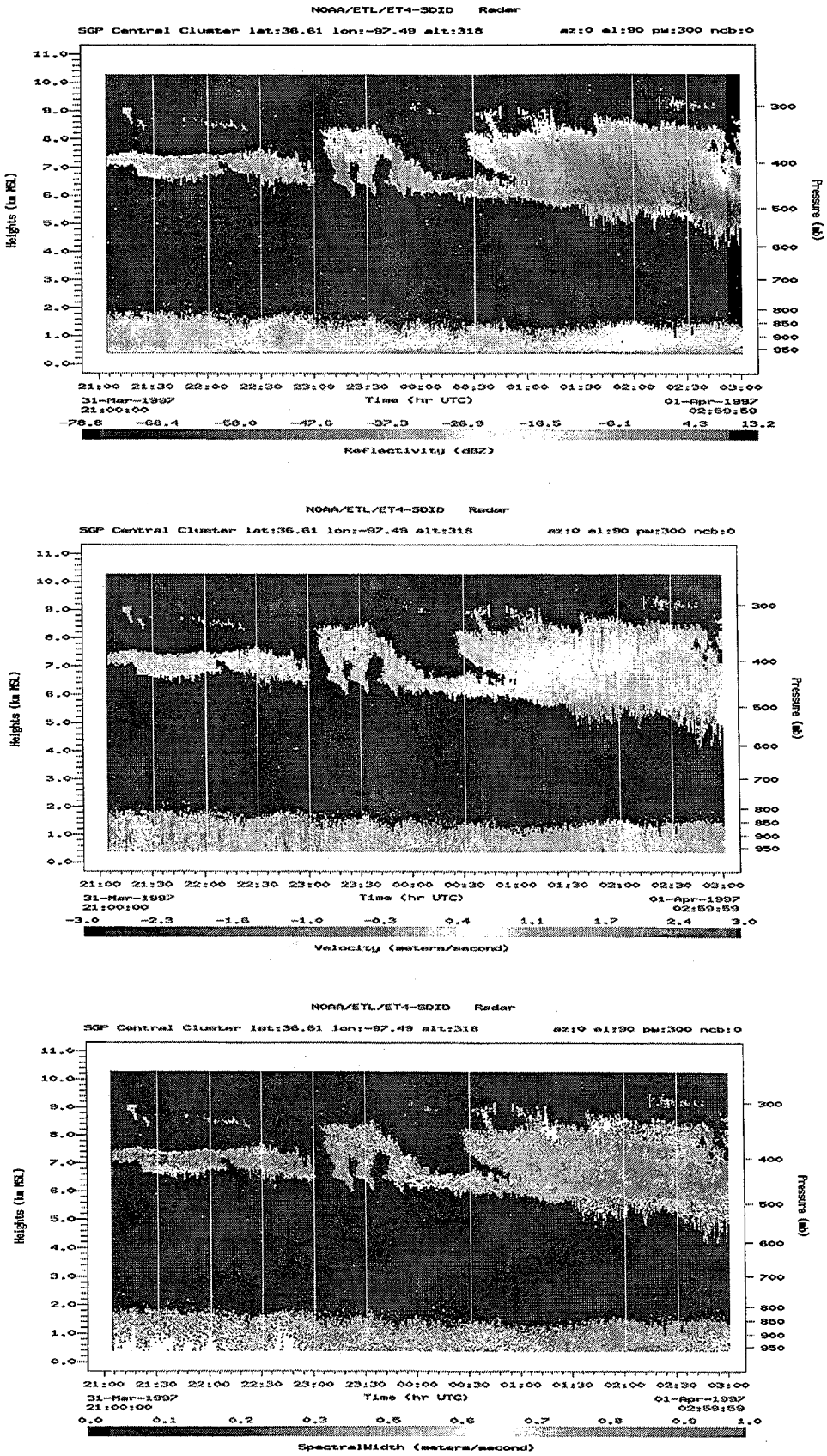

Fig. 4. Representative ARM cloud radar reflectivity (top), vertical velocity (middle), and velocity standard deviation (bottom) measurements at SGP for a 6-hour period beginning 31 March 1997. Data shown are for one of the two uncoded modes. No liquid stratus clouds are present, but these types of cloud observations are needed to properly retrieve liquid stratus cloud microphysical properties.

A System for Meteorological Analysis in Real Time (SMART) for Doppler Weather Radar

Donald Burrows, Enterprise Electronics Corp., Enterprise, Alabama, USA

Introduction

Modern Doppler radar systems acquire large volumes of data in short periods of time. This data consists of three or more different data moments collected from a large volume of space at intervals of a few minutes. To be of use to operational meteorologists the data must be made available in a meaningful manner often within a matter of minutes. The standard approach has been to automatically generate a series of pre-selected products, but inevitably there will be times when the desired product is not available. SMART (System for Meteorological Analysis in Real Time) was developed to provide a means of analyzing radar data in real time by a meteorologist without having to rely on the standard products. In addition it can be used as a means of training meteorologists to learn what products are available and how and when to use them. The products that are available range from simple reflectivity PPI displays to sophisticated products which process entire volume data files for storm tracking or severe weather detection. It was originally designed to work in conjunction with the Enterprise Doppler Graphics Environment (EDGE) radar controlling software, but an interface between the EDGE volume file format and the Tropical Rainfall Measurement Mission's (TRMM) Radar Software Library (RSL) makes it possible to use a wide variety of radar file formats including NEXRAD level II archive data.

User Interface

SMART has a mouse oriented graphical user interface written using the Interactive Data Language (IDL) version 5.0. The main screen for SMART is shown in Figure 1. The available volume data files are displayed in the **Current Volume** window and the user selects the file he wishes to examine. When a file is selected, a brief summary of the contents of the file is displayed in the **Volume Information** window.

Products, moments and elevations are specified using list file buttons. When the desired selections have been made then the **Load** button is pressed to perform the operation using the selected volume data file. Information about the product appears in the **Product Information** window.

The **Options** and **Color** buttons are used to customize product computation and display. The **Options** screen allows the default settings for product generation and screen display formats to be changed.

SMART uses a total palette of 256 colors divided into 13 groups of 16 colors each for moments and products, plus 32 colors for the underlay map and another 16 colors for overlays.

The **Print** button on the tool bar allows the user to print out any generated products. One option allows the **Print** button to be changed to a **Save** button which writes the product to disk as an image file rather than sending it to the printer.

The TRACK product identifies and stores information about storm cells in a storm history file. The **Storm Analysis** button provides access to much of the information in this file. The changes in location, height and reflectivity with time can be examined as well as the storm track and three-dimensional structure of the storm cell.

Product and Algorithms

The products, which SMART generates, are of three different types:

1. Products which display a single moment of radar data
2. Products which calculate new data values from the basic radar moments
3. Products which process a time series of radar volume data

The products in the first group are:

1. PPI
2. CAPPI
3. Base Reflectivity, BASE
4. Column Maximum, CMAX
5. Layer Reflectivity Average, LRA
6. Cross-Sections, XSEC

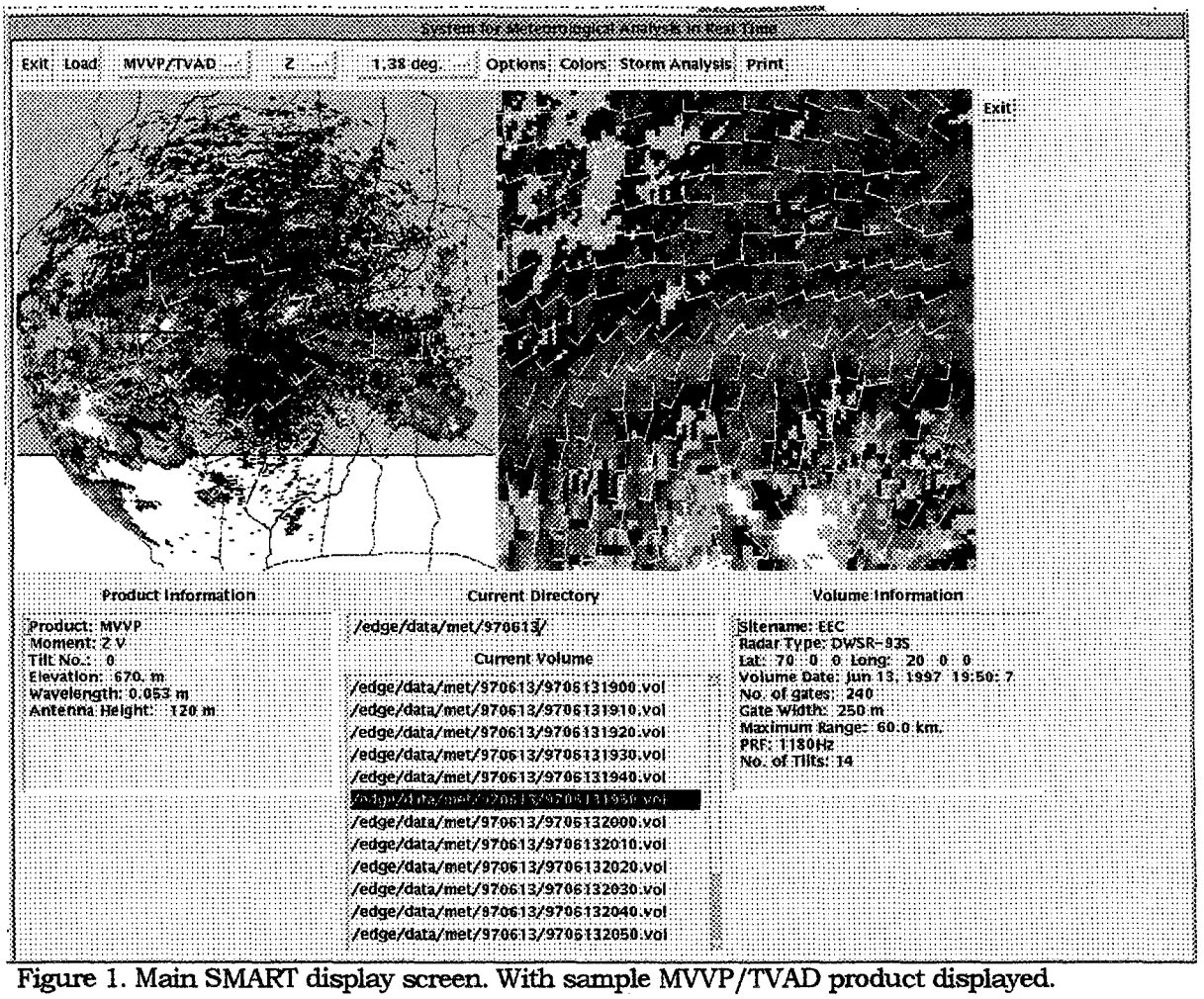

Figure 1. Main SMART display screen. With sample MVVP/TVAD product displayed.

The moments available for these products, depending on the radar system, are:

1. Uncorrected Reflectivity, U
2. Corrected Reflectivity, Z
3. Radial Velocity, V
4. Spectral Width, W
5. De-aliased Velocity, DV
6. Differential Reflectivity, Zdr
7. Radial Shear, S
8. Combined Shear, C
9. Hydrometeor Classification, H
10. Rainfall Rate, R

The products in the second group are:

1. Echo Tops, ETOPS
2. Vertical Integrated Liquid Water, VIL
3. Height of Maximum Reflectivity, HMAX
4. Gust Front, Microburst and Mesocyclone Detection, GUST
5. Hail Probability, Hail Prob
6. Hail Signal, HDR
7. Combined Moments Mapping, CMM
8. Modified Volume Velocity Processing / Tangential Velocity Assumed Display Wind Field, MVVP/TVAD
9. Velocity Azimuth Display Winds, VAD

The products in the third and final group are:

1. Storm Identification and Tracking, TRACK
2. Vector Displacement Forecasting Product, VECTOR
3. Precipitation Accumulation for 1,N, 3 and 24 hours, PCP_1, PCP_N, PCP_3, PCP_24
4. Precipitation Subcatchment Accumulation, SUBC

As there is not space to discuss all the algorithms, only a few key products will be described here.

TRACK – The TRACK product is generated using two algorithms, storm cell identification and storm history and tracking. A storm cell is defined by a reflectivity threshold value. Each elevation scan is searched for areas of reflectivity exceeding the threshold. These areas are matched vertically to areas from the preceding scan to link the areas and form cell volumes. When all scans have been processed, the total volume of each cell is calculated, together other statistics. Cells not exceeding the minimum volume threshold are eliminated from further consideration while the larger cells are passed to the tracking algorithm. In the history and tracking section, the new cells are compared with the storm data in the history file. Using location and size, an attempt is made to find the best match possible between the new storm cells and the older ones. New values for velocity and direction of motion are calculated when matches are found and the storm history file is updated. New storm cells that cannot be matched to old cells are assigned new storm numbers and appended to the end of the storm history file. This identification and tracking procedure is based on the procedure used in the TITAN (Thunderstorm Identification, Tracking, Analysis and Nowcasting) system, (Dixon and Wiener, 1993). A display product summarizing the results of the identification and tracking routines is then created.

GUST – At present this product consists of three separate algorithms that are processed together. Prior to running these algorithms the velocity data are sent for de-aliasing using the method developed for NEXRAD by Eilts and Smith (1990). The gust front and microburst detection algorithms are based on the Terminal Doppler Weather Radar (TDWR) algorithms, (Hermes et al. 1993).

1. The gust front detection algorithm searches the two scans, which are lowest in elevation, for radial convergence features with a linear shape.

In addition to shape, convergence and shear criteria have to be met as well.

2. The microburst detection algorithm searches the scan with the lowest elevation for compact shaped radial divergence features. Size, total velocity change, and peak wind shear criteria have to be met.

3. The mesocyclone detection algorithm searches all the scans in the volume data looking for rotation features that meet the criteria for mesocyclones established by Zrnic et al. (1985).

MVVP/TVAD –This is a double algorithm producing two displays. The first utilizes a Modified Velocity-Volume Processing (MVVP) based on Smith and Rabin (1989). Velocity unfolding is accomplished by using the method of Siggia and Holmes (1991). The analysis volumes depend on the maximum range setting for the radar. In the vertical they include 2 elevation scans and horizontally are arranged in annuli of width (maximum_range)/5. Three annuli are used encompassing the range from (maximum range)/5 to 4×(maximum_range)/5. Each volume extends 120° in azimuth and 12 volumes within each annulus are used centered at 30° intervals about the circle around the radar. This means that each volume has a considerable overlap with the adjacent volumes. The large range in azimuth seems to reduce some of the error in the wind velocity solutions. From the MVVP a display is produced showing the wind direction and speed at each volume center together with contours of divergence overlaid on a radar reflectivity PPI. An example is shown in the left-hand SMART window in Figure 1.

The result of the MVVP is a smoothed wind field. Many of the small-scale wind variations contained in the radial velocity measurements are lost. Some of this detail can be recovered by using a technique described by Takahashi et al. (1991), which they called Tangential Velocity Assumed Display (TVAD). Takahashi et al. used a single tangential wind component obtained from a Velocity Azimuth Display (VAD) to combine with the radial wind field to get estimated wind velocities. In the TVAD algorithm used in SMART, however, each MVVP wind is separated into its radial and tangential components and a standard kriging algorithm is used to produce a smoothed tangential wind component field. Interpolated values of the tangential wind component are then combined with interpolated values from the measured radial velocities to produce estimates of total wind velocity over a limited area, which can be selected by the user with a mouse. An example of the TVAD is shown in the right-hand window of the SMART display in Figure 1.

PCP/SUBC – Precipitation can be accumulated from a time series volume data products. The accumulation can be performed either for each pixel in the radar display range (PCP mode) or as a mean precipitation with in a user defined subcatchment basin (SUBC mode). The user has a number of options available to control the processing. A range setting of either 120 or 240 km can be used. The PPI, CAPPI, BASE, CMAX, or LRA product can be used with either uncorrected or corrected reflectivity. The Z-R conversion factors can be set by the user as well.

Summary

SMART is a program that has been developed as a radar analysis tool for meteorologists capable of analyzing data in a variety of radar data formats. In addition to standard radar products it is capable of being used in real time to provide sophisticated meteorological analysis of radar data. This analysis includes winds, thunderstorm identification and tracking, and gust front, microburst, and mesocyclone detection.

SMART received its first operational testing during the Nagano Olympics where the forecasters utilized the VAD and MVVP/ TVAD products as an aid in forecasting winds for the ski-jumping events.

References

Dixon, Michael, and Gerry Wiener, 1993: TITAN: Thunderstorm Identification, Tracking, Analysis, and Nowcasting – A Radar-based Methodology. Jour. Atmos. and Ocean. Technol., 10, 785-797.

Eilts, Michael D., and Steven D. Smith, 1990: Efficient Dealiasing of Doppler Velocities Using Local Environmental Constraints. Jour. Atmos and Ocean Technol., 7, 118-128.

Hermes, L., A. Witt, S. Smith, D. Klingle-Wilson, D. Morris, G. Stumpf, and M. Eilts, 1993: The Gust Front Detection and windshift Algorithms for the Terminal Doppler Weather Radar System. Jour. Atmos. and Ocean. Technol., 10, 693-709.

Siggia, Alan D., and Joseph M. Holmes, 1991: One Pass Velocity Unfolding for VVP Analysis. Preprints 25th Conference on Radar Meteorology, Paris, France, Amer. Meteor. Soc., 882-884.

Smith, Steven D., and Robert M. Rabin, 1989: Estimation of Divergence in the Prestorm Boundary Layer. Jour. Atmos. and Ocean. Technol., 6, 459-475.

Takahashi, N., H. Uyeda and K. Kikuchi, 1991: A Method to Describe the Fluctuation and Discontinuity of Horizontal Wind Fields by a Single Doppler Radar. Preprints 25th International Conference on Radar Meteorology, Paris, France, Amer. Meteor. Soc., 642-645.

Zrnic, D.S., D. W. Burgess and L. D. Hennington, 1985: Automatic Detection of Mesocyclonic Shear. Jour. Atmos. and Ocean. Technol., 2, 425-438.

Creating the North American Lightning Detection Network

J. Carr McLeod
Environment Canada
Canada

Jeffrey V. Tuel
Global Atmospherics, Inc.
United States of America

Project Description

Lightning kills an average of seven people and injures 60 to 70 others in Canada every year. It is also responsible for about 42 per cent of all forest fires, where damage to harvestable timber is enormous. For example, the cost of forest fires caused by lightning has been estimated at $US 9 billion annually between 1979 and 1993.

Environment Canada is in the process of implementing a $US 7.3 million lightning detection network that will result in better detection of thunderstorms across Canada and assist in earlier and more comprehensive weather warnings to the public.

The Canadian Lightning Detection Network (CLDN) will be seamlessly integrated with the existing US National Lightning Detection Network (NLDN), creating the North American Lightning Detection Network (NALDN). This will allow Canadian and American meteorologists to exchange weather data and work more closely together. In addition, the data collected provides commercialisation opportunities and will further support research on lightning and severe weather.

Global Atmospherics Incorporated owns and operates the US portion of the network and will supply and implement the new Canadian component of what is now referred to as the North American Lightning Detection Network.

In Canada, 81 remote sites will be built and deployed with sensing and satellite communications equipment. The entire NALDN, consisting of 186 sensors, will be operational by the summer of 1998.

Detection Theory

Lightning emits electromagnetic energy in a very wide range of bandwidths. As can be seen in Figure 1, the peak energy is transmitted in the higher end of the VLF (Very Low Frequency) spectrum. Unfortunately, VLF waves can and do reflect off of the ionosphere. Therefore, although they travel and can be detected at great distances, the location of the source of the waves cannot be known with great precision.

At the other end of the spectrum very high frequency waves will provide excellent location accuracy, but because of the low energies emitted in this band and the low propagation distances sensors must be closely (< 100 km) spaced.

The NALDN uses sensors that detect in the mid-range of the frequency spectrum shown in Figure 1. This allows a fairly sparse network density (about 600-km spacing in the Canadian network) while still producing high detection efficiency and unambiguous location accuracy.

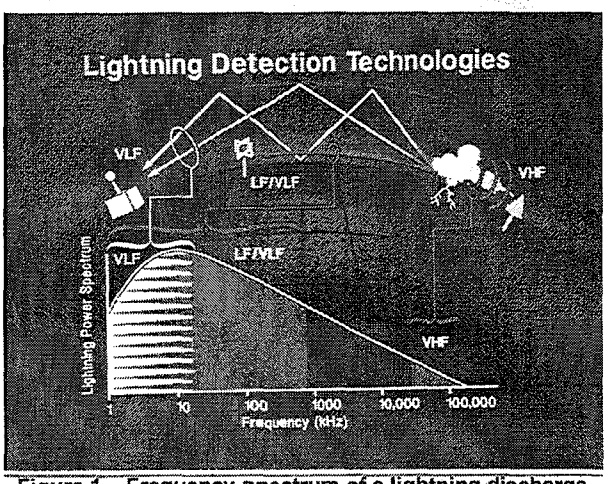

Figure 1 – Frequency spectrum of a lightning discharge

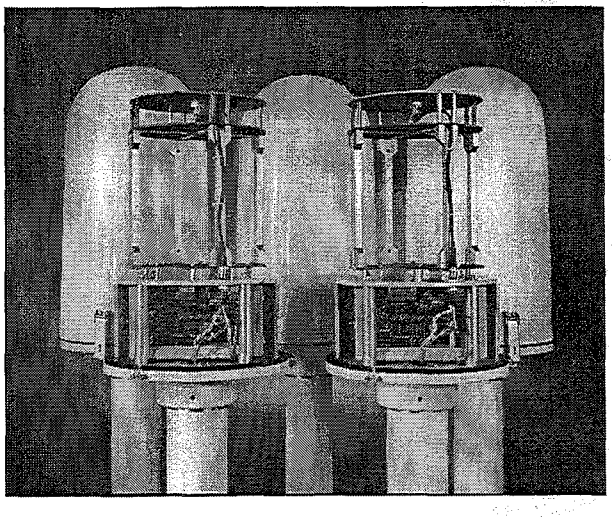
Figure 2 – IMPACT ES sensors

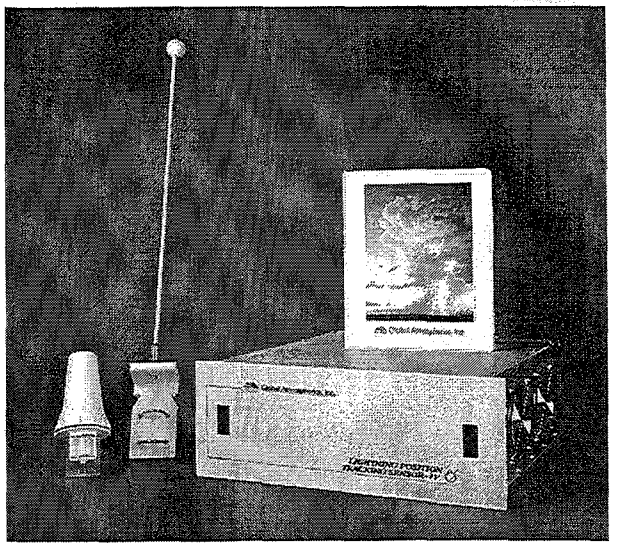
Figure 3 – LPATS IV sensor and hardware

Sensors Deployed

IMPACT ES

The next generation IMPACT (Figure 2) is an integrated lightning location sensor that combines the proven accuracy of Magnetic Direction Finding (MDF) technology with the beneficial elements of Time-of-Arrival technology to achieve greater location accuracy and detection efficiency than either technology could produce alone.

The IMPACT family of lightning sensors detects the presence of cloud-to-ground lightning events by employing both electric and magnetic field sensing. This unique combination of patented technologies allows GAI sensors to provide the most accurate estimates of location and peak currents of cloud-to-ground lightning discharges. All IMPACT sensors are self-calibrating and designed to perform continuous and comprehensive field diagnostics and are capable of automatically reporting their status to the central analyser. This built-in command and control intelligence minimises routine maintenance and diagnostic tasks while verifying the communications links and assuring user confidence in the system's reliability.

The real value of the IMPACT ES sensor is in its pinpoint accuracy, which commonly provides average system location accuracy of 500 meters or better. The high performance of the IMPACT Series is the result of Global Atmospherics' combined technology approach to lightning detection and location. All results are validated through extensive field-testing and independent third-party evaluations that no competitive system can match.

The IMPACT ES (Enhanced Sensitivity) sensor is the newest model of the IMPACT (Improved Accuracy from Combined Technology) sensor family. The IMPACT ES incorporates state-of-the-art electronics, increased range sensitivity, and waveform discrimination improvements to extend lightning detection efficiencies, particularly for low amplitude lightning events. Higher detection efficiency and better cloud and cloud-to-ground discharge discrimination provide end-users with more accurate and comprehensive information than ever before.

Lightning Positioning and Tracking Sensor – LPATS IV

These sensors (Figure 3) are based on a flexible, high speed multi-processor based transient analysis system capable of detecting and locating both cloud and cloud-to-ground lightning discharges. The basic sensor detects the wide-band VLF electric field signature of lightning discharges, extracts features from these transient waveforms, time-stamps this information with 50-nanosecond

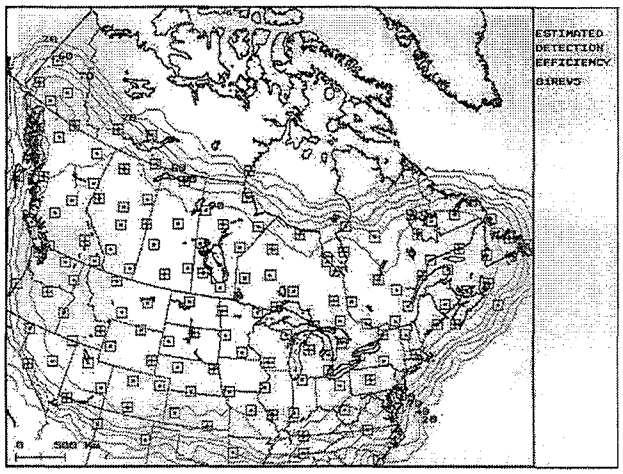

CLDN - Estimated Detection Efficiency (Rev-5)

Figure 4 – Network detection efficiency. Innermost contour is 90% detection efficiency.

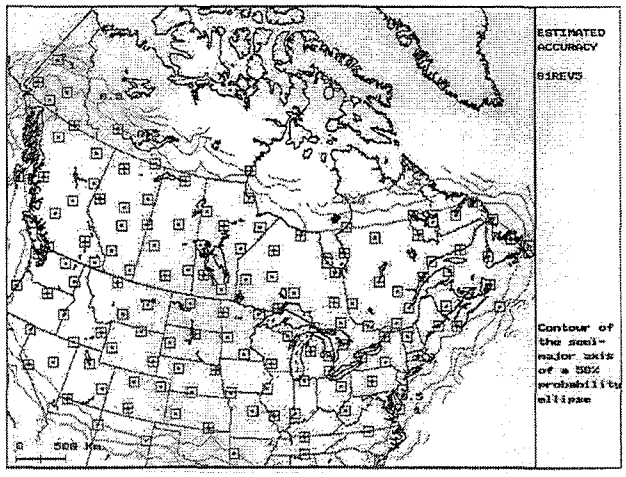

CLDN - Estimated Accuracy (Rev-5)

Figure 5 – Estimated location accuracy. Innermost contour is 500 m.

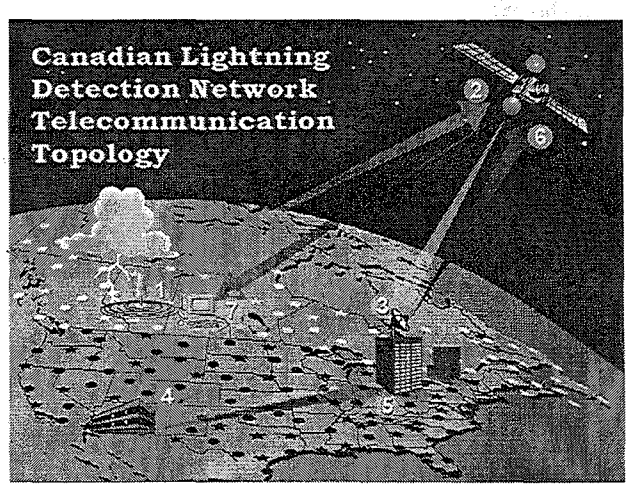

Figure 6 – Communications topology for the Canadian portion of the NALDN. Data from sensors (1) is sent via satellite (2) to a ground station in Toronto (3). The raw data is transmitted to GAI in Tucson (4) where it is merged with all other sensor data to produce lightning data solutions. These are transmitted back to the ground station in Toronto (5) and broadcast by satellite (6) to any number of end users (7).

resolution, and forwards the resulting information in digital form to the central analyser for interaction with information from other sensors.

The approach to lightning location using time-of-arrival only is to measure the absolute arrival time of the lightning discharge at each sensor, and to employ a location method which estimates both the location and time of the lightning discharge. Each sensor provides information that can be viewed as establishing a distance (range) of the discharge from the sensor, thus producing a circular locus of possible locations for each sensor. The radius of each circle is based on the difference between the estimated time of the discharge and the measured time of its arrival at the sensor site. A GPS clock in each sensor provides absolute timing of lightning events to a few hundred nanoseconds for correlation with other sensors. The initial location is determined by the central processor (LP2000), system using conventional hyperbolic intersections. When more than three sensors report, the method of circular intersections produces an optimised solution by employing a proprietary optimisation algorithm. The combination of high-speed multi-processors, patented waveform discrimination and location algorithms, along with cloud lightning detection capability makes the LPATS IV critical to the successful implementation of the NALDN.

Performance Requirements and Network Design

The network performance criteria are to detect 90% of all cloud-to-ground flashes and to locate the point of ground contact within 500 meters. These stringent criteria are needed to provide meteorologists with the data needed to assist forecast production. Demanding commercial clients in the USA and Canada such as forestry agencies, insurance companies and power transmission utilities also requires the criteria.

The planned detection efficiency is shown in Figure 4. It shows most of the USA and Canada within the 90% detection efficiency contour.

Location accuracy is shown in Figure 5. It shows most of USA and Canada within the (better than) 500 meters location accuracy.

Data Communications and Processing

Raw data from the remote sensor sites is transmitted via satellite to a central ground station (HUB). The data flow in the Canadian portion of the network is shown in Figure 6. Once the raw data is received at the ground station in Toronto, Canada, it is transmitted to the Network Control

Centre located in GAI's office in Tucson, Arizona. There it is combined with raw data from the US-based sensors and lightning solutions are produced. On average, each lightning solution is derived from raw data from 8-12 sensors that may be on either side of the Canada/US border.

Solutions are then returned to the satellite ground station and are uplinked onto a separate satellite data channel for broadcast. Users who subscribe to the data network require a very small aperture satellite (VSAT) receiving dish and controller hardware to receive the data. Software for the display of lightning data can be created by the user or purchased from GAI.

Data Users

The new NALDN will provide data to many users with a wide variety of applications. Meteorologists will make use of the data to help forecast severe weather. Power utilities will use the data to note where and when transmission lines will be adversely affected by lightning strikes. Forestry is also a large user of these data to assist in quick location of potential fire ignition and efficient fighting of forest fires.

Golf courses and other outdoor recreational institutions will use the data to warn their clients of impending danger. Infrastructure companies such as phone and gas pipelines have use for this data in a preventative or diagnostic sense.

Certain factories that are very power sensitive also need warning of impending lightning to allow a smooth and timely transition to back-up power.

The need for real-time lightning data for companies using or manufacturing explosives should be self-evident.

Finally, the aviation industry has significant need for these data for both in-flight and ground operations. Accurate lightning data and thunderstorm avoidance aid operations and crew safety, efficiency and passenger comfort.

A Large aperture scintillometer for routine observations of sensible heat flux

H.A.R. de Bruin, B.G. Heusinkveld, W.M.L. Meijninger and J.P. Nieveen

Department Of Meteorology
Wageningen Agricultural University
The Netherlands

1. Introduction

For various applications in meteorology, agriculture and hydrology, routine measurements of areally-averaged surface flux of sensible heat H are required. In addition, to verify or calibrate methods to derive H from satellite data these measurements are needed. Probably the best method to measure the area-averaged values of H is a network of eddy correlation stations. However, eddy-correlation equipment is still expensive and for maintenance and data handling a well-trained staff is needed. So there is still a need for a simpler approach.
Several studies carried out in the past decade have revealed that a remote-sensing technique, the scintillation method, is an attractive alternative for a routine observation of H (see e.g. McAneney, 1995; De Bruin *et al.*, 1995 and the cited papers). An important feature of this approach is that, because H is derived from the line-integral of the structure parameter of the refraction index, an average of H is obtained over a area formed by the path length of the light beam of the scintillometer and a line in the upwind direction. It is the objective of this paper to present some results of some measuring campaigns at Crete (Greece), in North Mexico (USA) and in New Mexico where a scintillometer has been used with a path-length of about 1 and 5 km. Comparisons with eddy-correlation equipment installed near the centre of the path will be presented also.

2. The Large Aperture Scintillometer (LAS)

A scintillometer is a device by which the turbulent intensity of the refraction index of air can be measured. To this purpose, a beam of light is transmitted over a (usually) horizontal path. At the receiver end the fluctuation of the light intensity is analysed. These fluctuations are occasioned by inhomogeneities of the refraction index along the path of propagation. The scintillometer used in the present study has been built at our department WAUMET. It has a large aperture-size of 15 cm (for that reason it is called a *large aperture scintillometer*), and the light source is a light emitting diode (LED: TIES16, Texas Instruments, Texas, USA) operating at a wavelength of 0.94 micron. The electronics are according to the design by Ochs and Wilson (1993). Improvements were achieved concerning the signal-to-noise ratio and sensitivity of electronics to temperature. The latter was tested in the field by comparing the analogue output with a digital data processing carried out on a data logger (Campbell Scientific Ltd, 21x). Note that this application of the Campbell 21X data logger is new. It allows data processing using only the demodulated signal from the detector in the receiver of the scintillometer. The demodulation requires only simple and cheap electronics.

3. Experimental

In this paper some results of three measuring campaigns will be shown.

a. Crete (Greece)
The field campaigns took place in 1995 in the Messara valley at Crete mid April through mid May and September. The receiver and detector of the scintillometer were installed at about 70 m above the valley floor at two opposite slopes of the mountains enclosing the valley. The path length was about 4.8 km. Near the centre of the scintillometer's light beam we installed a 3-D sonic anemometer (Gill instruments Ltd, Solent research), which with the sensible heat flux was obtained with the eddy-correlation method using the sonic temperature.

b North Mexico
LAS data have been collected at La Posa over the rangeland about 30- km south of Hermosillo (Sonora, Mexico) near a micrometeological mast of the Institute of Hydrology (IH) at which sensible and latent heat fluxes were observed using the HYDRA (eddy-correlation) system. Two sub experiments were performed, i.e. from 18 September - 17 October , and from 17 October - 24 November 1995. and The first period was wet (precipitation exceeded 100 mm) and the second period was dry.
In the first period the path length of the light beam was 3.2 km, but the light beam was not parallel to the surface. This non-ideal set-up was chosen to avoid saturation according to our calculation at 12 m it could be possible that around noon saturation of the signal could occur. At the effective height of 26 m saturation is unlikely. A correction procedure to account for the non-horizontally light beam.
During 10 October - 24 November the LAS was installed at the slopes of two hills at several kilometres from the HYDRA mast, but over similar terrain, at 30 m above the ground and a path of 1.1 km.

c. New Mexico (USA)
The third experiment was carried out in September 1996 at the Jornada experimental farm near Las Cruces, New Mexico, USA. The average light beam height of the scintillometer was 3 m and the path length was 675 m. At about 50 m from the receiver eddy correlation measurement were performed by the group of Dr. Larry Hipps and others.

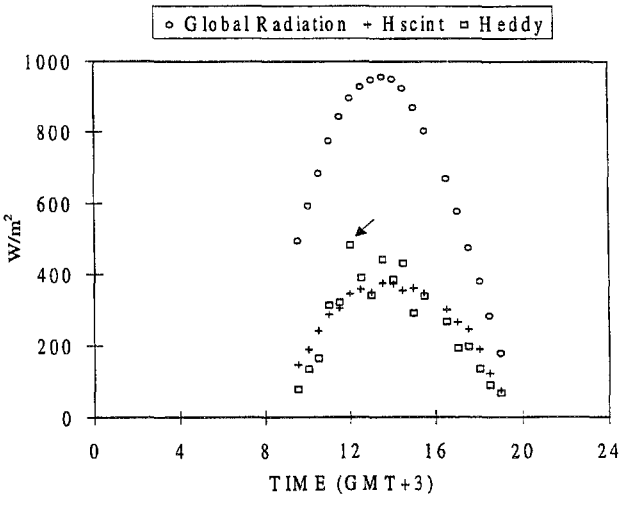

Figure 1. Daily course of H_{LAS} and H_{eddy} along with global radiation on 3 May.

4. Discussion and conclusions

In Figure 1 the diurnal course for 3 May of *H* is depicted, measured with the LAS and the eddy-correlation method at Crete. It is seen that the general agreement is good, but the LAS curve is much smoother than that of the eddy-correlation system. This is due to the fact that the LAS reveals a line-averaged value, whereas eddy-correlation refer more to a point.

In Figure 2 a similar plot is given for the New Mexico experiment. Also, here the agreement is good, except for the data around 14.30 hr. At that time scattered clouds were present. The eddy-correlation system was not located under the LAS beam, so it might be possible that by change the eddy-correlation experienced less clouds than the LAS.

The results for the two sub experiments in North Mexico are shown in Figure 3a and b, in which half-hourly values are plotted. The first refers to the wet and the second to the dry period. It is seen that the agreement is good.

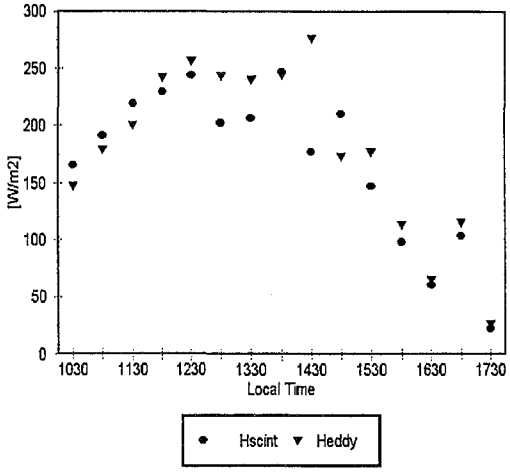

Figure 2. Daily course of H_{LAS} and H_{eddy} on 10 September.

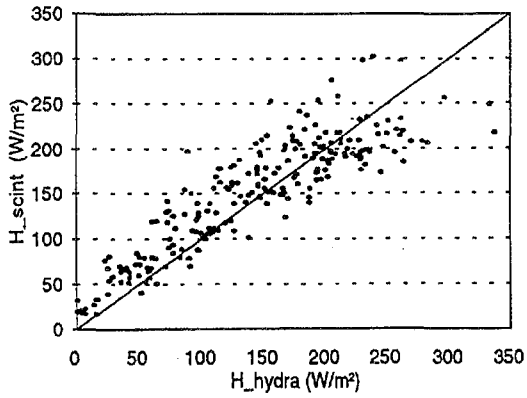

Figure 3a. H_{LAS} versus H_{eddy} during the wet period at North Mexico.

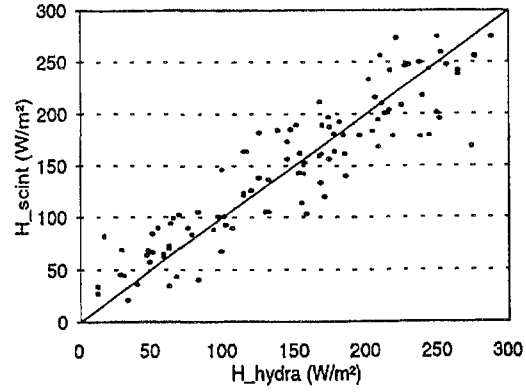

Figure 3b. As Figure 3a but now durig the dry period.

In Figure 4 the diurnal course of the sensible heat flux as determined with the scintillometer is depicted for a day in May and in September (Crete). It is noted that there was no rainfall in the area since March 1995, so one would expect that sensible heat fluxes increases during the season in virtue of the fact that the surface dries out and thus evaporation decreases with time The opposite is observed. This indicates that evaporation certainly did not drop during April to September, which must be due only to irrigation. Note that direct measurements of actual evaporation carried out by the Free University of Berlin confirm this picture: in September 1994 more evaporation was measured than in April/May 1995. One of the problems in the area is that for irrigation purposes too much water is extracted from the ground by which the ground water table dropped more than 25 m in the last decade. The example shown in Figure 4 illustrates a possible application of the long-path scintillometer. It can serve as a tool for a governmental body to check independently the total water use of an entire area with a relatively low-cost instrument.

One of the problems of testing procedures to derive H from those satellites is that with conventional methods only point ground-truth observations can be obtained. A long-path scintillometer yields H on the scale of a satellites pixel.
In the framework of a project supported by STW/GOA (projectnr. 790.541.33), which started in April 1997, and another EU-project (starting this year) the various applications of a LAS will be explored further in collaboration with potential users.

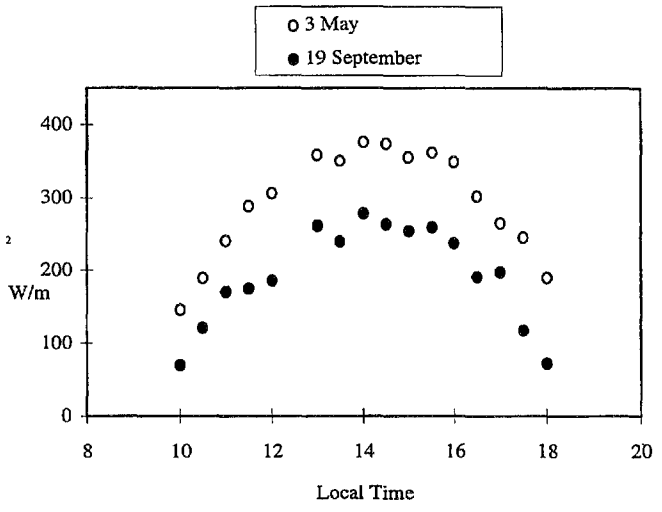

Figure 4. Diurnal course of sensible heat flux measured with the scintillometer on 3 May and 19 September 1995 at Crete.

6. Acknowledgement

The experiments at Crete, N-Mexico and New Mexico were partly sponsored by the EU (contract nr. EV5V-CT94-0466 and CI1*-CT94-0059) and by the Dutch Board for Remote Sensing (BCRS; the EOS project). We also would like to thank the support of Wim Kohsiek (Royal Netherlands Meteorological Institute, KNMI).

7. References

De Bruin, H.A.R., van den Hurk, B.J.J.M and Kohsiek, W. 1995: The scintillation method tested over a dry vineyard area. *Boundary-Layer Meteorology* **76**, 25-40
McAneney, K.J., Green, A.E. and Astill, M.S. 1995: Large-aperture scintillometry: The homogeneous case. *Agricultural and Forest meteorology'* **76**, 149-162.
Ochs, G.R. and Wilson, J.J. 1993: A second generation large-aperture scintillometer, Boulder, Colorado.

A multi-static Doppler weather radar to measure severe weather

J.J. VAN GORP[1] and L.P. LIGTHART
IRCTR, Delft University of Technology, PO. Box 5031, 2600 GA Delft, The Netherlands [2]

Abstract.
Airport operations and capacity are heavily influenced by the prevailing weather situation. Abrupt changes in the wind near the ground pose serious hazards to an aircraft during approach for landing or departure. The aircraft pilot and traffic controller may perceive different environment conditions. Inconsistent information between pilot and controller increases voice communications. Ad hoc decisions result often accompanied by negotiations. These will lead to delay and higher workload, especially in critical time periods of bad weather. One of the most dangerous weather hazard is wind shear. The hazard from wind shear is the resultant change in the lift of an aircraft. When sustained for a significant duration, the loss or gain in lift can lead to performance problems, especially hazardous at low altitudes. In this paper we propose to detect wind shear in the terminal area of an airport, by means of a cost-effective radar network. By advanced technology it is possible to worn the pilot well before a possible encounter.

1. INTRODUCTION

At Christmas Eve (25 December 1997) an airplane accident just missed to happen at Amsterdam airport. A Boeing 757, owned by the Dutch airliner 'Transavia', breaks its nose wheel and ended alongside the runway. The landing of the airplane took place in severe weather with wind from southwest, accompanied by strong wind shear. The nearly accident triggered discussions about choosing the right runway for bad weather conditions. The north-south runway (Zwanenburgbaan) was chosen instead of the northeast runway (Buitenveldertbaan). Under given conditions the last one has a headwind approach that used to be safer. The other runway was chosen because of environment claims: inconvenience of noise pollution for the dense population under the approach. The matter is under investigation office of the Dutch Department of Civil Aviation.
However, the nearly accident, ones more, urged for a more detailed a-priory information about the local weather conditions on an airport. The wind regime on the ground level is known by results of an extensive wind measurement network of wind vanes and anemometers, at and around the airport. Generally the upper air is sensed in a coarser way: at distance, the National Weather Service performs specific measurements, using Doppler weather radars, radio sondes and windprofilers. In case of the Faro aviation accident (Portugal, 1992, [1]) the upper air data were retrieved at a distance of about 300-km (at the Meteorological Office in Lisbon). It may be clear that it is more effective to measure the windfield as close as possible to the runways at an airport.
A Doppler radar can detect the wind velocity in only one direction (radial, alongside the radar ray). To measure the three-dimensional wind field a network of at least three weather radar's is needed. However, this is very expensive.
Using a bi-static radar concept, three dimensional wind fields can be measured with reduced cost. We propose to apply multi-static radar systems, compromising one transmitter and three or more receivers. In this paper we describe such a special radar system, for the measurement of severe weather phenomena for aviation.

2. SEVERE WEATHER IN RELATION TO THE SAFETY OF AVIATION.

Wind shear is a generic term referring to a wind change, direction and/or speed, over a small distance or in a little time difference. It is not a serious hazard for aircraft's en-route between airports at normal cruising altitudes. But in the terminal area low-altitude wind shear can be deadly for an aircraft, especially during take off or approach for landing. There are a number of sources of wind shear: temperature inversions, surface obstructions, and thunderstorms. Two special forms of low-altitude wind shear in relation to thunderstorms are: the "downburst" and the "gustfront". We will start our explanation with wind shear related to these hazardous meteorological phenomena.
The downburst is a strong short-lived outflow produced by strong thunderstorms. When this cold downward rushes of air reach the ground, they spread out, or burst, horizontally in all directions. Thus the downburst creates a locally intense divergent wind shear, illustrated in Fig. 1. Such a downburst can be imbedded in the thunderstorm heavy precipitation, but also within a benign-appearing virga. Those are wisps of precipitation streaming from the cloud but evaporates before reaching the ground. This makes a 'dry'-downburst more difficult to observe.

[1] Formerly: Royal Netherlands Meteorological Institute
[2] Phone: +31-15-278 78 60, Fax: +31-15-278 40 46, E-mail: J.J.VANGORP@ET.TUDELFT.NL, Internet: http://irctr.et.tudelft.nl

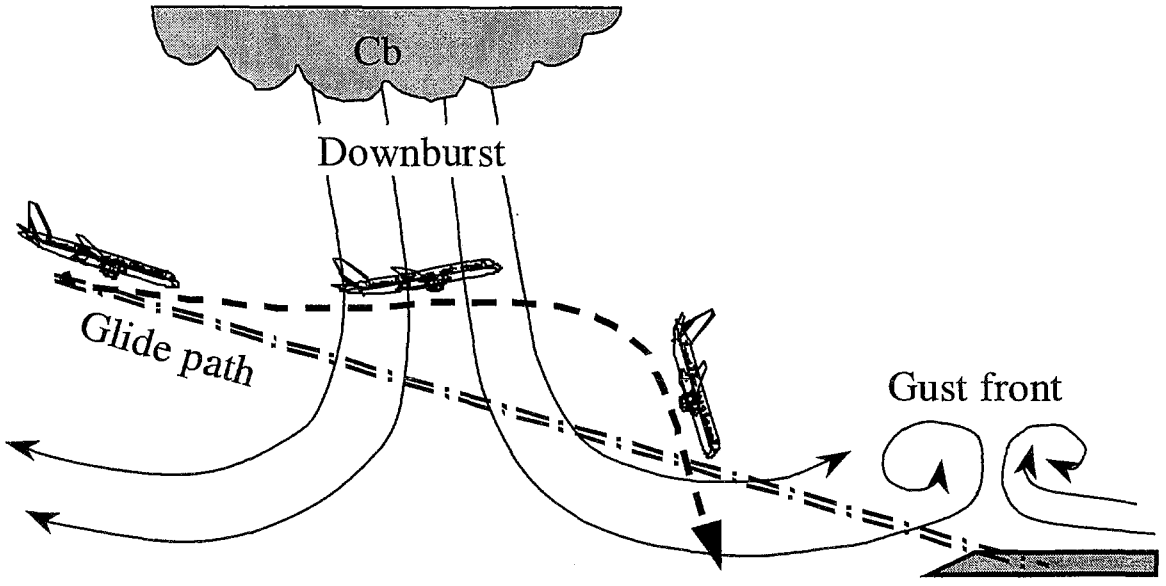

Figure 1. Downburst and gust front produced by a powerful Cumulonimbus and the impact on aviation.

The figure, above, illustrates a potentially hazardous encounter of a downburst by an aircraft on its final approach. Upon entering the downburst, an aircraft first experiences an increase in head wind. This increase causes the aircraft to fly above the glide slope. The pilot, who is unaware of the downburst, may attempt to return to the glide slope by reducing air speed and angle of attack. As the aircraft continues through the downburst, it encounters a strong downdraft and then a tailwind, which results in a loss of lift acting on the wings. The airplane falls beneath the glide slope and the pilot must increase power and angle of attack to bring the plane back to the glide slope. The aircraft, which requires a finite amount of time to respond to the controls, crashes if it is too close to the ground to recover. The lack of lift may cause a crash, even if maximum control and maximum power is used. The same mechanism can be applied to a take-off.
Another wind problem mentioned earlier, the "gust front", is also downdrafts related, as illustrated on the right hand side of Fig. 1. A gust front is formed at the leading edge of the outflow, where the cooler air from the downdraft meets the warmer air of the environment. Convergent wind shear pattern and very strong low altitude updrafts characterize them. An unsuspected pilot descending into the outflow will find his airspeed suddenly falls as he comes down into a tail wind during the last few hundred meters. Moreover gustfronts are mostly accompanied with severe turbulence, and that can cause fatal accidents. They do often cause a change of wind direction, necessitating a change of the runway in use. While downburst are short in duration and occur with little warning a gust front can last for hours as they travel away from the generating storm system.

3. DETECTION OF WIND SHEAR.

For the safety of aviation it is important to know the wind shear near-by the runway in an area of about 10 km. The horizontal surface wind is measured with a network of anemometers and windvanes. These instruments, which are mounted on 10-meter height masts, can analyze the wind regime near the surface. However, airplanes are flying at a higher level. Thus the wind in the upper air (0-1km) must be measured too. This can be done with traditional Doppler weather radars: the Doppler principle makes it possible to measure the movement of weather targets towards and away from the radar antenna (in radial direction). That implies the radar system must be located under the flight path looking across. Under very specific (and known) circumstances it is possible to measure the wind field aloft. However, such systems, like Velocity Azimuth Display (VAD) and Volume Velocity Processing (VVP), are based on linearly varying windfields. In convective storms this assumption is suspect. In fact, these approximated wind analyses is grown out of the restriction of having only a single radar system.
The following step is to apply two radars: dual Doppler radar systems. Again, this forms estimation: the vertical velocity must be computed from kinematics (mass continuity equation).
The ultimate solution for measuring the three-dimensional windfield is applying consequently three Doppler radars. The National Center for Atmospheric Research (NCAR, Boulder, CO, USA) and the University of Chicago (Prof. Fujita) has conducted such a research project, in a Joint Airport Weather Studies (JAWS) project low-level wind shear effects on aircraft performance. The fine structure of thunderstorm kinematics in the vicinity of the Denver (CO, USA) airport was examined. In this specific research project three independent scanning weather radars were

used. Deploying two or more conventional weather radar systems is very expensive in purchase and maintenance. Moreover, synchronizing the scan strategies of the individual radar's is very complex, if possible [3].

4. PROPOSAL FOR A MULTI-STATIC WEATHER RADAR TO DETECT WIND SHEAR.

The radar systems we mentioned before are of mono-static character, which means they have the same path for transmit and receive. By leaving this mono-static principle a considerable reduction in cost can be achieved. We propose to introduce the multi-static radar system, defined by the separation of transmit-axis and receive-axis. In Fig. 2 an example of such a radar system: one transmitter only and three receivers at different locations.

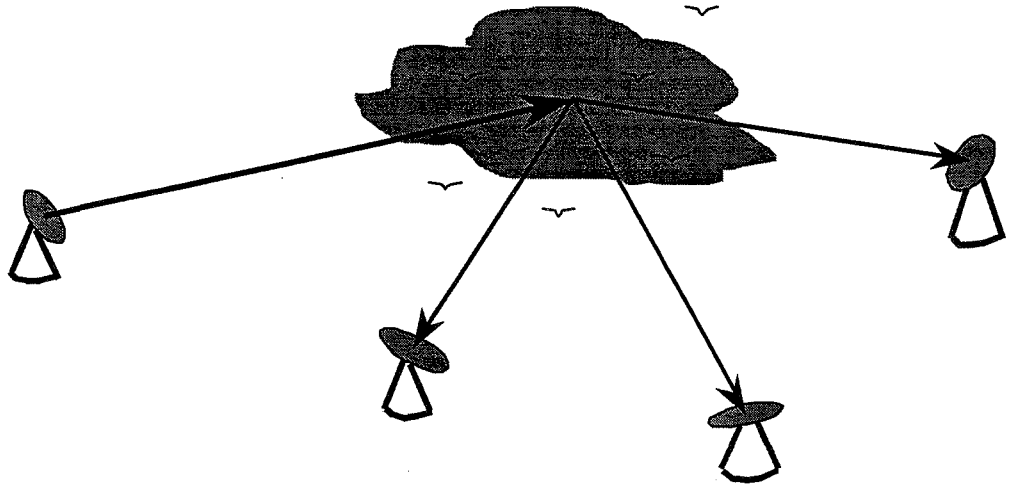

Figure 2. A multi-static weather radar system for the detection of the three-dimensional windfield.

The transmitter must operate within a very small beam width (pencil beam, ~1°) to retrieve the exact location of reflection. In contrary the receiver's antennas may have wide angles. That means wide in azimuth direction (60°), but limited in elevation direction (1°-30°). However, the low gain receive antennas will be highly contaminated by reflected radiation from the sidelobes of the transmit antenna. These adverse effects are reduced by introduction of more advanced radar technology: wide angle antennas with higher gain. Moreover, electronic arrays makes it possible to divide the receive antenna into several small angle ones. Coordination with the scanning transmit antenna can be controlled by electronic switching of the corresponding receive antenna sections. Electronic switching put into hand more rapid scanning scenarios as is the case with the traditional mechanical rotation of the radar antenna. This implies an important issue for detecting the fast changing weather situation. Within minutes a dangerous hazard may arise and rage itself out. Again, downbursts are very local and have a short lifetime.
Modulation of the transmitter pulse yields specific improvements: high range resolution (~20m), low minimum range (~200m.), accompanied with a reduction in transmit power (~100 W). This principle of pulse modulation reduces the maximum range (~50km), but that is not a handicap for measuring in the terminal area of an airport.
In the extreme case hundred percent modulation results in a FM-CW (Frequency Modulation-Continues Wave) radar. At the Delft University of Technology we have an outstanding experience in this radar principle [2], as well as with multi-static radar systems (in anti collision systems, with electronic arrays). The major disadvantage of FM-CW radar requiring two separate antennas (Tx and Rx) is eliminated gracefully in this proposal. The sensitive FM-CW principle makes it possible to detect and warn for bird's migration in the terminal area of an airport.
The installation of the multi-static receivers at different locations (and separated from the transmit antenna) demands for specific technical solutions of synchronization. Locking the (highly stable) frequency sources, of transmitter and receivers, makes it possible to maintain the necessary coherence. This can be done be linking the sites to the Global Position Satellite (GPS) system. A more accurate solution may be found in applying advanced telecommunication systems between the sites directly; e.g. by extremely high frequency radio transmission or by optical transmission via glass fiber cables. Research in this field is done at IRCTR.

5. WARNING FOR SEVERE WEATHER.

Last but not least, as result of the extensive measurements the pilot must be warned for wind shear hazards at the right moment and without misunderstanding. One picture says more then thousand words. A fascinating example forms the Three Dimensional Viewer (3DTV), in development at NCAR [4], see Fig. 3.

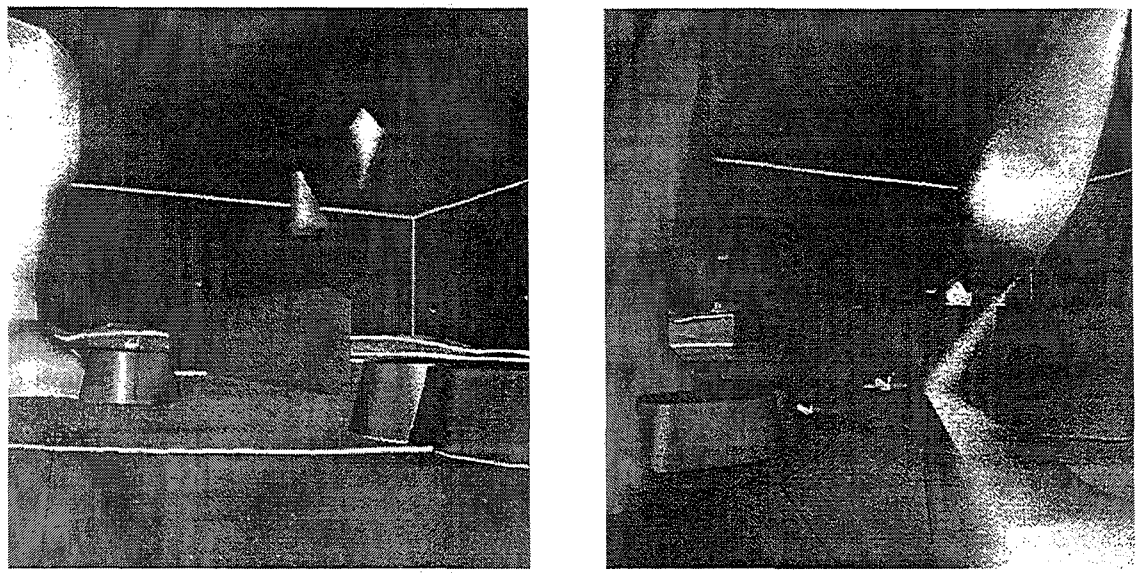

Figure 3. Approach to runway with precipitation (white), microburst (red) and gust fronts (blue).

It enables an intuitive understanding of dynamic weather phenomena, better communications among users (especially flightcrew and ATC), and its impact on a terminal area or en route airspace. It integrates topographical data from LANDSat imagery with ATC radar data and information from a variety of weather sensors. The result is displayed in high-resolution images and in real time. The virtual environment can be viewed from approach or departure end of the selected runway. By transmitting the image to the cockpit, a pilot could find himself immersed into the virtual environment of the terminal area

CONCLUSIONS

Three-dimensional measurement and display of wind shear would minimize traffic disruption and supervisor workload by providing advance-warning capability. This would permit air traffic supervisors to reroute before the severe weather take place with attendant workload reduction and capacity benefits.
The improvement of the safety of aviation, in relation to the weather conditions, is not a one-party problem but of all world urgency, so cooperation between the authorities of airports and airlines of different countries is necessary. In order to meet future airport capacity, efficiency, and safety requirements, new techniques and systems had to be introduced. Above a proposal to measure local severe weather at an airport with the application of currently new radar and telecommunications technology.

ACKOWLEDGMENT

The authors would like to thank Bill Meyers of NCAR and Joshua Wurman of the University of Oklahoma for carry over their experience.

REFERENCES.

[1] Van Gorp, J.J. and L.P. Ligthart, 1994: To be are not to be a microburst, that is the question. *27th International Conference on Radar Meteorology*, Vail, USA, AMS, 536-538.

[2] Van Gorp, J.J. and L.P. Ligthart, 1994: An operational weather radar network based on FM-CW. *COST-75 International seminar on advanced weather radar systems*, Brussels.

[3] Wurman, J., 1994: Vector Winds from a Single-Transmitter Bistatic Dual-Doppler Radar Network. *Bulletin of the American Meteorological Society,* Vol. 75, No. 6, June 1994.

[4] Annual Report-1992, *National Center for Atmospheric Research*, Boulder, USA.

Microwave radiometer for profiling tropospheric temperature, water vapor, and cloud liquid water

FREDRICK SOLHEIM and JOHN R. GODWIN

Radiometrics Corporation, Boulder, Colorado

Summary. An advanced microwave radiometer for profiling atmospheric parameters is described in this paper. The innovations of the radiometer system, including utilization of a stable frequency synthesizer and the calibration system, are described. Accuracies are significantly improved over current designs. Application to remote detection of aircraft icing is discussed. Modeled performance and comparisons with radiosondes are presented.

1 Introduction

Radiosondes are still the fundamental method for atmospheric temperature, wind, and water vapor profiling. Because of their cost, sparse temporal sampling, and logistical difficulties, a better technology has been sought for decades, but until now, no accurate continuous all-weather temperature and water vapor profiling technology has been demonstrated. Laser radars (lidars) and Fourier transform infrared spectrometers can profile temperature and water vapor, but not beyond cloud. Radar Acoustic Sounding Systems (RASS) can profile virtual temperature, but is limited in height. The radiometric temperature and water vapor profiler described herein gives continuous unattended profile measurements in all sky conditions (except precipitation), and also has the capability to profile cloud liquid water, a capability absent in radiosondes. Except for *in situ* aircraft measurements and values inferred from radar reflectivity by estimating droplet distribution, there are no other sensor systems that can profile cloud liquid water.

Under funding from the United States Department of the Army and the Department of Energy we have developed an advanced passive profiling microwave radiometer design based on a highly stable tunable synthesized local oscillator in the receiver. This design overcomes errors induced by receiver frequency drift in other current generation designs, while allowing observation of a large number of frequencies across wide tuning ranges. The number of eigenvalues in the radiometer observations, and therefore the information content, is thereby maximized. The result is more accurate and resolute atmospheric temperature, pressure, water vapor, and cloud liquid profiles than currently deployed microwave radiometers. Temperature profile rms errors are nearly halved relative to 4-channel Gunn-based radiometers (Solheim, 1995; Han and Thomson, 1994; Askne and Westwater, 1986).

Applications for this passive profiling capability include weather forecasting and nowcasting, detection of aircraft icing and other aviation related meteorological conditions, determination of density profiles for artillery trajectory and sound propagation, refractivity profiles for radio ducting prediction, corrections to Very Long Baseline Interferometry (VLBI) and GPS measurements, atmospheric radiation flux studies, and measurement of water vapor densities as they affect hygroscopic aerosols and smokes.

2. Advantages of the receiver design

The radiometer design is an advance over other current designs in several respects. The previous state of radiometric art was to employ Gunn oscillators as the local oscillators for the receiver mixer. A separate oscillator was generally utilized for each frequency to be observed, imposing a practical limit on the number of frequencies observed. Additionally, Gunn oscillators drift in frequency, even when temperature stabilized, and can induce errors in the retrieved temperature as large as 1C. The highly stable frequency synthesizer utilized here eliminates frequency drift, and allows a large number of frequencies to be observed. The number of eigenvalues, and therefore the information content of the observations, is thereby maximized.

Dicke-switched hot and ambient temperature loads are commonly used in radiometers as a calibration reference. This system switches from antenna to reference load, thereby excluding the antenna from the calibration. Dicke switches are ferrite waveguide devices with imperfect switching qualities, having isolation of about 20 dB and an "on" insertion loss of about 0.4 dB. They can therefore be a source of receiver noise and error. Hot loads are generally operated at 100 to 150C above ambient, with an ambient load giving a second measurement for determining the gain and offset of the receiver. As shown in Figure 1, although the load temperatures can be known very accurately, non-square-law be-

havior of the detector and signal compression of the receiver at higher antenna temperatures (higher signal values) can cause nonlinear behavior that can induce an error when the calibration is extrapolated to the range of sky observables.

We utilize a highly stable noise diode and an ambient target as a calibration reference. Although the noise diode raises the antenna temperature to well above ambient by injecting power into the antenna circuit, we utilize tipping curves or a second liquid nitrogen target at 77K for calibration of gain and offset of the radiometric receivers.

This calibration is then transferred to the highly stable noise source for field use. The nonlinearity of the receiver is present in both this calibration transfer and in sky observations, is common-mode to both measurements, and is therefore cancelled. The antenna system is included in the calibration, and the fundamental calibration spans the range of sky observables rather than being extrapolated.

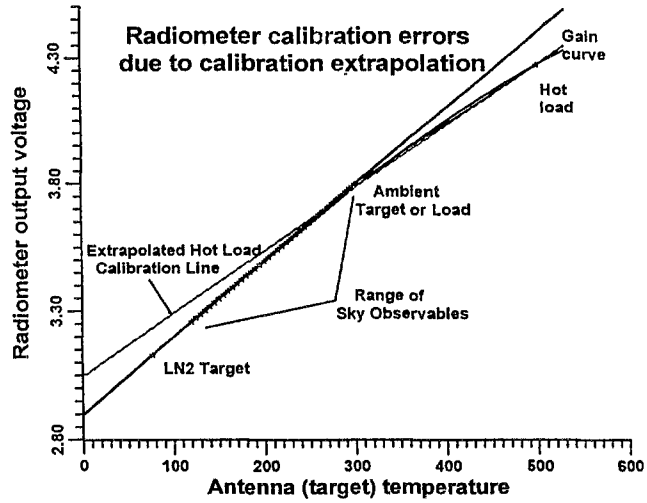

Figure 1. Cold target absolute calibration minimizes extrapolation errors and receiver nonlinearity.

3. Modeled profile results

The rms errors of the radiometer calculated from a study of 10 years of radiosondes at three sites are shown in Figure 2. This study, and the mathematical methods utilized to invert radiometric spectral information into atmospheric profiles, are described in Solheim et al., 1998. Several profiles retrieved by various inversion methods are shown in Figure 3. Note that, although surface inversions are well resolved, passive remote sensing will not resolve elevated inversions very well. Also, sensitivity is greatest near the surface, and diminishes with altitude, with the practical altitude limitation of 7 to 10 kilometers. At these higher altitudes the profiles tend toward a climatological and seasonal mean value.

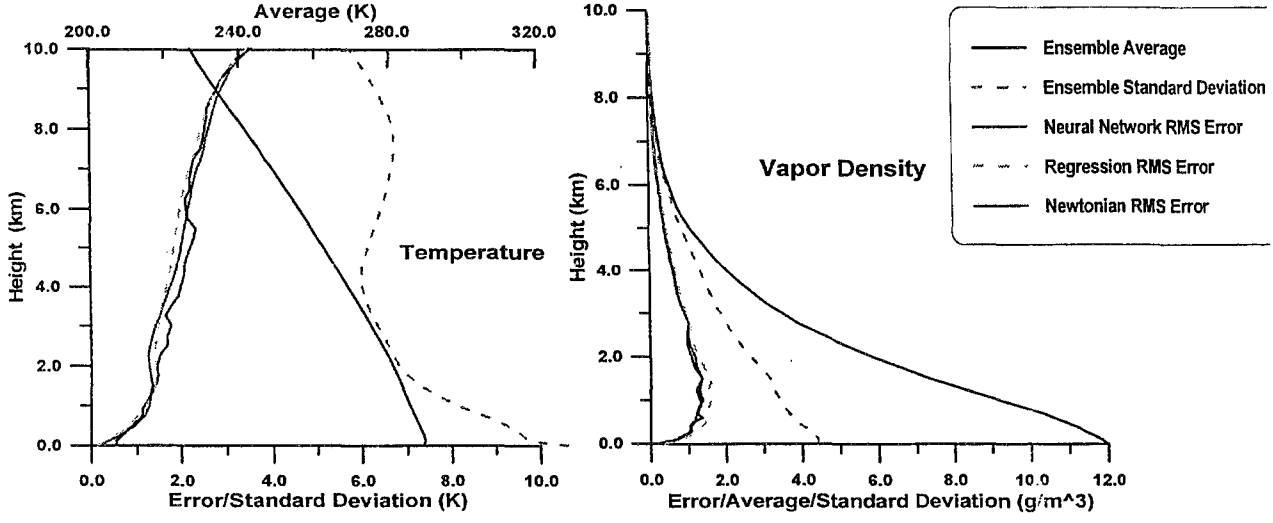

Figure 2. RMS errors of retrieved temperature and water vapor profiles. Also shown is the standard deviation of the set of soundings and the average sounding profile.

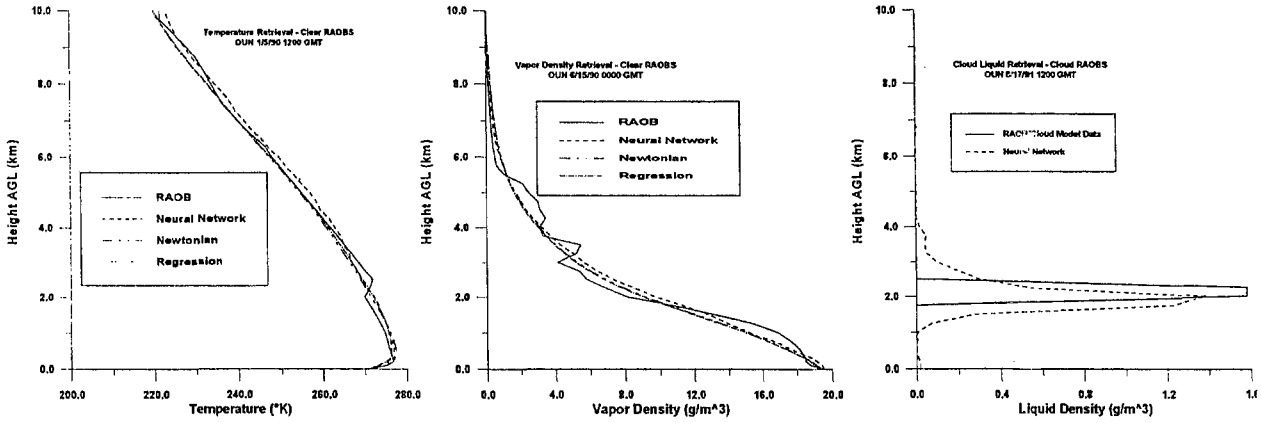

Figure 3. Sample profiles of temperature, water vapor, and cloud liquid water retrieved by modeling instrument performance.

4. Comparisons with radiosondes

Figure 4 show examples of the temperature and water vapor profiles retrieved by our prototype radiometer compared with concurrent radiosondes at the National Weather Service site in Denver Colorado.

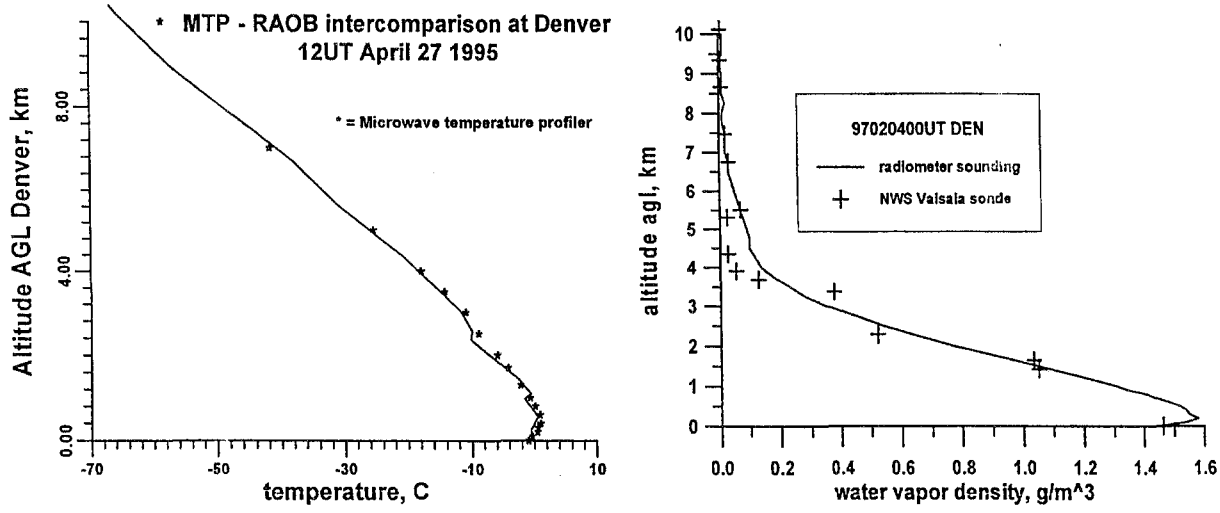

Figure 4. Actual temperature and water vapor profiles compared with concurrent National Weather Service soundings.

5. Detection of aircraft icing conditions

One of the capabilities of a multifrequency multiwaveband microwave radiometer is the detection and profiling of supercooled liquid water. Aircraft icing occurs in the presence of supercooled liquid water droplets. Because such droplets are generally very small in size, they are not easily detected by radar. Because this radiometer can profile temperature, water vapor, and cloud liquid, it can determine the presence and location (altitude) of supercooled liquid water by two separate mechanisms:

(1) The saturation vapor pressure can be calculated from the temperature profile, and when the measured vapor pressure goes to saturation, cloud liquid is present.

(2) The cloud liquid profiling capability defines the region of liquid water, while the temperature profile determines if the water is supercooled.

If the measured temperature profile shows that the water is at a temperature below freezing, it is an aircraft icing hazard. . Shown in Figure 5 at right is a case of aircraft icing wherein the pilot lost control of the aircraft and crashed into Denver Colorado. National Center for Atmospheric Research aircraft were probing this winter storm and defined the icing layer between 2400 and 3300 meters above sea level. The RAOB did not accurately define the cloud layer because of deficiencies in the humidity sensor; the measured water vapor density should have been at saturation in the cloud layer. Additionally, radiosondes cannot detect liquid water.

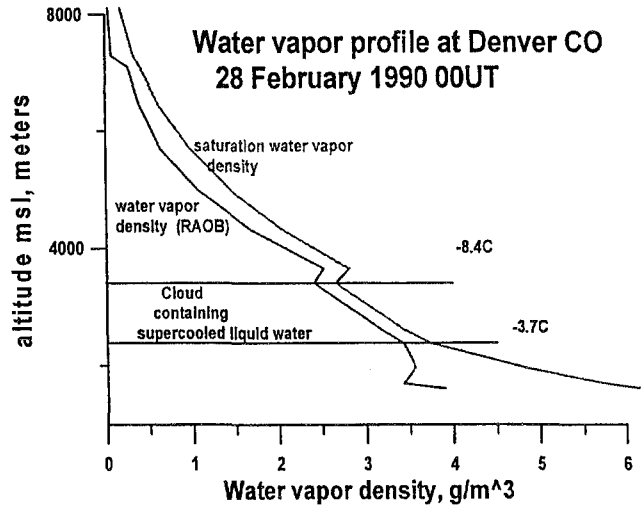

Figure 5. Measured water vapor profile and calculated saturation vapor density profile from radiosonde sounding at Denver Colorado

6. Conclusions

We have described an advanced radiometer for passive remote sensing of atmospheric temperature, water vapor, and cloud liquid profiles. We have shown that the radiometric observations can be inverted into accurate tropospheric profiles. The radiometer is based on a highly stable synthesized local oscillator that allows a large number of frequencies to be selected. The atmospheric profiles are useful for weather and artillery trajectory prediction, aircraft icing hazard and radio ducting detection, astrogeodetic measurements, and atmospheric radiation flux studies.

Acknowledgments.

This study and subsequent hardware development was supported by the U.S. Army Research Laboratory White Sands Missile Range and the Department of Energy under Small Business Innovation Research funding.

References

Askne, Jan I. H. and Ed R. Westwater, 1986: A Review of Ground-Based Remote Sensing of Temperature and Moisture by Passive Microwave Radiometers, IEEE Transactions on Geoscience and Remote Sensing, Vol. GE-24, No. 3.

Han, Y. and Dennis W. Thomson, 1994: Multichannel Microwave Radiometric Observations at Saipan during the 1990 Tropical Cyclone Motion Experiment, Jour. Atmos. and Oceanic Technology, Vol. 11.

Solheim. F., J. Godwin, E. Westwater, Y. Han, S. Keihm, K. Marsh, and R. Ware, 1998: Radiometric Profiling of Temperature, Water Vapor, and Liquid Water using Various Inversion Methods, Radio Science (in press).

Solheim, F., 1995: Ground-based microwave atmospheric temperature and water vapor profiles, Proceedings of the 33rd Aerospace Sciences Meeting and Exhibit, Reno, NV.

Corresponding author:
Fredrick Solheim
Radiometrics Corporation
2840 Wilderness Place Unit G
Boulder, CO 80301
(303) 449-9192 fax: (303) 786-9343
email: solheim@radiometrics.com

STATIC WINDSENSOR
FOR SURFACE-BASED REMOTE SENSING SYSTEMS

Ernesto Burgos, Kurt Nemeth

Wilh.Lambrecht GmbH
Friedländer Weg 65-67
D-37085 Göttingen, Germany
Tel. (++49) (+551) 49 58 0
Fax (++49) (+551) 49 58 312
email wilh.lambrecht@t-online.de

1 INTRODUCTION

The LAMBRECHT Static Wind Sensor incorporates an innovative wind velocity and direction measurement system that detects thermal field variations (TFV) caused by the wind flowing past a heated cylinder.

The TFV technique is very accurate, responds rapidly to wind changes and has a zero starting threshold. Most importantly, the instrument requires no calibration, no bearing replacement or any other periodic maintenance to maintain its accurate performance.

The STATIC WIND SENSOR is a compact and completely self-contained meteorological instrument. All components are enclosed in a sealed, ice-free and weather-proof cylinder. The package contains a micro-processor for determining weather parameters, performing self-diagnostic test and transmitting data and status information. The system is an intelligent device capable of transmitting data over an RS-485 serial digital interface.

2 GENERAL

The Automatic Digital Weather Station, rugged and reliable, all solid-state with no moving parts, is intended for meteorological services and naval use but will also find application in the fields of air pollution control, environmental sciences and industry in general. With no moving parts, the sensor features a high professional quality, both in its rugged construction and in the electronics design. For cold climates a sensor heater version is available.

3 THEORY OF OPERATION

Unique to the Meteorological Sensors is its patented Thermal Field Variation (TFV) technique for measuring wind speed and direction. The station detects thermal field changes caused by wind passing by a heated cylinder exposed to the winds. This principle is easily demonstrated when using a wet finger to sense the wind speed and direction. The TFV transducer is a small, rugged cylinder with several minute vertical transducers mounted symmetrically around its outer surface. The cylinders core is heated to a controlled, constant temperature of 50 °C above the ambient temperature. When there is no wind, the cylinders thermal field radiation from the central heated core is homogeneous and all the vertical transducers sense the same signal level.

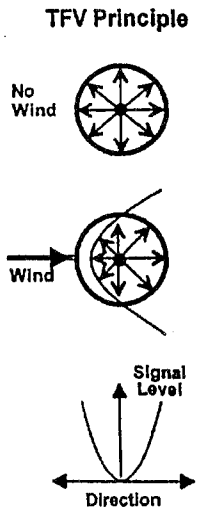

When the wind blows, the cylinders thermal field changes. Because the TFV transducers are cylindrically shaped, its thermal field forms a symmetrical parabola shape in the wind. The signals from the vertical sensors are used by the microprocessor to determine the parabolic form and drive the wind direction. The amount of energy required to maintain the cylinders central core at a constant temperature is the main information used to determine wind velocity. Since thermal radiation and convection are influenced by ambient temperature and barometric pressure, measurements of these parameters are used in the wind determination. Even under extreme meteorological conditions or low wind velocity.

4 TECHNICAL DESCRIPTION

The Static Wind Sensor is an all solid-state design with no moving parts. It contains five main elements: 1) transducers, 2) signal conditioning, 3) digital communications interface, 4) DC power supply, and 5) weather-proof enclosure.

The sensors transducers consist of TFV wind transducer, a thermistor temperature measuring device and a silicon piezoresistive absolute pressure transducer. The signal conditioning circuits transform the transducer signal into an analog form for digital conversion by the internal microprocessor. The signals are samples every 10 msec, compensated or corrected, and converted into measurement units. In addition to data acquisition, the microprocessor handles data communications and performs continuous tests on all elements of the instruments. This self-testing allows the station to identify, diagnose and report any failure without human intervention.

The transducers, conditioning circuits and power supply are packaged in a sealed, completely weather-proof cylindrical enclosure. The enclosure is made from non-corrosive materials and is coated with a protective, powder-baked enamel finish.

Functional block diagram

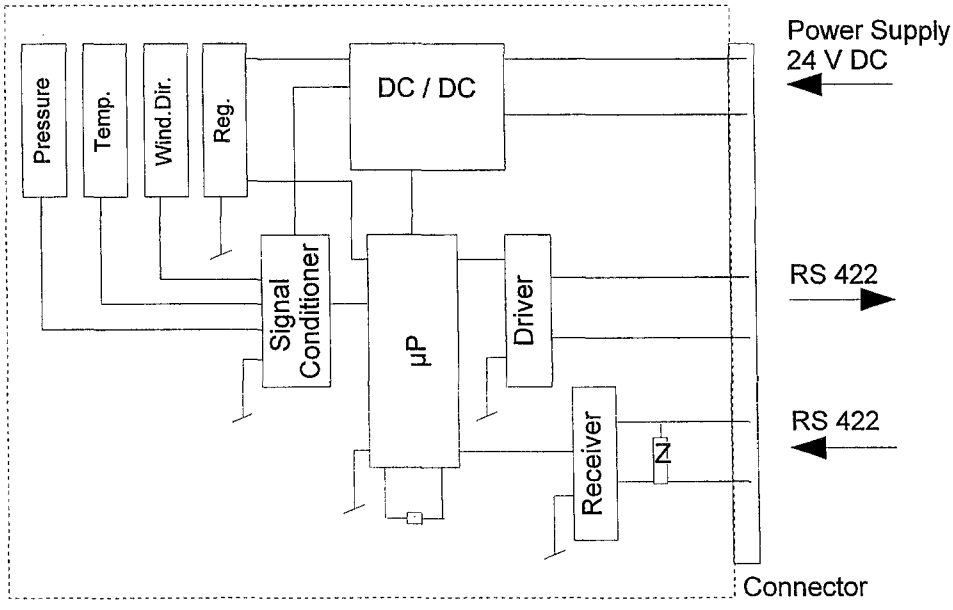

5 PERFORMANCES & MEASUREMENTS

	Functioning range	Resolution	Accuracy*
Wind speed	0 to 50 m/s	0.1 m/s	±(5 %+0.5 m/s)
Wind direction	0 to 360 °	1 °	±5 °

* These values are true for the results between -1.50 and +1.50, according to the Gauss law distribution, which represent 87 % of them.

Temperature range:	-40 to +60 °C	
Pressure range:	600 to 1100 mbar	
Power consumption:	at 0m/s	< 5Watt
	at 50 m/s	approx. 20 Watt
	at power on	approx. 30 Watt

6 DATA COMMUNICATION

The electronic interface meets the requirements of EIA RS-422 at 9600 baud. This type of interface provides complete immunity against interference due to cable lengths and common mode voltages that might otherwise be troublesome. The sensor is capable of transmitting data over cable lengths exceeding 1.200 meters (4.000 feet). The RS-422 signal is easily converted to RS-232 for connection directly to the Com port of the data acquisition and processing system SYNMET.

6.1 SYNOP Code generation

SYNMET generates the weather reports: SYNOP / METAR / SPECI.
It works in two operating modes: 1) on request at predefined time or 2) in active dialing mode with time schedule.
The weather reports are sent out with different communication units: GSM-Modem / telephone modem, satellite modem

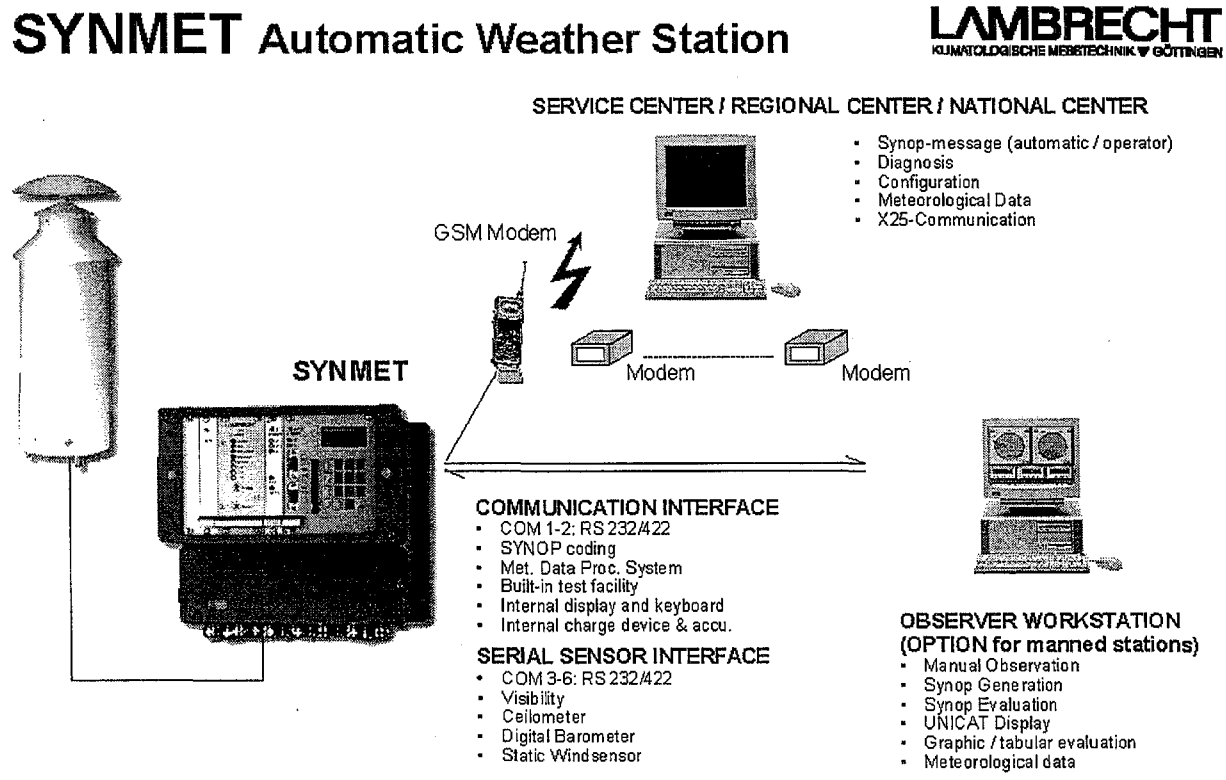

7 SYNMET TECHNICAL OVERVIEW

7.1 Features

- 2 communications ports
  (Station PC and modem)
- Real time clock:±30 s / month
- Power consumption: approx. 1 W
- Watchdog
- Multilayer board with EMV layers
- No potentiometers, no jumpers
- Reparable IC technology (no SMD technology)
- Measured value collection with precise internal reference measurement and automatic line-up
- 12 analog inputs*)
- Power source: 1/10 mA
- Res. meas.: 125/250/500/1250/2500/5000 Ω
- Programmable differential amplifier:
  50 mV/1.25 V/2.5 V/5 V/±25 mV/±2.5 V
- 3 digital inputs
  High/low level: 0.5...50 V
  Frequency: 10 kHz
  Proximity switch: according to Namur
- 2 digital status inputs
- 4 serial sensor interfaces
- LC-Display and keyboard
- Solar power system and uninterruptable power supply
- Sensor excitation by DC/DC-converters
- Integrated modem with active dialling mode

*) Resolution: 14 bit oversampling
Accuracy: ±0.02% with automatic correction
Current measurement 0...20 mA: ±0.1% over internal shunt resistors
Digital gain and filter control for change of measuring range

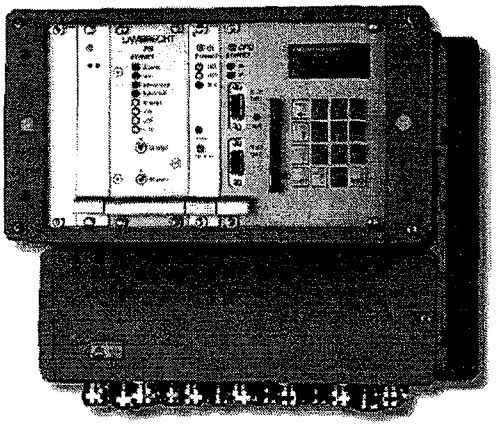

CPU board

- Proven firmware and operating system (written in the TURBO PASCAL high-level language)
- with formula interpreter (calculated values)
- Processor: 16 bit NEC V25
- Clock rate: 16/8 MHz
- Memory: 512 KB EPROM
  8 KB EEPROM
  512 KB RAM,
  battery buffered

7.2 Applications

- Automatic or manned **SYN**optical **MET**eorological weather station (WMO)
- Weather information system for ...
  ...airports (ICAO) with RVR, MOR and cloud height
  ...industrial region monitoring
- Meteorological weather station for ...
  ...industry in general
  ...environmental protection
  ...agriculture and forest purposes, etc.
- Software for PC-network with server and workstation
- Test, configuration and diagnostic integrated or by station PC/central office

7.3 Standards

- Construction according to low voltage instruction 73/23/EWG and VDE 100
- EMC according to VG 95 773 and EN 50082/81
- ESD protection according to IEC 1000-4-2
- WMO regulation No. 306

OZONOMETERS USING NARROW-BAND FILTERS

MARIAN MORYS* AND DANIEL BERGER
SOLAR LIGHT CO.,INC., PHILADELPHIA, PA 19126

Attempts to use filter-based sunphotometers to measure the total ozone column date back to at least 1963. Inadequate accuracy and stability of components then available made results only marginally useful. A pilot study by Mims in 1990 produced the Microtops ozone monitor which showed that improved technology allowed construction of a filter-based instrument with an accuracy comparable to more expensive spectrophotometers.

A more advanced ozone monitor, Microtops II, was introduced in 1996. A series of inter-comparisons with Dobson and Brewer instruments agree within 1-2% over a wide range of conditions.

Two calibrations of reference Microtops II S/N 3103 conducted at the Mauna Loa Observatory 13 months apart were within 0.7%.

In that same period of time, to further improve the range of solar zenith angles and of atmospheric conditions over which accurate ozone readings can be made, the shortest wavelength measurement at 300 nm was eliminated and one at 320 nm added. Shifting the range of measurements towards longer wavelengths made aerosol scattering effects more significant in relation to the ozone absorption cross-section. This was compensated by modifying the built-in algorithm. As a result Microtops II performance more closely resembles that of the Dobson instrument.

*Now at Numar Corp., Malvern, PA

Session V

QUALITY MANAGEMENT

Simple Tools for Effective Project Management

Ralph A. Pannett[1]

Meteorological Service of New Zealand Limited

An effective methodology for project management is a valuable capacity building tool. Projects differ in complexity and may include a diverse range of inter-related tasks carried out by several staff and contractors over different time scales and involving significant financial commitment and legal obligations. Good project management ensures that, despite complexity, the client's needs are met on time and within budget, and that the Project Leader is confidently in control of his or her task.

An effective Project Management Procedure will be an essential component of the Quality Management System operated by a National Meteo-Hydrological Service (NMHS), to ensure working results of predictable performance, without waste of resources, and within legal frameworks.

The competent management of other than simple projects is a discipline which requires the learning of a number of skills. It requires good overall appreciation of the technical solutions which may be applied, ability to visualize the project progress and result, good personal communications and negotiation skills, attention to detail, lateral thinking and problem solving, sound decision-making, ability to manage budgets, good record keeping and report writing— all components of capacity building. For small projects all the work may be done by one person, the Project Leader. Even so there is a need for planning and control of the process. The 'tools' described here are working aids to effective project management.

Project management is best learned 'doing it', learning to use the tools and thinking about the process, often under an experienced mentor or alongside a competent consultant.

Some Definitions

Project: the planned activities which result in some defined outcome to meet the needs of the client, employing personnel and designated material resources within a given time-scale. As an example we shall consider the installation of an automatic weather station, but projects may also be defined to produce non-material outputs like software or an instrument evaluation report. Large projects may be comprised of several sub-projects.

Project Procedure: the particular steps or actions that are required by the Management of the Meteo-hydrological Service of its Project Teams in executing projects; including approvals for significant elements of the project and to expend finance, adherence to legal and safety requirements, preparation of budgets, use of standard planning tools, and progress reports to the responsible manager or Sponsor.

Client or Customer: the person or group (e.g. the NMHS weather forecasters and climatologists) for whom the project is initiated and who expects real benefits from it. The customer must be consulted in the production of the Project Brief , which is the description of what the project is intended to achieve.

Project Sponsor: a senior manager who has the responsibility to ensure that the client obtains the desired results from the Project. The Sponsor prepares the Project Brief, ensures that the guidelines of the NMHS Project Procedures are complied with, and receives progress reports from the Project Leader.

Project Leader and Project Team: The Leader is responsible for all aspects of the management and carrying out of the project within the Service's Project Procedure, to achieve the required outcomes, and for assigning work to members of the Project Team. The Team is selected for the knowledge and skills needed on the project and to ensure that it is completed on time.

Contractor: a person or company outside the NMHS who is contracted to supply equipment; to do specified project work, or provide a service (e.g. communications) for an agreed price and terms. Contractors are used when the NMHS does not have the skills or staff resources to achieve the project on time. They are expected to provide services in accordance with formal specifications under a legal contract agreement.

---

[1] CIMO Rapporteur on Capacity Building

Commissioning: the act of putting the project system into operational use (e.g. adding an automatic weather station to the network) under routine maintenance following agreed Acceptance Tests, the completion of project documentation, and training for operation and maintenance.

The Tools

Project Management itself adds some necessary overhead to the project work. In the choice and use of the tools, the Project Leader should apply only the administrative effort appropriate to the complexity and financial value of the project, and the requirements of the NMHS Project Procedure. The following tools are simple in concept. They need to be selected and adapted to the context of the NMHS. Used together they are a powerful aid to the achievement of successful projects. Here they are illustrated with reference to a project for the installation of an automatic weather station (Figure 1).

1 Project Procedure

The NMHS should have a Project Procedure which defines policy for the use of significant financial and staff resources. Under this Procedure, the Project Team knows what is expected of it to achieve results and use resources efficiently. Figure 1 includes procedural requirements, including responsibilities (Item 30, etc), reports (140), approvals (150), financial controls (250) and checks (240) to avoid expensive or dangerous mistakes.

2 Project Brief

The Sponsor, in consultation with the Client, writes a concise, simply-worded statement of the purpose, objective and scope of the Project. It will include a target date for completion and state the budget and other resources available. The Brief may need to be refined by means of interviews with Client representatives to clarify their expectations and to discuss alternative technical solutions. One of the most important requirements for the successful outcome of a project is a clearly understood brief.

Changes in customer requirements and other circumstances are a normal part of project experience. The Project Leader will check that changes that may effect project outcomes or expenditure are properly recorded in writing and agreed by the Client and/or Sponsor.

3 Project Plan

The Project Leader and his/her Team draw up a plan or chart (Figure 1) indicating the way the project will be carried out. It includes all the **Tasks** required, **Resource** estimates, **Who** is responsible for them and the estimated **Times** to carry them out. The Start Time (<) for a task depends on the completion of other work which feeds into that task and the resources available to begin. The Finish Time (>) depends on the date when the task output is needed and the resources available to do the work. At the current date (30 April in the example) some tasks may be ahead of schedule (Items 190, 230) and some behind (310). The example plan is drawn up using a spreadsheet program on a personal computer, but a large sheet of graph paper could have been used. The Plan will help manage the resources so that the tasks and Project are completed on time. The Plan must be revised and updated at least at each Project Meeting (Item 40). The Plan shows the use of several other tools.

4 Task List

The Project Leader divides the Project work into easily managed tasks with well-defined outputs and responsibilities. These are listed in logical groupings with numbers for easy reference. Tasks will include attention to safety and regulatory matters, e.g. electricity supply, radio frequency licences. The Project Leader will give clear written instructions to Team members for most of the tasks.

5 Staff Resource List

The Project Leader, aided by the experience of the Team, contractors and others, estimates the skills required for each task and the resource, i.e. (number of staff) x (number of working days), to complete it. The Total Resource will indicate whether it is possible to achieve the desired target date. Resource estimation is difficult and requires varied experience of similar work. Recording the Actual Resource used will build that experience.

6 Task Assignment List

After discussion with his/her Team, the Team Leader '**AB**' (Item 30) assigns tasks to one or more Team Members (CD, EF, GH) based on the skills and staff days resource required, and the staff availability. (They will have other work to do, and may go on vacation.)

7 Project Budget

The Project Leader creates a Project Budget, based on known or best estimates of costs for equipment and services. S/he monitors and controls expenditure on the project against the total finance allocated. This is most easily done with a computer spreadsheet which will automatically re-calculate totals as actual expenditure is entered.

8 Project Meeting and Report

At regular intervals during the project the Project Leader and Team meet to review progress and budget, identify problems and discuss solutions. At particular times the Sponsor or Client representative and contractors may be present. By this means the Leader monitors the Project progress and can make resource decisions. The minutes of the meeting should be a simple record of the degree of project completion and decisions taken. As the Sponsor requires, the Leader will make formal written reports on project status.

9 Project Documents

The Project Leader ensures that Equipment Suppliers and Contractors are given explicit detail on the equipment and services required by means of carefully drafted and checked, clear technical specifications and drawings. Together with other formal correspondence and documentation governing purchase and supply (warranties, terms of payment, etc) they will define the legal contracts which are entered into.

10 Training Schedule

A schedule is drawn up identifying the specific skills required for operation and maintenance of the new system, manuals and other training resources, the staff members requiring training, the trainers, and the dates by which training should be given to achieve full operational status. Trainers may include equipment suppliers, consultants and NMHS staff.

12 Maintenance Plan

Based on information from equipment suppliers, other users, and local experience, a maintenance plan for the new system is drawn up which identifies frequency of routine maintenance; documentation; spare parts and consumable items; special tools and test equipment (320); need for factory-based repair; and local skills and training required. From this information (and other items like electric power and travel costs) it should be possible to form an estimate of the annual cost of running the equipment.

13 Acceptance Test Schedule

Lists of system tests and check criteria are drawn up and agreed between the Project Leader and major Contractors to demonstrate that the specifications and contractual requirements have been met (Items 240, 380). On passing Acceptance Tests contract payments may be approved. An Acceptance formality is also part of the Commissioning activity (810), where the Sponsor and Client are given evidence that the desired outcomes of the Brief have been achieved and can agree that the Project is complete.

14 Project File

The Project Leader maintains a well-organized file divided into sections for all documents relating to the particular named or numbered Project. The file includes the Project Brief; updated Project Plan and Budget; design notes and calculations; master copies of specifications and drawings; notes of discussions with Client and Sponsor; minutes of project meetings and reports; contract documents; correspondence with contractors; estimates, quotations and copies of invoices for payment. At any time the file should give the up-to-date status of the project.

Some Other Tools

There are several computer programs designed for project management. They provide facilities for drawing flowcharts, optimizing the project 'critical path' and re-scheduling resources. However, the overhead to set them up and update them may not be warranted except for the very largest projects. Personal computer word processing and spreadsheet programs together with rapid communications (telefax, email) will be valuable tools for the NMHS Project Manager.

Conclusion

Each new project brings challenges and learning for the Project Leader and Team as new problems are met and overcome. The reward is great satisfaction— in using effective management tools, meeting targets and knowing the job is well done, coupled with the appreciation of clients who are well satisfied.

Automatic Weather Station Installation Plan

Item	TASK	RESOURCE staff days (Estimated)	RESOURCE staff days (Actual to Date)	WHO?*	Jan 98	Feb	Mar	Apr	May	Jun	Jul	Aug	Sep	Oct	Nov	Dec
00	**Planning**															
10	Network site locality identified	2.0	3.0	MDS, FM, DA												
20	Draft Project Brief	0.5	0.3	MDS												
30	Project Leader & Team named	-		**AB**, CD, EF, GH												
40	Project Team Meetings (date)	8.0				16	27	24	29	26	24	28	25	23	27	
100	**Site & Works**															
110	Survey sites/select preferred site	5.0	4.5	DA, GH												
120	Define transport access, power & communications needs	2.0	1.0	GH, CD												
130	Estimate project cost/resources	0.5	0.5	AB												
140	Report options/cost	1.0	0.7	AB			R									
150	Get Approval to Proceed & Financial Approval	1.0	2.0	AB, MDS				A								
160	Get site owner's approval for installation	3.0	2.0	DA												
170	Obtain Local Authority Planning Consent	5.0	2.0	DA												
180	Arrange site purchase or lease	5.0	1.0	DA												
190	Write/revise installation works specification (roading, fence, mast, cabling)	4.0	3.0	CD, EF												
200	Contract for site works	2.0		EF, Workcon												
210	Contract for mains power to site	1.0		GH, Powercon												
220	Contract for telephone line to site	1.0		GH, Telcon												
230	Arrange for site maintenance	1.0	0.5	GH												
240	Inspect site works	1.0		EF												
250	Approve payments to contractors	0.5		AB, MDS									A			
300	**Equipment**															
310	Market survey of AWS/sensors if required	5.0	6.0	AB, CD												
320	Write/revise equipment specification (AWS & sensors, spare parts, tools, test equipment)	15.0		AB, CD												
330	Call tenders for supply of AWS & sensors, etc	0.5		CD												
340	Report options & prices ref. Requirement Brief	0.5		AB						R						
350	Get Approval for purchase	0.2		AB, MDS						A						
360	Arrange purchase contract for AWS & sensors,etc	2.0		CD, AWScon												
370	Liaise with equipment supply contractors	2.0		CD												
380	Do equipment acceptance checks/tests	4.0		CD, EF												
390	Check equipment manuals	4.0		CD, EF												
400	Approve payments to suppliers	0.1		AB, MDS											A	
500	**Installation**															
510	Install sensors	1.0		GH												
520	Test sensor installation	0.2		GH, EF												
530	Install AWS data acquisition unit	1.0		EF, GH												
540	Do field programming, time setting, etc	0.1		EF, GH												
550	Test AWS + sensors	0.4		EF, GH												
560	Test AWS + communications	0.2		EF, GH												
570	Do sensor on-site acceptance checks	0.5		GH												
580	Report field installation complete	-		AB, EF										R		
600	**Training**															
610	Do field maintenance training	2.0		EF												
620	Do workshop maintenance training	4.0		EF												
630	Do sensor calibration training	4.0		CD												
700	**Maintenance**															
710	Draft Maintenance Manuals & Procedures	25.0		CD, EF												
720	Create/update maintenance records	0.5		GH												
730	Schedule site maintenance	-		GH												
740	Schedule field AWS & sensor maintenance	-		GH												
750	Schedule sensor calibration	-		CD												
800	**Commissioning**															
810	Check performance ref. Requirement Brief	0.5		AB, CD												
820	Amend Network Hub data base software	0.2		IT												
830	Check reporting, coding & message format	1.0		IT, CD												
840	Get Approval to put AWS on line	-		AB											A	
850	Advise WMO new station	-		DA												
860	Report project complete	0.2		AB												R
	TOTAL RESOURCE (staff days)	115.7	26.5													
900	**Project Completion Target:** mid Nov. 1998							Current Date >								T
	Sign & Date on completion:															

R= Report required
A= Approval requ'd
T= Target date

Resource estimates and time durations are examples only

Task duration <->

Task Complete <->

* staff and contractors

Version Date: 30 April 1998

Figure 1

Quality Data— Application of the ISO 9001 Quality Model

Ralph A. Pannett[1]

Meteorological Service of New Zealand Limited

The efforts of instrument specialists are directed primarily towards the goal of improving the quality of measured data. There is continuing emphasis on better sensing systems, improved methods of processing and delivery of the data. This paper looks rather at a management system for maintaining and improving data quality which is independent of sensing and data acquisition technologies. It draws on the experience of Meteorological Service of New Zealand Limited (MetService), which is certified (for all its services) as compliant with international Standard ISO 9001 *Quality systems—Model for quality assurance in design, development, production, installation and servicing* [1].

'Quality' in this context does not mean the best possible result or the most accurate measurement, but is always relative to some standard of requirement. The International Organization for Standardization (ISO) defines '**quality**' as **the totality of characteristics of an entity that bear on its ability to satisfy stated and implied needs**. (An 'entity' may be for example, a product, a process, or an organization; or in this context a wind observation, the maintenance of a radiotheodolite, or the data collection division of a national meteo-hydrological service (NMHS)).

A short definition of 'quality' is 'fitness for purpose'. An appropriate choice of quality in measurement, for example, is important, since obtaining a particular level of accuracy costs significant resources in capital and operating costs. Unnecessary accuracy is therefore wasteful.

- **Quality management** includes all those activities that determine for the organization its quality policy, the objectives and responsibilities; and implements them by quality planning, quality control, quality assurance and quality improvement, all within the quality system.

Knowing the Customer

The relationship between the supplier of a service and the customer or client is critical to this way of thinking about quality. A national meteo-hydrological service will have as clients both government and non-governmental agencies, concerned with public safety, transportation, agriculture, tourism, civil works, university research, to name a few who will be clients with specific and differing needs. At the international level, the World Meteorological Organization is an important client which specifies accuracies and code formats of data products for international exchange.

There are also supplier/customer relationships internal to the NMHS, reflecting that each working group is a supplier to clients for its work output, and in turn is client for the output of other groups who supply products or services.

The quality model requires the identification of the client for each work procedure and an adequate specification of the work output, based on client requirements. So for example, the installation of a particular anemometer is a procedure which has specifications for meteorological exposure, mechanical mounting, electrical connection and testing performance.

The Quality System Model

ISO 9001 is the most comprehensive of the ISO standards for quality assurance purposes and should be applied when the activity includes any aspect of design and development (e.g. observing network, instrument or calibration systems design; project management). The ISO 9001 quality system model is generic rather than prescriptive. The model must therefore be interpreted and adapted for a particular business or a service like data acquisition for meteo-hydrology.

The clauses of the ISO 9001 Standard include requirements in the following areas: management responsibility; the quality system; contract review; design; purchasing; product identification and traceability; process control; statistical techniques; inspection and testing; nonconforming products; corrective and preventive action; product handling, storage, packaging and delivery; training; servicing; control of documents, data, records, calibration and test equipment; and internal quality audits.

---

[1] CIMO Rapporteur on Capacity Building

How the Model Works

The flowchart of Fig. 1 shows how the model works as a dynamic feedback activity with continuous comparison of output against customer requirements, and management actions to ensure conformity. Note that all staff exercise 'management' of the processes for which they are responsible.

Consider the calibration of a batch of barometers. The Process is driven by the written Customer Specification, which would include the number of units of a particular sensor required by a certain date, accuracy over a stated temperature range and stability with time.

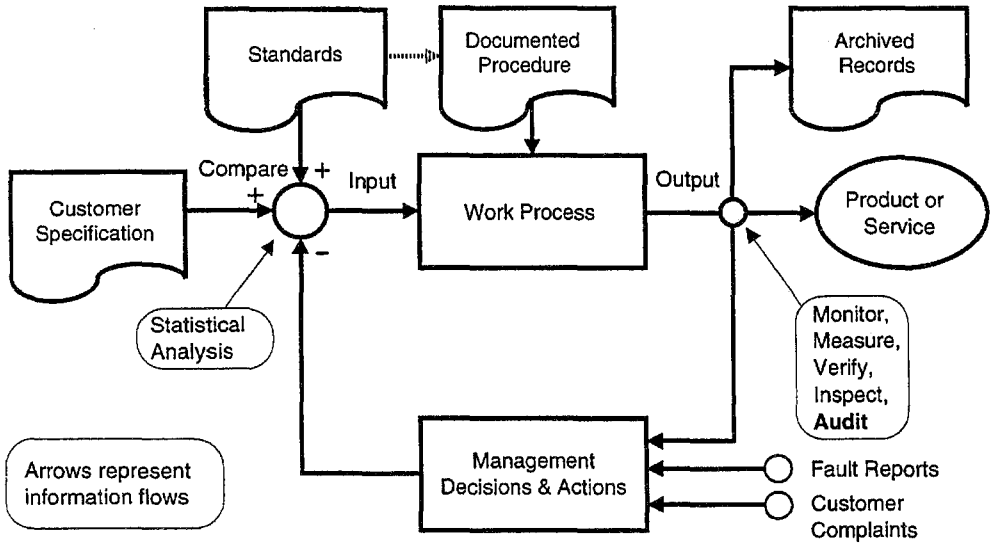

Figure 1 Operation of the Quality Model

Standards include a Working Standard Barometer, the WMO-No.8 Guide, and manufacturer's specifications. The Work Process, i.e. the calibration activity, is defined in a Procedure document supplemented by the manufacturer's manual and a local workshop manual which give the necessary detail of the operation.

Calibration adjustments are made via the feedback loop so that the barometer outputs conform to the input pressures within the accuracy tolerances. Good barometers are marked as calibrated, while any nonconforming instruments are tagged for maintenance attention. Along with calibration certificates for each instrument, an archive of statistics is maintained so that historical trends may be traced.

Fault reports are acted upon to remove defective sensors from use and client complaints are dealt with (both by defined procedures). Both faults and complaints are recorded and analyzed to discover trends which might indicate faulty manufacture or handling of the instruments, leading to a quality improvement activity. At intervals of 12 months, an independent NMHS auditor examines the calibration process to discover if it conforms to the documented Procedure, that up-to-date Standards are used and that customer needs are still met. Nonconformities will be the subject of a report to the responsible manager and the Quality Manager, and will initiate quality improvement action.

The Model Applies to all Activities

The familiar calibration example has been described in some detail because the quality model principles of customer orientation, written specification, reference to standards, proper training, documented work practices and production records, and feedback mechanisms (both on the job and through audit sampling at longer intervals) to ensure that the work output agrees with the client requirement, also apply to all data acquisition work activities. Thus management meetings, network planning, system design, project management, contract administration, installation and maintenance, network performance, processing and delivery of the coded data messages are all subject to the model to ensure quality data. Project management, which often has a high design content, provides a good illustration of the application of the quality model. [2]

Management Information

The compilation and intelligent use of process statistics for management information are an essential part of the quality system. Statistics for the performance of major systems (surface AWS, upper air stations, weather radars) in the data acquisition network are reviewed in MetService monthly and may reveal gradual changes in quality or anomalous behaviour. For example, in Figure 2, the low percentages of upper air soundings reaching target height in October and November 1996 was revealed to be due to a batch of poor quality balloons.

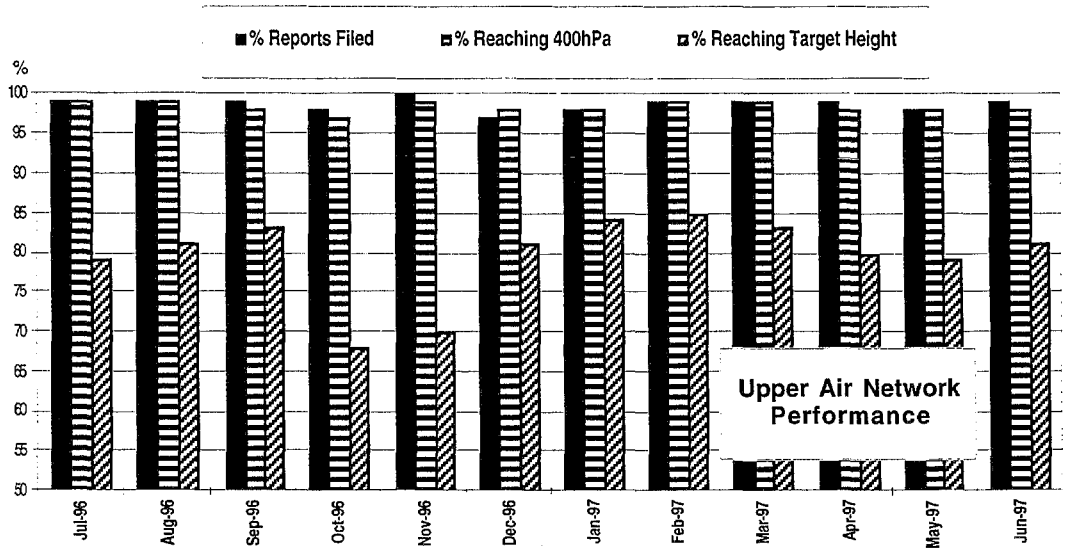

Figure 2 Overall Upper Air Network Performance

The MetService data-base computer calculates percentages of SYNOPs and METARs received and filed later than five minutes after the nominal reporting time. Figure 3 depicts a time series graph for the latter over a 12 month period. It is evident that for the months July to September, the delay from MetService stations increased relative to those from a major contractor. Once the trend had been noted, action was taken to investigate and improve delivery performance.

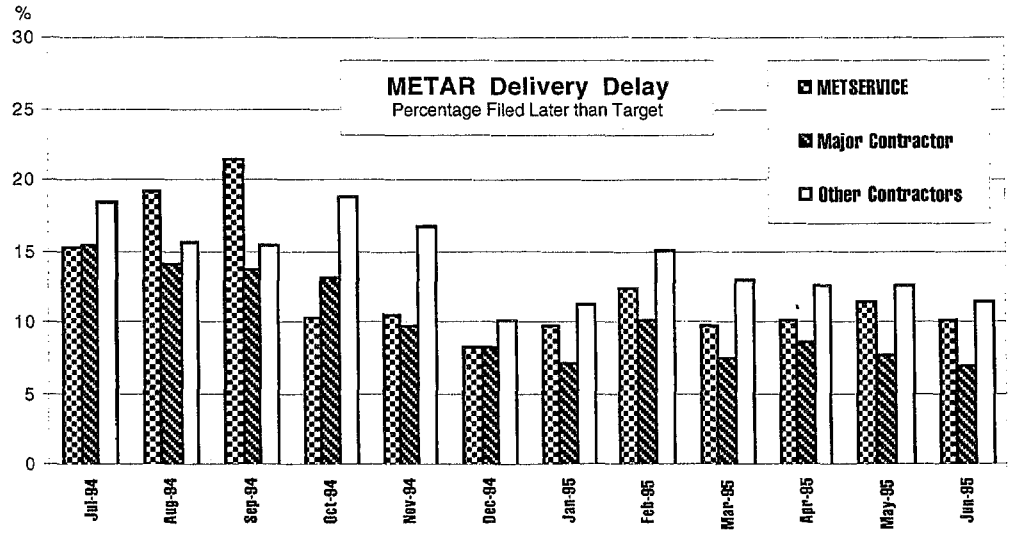

Figure 3 Delivery delay times for filing METARs

Developing the Quality System

The unambiguous commitment of all levels of management to the quality management programme is vital to its success. The programme becomes an integral part of the management activity. A **Quality Manager** is appointed to co-ordinate the development of the quality system and to oversee its operation.

Initially, an external quality consultant may provide valuable assistance in helping to interpret the ISO requirements for the particular NMHS to facilitate a smooth introduction. An early task is to document the work processes in the form of the Quality Manual.

The Quality Manual

The Quality Manual defines the working of the operational quality system, relating closely to the clauses of the ISO 9001 Standard, and is actually a hierarchy of documents. At the top level a policy manual represents the undertakings of management and describes the organizational structure.

The next level is the Procedures Manual, containing in a standard format, an outline description of each work process and its purpose, client, responsible staff and their training. Reference documents and interfaces with other procedures and work groups are indicated. There will be Procedures covering management functions; the making of surface and upper air observations; inspection of meteorological stations; installation and maintenance of instrument systems; and sensor calibration.

The third level consists of the Operational Manuals which probably include material originating from WMO, manufacturers, and the NMHS. They give complete detail on how a trained person should carry out the tasks, e.g. the making of a TEMP sounding or the maintenance of a rain gauge.

All documents must be issued and amended according to certain formal control procedures so that they always contains accurate and authorised material.

MetService has found that converting its Policy and Procedures manuals from printed form to computer-based hypertext format available to staff via the company Intranet has made it much more accessible and easy to maintain.

Auditing and Certification

Regular examination by trained NMHS auditors compare process outputs with client requirements (which will change with time) as described in the Procedure documents. They report nonconformities and make quality improvement recommendations to the relevant managers.

It is usual for organizations that accept the discipline of an ISO 9000 programme to seek formal certification from an authorised Certifying Body which itself must comply with an international framework. The Certifying Body conducts a detailed examination of the operation of the quality model in the organization, and may require remedial work before awarding the prized ISO 9001 Certificate.

Benefits of Quality Management

MetService has found that a quality system enables the Service to be confident that data and forecast products are delivered to client specifications on time and with efficient use of resources. [3]

It encourages a systems view of the meteorological enterprise and emphasizes the interdependence of various activities and work groups. Staff are motivated to think about and check their own work in an environment where innovation and improvement is encouraged. Waste of resources (time, materials, finance) is reduced or eliminated. On those few occasions when performance falls below the specified quality, or a client complains, the system provides a rapid and sure response to fix the problem within an acceptable time.

The Quality Culture

All staff are in the business of creating a quality-conscious community. The idea of collective ownership of the quality programme is crucial to success. Rewards are the great personal satisfaction in knowing that the job is done well; that clients are pleased with the products and services supplied; and that the NMHS is excelling at its appointed national role.

References

[1] ISO 9001:1994 *Quality systems—Model for quality assurance in design, development, production, installation and servicing,* International Organization for Standardization, Geneva.

[2] Pannett, R. A.: Simple Tools for Effective Project Management, Proceedings WMO TECO-98.

[3] Pannett, R. A.: The ISO 9001 Route to Quality Data, *WMO Bulletin* **47** (2), in publication.

Quality management in the modernised ground based observing network of the Deutscher Wetterdienst

Jochen Dibbern, Deutscher Wetterdienst, Offenbach/Main

1 Introduction

The Deutscher Wetterdienst is currently modernizing it's ground based observing network ("Network 2000"). The number of manned stations will be reduced, new sensors and software algorithms will be used to replace eye observations. In such an automated observing network quality management plays an important role.
The quality of the data, archived finally in a data bank, depends on the whole chain of data acquisition. Therefore it is necessary to build up a quality control system which includes all parts of the data production process from the sensor to the final archiving in the data bank.
Within our service the project "Network 2000" is a pilot project for the implementation of quality management. Necessary steps for the implementation are:

- building up a remote maintenance monitoring system
- using the network management system for the monitoring of the communication network
- building up a quality control system in different steps, at the site, at regional network groups and in the headquarter.

Control and comparative measurements will also be a part of the quality management system.
In this paper we outline the quality management system which will be implemented within the next years in the Deutscher Wetterdienst.

2 Data monitoring and quality control

Data monitoring and quality control are basic parts of the quality management. The quality management will be done in four different steps, separated in location and time.

- step I at the station
- step II in the headquarter
- step III at the regional network group
- step IV in the research department

The time schedule for the quality control steps is given in the following figure.

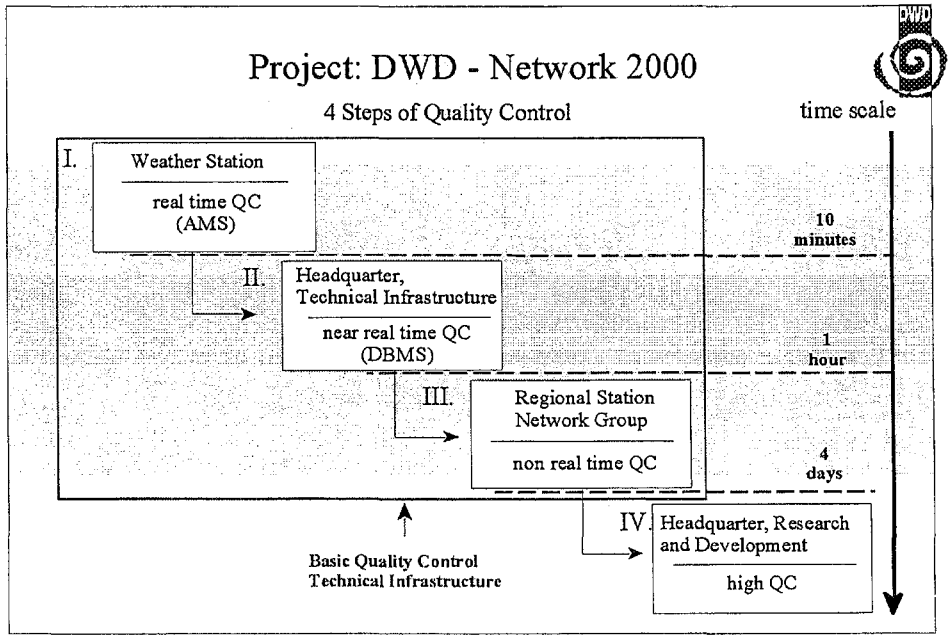

During the different quality control steps the data will be flagged to identify the quality level. The quality control of step four will only be used for special data sets to assure high quality for climatological purposes.

2.1 Quality control step I

The main steps of the automated quality control procedures at each station site are:

- formal checks (sensor voltage, sensor heating etc.)
- climatological extreme values
- variability in time
- consistency (cross checks between different meteorological parameters)

The aim of this very basic quality control is to identify sensor faults and system trouble very rapidly. Quality bytes identifying faults give rise to a appropriate message in the maintenance monitoring system. So the loss of data can be reduced to a minimum.

2.2 Quality control step II

The second step of the quality control is done in the headquarter with the following contents:

- formal checks to guarantee complete data sets
- data storage

These control steps have to be done quasi real time since WMO coded messages like SYNOP will be generated from these data.

2.3 Quality control step III

The third step of the quality control is a man-machine mixture, done at the regional network groups. A copy of the headquarters data bank will be available at the regional network groups. The following quality control procedures, which are a man-machine mixture, will be used:

- formal checks
- climatological extreme values (depending on seasons, climatological regions)
- consistency (internal, time, space)
- corrections, closure of data gaps

Data which have a corresponding quality byte from the automatic control steps will be displayed on a workstation and will be corrected through a man–machine interaction. For this task an advanced software with state of the art graphical display is necessary. At the end of this control step the corrected regional data set is restored to the headquarter's data bank.

2.4 Quality control step IV

This climatological quality assurance will only applied to limited data sets for special scientific purposes. Control steps can be:

- homogeneity checks
- spatial distribution
- statistics
- time series

3 Network management and maintenance monitoring

To operate an automated observing network in an efficient way it is necessary to implement an cost effective maintenance monitoring system. For this task the existing network management system will be extended down to the data acquisition systems at the measuring stations.
Currently a network management system on the basis of HP Open View is in operation. This software is a tool to monitor and display the status of the communication network of our service. If the station itself produces an SNMP-agent it is possible to use this management tool also as a maintenance monitoring system. The SNMP-agent can include status information from sensors,

from the data acquisition system and on quality bytes of the measurements. SNMP-agents will be added to every regular message or will be transmitted on request. If a sensor fault is detected in step I of the quality control the data acquisition system sends out an SNMP-Trap.
On the main SNMP management server the agents will be analysed and depending on the contents of the SNMP-agent several automatic procedures can be defined. The advantage of this kind of management tool is, that this software is widely used and that numerous tools are available for the special design of the whole system.

Thereby all information regarding the status of the sensors and data acquisition systems of the weather stations together with the status of the communication network will be made available at our maintenance sites.

Remote control of the stations does also mean that the following procedures must be possible:

- software downloads
- remote parameter setting
- disconnecting control sensors
- Remote calibration of intelligent sensors

4 Control and comparative measurements

Control and comparative measurements are part of the quality management. To identify sensor drifts control measurements will be performed. For temperature and humidity sensor drift will be controlled by doubling the sensors. Meteorological data from both sensors will be transmitted and archived in the data bank. If one of the sensors fails the quality control step I at the station, the data from the other sensor will be used for further processing. If the data from both sensors are flagged by an error byte, the consistency of the values will be verified in quality control step III at the regional network groups. For quasi real time applications like the distribution of SYNOP and related code only data without any error flags can be used.
At manned stations the automatic measurements of precipitation and pressure will be controlled by conventional measurements with the Hellmann rain gauge and the mercury barometer, respectively.

At about 15 manned stations in Germany conventional measurements will be conducted parallel to the automatic measurements for a period of at least 10 years. The reason for this is to find algorithms to homogenize time series of data from the old and new sensors. The station sites will be selected from different climatological regions. Comparative measurements shall also be conducted between eye observations and present weather sensor output.

5 Conclusion

Quality management will play an important role in the modernized ground based observing network of the Deutscher Wetterdienst. Within the next years we want to implement for the "Network 2000":

- Quality control in 4 different steps
- Control and comparative measurements
- Network management and maintenance monitoring

It is to be expected that data availability of reliable data sets will be well above 95 percent.

EQUIPMENT FOR DEVELOPMENT INITIATIVES

C.J. STIGTER[1] AND C.L. COULSON[2,*]

[1] TTMI-Project, Department of Environmental Sciences, C.T. de Wit Graduate School for Production Ecology, Wageningen Agricultural University, Wageningen, Netherlands

[2] TTMI-Project, School of Engineering & Information Technology, University of Lincolnshire & Humberside, Kingston upon Hull, UK
[*] Corresponding author: <ccoulson@humber.ac.uk>

With many years of Third World field research between us, and after many discussions with colleagues with similar experience (see references), particularly in Africa and India, the authors a year ago launched the idea of "equipment for development initiatives" (EDI, see web page mentioned at the end). EDI was conceived to tackle difficulties in equipment maintenance, trouble shooting, repair and calibration as well as in the use of basic workshop equipment. Already in the second phase of the TTMI-Project special attention was paid to equipping simple electronic and mechanical workshops/laboratories and to providing preliminary technician training. However, rationalizing the provision of strategic, tactical and operational solutions appears appropriate when so many national and international research systems face the same serious limitations in quantitative field research in developing countries.

Our initial aim was to develop more or less standard packages of equipment that can be used for maintenance, trouble shooting and repair of sensors, recorders, data loggers etc. as well as auxiliary office equipment like computers in the countries where the research is taking place. In order not to duplicate efforts in solving these equipment problems and to get a better feel of what our colleagues have experienced, last year we used a questionnaire that we sent to something like a hundred and fifty addresses, from which we got about a 50% reply rate. In this paper we discuss the replies to this questionnaire, of which the results are graphically displayed in the figure on the last page of this contribution. Where appropriate, "Yes" had three grades, with "Yes 3" expressing the highest level of importance.

Q1 shows the reply to the question whether the organizations of the respondents find the maintenance and/or repair of field and supportive laboratory research equipment a poblem. Two thirds found this serious problems and another more than 25% rated them as just problematic.

It was indicated that we had three packages in mind: (i) a low budget minmum kit, containing only very basic equipment to solve simple problems of equipment use; (ii) a medium budget intermediate or "core" kit, for solving more complex equipment problems and (iii) an advanced or specialized kit, which would be a client specific upgrade of the "core" kit. Q2a gives the reply distribution to the question whether provision of an equipment kit would help to solve maintenance/repair problems, showing that close to 70% finds this a very good idea while most of the remaining respondents indicate that this would be of (some) help. Close to 50% would be sufficiently assisted by a "core" kit, nearly 35% would need an upgraded specialized kit while just over 15% would be sufficiently assisted with a minimum kit (Q2b).

The questions 3 to 7 concerned the assistance that would be rendered by provision of (Q3): general electrical spares for maintenance and/or repair; (Q4): service manuals, circuit diagrams etc.; (Q5): guarantees of "fitness for use" in the conditions under which respondents had to work; (Q6): training on maintenance, trouble shooting and repairs and (Q7): advice, including manuals, for maintenance etc. of specific equipment. Nearly 80% of respondents said that they would be highly assisted by the provision of training (Q6), only a few saying training wouldn't matter (Q6). Almost the same reply distribution occurred for advice on matters surrounding specific equipment (Q7). The two top priorities are thus clearly known. The other provisions would highly assist from more than 50% to about 60% of the respondents, while an additional 20 to 30% would be much helped out with such assistance (Q3, Q4, Q5).

The following three questions (Q8 - Q10) had to do with problems in obtaining field and supportive laboratory research equipment and/or spare parts. We asked whether provision of advice for obtaining commercially available equipment would be of any assistance and this was the case for close to 90% of our respondents, more than half of whom would be most highly assisted with such help (Q8). The same question for "custom-built" specific non commercially available field research equipment was very positively replied to in more than 70% of the response, of which a clear majority would be most highly assisted (Q9). Provision of guarantees that spare parts will remain available for commercially obtainable and custom-built equipment alike, was rated as of much to very much help for again 90% of those that had problems in obtaining equipment, with a large majority in the highest class of importance of such provisions (Q10).

Our last group of questions (Q11 - Q13) had to do with projects, donors and budgets. A hundred percent of those recognizing the problems in our questionnaire would include the provisions that we listed in a project budget when such provisions indeed became available (Q11). Also a hundred percent of positive response was obtained on the question whether donors should allow and accept such provisions as budget items (Q13). However, slightly more than 20% of them thought that currently donors would not accept these provisions as budget items when included in the project budgets (Q12).

Where does the above study bring us to? It should first be indicated that we initially aim mainly but not exclusively at undertakings in the environmental and agricultural sciences. If indeed we want to rationalize the provision of solutions - to which aim so many of our respondents have subscribed - development of the "basic" and "core" kits should get priority. The exact nature of any upgrade to a specialized kit will of course be established with reference to the particular equipment used in the field research.

We also would like to propose that the EDI-project acts as "centre" to co-ordinate the sourcing, ordering, delivery, export paperwork and transport of equipment. This service would also include the provision/search of/for spare parts, manuals etc.. We would expect to negotiate with manufacturers to ensure high quality after sales services and backup. We would also want to address training needs for equipment maintenance and specialist advice on equipment repair etc. and spare part acquisition.

We may at a later stage want to address problems of collecting information from the type of field research which uses sensors and loggers under difficult field conditions. It may be expected that this will lead to the improvement of certain sensors as well as in their actual field use and sampling methodologies.

It appears possible for the EDI-Project, in the long run, to work commercially, paid by client project funds and supported by manufacturers interested in playing by the rules of customer orientation, delivering and services. However, the development of the kits and setting up a small organization need sponsoring and that will not so easily be obtained solely from manufacturers. Also single donor organizations may not see the advantages, because funding equipment is not their first priority. A consortium of donors, an umbrella secretariat of national or international research institutes, a bureau establishing large scale research funding within the World Bank, the European Commission, a UN-organization etc. are most likely sponsors.

We invite anybody interested in the EDI-Project and with ideas on its starting-up, to contact the corresponding author at the e-mail address given on page 1 or to visit our well illustrated web site under http://seit.humber.ac.uk/~ccoulson/edi.htm.

Coulson, C.L. and Stigter, C.J., 1988. Appropriateness of instrumentation for agro-ecological research in low-income developing countries. Funct. Ecol. 2: 109 - 113.

Coulson, C.L. and Stigter, C.J., 1989. Appropriateness of instrumentation in agroforestry/agricultural research in developing countries. In: W.E. Reifsnyder and T. Darnhofer (Eds.), Meteorology and Agroforestry. ICRAF, Nairobi, Kenya, pp. 305 - 314.

Stigter, C.J., 1994. Conditions, requirements and needs for outdoor measurements in developing countries: the case of agrometeorology and agroclimatology. Proceedings TECO-94, Instruments and Observing Methods Report No. 57, WMO/TD - No. 588, WMO, Geneva, pp. 1 - 2 (full text available from WMO/CIMO or the author, on request).

Stigter, C.J. and Coulson, C.L., 1988. Environmental measurements in Africa. In: Applicability of agricultural physics and meteorology in Africa, ISAPAM/ICTP Workshop, Addis Ababa University, Ethiopia.

Stigter, C.J. and Darnhofer, T., 1989. Quantification of microclimate near the soil surface. Appendix F in: J.M. Anderson and J.S.I. Ingram (Eds.), Tropical Soil Biology and Fertility: A handbook of Methods, IUBS/UNESCO (MAB), CAB International, Wallingford, UK, 144 - 157.

Stigter, C.J., Coulson, C.L., El-tayeb Mohamed, A., Mungai, D.N. and Kainkwa R.M.R., 1989. Users' needs for quantification in tropical agrometeorology: some case studies. In: Proceedings of TECIMO-IV, Instruments and Observing Methods Report No. 35, WMO/TD - No. 303, WMO, Geneva, 365 - 370.

EDI SURVEY RESULTS

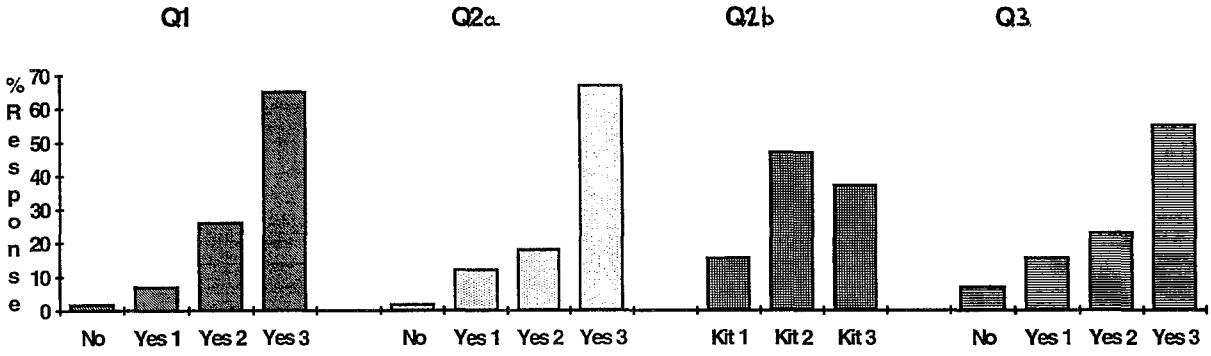

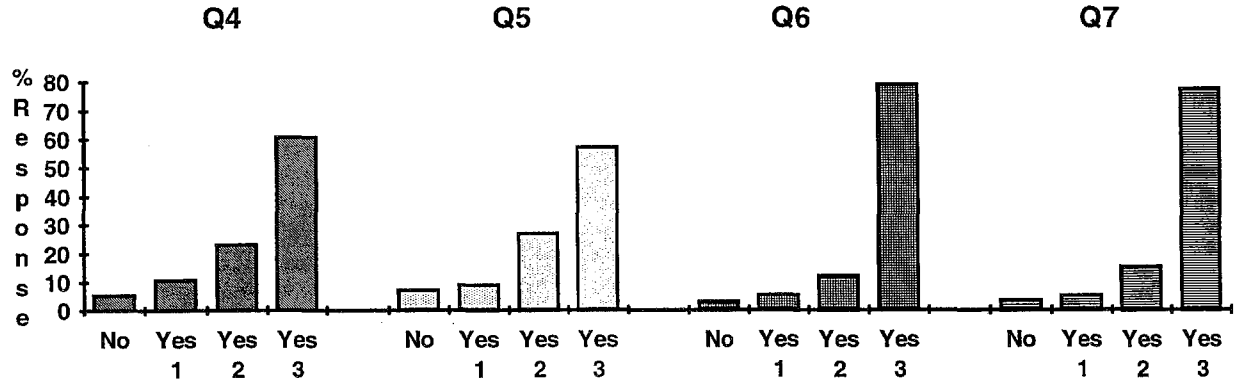

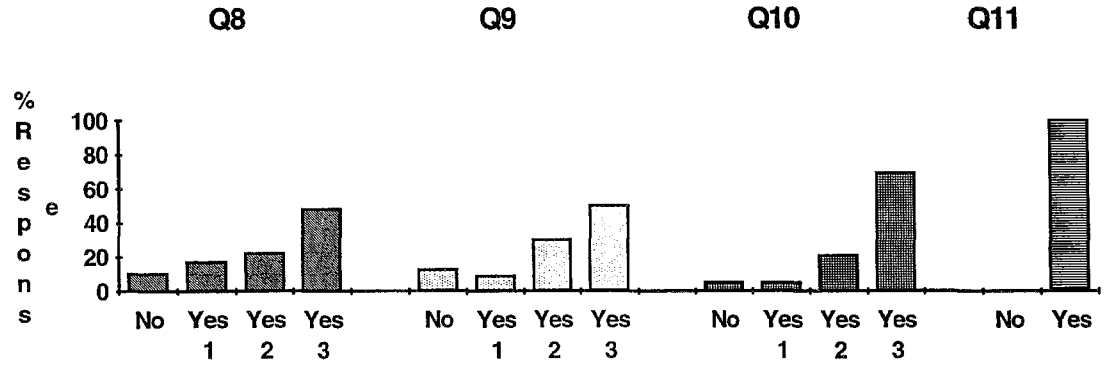

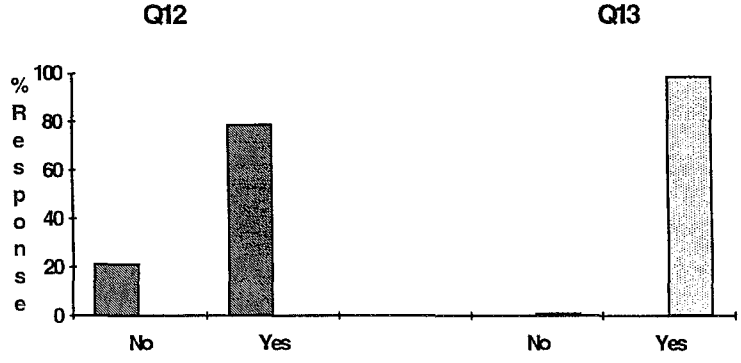

Wake Vortex Induced Wind Measurements at Airfields:
- A Simple Algorithm to Reduce the Vortex Impact

Jitze P. van der Meulen,
Royal Netherlands Meteorological Institute,
Postbus 201, 3730 AE de Bilt, Netherlands
meulenvd@knmi.nl

1. Introduction

At airfields, wind information is provided for specific locations. The WMO Technical Regulations, Vol. II (WMO-No. 49), equal to ICAO Annex 3, give detailed recommendations for observing and reporting of surface wind (TR[C.3.1]4.5). It is recommended that "Surface wind observations for take-off and landing should be the best practicable indication of the winds which an aircraft will encounter during take-off and landing." Particularly, in the Guide on Meteorological Observation and Information Distribution Systems at Aerodromes (WMO-No. 731) detailed information is presented concerning to operational requirements of surface wind observations. The most important statement is that for the take-off and landing operations, the observations should be *representative* of the conditions along the runway, particularly of 6 to 10 m above the runway. To generate this, it is stated that representative surface wind observations should be obtained by the use of sensors appropriately sited as determined by *local conditions.* (see TR[C.3.1] 4.52-3). Another manual, the ICAO manual of Aeronautical Meteorological Practice (ICAO Doc. 8896-AN/893/4; 1993) contains a table on the "Locations of Meteorological Instruments" (Table D-3). In this table it is remarked that the site should not be affected by buildings, etc., or by aircraft operations (*e.g.* jet afflux during taxiing). We may conclude that these manuals and guides give appropriate information, but there is a significant lack on detailed, quantitative information on this subject since the statement "representative" is not clarified in detail.

In practice, the determination of an appropriate location to measure wind is not a very trivial one. Since conditions, like buildings, airplanes on taxiways and other local systems, may affect the measurement, the finding of a suitable location is often not so easy. As a result, compromises seem to be necessary in spite of primary safety precautions, and the common sense is taken as the basic constraint. A fine location for wind measurements is about 225 m from the centre-line of runway, and far away from taxiways obstacles, etc.. However, in some cases, it turns out to be necessary to position the (frangible) wind system at about 105 m from the centre-line. As a consequence, wind measurements are significantly affected by the aircraft operations, *i.e.* by the wake vortexes. This happens especially in cases when the wind direction is so that measured wind comes from the direction of the runway.

2. The effect of Wake Vortexes on the measured wind speed

In fig. 1 a typical example of these effects are presented. In this figure not only the 12 s wind speed is presented as a function of time, but also the maximum windgust (FX), as it presented during 10 min at the user's display. Obviously a vortex may act as a spike (~ 30 s), but for the user the FX presentation will hold on for 10 minutes, which may have a significant impact on the air-traffic control.

3. The normalized wind speed as basic parameter for detection of a vortex

In the newest, sixth edition Guide to Meteorological Instruments and Methods of Observation (WMO-No. 8; 1996) information is presented on "Peak gusts and Standard Deviations" (par. 5.8.2). A basic dimensionless parameter for investigations on peak gusts is the so-called *normalized extreme wind*, indicated by u_n, and defined by:

(1) $$u_n = (u_{max} - U)/\sigma_U, \qquad (\sigma_U > 0)$$

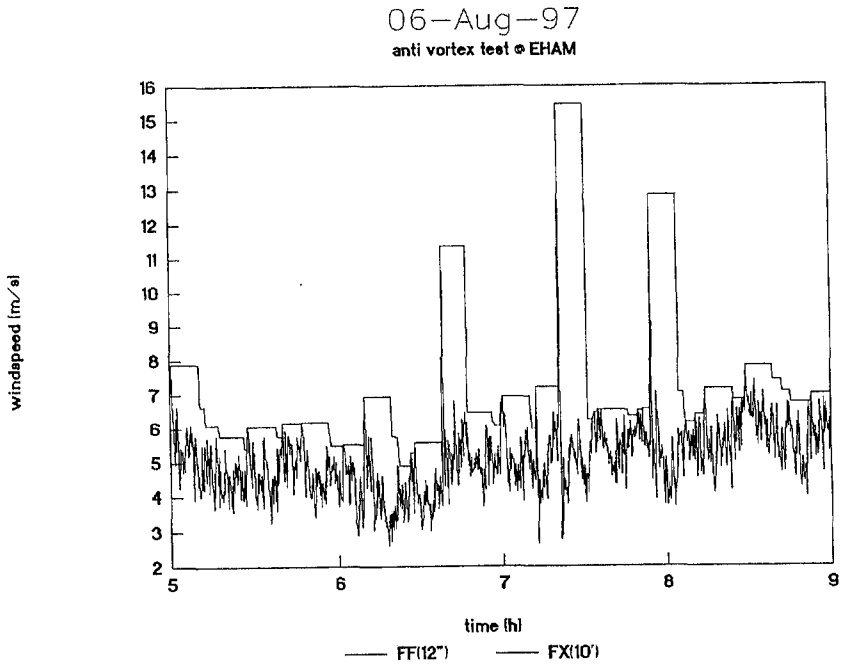

Fig. 1.
The measured windspeed as a function of time (on a 12 s interval base) and the presented 10 min FX. It is proven that FX is strongly affected by vortexes caused by large airplanes

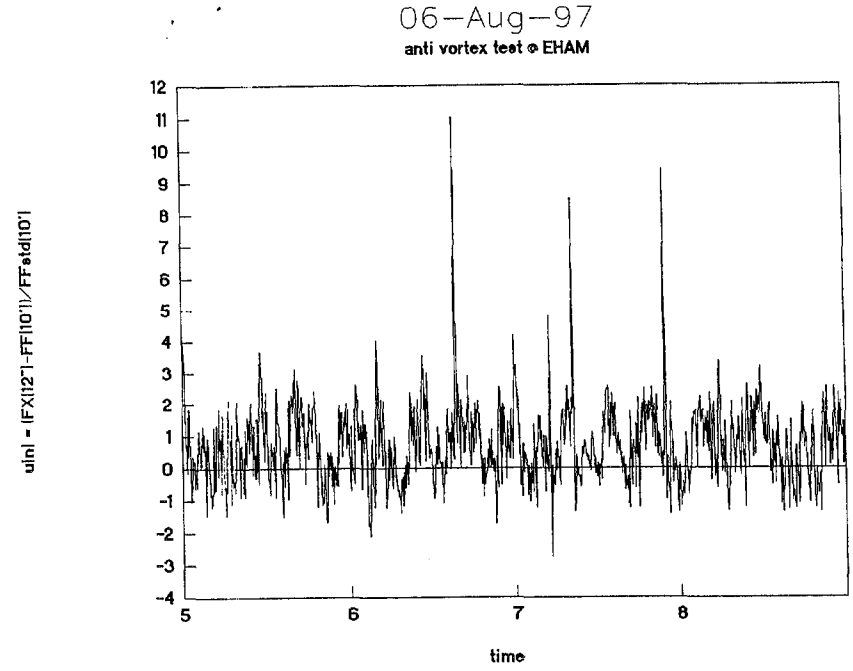

Fig. 2.
The dimensionless normalized windspeed u_n for the same period as with fig. 1. The artificial gusts from fig. 1, can easily be identified in this figure.

where u_{max} is the measured actual wind speed of the windgust, U is the time-averaged wind speed and σ_U is the with U related standard deviation. The averaging window for U and σ_U is optimal for $\Delta t = 10$ min as explained by Beljaars [1] and Wieringa [2]. When using the 3 s windgusts measured within a 12 s frame in relation (1), this will result in a time series of u_n, which can be plotted versus time. In fig. 2 such a plot is presented for the same period as in fig. 1. Investigations on u_n demonstrate that this parameter is rather independent of the actual windspeed itself, *i.e.* for natural winds. Artificial winds, however, like those produced by wake vortexes do affect u_n significantly as is demonstrated by the peaks (with $u_n > 5$). There is a significant correlation between the vortexes and those peaks > 5 in fig. 2. For a day without aircraft operations on the runway we can present a frequency distribution of u_n based on a whole day of 12 s samples (N = 7200). Such a *BAR*-plot is presented in fig. 3.

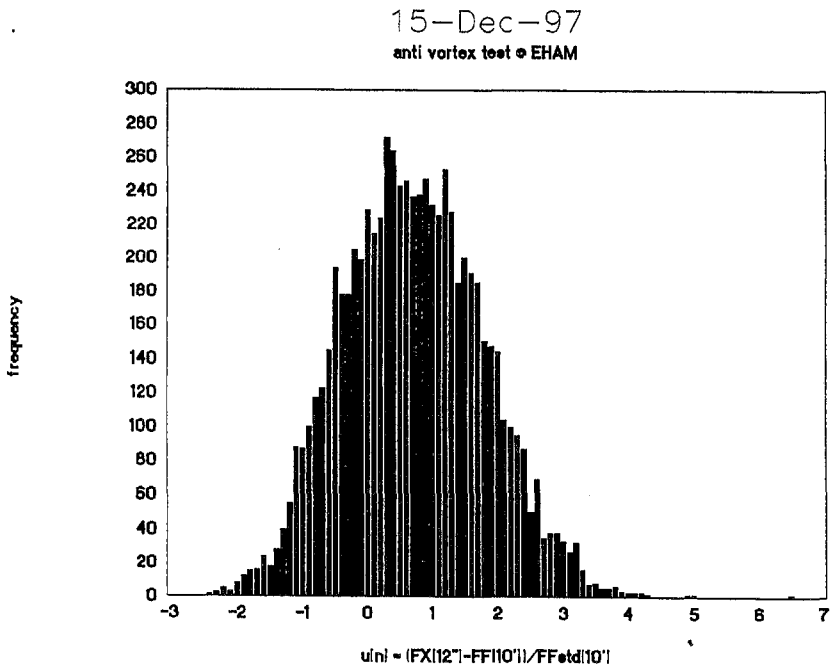

Fig. 3.
A typical BAR-plot for u_n for a day without affection by aircraft operations. This plot demonstrates clearly that a normal distribution holds for u_n

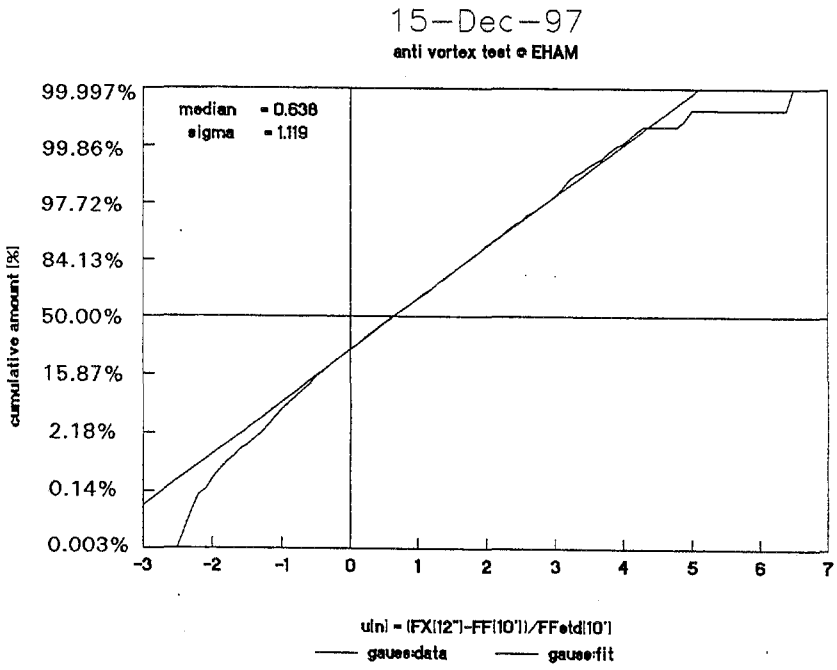

Fig. 4.
The cumulative frequency distribution on presented on "normal-graph" format based on the same data as for fig. 3. The straight curve fit indicates around the median (50% line) demonstrates that u_n confirm significantly to a normal distribution

Clearly, u_n confirms to a normal distribution. This can better be demonstrated by plotting the frequency distribution of u_n in a cumulative way on so-called "probability"-paper. Fig. 4 shows such a plot based on the data used for fig. 3. It is very clear that main part of the data confirms to a normal distribution, because the linear fit to the data is very significant. It should be noted that such a fit holds for all types of weather, inclusive thunderstorms. Moreover, the median value of the distribution is always within 0.3 and 0.8, the sigma between 1.0 and 1.6 (measuring period: 970501 to 971202 at EHAM, Amsterdam International Airport Schiphol, RWY 19R).

4. On the reduction of windsspeeds affected by vortexes.

As a consequence it is possible to detect a significant wake vortex and reducing or validating the value automatically. Tests at EHAM have demonstrated that a simple algorithm based on the principle that $u_n > 5$ is very helpful on this matter. In this case we have made restrictions to a specific range, *i.e.* $U > 0.5$ m/s, $\sigma_U > 0.5$ m/s and $u_{max} < 15$ m/s. This is done because at low values of the actual wind speed, the parameters U and σ_u may become zero, for which u_n is not defined. To avoid any risk, no reduction is carried out for measured windspeeds larger than 15 m/s.

In case of detecting any artificial windgust based on the above principle, the actual windspeed u is reduced to:

(2) $$u = U + b\cdot\sigma_U + c,$$

where the constants b may be about 2.5 and c = 0 to 0.5 m/s. The choice of the constants b and c is a matter of fine-tuning. The tests which we have carried out demonstrate successful results by using this procedure. During the test period, severe storms, including thunderstorms passed the test location and it is demonstrated that natural, heavy windgusts were not affected by the reducing algorithm.

5. Conclusion

By implementing a simple algorithm, which detects artificial windgusts caused by wake vortexes, the presentation of wind information can be improved by reducing the presented, not relevant gust. However it should be stated that principally wind measurements should be carried out free from artificial impacts. Only in particular circumstances a solution as described above may be used.

---

[1] Beljaars, A. (1988): "The Measurement of Gustiness at Routine Wind Stations," Instr. and Obs. Meth. Rep. 33 (WMO-TD No. 222) 311.

[2] Wieringa, J. (1973): "Gust factors over open water and built-up country," Boundary-layer Meteorology 3(1973)424

SQUALL IDENTIFICATION ALGORITHM

A.I. Mehovitch and V.V. Popov
Central Design Office of Hydrometeorological Instrument Production, Obninsk, Russian Federation
and
S.M. Persin
Main Geophysical Observatory, St. Petersburg, Russian Federation

INTRODUCTION

Most automatic weather stations report meteorological parameters with intervals considerably exceeding those of the measurement results output required by the users. This is done with a view to simplifying measurement algorithms, quality control, obtaining averages, etc.

Higher frequency measurements provide for data redundancy and enable creating algorithms for determining additional characteristics and phenomena on the basis of the time variations of the parameter. Known algorithms for determining pressure tendency characteristics, cloudiness characteristics from cloud height measurements (cloud amount in tenths, cloud height and amount by layers) can be given as examples.

The squall identification algorithm is based on the analysis of the sequence of the anemometer output data. The algorithm can be implemented by means of the software with no additional hardware required if microprocessor is used.

ORIGINAL DATA

Observations of squalls are made by all the land and sea-based hydrometeorological stations. Squall reports are given in Group 7 of Section 1 of Code FM-12-VII SYNOP and FM-13-VII SHIP - "Present weather or past weather during the hour immediately preceding the observation hour". Besides, squalls are dangerous or a marginal weather phenomena and they are included in special storm warning messages. Squalls are identified by the observer visually according to its description in Manual on Codes (1), Guide (2) and Manual (3). The observer is to be guided by the following criteria when reporting a squall: "...a sudden increase of wind speed of at least 8 m/s or more during 2 minutes at the most, with the wind speed rising to 11 m/s or more and lasting for at least 1 minute".

On the one hand the above squall description is sufficiently detailed for visual identification of the squall using the wind speed registration on the paper tape of the recorder and it is less likely that the squall description could be made more specific on the basis of visual observations. On the other hand, it is necessary further detailing of the squall description for the purpose of it automatic identification.

SQUALL DEFINITION DETAILING

In order to develop the algorithm for automatic squall identification, the definition given above have been made more detailed by following assumptions:

- "a sudden increase of wind speed" means that the squall preceding period of time is much longer than squall itself (including the time of increase) and is no less than 7-10 minutes;
- squall wind speed is assumed to be a 1-minute speed average according to the minimum squall duration;
- the wind speed build up front does not exceed 2 minutes during which 1-minute average wind speed does not amount to values corresponding to squall meanings;
- the excess of wind speed during squall (8 m/sec or more) is defined with respect to the wind speed preceding the squall and averaged over a time considerably exceeding the minimum squall duration;
- absolute value of wind speed during squall (11 m/sec or more) is defined using a 1-minute wind speed average.

The algorithm given below has been developed in terms of this more detailed definition.

MAIN OPERATIONS OF THE ALGORITHM EXECUTION

Squall can be identified with the help of software through performing the following manipulation with the electric signal of the anemometer which is proportional to the wind speed:

- the signal is integrated continuously over the 1-minute averaging period (which is equal to minimum squall duration) in order to obtain the average value of increased wind speed in case that the time of increase is no less than 1 minute;
- the signal is integrated continuously over the averaging period which is much longer than minimum squall duration (7-10 min) to obtain the average wind speed preceding a squall;
- the first integrated signal is compared with the specified limit (11 m/sec) and if it is exceeded, the following is performed:
- the difference between the first and the second integrated signals is determined for estimating the wind speed increase value;
- this difference is compared with the second squall specified limit (8 m/sec) and in case of its exceeding squall appearance is registered.

In case of squall registration some of its additional characteristics (like the moment of appearance, maximum instantaneous wind speed, wind direction changing, etc.) are registered as well.

CONCLUSIONS

The squall identification algorithm has been developed with a view to further automation of synoptic observations. The algorithm described above has been checked up by computer modelling. When the input data was being entered according to the squall description, the squall was identified by computer every time.

According to the traditions it would be highly desirable that intercomparisons should be carried out using new instruments and conventional observations. However, the squall is rather a rare and local phenomenon and a large network of stations would be required for such intercomparisons operating for a long period of time alongside with observers.

It could be reasonable to introduce a minor addition in a squall identification algorithm so that stations and instruments did not only report of squall but also automatically record all the wind speed data preceding and accompanying the squall. On the basis of such records the decision about improvement of a squall description should be taken.

REFERENCES

1. Manual on Codes, Volume II, 1982, supplement No. 9, WMO-No 306.

2. Code for transmitting data from surface and sea-based hydrometeorological stations KH-01; Leningrad, 1989 (Russian Manual on Codes).

3. Russian patent ¹ 1654757 "Method identification of squall and instrument for its realization".

****

AN ACCEPTANCE TEST METHOD FOR SONIC ANEMOMETERS

Michael C. Sturgeon*

National Oceanographic and Atmospheric Administration
National Weather Service
Surface Observation Modernization Office
Sterling Research and Development Center
Sterling, Virginia
USA

1. Introduction

The Automated Surface Observing System (ASOS) Program Office of the United States (US) National Weather Service (NWS) has established a Planned Product Improvement (PPI) Program to enhance sensor performance in the ASOS. The current ASOS anemometer, which is a conventional cup and vane design, was determined to be deficient under severe icing conditions and is a candidate for replacement under the PPI Program. A sensor technology was not specified in the requirements for a replacement ASOS anemometer. However, the technical proposal evaluation resulted in the selection of four candidate anemometers all of which were based on sonic technology.

Sonic anemometers have systematic direction and speed errors as a function of both azimuth orientation and wind speed, due to the shadow effects of the transducers and the flow distortion caused by the array assembly. The goal was to develop a standard test method to assess both speed and direction performance characteristics simultaneously and present the data to the user in as concise a format as possible.

The interdependent wind speed and direction performance characteristics of sonic anemometers presented several challenges at the start of the test. There are no existing NWS standard test methods that could be used for laboratory evaluation of sonic anemometers. The American Society for Testing and Materials (ASTM) currently has a standard test method D 6011-96, for determining sonic anemometer characteristics, but that test method is more appropriate for design and development verification than for end-user acceptance testing. The standard test method developed in this paper is concerned with the measurement errors in the horizontal wind field. However, this standard test method could be applied to the vertical wind component as well, with a suitable mechanical tilting fixture in the wind tunnel. This test method could be applied to other anemometer technologies which have interdependent speed and direction errors as a function of azimuth orientation.

Some anemometer manufacturers prefer to specify speed and direction accuracy either in terms of an average value or an overall root mean square (r.m.s.) error. This however, can hide large errors that may occur over certain azimuth ranges. The argument has been made that unlike the stream-lined air flow in the wind tunnel, the surface boundary layer wind is anything but uniform. Although the naturally occurring wind field is much more turbulent, wind tunnel tests have revealed significant speed biases over large azimuth ranges for some anemometers. In some cases these anomalies can exist over azimuth ranges as great as 20 degrees. These errors could result in significant reporting biases for the real world scenario. In some cases these biases may exceed 8% of the true wind speed. These sensor biases can cause significant data errors depending on the prevailing wind direction at a particular geographic location.

The current ASOS wind sensor requirement for laboratory wind speed accuracy is ±1 m/s or ±5% of the true wind speed, whichever is greater. The maximum operational wind speed requirement is 65 m/s. For wind direction the laboratory accuracy requirement is ±5 degrees at wind speeds of 2.6 m/s and above.

*Corresponding author address:
Michael Sturgeon
NOAA National Weather Service
44210 Weather Service Road
Sterling, VA 20166 USA
email: michael.sturgeon@noaa.gov

2. Wind Tunnel Test Setup

The test sonic anemometer is installed in the 1.2 by 1.2 meter calibration test section of the NWS Sterling Research and Development Center (SR&DC) large wind tunnel. The wind tunnel reference air speed is measured by a pitot-static tube mounted 305 mm from the wind tunnel side wall and 457 mm from the wind tunnel ceiling. The sonic anemometer is mounted in the center-line of the wind tunnel, 915 mm down wind of the pitot-static tube total pressure port and is typically 305 mm below the center-line of the pitot-static tube. The center-line of the sampling volume for the test sonic anemometer is typically 457 mm from the floor of the wind tunnel. The sonic anemometer is mounted to an adapter which passes through the floor of the wind tunnel to a commercial antenna rotator with a resolution of 0.1 degree and a repeatability of ±0.5 degrees.

The wind tunnel air speed is measured by means of a 12.7 mm diameter hemispherical nose pitot-static tube mounted in the calibration section of the wind tunnel. The pitot-static tube pressure is read by a differential pressure sensor with a range of 2491 Pa, stabilized with a thermal base heated to 35°C. Correction factors for air density are applied to the pitot-static tube readings. Standard conditions for the wind tunnel are 15°C, 1013.25 hPa, and 0% relative humidity. A correction factor is also applied for the compressibility of air. A location correction factor is applied to the wind tunnel air speed to account for the speed difference between the pitot-static tube location and the air speed at the test sensor location based on transfer standard calibration data from the U.S. national laboratory, the National Institutes of Standards and Technology (NIST). The tunnel air temperature, barometric pressure, and the pitot-static tube differential pressure sensor are sampled at a 3 hertz rate. The tunnel dew-point temperature is sampled five times during each one-minute calibration run. All wind tunnel reference data are processed by a 10 MHz 80286 computer.

3. Test Method

As previously mentioned, significant speed and direction biases can exist over certain azimuth ranges with a sonic anemometer. The problem is how to characterize the overall anemometer performance in a concise manner. Analysis of preliminary sonic wind tunnel test data led to the concept of using the best-case and worst-case performance as the test conditions. A decision can then be made to see if the sensor's test performance meets the user's accuracy requirements under worst-case conditions. The best-case performance gives the user an estimation of the performance capability of a particular sonic anemometer with full correction of the systematic errors due to the wind speed and azimuth orientation of the sensor.

Wind tunnel calibration tests are conducted in two separate steps:

1) Wind direction tests at fixed wind speeds to determine test sensor directional biases for wind speed and direction.

2) Full range calibration tests based on best-case and worst-case wind direction orientations identified in step one.

The sensor directional accuracy is measured by varying the sensor orientation with respect to the air flow at discrete wind tunnel air speeds. The anemometer is rotated in five-degree increments around the full 360 degrees. The 360-degree test has three separate parts: from 0 to 120 degrees, from 120 to 240 degrees, and from 240 to 360 degrees. Each data point is a one minute average based on 20 three-second samples from the anemometer under test. The direction tests are conducted at fixed speeds of 30 m/s, 20 m/s, 10 m/s, 5 m/s and 3 m/s.

The directional test data are analyzed for the best-case and worst-case direction orientations. Wind speed calibrations are performed at these two direction orientations. Wind tunnel data for anemometer wind speed calibrations are taken for three 60-second time intervals at each individual speed. Each data point is a one minute average based on 20 three-second samples from the anemometer under test. Calibration data are acquired at ten speeds over the operational range of the anemometer for a total of thirty data points. For all runs, test anemometer speed, direction, and sensor status are recorded on a separate computer.

Five-degree increments were chosen for the wind direction test to match the 10 (±5) degree window used for synoptic wind direction reporting used by the NWS. The fixed speeds were chosen to represent the normal range of wind speeds that occur at most NWS sites. The higher speed ranges, 30 to 65 m/s, are checked as part of the wind speed calibration tests.

Figures 1 through 3 are typical graphs for the wind direction tests at 30 m/s. The X-axis depicts the test sensor orientation at a constant wind tunnel air speed. The primary Y-axis is the delta speed, unit under test (UUT) - tunnel, in m/s while the secondary Y-axis is the delta wind direction, UUT - tunnel, in degrees.

Figures 4 and 5 are typical graphs of the full range anemometer calibration tests conducted at the best-case and the worst-case orientations. The X-axis is the wind tunnel air speed with the sensor at a constant azimuth orientation. The primary Y-axis is the delta speed, UUT - tunnel, in m/s while the secondary Y-axis is the delta wind direction, UUT - tunnel, in degrees.

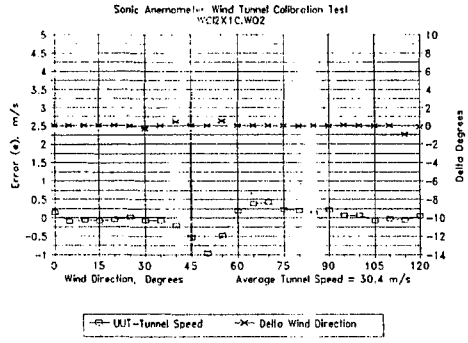

Figure 1. Sonic anemometer test data from 0 to 120 degrees @ 30 m/s

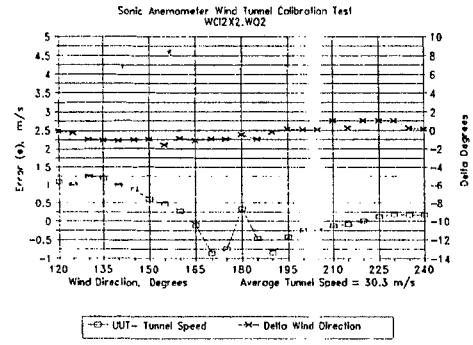

Figure 2. Sonic anemometer test data from 120 to 240 degrees @ 30 m/s

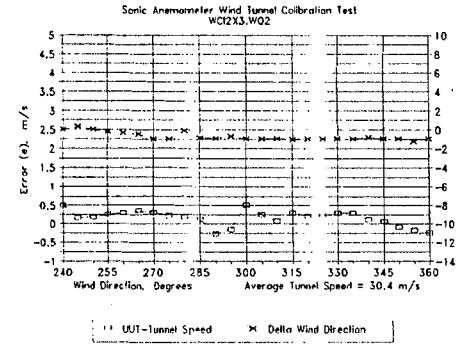

Figure 3. Sonic anemometer test data from 240 to 360 degrees @ 30 m/s

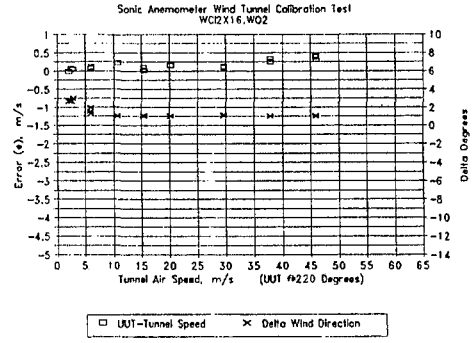

Figure 4. Sonic anemometer wind speed calibration test, best-case orientation

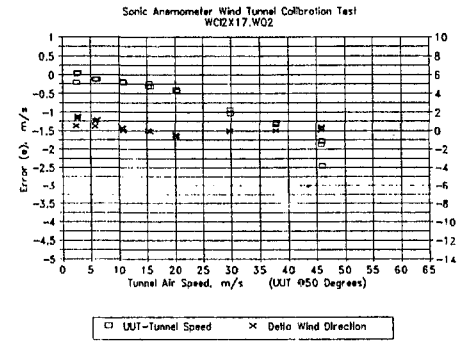

Figure 5. Sonic anemometer wind speed calibration test, worst-case orientation

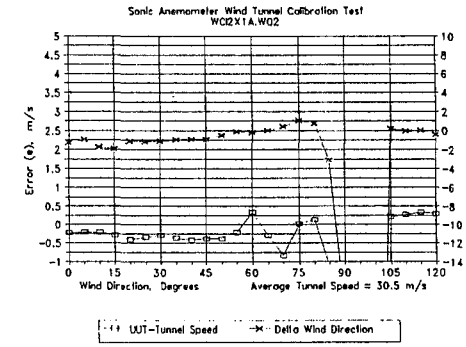

Figure 6. Sonic anemometer test run with anomalous data from 85 to 100 degrees

4. Test Results

Based on the analysis of the wind direction graphs for all the test speeds, the best-case wind direction orientation was determined to be 220 degrees for this test anemometer. Figure 4 presents the best-case wind direction orientation for the full range speed calibration test. Likewise, based on the analysis of all the wind direction graphs, the worst-case wind direction orientation was determined to be 50 degrees for this anemometer. Figure 5 presents the worst-case wind direction orientation for the speed calibration test.

This test method has uncovered various sonic anemometer deficiencies such as:

1) Significantly different wind speed errors at best-case and worst-case orientations. Using least squares analysis, the slope of the speed differences is 1.0059 (0.59% high) for the best-case orientation (figure 4) of this test anemometer versus the wind tunnel air speed. Likewise for the worst case orientation (figure 5) the slope is 0.9557 (4.43% low). The speed error difference between the best-case and worst-case orientations for this test anemometer exceeds 5%.

2) Lack of full range high speed performance to 65 m/s as shown in figures 4 and 5. (The test anemometer data went missing above 47 m/s.)

3) Anomalous wind speed and direction performance at certain azimuth orientations as shown in figure 6 between 85 and 100 degrees.

5. Conclusions

This method has proven effective in discovering sonic anemometer performance anomalies in individual sensors and manufacturers. Pretest checks could be added to validate the anemometer as ready for test:

1) Zero wind chamber check
2) Sonic path length check.

However, these checks are not absolutely necessary since the wind tunnel calibration test will reveal the anemometer performance anomalies.

The NWS results of using this standard test method indicate that, based on the sensors tested thus far, sonic anemometers can measure wind direction to ±2 degrees without much difficulty. However, overall wind speed measurement accuracies vary from 2% to 8% depending on the particular anemometer manufacturer. It seems that in some cases, better speed correction factors based on the wind direction data could be implemented to improve the sonic anemometer's overall speed measurement accuracy.

This test method has been accepted as the basis for a working draft standard by the International Organization for Standardization (ISO) Technical Committee 146, Subcommittee 5, Working Group 2 - Sonic Anemometers. The title of the draft test standard is: "Sonic Anemometers/Thermometers - Part 1 Acceptance Test Methods for Mean Wind Measurements".

6. Acknowledgements

The author wishes to thank Lynn Winans (NWS) and Anthony Leonardo (EG&G Inc.) for the numerous wind tunnel calibration runs and Michael Salyards (NWS) for technical discussions and editing of the draft manuscript.

7. References

American Society for Testing and Materials: "Standard Practices for Measuring Wind and Temperature by Acoustic Means", ASTM D 5527-94.

American Society for Testing and Materials: "Standard Test Method for Determining for Determining the Performance of a Sonic Anemometer/Thermometer by Acoustic Means", ASTM D 6011-96.

Kaimal, J.C. and Gaynor J. E., Zimmerman, H.A., and Zimmerman, G.A.: 1990 "Minimizing Flow Distortion Errors in a Sonic Anemometer", *Boundary-Layer Meteor.* 53, 103-115.

Wyngaard, J.C. and Zhang, S.F.: 1985 "Transducer Shadow Effects on Turbulence Spectra Measured by Sonic Anemometers", *J. Atmos. Ocean.Tech.* 2, 548-558.

Session VI

INTERCOMPARISONS FOR UPPER-AIR INSTRUMENTS

TRANSITION FROM OMEGA TO GPS FOR UPPER-AIR WIND OBSERVATION IN METEO-FRANCE

François Bonnardot
METEO-FRANCE SETIM, Trappes

1. INTRODUCTION

Météo-France radiosounding network consists in 23 stations (figure 2). Sixteen of them, located overseas or on transatlantic ships, were using the OMEGA radionavigation system for upper-air wind measurement. This system has been stopped on october first 1997. Météo-France, and many other weather services, had thus to find an alternative. By the end of 1995, Météo-France decided to use Vaisala's system with GPS for wind calculation. A lot of tests have been performed in Trappes (SETIM) in 1996 before settling in the stations. The first system was installed in Terre-Adélie (Antartica) in January 1997 and the last one in Kerguelen Island (Indian Ocean) at the end of September 1997. Since then, all stations continuously provide wind profiles for forcast models.

2. GENERAL DESCRIPTION OF VAISALA'S GPS SYSTEM

Global positionning system (GPS)

The GPS is a continuous world-wide navigation system. It is based on a constellation of 24 low orbit satellites sending navigation signals. Those signals are transmitted at two different frequencies L1 = 1575,42 MHz and L2 = 1227,60 MHz. Those signals are incoded to allow individual satellite identification by the receivers. The transmitted signals also provide satellites navigation data (position, speed..) to users.
A code correlating GPS receiver is able to decode those signals and to calculate its own position.

Vaisala's windfinding system

Vaisala GPS windfinding system is based on Doppler measurements done onboard the radiosonde. These Doppler shifts are due to the relative movement between the radiosonde and the GPS satellites. The simplified GPS module on the radiosonde is based on a codeless reception technique which enables the radiosonde to measure the Doppler shifts of the detected satellites signals but not to identify them.

The radiosonde sends the Doppler information to the ground station which is equipped with a code correlating GPS receiver. In addition to extract the satellites navigation data from the GPS signals, it also measures the local Doppler frequencies due to the satellites motions.

The satellites received by the radiosonde are identified by correlating the local Doppler measurements with those transmitted by the radiosonde.

The windfinding solution is calculated by the ground station GPS receiver. It is based on the following data :

- the relative speed amplitude from at least four satellites
  The sonde Doppler measurement gives the line-of-sight speed between the satellite and the sonde. Doppler shift due to the satellite motion, measured at ground level, is then substracted from the sonde one to obtain the Doppler shift caused by the sonde motion

- the relative speed direction from the satellites needs both radiosonde and satellite positions. The former is obtained by integration of the velocity vectors and is therefore only approximate, the latter is extracted from the GPS data by the ground station.

3. EXPERIMENTATION OF THE SYSTEM BY METEO-FRANCE

In order to test this new system and to integrate it into Météo-France STAR system, more than 100 radiosondes were launched from Trappes sounding experimental station in 1996.

The first tests occured in February 1996 with 21 launches. This experiment showed an important problem of availibility of GPS raw wind data. This problem leaded to important wind losses at all levels and more particularly above 15km. In average, wind data were definitively missing above 23km height, whereas the 400MHz sonde signals were received until 30km. Two causes were suspected for these losses :

- a too short distance between the radiosonde and the baloon causes a short period of radiosonde swing which degrades the satellites signals reception by the radiosonde. During the first tests, the length of the unwinder string was 30m.
- battery voltage weakness leaded to wind data losses at the end of soundings

During the second test period (October 1996), GPS radiosondes equipped with a new unwinder (60m string) and a new battery (longer lifetime) were used. Twenty soundings have been performed. The

losses have been partly reduced and wind data were available with a rate of 90%.
For six of those soundings, the cumulated wind data losses exceded 15 mn with a maximum loss of 40 mn (this particular sounding is analysed further, see figure 1). Wind data losses did not exceed 10 min for the 14 others.
During those tests, it appeared that it needs 2 or 3 mn after launching to get the first wind data. This gap was partly reduced by waiting 2 or 3 mn before launching. This gives enough time to the radiosonde to lock on GPS signals before launching. However this operation is almost impossible in strong wind conditions.

Analyse of a sounding presenting important wind data losses

The graph below shows the number of raw wind data per minute provided by the GPS receiver during a flight. The system normally provides 120 data per minute. We observe that, during the first part of the sounding, this number does not exceed 40 and is often near zero. The number of raw data were then too small for a good processing. During the second half of the flight, the number of data per minute was close to 120 and the wind could be calculated.

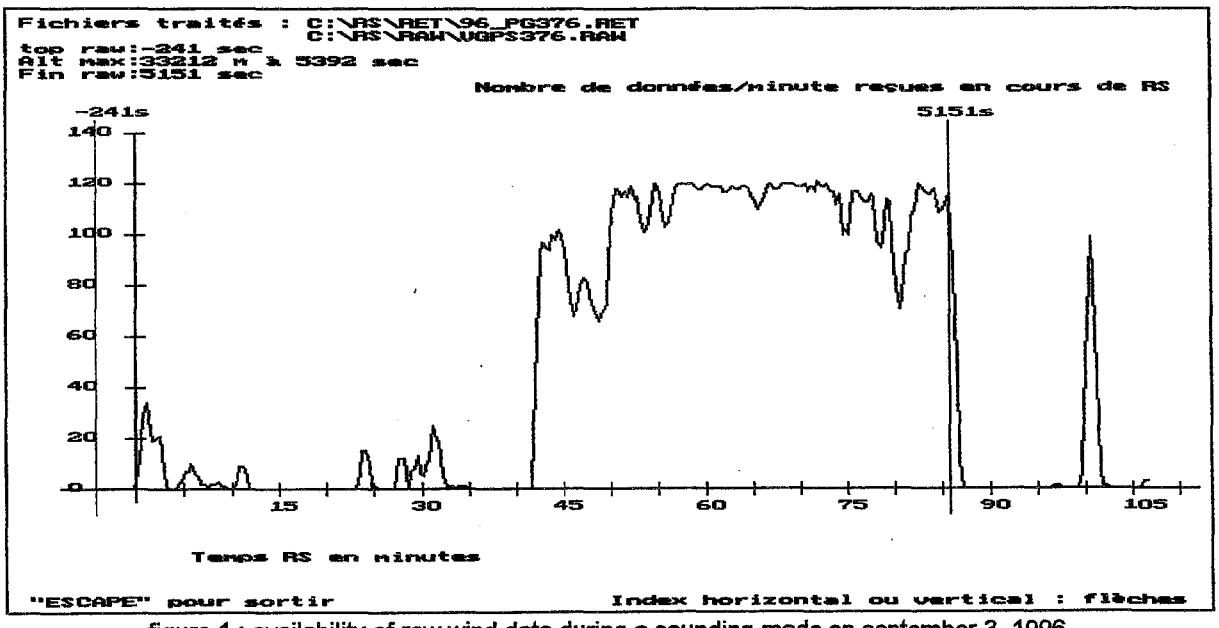

figure 1 : availability of raw wind data during a sounding made on september 3, 1996.

By checking raw data files, and particularly the state of the 8 reception sonde channels, we can identify 3 different situations :

- none of the 8 channels can lock on a satellite. No wind is calculated
- some channels are locked on satellites signals but the ground GPS receiver can not identify the satellites corresponding to those signals. No wind is calculated.
- at least four channels are locked on a signal and the corresponding satellites are identified by the ground GPS receiver. In this case, the system can calculate a wind.

The critical points seem to be the ability of the radiosonde receiver to separate satellite signals and the software procedure to identify the satellites. We have observed false winds due to bad satellite identification.

4. EQUIPMENTS SETTLING

Sixteen stations were concerned (see the map in figure 2). The main problem was to ship in time the equipement to some overseas stations.
For instance, Terre-Adélie (Antartica) is reachable only one month per year. Therefore, taking in account the ordering and shipping delays, we had to order in August 1996 for starting up in october 1997.
The second difficulty was to adapt the utilisation protocole to the roughness of local conditions. Four stations installed on transatlantic ships are now equipped with this new system.
For the 16 concerned stations, specialized staff made the installation and trained the local staff to the utilisation and the maintenance of the new system.

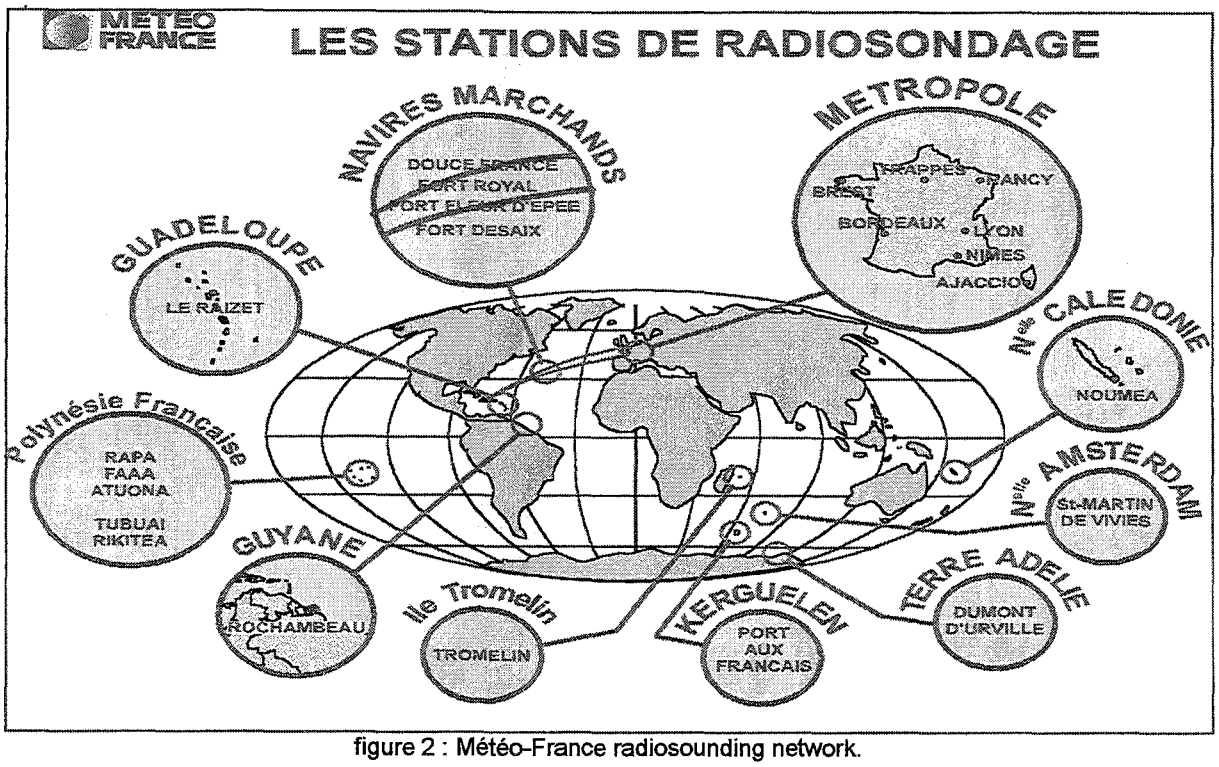

figure 2 : Météo-France radiosounding network.

4. FIRST RESULTS AFTER A FEW MONTHS OF EXPLOITATION

Since october 1rst 1997, the 16 stations are using Vaisala's GPS system for upper-air wind measurements. The monitoring (comparison with numerical forecast) of the data quality does'nt show more problems with GPS wind than with OMEGA's.

On the other hand, we have observed (table 1) a decrease of quality for the availability of wind data. In average, this rate is about 90% between 1000hPa and 300hPa, and closer to 80% above this level.

Level in hPa	% wind data availability with Vaisala's GPS system	% wind data availability with OMEGA system
925 hPa	90	98
500 hPa	92	99
250 hPa	87	99
100 hPa	81	97

Table 1

Notice that those rates vary quite a lot from a station to another due to different geographical positions (and various exploitation conditions).

Strong winds and turbulences may disturb a correct unwinding of the string between the sonde and the balloon. This may cause wind data losses due to a short period pendulum motion.

The system can also be disturbed by non GPS signals. For instance, WAAS signals transmitted by INMARSAT geostationary satellites have the same frequency than GPS signals. Consequently the codeless GPS radiosonde receiver is not able to reject the signals and gives false Doppler measurements to the ground station. This issues in false wind data or wind data losses. This problem occurs more especially in the West-Atlantic area at low latitudes since October 1997.

Radars interferences can also disturb the system if the transmitter is close to the station.

5. FUTURE PROSPECTS TO OBTAIN BETTER PERFORMANCES

From our experience, the remaining problems with Vaisala's GPS windfinding system come from three main causes :

- Some losses in wind data are due to a lack of sensibility of the GPS receiver onboard the radiosonde. A new receiver will be available in 1998.

- The unwinder used isn't always reliable and the needed distance between the radiosonde and the baloon isn't always reached. Vaisala is presently working on the improvement of the unwinder reliability.

- Many wind data losses or false winds are due to GPS satellite identification problems. A new software version is under developpement to solve these problems. More particularly, it should be able to reject unwanted WAAS signals.

Hopefully, those modifications in the system should improve its performances and more particularly reduce wind data losses during the soundings.

Comparison of GPS and OMEGA Radiosonde Measurements in Hong Kong

M.C. Wong, W. Y. Law and C.K.Chan
Hong Kong Observatory
Hong Kong, China

1. Introduction

The Hong Kong Observatory has operated an Upper-Air Meteorological Station at King's Park (station code: 45004, location: 22.31N, 114.17E) since 1951. In 1981, a Vaisala MicroCORA system was installed to automatically track the radiosondes. The computation of winds was made using the VLF signals in the very low frequency range of 10 - 13 kHz of the OMEGA windfinding system. Data reduction was carried out in real time by a minicomputer. The MicroCORA was replaced by the DigiCORA in 1993. In 1997, the Observatory began to employ the GPS windfinding technology and the DigiCORA was upgraded to include a GPS windfinding module.

2. Comparison of simultaneous GPS and OMEGA Measurements

An inter-comparison exercise using the GPS and OMEGA windfinding systems simultaneously was carried out from February to September 1997 at King's Park. A total of 34 flights were conducted. In each flight, two radiosondes, one receiving GPS signals (a Vaisala GPS sonde RS80-15G or WS80-15G) and the other receiving OMEGA signals (a Vaisala VLF sonde RS80-15F or WS80-15F), were carried on a single balloon. A pilot programme was first conducted for different arrangements of the GPS and OMEGA sondes with a view to selecting the one least susceptible to interference for further study. Table 1 summarizes the launch time and the configuration of sonde arrangements for all the 34 flights in the exercise, the first 20 being flights in the pilot programme.

Flight	Launch Time (UTC)		Configuration	Flight	Launch Time (UTC)		Configuration
1	97/02/24	03	2-meter horizontal	18	97/08/05	06	tied together
2	97/02/25	02	tied together	19	97/08/07	06	40-meter vertical
3	97/02/27	03	2-meter horizontal	20	97/08/14	06	2-meter horizontal
4	97/02/27	08	tied together	21	97/08/26	06	40-meter vertical
5	97/06/17	06	40-meter vertical	22	97/09/04	00	40-meter vertical
6	97/06/20	08	40-meter vertical	23	97/09/04	06	40-meter vertical
7	97/06/23	03	40-meter vertical	24	97/09/05	00	40-meter vertical
8	97/06/25	06	2-meter horizontal	25	97/09/05	06	40-meter vertical
9	97/06/27	08	tied together	26	97/09/06	06	40-meter vertical
10	97/07/14	06	tied together	27	97/09/11	06	40-meter vertical
11	97/07/15	06	2-meter horizontal	28	97/09/13	00	40-meter vertical
12	97/07/17	06	40-meter vertical	29	97/09/13	06	40-meter vertical
13	97/07/28	06	2-meter horizontal	30	97/09/14	06	40-meter vertical
14	97/07/29	06	40-meter vertical	31	97/09/18	02	40-meter vertical
15	97/07/31	06	tied together	32	97/09/18	06	40-meter vertical
16	97/08/01	06	40-meter vertical	33	97/09/19	00	40-meter vertical
17	97/08/04	06	40-meter vertical	34	97/09/19	06	40-meter vertical

Table 1: List of flight numbers, launch time, and configurations of the GPS-OMEGA flights

In the pilot programme, three configurations were tried, namely the "tied-together", the "2-meter horizontal" and the "40-meter vertical" configuration. In the "tied-together" configuration, the sondes were tied together side-by-side and lifted by a TOTEX TA500g balloon. In the "2-meter horizontal" configuration, the sondes were mounted at the two ends of a 2-meter horizontal wooden pole which was lifted by a TOTEX TA700g balloon. In the "40-meter vertical" configuration, the OMEGA sonde was mounted on a TOTEX TA500g balloon with the GPS sonde hanging downward by a 40-meter long string. In the pilot programme, a total of six, six and eight flights were launched for the three configurations respectively. As both the "tied-together" and the "2-meter horizontal" configurations were found to experience larger interference, the "40-meter vertical" configuration was used for the rest of the exercise (flights 21 to 34 in Table 1).

3. Results from the "40-meter vertical" configuration

Including those made in the pilot programme, a total of 22 flights with the "40-meter vertical" configuration were conducted in the exercise. Winds were calculated at 14 standard pressure levels, namely at 925hPa, 850hPa, 700hPa, 500hPa, 400hPa, 300hPa, 250hPa, 200hPa, 150hPa, 100hPa, 70hPa, 50hPa, 30hPa and 20hPa. The wind speed and direction data from the two sounding systems were compared to investigate any possible correlation in wind measurements of the two systems.

Figures 1 and 2 show the direct differences (see, e.g. Kurnosenko 1996) of the GPS data minus the OMEGA data (GPS-OMEGA) in the wind direction and speed as well as the respective standard deviations at each standard pressure level. In both figures no significant systematic differences in the GPS and OMEGA measurements were observed. The direct differences in direction and speed were in the range of -3 to +4 degrees and -0.2 to +0.8 m/s respectively. The standard deviations of the direct differences were within 5 to 25 degrees for wind direction, and within 0.5 to 3 m/s for wind speed. Similar to the observations of Nash and Schmidlin (1987), the magnitudes of the direct differences were much smaller than the respective standard deviations.

Figures 3 and 4 give the direct differences (GPS-OMEGA) along the east-west and the north-south wind components, as well as their standard deviations. In this report, the winds from the east and north were taken as negative, following usual meteorological convention. The direct differences in the east-west component ranged from -0.4 to 0.6m/s and in the north-south component -0.8 to 0.6m/s. It was observed that the GPS system in general measured a slightly larger value than the OMEGA system in the east-west component below 100hPa but exhibited a negative bias above. The direct differences in the north-south component showed more evenly distributed positive and negative biases. The standard deviations of the direct differences of the east-west and north-south components behaved quite similar to each other except at the very high levels, with a range of 0.7 to 2 m/s for the east-west component differences and a range of 0.6 to 3m/s for the north-south component differences.

Figure 5 shows the scatter diagrams and the least squares best fit of the east-west component and the north-south component measured by the GPS versus that by the OMEGA sondes. Each data point in the scatter diagrams represented a component value measured at a standard pressure level of an individual launch. The correlation coefficients for both components were close to 1. The least squares best fit for both components exhibited a slope close to 1 and an intercept close to 0, indicating no significant systematic difference between the two windfinding systems.

4. Conclusion

This comparison exercise of 22 soundings with GPS and OMEGA sondes paired in the "40-meter vertical" configuration showed very good agreement between the GPS and OMEGA wind measurements. The direct differences in direction were in the range of -3 to +4 degrees for the 14 standard pressure levels with the standard deviations ranging from 5 to 25 degrees. The direct differences in speed were in the range of -0.2 to +0.8 m/s with standard deviations within 0.5 to 3 m/s. No significant systematic difference could be found in the wind measurements of the GPS and OMEGA windfinding systems. There was a strong positive relationship in the east-west and north-south components themselves for the two windfinding systems, with a correlation coefficient of 0.98 for the east-west component at all pressure levels and 0.95 for the north-south component.

Acknowledgments. We thank Ms. S.W.Yeung, Mr. K.C.Tsui and the staff at the King's Park Upper-Air Meteorological Station for making extra efforts to launch the additional radiosondes for this exercise.

REFERENCES

1. Kurnosenko, S., 1996: Description and User Guide for the Radiosonde Comparison and Evaluation Software Package. WMO Instruments and Observing Methods Report No.60.
2. Nash J., and F.J.Schmidlin, 1987: WMO International Radiosonde Comparison (U.K. 1984, U.S.A. 1985). Final Report. WMO Instruments and Observing Methods Report No.30.

Figure 1: Direct Differences (GPS -- OMEGA) in Angle and their Standard Deviations

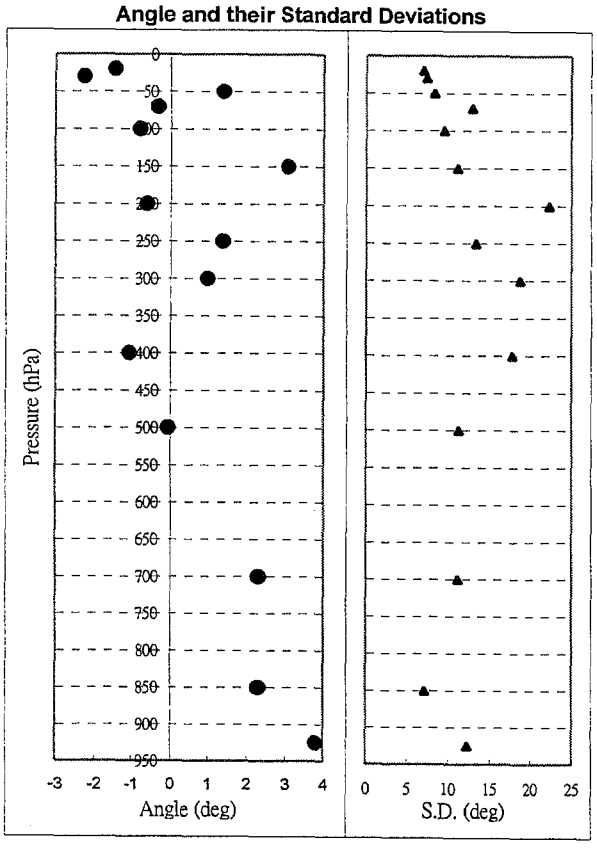

Figure 2: Direct Differences (GPS -- OMEGA) in Speed and their Standard Deviations

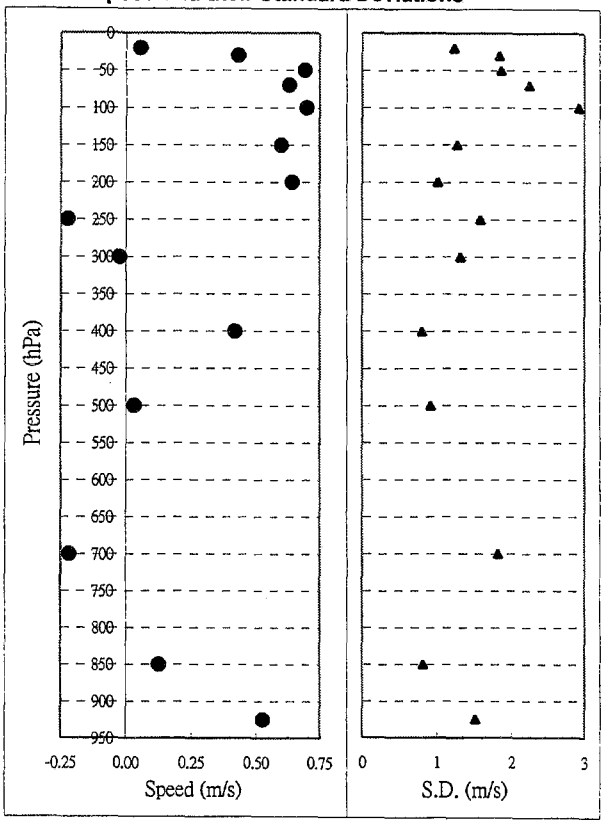

Figure 3: Direct Differences (GPS -- OMEGA) in the East-West Component

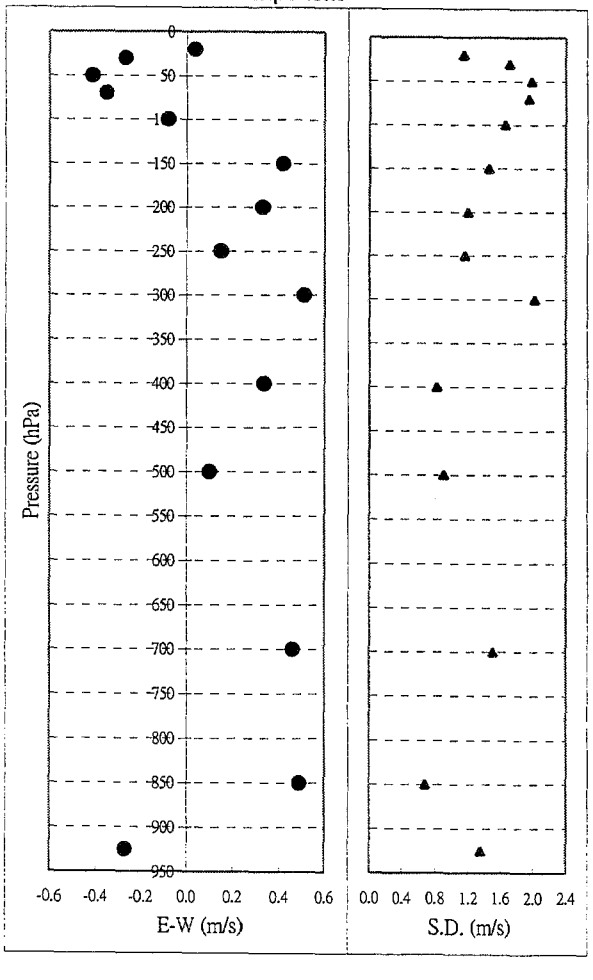

Figure 4: Direct Differences (GPS -- OMEGA) in the North-South Component

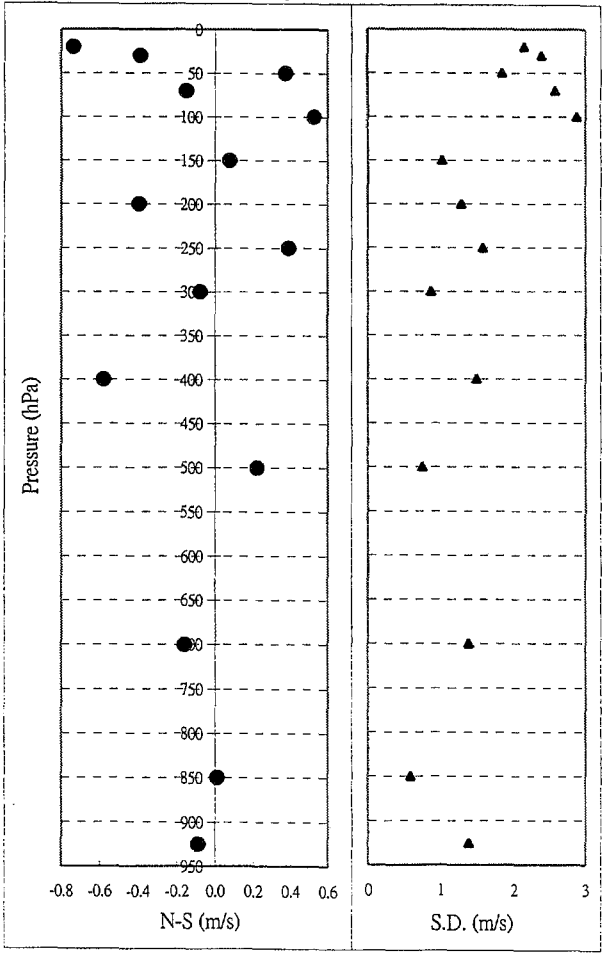

Figure 5: Scatter Diagrams of the East-West and North-South Components Measured by the OMEGA and VLF Wind-finding System

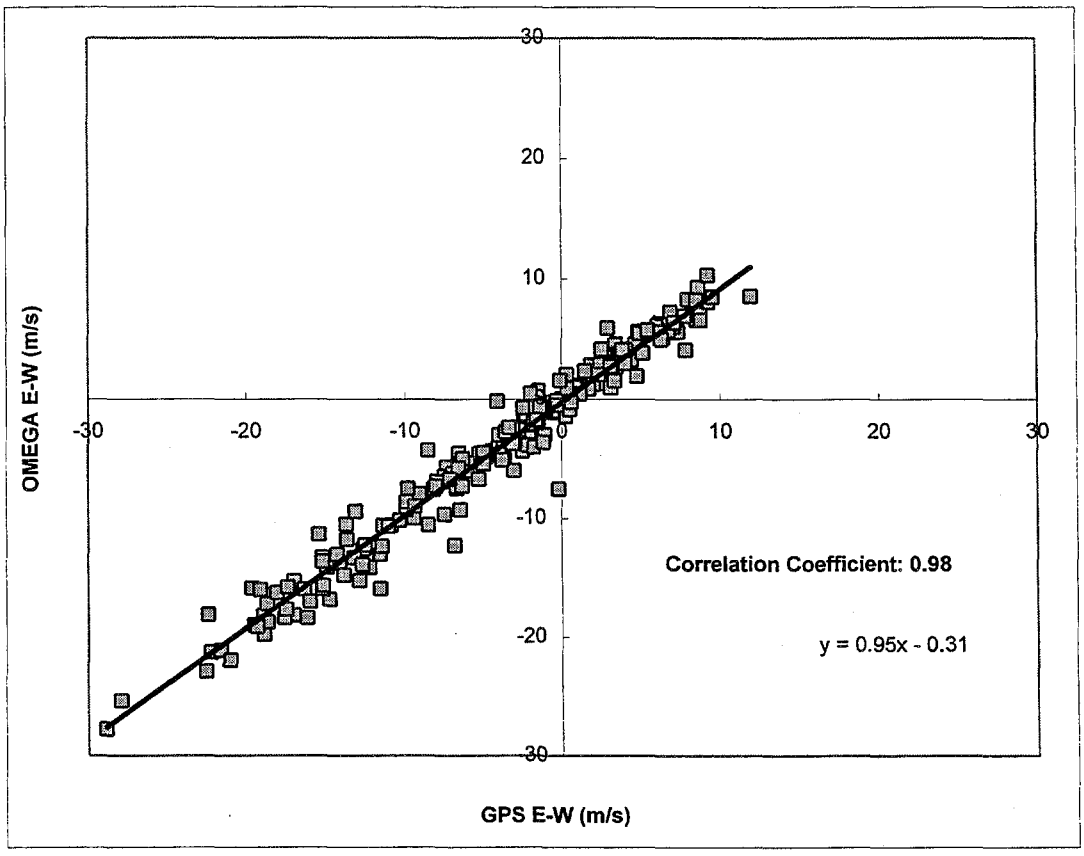

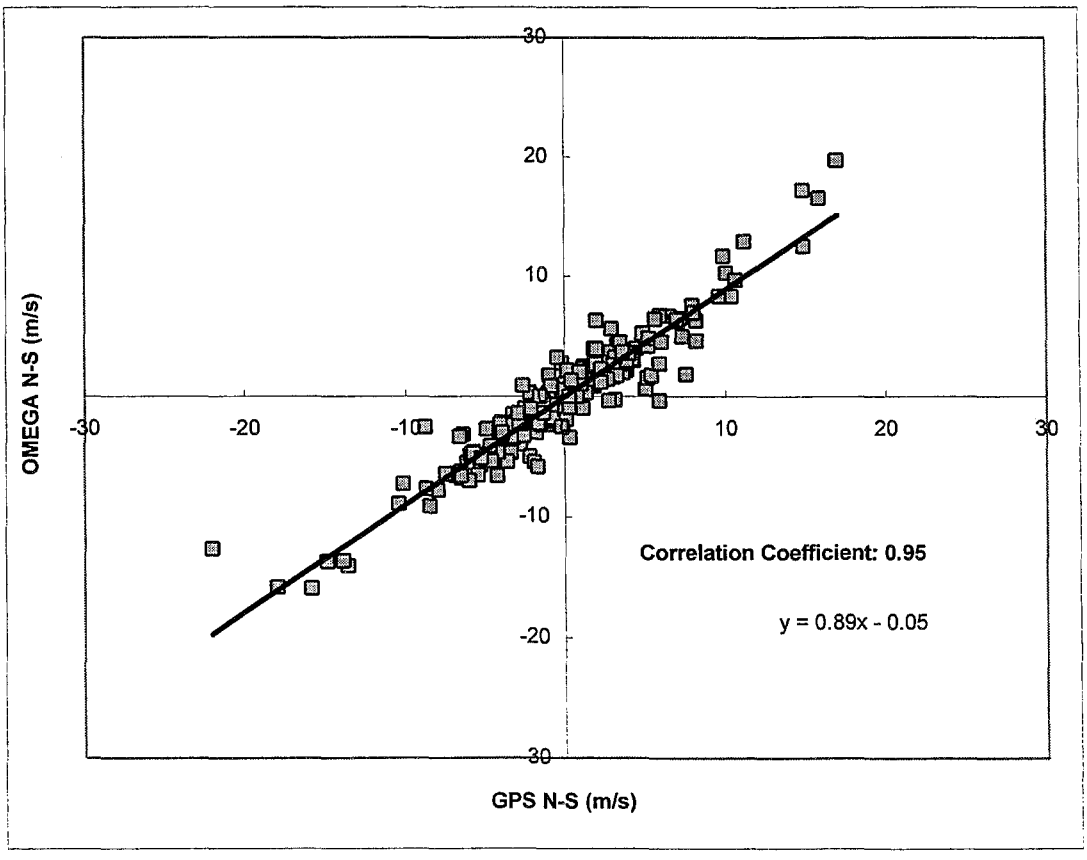

GPS RADIOSONDE TESTS AND OPERATIONAL EXPERIENCE FROM UK METEOROLOGICAL OFFICE AND OVERSEAS STATIONS

J. B. Elms, John Nash and R. Smout
The Met. Office, Bracknell, Berks, RG12 2SZ, UK

1. INTRODUCTION

The closure of the Omega navigation service on 1 October 1997 has caused a major problem to many national meteorological services who were relying on this system for automated upper wind measurements.

By late 1993, it was realised that there was a good probability that the Omega navigation service would cease within a few years. Thus, arrangements were made to test candidate windfinding systems to replace Omega. The tests were intended to allow the UK Met. Office to make an informed choice of equipment. As a spin-off, results could be supplied to WMO to aid the choices of other national meteorological services. In 1997, test reports were provided to the World Weather Watch, WMO in Geneva on:-
- AIR inc. radiotheodolite (USA), tested 1991/3 + operational use in Antarctica, Elms (1997)
- the ATIR radiotheodolite (Israel), tested twice in 1994, Elms, Nash and Glennie (1997),
- AIR Inc. GPS radiosondes (USA), tested in 1995 and 1996, Elms (1997)
- Vaisala Öy, GPS radiosondes (Finland) tested twice in 1996, Elms, Nash and Stancombe (1997).

All systems tested could be used as viable replacements for Omega windfinding. However, the UK Met. Office has purchased Vaisala MW15 ground systems and RS80-15GH GPS radiosondes to replace Omega wind finding at Falklands, Gibraltar and St. Helena. A GPS windfinding system was chosen so that a similar system could be used at all three sites. This was to minimise the number of system types requiring support from Bracknell. The radiotheodolite option could not be used because of the very strong upper winds over the Falklands.

2. INSTALLATION SCHEDULES

50 successful test flights were required from the operational systems in the UK before shipment commenced to the sites outside the UK. Fortunately, there were no major problems with the GPS radiosonde system or the radiosondes supplied in June 1997. Thus, it was possible to commence shipping systems in early July 1997, ready for installation, operational testing and local staff training by late July in the Falklands, early September at St. Helena and late September at Gibraltar.

Upper wind observations at the three sites were sustained without interruption by the closure of the Omega network .

3. TEST FACILITIES

The main site for test activities within the UK is now located at Camborne, an operational radiosonde station in the extreme south-west of England, located a few kilometres from the Atlantic coast. The operational staff at this station have been trained in test procedures and perform a large number of tests with only limited supervision from the instrumentation specialists in Bracknell.

The station has retained the windfinding facility that was used to provide operational wind measurements before the introduction of the automated Loran-C measurements. Thus, it is possible to track a target attached to the balloon, as well as measuring winds with the operational Loran-C radiosondes. Winds from the radar can be processed using Vaisala software or an independent Met. Office program, as in the examples shown here.

Testing of GPS radiosondes flown together with other radiosondes is not straightforward, since the GPS radiosondes tested to date appear more susceptible to interference from nearby radiosondes than other types of navaid radiosondes. In some cases the motion of the radiosonde relative to the balloon can impact on GPS tracking capability. Thus, real time processing of the comparison data is essential to check for problems. This was achieved in this exercise by staff from Bracknell, using the display and processing software developed by Kurnosenko, Kurnosenko and Oakley (1996).

4. TESTING AT CAMBORNE

The acceptance testing at Camborne combined a mixture of test configurations. Some GPS radiosondes were launched individually in normal operational mode to establish that the systems functioned adequately in standard operational mode. In addition, a series of twin radiosonde flights were performed with the GPS radiosonde suspended 60m below the balloon as recommended by Vaisala, but with a radar target a few metres underneath the balloon and a Loran radiosonde suspended about 30 m below the balloon between the radar target and the GPS radiosonde. Simultaneous wind measurements from the GPS, Loran and radar systems were

compared for each flight. A quantitative evaluation of the GPS measurement errors can be derived, if the error characteristics of the radar and Loran wind measurements are known. All the measurements have a vertical resolution of about 300m, as used for operational upper wind measurements in the UK (i.e. winds were derived from tracking data samples of duration 1 minute). While agreement was generally very close, there were a finite number of flights when the GPS measurements showed pronounced anomalies relative to the measurements from the other two systems. In these cases the anomalous winds were often followed by a period when the Vaisala ground system indicated that the radiosonde processor could not recognise the incoming GPS signals. Thus, operators should check if there are problems with GPS signal reception in flight, and be wary of reporting significant variation in the vertical when wind measurements are interpolated or reported immediately before a period of interpolation.

In the early stages of acceptance testing the temperature and humidity measurements were checked before launch by placing the GPS radiosondes near the station surface sensors. The temperature screens were relatively close to the tracking radar on top of the station building. On some occasions, the radar produced interference in the GPS signals received by the radiosonde and the GPS tracking prior to launch was clearly disturbed. Subsequently valid winds were often not reported until a considerable time after launch. Radiosondes with disruption in GPS tracking before launch [signals from far too many GPS satellites apparently being received] also produced a greater number of wind anomalies than usual during flight.

The weather during the GPS acceptance testing in June and July was not associated with strong upper winds so that slant ranges from the tracking radar remained relatively small. Earlier tests of Met. Office radar winds against high precision radar winds at another site in the UK showed that random errors in both westerly and southerly wind components of the radar should be less than or equal to 0.3 ms^{-1} at these slant ranges.

The standard deviation of the differences between simultaneous navaid (GPS or Loran) winds and radar winds are plotted as a function of pressure in Fig. 1. The data are taken from at least 40 comparison flights. The number of flights providing data at pressures lower than 14 hPa was small. Any apparent variation in measurement quality at pressures lower than 14 hPa is not significant.

There were no significant systematic biases between Loran-C or GPS winds and the radar winds. Thus, the statistics in Fig. 1(a) demonstrate that the automated GPS wind measurements were of suitable quality for operational upper wind measurements (since random errors in the unmodified data were generally better than 1 ms^{-1} in each wind component). However, the random errors in the GPS winds without quality checking, were not smaller than the Loran-C wind errors.

Fig 1(b) shows the results of flagging out the largest GPS wind measurement anomalies. It is assumed that an alert operator might be trained to identify and eliminate these anomalies. At pressures higher than 100 hPa the GPS winds could be of better quality than Loran-C winds given operator intervention. Here, GPS random errors were about 0.2 to 0.3 ms^{-1} in each wind component, compared to about 0.5 to 0.6 ms^{-1} for Loran winds. However, at pressures lower than 50 hPa the random errors in the GPS winds were still similar to or larger than the errors in Loran-C winds even after anomalies were flagged.

5. OPERATIONAL EXPERIENCE

In the Falkland Islands, it was discovered that a transmitter was in use near the radiosonde station that prevented operation of the GPS windfinding system. Fortunately, it proved possible to obtain an agreement about the use of the transmitter that allows GPS windfinding to work when required.

During installation testing, it was found that the GPS radiosondes would often not work very reliably during daytime flights [large amounts of missing winds during a flight] when flown in the twinflight configuration as used at Camborne.. On the other hand , when flown independently, a continuous measurement was usually obtained with the GPS radiosondes. Using the twinflight configuration seemed to hinder GPS tracking to some extent, although this was not the case at Camborne. Vaisala have indicated that in the Falklands there may be some problem with interfering signals from a satellite located over South America, and updated software to improve the GPS signal processing is to be delivered soon.

Installation and flight testing at St Helena and Gibraltar was relatively trouble free and satisfactory twin flight comparisons were obtained indicating that satisfactory GPS winds were being produced at both locations.

However, the following was noticed:-

- Faulty unwinder operation

It is critical for the Vaisala GPS radiosondes that the unwinder works correctly. Some of the Vaisala GPS radiosondes supplied had a very rough suspension cord that frayed easily. When this happened the suspension cord often became trapped on the edge of the plastic unwinder , and the radiosonde did not deploy to the full suspension length. Wind measurement quality was then very poor.

- Locking onto GPS signals prior to launch.. There was a better chance of obtaining wind measurements in the first few minutes of flight if the radiosonde was left standing outside the balloon shed so that it received GPS signals continuously prior to launch. This is possible at St Helena where one operator brings the balloon out of the balloon shed into the lee of the shed , whilst the other operator looks after the radiosonde and checks the ground system. The ground system should show that zero winds are being reported from the radiosonde prior to launch. Using this method about half the operational flights at St Helena reported winds from immediately after launch. At the other stations this level of checking prior to launch is not practical. The average height of the first reported wind above the ground was 500m at Gibraltar and 700m at the Falklands Islands.

Operational experience at all the sites in the last three months has shown that the Vaisala GPS system will generate very spurious winds when the GPS signal reception is poor. The operator must be alert to this possibility and check signal quality and the plausibility of the reported winds before the TEMP message is transmitted.

The amount of wind data loss during flight has been reviewed during the same period . Data loss is defined as no winds reported or data interpolated without reliable GPS signals.

- Data loss at Falklands 12 per cent
- Data loss at Gibraltar 4 per cent
- Data loss at St Helena 4 per cent

In testing Vaisala GPS radiosondes, it was found that wind data were often lost towards the end of the flight for flights ascending to pressures lower than 20 hPa. This has been attributed to limited battery life. For high flights, the preparation time for the radiosonde needs to be kept as short as possible ,once the battery is energised.

6. CONCLUSION

Vaisala GPS windfinding systems have been successfully implemented at all three UK GUAN stations in the Atlantic.

Test results indicate that errors in GPS winds should not be larger than the errors in the Omega measurements that are being replaced. The potential for very low errors in GPS winds is apparent (random errors better than 0.2 ms^{-1} in each component) but has yet to be reliably achieved in the Vaisala system tested.

Problem free deployment of Vaisala GPS radiosondes in comparison tests cannot be guaranteed with the Vaisala equipment. Optimum reliable operation may be over-dependent on the full deployment of the unwinder supplied with the radiosonde. Unfortunately the implementation of this unwinder in the operational radiosondes delivered to the UK was less satisfactory than that found in the prototype radiosondes tested earlier. In some cases the unwinder was not deploying to the full suspension length, following launch, and poorer wind measurements resulted.

ACKNOWLEDGEMENTS

R. Smout, J. Elms, J. Stancombe and D. Lyth performed all the testing and installation outside the UK. The staff at Camborne, managed by D. Drew, supported the UK acceptance operations.

REFERENCES

Nash, J. and Oakley, T. (1992) Experience in the use of Loran-C windfinding in the UK. Proceedings of the Wild Goose Association, 21st Symposium, Birmingham, England.

Elms, J. B. (1997) GPS radiosonde system trial, Camborne, January 1996 : Evaluation of AIR System and summary of Vaisala system, RS Tech. Memo No. 5.1, Met. Office, Bracknell.

Elms, J. B. (1997) AIR Radiotheodolite windfinding trial, Crawley 1991, RS Tech. Memo No. 5.4, Met. Office, Bracknell

Elms, J. B. , Nash, J and A. Glennie (1997) ATIR Radiotheodolite System Evaluation, 1994, RS Tech. Memo No. 5.3, Met. Office, Bracknell.

Elms, J. B. , Nash, J. and J. Stancombe (1997) Second evaluation of Vaisala GPS Radiosonde System, Camborne, RS Tech. Memo No. 5.2, Met. Office, Bracknell

Kurnosenko, S. and Oakley, T. (1996) Description and user guide for the radiosonde Comparison and Evaluation Software Package. WMO Instruments and Observing Methods Report No. 60, WMO/TD- No. 771

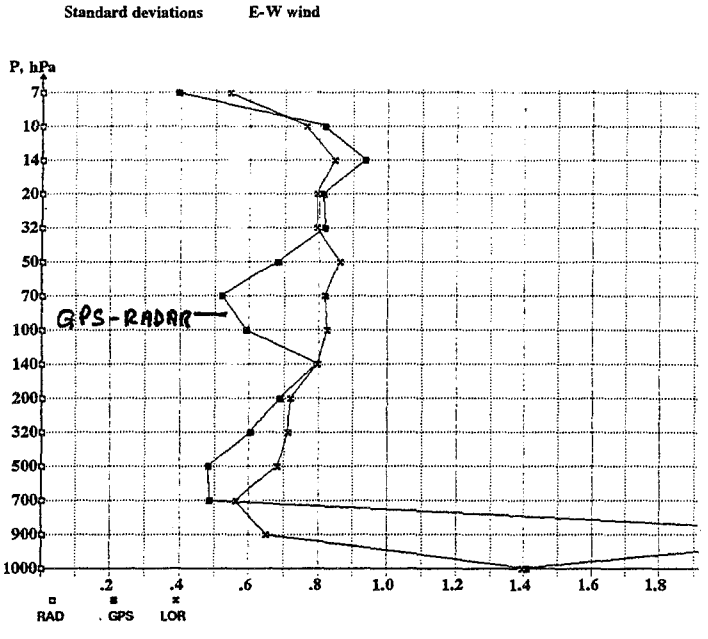

FIGURE 4 (a) CAMBORNE JULY 1997 GPS TEST

STANDARD DEVIATION OF GPS AND LORAN E-W WIND
FROM RADAR WIND REFERENCE (M.S-1)

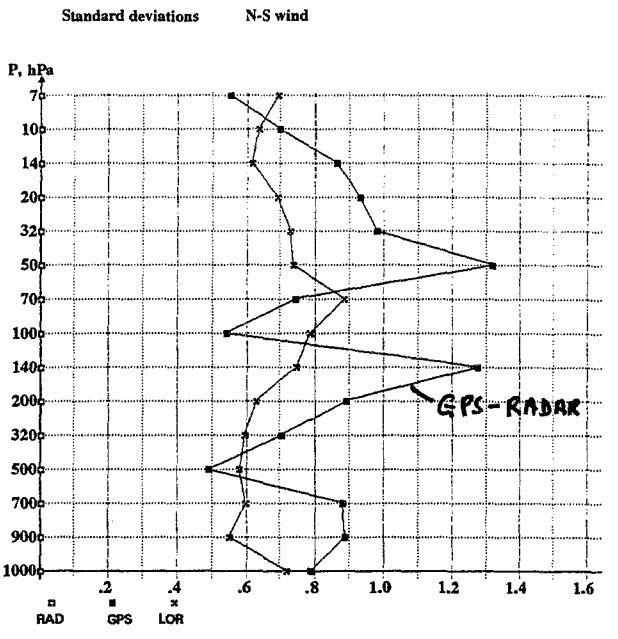

CAMBORNE JULY 1997 GPS TEST

STANDARD DEVIATION OF GPS AND LORAN N-S WIND
FROM RADAR WIND REFERENCE (M.S-1)

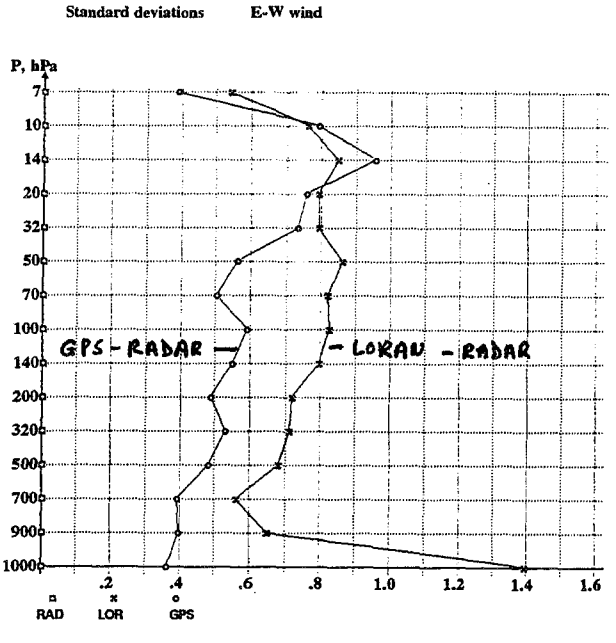

FIGURE 4 (b) CAMBORNE JULY 1997 GPS TEST

STANDARD DEVIATION OF GPS AND LORAN E-W WIND
FROM RADAR WIND REFERENCE (M.S-1)
***** ANOMALOUS WINDS EXCLUDED

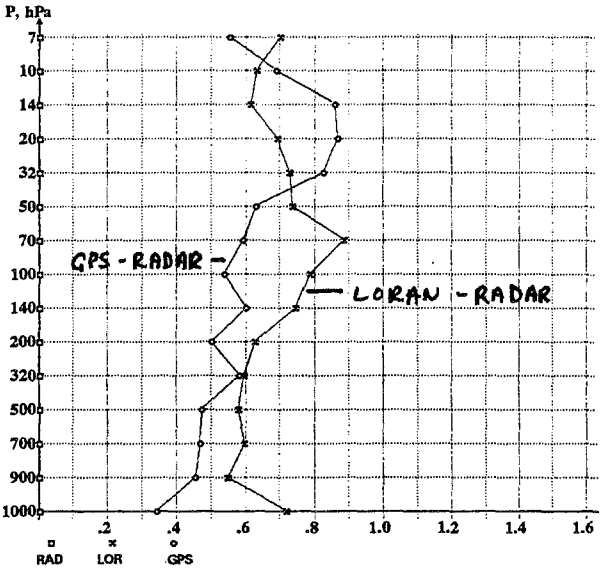

CAMBORNE JULY 1997 GPS TEST

STANDARD DEVIATION OF GPS AND LORAN N-S WIND
FROM RADAR WIND REFERENCE (M.S-1)
***** ANOMALOUS WINDS EXCLUDED

STATISTICAL ANALYSES OF PRESSURE, TEMPERATURE, RELATIVE HUMIDITY, AND GEOPOTENTIAL HEIGHT DIFFERENCE PROFILES OBTAINED FROM FLIGHT TESTS OF CO-LOCATED AIR, INC GPS AND VAISALA RS-80 RADIOSONDES

Dr. William J. Kohri
The Johns Hopkins University/Applied Physics Laboratory
Laurel, Maryland, USA

Abstract

A series of dual radiosonde comparison test flights were conducted at Cape Canaveral Air Station, FLA during September 1997 using the AIR Inc GPS sonde and the Vaisala RS-80 radiosonde. Twelve hundred gram weather balloons were used to obtain 100,000 ft maximum test flight altitude. The two sondes were separated horizontally by 2 m and located approximately 30 m below the balloon. Results of statistical analyses which address the functional comparability of the sonde sensor measurements will be presented.

****

STATISTICAL ANALYSES OF CO-LOCATED WIND MEASUREMENTS OBTAINED FROM AIR, INC GPS SONDE VERSUS JIMSPHERE TEST FLIGHTS

Dr. William J. Kohri
The Johns Hopkins University/Applied Physics Laboratory
Laurel, Maryland, USA

Abstract

Tests were conducted at Cape Canaveral Air Station, FLA during September 1997 to compare GPS derived wind profiles produced by the AIR, Inc GPS sonde with co-located radar-derived JIMSPHERE wind profiles. Results from statistical analyses of these comparative profiles will be presented. Differential and non-differential GPS wind profiles were obtained by using multiple GPS sonde base station receiver/processor units during testing. For a subset of the test flights, the effects of radar errors on radar-derived JIMSPHERE winds were evaluated by tracking the JIMSPHERE with multiple radars and comparing the wind profiles produced from each radar's track.

****

COMPARING THE WINDFINDING PERFORMANCE OF A NEW PHASED ARRAY RADIOTHEODOLITE WITH GPS RADIOSONDES

David B. Call
A.I.R. Inc.
Boulder CO, USA

ABSTRACT

This paper will describe a new phased-array, 1680 MHz radiotheodolite. Presented are radiosonde flight comparison test results using the precision winds derived from a GPS radiosonde as a reference. Single balloons equipped with both a 1680 MHz radiosonde and a 403 MHz GPS radiosonde were released and tracked simultaneously to provide winds. Of particular interest is the performance of the radiotheodolite at low elevation angles, where existing tracking antennas have poor performance due to ground reflections and multipath. Figure 1 shows the Diamond Array[tm] radiothodolite.

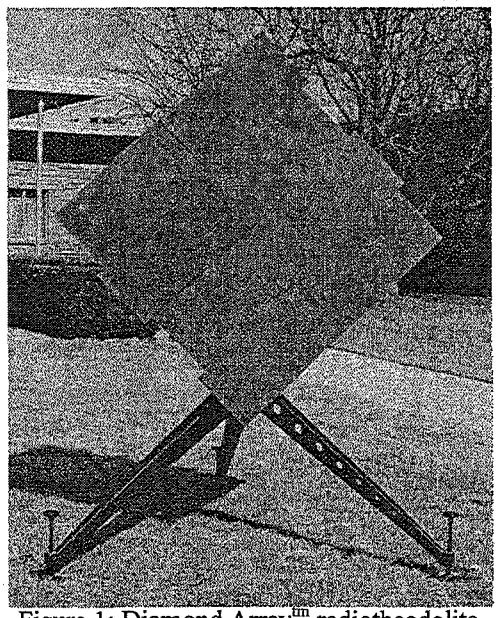

Figure 1: Diamond Array[tm] radiotheodolite

INTRODUCTION

Measuring synoptic scale winds by tracking radiosondes with Radio Direction Finding (RDF) equipment (radar or radiotheodolite) is the most widely used windfinding technique in the world weather network. The United States, states of the former Soviet Union, China, India, Australia and many other countries, all use RDF as the primary windfinding method for their national weather services. They account for more than two thirds of the WMO weather reporting stations.

The selection of RDF windfinding for a national, upper-air weather network is a combination of historic, economic, technical, and security considerations. Rawinsonde networks were introduced in the 1940's. At that time, only radar and radiotheodolite were available as practical methods for automatic radiosonde tracking. The navigation aide (NAVAID) methods such as, LORAN, OMEGA, and GPS did not yet exist. In addition, the cost of sensitive electronic components necessary for an expendable NAVAID receiver on the radiosonde was high before the semiconductor age and impractical for use in radiosondes. NAVAID windfinding is also very computer intensive and no computer means was available to process the volume of data generated by NAVAID receivers. Many rawinsonde networks were assembled from surplus military RDF weather equipment that became available between 1945 and 1955. Finally, for the military organizations, with close alliances in many countries to their weather service, security considerations require the primary source of weather information be under national control. RDF methods meet this requirement. Navigation aides do not.

ERRORS THAT DETERMINE RDF WIND ACCURACY

Errors that determine the performance of RDF systems are primarily related to their ability to measure the azimuth and elevation angles to the radiosonde they are tracking. Radar systems, operating at 5 to 10 GHz, have advantages in tracking accuracy because they measure range to the target and also because they operate with very narrow main-lobe beam-widths, typically 0.5 to 2 degrees. Radar tracked winds are considered the reference against which other techniques are compared.

Radiotheodolites operate at 1680 MHz with antenna apertures of 1 to 2 meters and have main lobe beam-widths of 6 to 12 degrees. These wide main-lobes and their side-lobes at low tracking elevation angles permit the effect of multipath reflections from the ground in front of the antenna to cause pointing errors, and hence wind errors. Reflections, from the ground or from nearby

objects, are the major wind error source for radiotheodolites. Figure 2 shows the geometry of multipath ground reflections.

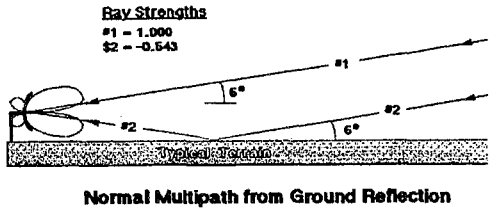

Figure 2: Multipath reflections enter the antenna at 2 times the elevation angle

The Diamond Array (DA) described in this paper is designed to significantly reduce the effect of these ground reflections on tracking accuracy.

When the elevation angle is above about 17 degrees, multipath reflections have little effect. The Brewster angle, at 1680 MHz is close to 17 degrees, depending on soil and surface conditions. Above 17 degrees elevation angle little energy is reflected from the surface and radiotheodolites provide accurate winds to high altitude. Figure 3 shows a comparison between a GPS radiosonde and a radiosonde tracked by the Diamond Array on the same balloon.

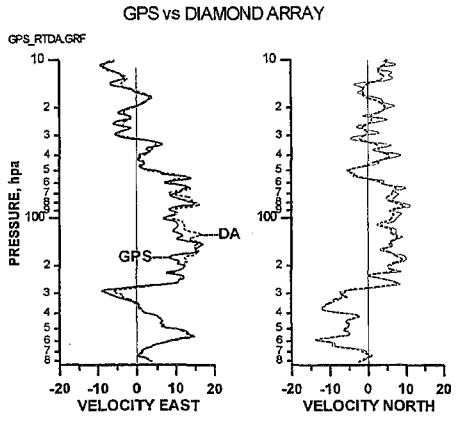

Figure 3: GPS and Diamond Array comparison at elevation angles above 17 degrees.

ANTENNA DESIGN

Below 17 degrees, multipath can be the primary cause of wind errors. Reflections from the surface, reach the antenna at an angle, measured from the antenna bore-sight, that is twice the elevation angle, as shown in figure 2. For example, if the elevation angle is 10 degrees, then multipath will be reflected into the antenna at 20 degrees off of bore-sight. This reflected radio frequency energy is vector summed with the signal along bore-sight and the antenna tracks low. Error can approach and exceed 1 degree and produce large wind errors, especially at long range.

ANTENNA SIDE-LOBES

All antennas are sensitive to radio energy in more than one direction. These directions of lower sensitivity than the main lobe at bore-sight are called side-lobes. Figure 4 shows an antenna pattern that is typical of a parabolic dish antenna or a conventional uniform illuminated phased array. The first and second side-lobes are less sensitive by -12 to -15 decibels than the main-lobe, when the beam is electronically steered down or up. They occur at 18 and 28 degrees off bore-sight. This means that the antenna will be somewhat sensitive to reflected energy at elevation angles of half these side-lobe angles, or 9 and 14 degrees. Experience bears this out. These radiotheodolites have significant wind errors when the elevation angle is about 14 degrees and are essentially unusable at 9 degrees and below. At these angles the antenna tracks low or high by up to one degree.

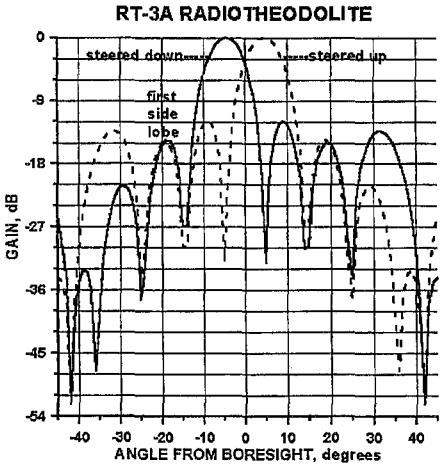

Figure 4: Antenna pattern, elevation cut, for a typical 1.2 meter radiotheodolite antenna.

To illustrate the effect that these second and third side-lobes have on wind accuracy, Figure 5 shows an example of severe multipath. In this comparison flight, one 1680 MHz radiosonde was tracked by two radiothodolites. The solid line is the Diamond Array and the dashed line is an AIR Inc. model RT-3A. The RT-3A is a 1.1meter conventional phased array antenna and has an antenna pattern very similar to a 1.2 meter parabolic dish. The dashed line is representative of multipath effects at 14 and 9 degrees. The missing wind information is deleted automatically by software when the

elevation angle is below 8 degrees. At these angles the RT-3A winds are no longer usable.

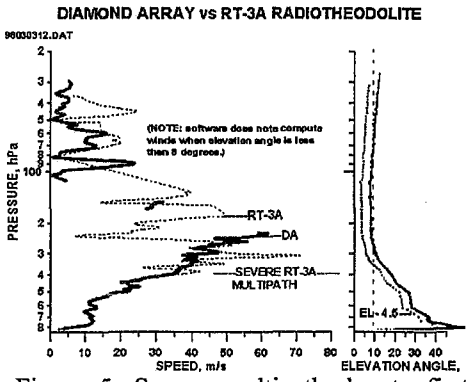

Figure 5: Severe multipath due to first and second side-lobe reception.

These tests were conducted at a site where the terrain is gently slopping upward to the east, direction of the radiosonde track. Slope of the land was measured with a radiotheodolite telescope to be + 2 degrees up. Homes and trees at about 200 meters raise the effective horizon to about + 4.5 degrees. The US National Weather Service Guidelines for siting a radiotheodolite, specify the horizon as the highest visible object. The elevation angles plotted on the right-hand graph in figure 5 should therefore be 2 to 4.5 degrees less than shown. The RT-3A shows significant multipath at about 17 degrees and is unusable below 11 degrees, allowing for the terrain's 2 to 4.5 degree rise. The Diamond Array shows little multipath degradation until about 9 degrees. This would be about 7 degrees on level terrain and lower if mounted on the roof of a building where radiothodolites are frequently installed.

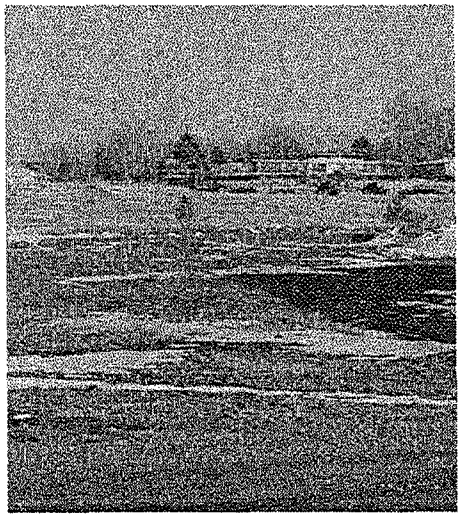

Figure 6: Terrain of 2 to 4.5 degree up-slope.

Figure 6 shows the gently rising terrain looking east, direction in which the radiotheodolites were pointing during the low elevation angle part of these soundings.

DIAMOND ARRAY PERFORMANCE.

The Diamond Array can track with precision well below elevation angles for radiotheodolites of comparable size. Figure 7 shows the size comparison for the RT-3A with a GMD-1 and Figure 8 shows the RT-3A with the Diamond Array. Measured along a vertical diagonal the Diamond Array is 1.7 meters, but each of its four antenna panel elements is a square 61cm on a side and 2 cm thick. It weighs less than 50 kg and requires less shipping volume than the RT-3A.

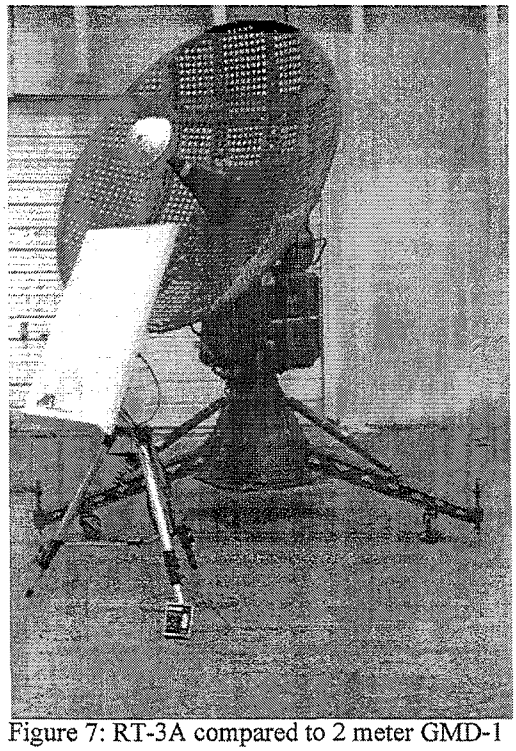

Figure 7: RT-3A compared to 2 meter GMD-1

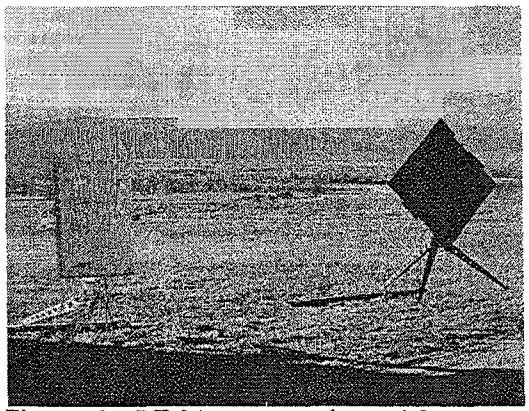

Figure 8: RT-3A compared to 1.2 meter Diamond Array

DIAMOND ARRAY ANTENNA PATTERN

Antenna pattern of the Diamond Array, shown in Figure 9, was designed to reduce sensitivity and increase angular distance between the main and first side-lobes. A third side-lobe at 45 degrees is well beyond twice the Brewster angle and has no effect. Taper produces a pattern that has a very deep null, more than 45 dB, between the main and first side-lobe when the beam is steered down. More important, the first side-lobe is –22 dB at 34 degrees versus -14 dB at 18 degrees for the first side-lobe for an RT-3A. Therefore, little multipath energy is received above 17 degrees elevation angle (1/2 of 34 degrees) because of the Brewster angle, and little between 17 and 7 degrees because of the deep null in the pattern.

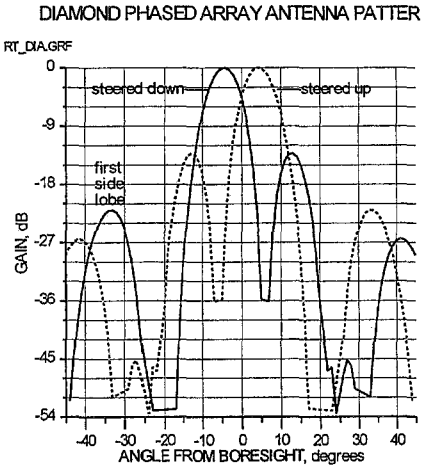

Figure 9: Diamond Array antenna pattern, elevation or azimuth cut.

DIAMOND ARRAY Vs GPS TEST DATA

Test results, shown in Figure 10, demonstrate that the Diamond Array tracks rawinsondes down to about 7 degrees elevation angle. A GPS radiosonde, tracked with differential GPS on a slowly rising, under-inflated balloon, provides wind velocity accuracy of better than 0.2 m/s. The Diamond Array tracked 1680 MHz radiosonde agrees with GPS until elevation angles are below at least 9 degrees.

Figure 11 illustrates that the Diamond Array produces a smooth trace of elevation angle and no multipath effects until pointing below 9 degrees-over terrain that rises 2 to 4.5 degrees (shown in Figure 6). In this sounding a radiosonde was tracked continuously to balloon burst and then tracked back to the surface in free fall.

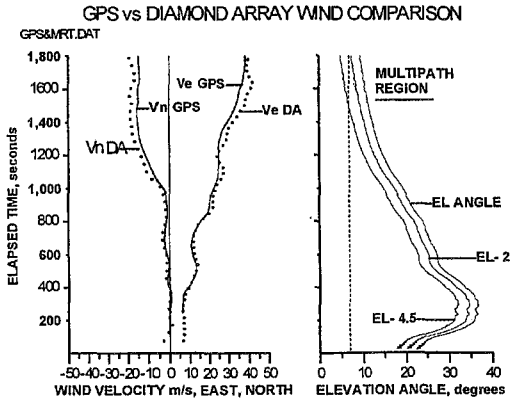

Figure 10: GPS and RDF radiosondes tracked on the same balloon

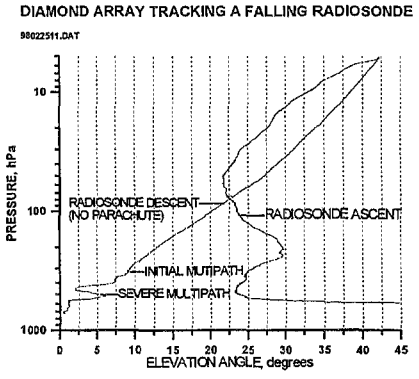

Figure 11: Evidence of no multipath effects until well below 9 degrees elevation angle.

CONCLUSION

The Diamond Array has demonstrated the ability to accurately track Radiosondes down to elevation angles of between 7 and 9 degrees, depending on the terrain and soil conditions. This performance is comparable with radiotheodolites that have much larger antennas. It is suitable for precision rawinsonde observations in synoptic weather forecasting.

REFERENCES:

Thompson, G. J., Giorgio, P. A., Penn, S. 971: Simultaneous GMD-1 Observations, Mesoscale Winds and Tracking Errors at High Levels. Proceedings of Second Symposium on Meteorological Observations and Instrumentation, AMS, 1972, pp40.

Todd, William, Circa 1965: RAWIN SET AN/GMD-1A
Lectures at Signal Corps Engineering Laboratories, Ft Monmouth , New Jersey.

Cole, H. L., 1979: Monographs on Techniques for Radiosonde Tracking, Simplified Range, Angle, Pressure Error Analysis.
NCAR, Monograph 79-38.

A COMPARISON OF RADIOSONDE WINDFINDING METHODS OMEGA, LORAN-C, and GPS

Wim Hovius, Wim A.Monna and Richard Rothe
Royal Netherlands Meteorological Institute KNMI
PO Box 201, NL 3730 AE De Bilt
e-mail: monna@knmi.nl

1. Introduction

When it became clear that the OMEGA network was going to be closed down, the replacement of the windfinding method of the operational radiosonde system at KNMI by another technique became necessary. In order to select the most suitable method, an intercomparison of various windfinding techniques, as offered by Vaisala Oy, was carried out in October-November 1995 and February 1996. The KNMI operational system, a MARWIN 11 groundstation and the RS80/15N OMEGA sonde, was compared with the RS80/15 versions for LORAN-C, GPS and OMEGA/VLF, using a MARWIN 15. With this groundstation one can choose between these three windfinding techniques. About 20 twin-flights were carried out at De Bilt and at the KNMI experimental research facility at Cabauw. As a reference we used data of the LAP-3000 1290 MHz wind profiler at Cabauw, and data of a tracking radar which was made available and was operated by the Royal Army. As a result of these comparisons, it was decided to purchase a MARWIN 15 system. At the acceptance test of this system, another 25 flights were carried out at KNMI in July 1997, when the MARWIN 11 was still in use, and the OMEGA network was still in operation too. At that occasion flights with a single OMEGA sonde were evaluated with the two ground systems in parallel. The experiences from these campaigns are presented in this paper.

2. Characteristics of windfinding methods

The three windfinding methods that were compared are briefly described below. A comprehensive overview of upper-wind observing systems is given by Nash (1994).

2.1 OMEGA

The OMEGA network consisted of eight radiotransmitters, distributed around the globe. Pulses are transmitted sequentially on frequencies between 10.2 and 13.6 kHz. An atomic clock is used for time control. The network was designed for global positioning. When used for windfinding with radiosondes, the displacement of a sonde is computed from the rate of change of phase of the OMEGA signals that are received by the sonde. An OMEGA receiver in the sonde receives the signals, that are retransmitted on the radiosonde carrier to the the ground system, where the wind computation is done. At least three OMEGA transmitters must be received by the sonde to allow wind computation. Because of the poor signal to noise ratio of the OMEGA signals, an integration time of 4 min is necessary, limiting the vertical resolution of the wind profile to about 1.2 km. The accuracy of the east-west and north-south wind components is usually better than 2 m/s. Having been the most widely used Navaid system to measure upper-air winds, the OMEGA network was closed down at September 30, 1997. In the former Soviet Union the Alpha-network, which is similar to the OMEGA network, is still in operation. Because this system is not operated continuously, it was not considered as a candidate for use at KNMI.

2.2 LORAN-C

LORAN-C is also a NAVAID system, somewhat similar to OMEGA. An important difference is the frequency used: around 100 kHz. At this frequency signal propagation is limited to some 1500 km, so LORAN networks, or rather LORAN chains, can only be used in limited areas. Each chain consists of one master station and some slaves. When at least three signals are received, wind computation is possible from the rate of change of the arrival times. When more than one chain is received the accuracy improves. In Northwest Europe LORAN-C windfinding performs well. The vertical resolution (about 300 m) is better than for OMEGA, because an integration time of 1 min is sufficient. The accuracy is about 1 m/s. The use of Navaid systems for windfinding is described by Lange (1985), while a recent discussion about the accuracy is given by Jaatinen and Pälä (1998). LORAN-C is guaranteed to be operational until 2003.

2.3 GPS

The Global Positioning System, based on L-band signals transmitted by a satellite network with global coverage, allows navigation with a very high accuracy. Only recently low-cost systems can be manufactured that allow the use in radiosondes at an acceptable price. When used for windfinding, the accuracy of GPS navigation is such, that the motion of the balloon relative to the atmosphere and of the sonde relative to the balloon is observed. Therefore additional smoothing is necessary to obtain representative wind measurements. This limits the vertical resolution to about 150 m. With GPS wind measurements an accuracy of better than 0.5 m/s can be achieved.

The measurements with the various windfinding systems described above were compared with wind measurements with a target radar, that were carried out by the Royal Army. A standard army procedure was used, with a rather poor vertical resolution of 500 m. The accuracy of the radar wind data is specified as 0.5 m/s. Due to technical problems, radar measurements were not available for all flights.

At the KNMI experimental research facility at Cabauw (Monna and Van der Vliet, 1987; Van Ulden and Wieringa, 1996) continuous wind measurements are carried out with a wind profiler radar. The wind profiler is a 1290 MHz LAP-3000 system. It measures hourly averaged wind profiles at 200 m intervals with a vertical resolution of 400 m. The height coverage is roughly 3 km, depending on atmospheric conditions. The accuracy is estimated to be 1 m/s. For an overview of wind profiler radar see Monna et al. (1998). The wind profiler data are compared with the sonde data not only for launches at Cabauw, but also for flights at De Bilt. However, the distance between De Bilt and Cabauw being 25 km, one must be careful when comparing these measurements, especially at lower altitudes where the wind field is more locally determined.

3. Measurements

In the test periods in 1995 and 1996 the production of GPS sondes was still very limited, and only 10 GPS packages were available. With 10 LORAN-C sondes, and the wish to carry out flights not only at daytime, but also at night and during twilight to test the influence of changing LORAN propagation conditions, only some ad-hoc comparisons were possible. Therefore proper statistics cannot be based on these flights. Because it became clear at the start of the comparison that a GPS sonde cannot be combined with a radar reflector, the reflector disturbing the reception of GPS signals, twin-flights were carried out with seperate balloons. For all flights 10 sec data were stored and plotted. The integration times used were 4 min for OMEGA, 1 min, and 2 min after 10 min flight time for LORAN-C, and 30 sec for GPS. The ascent rate of the balloons was about 300 m/min. After the purchase of the MARWIN 15 systems, flights with single OMEGA sondes were evaluated with the two ground stations in parallel, to compare the results of the two OMEGA computation versions.

4. Discussion

For discussion of the results, we refer to the three figures, that are representative for the flights. The figure at the top is a comparison of OMEGA and GPS, the second one a comparison of OMEGA and LORAN-C, and the lower figure is a comparison of the output from MARWIN 11 and MARWIN 15 for a flight with a single OMEGA sonde. As for the sonde types, G denotes GPS, L denotes LORAN-C and N denotes OMEGA.

Generally speaking, OMEGA and GPS compare well. GPS tends to showing more detail, as to be expected. When a GPS wind profile was recomputed with an integration time of 4 min, it came very close to the corresponding OMEGA profile. The large deviation of GPS in the first 700 m is a result of the launching procedure: the sonde should only be launched when at least three satellites are received. Since the sonde was prepared inside a hut, pre-launche satellite reception is often poor. The same precaution is also important for OMEGA and LORAN sondes.

The wind profiles compare well with the wind profiler data. It looks like the radar deviates most from the other systems. There are reasons to have some doubts about the accuracy of the tracking radar during these measurements.

OMEGA and LORAN compare well too. Because of the location of the transmitters of the LORAN-C chains, there were some doubts about the LORAN coverage over the eastern parts of the Netherlands. However, soundings during periods with stong westerly winds showed that LORAN-C coverage extends sufficiently eastwards to assure good wind measurements in these situations. Substantial influence of changing LORAN propagation conditions during the daily cycle were not observed.

It is remarkeble that MARWIN 11 and MARWIN 15 produce different wind profiles for the same sonde. The reason for this is not clear. One can hardly think of other possibilities than changes in the software.

5. Conclusions

OMEGA, LORAN-C and GPS are all three suitable as windfinding system in the Netherlands. LORAN-C performs slightly better than OMEGA, while GPS has the best accuracy. It is important that a sonde is only launched when at least three network signals are received by the sonde. A GPS sonde should not be used in combination with a radar reflector.

KNMI finally purchased a MARWIN 15 system, with which one can choose between LORAN-C and GPS (and OMEGA). For the moment LORAN-C sondes are used for operational measurement, since they are substantially more cost-effective than GPS sondes.

6. Acknowledgements

The authers wish to thank Mr Timmers and the 101 Fieldartillery Battalion for their support with a tracking radar, and Dr J.P. Van der Meulen for carefully reading the manuscript..

7. References

Jaatinen, J. and E. Pälä, 1998: Windfinding accuracy of terrestrial Navaids. Vaisala News, 146, 35-38.

Lange, A.A., 1985: Meteorological observations using Navaid methods. WMO Technical Note no. 185, WMO publ. no. 641.

Monna, W.A., R.B. Chadwick, J. Dibbern, J. Nash and H. Richner, 1998: Wind profiler radar: Operational remote sensing of upper-air winds. WMO Technic. Conf. Meteor. Environmental Instr. Methods Observation TECO-98, Casablanca, Morocco, May 13-15, 1998.

Monna, W.A.A. and J.G. van der Vliet, 1987: Facilities for research and weather observations on the 213 m tower at Cabauw and at remote locations. KNMI Scientific Report WR-87-5.

Nash, J., 1994: Upper wind observing systems used for meteorological operations. Ann. Geophysicae, 12, 691-710.

Van Ulden, A.P. and J. Wieringa, 1996: Atmospheric Boundary Layer Research at Cabauw. Bound.-Layer Meteorol., 78, 39-69.

RS80-15N, RS8015G, radar and windprofiler, 27-11-1995 14.00 at Cabauw.

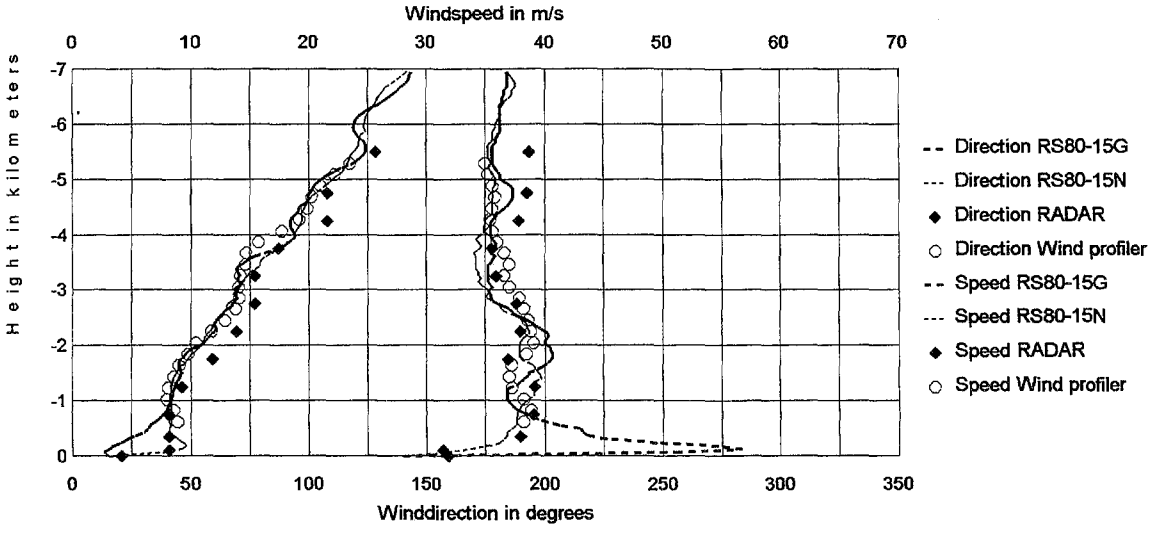

RS8015N and RS80-15L, 14-2-1996 15.50 GMT at De Bilt

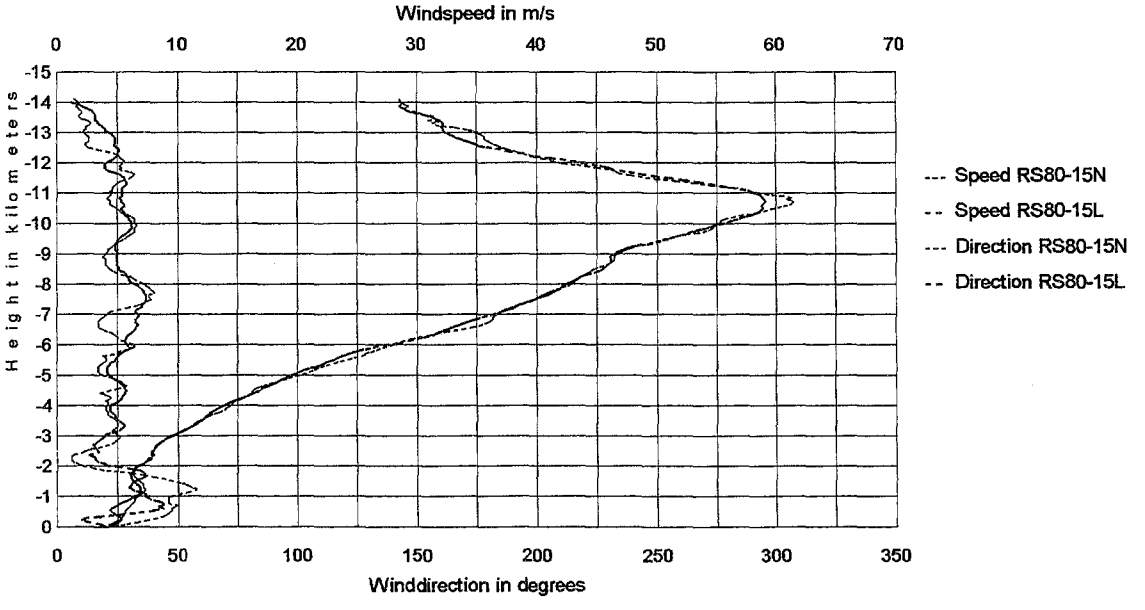

RS80-15N with MW-11 and MW-15, 23-9-1997 11.15 GMT at De Bilt

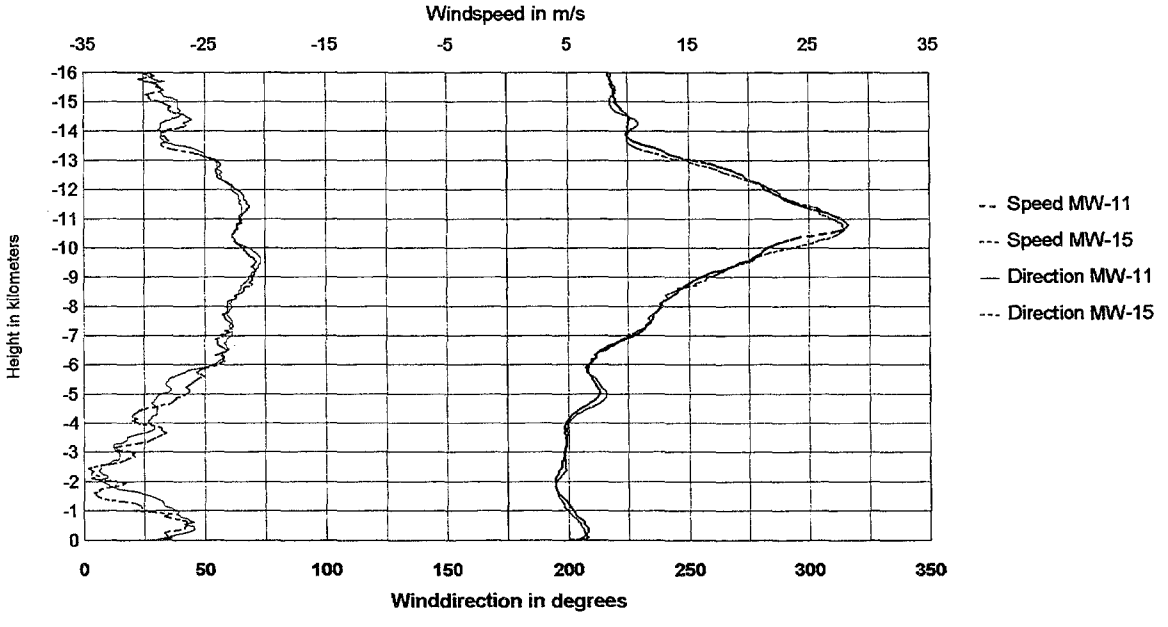

Improvement of radiotheodolite-based upper-wind calculation

Yuichi SAKODA
Japan Meteorological Agency
JAPAN

ABSTRACT

Japan Meteorological Agency(JMA) developed an improved algorithm of upper-wind calculation, which has the following functions;

(1)Automatic optimization of time spans for elevation-angle-smoothing

Time spans for elevation-angle-smoothing procedure are set to as short as possible fundamentally to express fine structure of wind profile, while they are extended to suitable length temporarily to remove elevation-angle-contamination caused by interference of reflected radio waves at the adjacent ground surface to directly received radio waves from the ascending radiosonde.

(2)Automatic restoration of unrealistic meandering in vertical profile of upper-wind

Unrealistic meandering in vertical wind profile that is sometimes found around the height of the maximum wind is detected and restored automatically based on the second finite differentiation of wind speed with respect to height.

This algorithm was introduced to the routine observation program in November 1996. Using this program, quality of observed data was improved and the burden of observer to manually correct contaminated elevation angles was reduced.

1. Introduction

In upper-air observation based on radiotheodolite, upper-winds are obtained from movement of radiosonde in a certain span of time. In JMA, this time span is set according to the pass time from the balloon launch, namely, one minute until 14 minutes, two minutes until 40 minutes, and four minutes after that. We call them "one minute method", "two minutes method" and "four minutes method" respectively. In these methods, averaged winds over the layers through which the balloon ascends during the time spans are obtained. Therefore, vertical resolution of the wind profile becomes considerably large, namely, about 400m from the ground up to about 6km, about 800m up to about 15km, and about 1600m at higher than that.

In winter in Japan, strong wind are apt to lower the elevation angles of the radiosonde and elevation angles are sometimes contaminated, which generate unrealistic meandering in upper-wind profile. In order to avoid these contamination, programs of upper-wind profiling calculation in JMA adopt smoothing procedure for time series of elevation angles. In the previous version, when elevation angles lower than 17° at after 10 minutes from the balloon launch, smoothing procedure using biquadratic approximation over ±8 minutes(totally 16 minutes) was adopted. But smoothing procedure over such a long span degrades the vertical resolution. The report of "WMO INTERNATIONAL RADIOSONDE COMPARISON -PHASE IV-" pointed out that "It was also observed that the peak of the maximum wind speed with JP2(Japanese radiosonde) is not so sharp as those with other systems. . . . the comparison results suggest the smoothing is too intense to obtain detailed wind profiles".

Under such conditions, the author started the study of an algorithm which can remove such unrealistic meandering in upper-wind profiles without degrading the vertical resolution.

2. Automatic optimization of time spans for elevation-angle-smoothing

2.1 Function to express fine structure of wind profile

First, the author investigated the periodic characteristics of both upper-wind profiling calculation and smoothing procedures based on biquadratic approximation. Fig.1 shows the result in two minutes method case. Ordinate of this figure is the amplitude of cyclic change in wind speed which were calculated from sinusoidal horizontal distance whose period is shown in the abscissa. It is expressed in ratio compared with the result of rigorous differentiation calculation. The top curve shows the periodic characteristics of upper-wind profiling calculation itself. The second to seventh curves which were shifted downward to avoid overlapping each other show the case when smoothing procedure over ±1 - ±7 minutes were applied to horizontal distance prior to the upper-wind profiling calculation. The curve of ±3 minutes seems to have the best characteristics of the seven because it has the least oscillation in the short period side and least decay in the long period side. Based on this result, the optimum smoothing time span for two minutes method was decided to be ±3 minutes. Similarly, ±1.5 and ±6 minutes were adopted for one minute method and four minutes method respectively.

2.2 Countermeasure for reflected wave interference

In winter, at stations where height of antenna measured from the ground is rather low, data of elevation angles are apt to be contaminated periodically like fig.2. Fig.3 is an elevation view which explains such contamination. When "E", elevation angles of radiosonde lowers below 15° or so, antenna of radiotheodolite located at "A" begins to receive radio wave reflected at "P" on the flat ground. This wave causes interference with directly received wave from the ascending radiosonde. "SPA", the propagation path of the reflected wave is longer than "SA", that of the direct wave by "QA'(=2h·sinE)". When actual elevation angle decreases, "n", the number of waves which corresponds to this path difference decreases and the phase of the reflected wave compared to the direct wave changes from same phase to opposite phase alternatively. This phase change generates cyclic contamination in elevation angles. Differentiation of "E" with respect to "n" indicates the difference of elevation angles which generates one cycle oscillation. It is expressed as "Δ E" and calculated by expression ①. It becomes a constant determined mainly by "h", height of the antenna. For example, Δ E=0.5,0.4,0.3,0.1° when h=10,13,17,50m, respectively.

$$\Delta E = \frac{dE}{dn} = \frac{180 \cdot \lambda}{2\pi h \cos E} \quad \cdots ① \qquad \Delta T = \frac{\Delta E}{\left| \frac{dE}{dT} \right|} \quad \cdots ②$$

Fig.4 is a schematic figure of time sequence of elevation angles contaminated by this interference. As it shows, "Δ T", period of elevation angle contamination expressed in time is estimated by expression ②. At stations where "h" is smaller than 20m or so, "Δ T" becomes considerably long when change of elevation angles becomes small so that the contamination cannot be removed by the pre-set smoothing time spans explained in 2.1. To cope with this situation, the improved algorithm has a function to check the value of "Δ T" always and to extend the smoothing time span temporarily with upper-limit of ±10 minutes when pre-set value is not long enough. This function is shown schematically by a polygonal line in the bottom of fig.4.

3. Automatic restoration of unrealistic meandering in vertical profile of upper-wind

At upper-air stations where interference by reflected wave occurs frequently, other types of contamination like fig.5 are sometimes observed in elevation angles. They have considerably long period, large amplitude sometimes reaches to 0.5° and cannot be explained completely by interference. They generates terrible unrealistic meandering in upper-wind profile. Thin dotted polygonal line in fig.6 shows wind profile calculated from fig.5 with elevation-angles-smoothing over ±4minutes. One can recognize unrealistic

meandering in wind speed between 10 and 15km. To cope this problem, the author developed a wind profile restoring algorithm which estimates the intensity of meandering quantitatively and keeps it less than pre-set criteria by adjusting the originating elevation angles.

In a vertical profile of upper-wind, gradient of wind speed with respect to height means wind shear. Therefore, intensity of meandering in wind speed can be expressed by the differentiation of wind shear with respect to height. Actually, that of radius component of wind at time "i" which belongs to two minutes method range can be estimated by expression ③. Si,Vi,Di and Hi are the vertical wind shear, radius component of wind, horizontal distance and geopotential height at "i" minutes.

$$\left(\frac{\Delta S}{\Delta H}\right)_i = \frac{\left(\frac{\Delta V}{\Delta H}\right)_{i+1} - \left(\frac{\Delta V}{\Delta H}\right)_{i-1}}{Hi+1-Hi-1} = \frac{\frac{Di+3-2Di+1+Di-1}{Hi+2-Hi} - \frac{Di+1-2Di-1+Di-3}{Hi-Hi-2}}{120(Hi+1-Hi-1)} \cdots ③ \left[= \frac{Di+3-3Di+1+3Di-1-Di-3}{120(2dH)^2} \cdots ④ \right]$$

In expression ④, denominators like "Hi+2-Hi" in expression ③ are assumed to be equal each other and expressed as "2dH". It shows that "Di+1" and "Di-1" have the largest effect to determine the intensity of meandering. Therefore, when the estimated intensity of meandering is large, it can be reduced by increasing "Di+1" and decreasing "Di-1" a little or decreasing elevation angles "Ei+1" and increasing "Ei-1". When the estimated value is negative, an opposite adjustment is effective.

In an actual program, meandering at all levels in the profile are calculated and the largest one is compared with the pre-set criterion mentioned later. When it exceeds the criterion, the meandering is judged to be too large and corresponding "Ei+1" and "Ei-1" are adjusted by either 0.01° or 0.02° depending the calculation method range that "i" belongs to. This adjustment is repeated automatically until the largest value meets the criterion. Elevation angles or upper-wind both before and after the adjustment are displayed on request in a same screen in different color. Observers can easily understand how automatic adjustment worked.

The candidate criteria of 30 m/s/km^2 for two minutes method range and 8m/s/km^2 for four minutes method range were proposed based on investigations of the restoration effectiveness. These criteria corresponds to a convexity of wind speed by 10m/s compared with adjacent points in the profile. To avoid too strong restoration, an investigation of automatic restoration frequencies using two winters data at all upper-air stations was carried out. At stations where unrealistic meandering had been observed very seldom, the percentage that automatic adjustments were executed was 0.5 - 1.0% in number of points (almost equals to pass time) or 5 - 20% in number of launch. This low percentage shows that the candidate criteria were in suitable level. They were accepted.

4. Effectiveness of improvement of upper-air calculating method

Fig.6 shows the results that the improved method processed the fig.5 data. Thin solid line is the result that only automatic optimization of time spans for elevation-angle-smoothing was executed. Fine structure of wind profile at 5km was expressed more in detail and meandering between 14 and 15 km was reduced. Bold solid line is the result that automatic restoration of upper-wind profile was executed additionally. All of unrealistic meandering were reduced to acceptable level.

5. Conclusion

An algorithm was developed that optimizes the smoothing time span and restores upper-wind profile automatically. The routine computer program of upper-wind profiling calculation was improved with this algorithm to express fine structure of wind profile fundamentally and to remove the unrealistic meandering in the wind profiles temporarily. It improved the data quality and reduced the burden of the observer to correct contaminated elevation angles manually.

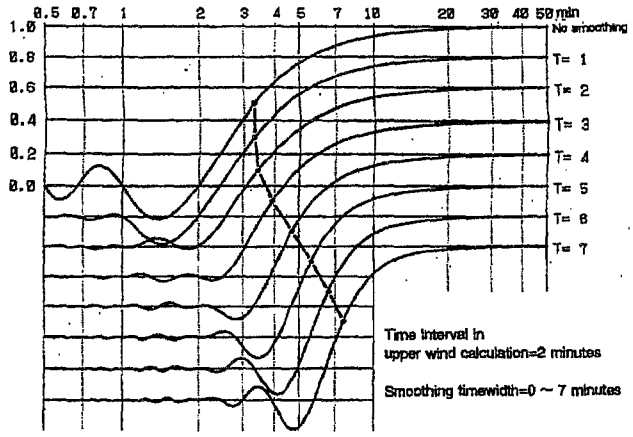

Fig.1 Periodic characteristics of upper-wind calculation and smoothing procedure

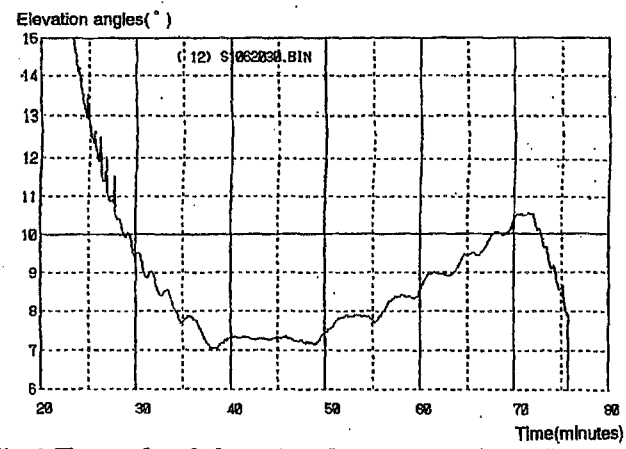

Fig.2 Example of elevation data contaminated by interference caused by ground reflected wave

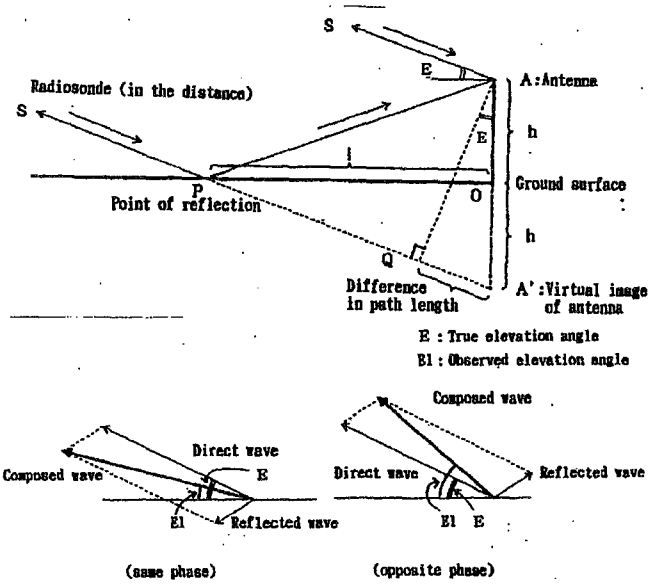

Fig.3 Schematic figure of interference caused by ground reflected radio wave

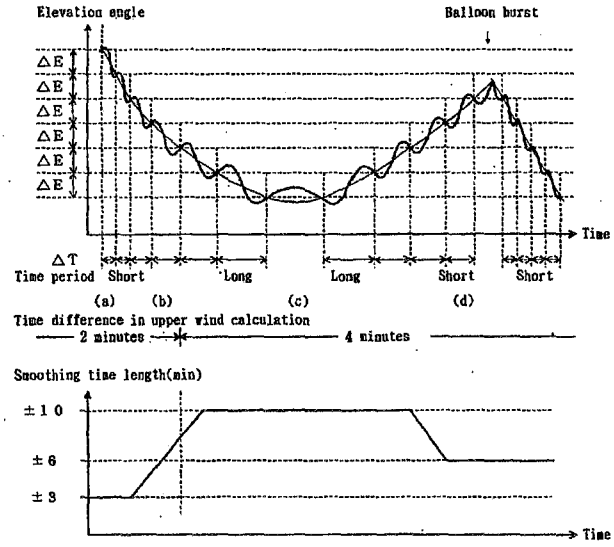

Fig.4 Schematic figure of
(top)elevation angles contaminated by interference caused by ground reflected radio wave
(bottom)extension of smoothing time span

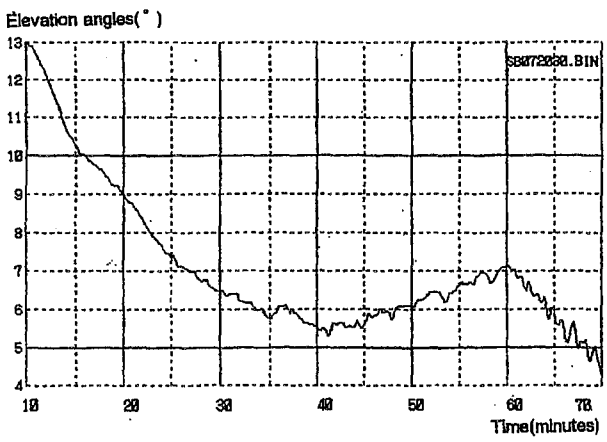

Fig.5 Example of long period random errors in elevation angles (35 - 40 min)

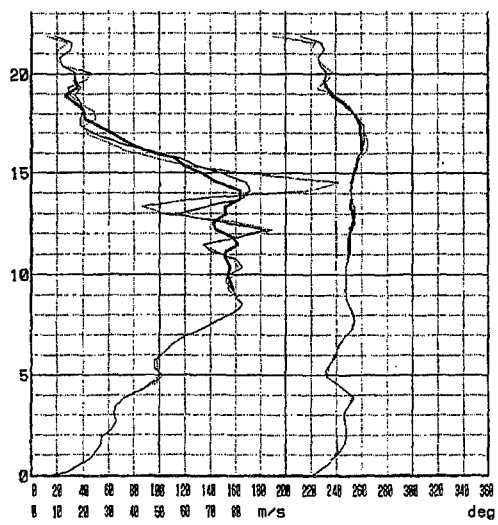

Fig.6 Upper-wind profiles calculated from fig.5 data
— same as pervious program(smoothing over ±4min)
— automatic adjustment of smoothing intensity only
— automatic restoration of wind profile additionally

RESULTS OF OPERATIONAL MONITORING OF RADIOSONDE RELATIVE HUMIDITY MEASUREMENTS IN THE UK AND ST HELENA

J. Nash and J. B. Elms
The Met Office, Bracknell, Berks, RG12 2SZ, UK

1. Introduction

Results from WMO Radiosonde Comparison tests[1] and from recent studies associated with TOGA-COARE [2] and the ARM sites [3] have provided conflicting views of the performance of most commonly used radiosonde sensors. This paper is intended to review the performance of relative humidity sensors used operationally in order to provide further feedback to the manufacturers. The Met Office has a network of 8 main upper air stations in the UK and stations in the Falkland Islands (88889), Gibraltar (08495) and St Helena (61901) In the past 2 or 3 years, several operational changes have affected the humidity measurements from UK controlled radiosonde sites:-.

(i) American VIZ W-9000 groundstation systems were installed during 1996 at Lerwick (03005) and Herstmonceux (03882) in East Sussex. Soundings from the VIZ Microsonde II Loran radiosonde are made at 6 hourly intervals from Herstmonceux and at 12 hourly intervals (alternating with Vaisala RS80 soundings at Lerwick).
(ii) All other sites in the UK radiosonde network using Vaisala RS80 Loran radiosondes have changed from "A" to "H" Humicap humidity sensors, with sounding made at 6 hour intervals
(iii) In September 1997 Vaisala MW15 groundstations were installed at the 3 overseas sites, with Vaisala RS80 GPS radiosondes incorporating "H" Humicaps used instead of the earlier Omega radiosondes with "A" Humicaps.

The "H" Humicap is expected to be more stable during flight than the "A" Humicap, although currently there is evidence that the calibration may change if the radiosondes are stored for any length of time. "H" Humicap calibration at cold temperatures is expected to be more realistic than that of the "A" Humicap.

2. Results from St Helena

The Met Office at St Helena is 436m above sea level and situated in the driest (north east) part of the island. Air from the south-east trade winds of the south Atlantic is orographically lifted to form stratus or strato-cumulus cloud capping the island on the majority of days in the year. Soundings from St Helena are made at 12 GMT each week day during the year. During the period studied, the sky was covered with at least 7 oktas of low cloud or fog on 75% of occasions. Launches into complete (8 oktas) cloud cover only occurred on about 10% of occasions. The marked increase in frequency of occasions 7 oktas compared to 8 oktas cover is due to small breaks in cloud towards the horizon and not over the launch site. The performance of the Vaisala relative humidity sensors was analysed using the raw data stored in the PC-CORA ground station (i.e. data adjusted following the pre-calibration ground checks, but not subject to the Vaisala editing routines that limit the maximum reported relative humidity to 100 per cent, and the minimum reported value to 1. The assumption was made that in the majority of cases when at least 7 oktas cloud was reported the radiosonde traversed through the cloud. Days when precipitation was reported by the observers were not included. Fig. 1 is a histogram of the maximum relative humidity reported for each of the flights assumed to pass through cloud. The average value for the maximum humidity recorded by the "A" Humicaps on 473 ascents between May 1995 and August 1997 was 94 per cent. Only 4 months of data, from September to December 1997, are available from the Vaisala 18GH radiosonde for analysis. The histogram in Fig. 2 shows that the average maximum humidity recorded by the "H" Humicap on the GPS radiosonde passing through low cloud in similar conditions was not significantly different from that measured by the "A" Humicap. In Fig. 3 the maximum reports for "A" Humicaps are summarised for days when precipitation was observed. There were about 40 occasions when RS80 "A" radiosonde was launched in precipitation and the average maximum humidity was about 96 per cent. Only 8 ascents using the "H" Humicap were launched in the wet during this period with the average of these values close to 100 per cent R. H.

During the changeover to GPS windfinding in September 1997, 31 simultaneous comparisons between the "A" and "H" Humicaps were made. The RS80 Omega and GPS radiosondes were suspended 30m and 60m below the same balloon and timing corrections were applied to ensure humidity measurements were compared at the same height. Fig. 4 shows an example of the simultaneous comparisons obtained. The systematic differences between "H" and "A" Humicap measurements are summarised as a function of relative humidity for temperatures greater than -20°C and below -20 ° C in Figs 5 and 6 respectively. The only significant differences were observed at temperatures below -20°C where the "H" Humicap recorded humidities between 5 and 12 per cent higher than the "A" Humicap for relative humidities above 5 per cent.

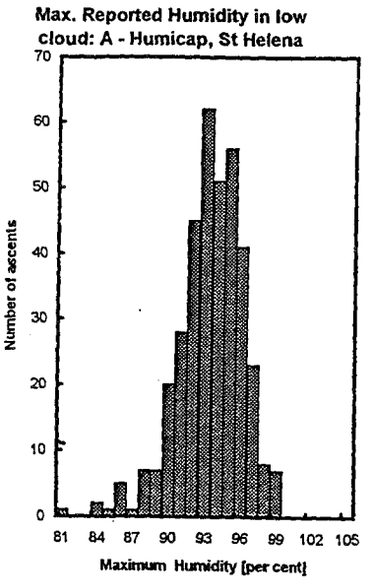

FIGURE 1

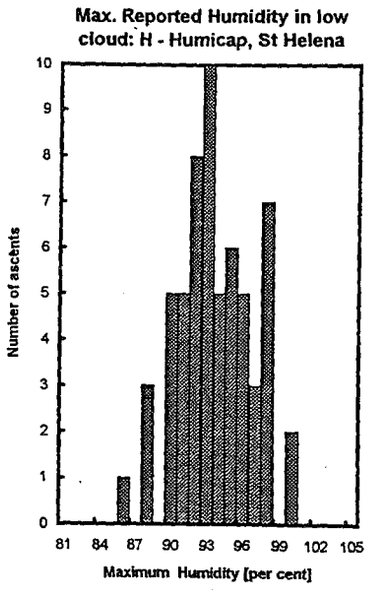

FIGURE 2

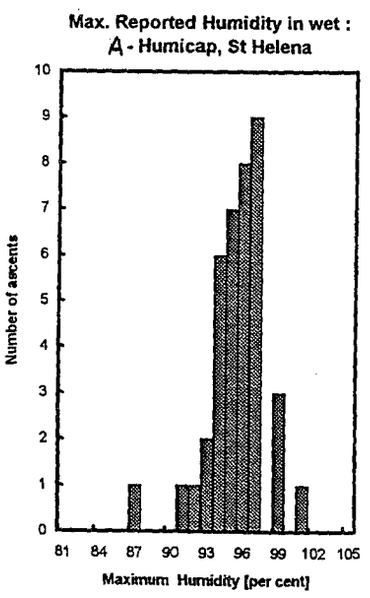

FIGURE 3

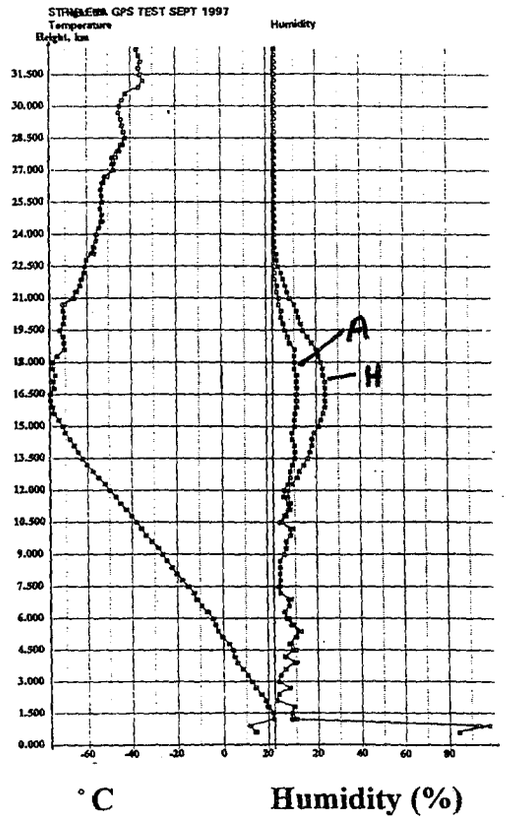

°C Humidity (%)

□ ■

RS80 "A" RS80 "H"

ST HELENA : FLT 55 SIMULTANEOUS COMPARISON AT 300m INTERVALS

FIGURE 4

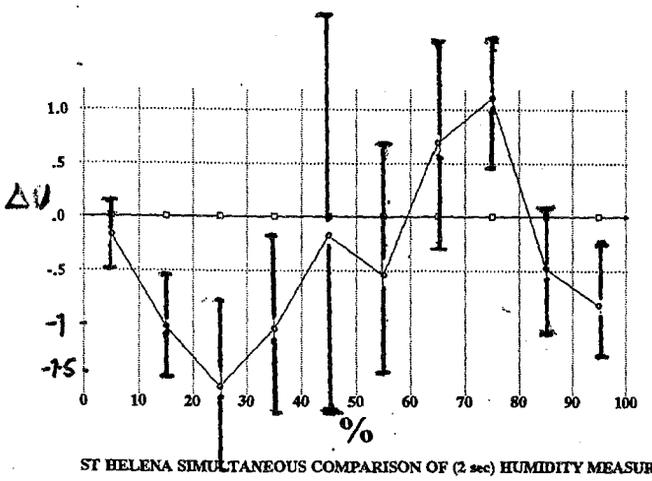

ST HELENA SIMULTANEOUS COMPARISON OF (2 sec) HUMIDITY MEASUREMENTS

DIRECT DIFFERENCES (GPS "H" HUMICAP - "A" HUMICAP)
(31 Twin Flights) NB Data Restriction: Temperatures > -20 C

FIGURE 5

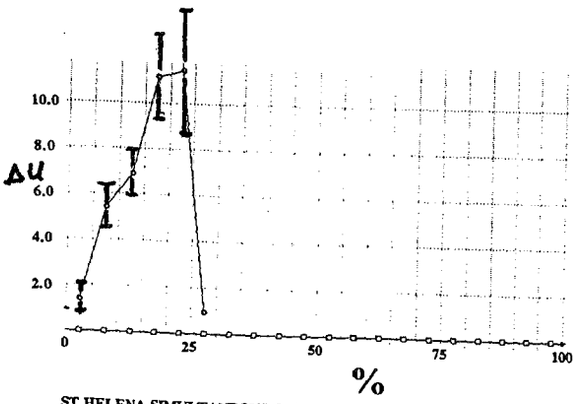

ST HELENA SIMULTANEOUS COMPARISON OF (2sec) HUMIDITY MEASUREMENTS

DIRECT DIFFERENCES (GPS "H" HUMICAP- "A" HUMICAP)
(31 Twin Flights) TEMPERATURES BELOW -20C

FIGURE 6

3. Results from the UK using the "H"- Humicap

Recent operational experience of "H" Humicap sensor performance in the UK has shown quite different results from St. Helena. Fig. 7 is a histogram of maximum humidity reported by "H"-Humicaps passing through 8 oktas of low cloud at Camborne (03808) during the first 9 months of 1997 . The mean maximum humidity was 101 per cent with a large number of recorded maxima of 105 per cent or higher. Fig. 8 gives a similar summary of the maximum humidity when there was precipitation at launch. The distribution of the maxima shifts even further into the supersaturated range of humidity. Further investigations will be made to determine whether the occasions of very high values can be attributed to particular radiosonde batches.

4. Performance of VIZ MKII

Prior to installations of the VIZ system at Herstmonceux and Lerwick, comparison test with the Vaisala RS80 were held at Hemsby (March/May 1994), Camborne (July 1995) and Lerwick (December 1995 to June 1996) to determine the differences between the VIZ carbon hygristor and the RS80 "A" Humicap. All flights were classified as either "Dry" or "Wet" , according to whether the sensors were exposed to liquid water during ascent.. Evidence of wetbulb cooling of the temperature sensor or complete low cloud cover was used to categorise the "Wet" ascents. Fig. 9 shows a "Wet" comparison ascent identified by the psychrometric cooling of the VIZ temperature sensor between 4 minutes and 4 minutes 20 seconds after launch. Cloud cover was reported as 4 oktas of cumulus cloud at 1800 feet. Whilst the RS80 indicated the likely presence of cloud after 1 minute 40 seconds, consistent with the surface observation, the VIZ MKII did not correctly indicate the cloud base level. Pre-flight tests of the two humidity sensors showed that the VIZ humidity sensor usually reported at least 5 per cent higher than independent surface sensors at humidity greater than 80 per cent. Figs. 10 and 11 summarise the differences between VIZ and Vaisala sensors as a function of relative humidity for the "Dry" and "Wet" ascents respectively. In dry conditions, the VIZ hygristor measurements in the later tests clearly shifted in performance relative to the first test, due to a refinement of the calibrations by VIZ. Further evidence of the a shift in calibration is given by the humidity (18% in 1994, 0% in 1995) by VIZ in the stratosphere (shown as spot values on the graph). Figure 11 shows that after the hygristor environment has become wet during passage through low level cloud the subsequent humidity measurements are significantly lower than those of the Humicap in the range 20 per cent to 60 per cent. Whilst some of the increased difference may be the result of positive bias in the Vaisala measurements on emerging from cloud, there is also plenty of evidence that the calibration of the hygristor also changes to give a negative bias at low humidity following exposure in cloud.

5. Influence of pre-flight ground checks on Vaisala measurements

The UK Met Office operational procedure is to make pre-flight checks on the RS80 Humicap by placing the sensor in the Vaisala Ground Check set containing desiccant for at least 10 minutes before check is performed. This gives adequate time for the conditions in the ground check chamber to approach the assumed 0 per cent reference provided by the desiccant. The correction applied by the Vaisala ground system software from the check is applied as an offset to all humidity over the full range of measurement from dry to wet conditions. If regular checks of the desiccant condition are not made, the desiccant may not reduce the relative humidity to zero in the chamber. Examination of operational procedures at some Met. Office stations showed that negative biases as high as 6 per cent were resulting from faulty desiccant. The effect of the reference instrument on the humidity measurements reported by the ground system was also recently seen in comparison trials of the Vaisala Autosonde system at Camborne. The automatic humidity ground checking of the RS80 Humicaps is made against a Vaisala Humicap reference sensor at the launch chamber humidity (typically about 50 per cent). Comparison ascents between operational RS80 radiosondes and Autosonde radiosondes from an identical radiosonde batch launched within 10 minutes of one another were compared. On the first 19 comparisons the automatic ground checks were used, whereas on a further 51 ascents the operator made the Autosonde humidity checks against the Ground Check Set reference. The lower curve in Fig. 12 shows the Autosonde - operational radiosonde humidity differences when manual ground checks were applied. The upper curve (automatic ground checks) shows a bias at all humidity levels of about 3 to 4 per cent. There is some evidence that the Autosonde reference was reading too high, but the practice of checking the operational radiosondes near 0 per cent is also questionable, since for most users improved sensor accuracy at relative humidity near saturation is important. Given the batch to batch fluctuations in sensor performance, possible sensor deterioration in storage, improved methods of checking the sensors prior to flight need to be implemented.

References

[1] Nash, J. and Schmidlin, F. J. (1987) *WMO International Radiosonde Comparison*, WMO/TD-No. 195.

[2] Zipser, E. and Johnson, R. H. (1998) *10 th Symp. on Met. Observ. & Instr.*, AMS, Phoenix, pp. 72 - 73

[3] Lesht, B. M. (1998) *10 th Symp. on Met. Observ. & Instr.*, AMS, Phoenix, pp. 80 - 83

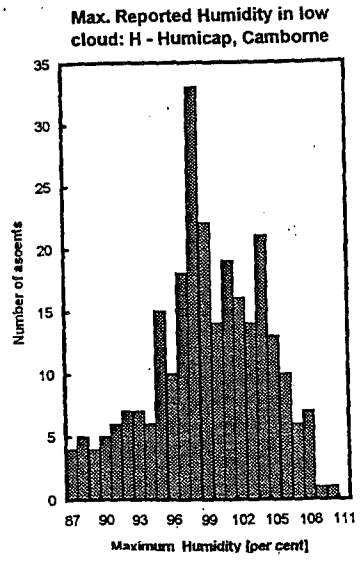

FIGURE 7

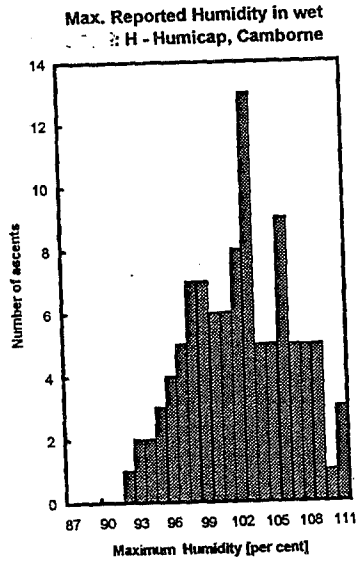

FIGURE 8

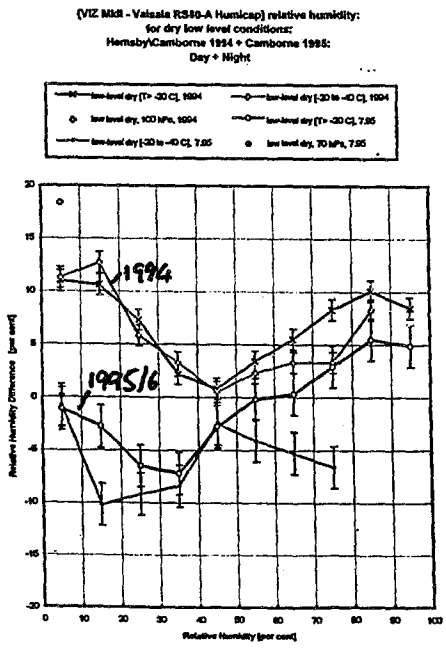

FIGURE 10

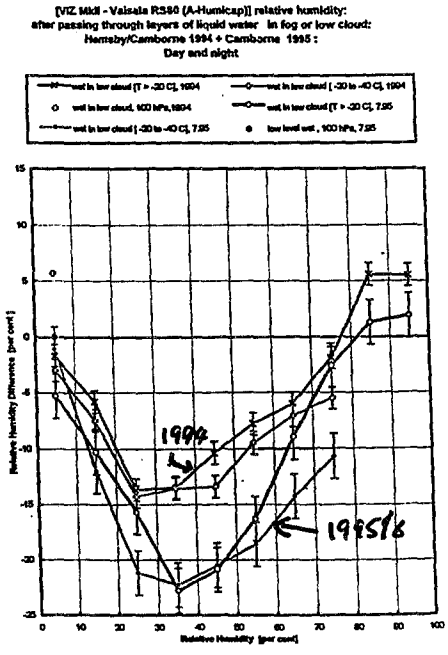

FIGURE 11

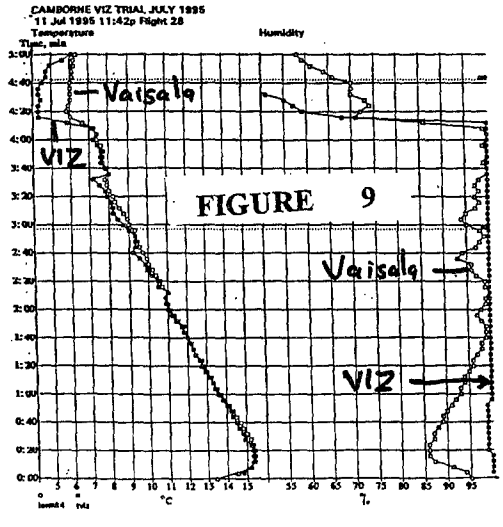

FIGURE 9

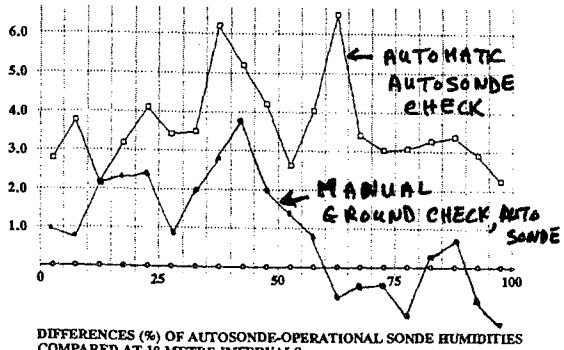

DIFFERENCES (%) OF AUTOSONDE-OPERATIONAL SONDE HUMIDITIES COMPARED AT 10 METRE INTERVALS USING AUTOMATIC GROUND CONTROLS (FLIGHTS 6-31)

FIGURE 12

IMPLEMENTATION AND RESULTS OF THE WMO RADIOSONDE HUMIDITY SENSORS INTERCOMPARISON (PHASE I LABORATORY TEST)

A. Balagurov[i], A. Kats[ii], N. Krestyannikova[i]
Russia

Phase I Laboratory Test of WMO Radiosonde Humidity Sensor Intercomparison was held under initiative of the Russian Federal Service for Hydrometeorology and Natural Environment in the Central Aerological Observatory, Dolgoprudny, Russia, since June 1995 till June 1997. 8 types of radiosonde humidity sensors from leading world manufacturers of radiosondes were presented onto intercomparison (see Table 1).

TABLE 1. SENSORS PARTICIPATED IN INTERCOMPARISON.

Manufacturer	AIR Inc. USA	Vaisala Oy Finland	Vaisala Oy Finland	Vaisala Oy Finland
Cond. designation	AIR	RSA	RSH	RS9
Type/model	thin-film polymer capacitor	thin-film polymer capacitor A-Humicap	thin-film polymer capacitor H-Humicap	thin-film polymer capacitor H-Humicap
Radiosonde	IS-5A	RS80	RS80	RS90
Manufacturer	VIZ Mfg Co. USA	Zond Co. Russia	Meteo Co. Russia	AMETO Co. Ukraine
Cond. designation	VIZ	DVR	GBS	UKR
Type/model	carbon film (hygristor)	thin-film polymer capacitor /APV	gold-beater skin	Ceramic capacitor /DV-01
Radiosonde	MARK-II	MRZ-6 MRZ-3AM	MRZ-3A MARZ-2	METEOR-1

The objectives of Laboratory Test were:

· To specify the metrological characteristics of humidity sensors of various radiosonde types under laboratory conditions;

· To evaluate the compatibility of humidity measurements of the tested systems in the temperature range from 20 to -60°C under laboratory conditions.

Brief description of used reference instruments and facilities is given in Table 2.

TABLE 2. COMPARISON REFERENCES AND FACILITIES

Installation	Working range	Accuracy	Other
Universal generator of moist air "DIPOLE", certified as working standard	Humidity: 1..95 %RH at $T \geq 0$ °C 5..95 %RH at $T < 0$ °C Temperature: -70..30 °C Pressure: 1100..10 hPa	maximum error: ±1 %RH (0..30 °C) ±3 %RH (-20.. 0 °C), ±5%RH (-70..-20 °C)	ventilation: 0.5..7 m/s, stepwise jump of humidity in microchamber- 15%RH/0.2 s volume of working-chamber: 10 dm^3, volume of micro-chamber: 0.02 dm^3
Condensation hygrometer "TOROS", certified as	Dew(ice) point: -80..29 °C, pressure: 1100..10 hPa	maximum error: ±0.15 °C (positive dew point) ±0.3 °C (ice point)	sensitivity: 0.01 °C

[i] Federal State Unitary Enterprise COMET, Russian Federal Service for Hydrometeorology and Natural Environment

[ii] Central Aerological Observatory, Russian Federal Service for Hydrometeorology and Natural Environment

mediate standard			
Condensation hygrometer "THYGAN" (granted by Meteolabor)	dew(ice) point: -65..50 °C	maximum error: ±0.15 °C (-20..50 °C) ±0.25 °C (-65..-20 °C)	resolution: 0.1 K
Dynamic test unit "CASCADE	humidity: 20...90 %RH, temperature: laboratory surroundings	systematic error: ±5 RH / 1s	stepwise jump of humidity: 15 % RH / 1 s ventilation: 0.5..7 m/s volume of working chamber: 1.0 dm^3
Platinum thermometer "TSP", used in "FEUTRON"		maximum error: 0.02 K	nominal resistance: 100 Ohms
Reference platinum thermometer "TSPN-3", used in "DIPOLE"		maximum error: 0.001 K	nominal resistance: 100 Ohms
Industrial climate chamber "FEUTRON"	10-95 %RH at normal conditions	Temperature regulation error – about 0.2 °C, humidity regulation error – from 2 to 5%RH	working volume: 0.5 $meter^3$

During intercomparison were fulfilled Test stage and Research stage. The Test stage included verification at normal conditions the correspondence of the actual metrological characteristics of sensors to the design specifications given in the technical documentation for these sensors. At the Test stage basic error was checked at "FEUTRON" using "TOROS" and "THYGAN" at humidities (10, 20, 30, 40, 50, 60, 70, 80, 90, 95 %RH) ±3 %RH under temperature 20 °C±2 °C and response time was checked in "CASCADE" under normal conditions. Totally at the test stage there examined in "FEUTRON" following amount of sensors: AIR - 12; RSA - 4; RSH - 4; RS9 - 8 (two sensors per sensor unit); VIZ - 15; DVR - 10; GBS - 10; UKR – 5, - and by three sensors of each type were examined in "CASCADE".

The Research stage included the determination of difference of sensors measurements against references at temperatures from 20 °C down to -60 °C in installation "DIPOLE" using reference hygrometer "TOROS" and time response examination at temperatures at +20 and -20 °C in installation "DIPOLE" too. The amount of experiments was limited by possibilities of sensors' arrangement in "DIPOLE" and duration of tests: temperature influence on performance was investigated for one AIR, RSH and DVR sensors and for two RSA, RS9, VIZ and GBS sensors, time response was examined for one sensor of each type except RS9 (UKR did not participated in the Research stage).

Fig. 1-2 present for each humidity category mean differences and root-mean square deviations for each participated sensor design against "TOROS", obtained in the Test stage. Generalized results from the Test and Research stages are summarized in Table 3.

Some notes, concerning sensor's performance can be cited here:

AIR has rather a good performance at normal conditions, however essential bias appears at negative temperatures, as well as slow response, caused, apparently, by design of cover cap.

RSA reveals some hysteresis and noticeable bias at -60° C, while other characteristics are very good. Despite they have the same polymer of sensitive elements, RS9 shows better performance than RSH, RS9 has minimal bias and reproducibility as well as response time.

VIZ - has an excellent response and reproducibility, however it should not be forgotten, that VIZ sensors were calibrated during intercomparison. Nevertheless, after influence of high humidity sensors don't come back to resistance at calibration point (33 %RH), that explains growing scatter at low humidities on Fig.2. VIZ completely looses sensitivity at -60° C.

DVR shows large scatter and response time and the most poor reproducibility as well as hysteresis, at -60° C it looses sensitivity.

GBS has rather a big scatter, especially at low humidity, large response time, that drastically grows at negative temperature, as well as bias, actually GBS as well looses sensitivity at -60° C.

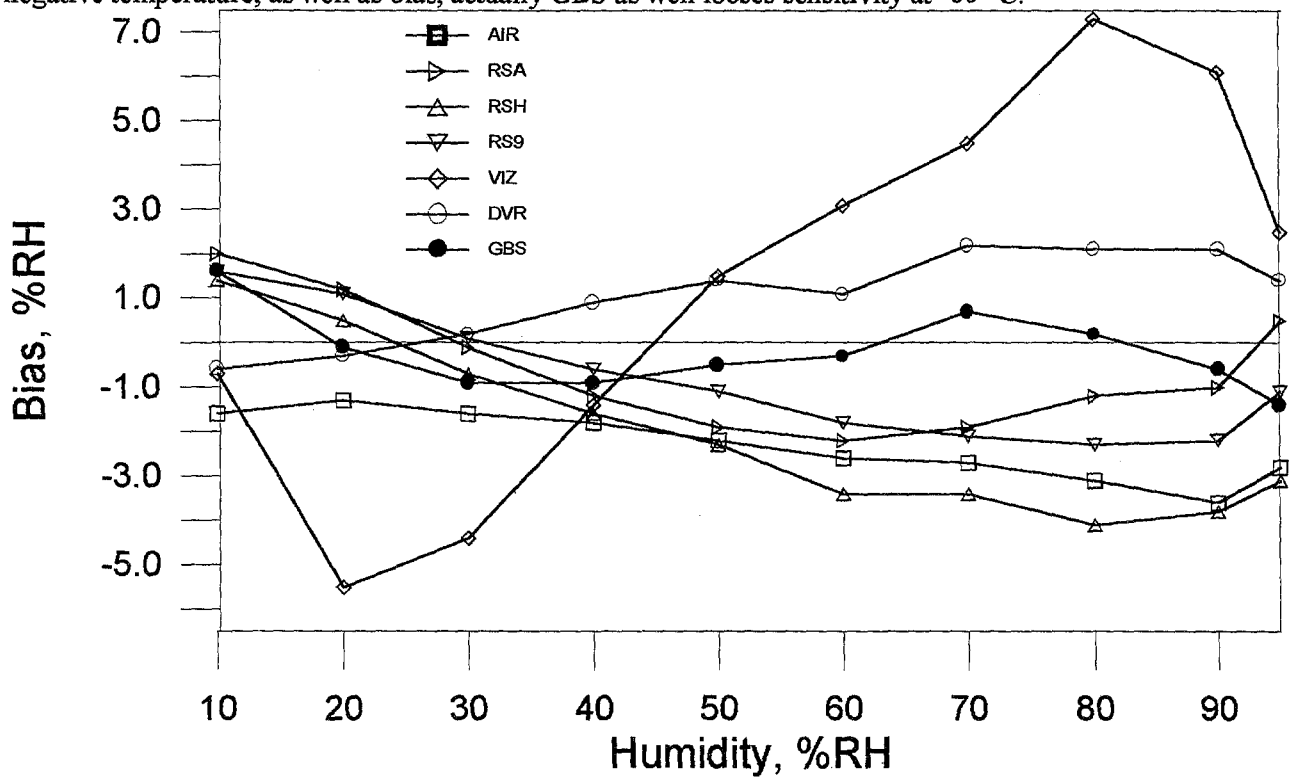

Fig. 1. Mean differences of participated sensors against "TOROS" at normal conditions.

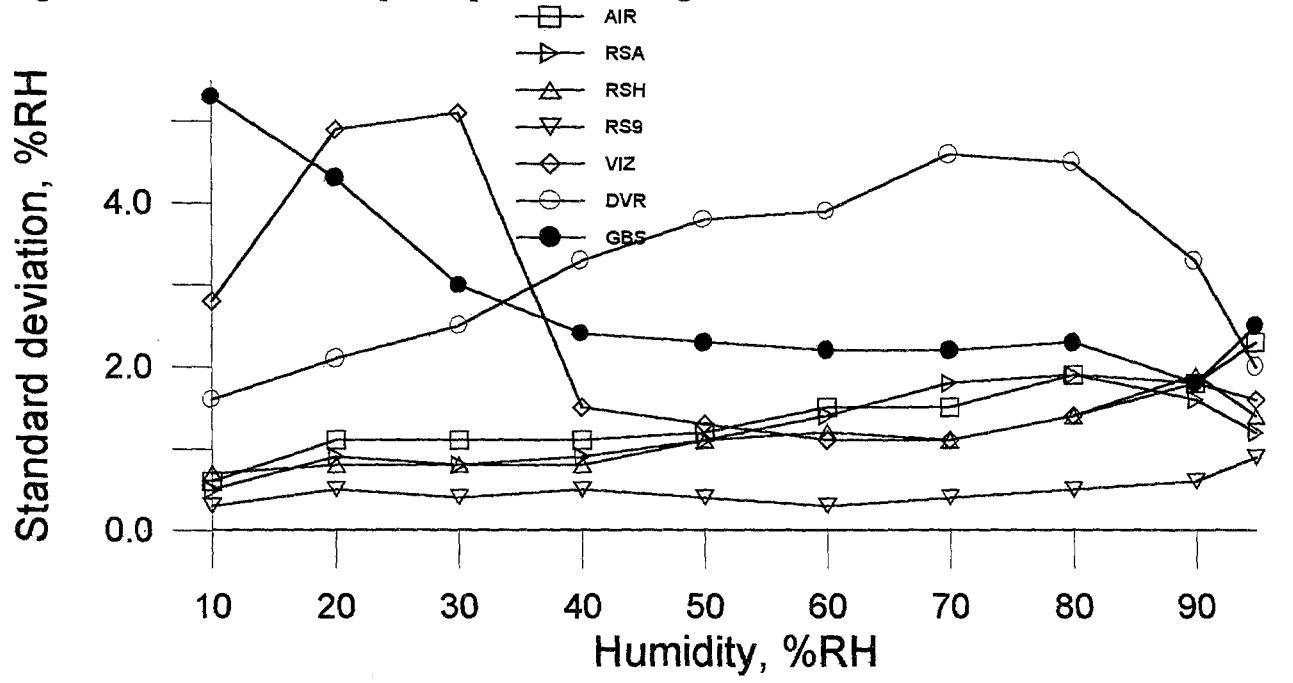

Fig. 2. Root-mean square deviations of participated sensors against "TOROS" at normal conditions.

Some conclusions could be made from intercomparison results:

Performance of sensor examined was evaluated for temperature range from 20 to -60 °C. Almost all participated sensors were satisfied to WMO accuracy requirements (5 -10 %RH) under temperatures ≤40 °C. For the whole range of conditions, reproduced in Laboratory Phase, only Vaisala H-Humicap sensors tolerated these requirements.

Despite of relatively small amount of results obtained at -60 °C it is possible to state that humidity measurements, produced by the better humidity sensors are reasonable, and therefore it is necessary to consider extending the temperature range for WMO legal approximation of saturation water vapour above water surface.

Taking into account increased performance of modern radiosonde humidity sensors it's necessary to consider the matter of improving practice of dew point depression reporting in TEMP messages for better representation of information.

All sensors showed more or less satisfactory performance at normal temperature while began essentially diverge at lower temperatures. That means to customers and members not to rely upon sensor's specifications at normal temperature but to interest in ones for the whole range of conditions.

The similar design of sensor doesn't guarantee itself the same or similar performance as it could be seen from comparison of thin-film capacitive sensors: AIR sensors and, especially, DVR sensors substantially concede to HUMICAP sensors.

It is very difficult if ever possible to reproduce in laboratory several environmental conditions, such as saturation, especially at negative temperatures, and simultaneous drastic changes in both humidity and temperature. In-flight intercomparisons between different sensors can give only comparative results. At the same time humidity sensors performance under such conditions is critical either for routine synoptic tasks or environmental studies. Therefore future intercomparison should involve in their flight phase direct comparison with balloon-borne humidity reference, although it is much more expensive.

TABLE 3. Radiosonde humidity sensors performance

	AIR	RSA	RSH	RS9	VIZ	DVR	GBS
Static characteristics at normal conditions (Test stage)							
Bias, %RH	-2.2	-0.5	-1.6	-0.7	0.9	1.0	-0.2
RMSD, %RH	1.6	1.9	2.2	1.5	5.2	3.4	3.2
Reproducibility, %RH	1.1	0.8	1.2	0.3	0.4	3.1	2.5
Hysteresis, %RH	2.6	3.1	-	-	-	6.5	-
Max. Error, %RH	1.9	3.3	3.0	2.3	10.4	14.8	10.1
Min. Error, %RH	-7.1	-4.4	-6.1	-3.7	-17.8	-7.6	-12.3
Temperature influence on static characteristics (Research stage) +20° C							
Bias, %RH	1.3	-0.8	-0.7	1.0	6.9	4.5	5.4
RMSD, %RH	1.0	1.8	1.6	1.7	4.2	2.2	3.7
-10° C							
Bias, %RH	-2.7	-0.5	-0.7	0.6	-2.1	-3.5	13.6
RMSD, %RH	2.4	2.1	2.0	2.2	3.8	2.4	3.4
-40° C							
Bias, %RH	-8.4	-3.3	-2.8	-1.9	1.2	-14.7	10.1
RMSD, %RH	2.6	3.2	3.0	2.8	7.6	4.1	6.1
-60° C							
Bias, %RH	-15.9	-6.9	-4.3	-1.9	5.3	-18.4	20.0
RMSD, %RH	4.9	5.1	2.7	3.6	14.3	8.5	10.0
Dynamic characteristics +20 °C ("CASCADE" and "DIPOLE")							
τ_{63}, sec	2.0	1.0	1.0	0.3	0.2	2.0	8
τ_{90}, sec	10	4	5	3	1	8	18
-20 °C ("DIPOLE")							
τ_{63}, sec	17	5	8	-	3	18	50
τ_{90}, sec	35	11	18	-	7	40	90

SUMMARY OF THE WMO INTERNATIONAL RADIOSONDE RELATIVE HUMIDITY SENSOR COMPARISON - SEPT, 1995

Phase II "Field Test"

Francis J. Schmidlin
Laboratory for Hydrospheric Processes
Goddard Space Flight Center, Wallops Island, Virginia 23337 USA

The World Meteorological Organization's (WMO) Commission on Instruments and Methods of Observation (CIMO) agreed in February 1994 to a proposal from the Upper Air Working Group that a relative humidity sensor comparison was needed. The Intercomparison Organizing Committee (IOC) had responsibility for organizing and overseeing the intercomparison. The IOC also solicited cooperation and participation of Members. The comparison was to be accomplished in two phases. Phase 1 was a laboratory calibration of participant's sensors in controlled chambers. It was agreed that the calibrations take place at the Central Aerological Observatory (CAO), Moscow, Russian Federation. Relative humidity sensors normally flown on various operational radiosondes as well as two radiosondes under development were calibrated. Phase 1 was initiated during June 1995 and was completed during early 1997. Phase 2, was a field measurement comparison of operational radiosonde instruments using the same sensor types calibrated in Phase 1. Phase 2 took place over a three week period during September 1995 at the National Aeronautics and Space Agency's Wallops Flight Facility of the Goddard Space Flight Center at Wallops Island, Virginia. The instruments were provided either by national weather services or by manufacturers willing to participate. Table 1 lists the types of sensors calibrated in Phase 1 and radiosondes flown during Phase 2.

Table 1. Relative humidity sensor types participating in the WMO intercomparison. The MRZ-3 temperature sensor was replaced with the capacitive humidity sensor.

Radiosonde	Pressure Sensor	Temperature Sensor	Humidity Sensor
VIZ MK 2	Capacitive Aneroid	Resistive Rod	Carbon Hygristor
RS80	Capacitive Aneroid	Capacitive	Capacitive 1. A-Humicap 2. H-Humicap
RS90	Capacitive Aneroid	Capacitive	Capacitive Dual Sensors
AIR	Capacitive Aneroid	Resistive Bead	Capacitive
MRZ-3	None	None	1. Capacitive 2. Goldbeaters

Two daytime and two nighttime balloon flights were conducted from Wallops Island each day. The radiosondes' transmitted on 403 MHz (the exception was the Russian Instrument which transmitted on 1790 MHz). The large number of radiosondes transmitting on 403 MHz limited each balloon flight to four instruments. The balloon release schedule was designed to obtain as many pairs of profiles as possible.

With a few minor exceptions all radiosondes performed well. There were occurrences when data were lost, but these were minimal. Since relative humidity sensor performance was the primary objective of the comparison there was little incentive to measure very high in the atmosphere. Humidity values at altitudes above approximately 200-300 hPa are small and the present sensors do not respond well at low humidities. Therefore, a balloon flight reaching the 50-hPa pressure level was considered successful.

Sixty-one balloons were released with each balloon carrying a minimum of three radiosondes and sometimes five. The number of pairs of profiles vary for the different radiosondes but there were 58 VIZ radiosondes flown, 54 Vaisala RS80 A-Humicap, 46 Vaisala H-Humicaps, 29 Vaisala RS90, 37 Air, and 24 Russian MRZ-3. Comparisons of relative humidity measurement vs temperatures were made over a 5°C bandwidth between 35°C and -45°C during day and night. These are shown in Figure 1 for daytime

observations and in Figure 2 for nighttime. The Vaisala RS80(A-humicap) sensor was adopted as an arbitrary reference (this does not imply that the A-humicap data are correct or better than that of the other instruments).

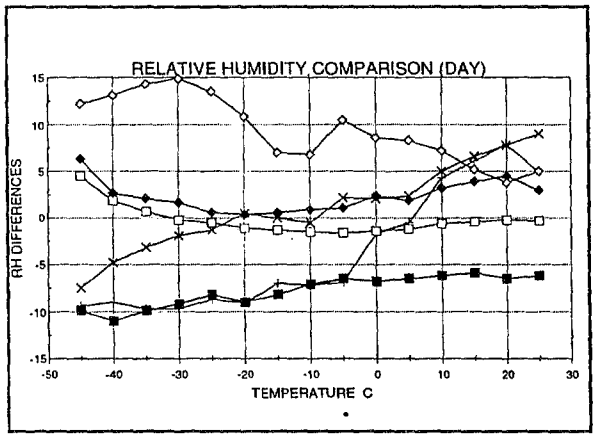

Figure 1. Differences as a function of temperature. VIZ (+), AIR (■), H-humicap (□), RS90 (♦), Russian capacitive (x), and goldbeaters skin (◇).

Comparisons of relative humidity measurement differences vs temperatures were made over a 5 °C bandwidth between 35 °C and -45 °C during day and night. These are shown in Figures 1 and 2. The Vaisala RS80(A-humicap) sensor was adopted as an arbitrary reference (this does not imply that the A-humicap data are correct or better than that of the other instruments).

Examination of differences between the MRZ-3 capacitive sensor and the A-Humicap as a function of temperature in Figure 1 shows that it measures more humidity at temperatures higher than -10 °C and lower humidity at lower temperatures. The differences beginning from approximately 10 percent at 25 °C slope to about -8 percent at -45 °C, with the slope rapidly departing from the reference below about -20 °C. This raises a question whether either sensor manufacturer is compensating for ambient temperature effects. The VIZ hygristor shows more humidity that the A-Humicap at temperatures higher than 5 °C and less humidity at lower temperatures. The AIR capacitive sensor measures lower over the full range of temperatures. But, when the nighttime measurements are examined the AIR sensor is experiencing a day-night temperature error. Further, Figure 1 also shows that below about -25 °C the differences relative to the reference rapidly diverge. Although goldbeaters skin is an exception it is best that it not be considered as a viable sensor after 20 minutes of flight. The Vaisala H-humicap and RS90 measurements agree with the reference sensor, except the RS90 reports higher humidities.

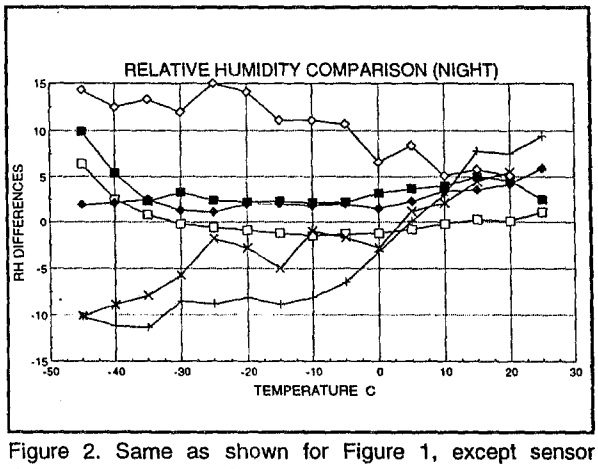

Figure 2. Same as shown for Figure 1, except sensor differences are shown for nighttime.

Relative humidity sensor differences vs temperature for nighttime are shown in Figure 2. The VIZ hygristor and the Russian capacitive sensor indicate more humidity at temperatures higher than about 0 °C. At colder temperatures the humidities are lower than the A-Humicap. It is obvious that goldbeaters skin is not responding at temperatures, e.g., below -25 °C. The relative humidity measurements diverge at temperatures lower than -25 °C, similar to the daytime measurements shown in Figure 1.

The WMO International Relative Humidity Sensor comparison provided unique and interesting results. This short report addresses the most obvious deficiencies noted. Except for the Vaisala RS80 A- and H-Humicaps the sensors did not correlate well with chamber measurements. Either lack of humidity sensing capability or temperature sensitivity, especially at cold temperatures, might be considered a problem. The A-Humicap correlated well with the chamber values, even at -60 °C, however, the actual flight tests presented in Figures 1 and 2 suggest that the A-Humicap's accuracy probably suffers at temperatures lower than -25 °C. Summarizing the results we find:

1. None of the humidity sensors reported identical values. The H-humicap agreed best with the reference, suggesting that the A- and H-humicaps are interchangeable.

2. At high relative humidities, the VIZ hygristor and the Russian MRZ-3 capacitive sensors have a moist bias relative to the reference sensor humidity and a dry bias at low ambient humidities. Nonetheless, the VIZ hygristor was judged the fastest responding sensor.

3. Goldbeaters skin gives viable relative humidity measurements at temperatures higher than 0 °C.

4. All sensors appear not to respond to humidity changes at temperatures lower than -30 °C.

A report of the laboratory calibration phase has been prepared by Balagurov, A., A. Kats and N. Krestyannikova. The draft of the field measurement comparison has been submitted to WMO. Both parts of the intercomparison report are expected to be available during early 1998.

Session VII

RADIOSONDE TECHNOLOGY

THREE YEARS OF OPERATIONAL EXPERIENCE OF AUTOMATIC BALLOON FILLING AND LAUNCHING SYSTEMS IN SWEDEN

Ture Hovberg, Bo Rosén and Stefan Ståhl
Swedish Meteorological and Hydrological Institute (SMHI), Sweden

1 Introduction

During the last four years, the total observational network in Sweden has been totally reconstructed. In the synoptic network the number of manned stations have been reduced from 140 to 45, and 115 new automatic synoptic stations owned by SMHI and 35 external automatic stations have replaced the old automatic stations and the withdrawn manned stations. The upper air station network has been remodelled, as well, in order to have more frequent observations and to obtain a more dense network in the data sparse area in the North Atlantic region. One station, Bromma Airport, has been withdrawn in favour of increased number of daily observations at the remaining stations, and one Icelandic merchant ship at the route Iceland - North America has been equipped with an ASAP container in collaboration with the Icelandic Meteorological Institute.

For the remaining, landbased civil upper air stations, SMHI has procured two Automatic Balloon Filling and Launching Systems of type Vaisala Autosonde. The systems were installed at Sundsvall/Härnösand Airport (62°31'N; 17°26'E) and Landvetter Airport (57°40'N; 12°17'E) late in 1994, and were used as "remote launchers" from November 1994. The fully automated function was implemented in March 1995. The reliability test at Sundsvall/Härnösand Airport, stipulated in the procurement agreement, was succesfully finished during Spring 1996.

The objective for the procurement was to make a further rationalization of the radiosonde stations in order to reduce cost, to make it possible to increase the number of daily radiosonde observations at a moderate increase of cost and to get a more safe balloon filling procedure. The quality goal was to have at least 95% data availability from the stations, expressed as an one year mean value of monthly data recovery, measured in the central data archive of SMHI.

The two Automatic Balloon Filling and Launching Systems now have been in operational use during three years. In this presentation, the experience from the three years will be summarized and discussed from an economical and qualitative point of view.

2 Brief system description

SMHI's Autosonde systems are fully automated ballon launchers including following equipment:

- shelter including operator room and UPS
- balloon launcher
- balloon filling equipment (filling from outdoors situated hydrogen cylinders)
- compressed air system

- robot system including loading trays for balloons and sondes (18 trays in Sundsvall/Härnösand and 22 in Landvetter)
- local and remote control computer (PC, Windows NT environment)
- Marwin Radiosonde System including Loran-C equipment for wind measurement

After fulfilled loading procedure by the local operator, up to 18 respectively 22 radiosonde observations can be performed fully automatically, or remotely controlled via telephone line from the Production Supervision Centre at SMHI in Norrköping.

3 Operation and maintenance organization

In SMHI's organization, the service at the radiosonde station has been and is still an integrated part of the meteorological routines at the Regional Meteorological Office. The local organization for Autosonde operation consists of 4-5 operators from the shift working assistant meteorologist staff, who prepare and load sondes and balloons as well as carry out simple maintenance. At Sundsvall/ Härnösand Airport the Autosonde equipment is situated at a rather short distance from the Met Office, and the work with loading the Autosonde is performed four to seven times a week. After a reorganization one year ago, the Regional Meteorological Office at Landvetter Airport moved to Gothenburg City, 30 kilometers away from the airport. Thus, the work with loading the Autosonde is performed only twice a week, in order to save man time and travelling expences.

The system supervision is performed from a remote PC computer situated at the Production Supervision Centre in Norrköping. The daily supervision is carried out by the computer operator staff at the Centre. During normal operational conditions, the work consists of pressing a button at the PC keyboard eight times a day, to confirm the balloon launchings at the two Autosonde sites. There is no longer a need for a dialogue between the operator and the actual Airport Tower before the ballon launching, and the possibility to run the Autosonde systems in the fully automated mode is now discussed. From the central operators position, alarms from the Autosonde sites also are handled, as well as measures in order to start a second radiosonde observation, if needed.

The local maintenance organization at each site consists of some of the local operators, which have recieved a deeper technical training, in order to be able to take care of simple routine maintenance. They are supported by a couple of engineers with Autosonde and Windows NT education, located at SMHI in Norrköping. A basic set of spare parts is available at each Autosonde site. For more sophisticated technical support, the Vaisala Autosonde specialists are accessible by phone or E-mail. The Vaisala specialists are also available for advanced corrective maintenance at the site .

4 Experiences, qualitative and economical result

The radiosonde operators had good experiences from the new system already at the early Autosonde prototype test at Sundsvall/Härnösand Airport in 1993 *(see Reference)*. The work is concentrated to daytime, and normally no work has to be carried out during weekends. The automated hydrogene ballon filling is an important safety factor.

The number of disturbances since the systems were installed late in 1994 is rather high, but most of the faults were "teething troubles" that ocurred before the fulfilled reliability test in Spring 1996. Those faults are corrected and the systems are now reasonable stable, disregarding some

communication problems. The quality goal of least 95% data availability is not yet fulfilled, see *Table 1.*

Site	**Before**	**After**		
Year	*Nov 1993 - Sept 1994*	*1995*	*1996*	*1997*
Landvetter	97,8	82,8	93,0	91,6
Sundsvall/Härnösand	94,9	83,6	96,2	91.8

Table 1: *Data availability in % from Landvetter and Sundsvall/Härnösand Upper Air Stations before and after Autosonde introduction. During 1997, the monthly figures have varied between 80,6% and 98,0 % in Landvetter and 62,9 % and 99,2 % in Sundsvall/Härnösand. Source: Internal SMHI reports "Data Availability from SMHI's Obsevation System"*

It has to be pointed, that the availability in *Table 1* is measured in the central data archive of SMHI, and the figures are influenced not only by Autosonde functionality and Autosonde operator skill, but also sometimes by communication failure and malfunction in the internal data distribution.

After the automation of the upper air stations, there is a strongly limited possibility to change back to manual balloon launching if the Autosonde is out of order for some reason The reason is that the remaining staff with adequate education is too small and they are also involved in the meteorological routine shift work. If, for example, a complicated fault occurs in the automatic control system a Friday evening, it will not be possible to access the specialists at Vaisala until Monday morning. The local maintenance staff does not include technicians with deeper mechanical and control system engineering education, and thus the system will be out of order for at least 3 days. Those three days will cause a 10% reduction in the monthly data availability! It is not possible to make technical systems totally free from that kind of faults without expensive back-up systems, hence the problem has to be solved in another way. SMHI intend to find some local company with adequately educated repair staff, who can be contracted for a rapid maintenance performance.

At Sundsvall/Härnösand Airport, 3300 hours per year were used for the upper-air service with two daily TEMP observations and two daily PILOT observations before the implementation of Autosonde equipment. After the Autosonde introduction, the local work is reduced to 700 hours per year. The number of daily TEMP observations is now increased from two to four. This implies, that at Sundsvall/Härnösand Upper Air Station the local work per radiosonde observation has been reduced from 2,3 hours to 0,5 after the Autosonde introduction, see *Table 2.* At Landvetter, the figures are substantially the same, but the longer distance between the Autosonde site and the Regional Meteorological Office causes some more local work.

	Before	**After**
Local work; hours/year	3300	700
Number of soundings/day	2 wind + 2 PTU	4 PTU
Hours/sounding	2,3	0,5

Table 2: *Difference in local work at Sundsvall/Härnösand Upper Air Station before and after Autosonde introduction*

In the time study performed at the Autosonde prototype test 1993 *(see Reference)* the average time for local work for 1 radiosonde observation was determined to be 28 minutes. That figure corresponds well with the operational experience in *Table 2*, but this ½ hour is also including local maintenance

work, carried out by the local operators. The maintenance work carried out by the support engineers in Norrköping is approximately 600 hours per year. Generally speaking, the operational cost is kept within expected limits.

5 Summary

The performance of the two Autosonde systems have substantially met the expectations. The saving goals are fulfilled, but the quality goal of at least 95 % yearly data availability, measured in the central data archive of SMHI, is not yet fulfilled. Nevertheless, there is good hope for meeting the availability expectations with a better tuning of the routines in the long and complicated chain "local operator skill - local computer power- promptly local maintenance - telecommunications - central computer power - central supervising and maintenance - internal data distribution - archiving routines".

The radiosonde operators' experience of Autosonde is very good. Their work is concentrated to daytime, and normally no work has to be carried out during weekends. Furthermore, the automated hydrogene ballon filling is a substantial safety factor.

Reference:

Hovberg, T, 1994: Test of an Ballooon Filling and Launching System in an operational environment. Paper presented at the WMO Conference on Instruments and Methods of Observation (TECO-94), Geneva 28 February - 2 March 1994. *Instrument and Observing Methods report No.57, WMO/TD - No. 588*

SONDEX96: A FIELD EXPERIMENT CONDUCTED BY NASA AND SMI AT PAYERNE, SWITZERLAND

F. J. Schmidlin, G. Brothers, W. Michel, and P. Moore
Laboratory for Hydrospheric Processes
Goddard Space Flight Center, Wallops Island, Virginia USA

B. A. Hoegger, A. A. Joye, G. M. Levrat, and P. Viatte
Swiss Meteorological Institute
CH 1530 Payerne, Switzerland

S. Kurnosenko
Central Aerological Observatory
Moscow, Russian Federation

1. Introduction

The assessment of ozone trends is a prescribed method for determining the rate at which ozone depletion occurs. This presumes that the data used to estimate trends can be trusted to be accurate. Unfortunately, unresolved uncertainties in the absolute calibrations of many of the measuring instruments, especially the ozonesonde, have led to a number of tests and evaluations (Kerr et al, 1994; Torres and Bandy, 1978; Torres, 1985).Today, four ozonesonde-type instruments are available to make vertical measurements of ozone distribution. There are some observation sites having available long-time series of measurements useful for studying ozone depletion. There are satellite remote sensing instruments capable of obtaining global coverage of ozone. These measurements do not have the vertical detail that ozonesondes provide. Further, ozonesondes are used for the validation of measurements obtained from remote sensors. Thus the requirement that ozonesonde measurements be as accurate as possible is important. Measurement disagreement is a historical problem; as new, hi-tech instruments become available the older instruments, by definition, no longer serve their purpose. Usually, a reference instrument can aid in determining the accuracy and reliability of newer instruments. But, balloon-borne reference instruments do not exist mostly because they are too costly to expend on a non-recoverable balloon package. Calibrations against laboratory standards prior to balloon release are usually ignored except for minimal checking. It is erroneously assumed that changes in accuracy do not occur during flight. Quantifying the accuracy of a given balloon borne instrument against a reference instrument is known to be performed at two sites: Payerne and Wallops Island.

During the past few years a series of campaigns have been conducted to 1) determine whether ozonesonde performance is changing and, 2) whether systematic differences can be identified. A World Meteorological Organization sponsored comparison was conducted in Vanscoy, Canada (Kerr et al, 1994). One result was that the Brewer Mast (BM) ozonesonde reported 15 percent higher ozone than measurements obtained with the Electrochemical Concentration Cell (ECC) ozonesonde. Previous comparisons had indicated that the BM instrument reported less ozone in the troposphere than the ECC (Attmannspacher and Dutsch, 1981; Beekmann et al, 1994). When results such as these occur questions arise: whether the instruments have changed? whether calibrations are different? whether preparation procedures are different? or, whether the method

of data analysis changed? A test was conducted in early 1996 at the Institute for Chemistry of the Polluted Atmosphere in Juelich, Germany (Smit, personal communication) to compare ozonesondes with a μv photometer. Only ozone sensors were to be tested in the chamber since it was decided not to include the radiosonde in the data link. This means that only differences due to the ozone sensors themselves would be compared. Results are to be forthcoming.

Because of the preparation methods adopted by Swiss Meteorological Institute (SMI) and the National Aeronautics and Space Administration (NASA) it was agreed to conduct an intercomparison of balloon-borne ozonesondes. The Payerne Aerological Station of SMI and the Wallops Island Upper Atmosphere Instrumentation Research Project of NASA's Goddard Space Flight Center organized an intercomparison for May 1996. The balloon-borne ozonesondes were to be flown from the SMI facility at Payerne, Switzerland. Comparisons of the BM, the BM modified with an ECC pump (BMECC), and the ECC ozonesondes were arranged so that daytime and nighttime observations were obtained. A total of 33 balloons were flown, each with the three ozonesondes attached. Although the instruments were prepared properly and in a similar manner, considerable measurement differences occurred, especially above the level of ozone maximum.

2. Test Results

Operational details of the ozonesondes' preparation, launch, and data processing will not be discussed. Although the results obtained are important, the measurements are still being analyzed. A more complete report covering these details is in preparation. Profiles of the three ozonesondes (BM, BMECC, ECC) flown at 0736 UTC on 3 May, 1996 may be compared from Figure 1. At release of the balloon the ECC indicated an ozone value of 33 nanobars (nbar), the BM and BMECC indicated 9 nbar and 19 nbar, respectively. These differences are not unique to just this set of measurements. All observations revealed erratic differences for at least the initial 10-20 seconds after balloon release. Although the differences may be meaningful we believe that how the instruments are handled prior to release may have caused the discrepancy. The ozonesonde measurements up through minute 20 of the flight followed each other reasonably well, in general, although the BM revealed more detail than the other instruments. The BMECC indicated a smoother profile and recorded more ozone than the BM and ECC. The lowest recorded ozone was measured at about minute 21, the BMECC indicated 2 nbar more ozone than the other instruments. From minute 21 to the ozone maximum, near 50 hPa, the ozonesondes recorded very similar values, although the BMECC did indicate slightly more ozone. At altitudes above the ozone maximum, the ECC instrument clearly recorded the highest amount of ozone, while the BM recorded more ozone than the BMECC. The profiles shown in Figure 1 are characteristic of the majority of the data obtained during SONDEX96, however, very few balloon flights indicated comparable ozone values above the ozone maximum.

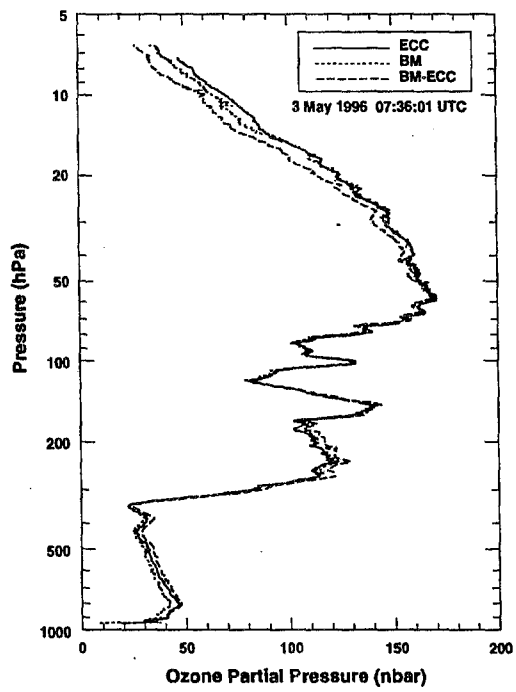

Figure 1. Example of a single balloon flight during daytime with three ozonesondes as labeled on the graph.

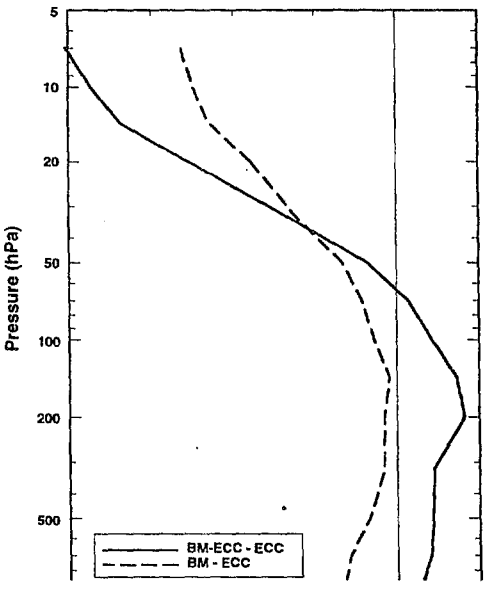

Figure 2. Mean differences between BM and BMECC and ECC ozonesonde

The mean differences formed between the ECC and BM and the ECC and BMECC ozonesondes are illustrated in Figure 2. The ECC ozonesonde was adopted as an arbitrary reference standard; either of the other ozonesondes could have been used as well. Means are plotted as a function of altitude. The data were sampled at different intervals for each instrument, e.g., the ECC sample rate was 2 second intervals, the BM sampled at 4 second intervals and the BMECC at 7 second intervals. Because of the different sample rates the data were interpolated at 2-second intervals.

Figure 2 indicates that, in the mean, the BM ozonesonde recorded less ozone than the ECC ozonesonde between the surface and ~7 hPa. Recorded ozone differences between the surface and about 40 hPa were between 1 to 3 nbars lower. At higher altitudes the differences increased, reaching almost 15 nbars less than the ECC near 7 hPa. The number of sample points also decreased at the upper altitudes. The mean measurement difference between the BMECC and ECC indicates that the BMECC recorded about 2-4 nbars more ozone between the surface and 60 hPa, above this point the differences change to negative values and mean measurements from the BMECC is about 20 nbars less than those of the ECC.

Since the ozonesondes drifted toward the East after the balloon launch, an ideal situation was present to obtain comparisons with total ozone measurements from the Arosa Dobson station. Figure 3 provides a comparison among the integrated total ozone of each ozonesonde observation with the Dobson's values. Because weather inhibited Dobson observations at some of the observation times, gaps or missing data is seen in the figure. Nonetheless, the pattern is clear.

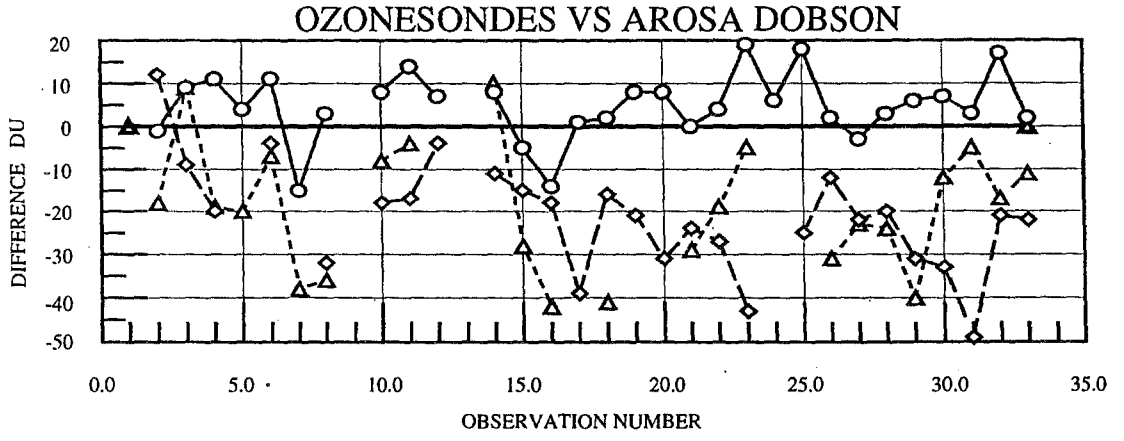

Figure 3. Comparison among SONDEX96 ozonesondes (BM shown by dashed line), (BMECC shown by dotted line) and, ECC shown by solid line and the Dobson spectrophotometer located in AROSA shown percentage differences of –5.8%, -5.2%, and 1.4%, respectively.

The overall difference between Dobson and integrated total ozone of the ECC instrument is about 1 percent. This is considerably good since the ozonesondes actually transverse over 150 km and did not make a direct overhead measurement at Arosa. Comparison between the Dobson and the BM integrated values indicate a -6 percent mean difference and the BMECC ozonesonde about a –5 percent difference. The latter two ozonesondes recorded less total ozone than the spectrophotometer.

3. Summary

It is clear that differences exist between the three ozonesonde instruments. What is not clear is why the BM and BMECC results are different from each other. The only change made to the BMECC is the substitution of the original BM pump with a Teflon pump typically used with the ECC ozonesonde. The ozone measurements from the BMECC were less than the ECC measurements. Furthermore, the BM recorded data also were less than the ECC, however, the comparisons conducted in Vanscoy, Canada a few years ago (Kerr, 1994) showed the BM measuring more ozone than the ECC.

It is now important that the SONDEX96 ozonesonde configuration be investigated further to determine the cause for the differences observed. It appears that the ECC ozonesonde fielded by the NASA team from Wallops Island provided total integrated ozone comparable to the total ozone obtained from the Arosa Dobson instrument. Consideration is being given to another laboratory test in Juelich that should provide additional information for the instrumental differences.

5. References

Kerr, J. B., et al, 1994: The 1991 WMO international ozonesonde intercomparison at Vanscoy, Canada. Atmospheres and Oceans.

Beekmann, M., G. Ancellet, G. Megie, H. G. J. Smit, and D. Kley, 1994: Intercomparison campaign of vertical ozone profiles including electrochemical sondes of ECC and Brewer-Mast type-a ground-based uv-differential absorption lidar. J. Atmos. Chem. 19: (3) 259-288.

Torres, A. and A. Bandy, 1978: Performance characteristics of the Electrochemical Concentration Cell ozonesonde. J. Geophys. Res., 83, pp.5501-5504.

Torres, 1985: ECC ozonesonde performance at high altitudes: pump efficiency. NASA Technical Memorandum 73290, 8 pages.

UPPER ATMOSPHERE INSTRUMENTATION RESEARCH

CONDUCTED FROM NASA/GODDARD SPACE FLIGHT CENTER,

WALLOPS ISLAND, VIRGINIA USA

F. J. Schmidlin
Laboratory for Hydrospheric Processes
Goddard Space Flight Center, Wallops Island, Virginia 23337 USA

1. Introduction

The National Aeronautics and Space Administration's (NASA) facility located at Wallops Island, Virginia is unique for conducting upper atmosphere instrumentation studies. Wallops Island is situated on the Atlantic Ocean and, for the most part, is located about 5-10 km east of any airlanes. Wallops Island also has available high precision tracking radars, superb telemetry antennae and receivers, excellent data reduction facilities, and skilled personnel well qualified to conduct meteorological instrument investigations. A variety of balloon types are at hand for use from the smallest rubber balloon to large plastic balloons. Major meteorological rocket-borne instruments and radiosonde systems are flown from Wallops, radar-tracked for position information thus enabling accurate altitude and winds to be resolved. Other parameters such as, temperature, relative humidity, and ozone are gathered for other studies. Special upper atmosphere instruments have been developed here, and additional sensors from various manufacturers as well as new techniques are periodically tested. Unique software is developed, as necessary, to meet research requirements.

A brief description of the type of meteorological instrument research carried on at Wallops Island is given below. The areas of study are separated into unique instrument disciplines to enable detailed description of each classification.

Meteorological Rocketsondes between 1960 and 1980 were routinely launched on average 3-5 times per week. There were two purposes for launching these instruments. Firstly, to enable atmospheric climatology to be developed for engineering use in the development of large rocket vehicles such as, Saturn, Atlas, Space Shuttle. The information gathered primarily provided the material necessary to establish safely factors required in the spacecraft design. Secondly, the data validated many remote measurements from satellites. Thirdly, the data were used by different agencies, one primarily the National Weather Service in the preparation of hemispheric charts to the 0.4-hPa pressure level. The temperature and wind information set the stage for planning numerous experiments designed to confirm previous unavailable and unknown circulation features. The number of meteorological rocketsondes decreased, at first gradually, then at a faster pace, until today, rocketsondes are launched only for special experiments.

Because different United States (US)agencies and other countries were launching uniquely designed small rocketsondes, Wallops Island hosted intercomparisons aimed at describing differences in the measurements from each of the instruments. In 1967 and in 1968 comparisons between Japan and the US took place at Wallops Island; in 1971 the first part of a World Meteorological Organization sponsored comparison took place between Japan, France, and the

US. And, in 1977 a comparison between the Former Soviet Union and the US took place. The unique location of Wallops and the tracking radars were a large factor in the tests to be conducted from the Wallops facility on Virginia's Eastern Shore. One early result obtained from a comparison between large and small rockets, and between satellite remote sensors, caused investigators to be concerned by the difference found among all of the techniques. Arbitrarily, a single rocketsonde temperature sensor was established as a reference; differences reached 10°C in the upper stratosphere.

Radiosondes are flown for various purposes: support of rocketsonde temperature measurements and to provide initial level date needed to calculate pressure at the rocket altitudes, satellite validation, WMO intercomparisons, development of an accurate temperature measurement technique, study of relative humidity sensors, and analysis of radiosonde manufacturers ground stations and capability.

Comparison of different radiosonde sensors have led to improvements and a better understanding of the size of error that.can be tolerated for science studies or synoptic purposes. Comparisons between radiosonde-measured and satellite-measured temperatures have been significant in identifying bias in the profiles. However, these results also led to a search to determine the error of the radiosonde, since it still stands alone as the long-term reference for many studies. Recent studies include the Accurate Temperature Measuring (ATM) radiosonde and a chilled mirror sensor to measure humidity.

Ozonesonde observations are made weekly from Wallops Island, from Brazil through an agreement between NASA and INPE, and two times each week from Ascension Island. These instruments are calibrated in the Wallops ozone laboratory before being flown. All ozonesonde data are quality checked and placed in the ozone archive located in the World Ozone Data Center in Toronto. Various studies to improve instrument response and accuracy have been conducted from Wallops Island and elsewhere. Satellite validation is one objective of the ozonesonde effort. Low pressure chambers are used to verify the ozone sensors ability to accurately measure ozone. Other testing involve radio frequency interference of the instrument and temperature effects on the electronic components.

The Upper Atmosphere Instrumentation Research facility also has available a Dobson spectrophotometer, an aerosol lidar, hand holdable photometers (Microtops) for measuring total ozone, precipitable water, and aerosol overburden. These ground based remote sensing instruments provide data necessary to understand the in situ systems and also are very useful for other research carried out by the group here or others wishing the data. A primary reference standard, a three-meter long-path μv photometer, is used to calibrate Dasibi ozonemeters. The Dasibi performs as a secondary reference standard used to calibrate the ozonesonde.

Our plan is to further enhance our capability to study upper atmosphere instrumentation and to use this new capability to study of processes going on in the atmosphere. We are considering adding other instruments that may be utilized for upper air research.

THE PERFORMANCE OF THE RUSSIAN SUSTEM OF RAWINSONDE ATMOCPHERIC OBSERVATIONS AVK-MRZ

V.A. Yurmanov
Central Aerological Observatory (CAO), Russian Federation

1. ABSTRACT

The results are presented of investigaiting performance of the Russion autjmated radar system for rawinsonde observations of the atmosphere AVK-MRS under various climatic conditions in different regions (mid latitudes, Arctica, Antarctica). Experimental estimates are given of basic performance characteristics reflection the efficiency of the system AVK-MRZ and the Russion upper-air stations using it. The corresponding testing procedures are described. The main concern is with determining the reliability and efficiency of the hardware, algorithms and software for automated data processing employing a specialized micro-computer (SMC "Argon"), the quality of autput upper-air information, and estimation of the AVK-MRZ system precision.

2. ВВЕДЕНИЕ

В настоящее время основной системой радиозондирования атмосферы на аэрологической сети России является система АВК-МРЗ /1/ с автономной автоматической обработкой данных. Автоматизированная система АВК-МРЗ относится к классу радиолокационных систем радиозондирования атмосферы с активным ответом, который реализуется с помощью суперрегенеративного ответчика. Используется совмещенный радиоканал для передачи аналоговой радиолокационной и радиотелеметрической информации в дециметровом (17 см) диапазоне радиоволн. При разработке системы АВК-МРЗ на основе системного анализа проведена ее оптимизация в целом и отдельных элементов. Процессы сопровождения радиозонда и обработки данных радиозондирования полностью автоматизированы.

3. ОБЩЕЕ ОПИСАНИЕ СИСТЕМЫ АВК-МРЗ

3.1. Радиозонд МРЗ

Разработан легкий малогабаритный радиозонд (МРЗ-3А) с использованием существующих стандартных датчиков с нормированными метрологическими характеристиками. Для повышения помехоустойчивости и надежности передачи координатно-телеметрической информации по радиоканалу в радиозонде применена устойчиво работающая схема суперрегенератора, частотно-манипулированная модуляция (ЧМ) несущей частоты, повышен к.п.д. антенной системы и оптимизирована форма диаграммы направленности антенны радиозонда с целью снижения вредного влияния замираний сигнала. Питание радиоблока радиозонда осуществляется от специально разработанной активируемой батареи со стабильными электрическими характеристиками.

3.2. Комплекс АВК

В наземном аэрологическом информационно-вычислительном комплексе (АВК-1) для повышения устойчивости приема сигнала радиозонда при замираниях используется круговая поляризация антенны. Применен малошумящий СВЧ-усилитель. На основе теории оптимального приема сигнала радиозонда /2/ разработано оптимальное приемное устройство для сигнала радиозонда МРЗ-3А. Улучшены характеристики систем автосопровождения радиозонда по угловым координатам и дальности. Произведено исследование и нормирование метрологических характеристик АВК.

3.3. Система автоматической обработки

Для обеспечения надежной и устойчивой автоматической обработки данных стандартных аэрологических наблюдений используется специализированная цифровая вычислительная машина (СЦВМ) типа "Аргон" (А-15) и оптимизированы алгоритмы обработки первичных данных приенительно к ограниченным вычислительным возможностям СЦВМ, работающей в реальном масштабе времени. Программное обеспечение (ПО) жестко прошито в постоянной памяти. СЦВМ одновременно выполняет управляющие и контрольные функции, автоматизирующие работу АВК.

В процессе эксплуатации производилась оценка работоспособности системы, тестирование и отработка ПО в различных климатических и физико-географических условиях России, в том числе в Арктике и в Антарктиде. На основе этого за период 1986-1990 гг. разработаны четыре усовершенствованных версии ПО.

4. ЭКСПЛУАТАЦИОННЫЕ ХАРАКТЕРИСТИКИ СИСТЕМЫ АВК-МРЗ

Наибольший интерес при использовании конкретной системы радиозондирования атмосферы представляет изучение и оценка ее эксплуатационных характеристик не по технической документации или проспектным материалам, а в реальных климатических условиях. Это необходимо для определения ее фактического соответствия предъявляемым требованиям со стороны потребителей аэрологической информации, а также при сравнении различных систем радиозондирования и их элементов на национальном или международном уровне.

4.1. Методики экспериментальных натурных исследований

Для оценки эксплуатационных характеристик системы АВК-МРЗ были проведены экспериментальные натурные исследования /3/ по специально разработанным методикам. Методиками предусматривалось как оценка технических и метрологических характеристик системы в целом и ее элементов, так и качества функционирования оснащенных данной системой аэрологических станций и получаемой аэрологической информации.

Особое внимание уделялось оценке точности системы АВК-МРЗ и сходимости ее данных с данными системы МЕТЕОРИТ-МАРЗ, эксплуатирующейся на аэрологической сети России до настоящего времени. Натурные исследования указанных характеристик радиолокационного, радиотелеметрического каналов и системы в целом производились с использованием образцовых средств измерений, методом спаренных выпусков радиозондов, синхронных измерений двумя комплексами данных радиозондов, методом структурных функций по данным серий учащенных выпусков радиозондов.

4.2. Результаты экспериментальных исследований

В табл.1 приведены результаты экспериментальных натурных исследований основных эксплуатационных характеристик системы АВК-МРЗ, выполненных в различных климатических условиях и регионах (средняя полоса, Арктика, Антарктида). В ней отражены погрешности измерения координат и телеметрической информации.

Таблица 1

ОСНОВНЫЕ ТЕХНИЧЕСКИЕ ХАРАКТЕРИСТИКИ СИСТЕМЫ АВК-МРЗ

Рабочий диапазон частот, МГц	1775-1790
Радиус санитарно-защитной зоны, м	40
Минимальная дальность, м	70-100
Максимальная дальность, км	300-310
Максимальная высота, км	40-42
Минимальный рабочий вертикальный угол, град	5,5
Максимальный рабочий вертикальный угол, град	55-60
Среднее время выдачи частей A и B (КН-04), мин ...	55-73
Среднее время выдачи частей C и D (КН-04), мин ...	97
Вероятность получения телеграмм без редакции	0,945-0,984
Погрешность измерения дальности, м:	
систематическая (маломощный/мощный передатчик)..	16-27 / 5-14
случайная (маломощный/мощный передатчик)	2,0-8,1/3,0-17,3
Погрешности измерения угловых координат, град	
систематическая:	
азимута (6 град < d < 60 град)	0,08-0,10
вертикального угла	0,10-0,11
случайная:	
азимута	0,09-0,17
вертикального угла	0,10-0,15
Случайные погрешности измерения телеметрической информации:	
температура, не более C	0,06
относительная влажность, не более,%	0,17
Диапазон измерения параметров атмосферы:	
температура, C	от минус 90 до 50
относительная влажность, %	0-100
давление, гПа	1020-2,2
скорость ветра, м/с	0-112
направление ветра, град	0-360

В табл.2 даны средние значения случайных погрешностей измерения основных параметров атмосферы системой АВК-МРЗ на уровне стандартных изобарических поверхностей по совокупной статистике натурных исследований в различных климатических условиях и регионах, учитывающие влияние сложных условий проведения выпусков (замирания сигнала радиозонда, работа в зените, прохождение зоны нерабочих углов АВК, большие дальности, значения температуры ниже минус 80 С). В скобках приведены случайные погрешности метеоэлементов по данным синхронных измерений.

Таблица 2

ПОГРЕШНОСТИ ИЗМЕРЕНИЯ ПАРАМЕТРОВ АТМОСФЕРЫ СИСТЕМОЙ АВК-МРЗ

P гПа	T С	U %	DT С	H гпм	V м/с	d град
850	0,46 (0,08)	6,2 (1,10)	(0,17)	5,0 (0,00)	0,88 (0,33)	(1.92)
700	0,47 (0,09)	7,0 (0,39)	(0,23)	9,0 (3,46)	1,00 (0,54)	(0,76)
500	0,50 (0,21)	6,5 (0,73)	(0,18)	14,5 (3,46)	1,02 (0,45)	(3,28)
400	(0,22)	(0,54)	(0,19)	(2,68)	1,02 (0,50)	(0,96)
300	0,45 (0,13)	5,8 (0,64)	(0,25)	11,0 (4,09)	1,02 (0,54)	(2,30)
250	(0,11)	(0,67)	(0,28)	(3,46)	(0,35)	(0,93)
200	0,46 (0,24)	5,0 (0,29)	(0,12)	10,0 (7,58)	0,82 (0,00)	(0,86)
150	(0,19)	(0,45)	(0,30)	(5,34)	0,95 (0,73)	(1,52)
100	0,50 (0,10)	4,0 (0,64)	(0,39)	18,5 (7,58)	0,79 (0,35)	(1,85)
70	(0,28)	(0,41)	(0,17)	(8,58)	1,38 (1,76)	(5,80)
50	0,66 (0,23)	3,2 (0,00)	(0,16)	23,0 (5,94)	1,21 (1,42)	(2,68)
30	0,80 (0,11)	2,8 (0,58)	(0,33)	29,5 (11,86)	1,09 (0,71)	(2,08)
20	1,00 (0,24)	2,4 (1,74)	(0,18)	29,5 (12,88)	1,00 (0,90)	(2,00)
10	1,25 (0,28)	1,5 (1,23)	(0,30)	32,0	0,90 (0,70)	(0,71)

5. ВЫВОДЫ И ПЕРСПЕКТИВЫ

Анализ данных табл.1 и табл.2 показывает, что система АВК-МРЗ имеет реальные эксплуатационные характеристики, соответствующие современному уровню и требованиям ВМО к точности и качеству аэрологической информации, что подтверждается результатами международных сравнений систем радиозондирования атмосферы, проведенных ВМО на этапе III фазы в Джамбуле /4/, и данными мониторингов качества аэрологической информации, регулярно проводимых Европейским центром средне-срочных прогнозов погоды (ЕЦСПП).

На основе более чем десятилетнего опыта эксплуатации автоматизированной системы радиозондирования АВК-МРЗ в различных климатических условиях и физико-географических регионах, в дальнейшем предполагается разработать, на базе компьютеров типа PC, универсальные алгоритмы и программное обеспечение для автоматической обработки аэрологических данных в существующих и новых российских радиолокационных/радиотеодолитных системах радиозондирования атмосферы.

6. ЛИТЕРАТУРА

1. Методические указания по производству радиозондирования атмосферы системой "АВК-1(ТИТАН) - МРЗ". Под ред. к.т.н. В.А.Юрманова. Долгопрудный, ЦАО (препринт), 1987.

2. Юрманов В.А., Ермаков В.И., Кузенков А.Ф. Системы радиозондирования атмосферы. Гидрометеоиздат, Л., 1977.

3. Юрманов В.А. Результаты исследования эксплуатационных характеристик системы радиозондирования атмосферы "АВК-МРЗ". Тезисы доклада на научной конференции по результатам исследований в области гидрометеорологии и мониторинга загрязнения природной среды. Росгидромет, МСГ. М., 1996. С.29-31.

4. Ivanov A., Kats A., Kurnosenko S., Nash N., Zaitseva N. WMO International Radiosonde Comparison. Dzhambul, USSR, 1989. Instrumentation and Observing Methods. Report N 40. WMO/TD - N 451, 1991.

AUTOMATION OF UPPER-AIR OBSERVATIONS IN THE RUSSIAN FEDERATION

A.A.Ivanov, G.P.Trifonov, and V.A.Yurmanov
Central Aerological Observatory (CAO), Russian Federation

1. ABSTRACT

The stages of automating upper-air observations in the RussianFederation are described. Primary consideration is given to the fully-automated radar system of rawinsonde upper-air observations AVK-MRZ operating in an UHF range. The specifications are given of the computer complex AVK (AVK-1, AVK-1M), using a specialized micro-computer (SMC "Argon"), and those of MRZ-3A type radiosonde. The 1985-1997 progress in the development of software versions for the system of rawinsonde data treatment, using the SMC "Argon", is described. Basic guidance methodological documents for carrying out routine upper-air observations, using AVK-MRZ, are presented. The prospects are outlined for futher development of the automation of radar/theodolite systems of ravinsonde observations in the Russian Federation.

2. ВВЕДЕНИЕ

В мировой практике радиозондирования атмосферы автоматизация обработки данных осуществлялась различными способами, в зависимости от имеющихся технических возможностей и степени алгоритмизации и совершенствования метода и программного обеспечения обработки.

В своем развитии она прошла путь от технологии полуавтоматической и централизованной автоматической обработки на универсальных ЭВМ до автономной автоматической обработки с помощью микро-ЭВМ и персональных компьютеров (ПК). Эта тенденция характерна и для систем радиозондирования России.

3. СИСТЕМЫ АВТОМАТИЧЕСКОЙ ОБРАБОТКИ РОССИИ

Особенностью систем радиозондирования атмосферы является большой объем информации и достаточно сложные алгоритмы обработки данных, поэтому автоматизация обработки стала возможной только при появлении вычислительной техники. На первом этапе автоматизация могла быть реализована только по принципу централизованной обработки (телеобработки), когда первичные данные от нескольких аэрологических станций (АЭ) в цифровом виде передаются в общий вычислительный центр (ВЦ), оснащенный универсальной ЭВМ для вторичной обработки с выдачей аэрологических телеграмм.

3.1. Система "Атмосфера"

Впервые работы по автоматизации обработки данных были начаты в России в начале 60-х г.г. применительно к системе радиозондирования "Малахит - А-22". Централизованная автоматическая обработка реализовывалась с помощью универсальной ЭВМ "Урал". Первая программа обработки данных радиозондирования атмосферы была составлена на языке Алгол для ЭВМ М-20.

3.2. Система ОКА-3

Система ОКА-3 /1/ для централизованной автоматической обработки данных системы радиозондирования "Метеорит-2 - РКЗ" применялась в территориальных центрах в ВЦ, оснащенных универсальными ЭВМ "Минск-22" и "Минск-32". Технология централизованной обработки была полностью автоматизирована при переводе обработки на ЕС ЭВМ /2/ с автоматическим вводом данных из каналов связи. С 1973 г. комплекс ОКА-3 получил широкое применение на наземной и судовой аэрологической сети России. Важным этапом по оценке качества автоматической обработки были сравнения данных советской системы "Метеорит-2 - МАРЗ-2 - ОКА-3" и финской системы "Микро-КОРА", проведенные в 1984 г. в Минске /3/.

3.3. Система ОКТАВА

В 1984 г. разработана система ОКТАВА с автономной автоматической обработкой с помощью микро-ЭВМ типа ДВК-2 /4/, которая была внедрена на 40 АЭ России. ОКТАВА на

базе ПК IBM PC (в составе системы "Метеорит-2 - МАРЗ-2") факультативно участвовала в проведении международных сравнений систем радиозондирования в 1989 г. в Джамбуле.

Для радиолокационной системы зондирования разработаны алгоритмы вычисления давления по высоте с учетом поправок на рефракцию и кривизну Земли. Разработанные методы и алгоритмы автоматической обработки /5, 6 / были положены в основу устройства автоматической обработки данных системы АВК-МРЗ, получившей массовое внедрение, начиная с 1986 г.

4. СИСТЕМА РАДИОЗОНДИРОВАНИЯ АВК-МРЗ

4.1. Технические средства

Система радиозондирования атмосферы АВК-МРЗ относится к классу радиолокационных систем с активным ответом и работает в дециметровом диапазоне радиоволн (17 см). Основные элементы системы - радиозонд МРЗ-3А и автоматизированный информационно-вычислительный комплекс АВК (АВК-1, АВК-1М).

МРЗ-3А является легким малогабаритным радиозондом, выполненным на интегральных схемах и полупроводниковых элементах. В нем использованы стандартные датчики температуры и влажности, но с улучшенными метрологическими характеристиками. Переключение датчиков производится электронным коммутатором. Сверхрегенеративный приемопередатчик радиозонда
выполнен в виде специализированного СВЧ-модуля и совмещает функции высокочувствительного приемника запросных радиоимпульсов АВК, активного ответчика и передатчика телеметрической информации с использованием частотной манипуляции (ЧМ) несущей частоты.

В табл.1 приведены основные технические характеристики радиозонда МРЗ-3А .

Таблица 1

ОСНОВНЫЕ ТЕХНИЧЕСКИЕ ХАРАКТЕРИСТИКИ МРЗ

Рабочая частота, МГц	1782
Частота следования суперирующих импульсов, кГц	800
Девиация ЧМ, кГц	от 11 до 17
Длительность канальных интервалов, с	5
Датчик температуры:	
чувствительный элемент	терморезистор
диапазон измерений температуры воздуха, °С.....	от минус 80 до 50
СКО погрешности измерения температуры, °С	0,4
постоянная времени (5 м/с, 1000 гПа), с	10
Датчик относительной влажности:	
чувствительный элемент	животная пленка
диапазон измерений влажности воздуха, %RH	от 15 до 98
СКО погрешности измерения влажности, %RH	5
постоянная времени (5 м/с,1000 гПа,20 °С), с	10
диапазон рабочих температур воздуха, °С	от минус 40 до 50
Источник питания (водоактивируемая батарея)	28 МХМ-01
Масса с источником питания, г	360
Габаритные размеры (в собранном виде), мм	200x150x300

В процессе эксплуатации системы АВК-МРЗ была произведена модернизация наземного оборудования, состоящая в разработке второго поколения комплекса АВК-1. Основным отличием модернизированного комплекса АВК-1М является замена элементной базы и повышение надежности аппаратуры, применение СЦВМ второго поколения "Аргон" (А-15-1) с улучшенными характеристиками, совершенствование аппаратуры предполетной проверки радиозонда МРЗ-3А и комплектование комплекса пультом дистанционного управления антенной для обеспечения надежного сопровождения радиозонда в начальный момент выпуска при его прохождении через зенит .

В табл.2 приведены основные технические характеристики АВК.

Таблица 2

ОСНОВНЫЕ ТЕХНИЧЕСКИЕ ХАРАКТЕРИСТИКИ АВК

Рабочая частота, МГц	1782
Тип поляризации	круговая
Минимальная дальность, м	100
Максимальная дальность, км	300
Максимальная высота, км	35-40
Максимальная излучаемая импульсная мощность:	
маломощного передатчика, кВт	1
мощного передатчика, квт	10
Частота повторения излучаемых импульсов, Гц	416
Чувствительность приемной системы, дб/Вт ...	минус 127
Диаметр антенного зеркала, м	1,8
Ширина диаграммы направленности антенны	
на уровне половинной мощности, град	5
Погрешность измерения дальности, не более, м:	
систематическая	30
случайная (СКО)	45
Погрешность измерения угловых координат, не более, град:	
систематическая	0,12
случайная (СКО)	0,18

4.2. Программные средства

В комплексе АВК реализована автономная автоматическая обработка данных с применением СЦВМ типа "Аргон", работающей в реальном масштабе времени. Программное обеспечение (ПО) жестко прошито в памяти СЦВМ. В процессе тестирования и отработки ПО в различных местных и климатических условиях и физико-географических регионах России и зарубежных стран, применяющих систему АВК-МРЗ, в Арктике и Антарктиде, разрабатывались усовершенствованные версии ПО. Всего разработано четыре новых версий. В АВК-1М используется версия, обеспечивающая сопряжение с ПК IBM PC.

Основным содержанием работ по поэтапному усовершенствованию ПО, приводящему к отличиям характеристик соответствующих версий, является улучшение используемых и разработка более эффективных новых алгоритмов обработки с целью повышения точности и надежности получения аэрологической информации в реальных условиях радиозондирования атмосферы. При этом учитывались сложные условия проведения выпусков при работе системы АВК-МРЗ в зоне нерабочих углов АВК, в области зенита , при больших удалениях и сильных замираниях сигнала радиозонда, при температуре воздуха ниже минус 80 °С.

4.3. Методическая база

В процессе опытной и последующей эксплуатации разработана методическая документация, регламентирующая соблюдение методики и технологии производства аэрологических наблюдений с помощью системы АВК-МРЗ /7, 8, 9/, а также обеспечение ее безопасной эксплуатации /10/.

5. ПЕРСПЕКТИВЫ

В ближайшее время планируется совершенствование системы АВК-МРЗ. Будут модернизироваться МРЗ, используя новые российские и финские датчики, и система автоматической обработки АВК на основе ПК IBM PC. Большое внимание уделяется разработке универсальных алгоритмов и программного обеспечения для обработки данных от радиолокационной/радиотеодолитной системы зондирования, созданию базы тестовых данных по реальным выпускам для проверки работоспособности алгоритмов ПО на основе использования опыта эксплуатации системы АВК-МРЗ. Планируется также внедрение нового наземного микроэлектронного аэрологического комплекса МАРЛ в радиолокационном (МАРЛ-А) и радиотеодолитном (МАРЛ-Т) вариантах, работающего совместно с радиозондами на частоте 1680 МГц.

6. ЛИТЕРАТУРА

1. Комплекс ОКА-3 для централизованной автоматической обработки данных системы радиозондирования "РКЗ-Метеорит". Под ред. к.т.н. Г.П. Трифонова. Л., Гидрометеоиздат, 1979.

2. Трифонов Г.П., Плотников Г.А. Система автоматической обработки данных радиозондирования атмосферы на ЕС ЭВМ. Метеорология и гидрология, 1984, N 8.

3. Кархунен П., Трифонов Г.П., Юрманов В.А. Сравнения данных советской системы радиозондирования атмосферы "Метеорит-2 - МАРЗ-2 - ОКА-3" и финской системы "Микро-КОРА". Метеорология и гидрология, 1987,N 11.

4. Трифонов Г.П., Плотников Г.А., Кузьмина Т.В. Система автоматической обработки данных радиозондирования атмосферы на микро-ЭВМ. Метеорология и гидрология, 1989, N 6.

5. Трифонов Г.П. Математическое обеспечение ОКА-70 для автоматической обработки данных радиозондирования атмосферы. Л., Гидрометеоиздат, 1981.

6. Трифонов Г.П. Алгоритмы обработки данных радиозондирования для микроЭВМ. Доклад на симпозиуме соцстран. Варшава, ИМВХ, октябрь 1987.

7. Временные методические указания по эксплуатации радиозондов МРЗ-3А. Под ред. к.т.н. В.А.Юрманова. Долгопрудный, ЦАО (препринт), 1986.

8. Методические указания по производству радиозондирования атмосферы системой "АВК-1(ТИТАН) - МРЗ". Под ред. к.т.н. В.А.Юрманова. Долгопрудный, ЦАО (препринт), 1987.

9. Руководство по производству радиозондирования атмосферы системой "АВК-1-МРЗ". Под ред. к.т.н. В.А.Юрманова. Долгопрудный, ЦАО (препринт), 1990.

10.Методические указания. Контроль и нормализация электромагнитной обстановки, создаваемой метеорологическими радиолокаторами. Л., Гидрометеоиздат, 1990.

NEW SOUNDING SYSTEM FOR AIRCRAFT ATMOSPHERIC MEASUREMENT

M.Zéphoris[1], J.Villain[1], S.Quemener[1], F.Henaff[1], S.Eideliman[1], J.C.Biguet[1], F.Lavie[1]
K.Veltchev[2], A.Fougeron[3]

[1] Météo-France / SETIM, 7,rue Teisserenc de Bort
78190 Trappes FRANCE
[2] Institute of Meteorology and Hydrology 1184 Sofia BULGARIA
[3] Société LEREL, 78170 La Celle St Cloud FRANCE

1. INTRODUCTION

A reliable local forecast used for gliding and hang-gliding activities or for pollution dispersion, requires accurate local atmospheric sounding information. The french weather service network (Météo-France) proceeds to atmospheric soundings each 12 hours (0000 UTC and 12OO UTC) at seven locations throughout the country. Infortunately Météo-France's sounding stations are generally located too far from the area of interest, and rawinsondes are ofen not launched at the right time for accurate local convective forecasts.

Météo-France, under request of the Fédération Française de Vol à Voile (FFVV), the Fédération Française de Vol Libre (FFVL), the Service de la Formation Aeronautique et du Controle Technique (SFACT) and for its own needs, respectively, has designed a new sounding system, named SSBC (Système de Sondages Basses Couches). They have set up a specific sounding network campaign for the 1994 gliding and hang-gliding seasons..

Thanks to the SSBC system, any flyer can now acquire local atmospheric soundings very easily, in the flying area, and from O700 to O800 UTC. Using the results of various temperature and humidity profiles, measured over different areas, in addition with the synoptic meteorological data, the meteorologists remain able to retrival realistic cumulus base and the cloud top forecasts over any specific area or all along a planned flying route and during daytime.

2. SSBC DESIGN

SSBC system has been designed when taking into account specific requirements of meteorological data users and of course meteorologists.

The operational specifications are as follows:

* pressure measurements from 1100 hPa to 500 hPa with an accuracy of 0.5 hPa.
* temperature measurements within the -40°C to +40°C range with an accuracy of 0.2 °C.
* humidity measurements from 1% to 98% with an accuracy of 5%.
* incloud flight measurement capability of 10 seconds.
* vertical sounding requires the use of an aircraft, an ULM or an helicopter which carry the probe.
* the SSBC probe is fastened to the aircraft, and is consequently independent of aircraft instruments.
* during the sounding process, data are stored in the SSBC system.
* SSBC handling is minimized for the pilot manoeuvres precedures thanks an intensive automation of its using procedures.

Finally, the main innovation of the SSBC system consists in its two folds. First, its design for a specific speed range (15 $m.s^{-1}$ to 50 $m.s^{-1}$). Second, any of its functions or measurement quality are automatically tested before and after each flight.

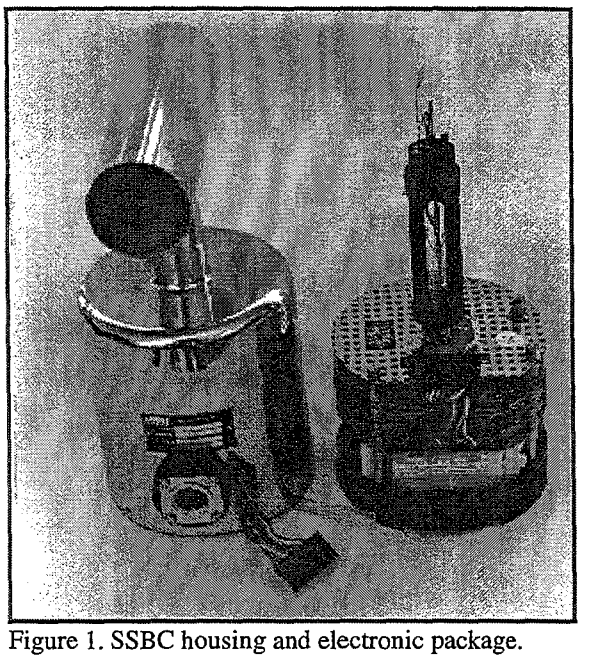

Figure 1. SSBC housing and electronic package.

The SSBC probe, which is fixed to the aircraft, is composed with the following parts (see figure 1):

* The probe housing, to protect the sensors location.
* integrated electronic unit.

* data storage.
* battery.
* fastening and bolting on aircraft system.

On ground, a calibration unit is avalaible including the following functions:
* atmospheric temperature, pressure and humidity measurements test using internal sensors référence.
* provide data transfer, through a serial communication link, from the probe to the data storage computer.

For that purpose, a specific software package have been implemented on the computer for emagrams ploting and for data transfer to a meteorological station through a modem link.

2.1 THE SSBC PROBE

The measurement spot is located behind a static helicoid jet deflector which rotates the air flow and throws the particles which could move throught the air intake, to the boundaries of the flow, thanks to the centrifugal effect (see figure 2). The measurement spot is therefore free of any droplets. The most interesting point is that the probe regains its meteorological characteristics as soon as it is back out of the clouds. The measurement sensors are located within the spot volume less than 5 cm^3 ;

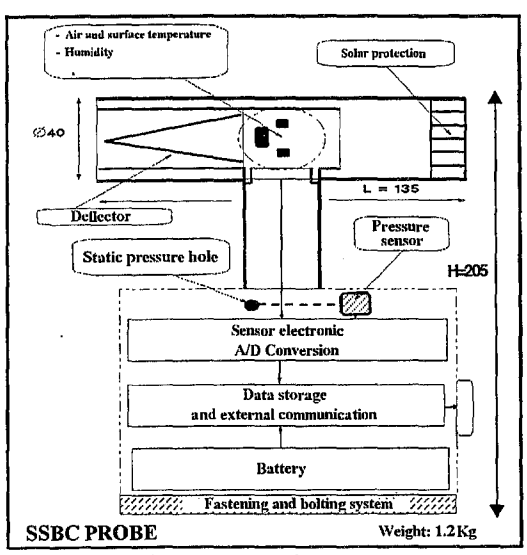

Figure 2. Sonde cut-away view.

Experimental study has been used for deflector design, material thickness, sensor location and positioning in the measurement spot. The main experimental tool was a wind tunnel which allows fast thermal and relative humidity variations (less than 0.1s). With this wind tunnel, it has been possible to inject droplets (8 to 20 micrometers diameter) into the flow in order to simulate cloud measurements intakes.

Fatigue tests in vibrating and contaminating surrounding environment (rain, particles, dust...) have been processed on instrumented vehiculs. Comparative flights have been made with the Piper Aztec aircraft of Météo France's Meteorological Aviation Center to assess the performance of the SSBC probe penetring in clouds.

2.2 THE SENSORS

* A 50 ohm thin film nickel resistor is used for temperature measurements. A similar sensor is used to measure the probe housing face temperature.
* A capacity sensor (CORECI) is used for relative humidity measurements. Its advantages are particulaly its fast response time (0.5 s to 0.8 s) and its reliability for aircraft measurements, as shown by Abadie (1991).
* A piezoresistive silicon sensor is used for the pressure measurements, compensated for temperature effects in 16 points. The sensor is calibrated at 4 pressures levels, from 1050hPa to 500 hPa and at following temperatures of +40°C, +15°C, -10°C and -35°C. The calibration procedure is similar to those used for the ERICA program, (see Norris and Lally - 1991). The static pressure intakes are located on the electronic housing.

Temperature, humidity and pressure calibration data are used for sensor response computation. This data are input in the SSBC calibration software.

2.3 THE ELECTRONIC UNIT

* Resistance variations of the air temperature sensor (Ta) and probe housing surface temperature sensor (Tp) are closely digitized of the sensors. A signals comparizon for each measurement cycle (320ms) is operated with a high stability resistor. The humidity sensor is operated at a frequency of 100 kHz and the atmospheric pressure sensor signal within 0 mV to 100 mV range.

* The whole measurement system ensures a 7 µV resolution with a stability higher than 10 ppm per degree within the -40°C to +40°C range
* P, Ta and R.H. Sampling rate : 3 Hz

* Tp and battery check sampling rate: 1 Hz
* all measurements are stored in a memory of 3x128 kB at 3 Hz.

3. RESPONSE TIME

The wind tunnel has been used to study the response of the SSBC probe with a stepped temperature variation of 1°C to 2°C and/or with relative humidity variation of 10% to 50%.

According to these previous tests in an air flow of 40 $m.s^{-1}$, the response time of the temperature sensor, at 90% of the scale, is around 0.4 seconds. Humidity response time at 63% of the scale is around 0.8 seconds.

4. PROBE FIXATION ON THE AIRCRAFT

The probe location and fixation on the aircraft is a tricky problem to solve, taking into account both antagonists requierments:

- a location where the aerodynamism behaviour do not alterate sufficiently any parameter under consideration.
- a location where it is easy to fix the probe, taking into account the aircraft type, its fuselage structure and the request of obtaining the official federal aviation clearances.

5. SSBC OPERATING PROCEDURE

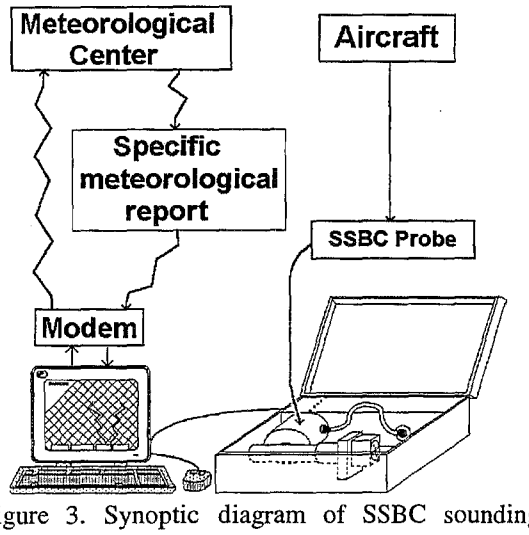

Figure 3. Synoptic diagram of SSBC sounding ground operations.

In order to ensure the measurements quality, sensors are automatically tested before running SSBC sounding. These quality controls are made, using a calibration unit,(see figure 3) which also can operate the data transfer from the probe to the PC.

Temperature, humidity and pressure measurements are controlled and compared with the internal SSBC calibration référence unit. The pressure value is adjusted before each flight thanks to the QNH provided by the meteorological station which is in charge of reporting. Quality controls are made for each use of the probe. The sounding can be accepted, corrected or rejected according to the tolerance range on temperature and humidity measurements. That measurement quality is garanted through that way.

Pre-flight and post-flight checking durations are 8 minutes and 5 minutes, respectively. Data are processed after post-flight checking. Thermo-dynamical diagram (see figure 4), TEMP A, TEMP B and TEMP SHIP (if any), respectively, are transmitted through the modem to meteorological station.

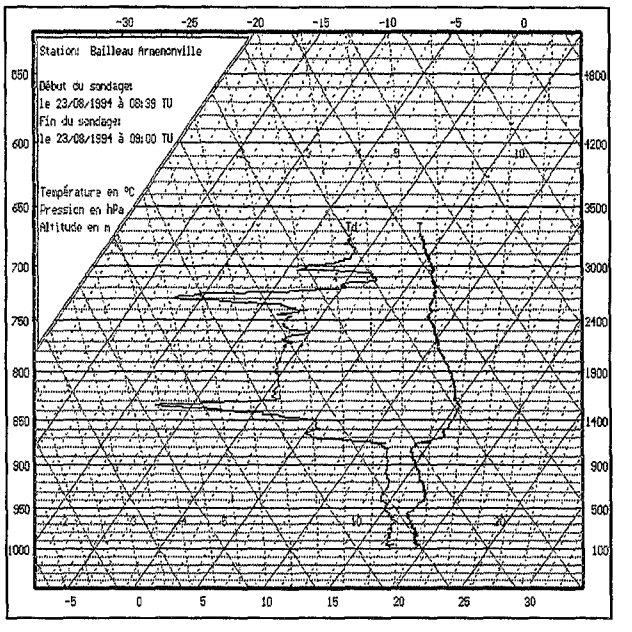

Figure 4. SSBC sounding standard plot of the thermodynamic diagram.

5.1 SSBC SYSTEM CARACTERISTICS

SSBC caracteristics and performances	
Temperature measurement	
Sensor	50 ohms nickel resistor
Accuracy	0,2°C from -40°C to 40°C
Resolution	0,05°C
Response time	0,2s at 40m/s (63% scale)
Relative humidity measurement	
Sensor	capacitive sensor
Accuracy	3% from 10 to 95%
Resolution	0,2%
Response time	0,8s at 40m/s (63% scale)
Pressure measurement	
Sensor	Piezo resistive silicon sensor
Accuracy	0,5 hPa from 1100 to 500 hPa
Resolution	0,1 hPa
Horizontal speed	30 to 220 km/h
Vertical speed	0 to 5 m/s
Incloud measurement	10 sec max
Autonomy	2h15
Weight	1,2 Kg
Batteries refilling	1 h

Table 1

6 COMPARISON BETWEN RADIOSONDE (R.S.) AND SSBC MEASUREMENTS

To evaluate the SSBC probe capability for atmospher study, a comparison betwen both probes has been operated with the RS 80 (Vaissala radiosonde). The area of study chosen was located over the CEL (Centre d'Essai des Landes) and the probe was operated at a distance of 10 ft from the helicopter canopy (Aerospatial Ecureuil type).

During the radiosonde launching, the helicopter was beginning its climb at an horizontal distance of 0.5 NM for safety. During the first flight segment, the helicopter's route was crossing the ballon's one till an elevation of 1500 ft. Then, the helicopter was following the balloon when flying with a serie of climbing spirals, the ground speed being maintened at 50 kt. The exact location in altitude was permanentely provided by CEL's radars with an accuracy of 15 ft.

Eight sounding tests having been proceeded throught that procedure. The results obtained show the accordance between both systems correctly correlated as predicted by manufacturers specifications (see figure 4 for measurements examples).

Figure. 4. Intercomparison RS/SSBC (3.19.1996).

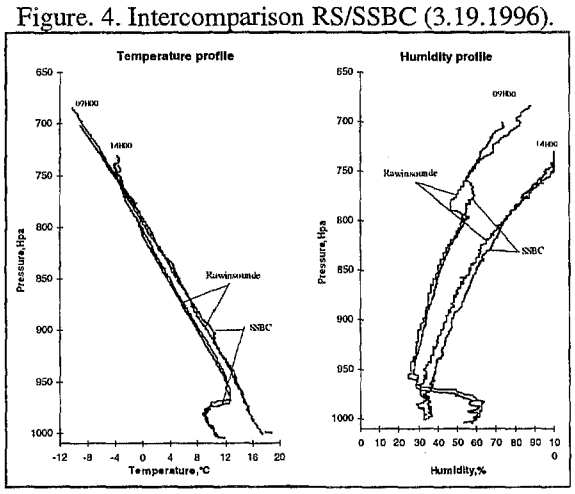

The standard deviation on temperature sounding between R.S and SSBC probe , at various altitude levels, show their good accordance (see table 2). Near the surface, which pressure was 1000 hPa, the observed difference is due to the distance of half mile between the area for the SSBC probe and the launching pad for the R.S. . and to an altitude which atmosphere pressure is 750 hPa, where the helicoptere have to maintain the flight in V.H.C. The temperature difference, ussually negative for any given altitude, can be misestimated because of the air disturbances due the helicopter's rotating blades wakes . Altitude provided by CEL radars confirme the bias previouly mentioned and it has been that during a smooth climb, the bias under cosideration does not vary very much (30 to 100 ft), , but can reach 600 to 1000 ft if the amplitude of the helicopter's route changes vary strongly.

Table 2. Difference of temperature beetween SSBC and the rawinsound (average on 8 flights)

pressure level hPa	1000	950	900	850	800	750
Δ(SSBC- RS) °C	-0.65	-0.05	-0.05	-0.16	-0.16	-0.39

To compensate that bias, the coupling between SSBC probe and differential GPS-3D has been studies. The altitude is directly provided by GPS with the new version of the sounding system, the temperature and humidity probe being inchanged. Excepted of being based on board an helicopter as part of the probe without any consequence on measurement probing, that new SSBC/GPS offer the choice of the place for the fixing on an aircraft, independantly of atmospheric pressure variation. .

5. CONCLUSION

The last four years of SSBC running have show the probe friendlyship for users as well as its reliability The comparison wiyh RS have also shown the measurements quality, at least equal to RS'ones.

Since 1995 an operational network of 7 SSBC lounch sites is conducted by their users during summertime. During the period 1994 - 1997, more than 4000 soundings have been operated.

The capability of using probe on board an helicopter have created a new categoriy of applications for SSBC system; particularly for low scale meteorological studies in low troposphere and for environnemental applications.

ACKNOWLEDGEMENTS

This work was sponsored partly by the Fédération Française de Vol à Voile (FFVV), the Fédération Française de Vol Libre (FFVL), the Service de la Formation Aéronautique et du Contrôle Technique (SFACT).

REFERENCES

Abadie.G, C.Berne, G.Cocher, 1991: Use of relative humidity sensors for plane measurement. *Proceedings Seventh symp. on Meteorological Observations and Instrumentation. Amer. Meteor. Soc.* New Orleans, LA. pp 247-249.

Norris D.K. and V.E. Lally 1991: An integrated circuit piezoresistive pressure sensor. *Proceedings Seventh Symp. on Meteorological Observations and Instrumentation. Amer. Meteor. Soc.* New Orleans, LA. pp 291-296.

The Impact of Year 2000 Problems on observing systems operated in the UK

J. Nash, S. Stringer and D. Brogden
The Met. Office, Bracknell, UK

1. Introduction

The UK Met. Office established a Year 2000 project in 1996 with the initial purpose of identifying the problems that might prevent the Met. Office functioning as a business and providing services to its customers in 1999 and the following years. These problems were expected to arise as a result of the representation of the year number in many computer systems and microprocessors by only the last two digits. Even if the year number is not a problem to the system, the attribution of leap year days in the following years may be corrupted. In some cases, software will interpret the transition from 99 to 00 as a backward step in time, and this may lead to a system failure. Date transitions which may cause problems with some hardware and software in use by meteorologists are:-

- 31 December 1998 to 01 January 1999
- 31 December 1999 to 01 January 2000
- 28 February 2000 to 29 February 2000
- 31 December 2000 to 01 January 2001

It needs to be recognised that the problem may occur in embedded control processors in systems where the date does not appear critical to the system function on a daily basis.

Unfortunately, the problem is not just limited to equipment under the meteorologists control. For instance, it is necessary to establish whether external suppliers of services (e.g. power supplies and communication services) to the meteorological organisation have also made the necessary checks to ensure continuous provision of their services as the transition occurs.

2. Current status of the UK project

The UK project has progressed from the initial phase through a second phase where 6 pilot projects on specific systems have been performed. On the basis of the experience gained with the pilot projects fifteen members of staff have been assigned to a central project team. This will manage and co-ordinate around 70 specialised projects charged with assuring year 2000 compliance for all the systems critical to the functioning of the meteorological service. The staff resources assigned to year 2000 issues during the remainder of the year correspond to about 5 per cent of the total work force. Central co-ordination is essential to ensure that all the critical links between services are considered. For instance, communication links for the data from an observing site onto the GTS and into the various numerical forecast data bases and local forecast display systems need to be examined, as well as the actual observing systems and the central computers.

The Observation division work has been subdivided into 6 projects. A full time project manager has been appointed by the branch responsible for operational logistics and the development of surface instrumentation. Part time project managers (committed for at least 30 per cent of available time in the next year) will be used in remote sensing, weather radar, upper air, data archiving, and data sales sections. The urgent tasks to be completed at this time are the complete inventory of hardware and software in use by critical observing systems operations. This inventory will be used to derive a list of all hardware and software that needs to be certified for Year 2000 compliance by Observation division staff. In addition, a list of the links of the observing systems to services supplied by other sections of the Met. Office will be used to check that no vital links between sections are missed. Thirdly, a list of the situations where compliance will be dependent on the supply of hardware and software from manufacturers (or other third parties) outside the direct control of the Year 2000 project will also be generated. The project managers will then agree time tables for the rectification of the Year 2000

problems with the engineers responsible for the individual observing systems. Ideally, this work should be completed by the end of 1998. However, in some cases where Year 2000 compliance will have to be obtained by replacing current hardware and software with upgraded systems, slightly longer lead times may have to be tolerated.

It will also be essential to set up improved methods of managing software so that Year 2000 compliance can be sustained, and the responsibility for the support of various software packages traced in future. The proliferation of operating systems and software used by different scientists or engineers for developments in the UK Observation division over the last twenty years will need to be rationalised to limit the requirements and costs of specialised software support in future.

3. Progress during the last year

The design of this final phase of the project was based on findings from the two earlier phases of the Year 2000 studies in the UK. As the resources required to carefully check all the existing software and all the systems in the Met. Office were very large, it was not practical to check all existing software in the time left. Thus, the systems and software packages that are essential were identified, so resources could be directed to these critical areas. Although much of the major critical system hardware was readily identified, some of the critical links between these systems had not been thoroughly considered in early stages. Similarly, significant effort was required to identify the critical software packages in use. Most of the observing systems managed by the observation division appeared on the critical list. Supply of observations from other Members of WMO via the GTS was also identified as essential for Met. Office functions.

Policy decisions were made about the PC operating systems and software that would be adopted office wide in order to ensure compliance through the Year 2000. The range of systems was to be minimised to reduce central support costs in future. In practice, it was decided that all critical systems using PC systems should use Windows NT operating systems. This has consequences for the upper air observing systems and some automated surface observing systems used by the UK, as will be discussed below. Standardised time and date algorithms were established for future use in all the divisions of the Met. Office.

In all recent equipment procurements, compatibility with the transition through the year 2000 was deemed essential. This is not completely effective since compliant systems and software may not yet be available, and upgrade of some systems purchased this year will be necessary within less than a year.

4. Issues affecting observing systems

4.1 Compatibility of individual observing systems with the year 2000 transition

A detailed review of the year 2000 status of the existing UK observing systems was begun in early 1997. Around 60 different observing system types were identified as potentially vulnerable to malfunction during the year 2000 transition. The observation support staff responsible for the systems were then asked to identify the systems that were required to function after 2000. This reduced the number of systems to be considered to about 40 different types. Of these 40, 30 systems were considered to be critical to Met. Office business. At this time, only 6 of the critical systems can be safely certified as compliant with the year 2000 transition. The central Year 2000 project has now requested more detailed information on the computer systems used with the equipment and detailed plans of the methods to be used to ensure year 2000 compliance. This will vary from system to system as can be seen from the following initial experience with pilot investigations.

4.2 Results of early pilot investigations

4.2.1 SAMOS

At the request of the central Year 2000 project, the main pilot project to establish year 2000 compliance for an observing system was performed on SAMOS. This is a PC based semiautomatic observing system. SAMOS functions as an automatic weather station at many sites where observing staff are only present for part of the day, and allows the observers to add more detail to the observation reports when they are on duty. There are more than 100 SAMOS systems within the surface observing network. The software is managed entirely by Observation division staff, and is not supported by an external manufacturer.

The SAMOS pilot project started in October 1997 and has been pursued in collaboration with an external consultant who advised on the methodology used. The project is expected to be completed by March 1998. It appears that the Year 2000 project management expected the testing and certification to be achieved more quickly than this, but the configuration of SAMOS software varies a great deal according to the different locations. This means that many more different configurations had to be tested than had been anticipated by the central project. Although many of the pilot projects in other areas of the Met. Office have used a specialised software package to check code for year 2000 problems, this was not used with SAMOS. Instead the areas of code that had date or time references were identified from existing software documentation and then checked in detail manually. Eventually, about 10 areas of the code were identified where there was a risk of problems in future because of timing issues. The software problems have now been rectified. The SAMOS manager feels that the software checks performed for the year 2000 project have been beneficial to the system and that the resulting software suite is much more suitable for future operations.

4.2.2 Radiosonde systems

In the case of its radiosonde systems, the Met. Office does not support its own software but relies on external manufacturers, mainly Vaisala Oy and VIZ INC. Discussions on Year 2000 compliance were started with the manufacturers in mid-1997. Vaisala assured the Met. Office that DigiCora / Marwin software compliant for the year 2000 will be issued by mid-1998. Arrangements for the software installation would have to arranged with Vaisala by individual customers. Recently purchased systems should be compliant, although the Metgraph facilities used with the MW15 GPS ground system purchased by the UK will need porting onto Windows NT machines.

Compliant software for PC-CORA systems , the system most widely used at stations in the British Isles, would also be issued by mid-1998. However, this assurance did not take into account compliance problems with the Windows 3.1 operating system used to host the SPU11 card in the Dell PCs used for PC-CORA in the UK. Subsequently, Vaisala have informed the Met. Office that the current PC-CORA hardware is not compatible with an upgrade to the Windows NT operating system, required by Met. Office compliance policy. Thus, it has been decided to bring forward the planned replacement of the PC-CORA systems by about 1 year. The Met. Office will go out to competitive tender for new upper air ground systems to be delivered in mid-1999, that will be compliant for the Year 2000 problem. These systems will have to be compatible with the Met. Office Information Technology policy for the future.

VIZ have assured the Met. Office that their ground systems are year 2000 compliant. This has not yet been thoroughly tested by Met. Office staff. VIZ ground systems have posed problems to the Met. Office in the last two years, since operational software problems in the ground system have not been resolved by the manufacturer in a timely fashion. In future, the current operating system used by VIZ would necessitate retention of specialised machines for internal software support, increasing the cost of this software support. Some standardisation in the operating systems used for PC -based upper air ground systems is desirable and would facilitate the operation of a dual supplier policy for national networks.

4.2.3 Long standing Automatic weather systems

The Met. Office has had a substantial network of automatic weather stations in operation for more than 10 years. These systems are still functioning reliably and there is no desire to replace them at this time. The software is not readily accessible, since it is housed in microprocessors that are not readily reprogrammed at this time. It is impractical to scan the code, although it is thought that year date was not included in the software.. In this case, examples of the systems have been tested through the various time transitions and have not experienced any disruption. This will probably be taken as adequate certification for these specific systems, although agreement of validation standards across all the different sections of the observation division has yet to be finalised.

5 Interaction with other operational services

The other operational meteorological services that are critical to the successful delivery of the observations to the users are communications and the central data bases where the observations are stored for access by the users. With some observing systems, the observation division is responsible for communication and archiving, but in most cases the responsibility lies within other areas of the Met. Office. The year 2000 issue has heightened awareness of this dependency and has also raised questions about how the interdependence is currently managed.

6. Dependence on observations from external sources

The UK Met. Office will be unable to meet its full business responsibilities in the year 2000 without the use of observations from all parts of the Global Observing system. Thus, the UK Project 2000 has attempted to improve the awareness of the international meteorological community to the year 2000 problem and associated problems in collaboration with WMO. WMO has a Year 2000 Information Web Page **(http://www.wmo.ch/web/www/y2k-info.html)** and WMO (D. McGuirk, WWW Department attended a recent WMO workshop) can also make available simple test programs to check PC compliance and provide additional information.

7. Future actions

We would encourage WMO members to:-

- Request the manufacturers of any observing systems containing modern control processors for information on the status of compliance with the year 2000 problem.
- Establish methods of checking observing systems where the observing system software has been generated by the national meteorological service or associated contractors.
- Establish a method of checking that new equipment and software are compliant and remain compliant in future.
- Circulate information on experience gained to other members, so that unnecessary duplication of detailed investigation is avoided.

IMPROVEMENTS IN RADIOSONDE HUMIDITY PROFILES USING RS80/RS90 RADIOSONDES OF VAISALA

U. Leiterer, H. Dier and T. Naebert
Deutscher Wetterdienst, Meteorologisches Observatorium, 15864 Lindenberg, Germany

1 Introduction

Accurate measurements of relative humidity in the free atmosphere are still lacking, especially for temperatures below -30°C. Fundamental atmospheric research and operational weather forecasting need high vertical resolution in relative humidity profiles provided by radiosondes in the troposphere. This requires small systematic errors in the radiosonde data. For instances, numerical analysis for regional and mesoscale weather prediction can not tolerate the large systematic underestimates of relative humidity also in cloud (Nash, 1995)! Thus, too low humidities used to assimilate into the models. Unpredicted high clouds are the result. The forecast can not be better then the basic data.
Over the past few years several authors have mentioned that there are deficiencies in radiosonde humidity observation. Recently the problems of different radiosonde humidity sensors have been discussed by Nash et al. (1995) and Sonntag (1994). These authors compare sensors like Humicap, carbon and LiCl-hygristor, goldbeaters skin, rolled hair sensor.
The last state of knowledge on the performance of humidity measurements from radiosondes has been investigated during the "WMO Radiosonde Humidity Sensor Intercomparison (Phase I Laboratory Test) 1995-1997", reported by Balagurov (1997) and in the "Summary of the WMO International Radiosonde Relative Humidity Sensor Comparison - September 1995" reported by Schmidlin (1998).

2 The New Measuring Philosophy

Technological progress in the development of new polymer materials opens new variants for precise humidity measurements. The general measuring technique is based on the capacity dependence of a thin polymer layer in relation to the quantity of water vapor molecules which are oozed into the polymer molecule structure. The capacity will be transformed into frequencies by a resonant circuit of the radiosonde transmitter.
The relative humidity in the range of 0 ... 100 % will be represented by about 200 Hz frequency difference which may be measured with 0.1 Hz resolution. In result one gets a dynamic range of 2000 units for the relative humidity U_w [%] $= e/e_w \cdot 100$. Because of this range the theoretical sensitivity will be about $\pm$ 0.05 % for a large temperature range. Especially for low temperatures up to -70°C one is able to measure relative humidities with respect to water with a better absolute accuracy than it is possible up to now as will be shown in section 4.
This report will give some new results and aspects of developments and new possibilities of relative humidity soundings with radiosondes, using a precise groundcheck and simple mathematical calibration relations between the raw data frequencies available by the new H-Humicap sensor of Vaisala. The results of the Vaisala investigators are also reported in publications of Antikainen and Paukkunen (1994) and Paukkunen (1995).
Besides the classical "thermodynamical" method of humidity calibration, e.g. as used by Vaisala or special humidity calibration laboratories as reported by Balagurov et al. (1997), the Lindenberg Observatory has begun to do research work to introduce the so-called standardized frequencies

$$F_n = \frac{F\,(0\ \%) - F\,(U\ \%)}{F\,(0\ \%) - F\,(100\ \%)} = \frac{F_H - F\,(U\ \%)}{F_H - F\,(100\ \%)} \qquad (1)$$

F (0 %)	:	dry frequency (no water molecules inside the polymere structure), produced inside the "Lindenberg container with use of molecular sieve MERCK"
F (100 %)	:	frequency of saturation water vapor partial pressure produced inside the "Lindenberg container with use of aqua dist. slowly cooling down"
F (U %)	:	measuring frequency
F_H	:	frequency if the H-Humicap is heated (in order of 70 ... 115 ... 180 mW)

The first result of the Lindenberg laboratory investigations is that the heated frequencies F_H are equal to the dry frequencies F (0 %) if the polymer works under optimized heating conditions.
The second important finding is that the difference F_H - F (100 %) is nearly unchanging over the temperature range (e.g. +40°C to -70°C).

The measuring frequencies F (U %) can converge to the both following extremes

$$F\,(U\ \%) \dashrightarrow F\,(0\ \%) \cong F_H$$

or

$$F\,(U\ \%) \dashrightarrow F\,(100\ \%).$$

The quotient of the differences (F_H - F(U %)) and (F_H - F(100 %)), see eq. (1), follows precisely the partial pressure relation e/e_w (our assumed hypothesis), which means the relative humidity, U_w [%], measured directly this way

$$\text{with} \quad U_w\,[\%] = \frac{e}{e_w} \cdot 100\,[\%] = F_n \cdot 100\,[\%] \qquad (2)$$

Relative small temperature corrections are derived from laboratory calibration. Deviations from this conformity with a natural law are caused by construction features of the H-Humicap chip and the used RS90 electronic. By using two reference capacitors and a stabilized power supply (e.g. 18 V) it is possible to eliminate these deviations. The physico-chemical background of solid-state moisture sensors has not been widely discussed in the literature. Only Denton et al. (1985) gave a plausible interpretation of the microphysics.

The supposition of our measuring philosophy is:

- The dielectric properties of the water molecules within the polymer material are close to these of free liquid water (Denton et al., 1985).
- The polymer material in the H-humicap (as a hydroactive sponge) responds to the relative humidity with respect to water in a wide temperature range between +40°C up to -70°C.

The water vapor molecules within the cavities of the polymer film are in thermodynamic equilibrium with the water molecules adsorbed in a hydroactive surface on the walls of the cavities.

Only the mechanism of a weak physical adsorption (described as Van-der-Waals-Interaction) is probably dominant in the interactions between the free water molecules, which do not lose their identity, and the "solid" polymer molecules (Atkins, 1987).

More details on fundamental calibration procedures to derive the "Calibration Matrix of standardized RS90 frequencies" are reported in Leiterer et al (1997).

3 The Calibration Matrix of Standardized RS90 Frequencies

Figure 1 demonstrates the main features of our hypothesis for H-Humicap (RS90) humidity calibration. In figure 1 the results from groundcheck experiments and test soundings are composed. They are confirmed by simulation chamber experiments in Lindenberg, Moscow and Jülich. The results of the chamber intercomparisons will be published in an extra paper.

Relative humidity (ordinate), temperature (abscissa) and the standardized frequency F_n (as parameter) show the general working principle of the new polymer together with our new raw data evaluation method.

During the radiosonde flight one measures with two (alternatingly heated) sensors the heated frequencies F_H (40 s heating) and the measuring frequencies F(U%) (100 s measuring). The frequency F (100 %) saturated with respect to water is a stable value derived from the ground check.

With a sequence of 1 s one gets the frequencies F_H and F(U%). Using the relations (1) and (2) for the standardized frequency F_n and a given temperature (measured by the thermocap sensor of the RS90) one directly gets the relative humidity U_w[%] with respect to water controlled by the heated frequency $F_H = F(0\%)$.

The standardized frequencies F_n have the temperature dependence illustrated in figure 1. $F_n \equiv 1$ is not possible for negative temperatures. The lower the temperature, the earlier the point of ice saturation begins; e.g. the relative humidity $U_w = 70$ % for -36°C corresponds to a relative humidity of $U_i = 100$ %. The area above the dotted line is the region of supersaturation with respect to ice which is an often-observed feature in high clouds (cirrus).

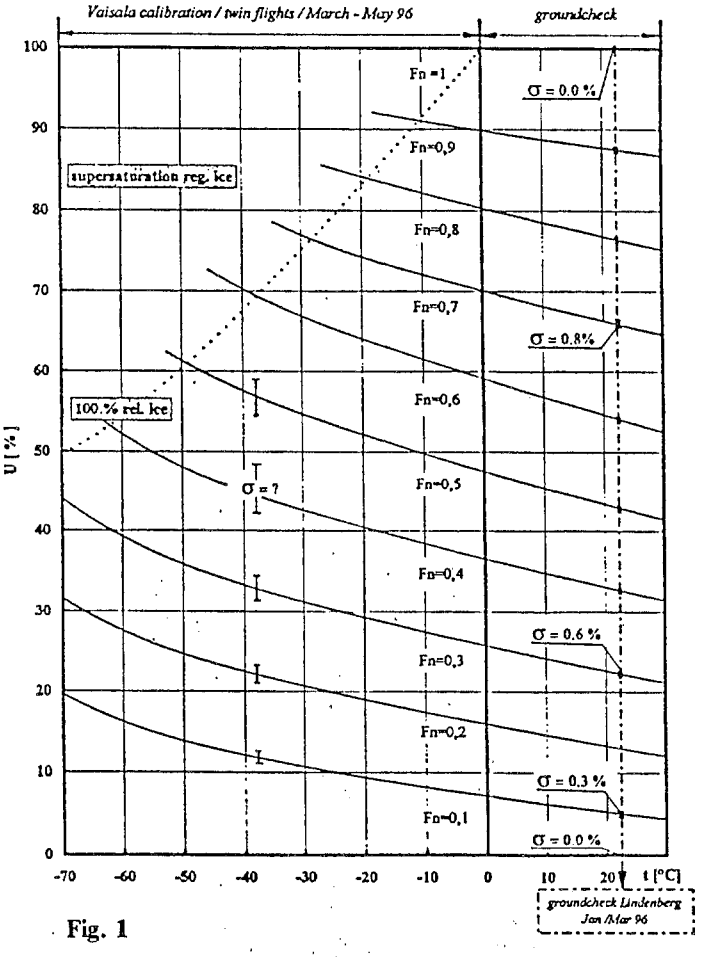

Fig. 1

4 Examples of RS80/RS90 Soundings

Using the raw data processing algorithm developed in Lindenberg for a research version of the RS90 sonde the results of tandem soundings with the conventional RS80 sonde are shown in figure 2 to 5. Due to this observation gaps emerge above 400 hPa reaching observation distances of ca. 300 m at 14 km (150 hPa) height. The normal measuring sequence is about 1 value per second, the observation distance 5 m. For better demonstration we summarized the measured data in figure 2 to 5. For the RS90 one depicted value corresponds to 3 s of measuring ($\approx$ 15 m vertical resolution), for the RS80 one depicted value corresponds to 10 s of measuring ($\approx$ 50 m vertical resolution). We can make no final statement about the absolute accuracy of the relative humidities in the temperature range demonstrated in figure 2 to 5 because so far we have used a preliminary calibration matrix of our standardized frequencies F_n (see figure 1), with the error bars depicted in figure 1. After the final evaluation of Jülich, Moscow and Lindenberg chamber experiments we expect the error bars for -70°C to be as small as the error bars for groundcheck conditions near 20°C.

Nevertheless the RS90 humidity profiles based on our preliminary standardized frequencies look plausible also for very low temperatures. A noteworthy result is that the RS90 sensor is still sensitive above the tropopause and measures realistic relative humidities in the range 1...2 %. Generally, the high measuring sensitivity is obvious. This feature allows to detect water vapor layers with small vertical extension also above the tropopause.

Figure 2 shows the comparison RS80/RS90 for the **cloudless case**. The relative humidity profiles of the RS90 and RS80 agree well in the lower and middle region of the troposhere. However, for temperatures lower than -30°C RS80 measures incorrect data, that means the RS80 sensor (A-Humicap) becomes insensitive. At first the values measured by RS80 are remarkably too low (12-18 % at 300 ... 250 hPa or -50 ... -60°C).

Figure 3 is an example for the **cloudy case** with one stratiform cloud layer near 520 hPa (Ac str tr) which has also been checked by observers and synchronous ceilometer measurements. Both radiosondes measure the profiles typical for each of the sensors (A-Humicap (RS80) and H-Humicap (RS90)). It is evident that the RS90 follows the vertically strongly structured humidity field better than the RS80. At temperatures lower than -30°C the RS80 becomes unsensitive, the typical behavior of the A-Humicap. The RS90 profile shows two layers with supersaturation with respect to ice (near 470 and 410 hPa) above the Ac-layer, probably thin cloud layers, which were detected by the ceilometer half an hour before the radiosonde ascent.

Figure 4 is an example of the **cloudy** and **icing case**. The icing only refers to the A-Humicap of the RS80 sonde which is usually used in observation routine. According to our experience cloudy weather causes in approx. 10 % of the cases icing of the A-Humicap. The problem of this error is the inability to recognize this icing case without much experience. Very often an unsystematic falsification of the vertical profiles occurs; the icing can start in all heights, that means even near ground level. This unsystematic error (contrary to the systematic errors by lag and temperature effects) makes it more difficult to detect the systematic deviations between the old (e.g. RS80) and new (e.g. RS90) sondes, and also the adaption of time series dated back - a very important demand for trend investigations in the frame of climate research. The RS90 sonde, fitted out with the H-Humicap pair, alternatingly heated with only 75 mW, measures the humidity profile with a good quality from ground level to 100 hPa (16 km). Above approx. 500 hPa (-23°C) ice clouds occur in this case; a relative humidity (with respect to water) of 86 % corresponds to a relative humidity of approx. 106 % (with respect to ice), a plausible value of the relative humidity in ice clouds (cirrus).

Fig. 5 shows again the typical behavior of the RS80 sensor in comparison to the RS90 sensor. Near the tropopause the RS80 A-Humicap measures 12 % too low humidities with respect to the "correct" values of the RS90. As usual the RS80 measured too high values in the stratosphere. More interesting is the comparison of the **supersaturated** (with resp. to ice) **layers** at 440, 400 and 250 hPa with the **backscattering** profile (λ = 532 nm) of the LIDAR, Ansmann 1997, and the cloud measurements by the ceilometer (controlled by observers of the synoptic station).

Thin interrupted clouds (Ci fib) are only measured by the ceilometer in the layer near 440 hPa, also sharply marked by the LIDAR. In the next higher layer with supersatured air there are no clouds and no backscattering signal. This layer seems to be without particles. This example shows that in supersaturated layers aerosols or clouds do not follow inevitably.

In the supersaturated layer near 250 hPa below the tropopause the LIDAR detected a backscattering signal, but the ceilometer measured no clouds in this moment. Probably there are a aerosol layers with particles in the presublimation phase, soon converting into clouds as shown by the ceilometer one hour later.

References

Paukkunen, A.; 1995: Sensor heating to enhance reliability of radiosonde humidity measurement. Preprints 9TH SYMP ON MET OBSERV & INSTR of AMS; Charlotte, NC; March 27-31, 65-70.

Leiterer, U.; Dier, H. and Naebert, T.; 1997: Improvements in Radiosonde Humidity Profiles Using RS80/RS90 Radiosondes of Vaisala. Beitr. Phys. Atmosph., November 1997, 319-336.

Nash, J., Elms, J.B. and Oakley, T.J.; 1995: Relative Humidity Sensor Performance Observed In Recent International Radiosonde Comparisons. Preprints 9 TH SYMP ON MET OBSERV & INSTR of AMS; Charlotte, NC; March 27-31, 1995, 43-48.

Sonntag, D.; 1994: Advancements in the field of hygrometry, Meteorol. Zeitschrift, N.F. 3, 51 - 66.

Schmidlin, F.; 1998: Summary of the WMO International Radiosonde Relative Humidity Sensor Comparison - September 1995. Paper in this issue of WMO/TD - TECO 98 -.

Antikainen, V. and Paukkunen, A.; 1994: Studies on improving humidity measurements in radiosondes. WMO/TD-No. 588, Report No. 57, 137-141.

Atkins, P.W.; 1987: Physikalische Chemie, Übers. u. erg. von A. Höpfner, 1 Auflage, VCH Verlagsgesellschaft mbH 6940 Weinheim (BRD).

Denton, D.D., Camou, J.B. and S.D. Senturia; 1985: Effects on moisture uptake on the dielectric permittivity of polyimide films. Int. Symp. on Moisture and Humidity: Research Triangle Park. N. C., Instrument Soc. Amer., 505-513.

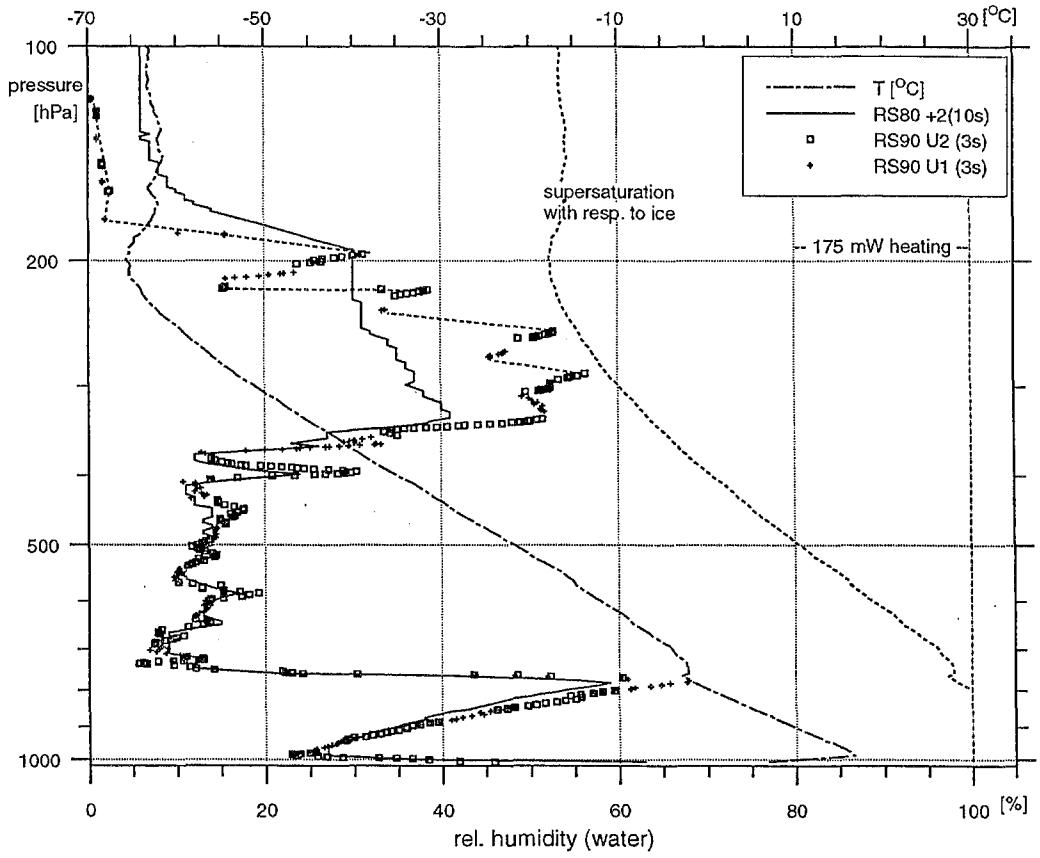

Figure 2: The cloudless case of RS80/RS90 relative humidity comparision. Lindenberg 19.04.96 07 UTC

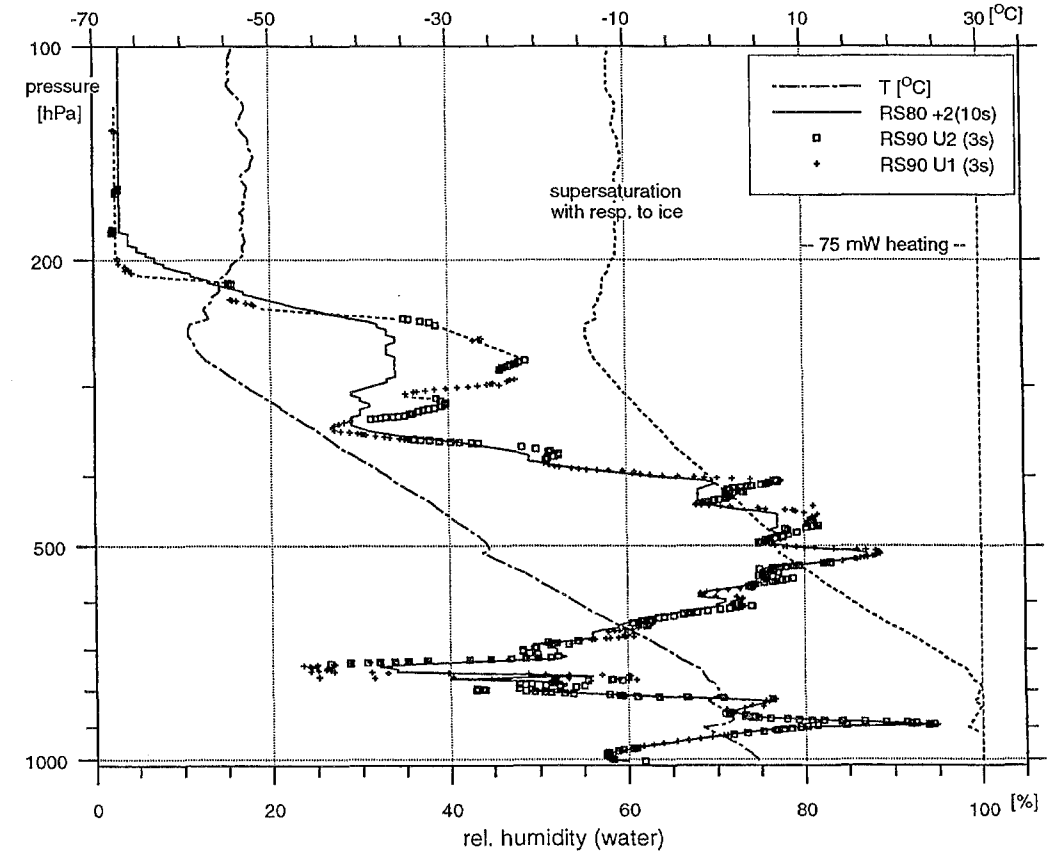

Figure 3: The cloudy case of RS80/RS90 relative humidity comparision. Lindenberg 18.03.96 18 UTC

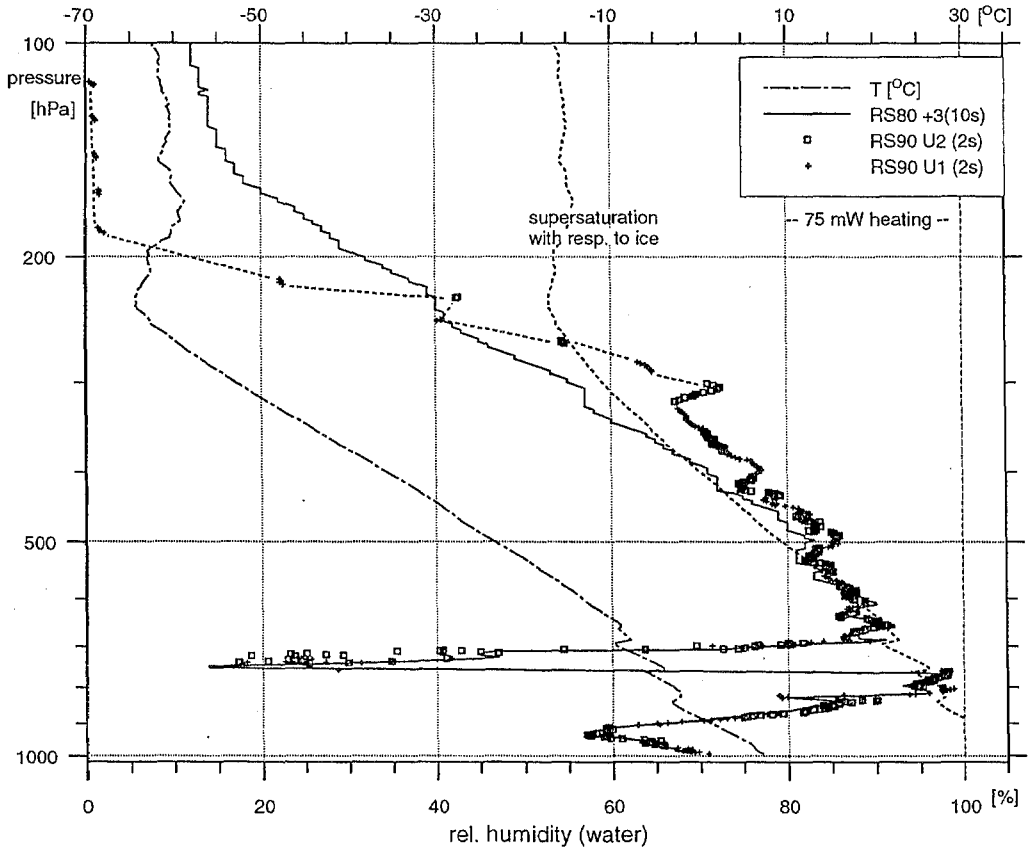

Figure 4: The icing case of RS80 relative humidity and no icing of RS90. Lindenberg 26.03.96 18 UTC

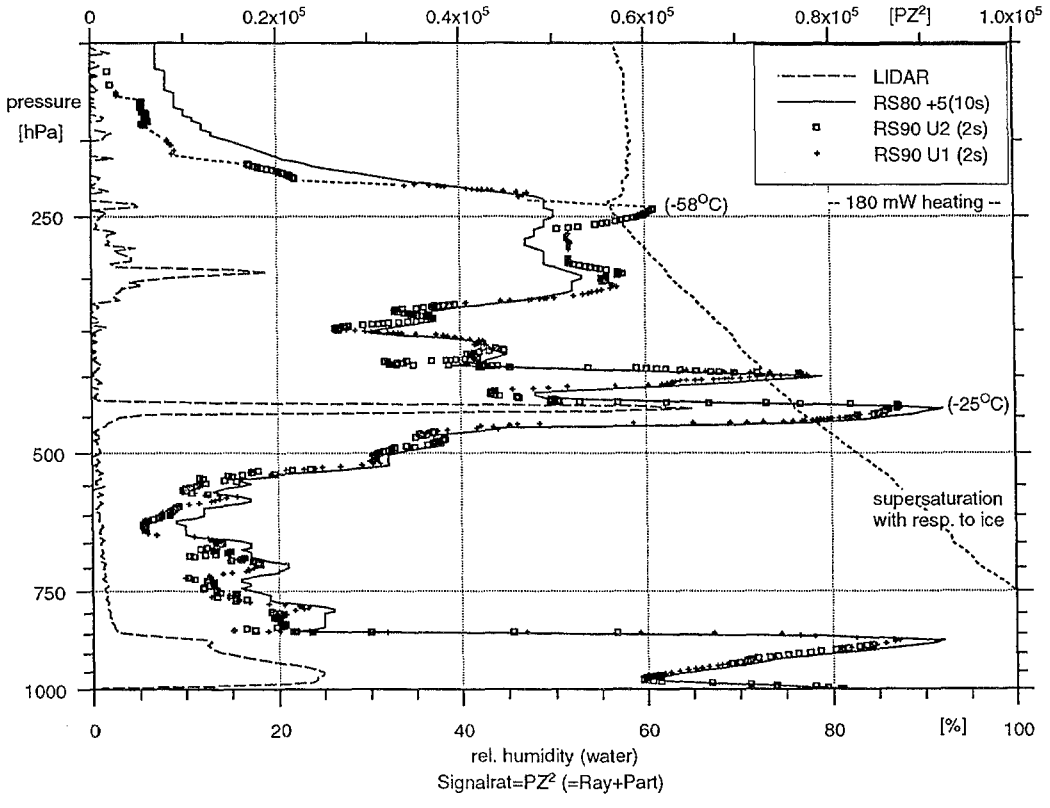

Figure 5: The comparision of RS80/RS90 relative humidity profile with the backscattering profile of the Ramann-LIDAR (IFT Leipzig). Lindenberg 20.09.96 (22:45-23:30 UTC)

The new generation of upper-air observation equipment

Vjacheslav Ivanov, Ph.D. & Vadim Kikin, Ph.D. (Ural State Technical University)
Yuri Losev (METEO Joint Stock Company)
Ekatarinburg, Russian Federation

Abstract

This report describes the new generation of upper air observation equipment that consists of the Breeze compact tracking radar system and associated radiosonde.

Compact upper-air radiosonde tracking radar integrates the beam switching antenna array, low noise receiver, pulse transmitter and digital systems for tracking, control and measurement. The beam switching antenna array and the switching phase shifter make up a precision system that measures the radiosonde tracking antenna elevation and azimuth angles. Application of the state-of-the-art electronic parts provides a means to attain the high receiver sensitivity better then 134 dBW.

The utilization of the tracked sonde active reply concept allows to cut the average transmitted power down to 0.1 W and to measure the slant range up to 200 km with high accuracy and low energy consumption. The mode of a radio theodolite sonde tracking is also available. Total power consumption is less then 300 W and total weight is no more than 120 kg.

Novel upper air sondes are equipped with the conventional transceivers for the slant range measurement and with pressure sensors for barometric altitude determination. Besides this, sondes incorporate thermistor and capacitor humidity sensors both complying with the WMO accuracy requirements.

The compatibility of the new equipment with the commercially available radiosondes and its low maintenance costs in conjunction with the high-end specification make it feasible for incorporating into meteorological observation networks.

1. Аэрологическая радиолокационная станция "БРИЗ"

Аэрологическая радиолокационная станция (АРС) "Бриз" предназначена для приема метео информации от радиозонда, запускаемого в атмосферу, и определения его координат: наклонной дальности, азимута, угла места.
АРС "Бриз" обеспечивает зондирование атмосферы как с помощью серийных радиозондов МРЗ (МАРЗ), так и специальных радиозондов, оснащенных датчиками атмосферного давления. При этом АРС обеспечивает возможность определения вертикальных профилей метео величин в следующих режимах:

- радиолокационном (измеряются наклонная дальность до радиозонда, азимут и угол места);
- радиотеодолитном (измеряются атмосферное давление, азимут и угол места радиозонда);
- радиолокационно-теодолитном (измеряются наклонная дальность до радиозонда, азимут и атмосферное давление).

Радио теодолитный и радиолокационно-теодолитный режимы работы могут использоваться как для специального зондирования атмосферы, так и для

повышения точности сетевого зондирования в экстремальных метеоусловиях.
В состав АРС "Бриз" входят:

- антенно-фидерная система;
- приемо-передающая система;
- система управления антенной;
- система обработки и управления;
- ПЭВМ.

При разработке АРС "Бриз" использованы последние мировые достижения в области радиотехники и электроники – фазированная антенная решетка, современные микроэлектронные компоненты, цифровые методы обработки данных и управления.
АРС "Бриз" имеет следующие основные технические характеристики:

- рабочая частота 1680 (1780) MHz;
- дальность сопровождения радиозонда, не менее 200 км;
- излучаемая мощность радиопередатчика, не более 0,1 W;
- мощность, потребляемая от источника питания, не более 200 W;
- масса комплекта станции 120 кг.

2. Новые аэрологические радиозонды для специального и сетевого зондирования атмосферы

В состав комплекта аэрологических радиозондов входят:

- первичные измерительные преобразователи (датчики) метео величин;
- радиоблоки, включающие в себя формирователь телеметрического сигнала и приемопередатчик;
- водоактивируемая батарея питания;
- теплозащитный корпус с элементами крепления.

В качестве первичного измерительного преобразователя температуры в радиозондах могут использоваться как серийный датчик радиозондов типа МРЗ (МАРЗ), так и датчики температуры повышенной точности ИПТ-Ф и ИПТ-ПО, выполненные на основе никелевого фольгового терморезистора и на основе платиновой микропроволоки.
В качестве датчика влажности используется измерительный преобразователь ИПВ с частотным выходом, выполненный на основе интегрального пленочного элемента влажности.
В качестве датчика атмосферного давления используется измерительный преобразователь ИПАД, выполненный на основе интегрального кремниевого элемента.
Возможно подключение к радиозонду датчиков других метео величин с выходными электрическими параметрами в виде емкости, сопротивления, напряжения и частоты. Подключение датчиков к радиоблоку производится перед выпуском радиозонда с помощью разъемных соединителей. Радиоблоки производят преобразование выходных параметров датчиков метео величин в частотные телеметрические сигналы и их поочередное подключение на вход приемопередатчика.

Сверхрегенеративный приемопередатчик обеспечивает передачу телеметрического сигнала на несущей частоте 1680 (1780) MHz и выработку ответного сигнала на запросный сигнал, излучаемый станцией сопровождения. Полный цикл передачи всех телеметрических сигналов содержит 8 равных по длительности канальных интервалов времени. Количество телеметрических сигналов и последовательность их передачи в цикле устанавливается в радиоблоке автоматически при подключении к нему определенного (необходимого для данного вида зондирования) набора датчиков метео величин.
В радиозондах могут быть использованы следующие наборы датчиков:

- температуры;
- температуры и влажности;
- температуры и атмосферного давления;
- температуры, влажности и атмосферного давления.

За счет применения в радиоблоках программируемых логических интегральных микросхем обеспечена возможность изготовления радиозондов с различной длительностью канальных интервалов, числом и последовательностью передачи сигналов в телеметрическом цикле, что обеспечивает возможность использования радиозондов с различными станциями сопровождения. Полетная масса радиозондов с полным комплектом датчиков метео величин не превышает 350 г.

3. Измерительный преобразователь температуры фольговый

Измерительный преобразователь температуры фольговый (ИПТ-Ф) предназначен для использования в качестве первичного преобразователя (датчика) аэрологических радиозондов и является законченным самостоятельным изделием с нормированными метрологическими характеристиками.с Термочувствительным элементом ИПТ-Ф является никелевый фольговый терморезистор типа ТРП2-1.
ИПТ-Ф имеет следующие основные параметры:

- диапазон измеряемых температур (-90 +60) ^{O}C;
- выходной параметр – электрическое сопротивление, в пределах (240 - 700) Ом;
- чувствительность, не менее 2,5 Ом/^{O}C;
- предел допускаемой основной погрешности измерения температуры, не более 0,5^{O}C.

Номинальная статическая характеристика преобразования ИПТ-Ф задается в виде математической формулы с двумя постоянными коэффициентами, определяемыми индивидуально для каждого образца ИПТ-Ф. Конструктивно ИПТ-Ф представляет собой проволочную рамку, на которой закреплен терморезистор, покрытый антирадиационной эмалью. Подключение ИПТ-Ф к радиозонду производится с помощью двухпроводного разъемного соединителя.

4. Измерительный преобразователь температуры проволочный образцовый

Измерительный преобразователь температуры проволочный образцовый (ИПТ-ПО) предназначен для использования в качестве первичного преобразователя (датчика) аэрологических радиозондов и является законченным самостоятельным изделием с нормированными метрологическими характеристиками. Термочувствительным

элементом ИПТ-ПО является неизолированная платиновая проволока диаметром 5 мкм.
ИПТ-ПО имеет следующие основные параметры:

- диапазон измеряемых температур (-90 +60)^{O}C;
- номинальное сопротивление при температуре 25 ^{O}C 500 Ом;
- предел допускаемой основной погрешности измерения температуры, не более 0,3^{O}C;
- радиационная погрешность на высоте 35 км, не более 0,5^{O}C

Номинальная статическая характеристика преобразования ИПТ-ПО задается в виде математической формулы с одним постоянными коэффициентом, определяемым индивидуально для каждого образца ИПТ-ПО. Конструктивно ИПТ-ПО представляет собой проволочную рамку, на которой V-образно растянута платиновая микропроволока. Подключение ИПТ-ПО к радиозонду производится с помощью двухпроводного разъемного соединителя.

5. Измерительный преобразователь атмосферного давления

Измерительный преобразователь атмосферного давления (ИПАД) предназначен для использования в качестве первичного преобразователя (датчика) аэрологических радиозондов и является законченным самостоятельным изделием с нормированными метрологическими характеристиками. Чувствительным элементом ИПАД является интегральный кремниевый тензорезисторный преобразователь давления.
ИПАД имеет следующие основные параметры:
диапазон измеряемых давлений (10 - 1070) гПа;

- выходные параметры - три знакопеременных напряжения, в пределах (0,1 - 2,5) V;
- предел допускаемой погрешности измерения давления, не более 1 гПа; разрешающая способность, не более 0,1 гПа;
- напряжение источника питания 5 V;
- ток, потребляемый от источника питания, не более 5 мА;
- диапазон рабочих температур (-15 +65)^{O}C.

Номинальная статическая характеристика преобразования ИПАД задается в виде математической формулы с несколькими постоянными коэффициентами, определяемыми индивидуально для каждого образца ИПАД. Конструктивно ИПАД выполнен на прямоугольной печатной плате с размерами 90х58мм^{2}. Подключение ИПАД к радиозонду производится с помощью семипроводного разъемного соединителя.

6. Измерительный преобразователь влажности

Измерительный преобразователь влажности (ИПВ) предназначен для использования в качестве первичного преобразователя (датчика) аэрологических радиозондов и является законченным самостоятельным изделием с нормированными метрологическими характеристиками.
Чувствительным элементом ИПВ является интегральный пленочный сорбционный преобразователь относительной влажности с емкостным выходом. За счет

использования структуры с верхним электродом из тонкого влагопроницаемого слоя золота, элемент влажности имеет высокую стабильность и воспроизводимость характеристик.
ИПВ имеет следующие основные параметры:

- диапазон измерений относительной влажности (2 - 99) % RH;
- выходной параметр - частота повторения электрических импульсов, в пределах (для всех модификаций ИПВ) от 50 Hz до 10 kHz;
- чувствительность, не менее $2,5*10^{-3}$ 1 % RH;
- погрешность измерений, не более 2 % RH;
- гистерезис, не более 1 % RH;
- напряжение источника питания (8,5 - 12) V;
- ток, потребляемый от источника питания, не более. 5 мА;
- диапазон рабочих температур (-60 +50) ^{O}C.

Номинальная статическая характеристика преобразования ИПВ задается в виде математической формулы с несколькими постоянными коэффициентами, определяемыми индивидуально для каждого образца ИПВ. Конструктивно ИПВ выполнен на прямоугольной печатной плате размером 50х35мм^2 с выносом чувствительного элемента на расстояние (40 - 150) мм от платы. Подключение ИПВ к радиозонду производится с помощью четырехпроводного разъемного соединителя.

В настоящее время проводятся лабораторные и полетные испытания описанного выше нового оборудования, которые подтверждают его высокие технические и метрологические характеристики.

OPERATION OF INEXPENSIVE ATMOSPHERIC SOUNDING NETWORKS IN DEVELOPING COUNTRIES

Michael W. Douglas
National Severe Storms Laboratory
1313 Halley Circle
Norman, Oklahoma USA

Walter Fernández
School of Physics
University of Costa Rica
San José, Costa Rica

Malaquías Peña
Cooperative Institute for Mesoscale Meteorological Studies
University of Oklahoma, Norman, Oklahoma USA

ABSTRACT

Sixteen pilot balloon stations are currently being operated in Latin America as part of a research program funded by the Pan American Climate Study program of NOAA. Although these observations are intended to satisfy research objectives, this network could also be of value for routine weather forecasting in the region. This paper describes the motivation behind the implementation of the network, some of the considerations involved in designing the network, and some of the difficulties to date in integrating this research network into local and regional forecasting systems.

Introduction

The National Severe Storms Laboratory (NSSL) is currently coordinating, with the assistance of a number of meteorological and educational institutions in Latin America, a network of 16 balloon sounding stations between Mexico and Bolivia. This activity is part of a research project supported by NOAA's Pan American Climate Studies (PACS) Program. These stations (see Fig. 1), most of which have been operating since May 1997, are intended to describe the windfield over Central and northwestern South America with better spatial resolution than with the routine radiosonde network observations. The overriding scientific objectives are to obtain observations that will help explain the rainfall variability in this region and to help determine the accuracy of the operational global analyses made for this domain.

The PACS - Sounding Network (SONET) has its precedent in previous field programs organized by NSSL in Mexico during 1990 and 1993. During these summer programs of 1-2 month duration 10 pilot balloon stations were operated to provide supplementary observations over north-western Mexico, where the radiosonde network was not sufficiently dense to describe the variability of the windfield and its relation to the local topography. These simple wind soundings were very effective in mapping the windfield in the arid regions under investigation.

Both the 1990 and 1993 Mexican programs employed pilot balloons for a number of reasons. The advantages of pilot balloons included: low cost (about $10 for balloons and gas), simplicity and ruggedness of the equipment, ease of data processing (personal computer for wind calculations), and simplicity of selecting observing locations (no electricity needed). Despite some reluctance with using pilot balloons to obtain wind soundings, these networks (see Reyes et al. 1994) proved useful for describing some previously poorly described phenomena, most notably surges and a low-level jet over the Gulf of California, and a numbers of papers have been based upon this data set. (Douglas, 1995, Douglas and Li, 1996, Stensrud et al. 1997).

The current Pacs-Sonet program

Because of the favorable experience with the Mexican field programs, a similar low-cost, simple technology program was proposed for making additional soundings in Central and northwestern South America. This observing network has been evolving over the past year, in part due to the strong El Niño event that has developed in the region. The dense spacing of stations along the coasts of Ecuador and Peru (Fig. 1) are an attempt to

resolve the meridional variation of the windfield in the transitional region between heavy rains and no rains. Most of these stations were not part of the original plan for the network.

The principal motivation for developing this network has been the need to improve the description and monitoring of intraseasonal and interannual variations in the atmospheric circulation in the Atmospheric Boundary Layer (ABL). The response of the ABL to variations in sea-surface temperature changes is not well described from in-situ observations and the network observations should improve this situation. In addition, there is currently only weak verification of the routine global analyses that are produced over this region, and the accuracy of the global analyses from NMC and ECMWF have been questioned (Schmitz and Mullen 1996, Stensrud et al 1995). Surface wind observations cannot be extrapolated much above the surface in most land areas, and cloud-tracked winds are quite uncertain or absent in many areas. The lack of radiosonde observations in the region has been accentuated recently by the termination of the Omega navigation system, and there is currently only one radiosonde station with windfinding capability along the Pacific littoral between Southern Mexico and northern Chile.

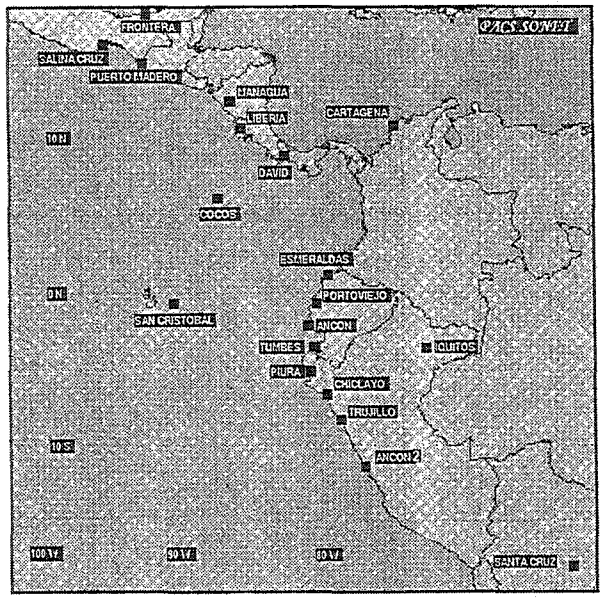

Figure 1: The current pilot balloon sounding network for PACS-SONET.

A second, though unofficial, impetus for better sounding networks over the PACS-SONET domain has been the desire to improve short-range weather forecasts in the region. Few of the countries in the PACS domain can claim much success in producing reliable short-range forecasts. Though not directly related to the objectives of this research study, it was recognized early on that if the network's observations were not converted to a near-real time data stream and the benefits of the observations not demonstrated to the host countries, then there would be little likelihood of long-term operation of the network. And the climate studies being considered by the meteorological community are in need of precisely these kinds of long-term records (see fig. 2). Thus the needs of both short-range weather forecasting and long-range climate forecasting are intimately connected through the joint data base needed for each activity.

It might be noted that this kind of multi-national sustained field program has not, to the author's knowledge, ever been carried out over such an extensive geographical domain, nor over such a long duration. Certainly, it has not been conducted in Latin America. Hence there were not many precedents for establishing the network, and a number of activities were essentially trial-and-error. For example, our efforts to identify suitable collaborators were made primarily via the internet, whereby we searched homepages of different institutions in order to identify possible individuals. This search ramified as our contacts increased, and eventually led to many contacts in National Meteorological Services. There were fewer meteorologists associated with universities than we had anticipated.

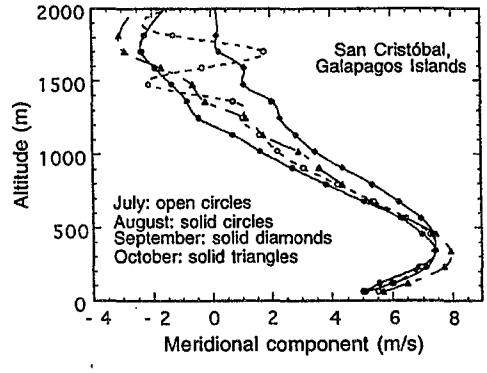

Figure 2. Monthly mean meridional wind profiles from San Cristobal, showng the similarity of the profiles from July through October. Differences above 1000m may be due to sampling uncertainty (many balloons lost into clouds above this level).

Experience from the PACS-SONET

The recent experience with PACS-SONET has made it clear not all of the experience gained during the Mexican

experiments could be directly applied to other regions. Cloudiness has been a more significant hindrance in PACS-SONET than in the Mexican programs, with some sites having persistent low cloudiness (Figs. 3,4). The assumption of inexpensive inflation gas has been valid for some countries, but not in some countries where prices could be two or three times that of other countries in the region. The difficulty in obtaining hydrogen gas in some countries was also not anticipated.

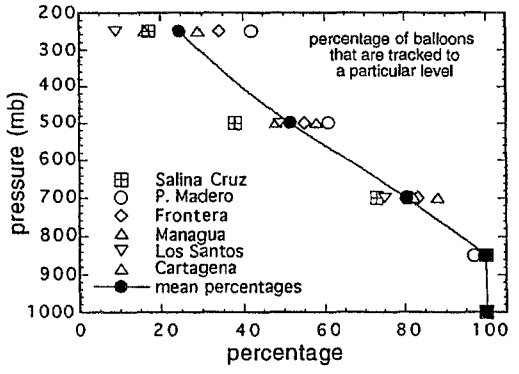

Figure 3: Percentage of balloons that were tracked to different levels at different PACS-SONET stations during a 4-month period.

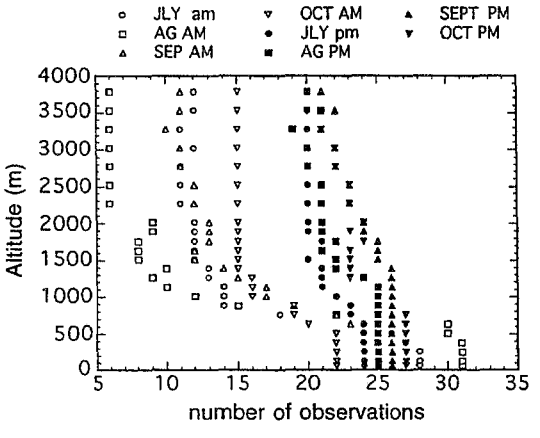

Figure 4: Monthly variation in number of soundings reaching different levels at Piura, Peru during PACS-SONET. Solid symbols are afternoon soundings, open are morning.

Some other observations made during the development of PACS-SONET included the following:

- The presence of special observations alone is no guarantee of their utilization. It has been noted that, almost universally, during the first 9 months of PACS-SONET, the participating Meteorological Services have under-utilized the special observations. The need for better training to use these observations has been apparent to every institution participating in PACS-SONET.

- Different meteorological organizations within each country do not always work closely together, and this impedes data dissemination and forecast development. Aviation weather forecasting activities often appear to have better-trained staff for carrying out daily weather forecasting activities and also often maintain better weather observer networks, yet the National Meteorological Services have the official meteorological functions and tasks before the WMO. Better communications and coordination is needed among the different weather services within these countries to improve the weather forecasts for the general public.

- There are often (though with some notable exceptions) less-than-ideal links between university or research personnel and the National Meteorological Services. Often data is available only for a substantial charge. Yet within the NMS's themselves there is often an absence of research personnel working to improve weather forecasting procedures. Thus, the PACS-SONET special observations, available without charge or restriction, may in some countries, not be readily complemented by other data sets collected by National Meteorological Services.

What has PACS-SONET suggested?

The SONET project has shown that an extensive network of pilot balloon sounding stations can be established and operated in developing countries with relatively modest resources. However, the sustainability of the project and its success as both a climate monitoring and a weather forecasting network is dependent upon many factors. Initially funded as a research activity, PACS-SONET has sought to demonstrate that the network could provide sufficiently valuable observations so as to justify its continued maintenance by the participating countries. This appears not to be the case so far, principally because it has yet to be demonstrated that the observations can indeed provide any measure of improved forecast skill. To do this will require a major educational effort to train personnel of the weather services involved with PACS-SONET how to use the observations to improve short-range weather forecasts. The success of such an educational effort, currently without major financial support, remains uncertain.

Where might PACS-SONET lessons be applied??

Any country where there is an insufficiently-funded weather service is a candidate for applying some of the lessons learned from the PACS-SONET and previous experiments. For example, t may not be financially feasible to move from a weather service without any atmospheric sounding systems to one with state-of-the art systems, especially without first evaluating the critical forecasting needs of the particular country. More often than not, the implementation of advanced observing system technology in a weather service whose personnel are not adequately prepared through training or education to fully use the new observations will yield results far less than anticipated, because the full requirements for making accurate forecasts have not been considered. Thus, a network of simple sounding systems, can be productive and assist in the development of a trained staff and a knowledge of the upper-air climatology (including variability of weather systems) of a particular region. Using this knowledge base, more sophisticated observing systems can be designed as observational requirements become clearer.

The greatest benefits from adopting simple sounding systems will accrue in regions where salaries are low, where inflation gas is readily available and not too expensive, where skies are more clear than cloudy, and where rainfall is modulated by synoptic-weather systems than can be resolved by the sounding network wind observations. These conditions have been discussed in Douglas (1991). Tropical regions are well suited for the pilot balloon observations such as employed during PACS-SONET. In low-latitudes small variations in boundary layer convergence or subtle changes in the orientation of the prevailing lower-tropospheric wind flow with respect to the local topography can produce large fluctuations in rainfall. Describing these variations with most other in-situ or remote sensors today is costly, hence local and regional weather forecasting suffers in many regions of Africa, South America, and Australia-Indonesia. These regions could benefit from an expansion of pilot balloon networks

Summary

The purpose of this paper has been to describe our experiences with implementing an inexpensive pilot balloon sounding network in Latin America, to discuss the problems encountered, and to consider the possibilities for practical implementation of such networks elsewhere in developing regions of the world. We recognize that the use of simple and inexpensive technology runs counter to the trends in most of the earth sciences today. We hope to demonstrate that for rapid progress to be made in many aspects of regional and local weather forecasting in the developing world, and for improved monitoring of inter-annual climate variability, relatively simple observations still can play an important role.

References

Douglas, M.W., 1995: The summertime low-level jet over the Gulf of California. Mon. Wea. Rev., 123, 2334-2347.

Douglas, M.W., 1991: Cost-effective upper wind observing networks for developing countries. The SWAMP example. In preprint volume for Lower-tropospheric profiling. Needs and Technologies. Boulder, Colorado, September 10-13, 1991.

Douglas, M.W., and S. Li, 1996: Diurnal variation of the lower-tropospheric flow over the Arizona low desert from SWAMP-1993 observations. Mon. Wea. Rev., 124, 1211-1224.

Reyes, S., M.W. Douglas and R.A. Maddox, 1994: El Monzon del suroeste de Norteamerica (TRAVASON/SWAMP). Atmosfera, 7, 117-137.

Schmitz, J.T., and S.L. Mullen, 1996: Water vaport transport associated with the summertime North American monsoon as depicted by ECMWF analyses. J. Climate, 9, 1621-1634.

Stensrud, D.J., S.L. Mullen and K. Howard, 1995: Model climatology of the Mexican Monsoon. J. Climate, 8, 1775-1793.

Stensrud, D.J., R.L. Gall, and M.K. Norquist, 1997: Surges over the Gulf of California during the Mexican Monsoon. Mon. Wea. Rev., 125, 417-437.

Acknowledgments

Many thanks are extended to the former Director of NSSL, Robert Maddox, for supporting the Mexican field activities, and to the NOAA PACS program for their support of the current observations in Latin America. Many thanks are due to each of the participating Meteorological Services, educational institutions, and individuals involved in the PACS-SONET activities.

The New NCAR GPS Dropwindsonde

Walter Dabberdt and Harold Cole
National Center for Atmospheric Research
Boulder, Colorado 80307-3000, USA
FAX: (+1 303)-497-1197

NCAR has designed a new GPS dropwindsonde to replace the Lightweight Loran and Lightweight Omega Digital Dropsonde (LD2) previously designed by NCAR in the 1980's. Here we describe both the unique design and performance characteristics of the sonde and its aircraft data system, as well as the application of the new GPS dropwindsonde in hurricane reconnaissance during the 1997 US hurricane season.

The dropwindsonde is composed of four main components: 1.) a Vaisala RSS903 Pressure-Temperature-Humidity (PTH) sensor module, 2.) digital microprocessor circuitry, 3.) a Vaisala GPS-111 codeless GPS receiver and 4.) a 400 MHz narrow-band, tunable telemetry transmitter. Pressure is measured over a range of 1060 to 20 hPa with an accuracy of +/-0.5 hPa; temperature is measured from -90 to +40 °C with +/-0.2 °C accuracy; and humidity is measured over from 0 to 100% RH with +/-2% RH accuracy. The electronics board uses surface mount technology, and contains a connector that serves as an RS-232 link with the aircraft data system for test and checkout, to set the telemetry transmitter frequency, and to download sensor calibration data. The transmitter can be set anywhere in the 400 MHz meteorological band in 20 kHz steps. A unique square-cone parachute is used to reduce the initial shock load and slow and stabilize the sonde during descent. The aircraft data system is a completely new design both in system software and hardware design. Perhaps the most significant aspect of the aircraft data system is its capability to simultaneously receive and process data from up to four dropsondes. This is a critical aspect at jet aircraft speeds when spatial resolution is crucial, such as obtaining profiles through a hurricane or other severe weather system.

Approximately 1500 of the new GPS dropwindsondes have been deployed in the first year of availability. During the 1996-97 field phase of the international FASTEX research program, the sondes were first used to map storm and frontal system structure over the Atlantic upstream of Ireland, and across the entire North Atlantic in a test of targeted observing strategies. Subsequent applications have involved their use in hurricane reconnaissance by the Hurricane Research Division of the National Oceanic and Atmospheric Administration. Because of the high measurement rates (2 Hz), high-resolution wind and thermodynamic soundings have been obtain to the sea surface for the first time. We discuss the some of the important new meteorological findings that have resulted from both of these two applications.

****

No-Transmission Ranging of Radiotheodolite

Li, Jiming and Feng, Dali
Shanghai No. 23 Radio Factory, China

Radiotheodolite windfinding system has a number of advantages in contrast to other windfinding systems such as primary- and secondary radars, and even navaids; Its simple structure, low cost, easy maintenance and less power consumption make it a most acceptible system for windfinding. And in addition, it possesses an inestimable value for millitary use, owing to its no-transmission nature.

For all its advantages the radiotheodolite system is negated by some users for its low accuracy during the lower elevation angle period. It is a vital problem. As we all know, windfinding is the process of assigning to wind speed and direction by estimating the sequential measurements of radiosonde positions. At least two of the three coordinates are needed for a position estimation. A radiotheodolite can obtain azimuth and elevation angle. But when the elevation angle is too low, the angle accuracy will lower to an unbearable level. So the third coordinate—slant range is needed.

The GMD2 system was thus made to give GMD1 its ranging function. They added GMD1 a transmitter of 403MHz with a modulation signal of 75KHz, and a transponder is set in radiosonde to answer the signal. By comparation of the phase difference of received and original 75KHz the slant rang can be obtained. However, such a design actually changes the nature of radiotheodolite; It becomes a seconary radar, and all the advantages the radiotheodolite owns are lost.

The contradiction is thus lying before us; to get ranging function or to keep no-transmission nature. Both are needed fo a good windfinding. It must be resolved through a new design, which our paper relates; To give radiotheodolite its ranging function without transmitting any radio wave.

Principle

Since radiosonde releases by the side of radiotheodolite (of course there is a certain distance between them, but it is a known constant), and goes aloft from near to far continuously, so we can move the emitter from radiotheodolite to radiosonde, and leave radiotheodolite its no-transmission nature. In reality we needn't add any emitter to radiosonde; we just use its transmitter. The thing we should do is to set a crystal oscillator in it, and yield a beacon signal of, say, 10KHz through frequency division. The beacon signal is modulated by TPU signals as subcarrier, and meanwhile modulates the carrier. And on ground equipment we also set a crystal oscillator with same characterics into ranging apparatus. As the subcarrier is transmitted to ground and demodulated, it is sent to the ranging apparatus to be compared with the local signal to get phase difference. After a series of calculation the slant range can be obtained.

From above we can see that although the two signals are of the same frequency and same phase(at the starting time), they are not from same source like what of GMD2; they are from different sources. So we call the means we design Seperate-Sourced Phase Difference Ranging.

Suppose the phase difference between the received and local 10KHz signals is τ, and it becomes larger and larger with the flight of radiosonde. When it is compared with the

local starting phase τ_0, the slant range S can be calculated through:

$$S=(\tau-\tau_0)\times 300(m) \quad \ldots\ldots(1)$$

Such an ideal ranging method must be based on abstract equality of the two 10KHz signals, otherwise τ_0 cannot be a constant. As a matter of fact, any oscillator has its temperature coefficient, so the frequency of 10KHz signals will certainly drift. Therefore, formula(1) is of no practical use. What we shall do must be more complex.

Calculation

Owing to the fact that the product of frequency and cycle is always 1 second, we needn't compare the two 10KHz; we just compare the after edge of radiosonde 10KHz signal with the "second-signal" yielded through frequency-division of the local oscillator.

Let F_K and T_K represent the frequency and cycle of radiosonde 10KHz signal respectively. Comparing F_K with second-signal, we get an f_K. Because f_K is the number of pulses measured between two second-signals, it is usually an integer; while F_K is not always an integer. Therefore there are three different cases between F_KT_K and f_KT_K:

$F_KT_K>f_KT_K$; $F_KT_K=f_KT_K$; $F_KT_K<f_KT_K$

To express the relationship clearly, we introduce a parameter ϕ named as "phase difference coefficient":

$\phi=F_KT_K-f_KT_K=10^6-f_KT_K$ unit: $\mu S/S$

When we input second-signal and F_K to an RS trigger, we get a series of pulses of τs.

If F_K is an integer, then $f_K=F_K$, so $F_KT_K=f_KT_K=10^6\,\mu S$. Thus we can know that the front edge of τ is a second-signal, then the difference between each τ's after edge is also 1 S. Therefore $\tau_i=\tau_{i+1}=\tau_{i+2}$.....etc. The magnitude of τ is determined by phase difference between F_K and second-signal. When they are synchronous, i.e. a certain pulse appears at the same time with second-signal, then $\tau=T_K$. It is the maximum of τ. The minimum value of τ is very close to 0, but cannot be 0. In this situation: $\phi=F_KT_K-f_KT_K=0$.

If F_K is not an integer, for example, $F_K=10000.1$Hz, then

$\phi=(10000.1-10000)T_K=0.1T_K$

How does value τ vary when ϕ is above 0?

Let's suppose the i-th second is synchronous with F_K:

$\tau_i=T_K$

$\tau_{i+1}=T_K-\phi=T_K-0.1T_K=0.9T_K$

$\tau_{i+2}=T_K-2\phi=T_K-0.2T_K=0.8T_K$

. . .

$\tau_{i+9}=T_K-9\phi=T_K-0.9T_K=0.1T_K$

$\tau_{i+10}=T_K-10\phi=T_K-T_K=T_K$

Hence we know $\tau_{i+n}=T_K-n\phi$. When τ_{i+n} is negative, a module $-T_K$ is introduced. For instance: $\tau_{i+12}=T_K-12\phi=T_K-1.2T_K=-0.2T_K=0.8T_K$. This is due to the fact that T_K is continuous, and RS trigger cannot create a negative τ pulse.

From above examples we can observe that value τ decreases gradually from T_K towards 0, and once it is very close to 0, it will jump to T_K. This circumstance occurs only under the condition that value ϕ is smaller than $0.5T_K$. If value ϕ is larger than $0.5T_K$, value τ increases gradually from near 0 towards T_K, and when it reaches T_K, it jumps to minimum value. For example, when $F_K=10000.7$Hz, we may first see how the measured value f_K varies. Suppose F_K is synchronous with the second-signal at i-th second, then from

i-th second to (i+1)-th second can measure a avalue f_K=10000; from (i+1)-th second to (i+2)-th second can measure a value f_K=10001; from (i+2)-th to (i+3)-th , f_K=10000;from (i+3)-th to (i+4)-th, f_K=10000.....etc. It should be noted that f_K has two values, and thus ϕ also has two values:

$\phi_1=(10000.7-10000)T_K=0.7T_K$

$\phi_2=(10000.7-10001)T_K=-0.3T_K$

No matter ϕ_1 or ϕ_2 is used, value τ is always the same. This is due to $\phi_1+\phi_2=T_K$, which we think is no need to certify here. In the following formulas, value ϕ will all be used as positive. If there is a negative ϕ, then a T_K will be added.

If T_K keeps unchanged when radiosonde goes aloft, we can use following formula to calculate slant range:

$$R_m=\tau_m-\tau_0-m\ \phi_0 \qquad \text{.....(2)}$$

where R_m is the slant range at second m, τ_0 is the measured value at the release of radiosonde, ϕ_0 is the measured value before release, and the maximum value of R_m is T_K (about 30Km).

When radiosonde goes aloft, the temperature of crystal oscillator changes, therefore F_K cannot keep unchanged. That means that the cycle of sub-carrier T_K also changes continuously. Let the variable of T_K be ΔT_K, so value τ contains three factors, ϕ_0, ΔT_K and R_m.

Let time be second 0, then $\tau_0=T_0-n\phi_0+R_0$

where T_0, ϕ_0 are, respectively, the cycle and phase difference coefficient of F_K at the release of radiosonde, R_0 is slant range (μS) at second 0. By the flight of balloon, T_K decreases with the dropping of temperature. Let variable per second be ΔT_K, then the calculation formulas for value τ of any one second can be derived:

Second 1 $\tau_1=T_0-\Delta T_1-n\phi_0-\{1-f_K(T_0-\Delta t_1)\}+R_1$

$=T_0-\Delta T_1-n\phi_0-(1-f_KT_0)-f_K\ \Delta T_1+R_1$

$=T_0-(n+1)\phi_0-\Delta T_1(f_K+1)+R_1$

Second 2 $\tau_2=T_0-\Delta T_2-(n+1)\phi_0-\Delta T_1(f_K+1)-\{1-f_K(T_0-\Delta T_2)\}+R_2$

$=T_0-\Delta T_2-(n+1)\phi_0-\Delta T_1(f_K+1)-(1-f_KT_0)-f_K\ \Delta T_2+R_2$

$=T_0-(n+2)\phi_0-\Delta T_1(f_K+1)-\Delta T_2(f_K+1)+R_2$

$=T_0-(n+2)\phi_0-(\Delta T_1+\Delta T_2)(f_K+1)+R_2$

Second 3 $\tau_3=T_0-(n+3)\phi_0-(\Delta T_1+\Delta T_2+\Delta T_3)(f_K+1)+R_3$

Secpnd m $\tau_m=T_0-(n+m)\phi_0-(\Delta T_1+\Delta T_2+\Delta T_3+\ldots+\Delta T_m)(f_K+1)+R_m$

Let $\tau_m-\tau=-m\ \phi_0-\sum_{i=1}^{m}\Delta T_i(f_K+1)+R_m$

then the formula for slant range at second m is:

$$R_m=\tau_m-\tau_0+m\ \phi_0+\sum_{i=1}^{m}\Delta T_i(f_K+1)+R_0 \qquad \text{.....(3)}$$

where R_m is slant range at second m;

τ_m is phase difference at second m, with scope of: $0<\tau<T_K$;

τ_0 is the measured value of phase difference at the release of radiosonde;

ϕ_0 is "phase difference coefficient" at second 0;

ΔT_i is cycle variable of subcarrier due to temperature effect at second i;

f_K is subcarrier frequency at second i;

R_0 is slant range at the release of radiosonde.

Now all the calculations are completed. It seems quite complex for us to do these calculations, but, we think, it is quite easy for a computer to do them.

Error Analysis

Now let's discuss the errors that formula(3) may bring to us.

The measure errors of τ_m and τ_0 depend on the frequency of count pulse. However, if we use 300MHz count pulse to measure τ_m and τ_0, the maximum error will be only 1m.

Value ϕ_0 is measured before release of radiosonde, and has a great effect on ranging accuracy. Some technical means must be adopted to put down the error of item $m\phi_0$. Also we use 300MHz pulse to measure the average value of τ_0 successively in 30 seconds, so that the maximum error of ϕ_0 can be lowered to 0.01m. If the sounding time is 1 hour, i.e. 3600 seconds, the, maximum error of item ϕ_0 is 36m.

As to the error of item $\sum_{i=1}^{m} \Delta T_i(f_K+1)$, it depends on the measure error of ΔT_i. We cannot measure ΔT_idirectly, but we can measure it indirectly, that is, to measure the temperature change per second of the local crystal oscillator. Then, we can figure out the needed ΔT_i in accordance with frequency-temperature relational expression made through local measurement.

If the accuracy of temperature measurement is 0.1°C, the error of ΔT_i per second can be estimated as 5×10^{-3}m. When m=3600, the maximum error of $\Sigma \Delta T_i$ is 18m.

Therefore, when m=3600, the maximum error of R_m is: 1+36+18=55m.

Comparing with the slant range error caused by the error of elevation angle measurement, we can see more clearly how our new design outweighs.

Let height be 25000m, and elevation angle be 15°. If the angle error is 0.05°, then the slant range error may be 320m.

Figures show that on height of 25000m the range error of radar is about 129m, and aneroid capsule(accuracy 0.5 hPa) through barometric height formula is about 100m.

Thus we know our new design Seperate-Sourced Phase Difference Ranging enhances the accuracy of radiotheodolite to a level that even equals to radars, especially that of lower elevation angles. Considering its low cost and other advantages, our new ranging means is certainly a very good option for windfinding system.

RS90 RADIOSONDE INTO OPERATIONAL USE

Ari Paukkunen, Hannu Jauhiainen
Vaisala Oy, Finland

1. INTRODUCTION

Pilot test results of the RS90 Radiosonde have been very promising, and a transition from RS80 to RS90 Radiosonde can be started. The RS90 Radiosonde introduces a new sensor unit, bringing several improvements to measurement results. The thin-wire new temperature sensor features a very short time lag and negligible solar radiation error. The new humidity measurement relies on heated twin-sensor principle and a new polymer. The silicon micromachined pressure sensor of RS90 provides an excellent dynamic range in the wide temperature profile of a sounding. Enhanced accuracy and reproducibility of the measurements with RS90 facilitate improvements in research and weather forecasting. This paper discusses the new calibration method, pilot test results and main features of the sensors. Additionally, typical differences between RS80 and RS90 are shown, which illustrates the reliability and overall performance of the RS90 Radiosonde.

2. RS90 CALIBRATION

Radiosonde accuracy is based on sensor quality and individual wide-range calibration. When development of the new-generation radiosonde began, a decision was made to optimize the calibration process and equipment. The objective was to take full advantage of the advanced features of this entirely new pressure, temperature and humidity sensor.

Vaisala's new CAL4 radiosonde calibration equipment was specifically designed for the RS90 Radiosonde. The result is a state-of-the-art calibration system that meets the highest performance standards, offering high accuracy with low short-term and long-term uncertainties. The following requirements for a good industrial calibration system were considered carefully in the development:

- Individual calibration of each sensor with sensor electronics
- Accurate and unbiased mathematical modeling of the sensors
- Stable and well characterized calibration chambers
- Internationally traceable low uncertainty working references and instruments
- Computer-aided test (CAT) instrument set-up
- High level of automation

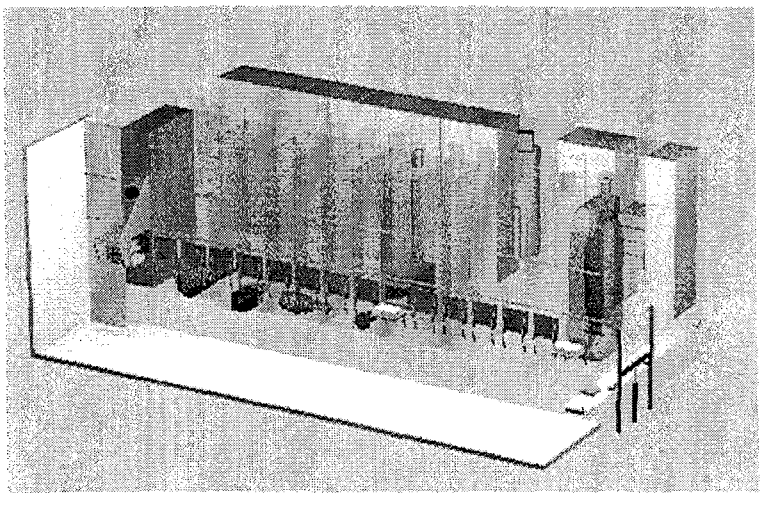

Figure 1. *CAL4 Calibration Equipment consists of 16 ventilated environmental chambers. All of them are temperature controlled, 3 humidity controlled and 4 pressure controlled. Calibration conditions: -90...+60 ° C, 0....90% RH and 0.....1090 hPa give good coverage of sounding conditions. The capacity is 180 sensor units per hour.*

The uncertainty presented below is calculated according to ref. 2 and ref. 3, where all the uncertainty factors are characterized by the estimated variations and degree of freedom or by the standard deviation. The combined uncertainty is characterized as the sum of the squares of the deviations.

Table 1. Estimated preliminary short- (σ_r) and long-term (σ_l) uncertainty of CAL4 calibration at different calibration points for a 2 sigma confidence level.

UNCERTAINTY	PRESSURE hPa	TEMPERATURE °C	HUMIDITY %RH
	0....1070	+60.....-90	0.....90
SHORT TERM (σ_r,k=2)	< 0.2	< 0.01	< 0.3....0.8
LONG-TERM (σ_l , k=2)	< 0.12	< 0.03....0.04	< 0.5....2
TOTAL	< 0.23	< 0.03....0.04	< 0.6.....2.1

Table 2. Measured preliminary values for the standard deviation of differences in repeated calibrations (σ_{rc}) for a 2 sigma confidence level.

	PRESSURE hPa	TEMPERATURE °C	HUMIDITY %RH
σ_{rc} (k=2)	< 0.4	< 0.1	<2
average	< 0.15	< 0.05	<1

3. RS90 RADIOSONDE IN CUSTOMER PILOT TESTS

One of the pilot tests was carried out as an intercomparison test, consisting a series of twin soundings with the new RS90 and RS80 Radiosondes performed at ZAMG in Vienna, Austria. The test and data acquisition was conducted by Mr. Kurt Zimmermann and Mr. Erwin Polreich from Zentralanstalt für Meteorologie und Geodynamik in Vienna, Austria.

The RS90 Radiosonde was evaluated in three areas of performance. The radiosondes were tested in Ground Check mode against ground weather references. The height and temperature data from RS90-RS80 soundings was compared with that of the ECMWF prediction model. Finally, the measured PTU values collected by RS90 were contrasted with those of RS80 using the WMO intercomparison software.

ECMWF Model Analysis

The 30, 50 and 100 hPa pressure heights for both radiosondes were compared against the ECMWF model. The results are presented in Table 3. For further information about the ECMWF forecasting system see Meteorological Bulletin M3.2, *User Guide to ECMWF Products,* edition 2.1. The specification for GRIB code can be found in *WMO Publications 306 Manual on Codes.*

The results in relation with the prediction models show improved accuracy. This is especially clear with the standard pressure level measurements that were compared to the ECMWF model's analysis data, mainly due to the faster temperature sensor. The RS90 gave lower standard pressure level heights than RS80 – typically 10 meters up to 30 hPa.

Table 3. Height differences against ECMWF model (radiosonde - model)

	RS80 Mean (m)	(n=32) Std.dev. (m)	RS90 Mean (m)	(n=32) Std.dev. (m)
100 hPa	-1.2	9.6	-10.1	8.1
50 hPa	2.0	15.8	-7.9	12.5
30 hPa	6.3	18.2	-1.8	13.6

Temperature differences against the model for both type of radiosondes were compared at 30, 50 and 100 hPa standard pressure levels, see Table 4.

Table 4. Temperature differences against ECMWF model (radiosonde - model)

	RS80 Mean (K)	(n=32) Std.dev. (K)	RS90 Mean (K)	(n=32) Std.dev. (K)
100 hPa	0.1	1.3	0.04	1.52
50 hPa	1.1	1.2	1.15	1.12
30 hPa	0.4	1.2	0.61	1.32

Comparison between RS90 and RS80

Pressure, temperature and humidity vs. height profiles were analyzed using WMO RS intercomparison software (WMO, *instruments and observing methods REPORT No:60*, WMO/TD_No.991, 1996). Figures 2 and 3 show the calculated RS90 - RS80 difference for temperature, pressure and humidity.

The differences between RS80 and RS90 temperature measurement are mainly due to the faster response of RS90 sensor and the wider deviation of the RS80 radiation correction. The difference in measured pressure is attributed to better thermal compensation of the RS90 pressure sensor. The small (0-3%) mean and standard deviation values for the humidity difference is related to dry weather conditions during the test. In cloudy conditions the difference was greater because of RS90's improved temperature dependency compensation and more accurate calibration.

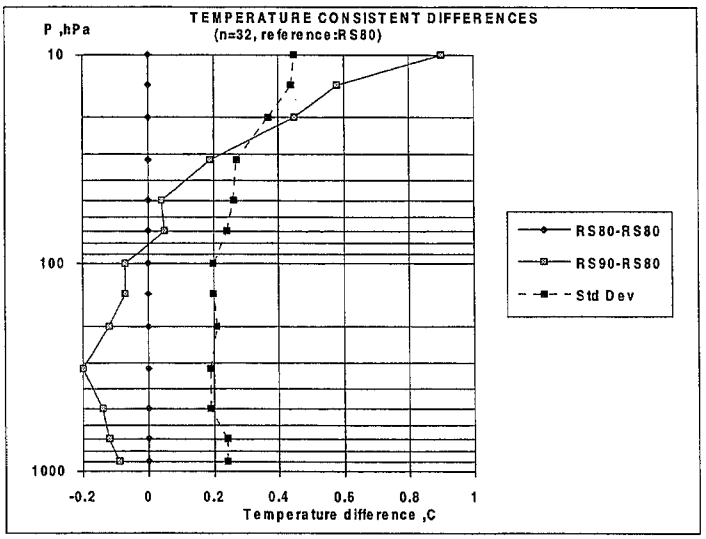

Figure 2. RS90 - RS80 temperature difference (mean value and standard deviation)

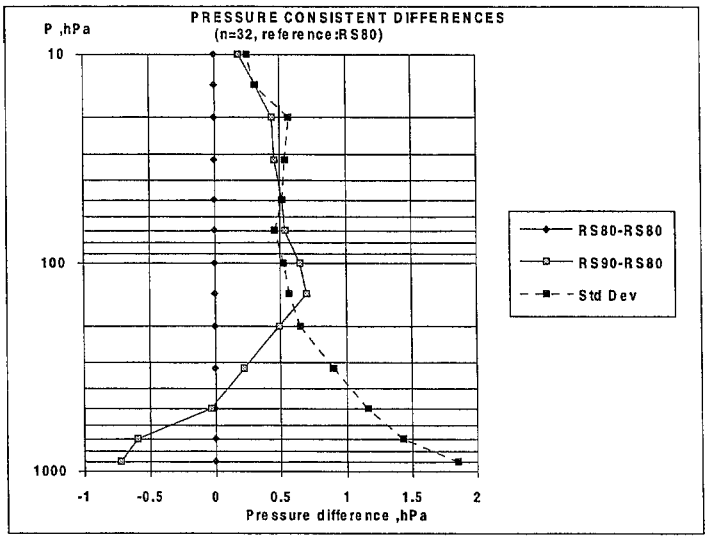

Figure 3. RS90 - RS80 pressure difference (mean value and standard deviation)

4. RS90 RADIOSONDE SENSORS

Various tests have shown that RS90 gives good measurement results. The new sensors have consistently outperformed their RS80 counterparts: improved measuring accuracy, faster response time and minimal solar radiation effects (see ref 3. for a report on preliminary tests for radiation correction). Through improved sensor electronics and calculation algorithm, the accuracy is further improved.

Humidity sensor is featured by new stabile H-polymer sensor with accurate calibration, resulting in excellent cloud detection ability compared to RS80 A-Humicap. Low drift during storage maintains the accuracy. Heating minimizes the adverse effect of frosting. The pressure sensor is shock-proof which eliminates transportation problems and the thermal compensation is improved.

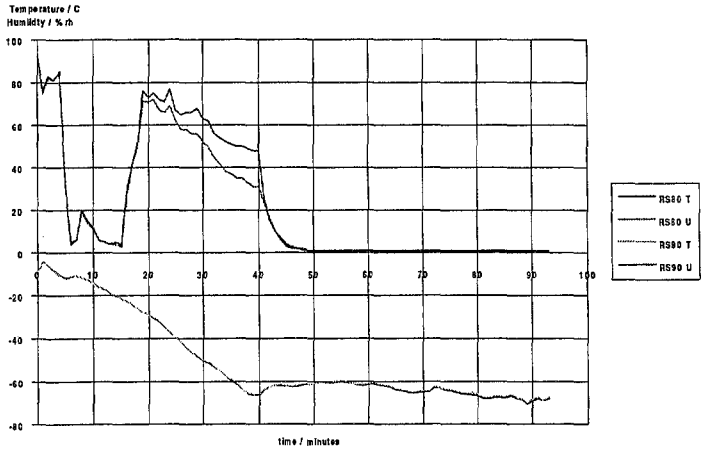

Figure 4. RS90 humidity sensor shows typically higher humidities at cold temperatures

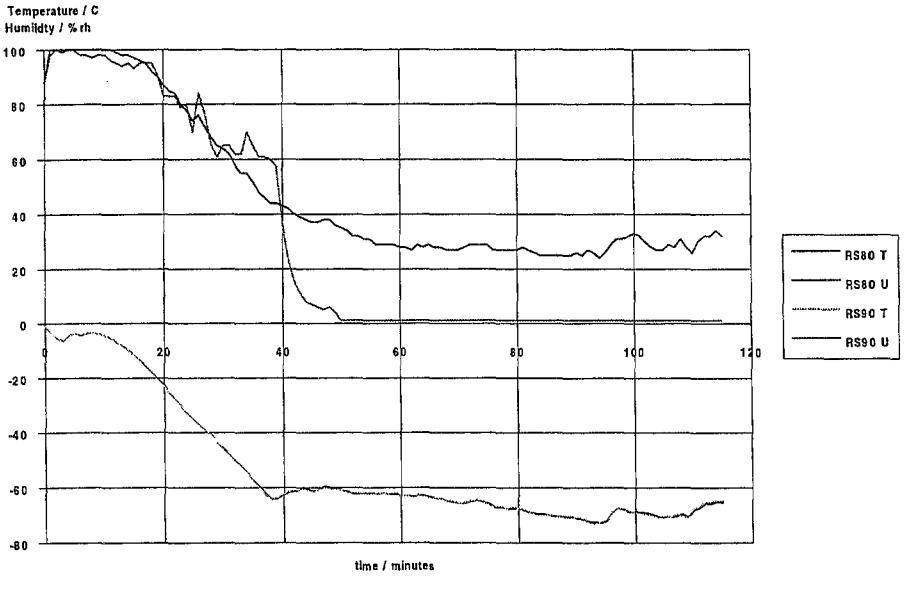

Figure 5. Heated RS90 humidity sensor prevents icing at low clouds

References:

1. Antero Pitkäkoski: Traceability of measurements at RSS production of Vaisala Oy, (22 September 1997) Vaisala Oy, internal report.
2. Guide to the Expression of Uncertainty in Measurements, First edition 1993, ISBN 92-67-10188-9, International Organization for Standardization.
3. Expression of Uncertainty of Measurement in Calibration (EARL-R2,1997) European Cooperation for Accreditation of Laboratories.
4. Guide to Meteorological Instruments and Methods of Observation, Sixth edition, WMO-No.8, 1996
5. James K.Luers : Temperature error of the Vaisala RS90 radisonde ,University of Dayton Research Institute, Jan. 1996.

AUTOSONDE – A RELIABLE WAY TO REDUCE SOUNDING COSTS

Hannu Katajamäki
Vaisala Oy, Finland

1. INTRODUCTION

The automation of meteorological observations reduces operating costs and allows greater scope for site selection and observation times, while maintaining the quality of observation data, and even improving data availability. The Vaisala AUTOSONDE system offers a cost-effective solution for upper air observations - a concept that has proven to work in tests and operational use in varied environments, harsh climates and remote locations around the world.

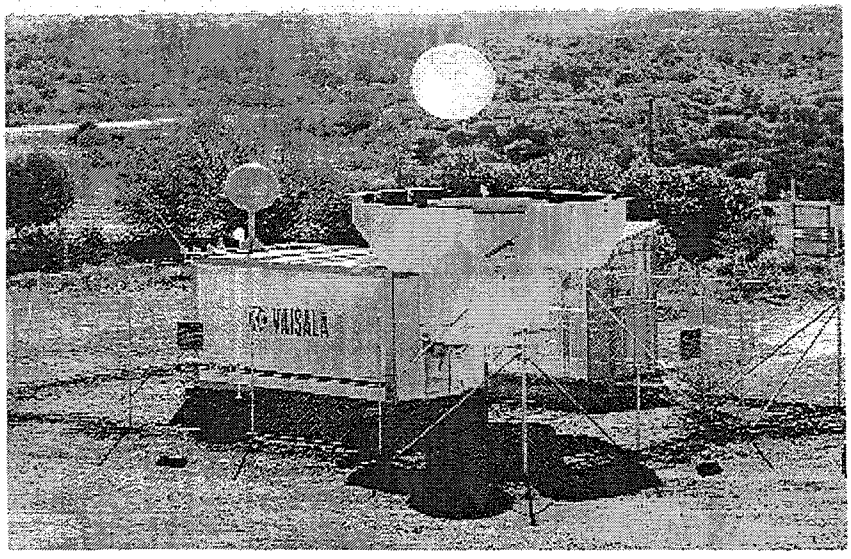

Figure 1 *AUTOSONDE System in Cobar, Australia, launching a radiosonde*

1.1. Increasing need for automation

The increasing cost of manpower, especially at weekends and night shifts has accentuated the need for automation of the observation tasks at synoptic upper air stations. Through full automation of the observation task, operating an upper air station becomes more of a periodic maintenance task. The AUTOSONDE concept also opens up new possibilities for extending the scope of upper air observations. Remote upper air stations can be set up in locations where manned operation is not feasible.

The need for operator attendance is limited to the days, when the AUTOSONDE is to be loaded with new radiosonde, balloons, and gas. For instance in a 24-tray configuration with two observations per day, attendance is needed only every 12 days. Full automation is especially suited also for e.g. research programs, and monitoring stations where the possibility to program the observations to be made at a short notice is very useful and valuable. Several radiosonde versions, including radioactivity sondes, can be used and launched with AUTOSONDE equipment in any sequence.

1.2. Background of AUTOSONDE development

The first semi-automatic systems that Vaisala developed date back to the early 1980's, when the ASAP (Automated Shipboard Aerological Program) observation containers were introduced. These systems automated the tasks of balloon filling and launching. Experience from this program, with some 20 ASAP systems operating around the world, proved that automation can improve data quality and lower the cost of operation. This encouraged Vaisala to develop the concept further into a fully automated system. The development of the AUTOSONDE was started in 1991, and a limited-autonomy prototype that was capable of handling 6 launches was exhibited at the TECIMO exhibition in Vienna in 1992.

2. System description

The AUTOSONDE system is a practically independent entity, an automated system that covers all stages of upper air observations, starting from pre-launch radiosonde preparation to data processing and meteorological message generation. The AUTOSONDE consists of several basic modular building blocks:

- radiosonde storage and preparation module,
- automatic radiosonde receiving and data processing system,
- control computer system,
- remote control terminal and
- system-housing container.

2.1 System shelter

The AUTOSONDE system is housed in an insulated shelter (dimensions 4.9 m (L) x 2.4 m (W) x 2.5 m (H), where the meteorological equipment is installed. Also the control computer that operates the robotics is located inside the shelter. The container is equipped with heaters or air conditioners, depending on the local climate. The system becomes its own building; thus allowing the freedom to locate the upper air station wherever is best for the operations.

The AUTOSONDE shelter interior is divided into two compartments: one compartment is allocated for the radiosonde storage and preparation module, whereas the other is used as working space during radiosonde loading, inspection and maintenance work. The control computer and the automatic rawinsonde set systems are installed in the working space. The balloon filling and launcher module is installed outside at one end of the container. A sub-processor controls the launcher and gas measurement. The antennas of the meteorological system are mounted on the roof of the shelter. The surface weather data for the AUTOSONDE system is supplied by a surface weather station MILOS, installed near the shelter.

The gas cylinders are situated in their own shed near the shelter and the gas piping is connected to the gas measurement system on the roof of the shelter. All the gas pipes and hoses are located outside the shelter. Hydrogen or helium gas is used. The container compartments meet the stringent safety requirements for hydrogen gas.

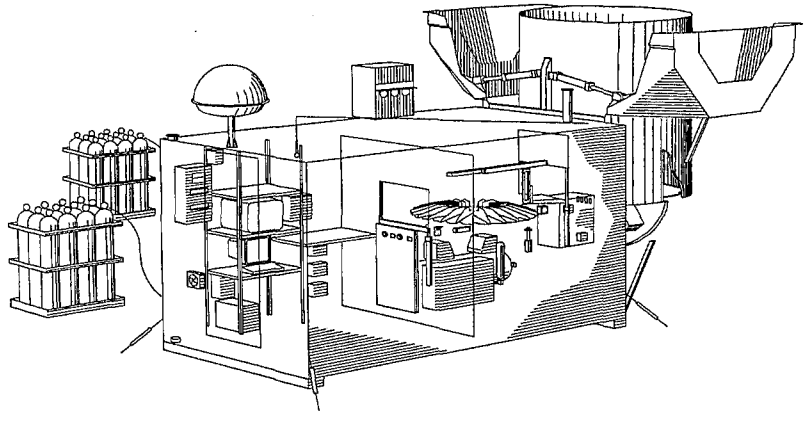

Figure 2 AUTOSONDE Shelter layout

2.3. Operation

The AUTOSONDE automatically prepares the radiosondes, fills the balloons, and launches them at preset times. The AUTOSONDE system can perform up to 24 automatic launches between charging (i.e. loading radiosondes). The maximum number of launches can vary according to system configuration. The AUTOSONDE system also receives the radiosonde signals and computes observation data automatically, including wind, which is then processed into a weather message. In addition to PTU and wind profiles, special sensor data can also be acquired with the AUTOSONDE.

The AUTOSONDE system can be remotely supervised, and launches can be fully automatic or remotely controlled. One person on duty can remotely control and monitor upper air observations that are carried out simultaneously at several locations. On-demand soundings can be ordered from the remote location.

2.4. Easy to use

The observation schedule and other settings for observations are defined in AUTOSONDE Graphical User Interface, running on the Control Computer. This allows modifying the settings quickly and easily. Soundings can be set up at a very short notice in unexpected weather situations. The AUTOSONDE User Interface handles the task of preparing radiosondes for launching, as well as manually controlling the AUTOSONDE launcher. Beside easy radiosonde loading, the user interface is designed for overall system control either from the sounding station or from a remote control station. The AUTOSONDE System Software runs in Microsoft® Windows NT™ environment.

2.5 Safety viewpoints

Safety is a major advantage of the AUTOSONDE, especially when it comes to gas handling. Because hydrogen is highly explosive, it is much safer and more convenient to use an automatic system to fill and launch balloons, especially during the night shift. In addition to the built-in safety features of the system, the AUTOSONDE system site is always fenced to protect the system against trespassing.

2.6. Variety of windfinding options

The AUTOSONDE offers a flexible choice of windfinding options: the same AUTOSONDE system can incorporate, Loran-C, VLF-NAVAID, and GPS windfinding methods. The operator can easily select the windfinding option to be used in a specific sounding through the graphical user interface. The local conditions and the availability of the various navigation networks are naturally to be taken into account in the choice of windfinding method, but now also the periodic maintenance breaks can be easily programmed into the system. This guarantees that data availability can be ensured.

2.7 In operational use all over the world

AUTOSONDE systems have been installed in seven countries in various parts of the world: Finland, Sweden, Denmark (including Greenland), France, Germany, and Australia. The wide variety of installation sites all over the world translates into an extensive record of operational experience from different climates.

The experience gained from the users all over the world has proven that the AUTOSONDE operates reliably in all kinds of weather and is well suited to remote locations with difficult access. The AUTOSONDE can perform radiosonde launches in winds up to 20 m/s (25 m/s with additional cover lids).

Figure 3 AUTOSONDE site map

3. OUTSTANDING RELIABILITY IN PERFORMANCE TESTS

The Swedish Hydrological and Meteorological Institute (SMHI) has tested Vaisala's AUTOSONDE systems in operational environment since 1994, most recently in Sundsvall and Gothenburg, Sweden. In May 1996, SMHI granted Vaisala AUTOSONDE systems final acceptance, and confirmed that the performance target set for the AUTOSONDE delivery had been achieved. Vaisala has delivered four AUTOSONDE systems to Sweden.

The AUTOSONDE observations made in Sundsvall and Gothenburg between 1 April and 5 May 1996 achieved a data availability of over 97.5 % which was one of the original targets. In the stability test at the Gothenburg site, an availability of 98.57 % was achieved, with just 2 missed soundings out of 140. The corresponding rate for the tests in Sundsvall was 99.44 %, with just 1 missed sounding out of 180.

The results from SMHI's test verify clearly that one of the key premises of AUTOSONDE concept works: improved data availability and lower costs can be reached with an automated system. However, it must be noted that to achieve data availability rates as high as 98 - 99 %, no major breaks in system operation are allowed. This in turn requires that personnel is well-trained and familiar with the system and that weather conditions do not prevent the system from performing observations as scheduled. Moreover, the service arrangements must be dependable and continuous to guarantee quick action in the event of a malfunction. Should the system operation fail, corrective action is to be taken without delay, regardless of the time of the day, to reach a data availability rate that exceeds the target set for the system (97.5 %). For instance, in a system with two observations made daily, not more than one sounding could be missed in a month to maintain high data availability.

3.1 Cost-effective soundings at unmanned stations

The automation of meteorological observations reduces operating costs and allows greater scope for site selection and observation times, while at the same time maintaining the quality of observation data. Because it minimizes the staff needed for radiosounding, the Vaisala AUTOSONDE system helps reduce costs. Consequently, flexible and cost-effective sounding operations are possible.

Session VIII

PRESENT WEATHER OBSERVATIONS

EVALUATION TECHNIQUE ET APPORT A LA PREVISION REGIONALE D'UN RESEAU DE STATIONS AUTOMATIQUES DE TEMPS PRESENT

Fabrice ZANGHI, Jean Louis GAUMET

Météo-France, Service des Equipements et des Techniques Instrumentales
Trappes, FRANCE

I - INTRODUCTION

Le projet SOLFEGE lancé à Météo-France en 1989 pour compléter l'observation météorologique automatique de surface est dans sa phase finale. Des capteurs de temps présent ont été développés dans ce but. Les instruments retenus pour constituer une station automatique d'observation SOLFEGE sont les suivants :

PRECIPIA : C'est un détecteur et identifieur de précipitation dont le principe de mesure est l'effet Doppler. Cet instrument est en fait un petit radar bi-statique émettant à 24 GHz, capable de discriminer les hydrométéores en différenciant les signatures des spectres de vitesse des particules précipitantes (Duvernoy et Gaumet, 1996).

SOLIA : Cet instrument qualifie l'état de surface d'une plaque de référence posée sur le sol. Il utilise le comportement optique d'un signal lumineux émis vers la plaque en analysant les quantités réfléchies et diffusées du signal émis par la plaque. Les variances des signaux sont aussi prises en compte (Gaumet et Salomon, 1991).

VISIBILIMETRE : Un visibilimètre est également nécessaire au fonctionnement complet d'une station SOLFEGE.

Ces nouveaux instruments viennent compléter la panoplie des équipements classiques disponibles sur les sites d'observation donnant: pression, température, humidité, vent, ...
Chacun de ces instruments prend en charge un aspect du temps présent (précipitation, état du sol, ..) et établit un diagnostic primaire qui est transmis à une station automatique SOLFEGE. Cette dernière élabore, à partir de l'ensemble des informations dont elle dispose, les différents messages de temps présent. Cette élaboration repose sur la combinaison des mesures des capteurs traditionnels et des diagnostics primaires issus des équipements observant le temps présent. En même temps, la station SOLFEGE accrédite l'ensemble des informations disponibles et fournit un indice de qualité sur leur contenu.
Le second rôle de la station est de transmettre les informations de temps présent vers l'extérieur en envoyant par un système de réseau interne ou par le réseau RTC des messages d'avertissement lors de la modification sensible du temps présent ou de l'évolution d'autres paramètres tels que l'état du sol, la visibilité, la force du vent, ...

L'ensemble des messages émanant d'un réseau de 5 stations SOLFEGE installées dans la région Centre-Est autour du Centre Météorologique Inter Régional (CMIR) de Lyon est évalué d'une part, du point de vue de sa qualité métrologique et météorologique (vraisemblance de l'information) et d'autre part du point de vue de l'apport à des prévisionnistes dont le travail d'exploitant se situe à distance des stations.

Le présent document traitera de la méthode utilisée pour tenter de qualifier les messages de temps présent SOLFEGE et pour estimer l'apport de ces informations sur le travail d'exploitation du prévisionniste.

II - ORGANISATION GENERALE D'UNE STATION SOLFEGE ET FONCTIONNEMENT

La figure 1 représente une station avec tous ses instruments (PRECIPIA, SOLIA, un visibilimètre) et les capteurs classiques donnant (P, T, U,..) connectés à une station météorologique automatique MIRIA ainsi que ses liaisons vers l'extérieur.

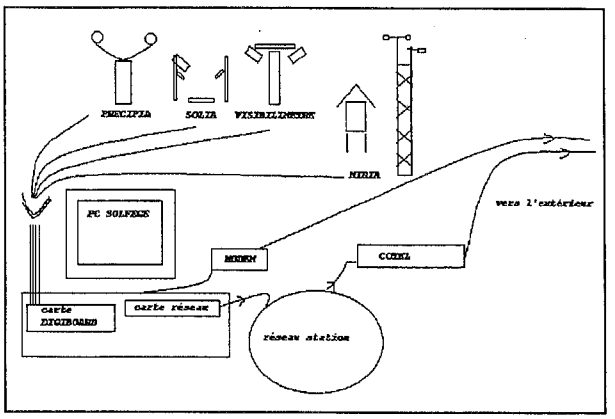

Figure 1. Schéma synoptique d'une station SOLFEGE

La station SOLFEGE procède aux tâches suivantes :

- elle effectue en priorité l'acquisition des données des différents systèmes que sont les capteurs de temps présent et la station MIRIA.
- elle élabore des messages horaires et d'avertissement.

Adresse de correspondance : F. ZANGHI Météo-France, SETIM , 7 Rue Teisserenc de Bort , BP 202, 78195 Trappes Cedex FRANCE

- elle décide de l'envoi des messages.
- elle stocke les informations primaires élaborées.
- elle transmet les messages
  - à des utilisateurs éloignés
  - aux utilisateurs sur place
- elle visualise en clair les informations avec une période d'actualisation d'une minute.

Les logiciels traitant ces différentes tâches sont les suivants :

SOLFEGE.EXE : Cette application est au cœur de la station SOLFEGE Elle est aussi appelée Validation **A**utomatique des **M**esures d'**Ob**Servation (VAMOS).
SOL_SEND.EXE (transmission des messages SOLFEGE)
SOL_VISU.EXE (visualisation des messages)
DEL_FICH.EXE (gestion des fichiers SOLFEGE)
SOL_RECV.EXE (réception des messages SOLFEGE)

Les instruments de temps présent délivrent leurs informations par l'intermédiaire de liaisons série RS. Ils sont branchés sur les différentes entrées d'une carte d'acquisition DIGIBOARD multisérie installée dans le PC SOLFEGE. La station MIRIA est elle même connectée sur cette carte.

Le schéma de fonctionnement du programme général (VAMOS) d'acquisition et d'élaboration des messages (SOLFEGE.EXE) est le suivant :

- Initialisations
  lecture VAMOS.INI (initialisation des voies série, des fichiers, ...)
  initialisation des variables ("999" si absentes)
  initialisation des fichiers tampons

- Boucle de fonctionnement général
  Examen permanent des voies série
  - Si données MIRIA correctes :
  - examen des messages capteurs disponibles
  - décodage des différents messages avec correction des éventuelles erreurs
  - prétraitement des données et validations croisées
    - Si assez de données disponibles :
    - étude des 59 minutes précédentes
    - phénomènes de brouillard (Oui/Non)
    - précipitations (Oui/Non)
    - élaboration du temps présent remplissage du tableau des codes de Temps Présent de 1 à 100
    - Fabrication et décision de l'envoi des messages horaires et d'avertissement
    - Ecriture des données sur les fichiers
    - Glissement d'une minute en arrière des 60 dernières informations
  Fin si données MIRIA correctes
- Pas de fin possible de boucle .

III - RESEAU EN PLACE

Cinq stations SOLFEGE sont en exploitation depuis plusieurs mois dans les Centres Départementaux Météorologiques (CDM) du Puy en Velay, de Mâcon, Montélimar et Embrun. Les données et messages sont concentrés et visualisés au CMIR de Lyon-Bron.

Les premiers résultats montrés ici comprennent l'ensemble des mesures et évaluations de début novembre à fin décembre 1997. Deux mois de mesures permettent de se faire une idée de la qualité de fonctionnement de SOLFEGE et de l'intérêt du système.

IV - VISUALISATION DES MESSAGES

Le poste de visualisation des messages est représenté figure 2. On peut y lire l'heure d'apparition des messages, leur nature (exemple: début de pluie,..) et d'autres paramètres classiques (P, T, U, ..) dont on peut visualiser graphiquement l'évolution temporelle.

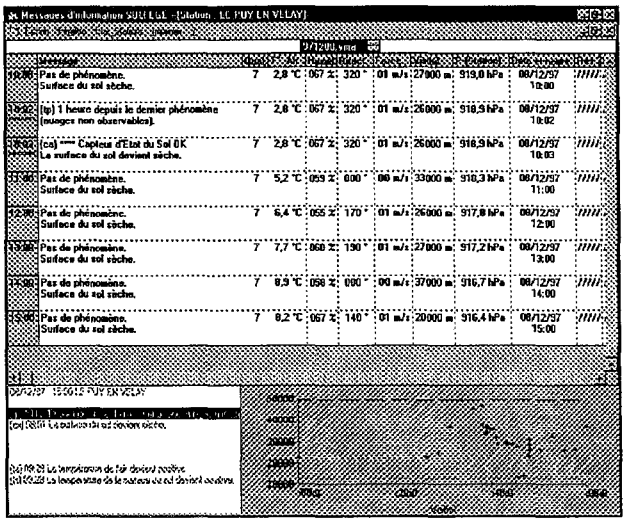

Figure 2. Poste de visualisation des messages SOLFEGE

V - METHODE ET PROTOCOLE D'EVALUATION

On se propose de faire deux évaluations, l'une technique en CDM où on compare les "sorties" SOLFEGE avec ce qui est effectivement observé à la station, l'autre effectuée en CMIR qui renseigne sur l'apport des messages SOLFEGE aux prévisionnistes éloignés du site de mesure.

Les évaluations sont effectuées au jour le jour, pratiquement en temps réel et les résultats sont consignés dans des fiches.

Les CDM comparent heure par heure (à l'heure ronde) les éléments suivants :

- Le temps sensible codé par l'observateur (table 4677) avec le temps sensible codé par SOLFEGE (table 4677) et décrit sur l'écran SOLFEGE (figure2). En cas de désaccord (codes différents), les deux codes sont notés.

Date HEURE/UTC	Temps SOLFEGE/OBS Sensible		si DESACCORD		Visibilité		si DESACCORD		Etat du sol Vemos/Plaque/Obs		si DESACCORD	
	Accord	Désaccord	PRECISER	si action N° FICHE	Accord	Desaccord	PRECISER	si action N° FICHE	Accord	Désaccord	PRECISER	si action N° FICHE
03/12/97												
04.00												
05.00		1	70/00			1	5000/10000					
06.00		1	71/72			1	5000/9000		1			
07.00		1	70/71			1	5000/10000					
08.00		1	70/68			1	5000/10000					
09.00	1				1				1			
10.00	1					1	2500/1000					
11.00	1					1	8000/5000					
12.00	1				1					1	sec/hum	
13.00	1					1	2000/5000					
14.00	1					1	2000/9000					
15.00		1	70/68			1	3000/8000			1	mou/hum	
16.00		1	70/68			1	3000/9000					
17.00												
18.00												
19.00												

Figure 3. Fiche d'évaluation journalière en CDM

- La visibilité mesurée par le visibilimètre relié à la station SOLFEGE. En cas de désaccord les deux visibilités sont notées.

- L'état du sol délivré par le capteur SOLIA relié à la station SOLFEGE. Le sol pris comme référence est celui habituellement évalué par l'observateur de la station et non celui de la plaque de SOLIA. En cas de désaccord les deux états sont notés.

En général, les observations en CDM vont de 05h à18h. L'ensemble des mesures par station fournit actuellement environ 800 comparaisons (heures).

Pour chaque type de mesure, les deux premières colonnes comptabilisent le nombre d'évènements où il y a accord ou désaccord. Puis dans une colonne "préciser" on écrit le code temps présent réellement observé / le code temps présent délivré par SOLFEGE (code temps présent Table 4677) ou la visibilité réellement observée / visibilité SOLFEGE, de même pour l'état du sol.

Pour le CMIR de Lyon, il ne s'agit pas seulement de comparer l'observation humaine avec les diagnostics de SOLFEGE mais surtout d'évaluer de façon plus subjective l'influence du réseau de l'ensemble des stations sur la prévision ou la connaissance à distance du temps sensible. Plusieurs bilans sont effectués, un le matin qui rassemble l'ensemble des messages de la nuit, un le soir pour les messages de la journée.

Les informations SOLFEGE d'évaluation du temps présent (sous forme de code), de visibilité et d'état du sol sont répertoriées de la manière suivante :

- SOLFEGE apporte t'il des informations ? :
  - justes et dans ce cas, elles modifient ou confortent l'analyse
  - douteuses
  - erronées
- Ces informations sont elles ? :
  - utiles
  - sans influence
  - néfastes

Des commentaires sont ajoutés si nécessaire. Les fiches correspondantes sont ensuite transcrites sur un fichier de type EXCEL et mises à disposition à tout moment.

Pour les CDM :

On a comptabilisé l'ensemble des accords et désaccords horaires complétés par des commentaires sur :

- le temps présent
- la visibilité
- l'état du sol

Dans les cas de désaccord, on en a précisé la nature.

Pour le CMIR :

On a comptabilisé les réponses par rubrique pour établir un bilan statistique de l'apport de SOLFEGE. (Exemple SOLFEGE apporte des informations qui confortent l'analyse dans 80% des cas).

VI - PREMIERS RESULTATS

VI.1 - Données techniques des CDM

- Etude du temps présent :

Le taux d'accord pour l'ensemble des stations se situe entre 80% et 90%.

- Etude de la visibilité :

SOLFEGE/VAMOS utilise les informations du visibilimètre en place. Celui-ci n'est pas identique dans chaque station. Il faut remarquer toutefois que le pourcentage de satisfaction pour des capteurs largement industrialisés n'est que de 90%. Ce score n'est guère meilleur que celui obtenu pour l'évaluation du temps présent.

- Etude de l'état du sol

Les résultats de bon accord se situent entre 80% et 95%. Il faut tenir compte du fait que les surfaces comparées ne sont pas équivalentes (état de surface du sol du parc instrumental et état de surface d'une plaque de référence SOLIA de 0,01 m²). L'enneigement du sol a été assez bien vu sauf lors de la formation de congères ou par vent fort lorsque la neige n'arrivait pas à s'accumuler sur la plaque. On n'observe pas de dégradation de la qualité de la mesure dans le temps.

Les résultats statistiques sont résumés dans le tableau 1 suivant:

Pourcentage d'accords	sur le WW	sur la Visibilité	sur 'état du sol
tous CDM confondus	**85**	**87**	**86**

Tableau 1. Pourcentage d'accords Observation humaine / Observation SOLFEGE

VI.2 - Bilan de l'apport SOLFEGE au CMIR

Les résultats statistiques sont résumés dans le tableau 2 suivant qui résume comment est actuellement "ressenti" SOLFEGE par les prévisionnistes régionaux.

Apport SOLFEGE		Appréciation subjective		
Conforte	Douteux ou faux	Utile	Sans influence	Néfaste
86	**14**	**17**	**80**	**5**

Tableau 2. Appréciations de l'apport SOLFEGE exprimées en %

Si on globalise l'ensemble des résultats de l'apport de SOLFEGE sur les deux premiers mois, il ressort qu'approximativement, 80% des informations sont sans influence sur la prévision qu'il s'agisse du bilan du soir ou du matin.

Le pourcentage d'informations utiles est de 15% à 20% tandis que les informations néfastes se situent entre 0% et 5%. Il est possible d'imaginer l'évolution de ces pourcentages si les données SOLFEGE n'avaient pas été entachées d'erreurs à cause des problèmes de détection des instruments de temps présent. Il est certain que les fausses alarmes génèrent la majorité des informations néfastes. En éliminant les erreurs importantes (fausses alarmes, non détection, confusion pluie/neige, ...), on peut estimer que le taux d'informations utiles passerait autour de 25%.

VII - CONCLUSION

Les premiers résultats de la phase d'évaluation sont encourageants avec un taux de qualité de 83% dans l'évaluation correcte du temps présent toutes périodes météorologiques confondues. On a pu montrer que ce taux pouvait atteindre 95% si on parvient à améliorer la qualité intrinsèque du capteur de temps présent PRECIPIA (élimination des fausses alarmes et meilleure identification des hydrométéores).
Compte tenu du fait que sous nos latitudes seulement 25% environ du temps sensible présente des épisodes d'hydrométéores en suspension ou en précipitation, un système SOLFEGE avec un instrument identifieur de précipitation plus fiable apporterait dans tous ces cas une information utile aux prévisionnistes régionaux.

VIII - REFERENCES

Duvernoy J., Gaumet J-L., 1996 Precipitating Hydrometeor Characterization by a CW Doppler Radar. *Journal of Atmospheric and Oceanic Technology.* Vol. 13, n°3, 620-629

Gaumet J-L., Salomon P., 1992 :Un nouvel instrument météorologique pour déterminer l'état du sol. *Conférence technique sur les instruments et les méthodes d'observation* (TECO-1992) *OMM* Vienne (Autriche)

METEOROLOGICAL SENSORS TO REPLACE THE OBSERVER

Olbrück, G.

Deutscher Wetterdienst
Abteilung Meßnetze und Daten, Meßsysteme
Frahmredder 95, D-22361 Hamburg 65

1.0 Introduction

The Deutscher Wetterdienst DWD started the project "Messnetz 2000" to rationalize the data receiving, processing and transmission in the surface network. The most challenging request of this enterprise is the automation of the visual and subjective observations in order to replace parts of the large staff of observers by automated systems. The preparation of specifications and the discussion of the spezialized requirements is accompanied by the development, test and evaluation of intelligent meteorological sensors. Along these lines are the tests of present weather sensors, laser ceilometers, backscatter and foreward scatter sensors beside lightning sensors and systems for the determination of the precipitation type.

The automating of the visual observations has to be carried out very carefully because we have to gain acceptance from internal and external users, that means, the forecaster and climatologist in our service has to accept the output of the new technic as well as the air traffic controller, the pilot and the users of different economic branches. Keeping this in mind, the DWD started to investigate the performance of systems which are provided by the market of today. Beside, feasibility studies the DWD has cooperations with manufac-turers accompanying developments of a lightning detector or automatic precipitation sensors.

2. Automating visual observations

2.1 Visibility

The task to replace the observer´s prevailing visibility by the information of a visibility sensor is one of the most difficult projects. The tests which have been conducted on different synoptic stations and in the test field at Hamburg demonstrated that in most cases the visibility distances of an observer and a sensor differ in a wide range. The reason for this result is the fact that the observer looks around and decides for the worst visibility sector, whereas, the sensor takes its information out of a small volume (tennis ball) at the same location.

Field tests showed that additional visibility sensors which were similarly placed did not increase the quality of visibility measuremnts significantly. So one may determine the information of a single point sensor to be representative. Nevertheless, the visibility information of a sensor does not replicate that of an observer. Therefore, the Deutscher Wetterdienst decided to place a feasibility studie on visibility measurement especially under

the condition of falling precipitation. The assessed representativeness of the information may in the end be the result of a modell calculation using the information of different parameters like temperature, humidity, light intensity, type of precipitation rain drop size distribution and the mass of solid hydrometeors.

2.2 Sky Conditions

The automatic detection of the height of cloud layers and their coverage in eighth is carried out by the laser ceilometer. Compared to the spatial averaging of an observer the data of the single laser ceilometer pointing upward have to be time averaged. For this reason thirty minutes of data are collected from a ceilometer and processed through statistical routines to form layers and to calculate the percentage of their coverage - see fig 1.

Similar to the results with some visibility sensors the comparison of the information from ceilometers in a test field stated that in most cases the results did not differ very much from each other. However, it is recognized that in low wind conditions with a small displacement of the cloud layers one ceilometer is not sufficient. The alternativ in these situations are multiple sensors or a tiltable sensor to provide a better observation.

New laser ceilometers offer the possibility to devide the information of cloud layer from precipitation hits with the help of special algorithms layed down in the processing software. Therefore, the information of the lowest cloud layer (ceiling) and its coverage is nearly garantied, whereas the detection of higher cloud layers is not complete due to loss of the small energy which is transmitted for security reasons only with 20 Watt. The detection of clouds with the laser beam needs vertical changes of the extinction coefficient. In difuse weather situations with high humidity degrees over a large vertical extension of the atmosphere (< 90 % RH) the laser detects sky clear whereas the observer encodes overcast. This technical problem in the processing software will be solved in close contact with the manufacturers.

2.3 Present Weather

Many studies which have been conducted over the last years especially the preliminary results of the WMO present weather sensor intercomparison which have been reported on the CIMO Expert Meeting on "Automation of Visual and Subjective Observations" in Paris, 14-16 May 1997, confirm that only a small proportion of the WMO table 4680 of the automatic weather code can be detected by a present weather sensor of today. There is the problem of detecting the intensity and typ of precipitation and the mixing of these types. Another question is the observation of shower or intermittent precipitation, the difference between hail and snow showers combined with rain. The test results of present weather sensors with regard to these informations are not satisfying.

Therefore, the DWD has decided to concentrate on special observation problems so for instance on an exact statement of the sensor on the type of precipitation. The Information of the precipitation intensity will be provided by automatic rain gauges operating on the weighing principle. The optical distrometer for measuring size and velocity of hydrometeors based on single particle extinction measurements is able to provide the information on

precipitation types. Today particles are detectable in the diameter range from approximately 0.3 to 10 mm having velocities of up to 10 m/s.

The advantages of low-cost distrometer measurements are that small drops down to the size of cloud drops are reliably detectable together with snow and hail particles. A 780 nm laser diode with a power of 3 mW produces a horizontal sheet of light. Particles passing through the light sheet of 160 mm by 30 mm cause a decrease of the output signal by extinction and therefore a short reduction of the initial voltage. The amplitude of the signal is a measure of particle size, the duration of the signal a measure of particle velocity.

The DWD cooperates with the development engineer in order to design a sensor which meets the requirements of an operational synoptic-climatilogical network.

2.4 Icing detector

One of the most critical informations at winter time is the icing situation starting with freezing rain up to the icing of cold grounds in a humid air. The DWD set up a feasibility study on the physics of icing detectors which had the following results - see fig. 2.

The method which meets best the requirements of an icing detector is the ultrasonic technic. The development of a ultrasonic sensor has to start from the knowledge that a spreading ultrasonic wave is interfered at a borderline. If this borderline separates a sensor block from the air the wave is reflected in situations of a plaine surface or scattered in situations of a rough surface.

If the surface of the sensor block is covered with water or ice the ultrasonic wave penetrates into the water or ice level by changing direction and energy. Reflection takes place at the borderline of the water or the ice to the air. The knowledge of the caused consequences on the reflected waves by the changes and differences of the acoustic impedance on borderlines leads to the identification of the contamination on the sensor block: water, ice, mixing of both. The study discussed different materials of the sensor block, the temperature dependence of the material and the angle under which the input and the detection of the acoustic waves are transmitted.

Today the DWD has to decide on the development of a prototyp of an icing sensor which will be installed on ground and perhaps 1 m above ground in order to detect freezing rain and ground surface icing. The ultrasonic method uses a 2 Mhz frequency detecting the conditions on the sensor surface by the measurement of the amplitude and the running time of the ultrasonic signal.

2.5 Lightning detection

A thunderstorm is one of the most significant weather events in meteorology and has ist influence on industrie, traffic and commerce. The information of a present weather sensor can only be used to report on a shower. Additional information on rain intensity and lightning is needed to find out that the observed shower is a thunderstorm. In cooperation with the manufacturer the DWD accompanied the development of two types of lightning sensors.

Electromagnetic wave detector

The electromagnetic wave detector measures the phase distance of the field strength of the electrical and magnetic signal. A small phase distance stands for a far distant lightning whereas a large phase distance near 90^0 points out a very near lightning. Local thunder-storms are detected by lightning events in a distance of 10 to 30 km, far distant lightnings are not detected. Cloud/cloud and cloud/earth discharges are measured, that means, audible and non-audible lightning events are reported. The antenna to receive the electromagnetic waves and the processing unit are installed out-doors and, therefore, they are protected against an overload.

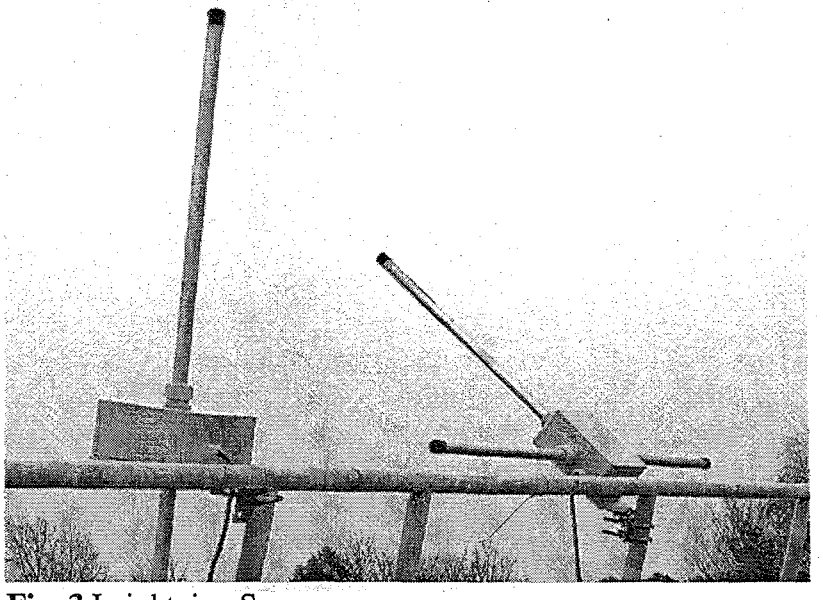

Fig. 3 Leightning Sensors

Acoustic and optical sensor

Beside the above mentioned parameters of lightnings like the field strength, the run time of the signal, its spectral composition and the phase difference a new development of a light-ning sensor with integrated optical and acoustic sensors detects also the echo and the flash light of a thunderstorm.This gives us the opportunity to decide between a weak and a strong thunderstorm.

The information of lightnings can also be taken from national or global lightning networks. But there is the difficulty to transfer the local information into the automatic weather station where the processing needs the lightning data for the decision shower or thunder-storm.

3. Outlook

The development and evaluation of new technologies will run in parallel with the enhance-ment of the actual technic. There are plans to set up additional algorithms in the area of present weather detection in order to integrate the information of a definite number of intelligent sensors. Automating the visual and subjective surface observation is also gaining acceptance by the different users, therefore, training and clear definitions of the products are needed to be understood.

EVALUATION of cloud levels with the data of Laser ceilometer according to DWD-algorithm

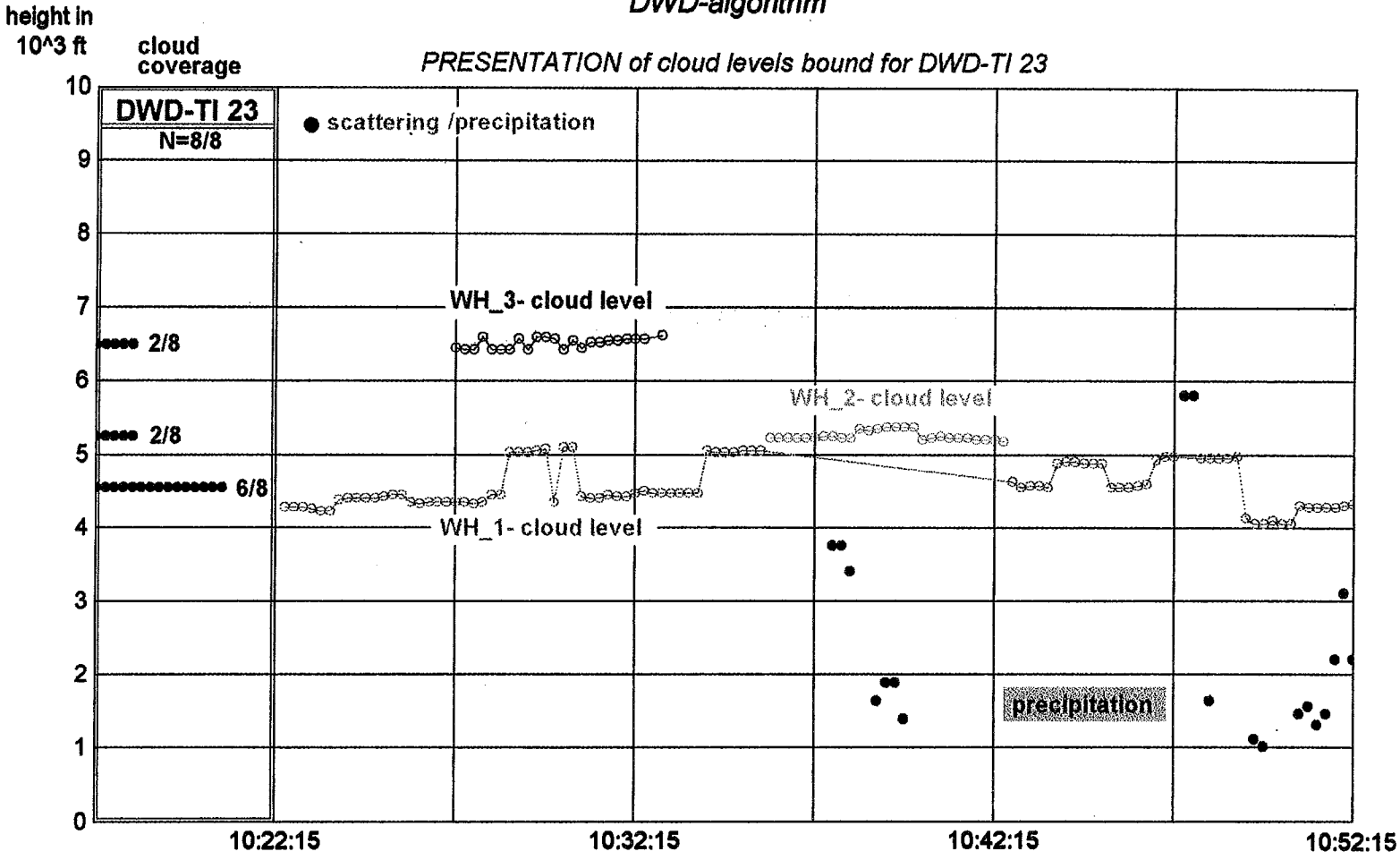

24.09.1996

DWD - Meßsysteme TI 23b

w6092407

Fig. 1

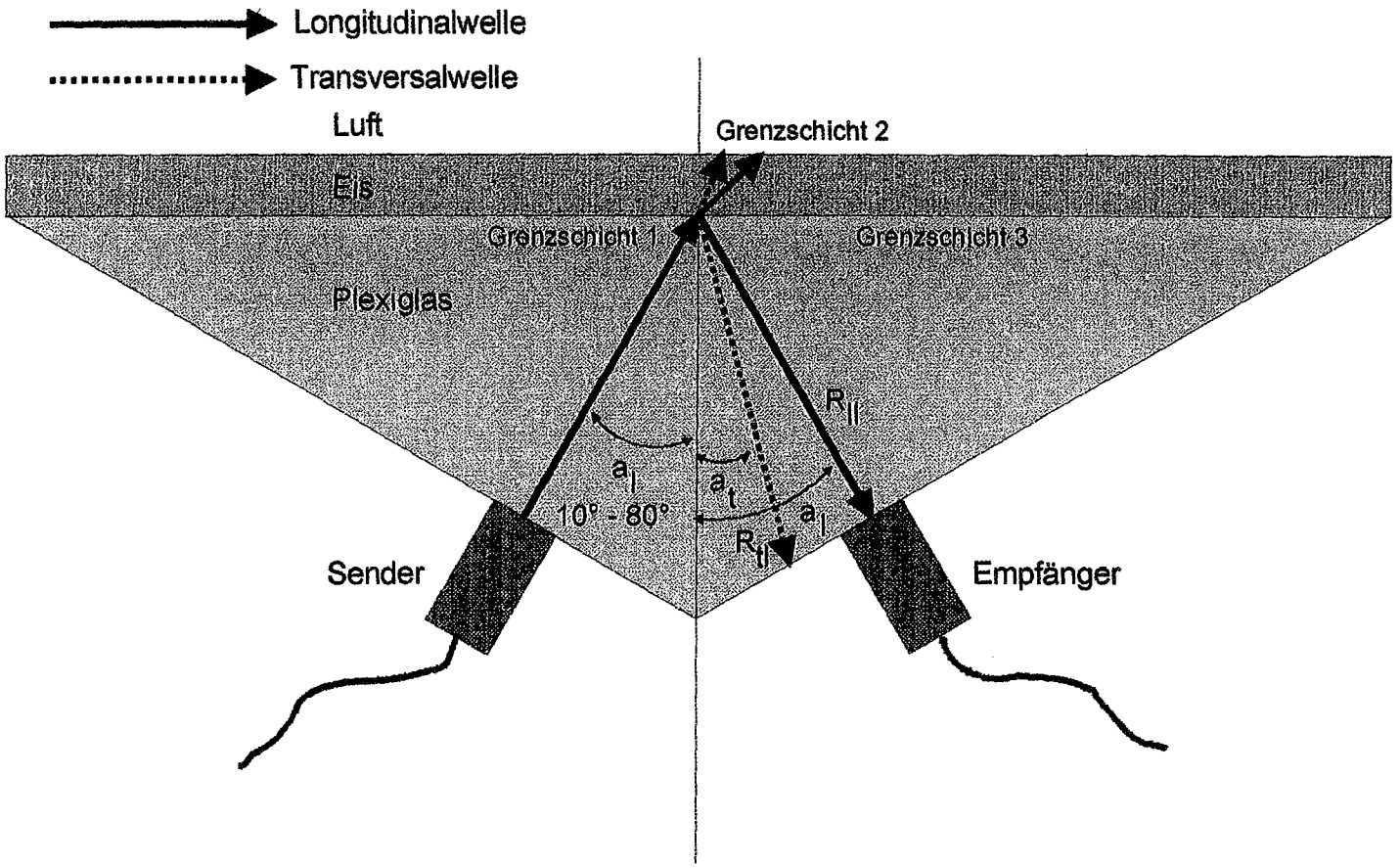

Modell für die Berechnung der Reflexionskoeffizienten von Grenzschicht 1

Fig. 2

The Remote Video Acquisition System
A Canadian Approach

by Dave Wartman and Ben Hunter
Environment Canada

INTRODUCTION

Operational weather observing programs are evolving and changing. This is particularly true in Canada where the presence of human weather observations in the hourly observing network which provides core support to Environment Canada's (EC) operational weather service is shrinking. In order to continue to meet its mandated demands and in fact expand its monitoring capacity, EC must look towards new and innovative technologies.
In response to these requirements, there is an increased emphasis placed on the role of automated weather observation stations (AWOS) which allows EC to meet budgetary requirements and expand the network for a much reduced cost. However, in some cases it is essential to augment and validate the AWOS information on a routine basis with other tools.
The Remote Video Acquisition System (RVAS) was developed to address this need.

THE REMOTE VIDEO ACQUISITION SYSTEM - PROCESS, CONFIGURATION AND ATTRIBUTES

The RVAS is a modular system first developed in the early 1990's to obtain full color video images from a remote meteorological observation site during daylight hours. The latest version, developed in-house by EC's Atlantic Region, uses commercial hardware and support software where possible.

The Process

There are two major parts to the RVAS: the "**office**" system and the "**field**" system. The **office** system, under the direct control of the user, requests and schedules images, reboots the **field** system when necessary and displays the images for review. The **field** system is used to capture images, save them on the hard disk, accept calls from the **office** system site and transmit the images as requested.

A video camera installed in outdoors-environmental housing captures images. Up to four of these cameras are installed at the observation site and pointed in different directions to allow complete field of view. The cameras are in turn connected to a personal computer which continuously captures still video images in compressed format and stores them locally. The PC also has a high speed modem and telephone line. Users, equipped with a similar PC, use the application software to initiate a telephone call to the field site and download one or several images, from the various video cameras, which are stored on the field PC. Multiple **field** sites can be accessed sequentially by the user. The frequency of these requests (calls) can be set automatically and individually for each of the **field** sites. The images are stored on the **office** system for review and are organized by site

and time. They can be converted to a number of standard formats and then viewed on standard PCs or automatically uploaded to the HP9000 HP-UX or another environment

System Components

The **office** system requires the following minimum hardware/software:

- Personal Computer - Pentium 120 with 16 mb memory, 1gb hard disk, 2 serial ports, SVGA monitor, keyboard, 28.8 baud modem, Windows95, mouse
- PC ANYWHERE (Win95) Communication Software $150

The **field** system requires the following minimum hardware/software:

- Personal Computer - 486DX-100 with 4 mb memory, 350 mb hard disk, at least 2 serial ports, VGA monitor, keyboard, 28.8 baud modem, DOS 5.0 or higher
- PC ANYWHERE (DOS) Communication software $150
- Videovue Image Capture Board and Video Switch Board (developed especially for RVAS) $800
- Optional Watch Dog Timer Circuit (developed especially for RVAS) $200
- Up to 4 video cameras, housing, mounting brackets, etc. $2300 each

RVAS Attributes

- The user has control of the **field** system through the **office** system modem and the PC ANYWHERE software. A watchdog timer resident at the **field** system is set to check communications at almost any interval desired allowing the **field** system to automatically reboot itself if necessary.
- The RVAS allows automatic retrieval of pictures from each of the individual **field** sites at a pre-set frequency. Monitoring of this automated retrieval can be done manually, with ease, through color-coded screens. Automated monitoring is also possible with an alert sent if no images are received over a pre-set time interval.
- A complete RVAS system is available at a relatively low cost, especially when compared to the potential value in augmenting an AWOS for establishing the veracity of different parameters or qualitative information about weather elements not observed by AWOS (eg. cloud type)
- The RVAS has archiving capability on the **field** system , the **office** system, or on a separate system.
- The Videovue Video Switching Board was developed especially for the RVAS and is commercially available.
- The resolution of the images from the RVAS is as high as 1024 x 786.
- The RVAS is totally Year 2000 compliant.

USE OF THE RVAS IN ATLANTIC CANADA'S WEATHER FORECAST CENTRES

There are presently **office** systems installed in each of the 3 Atlantic Canadian Weather Forecast Centres - Gander (Newfoundland), Fredericton (New Brunswick), and Halifax (Nova Scotia). There are **field** systems installed in 6 locations across the region: Churchill Falls, Burgeo, Cornerbrook and Port aux Basques (Newfoundland) and Amherst and Dartmouth (Nova Scotia).

The RVAS is used for several major purposes in the Weather Forecast Centres:

- to augment the weather information provided by the AWOS
- to validate the weather information received from the AWOS

The different situations in which the RVAS is used vary. Following are some examples of how the RVAS integrates positively with the forecast program:

- fog formation
    - illustrating the formation of patchy or shallow fog or fog over the sea or at a distance from the observation site. This is information not usually obtained from the AWOS.

- precipitation type
    - the occurrence of freezing precipitation is at times something that must be inferred from an AWOS site. The RVAS which can readily show ice accretion can be valuable in this regard.

- cloud type
    - cloud type is a parameter that is not available from the AWOS. However it can be discerned from the high quality images of the RVAS.

- low ceilings
    - at times the AWOS will indicate low ceilings with the occurrence of ice crystals even when there is no ceiling present at the site. The RVAS can aid in this situation.

- thunderstorms
    - the occurrence of thunderstorms away from the site cannot be discerned by the AWOS. However the RVAS can allow the forecaster to see the lightning strikes.

- snow depth
    - the AWOS does not provide information regarding snow depth. Through the use of several snow rulers or other measurement instruments, the snow depth at at the observation site can be estimated with RVAS.

The examples of the value added by the RVAS, as detailed above, apply to the broad spectrum of the forecast programs, including:

- Aviation Forecast Program
- Public Forecast Program
- Inshore Marine Program
- Media Broadcast Program
- Climate Program

NEXT STEPS

- Investigate the use of infrared cameras in order to extend period of coverage to a full 24 hours.
- Explore the use of tools which allow the use of 4 live video images from one sight and "panning".
- Develop software which will allow for animation of video images.

CONCLUSION

The Remote Video Acquisition System is a low-cost, reliable and highly automated tool which can provide value-added information to the operational forecast process in a variety of situations. Augmenting and validating the Automatic Weather Observing Station with RVAS during daylight hours can provide information nearly equivalent to that provided by a human observer. The effectiveness is evidenced by its use in Atlantic Canada as well as in dozens of locations through the Canadian provinces of Ontario, Alberta, Saskatchewan and Manitoba, in 5 "arctic" locations in the Canadian Northwest and Yukon Territories and in many sites through the northwestern United States.
Further information regarding the RVAS can be obtained from the following web page address:

http://www.ns.ec.gc.ca/video

or from Ben Hunter at Environment Canada (**ben.hunter@ec.gc.**ca)

Technical experiences of using a video camera to make remote weather observations

D B Hatton, D W Jones, C M Rowbottom
Meteorological Office, United Kingdom

1. INTRODUCTION

Since 1995, the UK Met Office has been exploring ways of making use of state of the art video camera technology as an aid to meteorological observers. These investigations have concentrated on using equipment primarily developed for the security market.

The initial consideration has been to enable a human to interpret camera images and to establish their usefulness.[1] Until this is proven, there is little hope in succeeding with the next step of exploring the possibilities of using a computer to interpret the images and produce an automatic observation.

2. TECHNICAL OPTIONS WIDELY AVAILABLE

2.1 VIDEO IMAGE TRANSMISSION SYSTEMS

We are used to watching broadcast quality television pictures which provide live video images. This technology relies on high speed communication links between sites, over media which are typically fibre optics or microwave. This is the ideal system which works well where the communication infrastructure is already well established. However, in order to communicate with weather stations that are often very distant from urban centres, the cost of providing a reliable wide bandwidth link rapidly rises as the separation distance increases.

Public telephone networks are capable of transmitting video images for the cost of the standard line rental and the telephone call. However, their limited bandwidth usually means that only single image transmissions (at least with useful image quality) with an update interval of a second or more are possible. Experience has shown that with the possible exception of real time precipitation, the advantages of live video are limited and it has therefore not been considered further as part of this study.

In the UK there is a well developed mass market for camera security systems. Good quality monochrome and colour video cameras are readily available at quite low cost, together with a variety of image transmission systems using data compression techniques to enable frequent picture updates at the image receiving site. The technology is continuously developing with smaller cameras and faster image transmission options being announced by the manufacturers almost every week.

The Met Office has tested two transmission systems in the past two years and both have produced images of very similar quality. Zoom lenses have been used to provide a range of views and to allow some assessment of what field of view is likely to be most useful when different subjects are being viewed. The quality of the images produced depends upon the losses due to image compression; most tests have been performed with the equipment set to give the best quality picture readily available.

Both systems were purchased from companies who normally supply the security market and were off the shelf products rather than being developed for meteorological use. Important features to note are:-

- The camera images are normally compressed in order to speed up transmission time.
- The amount of data compression can be preset. For a given system there is a visible trade off between image quality and the amount of data compression.
- Manufacturers tend to use different compression and transmission techniques so the equipment is not interchangeable between manufacturers.
- Some systems offer an option for conditional refresh, whereby only pixels that have changed are retransmitted in order to increase the rate of update from that for transmitting full video frames.
- Data were transmitted over dial up telephone lines (Public Switched Telephone Network, PSTN, or Integrated Services Digital Network, ISDN). Options for cellular telephone links are available but at present in the UK are very slow.

- The receiving equipment decompresses the data and provides images on a video monitor that are typically updated every five to ten seconds over PSTN and one to three seconds over ISDN.
- One transmitter is able to control several different cameras, each of which can be selected remotely.
- Manually operated remote control is available for moving the pan and tilt of the waterproof camera housing.
- Outputs are available for switching relays to operate equipment such as a windscreen wipers or lights.
- There are facilities for remote control of the lens zoom, focus and aperture (iris), however, there is no single manufacturer of transmissions systems, pan and tilt controllers, cameras and lenses. Integrating them can be complicated since different manufacturers use different protocols and, for example, difficulties have been experienced with obtaining remote manual iris control.
- There is a general reluctance from equipment manufacturers to provide information about the operating details of the equipment, making it difficult both to install and to evaluate its full potential. This is probably partly related to the standards required when working in security applications, and also a result of the competition among manufacturers in this fast expanding industry.

2.2 IMAGE COLLECTION

The technology used in these trials has a number of options, the use of which can have a different impact on the optimum image needed for different observational requirements.

2.2.1 Panoramic viewing

One application for cameras that has been explored is their use to produce images of the sky and the horizon to enable assessments of clouds (type and amount), and visibility. Artificial (street) lighting is quite sufficient to enable modern colour cameras to operate when observing nearby scenes but a full panorama capability is not possible at night.

- Experience has shown that a field of view for the camera lens needs to be chosen which enables sufficient sky to be visible without excessive distortion from a wide angle lens. An angle of about 50° to 60° is acceptable, which means that the camera has to pan to at least six different positions to encompass the full horizon. It also has to be pointed upwards to observe the sky, but as soon as the horizon is lost, humans have great difficulty in knowing where in the celestial dome the camera is pointing and then relating to the scale of whatever is within the field of view.
- Most cameras operate with an automatic iris setting and difficulties can be experienced on a bright day when light levels from the sky are significantly greater than those from the land. If an image includes both land and sky, the exposure will automatically adjust for one or the other depending upon the control settings in the camera. Manual control of the iris is then necessary to remotely adjust to suit the part of the image that is of interest. Having the sun in the image also makes viewing clouds in that region difficult or impossible.
- Colour images have been found to be more useful than monochrome, especially in distinguishing blue sky from a dark cloudy background, and where there are several layers of cloud. There are of course problems at night when both colour and monochrome cameras are not sensitive enough.

2.2.2 State of the ground

By using the pan, tilt, zoom and focus facilities it is also possible to view other phenomena such as present weather and the state of the ground. Interpreting images of the ground is not always easy as the colour balance due to lighting changes can alter appearances considerably. When trying to decide whether it is wet or dry the most reliable way has been to look for the presence of reflections.

2.2.3 Precipitation

When looking at panoramic views, it is rarely possible to detect precipitation on single frames. With '*live*' pictures it is sometimes possible, in certain lighting conditions, for the precipitation to be detected against the background by the change between successive frames and it may also be possible to see splashing on puddles when viewed at exactly the right angle. However, the systems under test did not have a full live

transmission capability; live images could only be studied in local mode. If individual frames from a live recording are viewed it soon becomes apparent that sometimes only one in ten show a splash during light rain, the remainder show either a smooth surface or ripples that could just be due to the wind. With transmitted frames only being updated every second or two, the chances of capturing a splash are quite low, and it becomes quite difficult to positively identify precipitation.

The most reliable way to detect rain has been to point the camera into wind and observe the water droplets on the window of the waterproof housing[1], however this is time consuming and doesn't work in light winds! However, the idea of using a transparent screen to collect precipitation is being explored.

Since all the transmitters that have been evaluated can accept several camera inputs, a better way of viewing precipitation has been to dedicate a second camera for this purpose. By using a dark uniform background, focusing in the near field, and providing suitable illumination, it has been possible to capture images with contrasting precipitation, by day and by night. A manually controlled iris is preferable to keep the background 'dark' and the camera exposed correctly for reflections or refractions of artificial light by the precipitation. The need for colour is less important, and work is now underway to see whether it is possible to use infra red light, or synchronised flash light for illumination of objects within a well defined, focused field of view.

3. FUTURE DEVELOPMENTS

3.1 THE EQUIPMENT AND SUPPLIERS

The use of video camera images to augment present weather observations has been shown to provide useful information to observers and forecasters during daylight hours.[1] The technology used in cameras and lenses is now adequate, with a wide range of makes and types readily available to suit any daytime application. However, the recent developments in digital camera technology may mean that they become more suitable than video cameras since the current applications detailed above are in effect using video cameras in a still image collection mode. Digital cameras also have the advantage of easier flash synchronisation and easier interfacing to a PC.

As previously explained, much of the work undertaken by the Met Office has been based on systems developed for the security market. There are *drawbacks* resulting from this:-

- The difficulty in adapting systems to anything that isn't completely standard.
- With the systems tested, it is not possible to gain access to the digital images after transmission, and so they are less suitable for computer analysis.
- Security equipment is normally supplied (in the UK) only through approved distributors who are generally security system installers. These people do have the advantage of knowing what is currently available from a range of manufacturers, but they are not normally in a position to discuss reliably the future developments for specific equipment. Experience has also shown that they do not have sufficient technical understanding of the equipment they are selling to enable them to deal with non standard applications.
- The manufacturers themselves have tended to be difficult to communicate with, and for the relatively small number of systems likely to be needed in the meteorological market there is little incentive for them start developing special products.

The *advantages* of using security systems have been:-

- The good choice of equipment.
- Low development costs.

The signs are that without further development of security equipment away from its intended design, it may never really be suitable for meteorological applications, especially automatic image collection.

It is notable that even in the two years that this study has been underway there have been significant developments in PC performance and their capability for image collection and processing. The authors feel that this is the way of the future.

3.2 IMAGE COLLECTION AND ANALYSIS

Time is an important factor when making manual remote observations; trials[1] have shown that it can take a person 10 minutes to manipulate a remote camera and make an observation. This process could be speeded up by carrying out automatic collection of images at the camera site particularly if this was under PC control. This would make it possible for the user to:-

- Access all the images from a desktop PC rather than through a separate controller/display.
- Control the camera and receive images via the Internet, though this might be too slow or unreliable for operational use.
- Have 'intelligent' iris control optimised separately for different parts of the image.
- Set a camera to automatically pan and tilt to preset positions, and so build up a whole sky and horizon scene, with images stored ready for immediate transmission when interrogated.
- Consider collecting fewer images using a wide angle lens, at a high resolution and apply mathematical corrections for distortion of wide angle lenses so that images match those expected by the human eye without a camera.
- Fit overlays to the video image to give the operator direction of view, heights of distant mountains, or visibility points for example.
- Remain as flexible as possible to enable future requirements to be met with minimum change to the system.

Images could be processed either at the remote camera PC or in the collection PC so that they are ready for immediate viewing by an operator.

Another important though perhaps longer term development is the use of the computer and for example neural network techniques, to analyse the images and recognise present weather phenomena such as cloud types, cloud amounts, visibility, precipitation type and precipitation intensity.

In theory anything that the human eye can define could be automated, but such techniques are likely to take some years to perfect.

3.3 NIGHT TIME OPERATION

This is probably our greatest challenge. Flood lighting and certain specific lighting configurations will enable local features such as state of the ground, or precipitation to be detected. However, panoramic viewing necessary for a full observation is not yet possible.

Image intensifiers have been tested but at present have severe drawbacks since they do not have the required resolution during overcast or moonless nights, and they are not able to distinguish clouds reliably. They also need to be carefully protected from permanent 'burn' damage caused by staring at individual lights and from operation in daylight conditions which causes rapid ageing. This would result in loss of sensitivity and increases in noise levels.

Infra red images may be an alternative. However, although monochrome cameras are sensitive into the near infra red, there is still not sufficient natural illumination available at night. Radiometers may be used to measure the temperature difference between cloud and clear sky to establish cloud cover, at least for low and medium height cloud. Specialised radiometers exist that will do this job, but at present they are very expensive and do not really come into the category of 'video cameras'. We will have to wait for technology and the development of modern materials to catch up.

4. REFERENCES

Operational experiences in the use of video camera images to augment present weather observations - C M Rowbottom, D B Hatton, D W Jones, WMO Instruments and Observing Methods Report, TECO-98, May 1998.

Operational Experiences in the Use of Video Camera Images to Augment Present Weather Observations

C M Rowbottom, D B Hatton and D W Jones
Meteorological Office, United Kingdom

1. Introduction

The UK Meteorological Office has been investigating the use of Closed Circuit Television (CCTV) cameras to meet observation and forecast requirements for monitoring the weather on remote sites. The aims are to automate and provide additional observations from data sparse areas and to provide information for short range forecasting and for site specific forecasting, e.g. forecasting for military low flying areas.

Trials of the system were started in spring 1997 with colour cameras installed at Eskdalemuir and Hemsby (manned observing stations), at Loch Glascarnoch and Plymouth (automatic weather stations) and at Bala (no independent weather observations). Loch Glascarnoch and Bala are situated in military aircraft low flying areas. At the receiving sites (shown on the map) users viewed the camera images as a series of still frames updated every 2-3 seconds and were able to control the cameras remotely.[1]

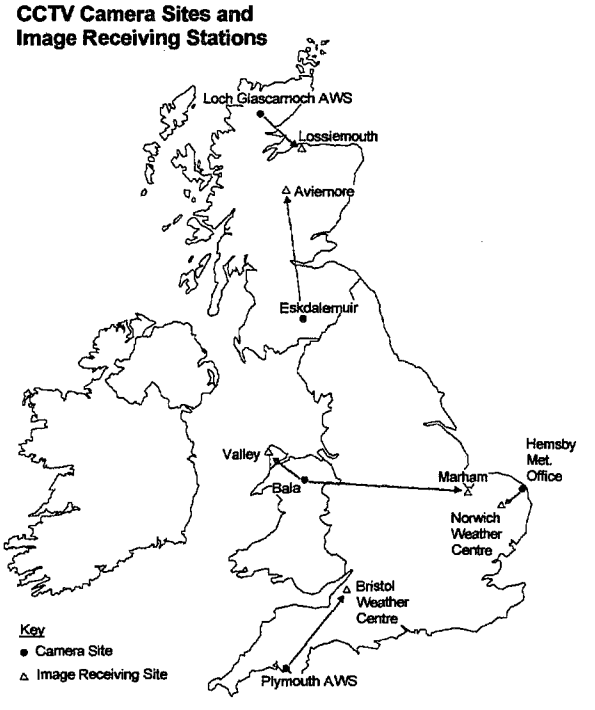

The objectives of the trials were:-

1. To determine the usefulness of CCTV images in identifying present weather, in particular precipitation.
2. To determine how well cloud type and amount can be identified from a CCTV image.
3. To compare the accuracy of visibilities reported from camera images with visibility sensors.
4. To determine which ground states can be distinguished from a CCTV image.
5. To estimate the potential usefulness of CCTV images in aiding a forecaster with responsibility for a remote site.
6. To identify methods of incorporating data from camera images into automatic synoptic reports.
7. To assess the number of camera observations that can be done within the observation period.
8. To determine if image processing could be used to automate the process of recognising the weather and reporting the correct code.
9. To determine if information from the camera could be used to improve present weather algorithms.
10. To investigate the practicalities of installing and maintaining CCTV systems and assess the reliability of hardware.

2. Results[2,3,4]

2.1 Present Weather Table 1 compares the present weather identified from the CCTV image with that reported by the observer. The number of times the present weather could not be detected on the image is also shown. Very few state of sky changes were recorded because they are not usually considered significant enough to be transmitted in the synoptic report. The table clearly shows that CCTV images did give useful information about present weather on a remote site when it was detected.

Table 1 - Reported Present Weather Codes (WMO 4677)

Present Weather Reported by Observer			Present Weather Reported using CCTV																														
			No Precipitation on site at the time of Observation											Events during preceding hour				Fog			Drizzle			Rain					Showers	No Report
			1	2	3	4	5	8	10	11	15	16		21	25	28	29	42	44	46	51	55	58	60	61	62	63	65	80	
		1	5	4																				1						14
	No ppn	2	1	5																										12
	on site	3	1	4	1																									4
	at the	5				1	78	1	16															2						86
	time of	10					1		8					2																4
	Obs.	11								2																				
		14																												1
		15		3								1			3															7
		16																												3
		17																												1
		20							2															1	2	1				2
	Events	21		1			6							15										4	2					15
	during	22																												3
	preceding	25		1										1	5															23
	hour	27										1																		2
		28							5							5														2
		29												2	2															1
		40					2																							
	Fog	42																1		1										
		43																1												
		44																	1											
		46					1												1	1										
		47																		1										
		50							4																					1
	Drizzle	51																							1					
		53																			1									
		58							2															2	7		2			
		59																								1				
		60	1				4		2					3	2									8	4				3	9
	Rain	61	2				2							1										3	11				1	1
		62																							1		1			
		63																							2		5			1
		65																										1		1
		67																												1
		80																					1						2	9
	Showers	81																											1	
		87													1															
		92															1													
		95																						1			1		1	
		96																											1	

Corresponding Codes

Note: Users found the most successful method for detecting precipitation was to point the camera into the wind and watch the droplets fall on the camera housing window!

There were discrepancies in the following types of report:-

- Characteristic changes in the state of the sky
- Events occurring within the previous hour
- Changes in visibility within the previous hour
- Identifying precipitation as continuous, intermittent or showery

However, this can be expected because of the limited periods of time that users were able to spend looking at the video images.

The main shortcomings in identifying present weather were:-

- Only 42% of the haze reports were correctly identified and 47% were unreported (Code fig. 5).
- Precipitation 'not at the station' was not visible using the cameras (Code figs. 15 and 16).
- Distinguishing whether the sky above fog was visible or obscured was difficult (Code figs. 40-47).
- Drizzle and slight rain were very difficult to detect using CCTV cameras and interpreted as mist on a few occasions (Code figs. 50-57 and 60-61). Rain and drizzle in combination, and moderate and heavy rain were easier to detect but estimating the rate was not always accurate (Code figs. 58-59 and 62-67).
- Thunderstorms (Code figs. 95-99) cannot be detected using CCTV alone, though the precipitation type reported with thunderstorms during this trial was usually correct.

2.2 Cloud The ease with which cloud type and amount was identified depended on the general weather conditions. When there was a high level of contrast between sky and cloud or when there was only a single cloud layer, identification was relatively simple. However on hazy days when there was low contrast or when there were large amounts of cloud in multiple layers, it was much more difficult. The majority of cloud, particularly low level clouds, was correctly identified.

The presence of a ceilometer on some camera sites made distinguishing types such as Cumulus from Altocumulus much easier. When there was full cloud cover there were occasions when it was difficult to distinguish Stratocumulus from Cumulus, and Stratocumulus from Stratus. Distinguishing thin Cirrus from blue sky or thin Cirrostratus also caused a few problems. Identifying the species and variety within each cloud genus was only accurate on a few occasions.

93% of total cloud amounts were correctly estimated to within 2 oktas or less. Very small amounts (< 1okta) were unlikely to be detected. Observers on site reported more cloud layers than those using the cameras. CCTV users also tended to overestimate the amount of cloud in lower layers and correspondingly underestimate the amount in higher layers.

2.3 Visibility CCTV cameras were not as accurate as visibility sensors but were useful to determine whether the visibility was typical of the whole area.

2.4 State of the Ground CCTV users felt confident in identifying ground state if the ground was covered in frost or snow. However, they were not always able to reliably distinguish between more subtle conditions, including the differences between dry, moist and wet.

2.5 Forecasting Tool Forecasters reported that CCTV provided useful information when placed strategically in data sparse areas. In the low flying areas cameras were proved to be a cost effective investment; a number of military flights were cancelled due to weather conditions in the low flying area that could only be seen on the CCTV image and were not reported from any other meteorological station in the region.

2.6 Image Analysis Until automatic image analysis has been developed the only method of incorporating data from camera images into automatic synoptic reports is by human interpretation and data processing. With the systems under trial at Bristol and Norwich, data can be added at the image receiving stations and the full synoptic report forwarded to the Bracknell telecommunications hub.

2.7 Data Enhancement Users were unanimous in confirming that co-location of the camera with other meteorological observing systems i.e. AWS and a knowledge of regional conditions made the interpretation of CCTV images simpler and quicker. Once proficient in the use of the camera system, it took 10 minutes to supplement and correct an automatic observation with visual data from the camera image.

2.8 Automatic Image Processing During the trial, work was concentrated on producing an image (particularly of precipitation) which was recognisable to a human operator. The trial did not reach the stage where automation of the process was possible.

2.9 Present Weather Algorithms It is expected that camera information will be used to improve present weather algorithms when the process of analysing the image and producing a present weather code has been automated. However codes for present weather other than 4677 e.g. 4680 or BUFR will be more appropriate for both CCTV and algorithm reports.

2.10 Technical Considerations The system chosen was a standard off the shelf security system. It was simple to install and use, and has been very reliable. The use of colour cameras was essential for identifying cloud and ground state but restricted operational use of the system to between approximately an hour before dawn to an hour after dusk.[1]

3. Conclusions

The use of CCTV camera images to meet requirements for observations and information for forecasters has been very successful. In particular, forecasters supplying short range forecasts to the military and to customers in other data sparse areas have found it most useful. Whilst not providing the level of detail available from a human observation it does provide useful information not currently available from automatic weather stations.
Work will continue to

- improve the detection and identification of present weather
- enable the system to be utilised during hours of darkness
- fully automate the CCTV process

Stations receiving images have requested the systems are left in at the end of the trial and there are plans to expand the number of CCTV systems across the UK, to meet the requirements for observations and from our increasingly diverse number of users.

4. References

1. Technical Experiences of Using a Video Camera to Make Remote Weather Observations - D B Hatton, D W Jones and C M Rowbottom, WMO Instruments and Observing Methods Report, TECO-98, May 1998
2. Present Weather Camera Project Feasibility Study - C Rowbottom, Met. Office Observations (Land) Technical Report No. 9.
3. Present Weather Camera Project - C Rowbottom, Met. Office Observations (Land) Technical Report No. 13.
4. Military Low Flying CCTV Project - I Cameron, Met Office Defence Provision Report.

Session IX

AUTOMATION OF SURFACE OBSERVATIONS

Canadian AWOS Evolution

Earle Robinson
Atmospheric Environment Service, Canada

Background:

The Canadian automatic weather station networks have continued to evolve from data logger applications for measuring basic parameters as observer aids; through remote, harsh environmental, low power applications to fill in the gaps in measurement where people do not exist; to complex systems at Canadian airports to replace human observers. The evolution has been largely cost driven due to decreasing resources to support these programs in Canada.

Each technological transition has lead to improvements in performance, increased flexibility and diversity in application, reductions in production and operating costs, increases in reliability and faster maintenance response.

In 1980 the AES introduced a multiprocessor system architecture known as READAC (Remote Environmental Automatic Data Acquisition Concept (1)) which was based on a distributed microcontroller technology. This system has been the backbone of the Canadian high-end automatic weather stations since then and it has gone through various stages of evolution which will be described in this paper. The current system, called AWOS (Automatic Weather Observing System), has lead to significant reductions in: investments for non-recurring engineering (NRE), time to market for feature enhancements and field upgrades, as well as in operational configuration management overheads.

Initial Considerations:

When we think of data acquisition systems, we generally consider a system configuration, such as shown in Figure 1, in which various sensors are connected to a generalized data acquisition system through appropriate interfaces which are compatible with each sensor type. These inputs would likely be a combination of analogue, parallel digital or serial digital signals. Analogue signals may be voltages, currents or frequencies among others (2). Parallel digital signals are typically binary or binary coded decimal (BCD) with typical logic levels of 5 volts or 3.3 volts. Serial digital inputs tend to be character oriented, such as ASCII data, in various signal modes such as; RS232, RS422, RS485, current loop, modem V.23, Bell 202 or others.

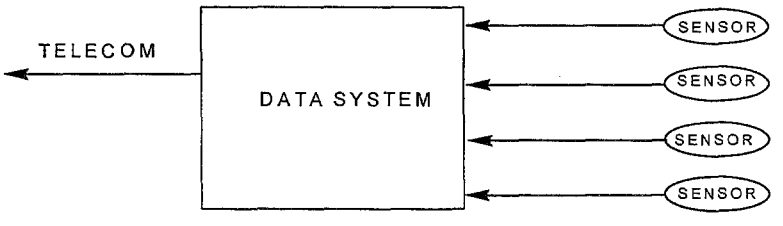

Figure 1 - Generalized Data Acquisition System

The "system" then acquires data from each sensor, performs some processing (data smoothing, averaging, conversion into engineering units...) and reports the data message via a communications medium or stores the data locally for later retrieval. Although today this is quite simplistic, it serves to emphasize the single processor or tightly coupled architectural concepts and limitations.

In tightly coupled architectures, as the system complexity increases, the incremental cost of adding a parameter of equivalent complexity increases non-linearly, as conceptually shown in Figure 2. More complex applications become entangled in sensor sampling, processing or timing considerations and real-time telecommunications overheads which must be merged into effective single operating systems. The incremental cost (C) includes the cost of design of the change (K) and a redesign cost to the initial system (B) to add the change. There is also a retrofit cost to *each* system (A), which excludes the procurement cost. This NRE cost can be approximated by $C = (K+NA)X + BX^2$, where N is the number of systems. Eventually the cost of incremental change prohibits further system enhancement as the processing capacity approaches its limit or the required budget approaches financial bounds. B is conservative at X^2.

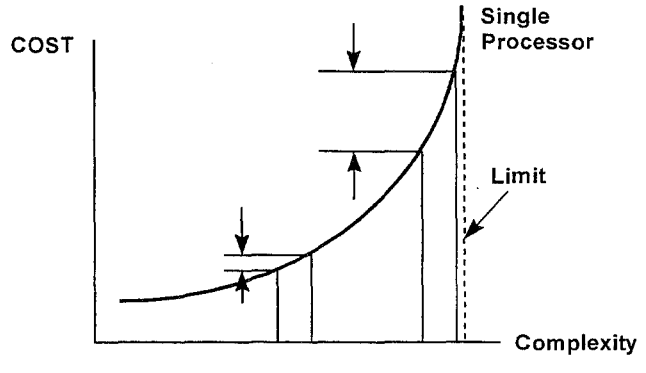

Figure 2 - Incremental development costs for tightly coupled architectures

Other practical considerations must be included when choosing system architectures for long term national networks such as radio frequency (RF) interference protection, RF emissions standards, electromagnetic interference and surge protection against lightning strikes, shock hazard, corrosion, connector keying for ease of installation or maintenance and a plethora of other field installation and maintenance considerations.

The AWOS architecture, as first introduced, illustrated in Figure 3, was designed to include solutions to these issues. It defined functional tasks and used standard, normalized protocols between modules which functionally isolated each module from the overall system design. This permitted the engineering design of each module to be broken into small, manageable tasks. The unique Peripheral Interfaces (PI) were completely self-contained thereby simplifying individual sensor connectivity and EMI protection solutions. System data collation was accomplished in the Shelf Controller with no data processing permitted at this level. Only simple message grouping was performed here for a variety of data types. System reconfiguration was automatic, requiring no insitu NRE effort when adding new parameters or features.

Telecommunications overheads were functionally isolated from the central collection tasks and completely self-contained in the Communications Controller module.

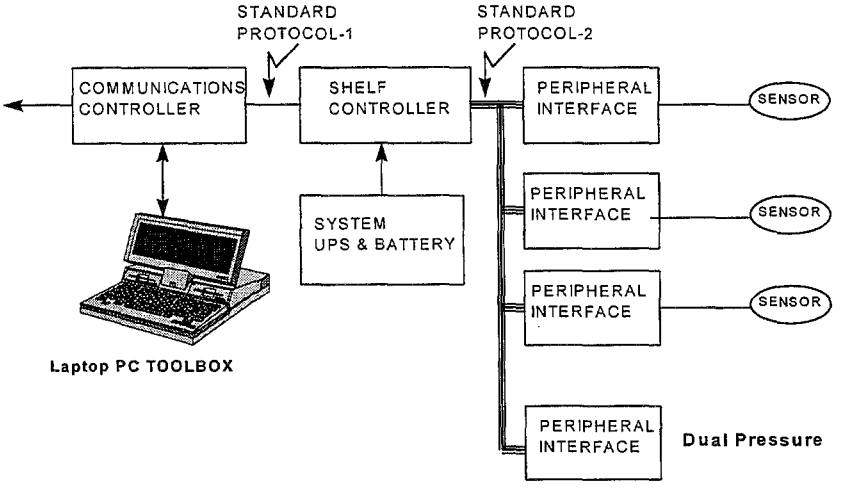

Figure 3 - Canadian AWOS Architecture

In a multiprocessor, loosely coupled architecture, since functional independence has been established for modules, variables A and B become zero, hence the NRE cost for incremental change is approximated by **C = KX**. The incremental NRE cost of adding a parameter of equivalent complexity increases linearly with overall system complexity and the system does not approach a limit due to processor capacity, as illustrated in Figure 4. There is, however, a real limit to the number of parameters which can be added by the physical design. This limit was set at 30 modules in the AWOS, where each module has the capacity to report a variety of *related* parameters. For example, a pressure Peripheral Interface can report station pressure, altimeter and mean sea level pressure which are all related to the pressure data. For our high-end national networks, since the requirements are not constant and the user expectations usually exceed current system capabilities, this linear incremental cost characteristic is critical to cost effective, long term system evolution. This is especially true when using automatic systems as alternatives for human observations.

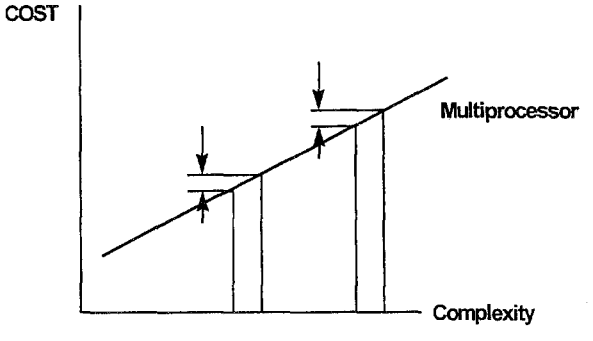

Figure 4 - Incremental development costs for loosely coupled architectures

Technology Availability Considerations:

Long term availability of technology is another critical factor when choosing system architectures. A typical technology availability ("bathtub") curve for the electronic component industries is illustrated in Figure 5. When new devices are first introduced they are in short supply and expensive. As the device becomes more widely known, and accepted, in the design industries several sources of supply come online for the manufacturing industries and the prices drop significantly. T1 is the first point of actual manufacturing availability for new products.

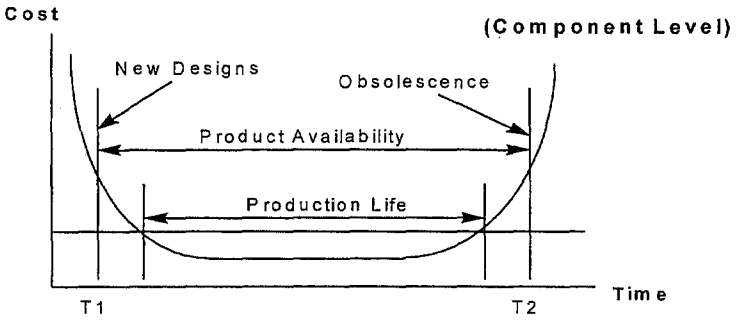

Figure 5 - Technology Bathtub Curve

When the device is in full production, the cost curve typically flattens throughout its production life. Later in the technology cycle, as newer devices become available and sales drop off for this technology, the prices begin to rise. At this point some of the manufacturing plants cease production and the supply drops thereby pushing prices even higher. When T2 is reached, all production has ceased and the only components available are those which are still within the distribution industry's inventory or those held by astute network managers who have procured enough spares to ensure that their life cycle requirements will be met. The interval between T1 and T2 depends on the component category but for common parts it is typically 10 to 15 years. For large scale integration (LSI) parts this interval can be less than 5 years.

In 1988, the AWOS technology was upgraded to CHMOS technologies with generic PI designs which were then programmed for full compatibility with existing modules. This extended the projected procurement life of the network by 10 to 15 years while further reducing costs and adding enhanced features for a low incremental NRE cost. These new modules were used with newer generation sensors to further enhance the AWOS performance. In 1996, a further redesign was initiated to add even more features including flash memory for remote software upgrades, high density RAM for data archiving and reprogrammable gate array logic which will permit significant field hardware changes through software uploads without opening a module. This adds much more flexibility to standard modules to take advantage of emerging sensor technologies. Surface mount technologies and multilayer printed-circuit boards were used for compatibility with new manufacturing practices and to meet tighter evolving EMI restrictions.

Commercial Realities:

Manufacturing industries provide a variety of board sets as well as complete data acquisition systems which are also based on these components. The length of the bathtub curve for commercial board sets is only 5 to 10 years, typically, and even shorter for system level equipment. This must be carefully considered in the network planning processes. For example, when system level equipment is purchased for networks, due to much shorter availability curves, it requires program managers to procure complete networks in a short time, including spares. This is neither pragmatic for implementation staff nor feasible for corporate financiers or telecommunications support infrastructures. It also makes long term technical system evolution strategies dubious and costly replacement strategies more likely.

Another factor which must be well understood by network planners is the technological state of the industry for system level products. Figure 6 illustrates a typical inverse relationship with commercial system suppliers versus system complexity. As the product complexity increases, the number of manufacturers drops off rapidly since sales and marketing strategies in these industries are linked to and prefer higher volume applications. When a certain complexity is reached (X), although there are commercial suppliers which claim product availability, there is always a "custom" element to these products which must be handled through NRE contracts. As the industries evolve, so do the requirements, so the gap between requirements and commercial availability continues for the high-end applications.

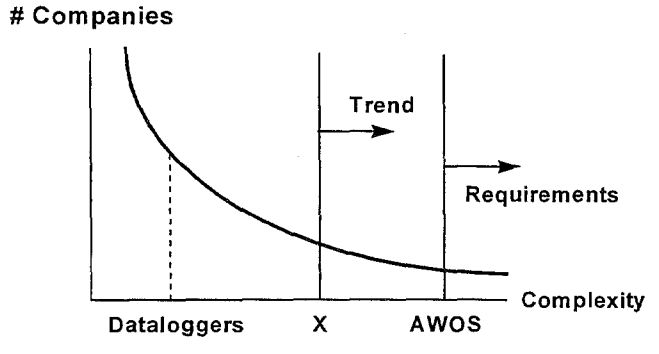

Figure 6 - Industrial Product Realities

AWOS Front-End Processors:

For high speed sampling and/or more complex processing at some sensors (3) or to meet increasing AWOS requirements for long line sensor remoting, or for economies of implementation, a series of front-end processors (FEP) were developed which mount directly at the sensors. These devices have been designed for low temperature operation with wide tolerances on DC power. These FEP's have also been standardized for serial digital, ASCII communications using low cost current loop methods which can be remotely connected to lines of up to 16 km. in length.

This FEP evolution has created smart sensors which significantly improve fast insitu processing for specific sensors such as complex FFT algorithms for precipitation detection and typing or wind pumping removal for shaft encoder applications for total precipitation. Simple FEP designs have also been created for temperature and dewpoint sensors, for example, to create low cost digital solutions for these analogue parameters as well as improving remoting options. FEP concepts have also been used for vector processing of wind information in the sensor head for many years.

AWOS Multiparameter Algorithms:

As AWOS moved more into human observer replacement modes the processing requirements became more complex. Multiparameter algorithms were developed to utilize shared raw data from other PI's. These algorithms have evolved through operational comparison studies with human observers, human observing practices and observed weaknesses in existing sensors and algorithms. Monitoring the presence, duration and rate of ice accretion along with air temperature during precipitation events, for example, permits the effective reporting of freezing drizzle and freezing rain with a high degree of confidence and low false alarms.

Some of the multiparameter algorithm work was necessary to deal with undesirable sensor characteristics and performance limitations. For example, laser ceilometer performance in precipitation events is degraded so using the presence of precipitation, precipitation type and visibility to selectively process the cloud data significantly improves probability of detection and reduces errors. Intensive field testing (4) and intercomparison studies (5) have proven multiparameter algorithm viability and limitations.

Default modes are built into these algorithms to follow a hierarchy of algorithm decisions in the event that a parameter is not available within a specific configuration. Diagnostic codes are also provided to advise operational staff of reduced functionality in these cases. The capacity of the AWOS to share data between PI modules, while maintaining functional independence, has been a powerful feature of the AWOS architecture.

Future AWOS Evolution:

With the industrial trend towards digital smart sensors which use new low cost microprocessor technologies, the AWOS FEP and PI algorithms will likely be merged in the future while maintaining full system compatibility. It is critical to ensure that parameter sharing capabilities continue in these new systems.

Higher speed inter-module communications will be required as new data groups are defined. More complex diagnostic tools will need to be developed to identify and resolve system problems quickly and effectively. Network telecommunications will need serious review as faster access and shorter temporal granularity become expected. We should expect new METAR code groups to be defined for probable data enhancements which will become technologically feasible and could enhance aviation safety.

The complex decision processes involved in human replacement strategies are forecast to include much more complex and integrated man/machine mix applications at major airports. New graphical displays in the future should provide humans with live, high resolution data on existing and new parameters as AWOS and sensor technologies evolve. Further investments into these diverse AWOS applications should rise to meet these challenges.

References:

(1) Robinson, C.E. (1980). "Automatic Weather Stations - Anatomy of a Concept". WMO Technical Conference on Evolution and Standardization of Observing Techniques in Light of Automation, Sept. 1980. Norkoping, Sweden.

(2) Robinson, C.E. (1981). "Microprocessors in Instrumentation". Second WMO Technical Conference on Instruments and Methods of Observation, October 1981. Mexico City, Mexico.

(3) B.E Sheppard and K.K. Wu (1985). "An Improved AES Precipitation Occurrence Sensor System". Third WMO Technical Conference on Instruments and Methods of Observation, July 1985. Ottawa, Canada.

(4) W. Peter Bowman and Roger Van Cauwenberghe (1985). "The READAC Field Test". Third WMO Technical Conference on Instruments and Methods of Observation, July 1985. Ottawa, Canada.

(5) Micheal Crowe, André Giguere, Stu McNair (1998). "AWOS Performance Evaluation Data Analysis Results". 78th American Meteorological Society, January 1998. Phoenix, Arizona, USA.

EXPERIENCES FROM A FULLY AUTOMATED OBSERVATION NETWORK, TWO YEARS OF OPERATIONAL USE

Britt Frankenberg and Ture Hovberg
Swedish Meteorological and Hydrological Institute (SMHI), Sweden

1 Introduction

During 1995, SMHI installed 115 new automatic weather stations. This was accomplished in a large project called OBS2000. The major goal of the project was to rationalize by automating the synoptic weather observations.

This automatic station network has now been in operational use for two years. SMHI operates the network with its own personnel in every aspect, by conducting service and maintenance, calibrations and programming of the automatic data collection unit.

In this presentation, experiences from these two years will be summarized, concerning quality assurance, cost efficiency, service and maintenance experiences and co-operation with data users and suppliers.

2 Quality assurance

Already during the installation of the 115 new automatic weather stations, the quality assurance work was thorough. This work laid the ground for the regular quality assurance work connected to these stations. The quality assurance within the daily maintenance and calibration work, is now built on the following main blocks:

1 Self-diagnostic equipment and automatic alarms
2 A register to follow up the equipment performance
3 Detailed working instructions
4 Continuous education of the technical staff

This quality assurance work is a part of the overall quality thinking at SMHI.

Ideas on how to implement the quality thinking in *practise*, have been obtained from the well known method within the production industry, called Total Productivity Maintenance (TPM).

2.1 Self-diagnostic equipment and automatic alarms

The automatic weather station used is a Milos500 from Vaisala Oy. The algorithms for measuring and calculating the parameters the data users request, have been implemented by our own staff at SMHI. Both the automatic weather station and some of the sensors used, run their own self-diagnostics and send alarms when there is something wrong. For the simplier sensors special alarm criteria have been implemented together with the measurement algorithms.

Data is collected from all the 115 stations via the switched telephone network every hour. The messages sent, contain both the measured parameters and the possible alarms. The alarms are automatically distributed via the system for collecting data to the maintenance

department. The alarms are then analysed by calling the alarming stations and reading service parameters on-line, before sending a service technician out to the station.

2.2 A register to follow up the performance

All information about every station is stored in a data base. The database is implemented in the data base software Access, with a user-friendly interface, and is used in the every day work of SMHI's technical staff, even in field conditions.

The database has tables for registering information about:

- the physical station e.g. site, position, telephone number and addresses.
- the location of each instrument and when it is moved to another station.
- every single measure taken for every piece of equipment, both concerning maintenance and calibration work.
- the program versions installed in each sensor and automatic station.
- the necessary documentation for the equipment.

The equipment performance is followed up by using the facilities of this database. The information obtained makes it possible to operate the station network in a more and more cost efficient way. For example:

- by studying the drift of the instruments between the calibrations, the interval between the calibrations can perhaps be prolonged.
- by tracking repetitive faults, the equipment performance can be improved in co-operation with the manufacturer.
- by analysing the faults, the routines for preventive maintenance can be improved.
- by keeping track of faults and how to solve them, the technicians learn more.
- the results give feed-back to the technical staff, which improve their motivation and responsibility.

2.3 Detailed working instructions

Since all the new stations have the same type of instruments and are built in exactly the same way, it has been possible to write instructions for the main part of the regular work done with the instruments. In these instructions SMHI´s working routines for these stations are combined with the useful parts of the technical manuals for each piece of equipment. The purpose of the instructions is to assure that the known work is done in the same way by every technician at every station. The instructions are easy to use and suited for the reader.

The development of these instructions have been accomplished more or less in field conditions, i.e. they have been worked with and revised by the technicians themselves while being at site doing maintenance work, and they are still improved bit by bit as the general knowledge of the technicians grows.

2.4 Education of the technical staff

During the introduction of the new equipment used at the stations, education was performed for those involved in the practical work, both at the manufacturer and by arranging our own courses at SMHI.

The education continues more or less automatically by self-learning, both through the follow-up of the maintenance work using the register and by improving the routines and

instructions as the practical experience grows. These two tools, the documented instructions and the register, make the development of competence natural and easy.

3 Economical results

The first period of operational use of these stations, has been evaluated both economically and technically, to see to what cost and what quality SMHI can run these stations. The cost of the maintenance work done at each station has then been studied. When the cost of the rest of the work done at SMHI to run these stations is included, the result is that the rationalization goal (a 20 % reduction of the annual cost for the whole network) is accomplished.

The economical evaluation also showed that running the network within SMHI is cost efficient, especially concerning the following important aspects:

- The economical benefits from using an external contractor for the maintenance, would only be a reduction of the cost for travelling to the stations. This cost only constitute < 5% of the total annual cost for the network.
- It will be practically more difficult and more expensive for a contractor to maintain the level of technical competence SMHI demand to run these stations.
- The benefits from daily contact between the network operators and the data users, cannot easily be measured. It surely effects the quality of the collected data, through better motivation for those who do the practical work, better feed-back to the data users and the possibility for SMHI to fully control the data quality through the whole production line.
- To employ a contractor for operating the network would be risky, since it would make SMHI dependant on the technical competence of another company.

4 Service and maintenance experiences

The service and maintenance organisation for the new network at SMHI, has so far consisted of two technical experts working as co-ordinators in the office and 5-6 technicians who travel to the stations for both preventive maintenance once a year and corrective maintenance when needed. At each station there is also a local person who conduct the simplier measures.

One main goal to achieve for the maintenance organisation, is to repair a faulty station or sensor within a time limit set by the data users. At SMHI, this time limit differs for different station locations and different parameters. For example a wind sensor at a coastal station must be repaired within three working days, whereas a whole inland station can stand still for up to 20 days if the neighbouring stations run properly. To accomplish these goals and to be cost efficient as well, the maintenance work need to be well structured and organised. The technical evaluation of the first period in operational use, showed that these goals have been met for most of the occasions. When the time limit has not been held, the reasons were mainly either that the weather made it impossible to reach the station or that spare parts could not be supplied in time.

The evaluation also showed that for the whole network, the number or service trips needed for corrective maintenance was 0.3 per station per year.

The data users at SMHI demand 95% data availability for the whole network. This goal has been met during the evaluation period. For 90% of the stations the data availability is as high as 98%. The stations which do not meet this criteria, are those who could not be supplied with a regular dialled-up telephone line, but had to communicate via mobile telephone networks.

5 Co-operation with data users and suppliers

During the first years of operational use, some complaints have arisen concerning the automatic weather data. These have been solved in mainly three different ways:

1. *Education of the data users*
   All meteorologists have received a four hours training in the new measurement technique, aiming at a better understanding for and more realistic interpretation of the new type of data received.
2. *Co-operation with the data users*
   Unexpected deviations in data have been dealt with within a so called reference group, consisting of data users and network operators. The deviations have been analysed and the best possible solution has been discussed. These discussions have been very fruitful, both for the performance of the network and for the education of both parties.
3. *Co-operation with the suppliers*
   Regular meetings between SMHI and the main suppliers (Vaisala Oy and Geonor A/S) for discussions of the problems that have come up, have resulted in good solutions for both parties. SMHI has experienced good support and the suppliers have been able to further develop their equipment, using the experiences from SMHI´s extended network.

Examples of problems solved in this way are:

1. *The Present-Weather sensor sometimes indicated snowfall falsely*
   A correction algorithm has been developed in co-operation with the data users and discussed thoroughly with the supplier. The algorithm uses the measured visibility, precipitation intensity, air temperature and humidity to judge whether the snow fall is realistic or not. The limits for these parameters were decided within the reference group and the implementation of the algorithm in the software of the automatic weather station, was accomplished by SMHI´s technical experts
2. *The precipitation gauge indicated precipitation on sunny summerdays*
   The reason for this fault was that the sensor readings varied (with up to 0.7 mm) over the day, especially on sunny days, but only at some locations. This problem was also discussed with the supplier and the reference group. Another correction algorithm was implemented in the automatic station. The algorithm uses the precipitation intensity measured by the Present Weather sensor to judge whether the accumulated precipitation amount is true or not.
3. *Manufacturing problems*
   of the barometer (extensive lacquer on capacitors), Present Weather sensor (leaking rain detector) and ceilometer (blower motor failures) have all been taken care of as Customer Complaints, which for SMHI is equivalent of receiving life-time guarantee for these faults.

6 Summary

As a summary, SMHI would like to recommend the following, to other similar organizations planning on automating their synoptic station network:

1. Develop tools for *practical* quality assurance from the start, like working instructions, a maintenance register and continuous education of all personnel involved. It takes time, but it will make the operation of the network more cost efficient.
2. Develop good relations to the suppliers, something both parties benefit from.
3. Develop good relations between the network operators and the data users, a possibility to improve the network performance continuously, according to the needs of the data users.
4. Develop and keep the technical competence for running the network within your organization. In that way you are able to fully control the data quality through the whole production line and you have the possibility to improve the performance of the equipment.

ASOS PROGRAM UPDATE

Vickie L. Nadolski
National Weather Service, ASOS Program Office

1.0 BACKGROUND

In the mid 1980s, an agreement was made between the National Weather Service (NWS), the Federal Aviation Administration (FAA), and the Department of the Navy for the development, production, and deployment of Automated Surface Observing Systems (ASOS). In 1994, the U.S. Air Force joined the program and began procuring systems for use on their bases. The acquisition contract, under the management of the Department of Commerce, National Oceanic and Atmospheric Administration entailed the development, design, test, installation, and acceptance of more than 950 systems in the United States and abroad. The design and development of ASOS centered around the need to provide automated observations at airports in lieu of an observation manually taken and recorded by an observer or an air traffic controller.

The ASOS design was based upon specific requirements established by the Joint Automated Weather Observing Program Council in 1981 (JAWOS, 1981). From that requirements document, a specification was developed and approved by the key partner agencies participating in the acquisition phase of the program. Through development and pre-production, extensive testing was performed to ensure that the systems met the specification. Discrepancies were discovered and fixed as early as possible before field implementation, but in fact, other deficiencies were noted in the early stages of deployment. Corrections were made and a major retrofit of sensor upgrades took place for several years between 1991 and 1994.

The first production system, manufactured by AAI Systems Management, Inc. of Hunt Valley, Maryland, was delivered and installed at Topeka, Kansas in August 1991. For more than six years the ASOS contractor has been installing systems to support the needs of the four federal agencies.

Table 1 shows the status of purchase, installation, and commissioning of all systems as of March 6, 1998. The production contract previously scheduled to end December 1997 has been expanded to accommodate congressionally mandated additional purchases for the FAA and the U.S. Air Force. These systems will be installed over the next year and it is anticipated that the production contract will conclude in late 1998. Some activities will be transferred to the government earlier, such as the life cycle software support, which includes routine software maintenance, as well as enhancements (new requirements). The National Weather Service has been primarily responsible for operations and maintenance of systems purchased by the FAA and the NWS since initial deployment. In addition, NWS provides logistics support for all agencies.

ASOS Production Contract Status as of March 6, 1998

Base Program	*NWS*	*FAA*	*Navy*	*AF*	*TOTAL*
Planned	314	569	76	34	993
Installed	313	538	76	29	956
Accepted	311	535	76	29	951
Commissioned: NWS - 261		*FAA - 246*			

2.0 SYSTEM ENHANCEMENTS

Program efforts are now primarily focused on system enhancements. With widespread use of the system and exposure to many different environments, areas where improvements are needed have been identified. A plan was developed in 1995 which detailed product improvement activities. The program office began budgeting for new and improved technology in that time frame and has continued to successfully acquire funds to support development and testing of new sensors and software to enhance the current baseline ASOS.

2.1 *Recent Improvements*

Since the first system deployment, two new sensors have been added at specific locations. One was the freezing rain sensor which was added to sites prone to the occurrence of freezing rain. Installation began in 1996 and all commissioned sites now have the capability to automatically report freezing rain. Secondly, a single site lightning detector was added to 26 National Weather Service ASOS locations in 1997 to support automation certification and closure activities as part of the NWS modernization. These sensors use the same technology as that of the large lightning detection network that covers most of the United States which detects cloud to ground lightning. In addition, the single site sensor can detect cloud-to-cloud lightning strikes in and around the station.

2.2 *Future Improvements*

Sensor development and test activities are underway for the following: sunshine duration, ice-free wind, dew point, all weather precipitation gauge, enhanced precipitation identification, and 25,000 foot ceilometer.

Corresponding author address:
Vickie L. Nadolski
National Weather Service, 1325 East-West Highway, Room 4348, Silver Spring, MD 20910, USA

2.2.1 Sunshine

Several years of testing were conducted on the EKO sunshine duration sensor. The testing started in 1990-1993, where sensors from the following manufacturers were also evaluated:

- Aanderaa of Norway,
- Atmospheric Environment Service (AES) of Canada,
- Vaisala, Incorporated of Finland.

The EKO sunshine duration sensor was the best performer.

Currently, the EKO sunshine sensor is being field tested at twelve sites. At four of the twelve test sites, the EKO sunshine duration sensor performance is compared with the collocated Eppley pyrheliometer which is the equipment used in the national solar radiation network. At the remaining eight test sites, the EKO sensor is compared with the current NWS reference sensor, the Foster-Foskett.

The sensor performance has met the NWS requirement and NWS is pursuing use of this sensor at forecast offices to replace aging technology. It is estimated that the sensor will be ready for implementation on a limited production basis, beginning 1999.

2.2.2 Ice-Free Wind

During the Winter 1995-1996, three ice-free wind sensors were evaluated, two ultrasonic and one heated cup/shaft sensors:

- SOLENT, Model Basic Heated Ultrasonic Anemometer, (Gill Instruments distributed by IN USA, Incorporated),
- Model 425AH Heated Ultrasonic Wind Sensor (Handar, Incorporated),
- WAA25 Cup/Shaft-Heated Anemometer, WAV15A Shaft-Heated Wind Vane, and WAC15 Cross Arm, (Vaisala, Incorporated).

The test results showed a need to further evaluate additional candidate ice-free wind sensors and to revise the ice-free wind sensor requirement. However, it was decided that the ultrasonic wind sensor technology was viable and further development work was warranted. One benefit of an ultrasonic wind sensor with non-moving parts is low maintenance and not prone to freeze-up. The ultrasonic sensors appeared to operate during the few winter events when the current ASOS cup and vane sensor did not.

Testing of ice-free wind sensors continued during Winter 1996-1997 with sensor technologies from the following four contractors:

- SOLENT Model 1172T Basic Heated Ultrasonic Anemometer, (Gill Instruments distributed by IN USA, Incorporated),
- Model 425AHW Heated Ultrasonic Wind Sensor, (Handar, Incorporated),
- USA-1 Model BH422 Sonic, (Metek distributed by AeroVironment Incorporated),
- Model 102263 Sonic Anemometer with Heater, (Climatronics Corporation).

The ice-free wind sensors were field tested at two test sites, chamber tested in the CRREL blowing snow wind facility, and tested in the wind tunnel at Sterling, VA. As a normal part of NWS testing, problems and/or anomalies were documented and communicated to the respective contractors.

Current plans are to complete the wind tunnel calibration testing and do additional field testing at Cheyenne, WY and Mount Washington, NH.

2.2.3 Dew Point

Initially the Rotronic Model MP 101A-C5 sensor was tested during the first part of 1997. For the most part the sensor tracked well when compared with the current ASOS chilled mirror dew point sensor. One concern was that laboratory accuracy tests for temperature and dew point revealed a calibration dependence on operating supply voltage. A second concern was that the sensor never reached 100% humidity during field testing. A third concern was a relative humidity calibration shift in the sensors tested at Fairbanks, AK.

Based on the above concerns, alternative vendor/technologies were identified. Subsequently, the NWS selected two Vaisala models, HMP 243 and HMP 45A. Preliminary calibration tests were favorable and planning for additional tests includes calibration tests, environmental stress tests, and field tests.

2.2.4 All-Weather Precipitation Accumulation Gauge (AWPAG)

Two candidate AWPAG sensor technologies were tested and evaluated during Winter 1996-1997:

- Hi-Capacity Precipitation Sensor, (Belfort Instrument Company)
- NOAH II Total Precipitation Gauge with ASOS Enhancements, (ETI Instrument Systems, Incorporated)

The testing was conducted at Sterling, VA; Johnstown, PA; and Boulder, CO. The winter test and evaluation showed good performance in liquid and dry snow precipitation events. However, both gauges exhibited the classic problem of underreporting the precipitation amount of wet snow and freezing precipitation. The precipitation sticks to the sidewalls of the unheated gauges. Once melting occurs and the precipitation falls into the measurement area, the precipitation is recorded. This produces an unacceptable delay in reporting precipitation amounts.

The NWS specification resulted in gauges that were not easy to maintain. Sensor calibration was not easily performed due to the cumbersome calibration equipment and software. Because of the experience gained in the during this phase of testing, the NWS specification is undergoing revision. Meanwhile, a second Request For Proposal (RFP) was issued in June 1997. One vendor gauge technology was selected, test and evaluation is undergoing during the Winter 1997-1998.

2.2.5 25,000 Foot Ceilometer

Evaluation of three manufacturer's sensors are currently underway. Those are: Handar (Model 450C), Belfort (Model 7013C), and Vaisala (Model 725K). There

are currently no plans to replace the ASOS 12K ceilometer, but as technology improves, the new sensors will be considered for integration into ASOS over the next five years.

2.2.6 Enhanced Precipitation Identification

During the Winter 1995-1996, the ASOS Program Office tested the following two precipitation sensor types:

- Enhanced Light Emitting Diode Weather Identifier (E-LEDWI) present weather sensor, (Scientific Technology Incorporated),
- FD12P Precipitation Sensor (Present Weather), Vaisala, Incorporated).

As a result of the performance of the FD12P, Vaisala requested time to work on their sensor after the Winter 1995-1996. Scientific Technology Incorporated made modifications to their sensor prior to the Winder 1996-1997 test season.

Winter 1996-1997 testing of the E-LEDWI present weather sensor yielded good performance in detecting and reporting ice pellets and hail. However, three concerns were identified with the E-LEDWI performance:

- Reporting snow as ice pellets.
- Reporting freezing drizzle and rain as snow.
- Problems due to snow blockage of the lens.

Particular attention is being paid to the sensor's performance during hail and light precipitation events. In addition, the NWS has not developed a formal requirement for the enhanced precipitation identification sensor. It is apparent that ASOS needs a sensor capable of detecting and identifying ice pellets, hail, and light precipitation (< 0.01 inch/hour). Therefore, the NWS plans to develop a requirement for the enhanced precipitation identification sensor and to conduct test and evaluation against the new requirement.

3.0 SUMMARY

The development and test cycle is an interactive one and often must be repeated several times on a given sensor as it is tested under different conditions. The task of exposing sensors to all types of weather phenomena is a difficult one. For example, a sensor might not perform satisfactorily in wet snow. The manufacturer is notified of the problem and a fix is derived. At that point, the winter season may have ended and validation of the fix must wait for the next winter. Where possible, chambers are used to simulate conditions and test sites from different parts of the country are used where feasible (Gifford 1997, Gifford 1998). Given the lengthy time period that is required to fully test and integrate a new sensor, many of the enhancements referenced above are still years away from implementation.

As previously mentioned, the National Weather Service has embarked on an extensive program for ASOS product improvements. These efforts will not only extend the useful life of this vast network of instrumentation, but will enhance air safety and provide more and better data to the research community and the general public. The ASOS Product Improvements Program will continue for at least the next five years as new sensors and better processing capabilities are brought online.

To summarize, the acquisition phase of the program is nearing completion and the production of ASOS is expected to end in 1998. The implementation of more than 950 systems has in itself been a challenging and lengthy process; however, the full benefits of this automated observation system are yet to be realized. More than 200 systems have been installed at airports that previously did not have weather observations. This alone increases the amount of data available for warning and forecast purposes. ASOS has the capability to generate both five minute and minute-by-minute observations and in addition, high resolution data can be archived and downloaded for special studies. Unfortunately, this data is not readily available or recoverable for widespread use, but perhaps someday in the future there will be a means of collecting and utilizing this valuable information.

4.0 REFERENCES

Joint Automated Weather Observing System (JAWOS), *Proposed Functional Requirements*, February 1981

Gifford, M.D., M.E. Laster, and C.L. Alexander, *Status of ASOS Planned Product Improvements*, 1st Symposium on Integrated Observing Systems, American Meteorological Society, February 1997, Long Beach, CA

Gifford, M.D., M.E. Laster, and J.L. Ball, Jr., 1998: *ASOS Planned Product Improvements*, 14th International Conference on Interactive Information Systems (IIPS) for Meteorology, Oceanography, and Hydrology. American Meteorological Society, January 1998, Phoenix, AR

****

High Precision Instrumentation For Meteorological Applications

Jerome M. Paros, Mark H. Houston

Paroscientific, Inc.
4500 148th Avenue N.E.
Redmond, WA 98052 USA
http://www.paroscientific.com

INTRODUCTION

Accuracy, stability, and reliable performance under difficult environmental conditions are key performance requirements for meteorological instrumentation. Accuracy and stability are required to assure data quality. Instrumentation reliability directly affects data network integrity as well as operating costs.

Barometers employing quartz crystal resonator technology were developed and commercially introduced over 25 years ago by Paroscientific, Inc.[1] The design and performance requirements included: (1) Inherently digital outputs, (2) Accuracy comparable to the primary standards, (3) Highly reliable and simple design, (4) Minimum size, weight and power consumption, (5) Insensitivity to environmental factors, and (6) Long-term stability.

These barometers are used in laboratory and field pressure standards of remarkable resolution, stability, and accuracy. Other meteorological applications include use on marine data buoys, atmospheric wave and turbulence detectors, and altimeter-setting indicators. More recently, the technology has been incorporated into automated surface observation systems that estimate atmospheric precipitable water vapor in conjunction with GPS (Global Positioning System) geodetic networks.

RESONANT QUARTZ CRYSTAL BAROMETER-CONSTRUCTION & OPERATION

The resonant quartz crystal barometers are designed to have resolution better than one microbar (<0.1 Pa) and a precision of better than 0.01% of reading (<0.1 hPa) maintained even under difficult environmental conditions.

The remarkable performance is achieved through the use of a precision quartz crystal resonator whose frequency of oscillation varies with pressure induced stress. Quartz crystals were chosen for the sensing elements because of their remarkable repeatability, low hysteresis, and excellent stability. The resonant frequency outputs are maintained and detected with oscillator electronics similar to those used in precision clocks and counters.

Several flexurally-vibrating, single or dual beam, load-sensitive resonators have been developed. The Double-Ended Tuning Fork consists of two identical beams driven piezoelectrically in 180° phase opposition such that very little energy is transmitted to the mounting pads. The high Q resonant frequency, like that of a violin string, is a function of the applied load; increasing with tension and decreasing with compressive forces. The digital temperature sensor consists of piezoelectrically-driven, torsionally oscillating tines whose resonant frequency is a function of temperature. Its output is used to thermally compensate the calculated pressure and achieve high accuracy over a wide range of temperatures.

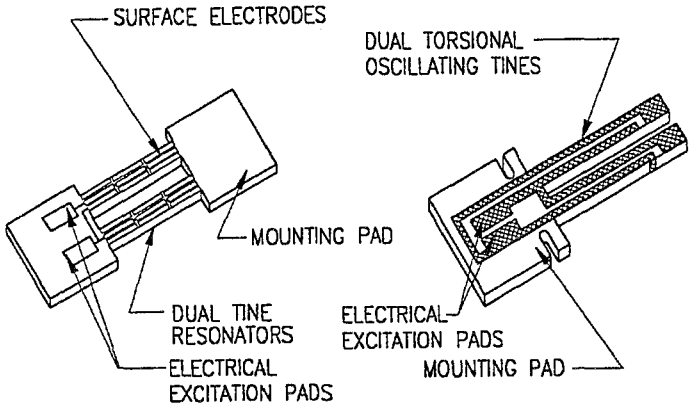

Figure 1 - Load and Temperature Resonators

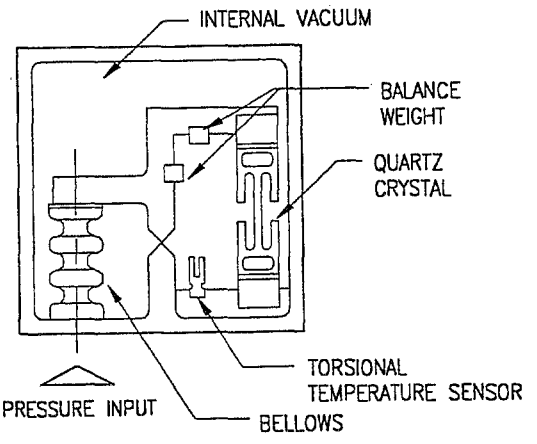

Figure 2 - Barometer Mechanisms

The barometer mechanisms employ bellows as the pressure-to-load generators. Pressure acts on the effective area of the bellows to generate a force and torque about the pivot and compressively stress the resonator. The change in frequency of the quartz crystal oscillator is a measure of the appplied pressure. Temperature sensitive crystals are used for thermal compensation. The mechanisms are acceleration compensated with balance weights to reduce the effects of shock and vibration. The transducers are hermetically sealed and evacuated to eliminate air damping and maximize the Q of the resonators. The internal vacuum also serves as an excellent reference for the absolute pressure transducer configurations. Since any changes in the reference vacuum directly affect the barometric output, great care is taken to ensure that there are no leaks and minimal outgassing in the evacuated housing.

Because the quartz crystal constrains total mechanism movement to several microns full scale, reproducibility is excellent. Pressure hysteresis tests on a group of 23 standard production Paroscientific barometers showed no measurable hysteresis when cycled over pressures from 827 to 1069 hPa. The mean observed hysteresis was 0.001 hPa and the largest observed value was 0.0077 hPa. The estimated measurement uncertainty of 0.008 hPa, was greater than all observed values.

RESOLUTION, NOISE, AND ACCURACY

Short-term measurements generally require high pressure resolution while longer term measurements need accuracy, stability, and insensitivity to environmental errors.

With a sensor of inadequate resolution, real signals can be obscured by noise, or sensor noise can be misinterpreted as real signals. The resonant quartz crystal barometer mechanisms, oscillator circuits, and digital interfaces are carefully designed for high resolution. Typical delivered resolution is better than one part per million, and under stabilized laboratory conditions, resolution can approach one part per billion. Applications where it is important to measure small pressure changes include measurements of wind-shear, wake turbulence, and atmospheric shock waves.

Noise levels as a function of frequency are generally expressed as spectral densities. Plots of this type are used to determine whether a sensor can measure a desired signal. The goal is to have the sensor noise levels much smaller than the expected real signals at all frequencies of interest.

Data from an evaluation by Hutt, Holcomb, and Agnew[2] of high quality sensors for use in atmospheric seismic studies showed that the resonant quartz barometers had power spectral density noise levels a factor of 100 lower (20 db) than the next best transducer.

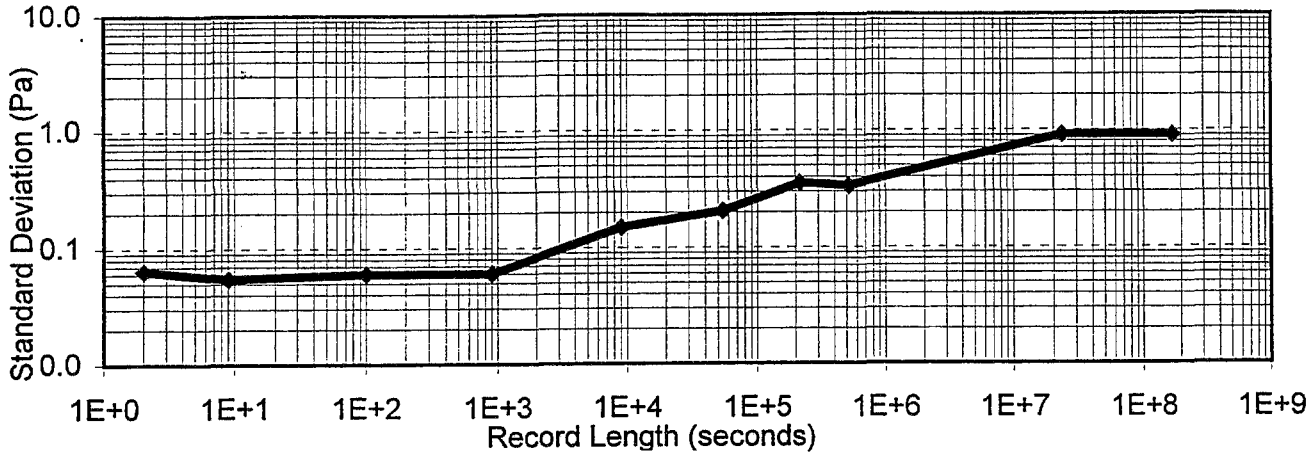

Figure 3 - Noise Versus Record Length

The ultimate resolution achievable with a transducer is limited by its noise level. Typically, the rms noise increases for longer data records because of sensor drift and because temperature and other environmental contributors to noise tend to vary more over a longer period of time. Typical rms noise levels for the quartz transducers are shown in Figure 3. For records shorter than about 1 hour, the rms noise level is less than 1 part per million (< 0.1 Pa). The rms noise rises slowly with record length, reaching approximately 10 ppm for records several years long.

LONG-TERM STABILITY

Generally, users who care about absolute accuracy also need to know how well the transducer holds its accuracy over time (long-term stability) and how sensitive it is to temperature and other environmental effects. Less stable devices need to be recalibrated more often or may be incapable of performing adequately under field conditions.

Paroscientific pressure transducers typically deliver accuracy better than 100 parts per million of full scale pressure over a wide temperature range and maintain this accuracy for a long time. Figure 4 shows cumulative drift on three resonant quartz barometers. All three are still within 0.01% of their original calibration while in their ninth year of service. Drift rates range from -3ppm to -11 ppm per year, with a median drift rate of -6ppm (-0.006 hPa) per year.

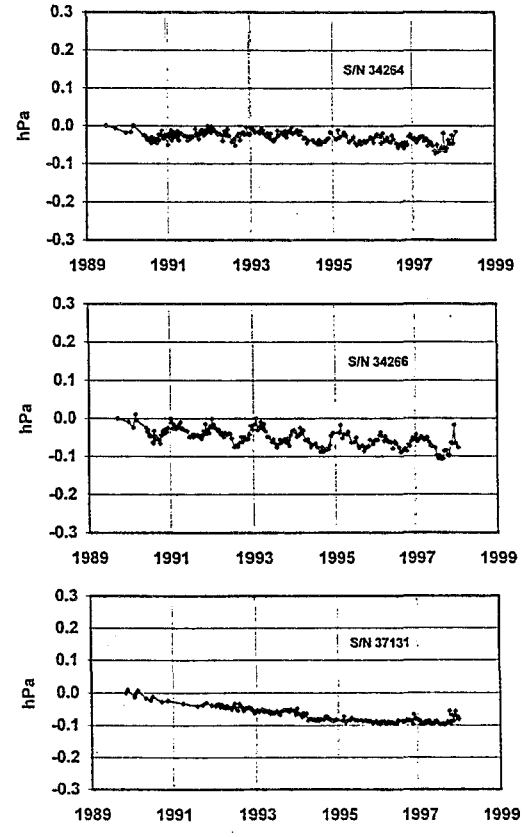

Figure 4 - Long-Term Stability

Thousands of the resonant quartz crystal barometers are used in applications where long-term stability is critical including transfer standards, digital altimeter setting indicators, air data computers, calibration systems, remote sensing stations, and drifting data buoys. An important new application is the determination of precipitable water vapor using GPS Meteorology.

GPS Meteorology

Global Positioning System (GPS) Meteorology is the application of GPS data to the monitoring and analyses of atmospheric conditions. Accurate, frequent, and dense sampling of water vapor is needed for operational weather forecasting as well as for weather and climatic research.

GPS satellites transmit radio signals that can be inverted to measure atmospheric profiles of refractivity. The refractivity profile can be transformed to profiles of tropospheric humidity given a temperature profile. Ground-based GPS receivers at fixed locations with accurate surface barometric pressure measurements can be used to gather data to determine vertically integrated Precipitable Water Vapor (PWV).[3,4]

GPS satellites transmit atomic-clock controlled L-band signals to receivers on the earth. Time delays of the signals can be directly attributed to the passage of the signals through the Earth's ionosphere and neutral atmosphere. The ionospheric delay is dispersive (frequency dependent) and can be determined by observing both of the frequencies transmitted by the GPS satellites (L1 & L2) using a dual-band GPS receiver. The neutral delay, is not dispersive and can be decomposed into a "hydrostatic delay" associated with the "dry" atmosphere and a "wet" delay associated with the permanent dipole moment of water vapor. The Zenith Hydrostatic Delay (ZHD) has a magnitude (equivalent GPS phase delay length) of about 2300 mm at sea level. The Zenith Wet Delay (ZWD) can vary from a few millimeters in desert conditions to more than 350 mm in very humid conditions. It is possible to predict the ZHD to better than 1 mm given surface pressure measurements accurate to 0.3 millibar or better. The wet delay may be estimated using Water Vapor Radiometers; however, these instruments are subject to rain spike contamination, expensive, and difficult to calibrate with sufficient accuracy. Most geodesists prefer to measure the hydrostatic component of the neutral delay using barometers and estimate the remaining wet delay during inversion of the GPS observations.[3]

The important ground-based measurements of barometric pressure, temperature, and humidity necessary to determine precipitable water vapor can be made with the Paroscientific MET3 Meteorological Measurement System which uses a resonant quartz barometer. This GPS Meteorological technique can recover precipitable water vapor with an rms error of 1.0 to 1.5 mm and represents a milestone improvement in environmental sensing technology. More accurate prediction of storm systems will improve surface, coastal, and air travel safety. Agriculture and farming will greatly benefit from these models by improving crop yields and better understanding micro-climates.

CONCLUSION

There are many important meteorological measurements that need high precision pressure sensors. Resonant quartz crystal barometers with high resolution, accuracy, and excellent long-term stability meet these demanding requirements.

References:

1. Paros, J.M., 1973, Precision Digital Pressure Transducer, *ISA Transactions: 12, p. 173-179.*
2. Agnew, D.C., 1995, Analysis of Microbarograph Comparison Data, *U.S.G.S. Internal Project Report, August 24, 1995.*
3. Duan, J., M. Bevis, P. Fang, Y. Bock, S. Chiswell, S. Businger, C. Rocken, F. Solheim, T. van Hove, R. Ware, S. McClusky, T. Herring, and R. King, 1996: GPS Meteorology: Direct Estimation of the Absolute Value of Precipitable Water, *Journal of Applied Meteorology, Vol. 35, No. 6, p. 830-838.*
4. Businger, S., S. Chiswell, M. Bevis, J. Duan, R. Anthes, C. Rocken, R. Ware, M. Exner, T. van Hove, and F. Solheim, 1996, The Promise of GPS in Atmospheric Monitoring, *Bulletin of the American Meteorological Society, Vol. 77, p. 5-18.*

NEW DIGITAL BAROMETER USING 3-D MICROMACHINING RESONANT PRESSURE SENSOR

Yoshikazu Hashimoto , Masato Yamamoto
Yokogawa Weathac Corporation , Japan

1. INTRODUCTION

The barometers using piezoresistive and capacitive type of pressure sensors are widely used these days. On the other hand the resonant type pressure sensor constructed by for example constructed by a cylindrical resonator[1] has been well known for it's high sensitivity and smaller temperature effect than the other. However the cost of conventional resonant pressure sensor is relatively high because of the fabrication process using conventional machining technology and complexity of it's construction. The new digital barometer described here uses the resonant type pressure sensor fabricated on the silicon chip using the unique three-dimensional micromachining technology. It improved the various characteristics of the conventional type such as linearity, repeatability and long term stability and realized more compact design and low manufacturing cost.

2. STRUCTURE

Fig.1 and Fig.2 show the structure of the pressure sensor of barometer. Atmospheric pressure is introduced through an inlet and a filter to a sensor chip. The filter removes dust or other substances from the air. Magnet gives the magnetic field to the resonators fabricated on the sensor chip. Vacuum chamber giving the absolute pressure reference is located at the opposite site of the sensor chip and sealed by electric beam welding.

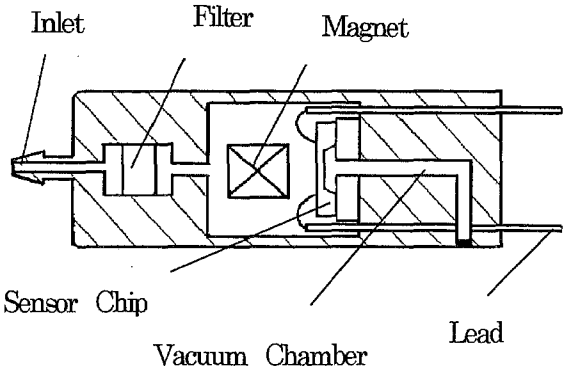

Fig.1 Structure of barometer Sensor

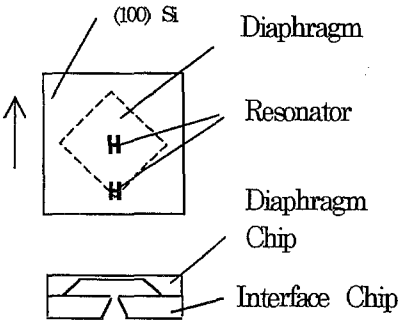

Fig.2 Construction of sensor chip

3. PRINCIPLE

The resonator is shaped like a capital H which is 20 μ m wide, 5 μ m thick and 500 μ m long and is constructed in the micro vacuum cavity and fixed to the sensor chip at the four edges of capital H. The pressure of the vacuum cavity is less than 0.1Pa. Fig.3 shows the operating principle of resonant pressure sensor. The AC drive current i applied to one side of the resonator vibrates the whole resonator under the magnetic field B perpendicular to the resonator. That induces the AC output e in the other side of resonator. Feeding back the AC output to the resonator constructs the self-resonant system. The atmospheric pressure change $\triangle p$ applied on the sensor chip causes the tension change $\triangle \varepsilon$. It changes the resonant frequency f of the resonator as shown in eq.1 and eq.2 . The resonator's very large mechanical Q factor (about 50000) realized higher accuracy and resolution than the conventional one. There are two resonators located on the sensor chip for

improvement of sensor characteristics. One is located at the center and the other is at the edge of the sensor diaphragm as shown in Fig.2. When the applied air pressure increases, the frequency of center resonator decreases and the frequency of edge one increases. The differential frequency of the two resonators amplifies the sensitivity and compensates the temperature effects of each resonator.

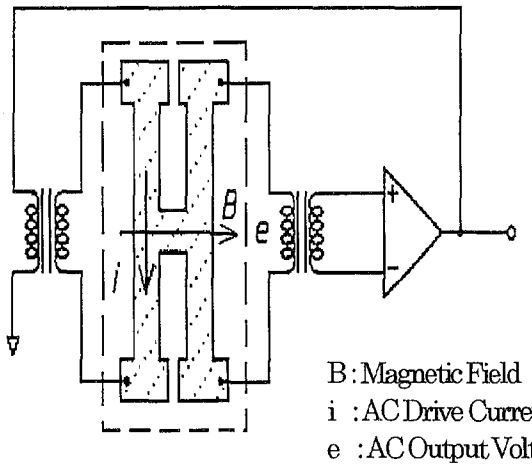

B : Magnetic Field
i : AC Drive Current
e : AC Output Voltage

H-shaped resonator
in vacuum cavity

$$\Delta\varepsilon = \frac{\kappa a^2}{t_0^2}\Delta p \qquad (1)$$

$$f = \frac{4.73^2 h}{2\pi L^2}\sqrt{\frac{E}{12\rho}\left[1+0.2366\left(\frac{L}{h}\right)^2(\varepsilon_0+\Delta\varepsilon)\right]} \qquad (2)$$

where ,

ε_0 : Resonator tension
$\Delta\varepsilon$: Change in resonator tension
κ : Constant
a, t_0 : Diaphragm diameter and thickness
Δp : Change in applied pressure
f : Resonant frequency
h, L: Resonator thickness and length
E : Young's modulus of silicon
ρ : Density of silicon

Fig. 3 Schematic diagram of resonant sensor

4. SENSOR FABRICATION

Fig.4 shows the sensor fabrication process. Sensor chip is constructed by diaphragm chip and interface chip. (100)n-type silicon wafer is used for both chips. After the anisotropic etching of Si wafer, the resonator and the cavity are made from highly concentrated boron p-type layer stacked by selective epitaxial growth technology (a). P+ layer are selectively etched after removing SiO_2 and makes the resonator and cavity wall (b). The etching clearances are sealed by additional n-type epitaxial layer and constructs the vacuum cavity (c). The remainder of the H_2 gas in the cavity is evacuated to less than 0.1Pa by the unique annealing process in high purity N_2 gas (d).The diaphragm is fabricated by anisotropic etching on the back side of the Si wafer (e). The diaphragm chip and the interface chip are bonded by a thermal oxidation process (f). Fig.5 shows a cross sectional SEM photograph of the resonator.

5. SYSTEM DESCRIPTION

Fig.6 shows the simplified block diagram of new barometer. Sensor driver controls the amplitude of the frequency signal of the resonators and transfer them to the counter. No A/D conversion realized more simple and accurate signal processing than the other type of pressure sensors. Frequency output of two resonators are directly measured in 0.5 sec sampling period, changed to the differential frequency to improve the sensor characteristics as described before and finally converted to the pressure value by the microprocessor. Residual temperature dependence and non-linearity of the sensor assembly is measured using the standard barometer at the different temperature situation, -20 to 50℃. Measured temperature effect is compensated using the temperature sensor located close to the sensor chip. Compensation factor for temperature and non-linearity are stored in the non-volatile memory. LCD display and RS-232 digital output have 0.01hPa resolution respectively. Barometer has the various kinds of operation mode such as continuous or intermittent measuring. They can be changed remotely through the digital communication using RS-232 line. There are some optional analogue output for signal recording. Fig.7 shows the outlook of the new digital barometer.

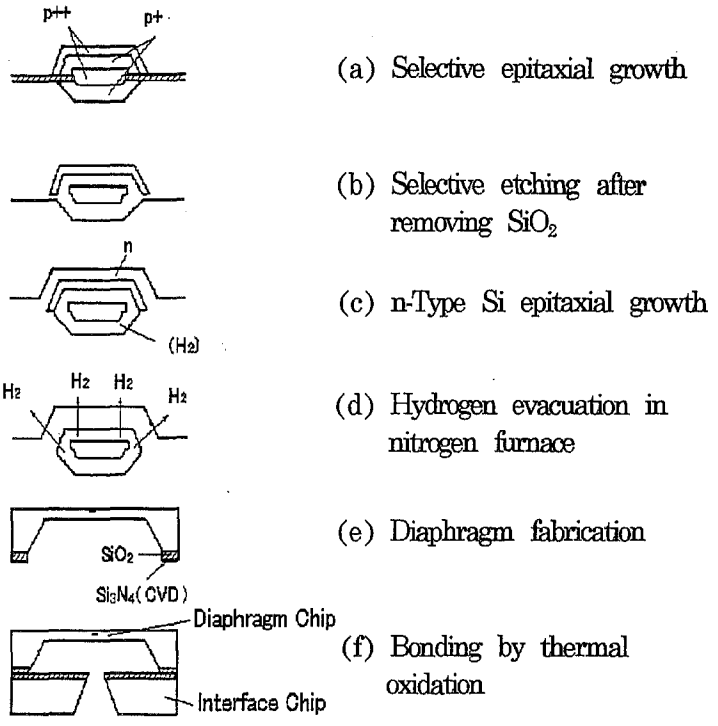

Fig. 4 Sensor fabrication process

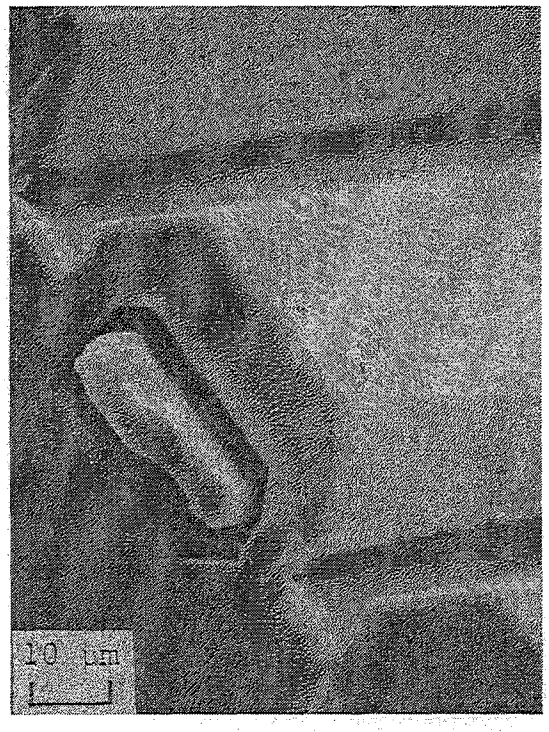

Fig. 5 A cross-sectional SEM photograph of the resonator

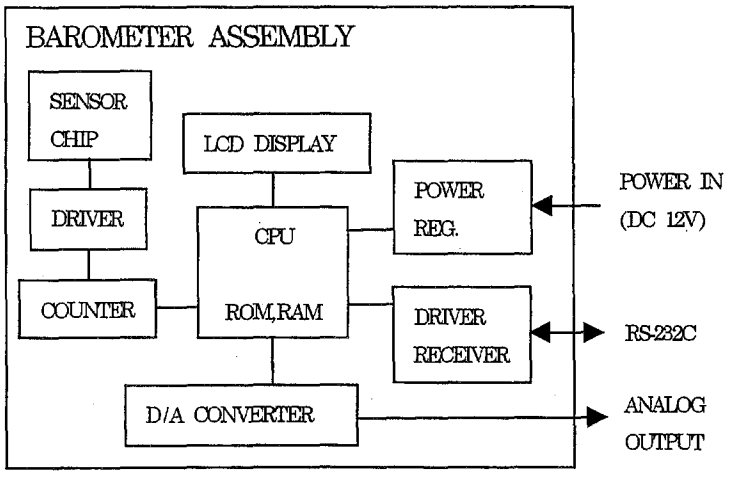

Fig. 6 Block diagram of new digital barometer

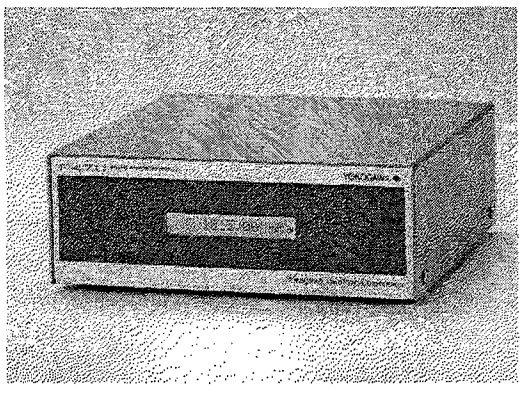

Fig. 7 New digital barometer F4711

6. CHARACTERISTICS

Fig.8 shows the input/output characteristics at various ambient temperature. New barometer has the excellent linearity at the 500 to 1300 hPa measuring range and -20 to 50 ℃ wide temperature range. Total error including Hysteresis and repeatability are less than ±0.15 hPa. These wide measuring range is introduced for the sake of using this barometer as the portable calibration standard. In the most popular operating range, 800 to 1100 hPa, however the linearity is improved to less than ± 0.03 hPa at 23℃.

Fig.9 shows the long term stability of the three units of new barometers at the room temperature. They all have been showing the very stable operation and their long term drift is less than ±0.03 hPa for two years and have no indication of drifting to one direction.

Comparison of various characteristics of new and conventional resonant type barometer is shown in table 1. New model improved almost four times as accurate than the conventional one in linearity and temperature dependence and also realized the compact design.

	F4711 New type	F-451 Conventional type
linearity including hysteresis	±0.05 hPa (800~1100 hPa,23℃)	±0.2 hPa (800~1060 hPa,23℃)
temperature depend	±0.0024 hPa/℃	±0.01 hPa/℃
size	180(W)×180(D)×63(H)	480(W)×400(D)×149(H)
weight	2kg	11.5kg

Table 1 Characteristic comparison of barometers

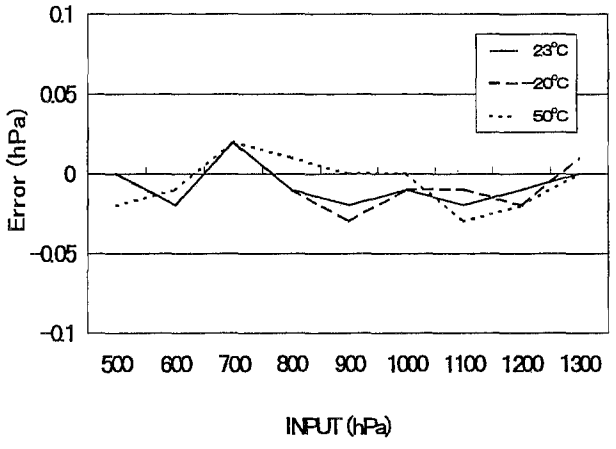

Fig.8 Linearity characteristics

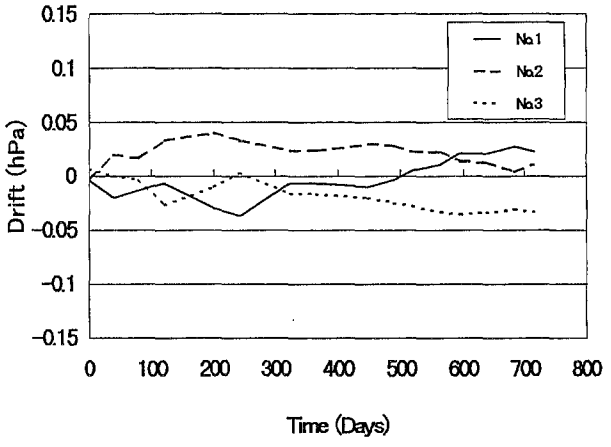

Fig.9 Long-term stability

7. CONCLUSION

We have developed the new digital barometer using resonant type pressure sensor which is fabricated three-dimensional silicon micro-machining technology. It utilizes the excellent characteristics of the resonant pressure sensor and improved them as well as the improvement of the weak points of the conventional one such as difficulty in manufacturing、high cost and portability. We would like to contribute more accurate and stable air pressure measurement using this new digital barometer.

8. ACKNOWLEDGMENT

The authors would like to thank to Mr. Kinji Harada (Yokogawa Research Laboratory), Hideki Kuwayama and Hidekazu Murayama(Yokogawa Electric Corporation) for their useful guidance.

9. REFERENCE

1)T. Tanabe, N. Numasaki, Precision Digital Barometer Using Cylindrical Resonator, WMO TECO85 Instrument and Observing Methods,(1985) pp.73-78

2)K. Harada et. all, Three-dimensional Micro-machining of Silicon Pressure Sensor Integrating Resonant Strain Gauge on Diaphragm, Sensor and Actuators, A21-A23(1990) pp1007-1010

Automation of the Observing System in Slovakia

Miroslav Ondráš, Branislav Gajar
Slovak Hydrometeorological Institute

NATIONAL PHILOSOPHY

New technology and techniques for monitoring of the meteorological and environmentally related data and its reliable performance leads to a new views on the structure and the composition of the National Observing System (NOS). This comes when increasing demands on exact, high-quality and frequent meteorological information in real time required improvement of the NOS.

Automation of the NOS was proposed in few steps (Projects) and few overlapping stages. Time scale was not fixed; it was rather loose depending on funds available and accomplishment of individual Projects. Time frame of the following Stages starts in 1990 but it should be mentioned that automation of the observations within SHMI goes back to 1974 when the first fully automatic measurement system for nuclear power plant Jaslovské Bohunice was introduced. Another automatic systems for measurement of sunshine radiation were implemented in 1980.

STRUCTURE OF THE SURFACE PART OF THE NOS

National Observing System comprises various observing systems for various purposes. That structure takes into account the historical development when individual observing systems were established for individual purposes. This is why surface part of the NOS has Partial Observing Systems (POS) for Aviation (10 aviation meteorological stations), for Synoptic meteorology (13 stations), for Nuclear safety (2 stations), for Climatology (851 stations). However as time passed partial observing networks have a mixed observing programme thus serving all users.

A. Partial Observing System for Aviation:

All 10 Aviation Meteorological Stations do the Aviation Observing Programme, Synoptic Programme, Climatological Programme, Rainfall Programme and Soil Temperature Programme. Seven of them do the Gamma Radiation Programme. The core is the Aviation Programme. However it differs depending on the importance of the airport and airport weather system. Three International airports are equipped with the comprehensive airport observing and monitoring systems MIDAS 600. MILOS 500 Automatic Station (AS) is installed at all 10 MS. All of them are manned but depending on the airport the observer may or may not be working 24 h a day. At those stations where observer is present 24 hours a day Automatic station works principally in a semiautomatic mode. The others operate in fully automatic mode when or where observer is not present (during the night in a manned station or in a pure field installation).

B. Partial Observing System for Synoptic Meteorology:

All 13 Synoptic Meteorological Stations do the Synoptic Observing Programme, Climatological Programme and Rainfall Programme. Some do one or a combination of the following Observing Programmes: Gamma Radiation Programme (11 stations), Sunshine Radiation Programme (4 stations), Soil Temperature Programme (7 stations) and Soil Moisture Programme (2 stations). The core programme is Synoptic Observing Programme. Four MS are equipped with the ESC 8800 AS and 9 with the MILOS 500 AS. All of them but two are manned stations. Automatic stations work either in semiautomatic or fully automatic mode depending of presence of the observer. Climatological Programme is performed manually both at Aviation and Synoptic Meteorological Stations.

C. Partial Observing System for Nuclear Safety:

Both Meteorological Stations at Nuclear Power Plant (NPP) do the Synoptic Observing Programme, Climatological Programme, Gamma Radiation Programme, Rainfall Programme, Sunshine Radiation Programme, Soil Temperature Programme and Special Programme for NPP. In addition one station does Soil Moisture Programme. The core programme is the Special Programme for NPP. Both MS are equipped with MILOS 500 AS and one with the Automatic system (VAISALA - MPS System - SHMI Production) for monitoring of the boundary layer of the atmosphere (sensors installed on 203.5 m high meteorological mast).

D. Partial Observing System for Climatology:

851 Climatological Stations do one or a combination of the following Observing Programmes: Climatological Programme (78 stations), Rainfall Programme (655 stations), the Sunshine Radiation Programme (2 stations), Phenological Programme (193 stations), Soil Temperature Programme (31 stations) and Soil Moisture Programme (12 stations). Automated were those two (plus 3 in other POS) that perform Sunshine Radiation Programme (using IS-32 AS, the SHMI production with Kipp-Zonnen and Li-cor. sensors for Global and Diffuse Radiation and FAR) and some rainfall stations serving Hydrology and Radar Meteorology.

PARAMETERS AND SENSORS

At the present SHMI is operating twenty one VAISALA MILOS 500 AS, four USA ESC 8800 AS, five SHMI IS-32 AS, three VAISALA MIDAS 600 and one VAISALA-MPS-SHMI Tower Automatic System in either fully automatic or semiautomatic mode. Older ESC 8800 will be replaced by MILOS 500 within 2 years. Automatic Stations, depending on the observing programme, are used to monitor some of the following meteorological and environmental related data (many other parameters are calculated further): surface wind speed and direction 10 m; wind speed and direction at 0.5, 2, 4, 6, 10, 20, 30, 40, 50, 60, 80, 100, 120, 160, 200 m height; vertical wind speed at 10, 100 and 200 m height; air temperature in 2 m; ground surface temperature; soil temperature in 5, 10, 20 and 50 cm; humidity at 2 m; humidity at 0.5, 2, 4, 6, 10, 20, 30, 40, 50, 60, 80,

100, 120, 160, 200 m height; barometric pressure; global radiation; radiation balance; diffuse radiation; FAR; UVB radiation; sunshine duration; precipitation; evaporation; horizontal visibility and MOR; background luminance; cloud base level; present weather; gamma radiation doses.

Different types of sensor are used because of the historical reasons. Nowadays there is a tendency to use one type of sensor or at least one producer is accepted:

In a semiautomatic mode MILOS 500 and ESC 8800 Automatic Stations are associated to an IMS (Integrated Meteorological System - PC based multipurpose system), making the interface with the human observer who can input its own observation and supervise the system. Data pre-processing, data check and control, archive, compilation of meteorological messages and data transmission are done automatically using IMS into the Message Switching System (MSS) of the National Telecommunication Centre.

In a fully automatic mode MILOS 500 Automatic Stations can work with or without the IMS. This means duplicity in performing some of the jobs, especially data pre-processing, data check and control, archive, compilation of meteorological messages and data transmission. When AS is installed in the site of normal meteorological station then IMS, situated at the observer room, is connected with AS. In such a case in full automatic mode both IMS and AS send compiled messages to MSS independently. In this case data from IMS have priority. This is a back-up in case of break down of IMS or lack of manpower. Obviously in a purely field installation AS works without the presence of IMS System. This gives us variability in all possible installations - fully manned, partially manned and unmanned meteorological stations.

Semiautomatic mode is used in a fully manned meteorological station with the 24 h/day of operation. Automatic mode is continuously running together with the semiautomatic mode therefore there is the possibility to switch automatically to the automatic mode in case of failure of an observer or the IMS System without loosing any of the measured data. Automatic mode is used in a partially manned meteorological stations with the 18 h/day of operation and in a purely field installation. As the total amount of the observers continuously decreases the automatic mode takes over the semiautomatic mode. In this respect SHMI works on a development of fully automatic station not only for synoptic but also aviation purposes. This is done by adaptation of existing hardware.

DATA CHECK AND DATA FLOW

Both AS and IMS process the raw data and produce 1 minute, 10 minutes and 1 hour data sets that are sent to MSS via Private Data Network. 10 minutes data are sent every 10 minutes, 1 minute data are sent once a day (soon every hour) or any time on request, 1 hour data are sent every hour. In addition there are compiled messages like SYNOP, METAR, CLIMAT or local type of messages and different pre-processed data in tables (monthly sheets). AWOS System at Bratislava Airport compiles messages on horizontal and vertical Wind Shear as well. Automatic data check routines are run in AS and IMS for internal validity and consistency of raw data and compiled messages. In three hour intervals manually measured parameters are compared with the ones from AS. It is an observer duty to make an action in case of any discrepancies. In future automatic check of all 10 min data will be introduced. From MSS all data are sent to local users on line and to the KMIS (Climatological and Meteorological Information System - RDB INGRES). All

data sets and compiled messages are stored in KMIS where sets of comprehensive data check are applied. In case of missing data or messages automatic routine is being developed for retrieving the data from the originating AS or IMS. Further post-processing is done in KMIS where other data control is applied and data corrected if necessary.

COMMUNICATION NETWORK

Private communication network of the SHMI is an integral part of the information system designed to satisfy needs for data and information distribution on national and international level (routine national data collection; data, product and information distribution to internal and external users; access to national central or distributed databases, international data exchange). It is designed as a packet-switching private network using the X.25 and TCP/IP protocols. There is an interface to PSDN, PSTN, INTERNET, GTS, and AFTN. All kind of data, products and information either character or binary could be distributed via the Private Network.

PROBLEMS

Automation is connected with the new observing methods and procedures that may differ significantly from the old ones. At manned stations the observations of weather phenomena or subjective parameters are estimated by the observer at a fixed location by integrating in space. An example is the observation of cloud amount and present weather. Contrary to man made observation automatic system estimates cloud amount or present weather from measurements made at a fixed location by integrating in time. Thus there is a principal difference between the behaviour of an observer and automatic system by estimating these weather phenomena. The crucial point in the development of new automatic weather station is therefore not only to find new sensors but also to find new algorithms, which allows calculation of the spatial distribution of a parameter from point measurements as well.

Automatic weather stations will inevitably introduce inhomogenities into the old climatic records because of changes in sensor design, physical principle of measurements, observation techniques, interrogation time and data processing algorithms. Therefore an effort should be aimed at the studies of the homogeneity of time series of data after the change of instrumentation.

CONCLUSION

Continuous increase of demands for regular, timely and on-line data from all over the national territory is the main driving force for automation and restructuring of NOS. Even if this is the main tendency, automation should be done very carefully with respect to present limitations and contradictory tendencies. One of them is the requirement for conservative approach from Climatology. This is why automation of the Partial Observing System for Climatology will be automated the last. Even then substantial amount of stations will keep the old instrumentation and observing methods.

The Swiss Atmospheric Radiation Monitoring Network CHARM

A. Heimo[1], R. Philipona[2], C. Fröhlich[2] , Ch. Marty[2] and A. Ohmura[3]

[1]Swiss Meteorological Institute, CH-1530 Payerne
[2]Physikalisch-Meteorologisches Observatorium, World Radiation Center, CH-7260 Davos-Dorf
[3]Institute of Geography, Swiss Federal Institute of Technology, CH-8057 Zurich

ABSTRACT

A major effort is presently being made in Switzerland for the establishment of a new radiation network CHARM (Swiss Atmospheric Radiation Monitoring), a joint venture between the Swiss Meteorological Institute (SMI), the Physikalisch-Meteorlogisches Observatorium Davos/World Radiation Center PMOD/WRC and the Institute of Geography of the Swiss Federal Institute of Technology GIETHZ. Its main objective is to make the best possible use of the presence of the Alps in Switzerland, one of the best instrumented natural mountainous laboratories in the world. For this purpose, a network of about fifteen operational stations is being installed, located at various sites representative for high and low altitudes, urban and rural environments, at the north and south parts of the Alps. Measurements of the solar global and direct irradiances, of the UV-A, UV-B and IR radiation and of the spectral optical depth at three/four, resp. twelve wavelengths are presently being implemented.

An overview of the actual state of installation is presented, especially concerning the new radiometric station located at the Jungfraujoch Observatory (altitude 3587 m a.s.l.). Preliminary results in the different spectral ranges are displayed, with emphasis on the information potential in regard of possible climate changes in the future.

1. Introduction

According to model calculations, an increase of the greenhouse effect will result in an elevation dependent change of the long-wave part of the surface radiation budget (SRB). This will certainly influence the dynamics over the Alps in a different way than for the lower parts of Europe. The energy balance at the surface is determined not only by the long-wave part of the SRB, but also, and as important, by the short-wave part. Both are influenced by clouds, although in a physically different way: an increase of cloud amount leads to a decrease of the shortwave irradiance because more radiation is reflected back to space, but to an increase of the downward long-wave due to an increased greenhouse effect which depends essentially on cloud base height. As the cloud climatology is not well established, the influence of clouds on the SRB is not well known and more experimental data are needed.

The short-wave part of the SRB is further influenced by aerosols and surface albedo. Both have a strong seasonal course, and again a reliable climatology is not yet established which would allow to predict the influence of long-term changes of the amount and type of aerosols. These two parameters are also important for understanding changes in the UV-radiation reaching the ground, apart from the influence of stratospheric and tropospheric ozone. Thus, the aerosol optical depth measurements are important, as well as the determination of a climatology (in space and time) of the properties of the surface albedo.

In the framework of the Swiss contribution to the Global Atmosphere Watch program WMO/GAW, the need for an increased synergy of the activities in the field of radiation measurement has led to the creation of the Swiss Atmospheric Radiation Monitoring program CHARM, a joint venture between the Swiss Meteorological Institute SMI, the Physikalisch-Meteorlogisches Observatorium Davos/World Radiation Center PMOD/WRC and the Geographic Institute of the Swiss Federal Institute of Technology GIETHZ. The objective is to make the best possible use of the presence of the Alps in Switzerland, probably one of the best instrumented natural mountainous laboratories in the world, and to investigate the basic nature and distribution of irradiance in montainous regions.

2. Configuration of the CHARM network

The CHARM network will ultimately consist of a set of eight radiometric automatic (RASTA-UV, [1]) stations with measurements of:

- direct irradiance (PMO6 absolute radiometers),
- direct spectral irradiance with three/four WMO standard wavelength sunphotometers/Precision Filter Radiometers with nine additional wavelengths added at four selected stations (Optical Depth OD stations) Jungfraujoch, Davos, Payerne and Locarno-Monti,
- direct, diffuse and global components of the broad-band erythema UV-ERY radiation (Solar Light UV-Biometers).

Infrared and visible global radiation are measured at eleven Alpine Surface Radiation Budget (ASRB) stations, including the Swiss Baseline Surface Radiation Network (BSRN) station at Payerne [2]. The stations are located within the Alps as well as on the Swiss Plateau and in the Tessin region in the southern part of Switzerland. Altitudes are ranging between 366 and 3587 m a.s.l.

About two thirds of the RASTA-UV stations, the BSRN station at Payerne, all the ASRB stations and two OD stations are presently operational. Meteorological data, when not directly measured, are available through the automatic networks of the SMI. Routine ozone measurements are performed at Arosa using two Dobson, two Brewer MkII and one Brewer MkIII spectrophotometers. Daily soundings are launched at the Aerological Station at Payerne to measure PTU profiles as well as ozone profiles three times a week.

Furthermore, in collaboration with the Swiss Federal Office of Topography, ground based Global Positioning System GPS stations will be installed in the near future at the four main stations: GPS satellite signals are delayed by the atmospheric refraction which is dependant, among others, on the water vapor content of the atmosphere. This so-called "wet delay" can be used to retrieve the integrated precipitable water vapor above the station on a continuous basis.

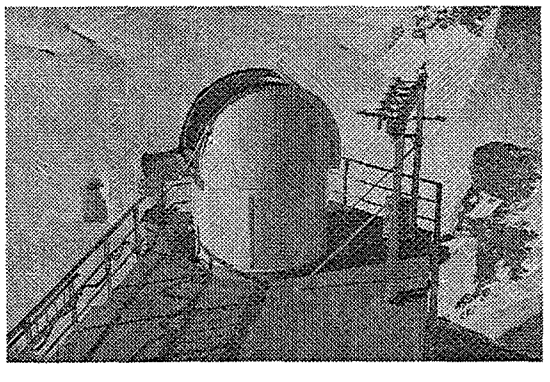

Picture 1: The Jungfraujoch station

A special mention must be made concerning the installation of the highest radiometric station in Europe, and one of the highest in the world, at the Jungfraujoch Observatory, which is operational since spring 1997. As far as the harsh environmental conditions allowed, all the CHARM components have been installed on this site, which can be most of the time considered as representative of free tropospheric conditions. A new dedicated Web page is now available which presents static and dynamic views of the installation as shown in Picture 1 (http://sma001.unibe.ch)

3. Data acquisition

Most of the measurements - existing or planned as described above - are or will be performed with the help of data-loggers (CR10, CR7 and, since 1998 CR23X from Campbell Scientific Ltd. CSL) which are widely used within the SMI and other institutions in Switzerland.

All the loggers are accessed either through normal telephone lines (MODEM, 1200 bauds) or directly through coaxial cables (BSRN station) or, more recently, through the internet (Jungfraujoch station) by common portable computers equipped with the software PC208W delivered by CSL. The software needed for the management of these special networks as well as for the programming and direct access to the logger is therefore unique.

For the time being, the networks' integration times have different values, ranging from 1 minute (BSRN station at Payerne) to 10 minutes for the automatic weather station network. The goal is to reach a common value of 2 minutes for all stations apart from the BSRN facility.

Furthermore, the BSRN experience has best shown that each average value should be escorted by the minimum, maximum and standard deviation over the integration period. This supplementary information, now implemented in the CHARM network, provides a good view of the variations of the natural phenomena during the integration time and is of great help for the subsequent data quality control.

4. Calibration and Quality Control

Much attention is being given to the calibration of the radiation sensors at all wavelengths. The PMOD/WRC houses the World Standard Group (WSG) and is responsible for the World Radiometric Reference (WRR). It also achieved recently a major improvement in the calibration technique for infrared instruments [3]. New methods for the calibration of Precision Filter Radiometers PFR and broadband sensors in the UV-ERY spectral range are presently being implemented at Davos.

Quality Control / Quality Assessment (QC/QA) procedures applied to the measurements are very important and carefully analyzed at the SMI. Among other tools, tentative use of Artificial Intelligence (Expert Systems) is presently being investigated. The data are centralized in a specifically developed database system, which allows for easy and rapid access to the whole set of information. Once the control procedures are completed, the final data set is transferred to the new National Radiation Monitoring Center, hosted by the GIETHZ at Zurich, where it is co-located with the World Radiation Monitoring Center of the BSRN network [4].

5. Preliminary results

To illustrate part of the information potential of the CHARM network, specific days are selected, for which the weather conditions were more or less clear over the four stations Locarno-Monti (OTL, altitude 366 m.a.s.l.), Payerne (PAY, altitude 491 m.a.s.l.), Davos (DAV, altitude 1610 m.a.s.l.) and Jungfraujoch (JUN, 3587 m.a.s.l.).

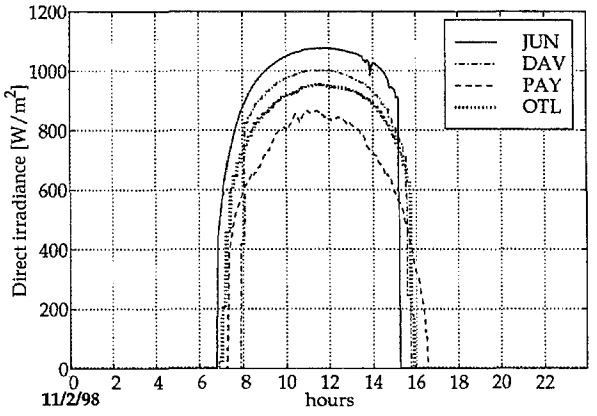

Fig. 1. Direct solar irradiance measured with absolute radiometers PMO6 at the four stations Jungfraujoch (3587 m a.s.l.), Davos (1610 m a.s.l.), Payerne (491 m a.s.l.) and Locarno-Monti (366 m a.s.l.) on the 11-Feb-1998.

Fig. 1 displays the direct solar irradiance measured at OTL, PAY, DAV and JUN by absolute radiometers for the 11-Feb-1998. The height dependent atmospheric extinction may be easily seen, with a relatively low intensity at station PAY, located in the Broye valley: local strong haze conditions are often existant at this site during the winter period. On the contrary, intensities up to almost 1100 W/m^2 are measured at the Jungfraujoch, even for high solar zenith angles in winter.

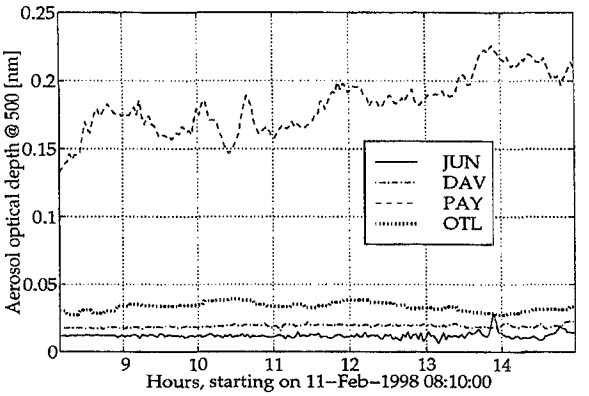

Fig. 2. Aerosol Optical Depth at 500 [nm] for the four stations JUN, DAV, PAY and OTL on the 11-Feb-1998.

Figure 2 displays Aerosol Optical Depth (AOD) at wavelength 500 nm for the same stations and the same day as in Fig. 1. Here again, the altitude dependence of the aerosol load in the atmosphere is clearly visible. The unusual low aerosol load at OTL as well as the strong hazy conditions at station PAY are best illustrated on this graph, with an AOD at PAY about 5 times higher than at OTL though the latter site's height is about 125 meters lower.

Figure 3 presents the UV-ERY global radiation measured by the broad-band Biometers for the stations PAY, DAV and JUN for four consecutive days (8-Feb-1998 to 11-Feb-1998). The altitude dependence is clearly seen on this graph. Furthermore, a major UV-ERY increase is observed at the three stations between the 8th and the 11th, well correlated with an ozone decrease from 363 DU to 299 DU. As mentioned in section 2, measurements of the direct and diffuse UV-ERY components are also available. A comprehensive study of the dependence of the UV-ERY broad-band measurements on the total ozone amount and the aerosol optical depth is presently being undertaken within the CHARM group.

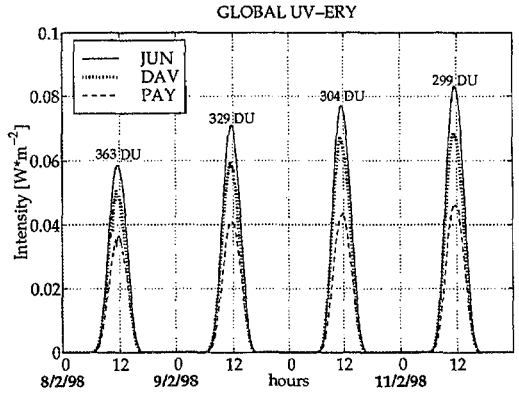

Fig. 3. UV-ERY global radiation measured at JUN, DAV and PAY for the period 8-Feb-1998 to 11-Feb-1998. The daily mean total ozone values [DU] measured at Arosa are displayed above the curves.

Figure 4 displays the downward infrared radiation measured at the four ASRB stations PAY, DAV, WFJ (Weissfluhjoch, altitude 2690 m a.s.l.) and JUN for the same day as in Fig. 1. These sites are selected because of the more or less constant altitude difference between them. In terms of greenhouse effect, the decrease of the downward flux, i.e. the decrease of the sky temperature with altitude, is a direct consequence of the contribution of the water vapor content which strongly decreases with decreasing temperature and therefore with the height of the stations. The small difference between DAV and PAY during the morning hours seems to be due to the strong heating of the atmosphere by the exposed steep mountain slopes around station DAV. No such daily cycle for the longwave downward flux can be observed at the two snow-surrounded mountain stations JUN and WFJ.

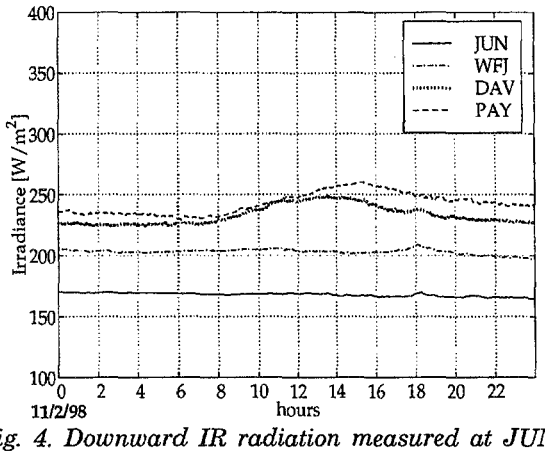

Fig. 4. Downward IR radiation measured at JUN, WFJ, DAV and PAY for the 11-Feb-1998.

The eleven operational stations of the ASRB sub-network are yielding basic evidence of this height dependance and studies are presently undertaken at the PMOD/WRC to evaluate these preliminary results on a statistical basis.

6. Conclusion and future activities

The CHARM network, which will be hopefully completed within the next 2 years, will represent a very powerful tool for the investigation of the radiation budget and its variability in the Alps. Altitude profiles will be available on a routine basis, for ultraviolet, visible and infrared spectral ranges, measured with broad- and narrow-band instruments. When enough data will be available, it will then be possible to evaluate statistically the influence of the atmospheric gases -, the geographical variability -, the local climate characteristics -, etc. on the radiation balance with instruments calibrated with the best possible accuracy. Furthermore, the diffusion of the data from a centralized database system will allow the scientific community to work on reliable, good quality data sets.

References

[1] A. Heimo, Ch. Thévoz, Ph. Renaud, R.W. Brusa, J. Sekler, C. Fröhlich
"RASTA, Radiometer for automatic stations"
Working Reports of the SMI, No. 183,
July 1995

[2] A. Heimo, A. Vernez, P. Wasserfallen
"Concept and Implementation of a BSRN Station"
WMO/TD-No. 579, November 1993

[3] R. Philipona, C. Fröhlich and Ch. Betz
"Characterization of pyrgeometers and the accuracy of atmospheric longwave measurements"
Applied Optics, Vol. 34 No. 9, 1598-1605 (1995)

[4] H. Gilgen, C.H. Whitlock, F. Koch, G. Müller, A. Ohmura, D. Steiger and R. Wheeler.
"Baseline Surface Radiation Network (BSRN) - Technical Plan for BSRN Data Management"
WMO/TD-No. 443, February 1995

SIOMA

An Integrated System for the whole range of airports

Un système intégré pour tous les types d'aéroports

François DUVERNET, Yves MERCADIE

SOFREAVIA (France)

General Presentation of SIOMA

SIOMA, is designed as a fully modular and evolutive airport weather system in accordance with the latest WMO and ICAO recommendations and standards.

It fulfils the operational requirements of every kind of airport, from small VFR airfields to large international CAT IIIc airports.

It can be easily upgraded to new technical and operational requirements (new runways, higher airport category etc.).

Présentation Générale de SIOMA

SIOMA est un système automatique d'observation météorologique d'aéroport modulaire et évolutif respectant les dernières normes et recommandations de l'OMM et de l'OACI.

Il convient aux besoins opérationnels des petits aérodromes VFR jusqu'aux aéroports internationaux de catégorie IIIc.

Il peut être facilement étendu en fonction de nouveaux besoins techniques et opérationnels.

Main Functions of SIOMA

Real-time management, storage, consultation and printout of MET data.
Automatic data recording of al parameters with one minute resolution.
Easy sensor set-up with selection/deselection and substitution.
Immediate access to one or more parameters and reports over a selected period. Data display and printout in both alphanumeric and graphic formats.

Comprehensive meteorological data display (AEROVIEW)
Real-time information (including wind shear alert report) available for all airport users through PC based network.
Personalised interface based on users' needs.

Easy encoding of WMO/ICAO standardised reports
Automatic data collection through CIBUS digital network, observed parameters input and computer-aided report edition of METAR, SPECI, SYNOP and MET REPORT.
Automated report transmission to ATC services, to AFTN or GTS network, to ATIS system and to local distribution networks.

Telecommunications

Interface with AFTN, and Meteorological network.

Automatic message wording(ATIS).

Principales fonctions de SIOMA

Gestion, archivage, consultation et impression des données en temps réel.
Enregistrement automatique des paramètres ou pas d'une minute.
Configuration aisée des capteurs raccordés avec possibilité de sélection/désélection et substitution.
Accès immédiat à un ou plusieurs paramètres/message sur une période choisie. Affichage et impression des données en mode graphique et alphanumérique.

Affichage de l'ensemble des paramètres météorologique (AEROVIEW)
Informations (y compris les alertes au cisaillement) disponible en temps réel pour tous les utilisateurs de l'aéroport par un réseau de PC.
Interface personnalisable selon les besoins des utilisateurs.

Assistance au codage des messages d'observation au format OMM/OACI
Acquisition automatique des données de piste par le réseau numérique CIBUS, saisie manuelle des paramètres observés avec codage assisté par ordinateur des messages METAR, SPECI, SYNOP et OBSMET.
Transmission automatique des messages vers les services ATC, sur les réseaux RSFTA ou SMT, vers un système ATIS et vers les réseaux de distribution locaux.

Télécommunications

Interface avec le RSFTA, le réseau météorologique.

Système automatique de bulletins parlés (ATIS)

Some SIOMA Sensors

Weather radar

SIOMA can be combined with SOFREAVIA weather radar data processing system offering display of both systems within the same workstation.

SANAGA provides users with detection and tracking, vertical analysis of storm systems and hail warning.

Wind profilers

SIOMA can automatically display upper-air wind observations provided by DEGREANE's UHF Doppler wind profiler through a real-time measurement of the 3 components of low layer wind vector.

SIOMA automatically displays wind shear alerts.

Specific aeronautic sensors.

SIOMA displays data from specific aeronautic sensors such as transmissometer or diffusometer for RVR, ceilometers etc...

Future Developments

It is planned to integrate other sensors, notably lightning detection system (DIMENSIONS).

Other development, on data program and telecommunications are going on ; for instance automatic integration of data into a CLICOM system, on the interface with the Internet.

Conclusion

SIOMA is the result of a common development of METEO-FRANCE, DEGREANE and SOFREAVIA.

Various versions of the system are operational in more than 25 countries.

Quelques Capteurs de SIOMA

Radars météorologiques

Le poste de travail SIOMA permet l'affichage des données radar transmises par le système de traitement radar SANAGA développé par SOFREAVIA.

Le système SANAGA permet aux utilisateurs la détection et le suivi des orages, leur analyse verticale et l'alerte de grêle.

Profileurs de vent

SIOMA peut afficher automatiquement les observations de vent en altitude issues du profileur de vent UHF Doppler DEGREANE. (Mesure tri-dimensionnelle du vecteur vent en temps réel).

SIOMA affiche automatiquement les alertes au cisaillement de vent.

Capteurs aéronautiques spécifiques.

SIOMA affiche les données des capteurs aéronautiques spécifiques comme les transmissomètres ou les diffusomètres pour la RVR, les télémètres de nuage pour le plafond, etc...

Développements futurs

Il est prévu d'intégrer d'autres types de capteurs, notamment les systèmes de détection d'éclairs (DIMENSIONS).

D'autres développements portant sur le traitement des données et les télécommunications, par exemple l'intégration automatique des données dans un système CLICOM, ou l'interface avec le réseau Internet.

Conclusion

SIOMA résulte d'un développement de METEO-FRANCE, DEGREANE et SOFREAVIA.

Diverses versions de ce système sont opérationnelles dans plus de 25 pays du monde.

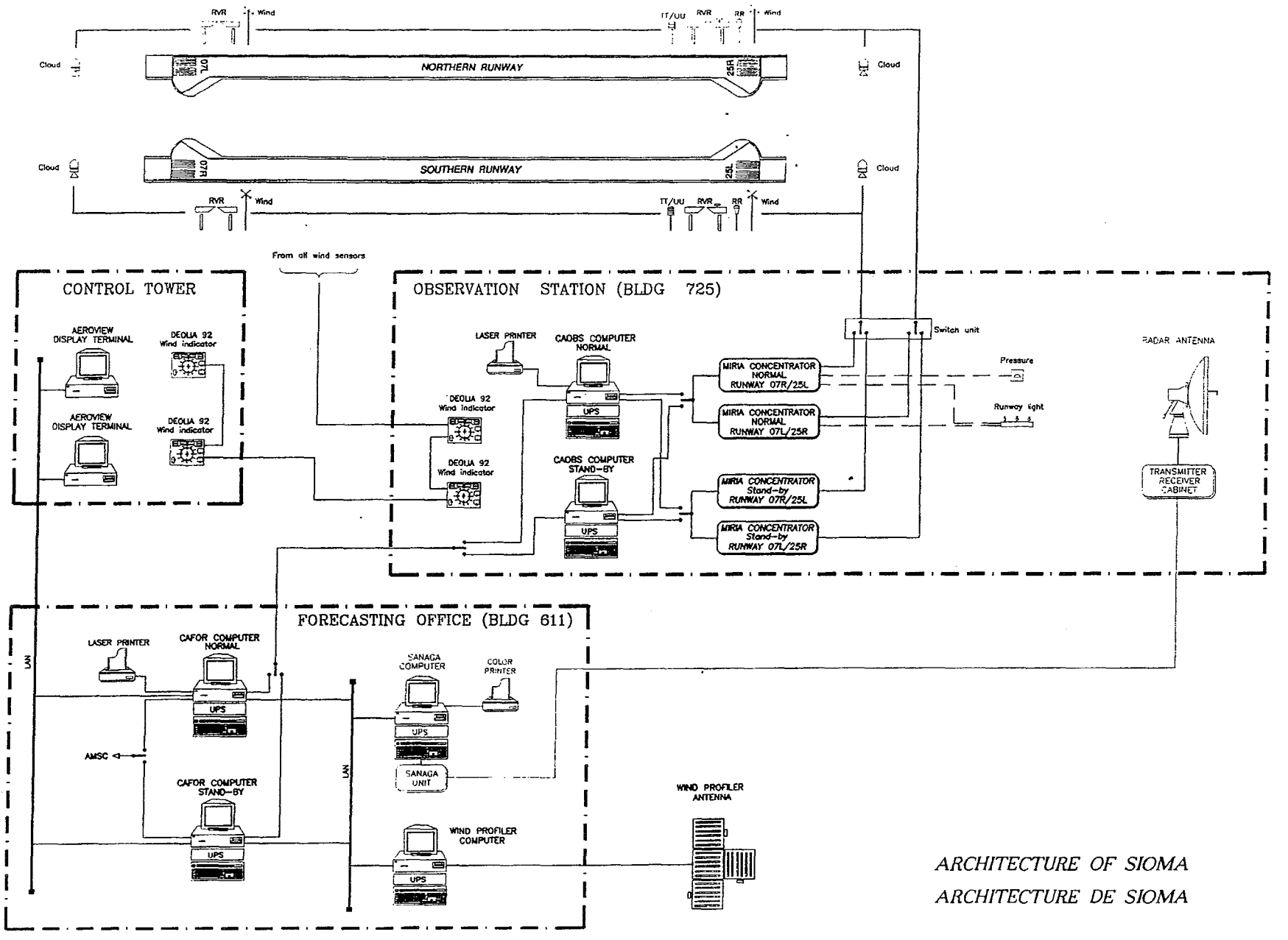

ARCHITECTURE OF SIOMA

ARCHITECTURE DE SIOMA

An Ultrasonic Anemometer for General Meteorology

R. Lockyer and S. Ammann,
Handar Inc., Sunnyvale, California

1. Introduction

The Handar Model 425 Ultrasonic Anemometer was designed to meet the needs of the general meteorology market by providing an alternative to the traditional cup and vane type products at a comparable price. The sensor offers users many advantages over the cup and vane or propeller and vane mechanical anemometers. The sensor has no moving parts, so threshold and inertia effects that hamper the performance of mechanical sensors are not present. The lack of moving parts also contributes to the need for substantially less preventative maintenance, since there is nothing to wear out or need refurbishment. Sensor accuracy is inherently stable, with no calibration required other than verification of the distance between transducers. The lack of moving parts to wear or degrade also provides a more stable and accurate measurement over the long run, and provides superior performance in regions prone to blowing dust or sand, as well as corrosive environments such as those found in marine applications. Unlike the mechanical sensor, which might report no wind when frozen or damaged, the Model 425 is an intelligent sensor with the ability to report a no data value if the measurement is not valid.

The novel design of this ultrasonic sensor, where three transducers are used instead of the more traditional four headed orthogonal approach, provides performance superior to other ultrasonic sensors. The three transducers are located on an equilateral triangle in the horizontal plane (see photo 1). The transducer shape provides a constant aspect ratio for all wind directions, which dramatically decreases the angular variation in measurement accuracy. The various sensor versions can provide serial data output via RS232, RS422, RS485, and SDI-12. The sensor is also available with a frequency output for speed and analog output for direction to provide signals commonly used with cup and vane type sensors. The standard sensor produces a new reading once a second, typical for the general meteorology market for which it was designed.

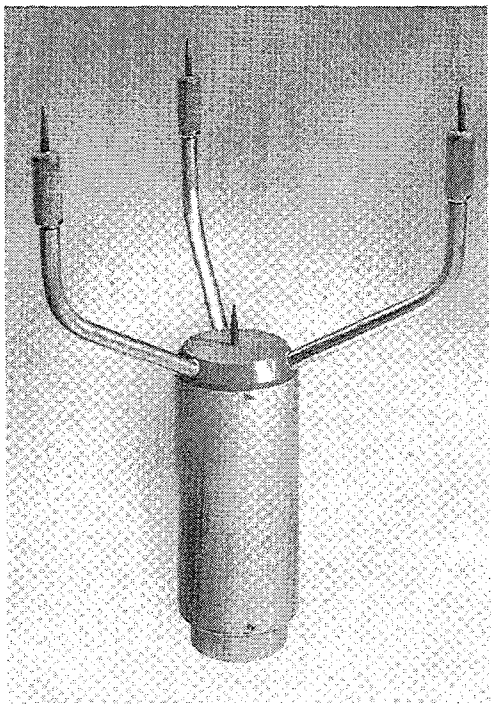

Photo 1

The Handar Model 425 Ultrasonic Anemometer was selected for the new U.S. FAA Low-Level Wind Shear program (LLWAS). The sensor has been extensively tested both in the field and in a wind tunnel by the U.S. NWS Sterling Test and Evaluation Center for use in the NWS ASOS system. The sensor is currently in the final stages of certification for use in the U.S. FAA AWOS system. Other U.S agencies that have performed their own wind tunnel testing include NASA Ames. Numerous U.S. governmental agencies have performed their own field tests. Performance has been verified at wind speeds from 0 to 125 knots. Actual and simulated environmental tests have been performed for operation in blowing rain and snow conditions as well as icing and freezing rain. Acoustic noise interference tests were performed at a major U.S. international airport. The sensor has been tested for and is fully compliant with CE mark requirements.

2. Sensor Operation and Advantages Over Other Sonic Anemometers

Vector analysis shows us that N basis vectors are required to span an N dimensional vector space. The polar representation of horizontal wind typically used in general meteorology is equivalent to a two dimensional vector space. Therefore, two basis vectors are required to provide a solution for horizontal wind. The typical approach to determination of 2-D wind with sonic anemometers is to place four transducers in an orthogonal geometry, providing only two basis vectors that are mutually perpendicular.

An infinite number of different basis sets exist for normal 2-D physical space. There is no requirement for each of the vectors in a basis to be mutually perpendicular; they must only be linearly independent. This simply requires them to not be parallel. Figure 1 shows a top view of the transducer geometry for the Handar Model 425 sensor. Bi-directional times of flight measurements are performed on paths on each side of the equilateral triangle formed by the transducers. The bi-directional measurements are used algebraically to remove the static speed of sound and cross wind effects, leaving the component of wind velocity in the direction of each of the three paths. Since no path is parallel to any other path, any two of the three paths may serve as components in a proper basis for horizontal wind velocity determination.

The unique geometry of the sensor thus provides an over-determined solution, since three vectors are available when only two are required. This gives the Handar approach a fundamental advantage over all four head 2-D sonic sensors. These sensors use the orthogonal approach that yields only enough information to make a solution when both paths can provide valid and accurate data.

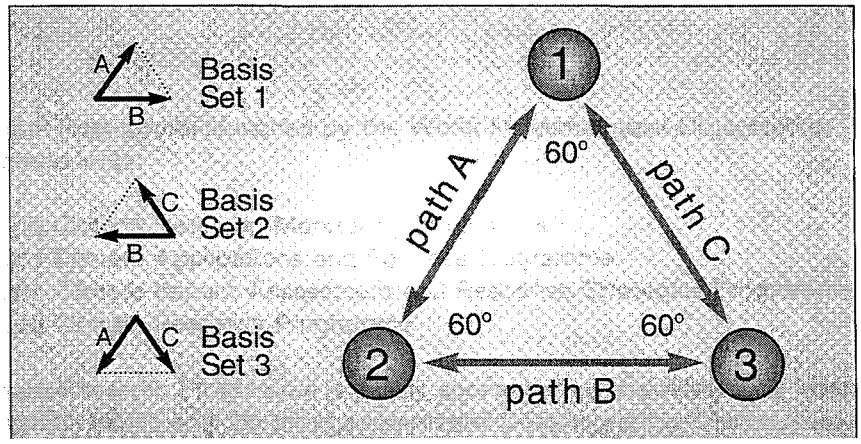

Figure 1

The primary difficulties in making accurate high wind speed measurements with sonic anemometers comes from effects created by the presence of the sensor components within the sample volume. The transducers block the natural flow of the air stream, causing pressure gradients in the sonic path, which modify the sonic propagation characteristics in a turbulent, non-stationary fashion. As wind speed increases, the received signal strength decreases while the acoustic noise increases. The decrease in signal to noise ratio and the turbulence effects combine to provide increased noise in the time of flight measurement, decreasing the accuracy of the speed and direction solution. Eventually, the wind speed increases to the point where there is insufficient signal to noise ratio to make a time of flight determination. At this point the sensor has no option other than to report the data as missing.

Wind tunnel tests show that all of these detrimental effects reach a maximum when the wind direction is in line with the sonic path between transducer pairs. This is where the over determined solution of the three-transducer approach provides its largest advantage over the four-transducer geometry. The Handar Model 425 internal algorithms discard the path that is most effected by turbulence and still have enough information to make a solution.

The orthogonal sensor, with only two vectors, must live with a highly jeopardized basis path when the path is co-linear with the wind direction at high speeds. At this direction the other basis path is broad to the wind, so its contribution to the wind speed solution is nearly zero. The sensor speed accuracy hangs almost completely on the accuracy of the path most effected by turbulence and pressure gradients.

At wind speeds below the extreme top end the redundant path of the Handar Model 425 provides useful information. The sensor internal algorithms use this information to verify and enhance the accuracy of the resultant solution.

The transducers used on the Handar Model 425 are made from cylindrical ceramic tubing metallic coated on their inside and outside surfaces. The cylindrical construction provides a radiation and reception angle wide enough to ìseeî the other two transducers. The rotational symmetry in the horizontal plane allows the transducers to provide a uniform cross section to the wind for all 360 degrees of wind direction. This greatly enhances the resultant wind directional accuracy and speed vs. angle accuracy, especially at upper wind speeds. Competitive 2-D four-transducer designs typically enclose their transducers within horizontal tubular constructions, which present a smaller cross section to the wind when impinged head on than they do from the side. This creates a greater angle dependent aberration to the airflow in the sample volume than is present with the Handar approach. Some of these sensors cannot meet the required accuracy without individual calibration of each sensor in a wind tunnel to create a two-dimensional correction table with both uncorrected speed and angle as input parameters, as well as costly periodic wind tunnel recalibration.

With all the advantages of the Handar approach set aside, the sensor shares the fact with all other sonic anemometers that the basic accuracy of the sensor is dependent on the distance between transducers and the accuracy of the time base used to make the time of flight determination. The Handar Model 425 time base is derived from its microprocessor crystal oscillator. State of the art crystal oscillator designs used in microprocessors either oscillate at a frequency tolerance orders of magnitude better than the sensor accuracy or do not oscillate at all due to component failure. The 425 will not report if the microprocessor oscillator is not running, so this leaves only the variation in the distance between transducers as a concern for sensor accuracy assurance. As mentioned above, the received signal amplitude drops as wind speed increases. Sensor operational validation and calibration verification can therefore be made at zero wind speed, without a wind tunnel, using a mechanism that slips over the transducers.

The Handar Model 425 Field Verifier allows users to verify proper operation of the sensor. It is a box which will only fit over the transducers if they are in correct alignment, and contains baffles in the sonic paths between each transducer which simulate the decreased received signal strength found at high wind speeds. The baffles verify the integrity of the transducers and supporting electronics. A near zero speed is expected with the Verifier in place, and a sensor command is available to calculate and retain in non-volatile memory subtle path differences within the sensor for later incorporation in the speed and direction algorithms.

Wind Tunnel Data

Figure (2) shows three minute averaged data (180 samples) for speed error vs. wind tunnel speed at a fixed direction of 180°. Figure (3) and (4) are data from a single wind tunnel run, where the angle was incremented by six degrees each data point with a constant wind speed averaged at about 120 knots. Each sample plotted is a single one-second reading. Figure (3) shows the speed error vs. angle, and Figure (4) shows angle error vs. actual angle.

Conclusion

Until recent times, the ultrasonic anemometer was little more than a research tool, used for fine structure wind studies because mechanical sensors lacked sufficient responsiveness. The clear advantages provided by a non-moving part anemometer had been outweighed by the price difference between the mechanical and sonic sensors. Research sonic anemometers also failed to meet the needs of general meteorology for top end speed and ability to stand up to the elements such as rain, snow, and icing. The Handar Model 425 was designed to provide a rugged, durable, cost-effective non-moving part solution to the general user knowledgeable to the long-term costs of providing accurate wind data. The advantages of the Handar approach over other sonic anemometers truly represents advancement in the state of the art.

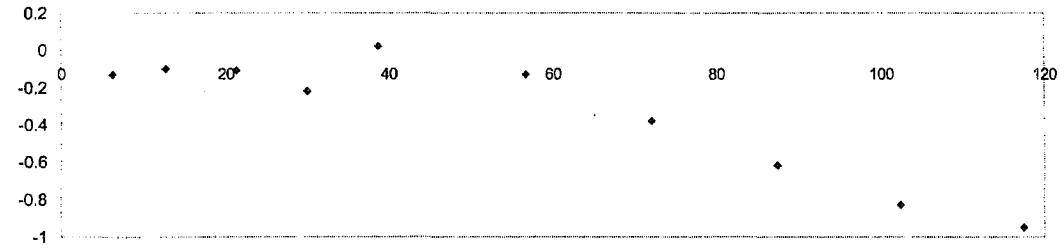

Handar 425 avg. speed error (knots)

Figure (2)

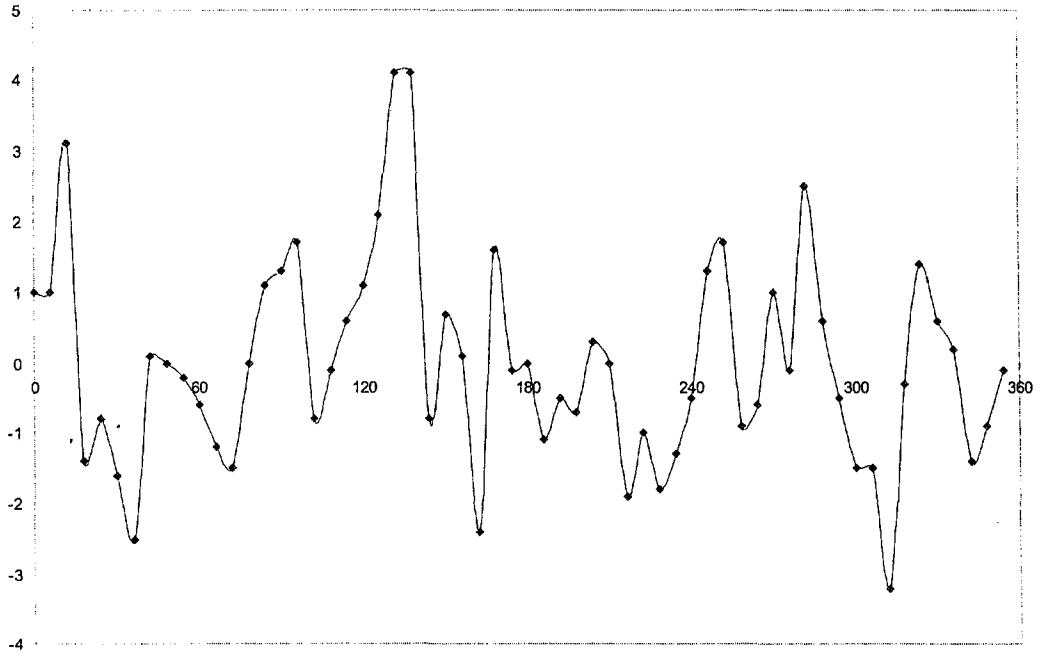

425 speed error @ 120 knots in knots

Figure (3)

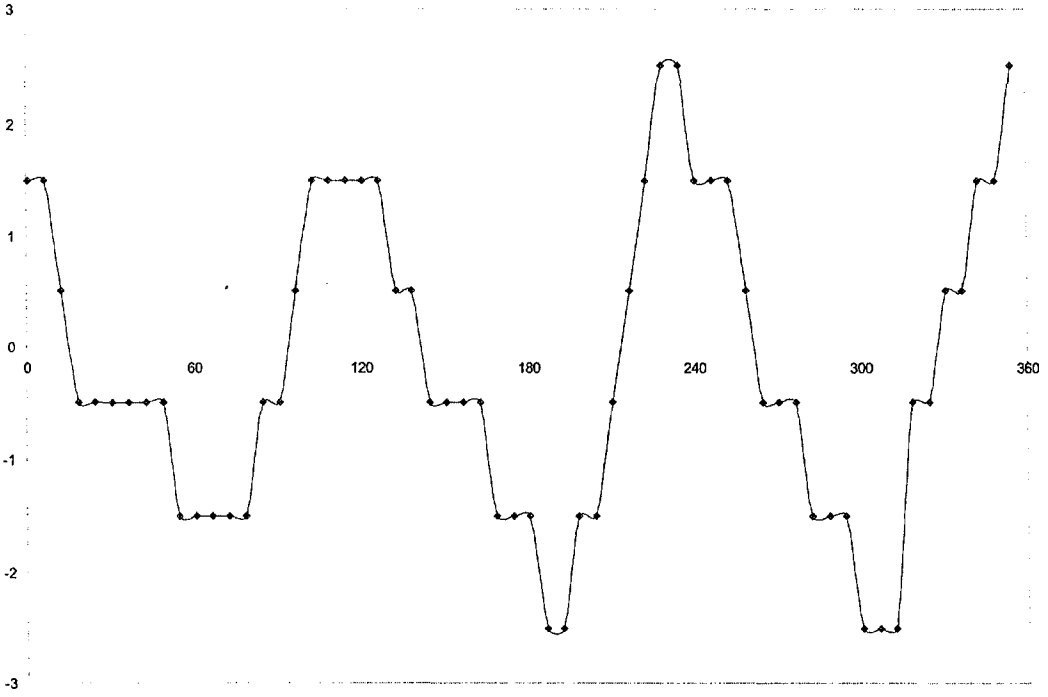

425 angle error (deg) at 120 knots

Figure (4)

The new concept of the Automatic Meteorological Observation System (AMOS)

Kunio Hoashi
Meisei Electric Co., Ltd., Tokyo, Japan

Abstract

Surface meteorological observation is the most fundamental means of observation for weather forecasting and climate changes. Meisei announced the newly developed Automatic Meteorological Observation System (AMOS) in 1995. The AMOS system is based on a new concept for improving observation accuracy, reliability and automatic observations. This AMOS is designed featuring the technical requirements (accuracy, time constant, averaging time, etc.) established by JMA(Japan Meteorological Agency) and WMO. Since 1996, the new system has been replacing the existing equipment in use in the meteorological observatories in Japan. More than 45 observatories have been substituted with the new AMOS system.

Introduction

The surface meteorological observation system is used in the local meteorological observatories throughout Japan. Fig.2 shows the block diagram of the AMOS .

The newly developed AMOS has two models. The AMOS-95 is installed in manned meteorological observatories. It monitors the present weather conditions, reports and processes climatic information statistically. It is further capable of data storage and multi processing such as printing, file maintenance. The AMOS-95 performs meteorological observation within the observatory and at the same time receives data from unmanned stations installed in the districted area. The collected weather data is converted into SYNOP(FM-12)report, domestic weather reports, etc., and output to the meteorological data telecommunication network (ADESS*[1]) which links all the meteorological observatories in Japan via leased land-line. All meteorological information available in Japan is sent to the headquarters via ADESS. In addition, the data acquired by the specified observatories are further linked to the WMO Global Communication System (GTS).

The AMOS-96 is installed in unmanned/automatic weather stations. The AMOS-96 is designed basically with the same concept as the above AMOS-95. The SYNOP (automatic) report of AMOS-96 is transmitted to meteorological observatory periodically via ISDN telephone line.
To enable unmanned (automatic) observation, the AMOS-96 system is provided with an uninterrupted power supply which can supply power for 24 hours. This also supports the small-size and power saving features of the AMOS-96 system.

This system has been originally developed for synoptic surface meteorological observation, but is also used for aviation weather observation system when optional sensors are added.

Design concept

The following design concept and features apply to both systems.

- *Fully automatic operation for SYNOP reporting*
- *Remote maintenance for unmanned weather station*
- *Built-in self-diagnosis and AQC*[*2] *for reliability*
- *Hot-standby computer system*
- *Advanced Data communications and networks*
- *Latest operating system(Windows-NT) for the multi-task processing*
- *New algorithm for present weather observation*
- *Substitute optical memory disc for analog recording papers*

---

*[1] ADESS :Automated Data Editing and Switching System *[2]AQC : Automatic Quality Control

Sensors

All sensors conform with the 6th edition of Guide to Meteorological Instruments and Methods of Observation(WMO-No.8). The AMOS system uses the following sensors:

a) Rain and Precipitation: Rain is measured in the unit of 0.5 mm with a tipping bucket type rain gauge with a collection funnel 200 mm in diameter. Precipitation intensity is determined by rain contact intervals. Presence of a precipitation phenomenon is determined by a droplet detector that detects resistance changes caused by rain drops.

b) Wind: A propeller type sensor is used to observe wind. The wind direction and the speed are converted into 8-bit gray code signals by a photo-encoder and optical pulses through a slit, respectively. This sensor is a heavy-duty with response characteristics similar to those of some lightweight cup and vane sensors.

c) Air Temperature: A 4-wire platinum resistance probe(Pt100) is used to measure air temperature. To reduce the time constant, a thin metal tube is used to protect platinum and the tube with the platinum is housed in a shelter ventilated at 5 m/sec.

d) Humidity: We tested many sensors of various measurement systems for three years to develop a practical system. Meisei confirmed that a polymer thin film capacitance type sensor has excellent accuracy and stability. The element is protected by a PTFE*3 filter using *GORE-TEX*™ because the sensor will be used in a dusty environment.

e) Air Pressure: After approximately two years of testing, we selected a sensor in which the deformation of a single crystal silicon diaphragm under the atmospheric pressure is detected by electrostatic capacity. This sensor has the smallest drift.

f) Solar Radiation/Sunshine Duration: The new AMOS system employs a newly developed sun tracking pyrheliometer-pyranometer. The both sensors measures the flux of direct and global solar radiation by a thermocouple. When the direct solar radiation is exceeded 0.12 kW/m^2, the sunshine duration is calculated by accumulator.

g) Snow Depth: An ultrasonic sensor of an excellent maintainability is used to measure snow depth. A transmitter is mounted on the top of a pole and ultrasonic pulses reflected from the surface of snow are detected by a receiver. The travel time of the ultrasonic waves is measured to determine the height, or snow depth.

h) Visibility and Present Weather: A forward scatter meter is used to observe MOR(Meteorological Optical Range) and present weather. MOR, precipitation and its intensity are observed every 1 and 10 minutes and every one hour.

Data Logger

The data logger converts sensor signals into digital signals, edits observation values that correspond with meteorological parameters, and stores the data in a memory. The number of sensors that may be connected is up to 20 elements. Conversion units corresponding to the number of sensors are connected to the CPU via the bus lines. The CPU for the data logger is based on a 16-bit microprocessor. To enhance software programs, a newly developed multi-task operating system (OS) has been installed. The multi-task OS allows real-time processing of all data.
All conversion units are provided with an individual 8-bit CPU for multiple data processing.

The self-diagnosis function checks the circuits for normal operation by periodically sending the standard signals to the conversion units of the system. To check the circuits, preset signals from a standard signal generator connected to the bus lines are used.

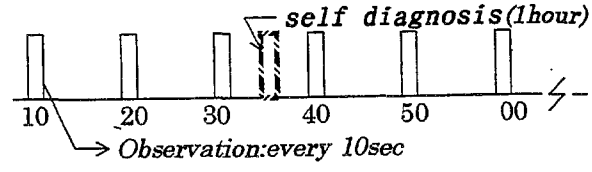

The checking is executed between observations as shown in the figure to the above. The self-diagnosis, real-time processing, can be executed without interrupting observations. The self-diagnosis function allows arbitrary inspection of the system from a remote place. It has enhanced the ability of automatic observation for unmanned weather station.

*3 PTFE : Poly-Tetra Fluorine Ethylene(Tefron™)

Dual Computer System

This system uses two personal computers which are interconnected via LAN (Ether-net of the IEEE*4 802.3 standard) to configure a duplex stand-by system. By using two low-priced personal computers, an economical system comparable to an Engineering WorkStation(EWS), a higher-level model, is realized. When main PC should fail, the other takes can be switched over to the stand-by computer, the system automatically resumes normal operation. As a result, reliability and function of the total system have been dramatically enhanced.

The CPU of the personal computers comprises a Pentium™ chip. The operating system is Windows-NT™. Both PCs always exchange data, and the data are mirror stored on respective hard disks. A HELP pop-up menu is provided to guide the user how to use the operations of the system. The user can use this menu like an instruction manual for the system. The adoption of Graphic Users Interface(GUI) has improved the operativeness of the system. Key operation and menu/tool bars on the display are the same as the standard Windows performances and are easy to use.

In a conventional and generally accepted surface meteorological observation system, real-time meteorological phenomena and long-term change trends are monitored on an analog recorder. With our new system, a CRT display replaces the conventional recorder to show graphical meteorological data in multiple windows allowing the operator to monitor data minutely. And the new software allows users to create the plural windows. Users can modify the display mode at any time.

Multi-task Processing

Fig.1 shows the multiple tasks.

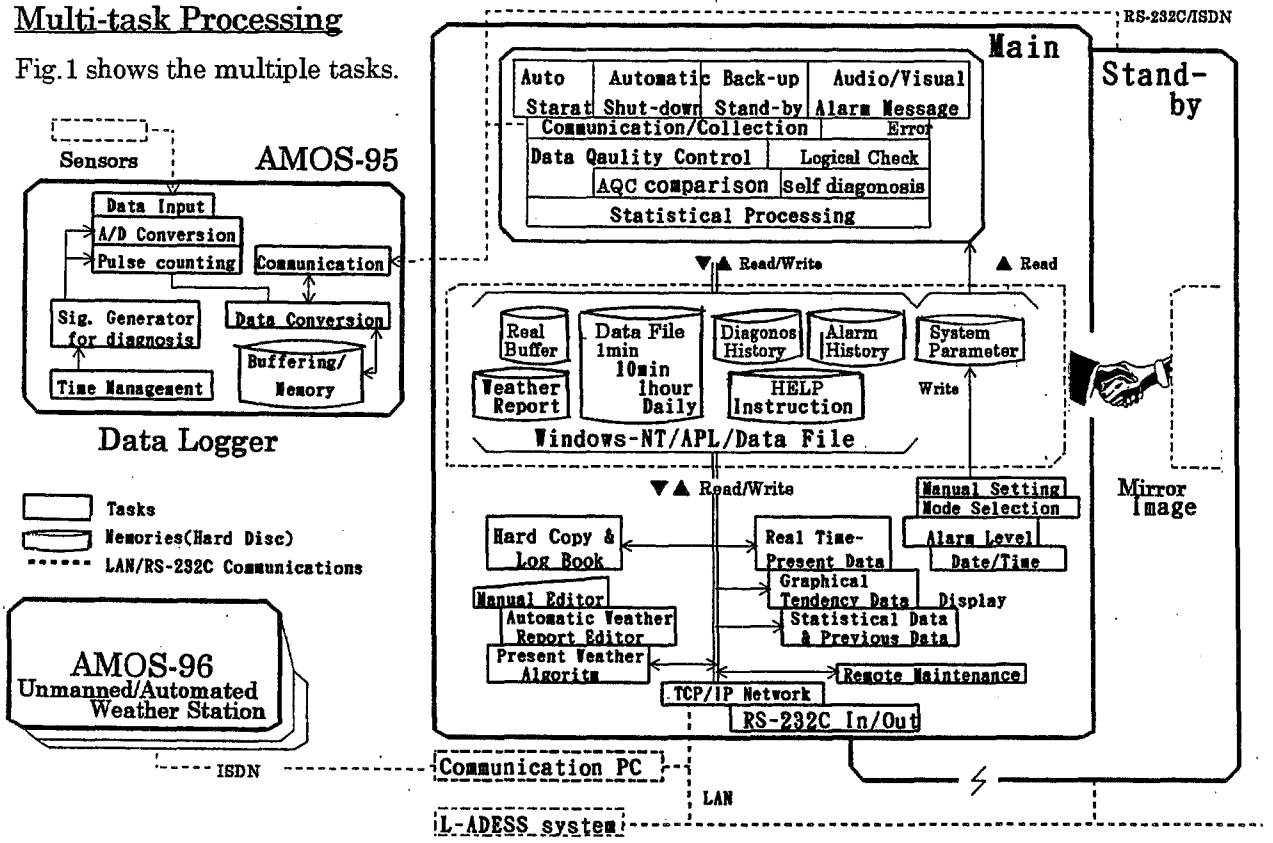

Fig.1 Software architecture of AMOS-95

Automatic Weather Report

In the new AMOS-96 unmanned weather stations, present weather information, which has conventionally been observed visually, is judged by the information derived from forward scatter meter and using a new algorithm in which air temperature, relative humidity and other data are combined. The result of the judgment is used to automatically edit ix (type of the observatory), VV (visibility), WaWa (present weather) and WaiWai (recent weather) which are the visual observation items currently being SYNOP reported. In this automatic process, the visibility values and weather are converted into 2-digit report steps and WMO-4680 codes, respectively.

The weather types are converted into symbols such as (●) for rain, (≡) for fog, (=) for haze and (*) for snow to show on the real-time monitor on the personal computers installed in the meteorological observatories and on the daily weather report.

Conclusion

At the automatic weather station, present weather, which has been observed visually, is coded and the SYNOP reports are automatically edited and generated making it possible to automate manual ion. In the aviation weather observation system, the necessary visual observation items include the directional lowest visibility, cloud(amount ,type) , thunderstorm, lightning and other important weather phenomena. The market is looking for the development of a new sensor and algorithm that take into consideration such factors as accuracy, reliability, maintainability and economy necessary for these meteorological elements.

It is now possible to optically/electrically observe precipitation in greater detail using a forward scatter meter. It is necessary to discuss correlation between visual and automatic observation. The difference between the results of observation due to different observation systems will be decreased when the current WMO expert meeting sets definitions for weather codes to ensure further development of automatic meteorological observation.

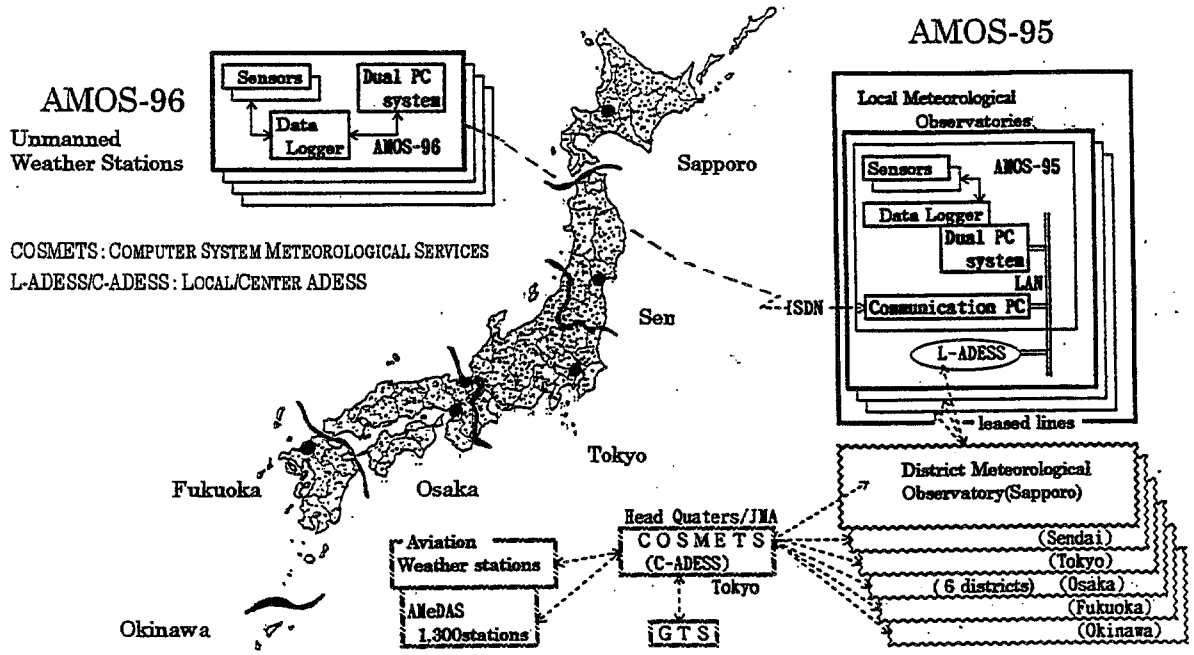

Fig.2 System Diagram for AMOS-95/AMOS-96 and Surface Meteorological Observation Network in Japan

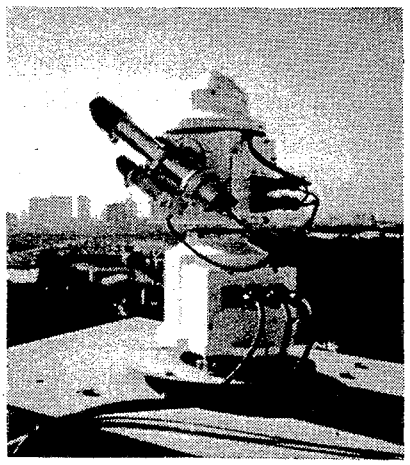

e.g. pyrheliometer-pyranometer

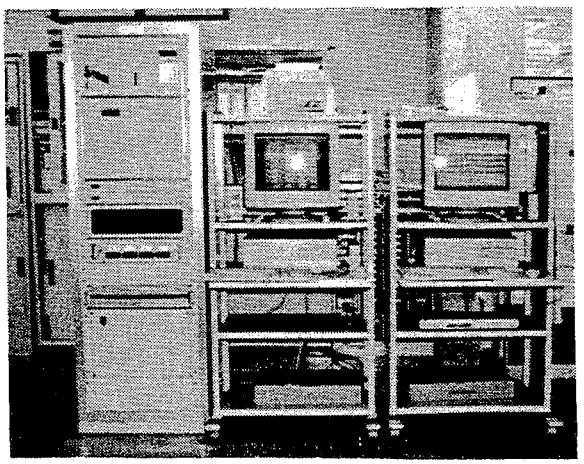

Data Logger Main & Stand-by Computer

Session X

VISIBILITY AND TEMPERATURE OBSERVATIONS

COMPARISON OF CEILING-HEIGHT AND VISIBILITY VALUES FROM OBSERVERS AND THE AUTOMATED SURFACE OBSERVING SYSTEM (ASOS)

Allan C. Ramsay
EG&G Services Corporation, Sterling, Virginia, U.S.A

Vickie L. Nadolski
National Weather Service, Silver Spring, Maryland, U.S.A.

1. INTRODUCTION

The United States Automated Surface Observing System (ASOS) has been criticized by some members of the aviation community for failing to provide representative reports of ceiling heights and visibilities that are important for flight operations. A joint National Weather Service (NWS) / Federal Aviation Administration (FAA) data-collection effort in 1995 provided a unique data set of over 10,000 hours of coincident ASOS and observer reports of ceiling height and visibility. This paper provides insight on the comparability of automated and manual observations, with special emphasis on differences in reports at the thresholds of 1000 feet (approximately 300 meters) for ceiling height and three miles (approximately 5 kilometers) for visibility, which define the breakpoint between Instrument Flight Rules (IFR) and Marginal Visual Flight Rules (MVFR) conditions.

Ceiling-height values from the ASOS are the result of a complex series of algorithms which process thirty minutes of data from a Vaisala CT12K laser ceilometer to generate a report with a maximum of three cloud layers each minute. The algorithms process two ceilometer reports each minute, successively group reports of cloud returns, and include provisions for surface-based obscurations, variable ceilings, and the reduction of data transmissions during rapidly-changing conditions.

Visibility values from the ASOS are the result of an algorithm which processes ten minutes of data from a Belfort Model 6220 forward-scatter visibility sensor; the algorithm computes a ten-minute harmonic mean of visibility values for a report each minute, and also includes factors for day/night and rain/snow conditions.

2. THE 1995 AVIATION DEMONSTRATION PROJECT

In response to concerns from the aviation community, the NWS and the FAA conducted a study of twenty-five ASOS installations throughout the country from mid-February through mid-August, 1995. The study was based primarily on manual input from observers who were required to record instances when ASOS reports were considered to be "unrepresentative." The results of the study provided strong evidence that, in the subjective opinion of on-site observers, the ASOS provides representative observations of ceiling and visibility.

A small part of the 1995 study involved the collection of concurrent human observations and un-augmented ASOS observations from four locations: Allentown-Bethlehem, Pennsylvania; Mobile, Alabama; Salem and Portland, Oregon. (Salem and Portland observations did not overlap in time, and were effectively treated a single data source which covered the full time period of the evaluation.) ASOS installations were typically three to four thousand feet distant from, and 30 to 70 feet below, the observers or towers. The arrangement at each location was that observers were not permitted to modify ('augment') the ASOS observations, even if those observations were considered to be unrepresentative. Just over 10,000 hours of observations were acquired, with more than 600 hours in IFR conditions. Although observers were not "blind" to the automated observations, the analysis was completed on the assumption that the automated data did not influence the observers' reports. Using the logic that an observation remains valid until it is replaced with a new observation, it was possible to compare manual and automated values of ceiling height and visibility for each minute of the day.

3. "CLIMATOLOGY" OF THE DATA SET

The manual and automated observations were highly comparable in their over-all reporting of ceiling height and visibility. Tables 1 shows the total number of hours with ceiling heights or visibilities below specific values, for both manual and automated observations.

Observers reported 641 hours of IFR conditions: the ASOS reported 658 hours of IFR conditions; some 501 hours of IFR conditions were reported concurrently by observers and the ASOS.

Ceiling Height (Feet)	Observer Hours	ASOS Hours	Joint Hours	Visibility (Miles)	Observer Hours	ASOS Hours	Joint Hours
No Ceiling	5006	6184	4769	≥5	9449	9463	9248
≥5000'	2569	1417	1080	<5	805	791	590
<5000'	2679	2653	2284	<4	510	589	380
<3000'	1502	1508	1271	<3	360	358	239
<1000'	448	463	358	<1	82.4	99	59.6
<500'	186	209	142	<0.5	39.0	58.3	28.7
<200'	45.7	85.7	35.6	<0.25	26.5	0.0	0.0

Table 1 Climatology of Observer and ASOS Ceiling-Height and Visibility

4. DISTRIBUTION OF VALUES

Although the over-all climatology of the data set indicated high comparability between manual and automated observations, a closer look at the distribution of specific values of ceiling height and visibility revealed significant differences. Figures 1 and 2 illustrate the differences between observer and automated observations: manual observations have a tendency to concentrate on specific values, while automated observations are more evenly distributed over the range of values, and appear to more closely represent a "natural" distribution of values. Preferential reporting of ceiling heights, in particular, raises questions because observers in this assessment had full access to the accurate (and commonly accepted) laser cloud-height measurements from the ASOS ceilometer. Of particular interest is the distribution of observer reports in the 900- to 1100-foot range of ceiling heights -- bracketing the ceiling-height threshold for Instrument Flight Rules.

When both the observer and the ASOS were reporting ceilings, why would an observer choose to differ from measured height values? Observers are conscientious professionals, but are also very conservative professionals, and members of an airport team whose primary mission is to ensure safe aircraft operations. An observer will not commonly "rush to judgment" to release a report of changing cloud heights until he or she is confident that the new cloud height represents a stable condition. This would be especially true when the cloud height is near an important threshold, such as 1000 feet.

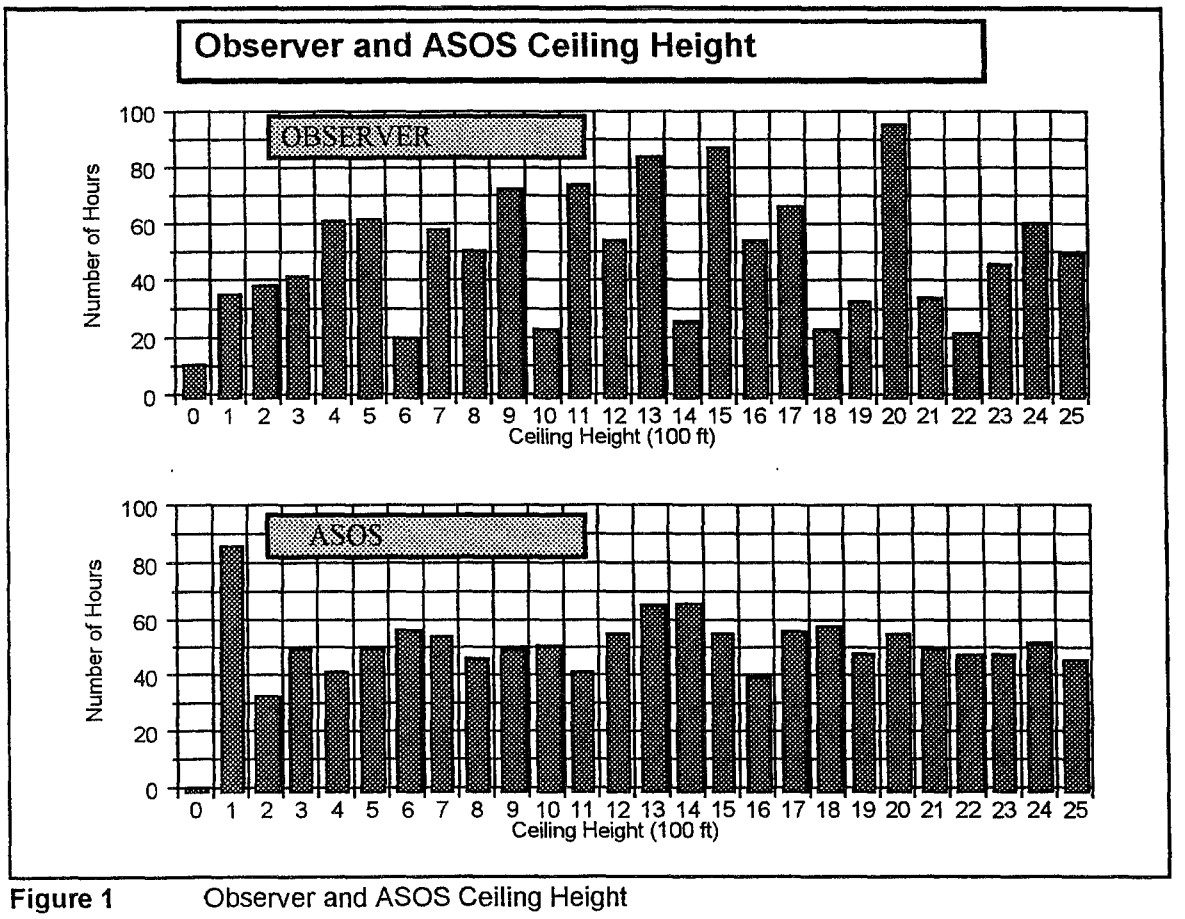

Figure 1 Observer and ASOS Ceiling Height

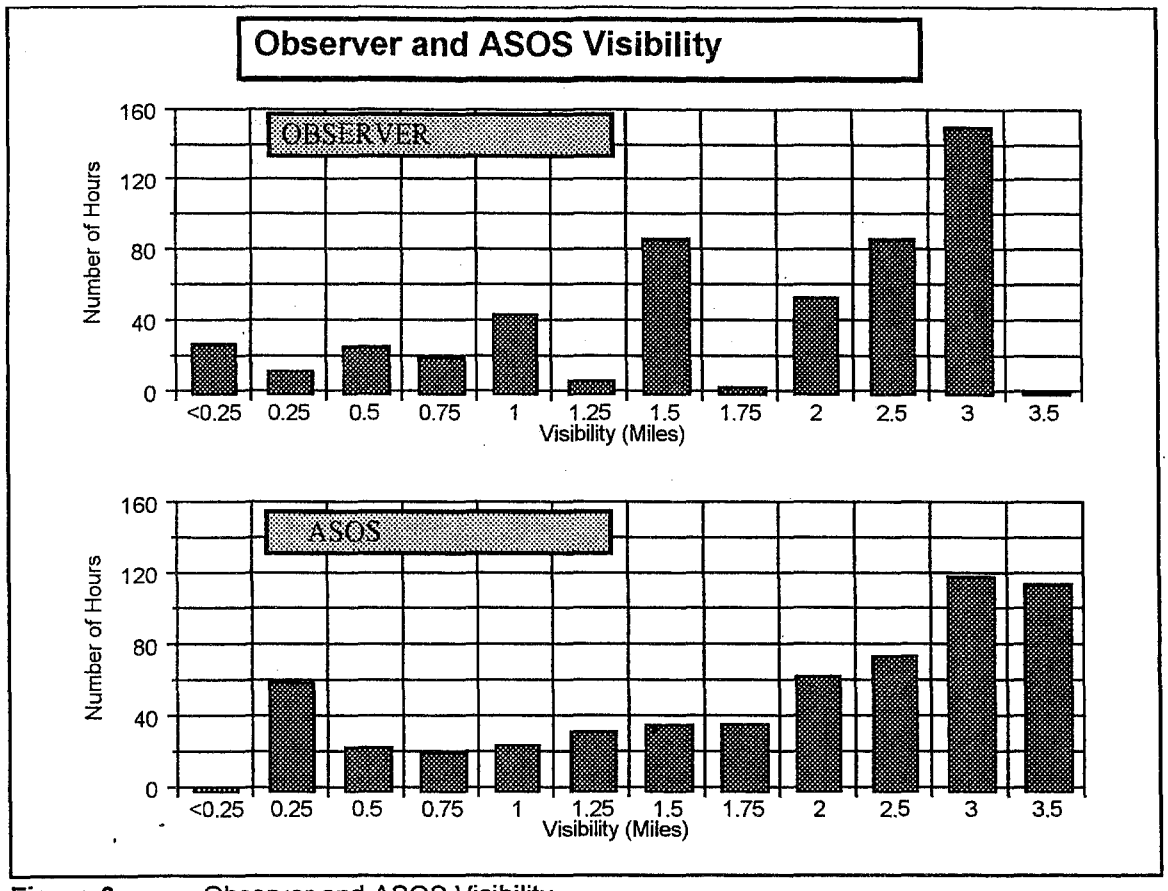

Figure 2 Observer and ASOS Visibility

Air traffic controllers and pilots in the local area would be highly unappreciative of reports which change between IFR / MVFR / IFR / MVFR, etc., every few minutes. Unfortunately, this is precisely what the ASOS may report: the automated system doesn't know or care how many aircraft are on final approach or waiting to take off, and the ASOS doesn't hesitate to transmit a new "SPECI" whenever it senses a change in cloud height from 1100 to 900 feet, or vice versa. (During this 10,000-hour evaluation, observers issued 1187 off-hourly "special" reports, compared to 3378 issued by the ASOS.)

5. DISAGREEMENTS BETWEEN OBSERVER AND ASOS

While the comparability between observer and ASOS reports is good from a climatological perspective, flight operations may be impacted by minute-to-minute differences between manual and automated reports. This data set provided an opportunity to examine minute-to-minute details of disagreements between observer and ASOS.

5.1 *Over-all Ceiling and Visibility Disagreement*

Table 1 and Figure 1, above, show significant disagreement concerning ceiling heights at or below 200 feet. This difference can be related directly to a characteristic of the ASOS laser ceilometer, which occasionally interprets partial ground-based obscurations as total obscurations (reported as Vertical Visibility, "VV") or as 100-foot cloud layers. The National Weather Service is aware of this ceilometer characteristic, and is evaluating technology which may provide more accurate reporting of vertical visibilities and cloud height in obscured or partially-obscured conditions.

Table 1 and Figure 2, above, show significant disagreements existed between observer and ASOS for values of visibility less than one mile. This category of disagreement is attributed to the different locations of the instruments (human eye vs ASOS visibility sensor) and also to the spatial variability of visibility values. It is probable that, in most cases, both the observer and the ASOS were reporting accurate values of visibility from their respective vantage points. As with real estate sales, the three most important issues regarding ASOS visibility reports are location, location, and location.

5.2 *Duration of Observer / ASOS Disagreements*

One characteristic of an observer/ASOS disagreement is the *duration* of the condition. Reports of changes in sky cover or visibility will be released as soon as they are identified by an ASOS, but may be delayed by an observer until the condition is determined to be stable. Delayed reporting may indicate a disagreement when all that is happening is a simple difference in responsiveness.

The median duration of episodes of significantly different values of ceiling height (±300 feet, for ceilings below 1000 feet) was 25 minutes; the median duration of visibility disagreements (±½ mile for visibilities less than 2 miles) was 20 minutes. Under the Basic Weather Watch criteria used for manual observations, it may not be possible for an observer to detect a change in ceiling or visibility of so short a duration, and even if detected, the observer would be likely to delay reporting to ensure that the conditions were stable.

5.3 *IFR / MVFR Disagreements*

Disagreements between observers and the ASOS are most important at thresholds which change flight rules; the IFR/MVFR thresholds of 1000 feet (ceiling height) and 3 miles (visibility) were closely examined to see if there were any possible explanations or patterns in the time periods when observer and ASOS disagreed.

- While observers reported IFR conditions and the ASOS remained above IFR, the ASOS frequently reported conditions very close to the IFR thresholds: for the 140 hours of disagreement, the ASOS reported 113 hours (81%) during which ASOS ceilings were at 1000-1200 feet, or ASOS visibilities were either 3 or 4 miles, or an ASOS scattered cloud layer was within 200 feet of the observer's ceiling, or there were showers creating different conditions at the different observation points.

- While the ASOS reported IFR conditions and the observer remained above IFR, the observer frequently reported conditions very close to the IFR thresholds: for the 157 hours of disagreement, the observer reported 108 hours (69%) during which observer ceilings were at 1000-1200 feet, or observer visibilities were either 3 or 4 miles, or an observer scattered cloud layer was within 200 feet of the ASOS ceiling, or there were showers creating different conditions at the different observation points.

6. CONCLUSIONS

This unique data set indicates that significant disagreements are typically of short duration, while long-term disagreements typically occur when the observer and ASOS are reporting values that are close, but may be on opposite sides of an important threshold (e.g., IFR / MVFR flight categories).

Users should remain aware of the potential for, and the character of, observer / ASOS differences. In particular, users should be aware of the ASOS ability to report changes in ceiling and visibility as often as changes are detected. The responsiveness of the ASOS to changing conditions is both a blessing and a curse: ASOS can report changes (especially at night) before they can be detected by an observer, but the ASOS proclivity to report frequent changes can create challenges for users of automated reports. In order to get a representative picture of conditions at an ASOS-supported airfield, users should learn to consider a series of ASOS reports rather than to assume a single ASOS snapshot is likely to represent the "smoothed" conditions typically reported by the observer.

Comparison of Forward Scattermeter and Short-Baseline Transmissometer For Runway Visual Range Use

Steve Collett, National Air Traffic Services, Ltd., UK
Deborah Lucas, Federal Aviation Administration, Washington, DC, USA
David C. Burnham, Scientific & Engineering Solutions, Inc., Orleans, MA, USA

1. Introduction

The United States (US) selected[1] a forward scattermeter for the Federal Aviation Administration's new generation runway visual range (RVR) system. After an extensive test program and two redesigns[2], the system was approved for deployment in 1994 and installation at US airports began. The final scattermeter design uses (a) a look-down scatter geometry that protects the windows from contamination and snow clogging and (b) a scattering angle (42°) that gives equal fog and snow response. The US forward scattermeter was validated against US requirements using the standard US transmissometer, which represents 1940s optical technology combined with 1970s electronic technology. Since the US transmissometer cannot measure the full RVR range of 50 to 1500 m, the scattermeter validation for RVR values below 200 m was carried out by analysis and by comparison with human observations.

The UK RVR system is based on a state-of-the-art transmissometer, which has been the conventional choice for RVR systems. The UK transmissometer uses a folded 20-meter baseline; its transmission measurement provides sufficient accuracy to cover the entire RVR range with a single instrument. This UK transmissometer is the end product of 30 years of ongoing development and evaluation, resulting in an instrument that is reliable and has no known deficiencies. The early instruments were validated against human observers and other transmissometers of different baselines. This validation has been carried forward to the current instrument by intercomparison trials[3] of successive generations of instruments. Periodically the current transmissometers are returned to a central location for calibration and recertification, where the calibration is traceable to national standards.

In 1994 the US and the United Kingdom (UK) agreed to conduct comparison testing of their respective RVR systems. This comparison testing provided an opportunity to study the performance of the latest transmissometer and forward scattermeter technologies under a wide range of conditions. Tests were conducted at three sites: (1) Birmingham International Airport (UK), (2) Otis Weather Test Facility on Cape Cod, Massachusetts and (3) Mt. Washington, New Hampshire. The three-year Birmingham test compared two US forward scattermeters to an operational UK transmissometer. A UK transmissometer was installed in the US at Site 2 for two years of testing, except for one summer at Site 3.

The following test results will be presented:

1. A comparison of US and UK transmissometers at normal airport fog densities will establish the equivalence of the US and UK transmissometers as reference standards for evaluating the performance of forward scattermeters.
2. A comparison of the US scattermeter and the UK transmissometer in dense fog will show how beam attenuation affects scattermeter performance.
3. The consistency of the scattermeter fog response will be addressed using data from all three sites. This issue has been raised[4] as a serious obstacle to the use of a scattermeter for RVR.
4. The US and UK accuracy requirements will be compared and applied to the US forward scattermeter.

2. Comparison of US and UK Transmissometers

The Otis test provided an opportunity to compare the UK transmissometer to the US transmissometers used to evaluate the US forward scattermeter. The US reference standard consists of two transmissometers with crossed baselines of 90 and 150 meters. The reference MOR is derived from the average extinction coefficient from the two transmissometers. The difference between readings is used to assess the homogeneity of the fog and to reject invalid transmissometer data. The US homogeneity criterion requires a difference less than ten percent of the average.

Figure 1 shows a box plot[5] comparing the UK transmissometer against the US reference standard. The box plot shows the distribution of the meteorological optical range (MOR) ratio of the test sensor to the reference sensor as a function of the MOR measured by the reference sensor. For each MOR bin, an X marks the median (50th percentile) of the distribution, a box marks the 25th and 75th percentiles, a heavy line marks the 5th and 95th percentiles, and a thin line marks the 2.5th and 97.5th percentiles. The results of the 10-percent homogeneity test are listed to the right of each bin; note that the fraction of the points rejected decreases dramatically for lower values of MOR. The ratio data for MOR < 600 m (MOR bins with "F" label) are consolidated into a bin labeled "FOG" at the bottom of the plot; 1287 minutes of homogeneous fog were experienced during the one-month test period. Five percentile MOR ratios are listed at the bottom of the plot for the FOG bin. The UK RVR accuracy limits (see Section 5) are drawn on the plot. The agreement between the UK transmissometer and the US reference is excellent; the difference in median fog calibration is only 1.2 percent.

Table 1 shows how the performance evaluation of a forward scattermeter differs when compared to the US and UK reference transmissometers; percentiles of the "FOG" bin (MOR < 600 m) are presented. The 50th percentile (median fog response) is almost identical for the two references. However, the spread between the 25th and 75th percentiles is slightly

greater for the UK reference than for the US reference. Some of this small difference may be related to the differing homogeneity criteria used for the two references: two-sensor comparison for the US and time variability for the UK (see next section). Two-sensor comparison can reject poor quality transmissometer data, while time variability cannot. One must conclude that the two reference standards are essentially equivalent for evaluating the performance of forward scattermeters.

3. Dense Fog Results

Homogeneous, dense fog occurs frequently on top of Mt. Washington. Figure 2 presents a box plot comparing the performance of a US forward scattermeter to the UK transmissometer as a reference standard. The MOR values in Figure 2 reach as low as 10 m. The data points included in the plot are subject to a 10-percent homogeneity test based on the time variability of the UK reference transmissometer; the MOR for the prior and following minutes must differ by less than 10 percent. The ratio data for MOR <300 m are consolidated into a bin labeled "FOG" at the bottom of the plot; a large amount (13,753 minutes) of homogeneous fog was experienced during the three-month test period, most with MOR below 50 m. The dense fog on Mt. Washington was less homogeneous (only half the points accepted by 10-percent criterion) than at Otis (see Figure 1). Figure 2 shows the US error limits (see Section 5) instead of the UK limits in Figure 1.

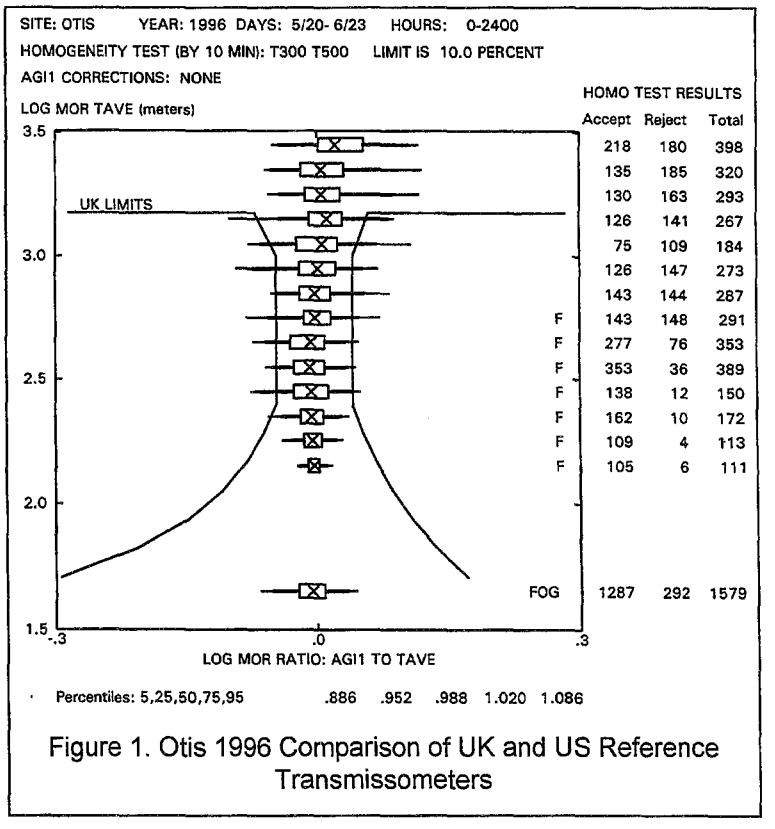

Figure 1. Otis 1996 Comparison of UK and US Reference Transmissometers

Table 1. Otis Performance of US Forward Scattermeter 3/5/97-8/11/97: FOG Bin MOR Ratios for Specified Percentiles

Reference	10 % Homogeneity	5th	25th	50th	75th	95th
US	By Two Sensors	0.875	0.928	0.960	1.000	1.093
UK	By Time Variability	0.835	0.903	0.958	0.997	1.061

The most notable feature of Figure 2 is that the median MOR ratio varies greatly with MOR for the five lowest MOR bins. This observation was not a surprise. The original scattermeter calibration corrected for attenuation over the 1.0-m path between the transmitter and receiver. Prior testing showed that this correction was too large and it was therefore removed from the deployed US system. When a beam attenuation correction was added to Figure 2, the best attenuation distance was found to be 0.5 or 0.6 m. Figure 3 shows the results with a 0.6-m correction; the median MOR ratios are consistent for all bins with more than 400 minutes of data. Updating the US system with a 0.6-m beam attenuation correction is currently under consideration.

The explanation for the reduced attenuation distance can be found in the way light scatters from fog. For each fog particle, the total amount of scattered light is equal to twice the amount of light hitting the particle. The light hitting the particle is scattered into *all* directions. The shadow of the particle in the incident light beam produces an equal amount of diffraction scattering, which is concentrated in the forward direction. The observed factor of two reduction in attenuation correction compared with the physical distance is understandable if the

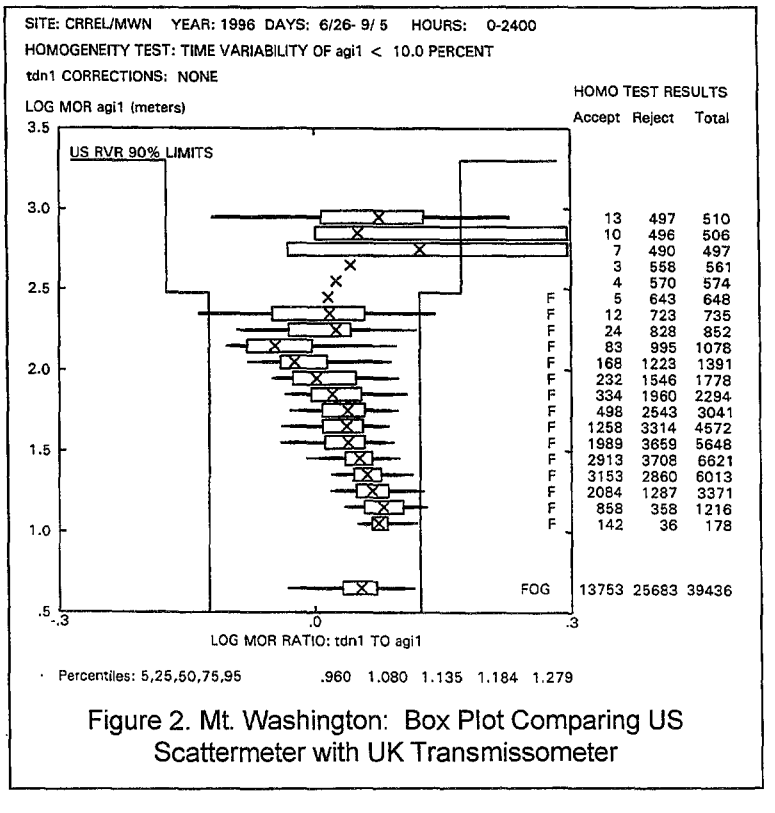

Figure 2. Mt. Washington: Box Plot Comparing US Scattermeter with UK Transmissometer

diffraction scattering does not effectively remove light from the beams of the sensor.

4. Scattermeter Fog Calibration Consistency

The unit-to-unit calibration consistency of a scattermeter depends upon the consistency of the scattering geometry. The production consistency of the US forward scattermeter was checked[2] using a precision measuring machine. A number of "golden" units, i.e., those with close to nominal scattering geometry, were selected for field testing (1) to determine the correct scattermeter calibration and (2) to assess the variation in fog calibration under different test conditions. All the data presented in this paper came from "golden" sensors. The current fog calibration for the US scattermeters was derived from early production sensors that were not golden. Field test data show that the typical calibration of the golden sensors is about five percent different (MOR ratio 0.95) from the reference transmissometers. A field calibration adjustment will be implemented as part of future system enhancements.

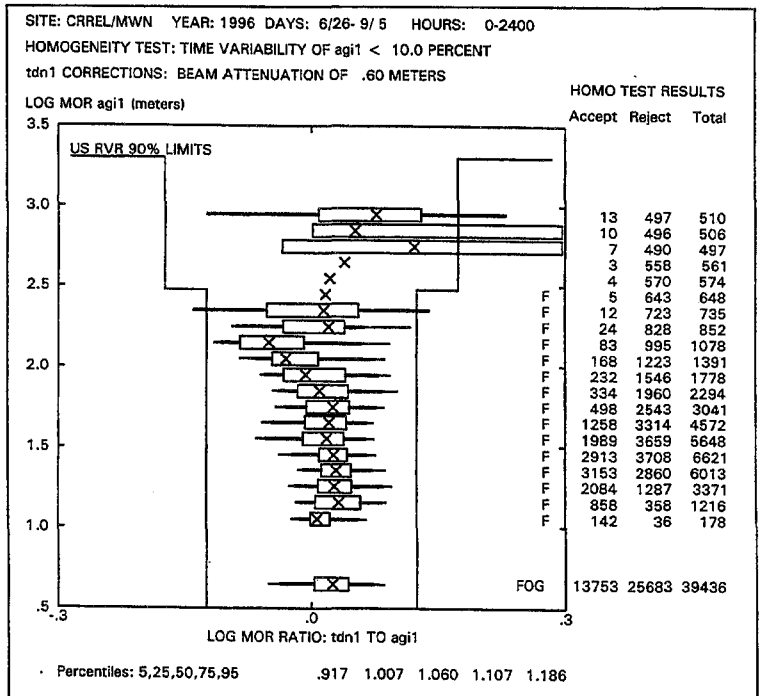

Figure 3. Comparison of US Scattermeter (0.6-Meter Attenuation Correction) with UK Transmissometer

The concept of the forward scattermeter assumes that the scattered signal in a particular range of scattering angles is proportional to the total extinction coefficient. For effective operational use, this proportion must be nearly constant for different fog conditions (i.e., different drop size distributions). Scattermeter designers have selected scattering angles in the range 30 to 50 degrees which, based on the angular scattering characteristics of fog, should provide performance approximately independent of the precise drop size distribution. The validity of this assumption was tested for the US forward scattermeter by (1) comparing the median fog response results for different sites and different test periods, (2) looking at the spread in the MOR ratio distribution, and (3) studying the variation in fog response with wind direction. Data from the first two analyses will be examined.

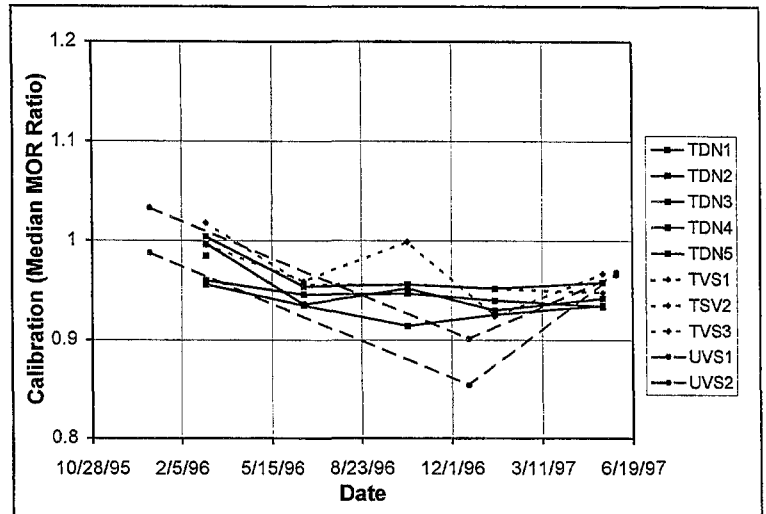

Figure 4. Calibration of "Golden" Forward Scattermeters at Otis (5 periods) and Birmingham (3 periods)

4.1. Median Fog Response

Comparing the median fog response from different sites will ensure consideration of different drop size distributions resulting from differences in geography Figure 4 shows the golden sensor test history over two years at the Otis (units with T--- names) and Birmingham (units with U--- names). Figure 3 shows the Mt. Washington test results. The test results for the three sites are somewhat different:

Otis - Five test periods - The total spread in median fog response is ± 5 percent. Periods 1 and 3 showed the greatest variation. The other three test periods showed a much smaller variation of ± 2 percent.

Birmingham - Three test periods - The total spread is ± 9 percent and the two units disagree by about 5 percent for the first two periods (which had the most data).

Mt. Washington - The median MOR ratio about 10 percent higher than the typical value noted for Otis

Although the variance is greater than at Otis, the Birmingham values bracket the Otis values and give no evidence for a systematic difference in fog type between the two sites. The reason for the greater variability of the Birmingham data is not known at present. The scattermeters tested at Birmingham are now being tested at Otis using US and UK reference standards.

The more significant difference in the Mt. Washington data is likely an example of scattering proportion variations resulting from a radically different fog type. Mt. Washington fog is typically generated by relatively strong upslope winds as opposed to Otis fog which is formed by advection over the cool ocean. Since the conditions encountered on Mt. Washington are not representative of operational airports, the differences noted are not considered to be significant.

4.2. *MOR Ratio Distribution*

A narrow MOR ratio distribution will indicate consistent performance at a single site where drop size distribution may vary from event to event and within each individual event. Table 1 presents data on the width of the MOR ratio distribution for scattermeter-transmissometer comparisons. For both references half the ratios (25^{th} to 75^{th} percentiles) lie within ± 5 percent of the median ratio. Likewise, 90 percent of the ratios (5^{th} to 95^{th} percentiles) lie within a spread of 23 percent.

5. Accuracy Requirements

The US visibility sensor accuracy requirements are listed in Table 2. The RMSE (root-mean-square-equivalent) limit says that, for a Gaussian error distribution, the standard deviation of the measurement must be less than the specified value at the 90% confidence limit. Specifically, this requirement means that 90% of the errors must be less than 1.65 times the RMSE accuracy value. The US accuracy criteria are shown as vertical boundaries in Figures 2 and 3 and are designed to be applied to experimental data using the two-transmissometer US reference standard with a 10-percent homogeneity criterion. In this accuracy definition, any errors in the reference standard are incorporated into the accuracy requirements. To meet the US accuracy requirement, 90 percent of a sensor's MOR ratios must lie within the accuracy limits. The US scattermeter meets[2] the US accuracy requirements.

Table 2. US MOR Accuracy Requirements

MOR	Accuracy
300-2000 m	20% RMSE
< 300 m	15% RMSE

Table 3 lists the UK RVR accuracy limits. The accuracy values are two standard deviation values (i.e., 95 percent of the RVR measurements must be within the limits). The UK accuracy criteria are more stringent than those of the US, but are not as easily applied to experimental data since they pertain to RVR system accuracy, which has contributions from light intensity and background luminance errors, in addition to MOR errors. Moreover, it may be difficult to account for errors in the MOR reference sensor. The analysis of this paper avoids these difficulties by applying the criteria of Table 3 to MOR rather than RVR. Figure 1 plots the errors of Table 3 under this assumption. If the reference sensor had no errors, then the UK transmissometer data in Figure 1 would appear to violate the accuracy requirement since the 95-percent lines (narrow lines for each MOR bin) are typically well outside the limits. However, a more reasonable assumption is that the US reference and UK transmissometer have comparable errors. In this case, the error limits should be expanded by $\sqrt{2}$ to include the reference sensor errors and will then encompass enough of the error lines to meet the UK accuracy criteria.

Table 3. UK RVR Accuracy Limits

RVR	Accuracy
<250 m	±25 m
250-1000 m	±10%
1000-1500 m	±(RVR/100)%

The application of UK accuracy criteria to a forward scattermeter is difficult because the assumption of equal test sensor and reference sensor errors is not necessarily valid for transmissometer-scattermeter comparisons. A deeper analysis of the test data summarized in Table 1 suggests that the spread in the MOR ratio distribution for a single golden scattermeter can be narrow enough to meet the UK criteria for MOR below 600 m, but probably not for higher MOR values. Moreover, variation in the mean response for non golden scattermeters may put some production run US sensors outside UK criteria at MOR above 250 m where high accuracy is required.

6. References

[1] Burnham, D.C. and Phillips, C.O., "Validation of a Forward-Scatter Visibility Sensor for RVR Measurements," WMO/TD-No. 462, Papers presented at the WMO Technical Conference on Instruments and Methods of Observation (TECO-92), 11-15 May 1992, Vienna, Austria, pp 320-324.

[2] Burnham, D.C., Spitzer, E.A., Carty, T.C., and Lucas, D.B., "United States Experience using Forward scattermeters for Runway Visual Range," DOT/FAA/AND-97/1, Volpe National Transportation Systems Center, Cambridge, MA, USA, March 1997.

[3] Brown, W.D. and Collett, S.R., "Close Agreement Between Two Transmissometers of Different Designs During Field Evaluation Trials," presented at TECO-92

[4] Brown, W.D., "Scatter Related Errors in RVR Atmospheric Optical Sensors," WMO/TD-No. 462, Papers presented at the WMO Technical Conference on Instruments and Methods of Observation (TECO-92), 11-15 May 1992, Vienna, Austria, pp 341-344.

[5] Griggs, D.J., Jones, D.W., Ouldridge, M. and Sparks, W.R., "The First WMO Intercomparison of Visibility Measurements, United Kingdom 1988/1989," Final Report WMO/TD-No. 401, 1990.

COMPARISON OF METEOROLOGICAL SCREENS FOR TEMPERATURE MEASUREMENT.

LEFEBVRE Guy, (FRANCE)
METEO-FRANCE/SETIM/QMR BP202 78195 TRAPPES
e mail: <guy.lefebvre@meteo.fr>

1 INTRODUCTION

The miniaturization of sensors and the wish to reduce manufacturing costs lead to consider smaller and smaller meteorological screens made of new materials. This explains interest of a technological follow-up regarding meteorological screens. The main purpose is to homogenize the effect of the screen upon temperature measurement in a meteorological surface network.

For any screen comparison, it's difficult to know the real air temperature. This comparison is used as a support and comments the elaboration of a standard relating to meteorological screens. It can also give the opportunity to discover a screen excluding any baneful influence and offering the sensor a maximal protection.

2 PRESENTATION

This comparison started in january 95 up to december 97. In this document, the data acquired during the period from 01/04/96 to 01/04/97 will be studied.

The site is that of the SETIM-TRAPPES, near PARIS. Its climatology is characterized by:
- Daily maximal temperature averages from +5.3°C in winter (Februar) to +23.3°C in summer (August),
- Absolute maximum +36.6°C and minimum -15.8°C,
- 54 frosty days per year in average,
- average precipitations per month ranging from 48 to 59mm, being 651mm per year,
- 12 to 17 precipitation (rainy) days per month,
- Average insolation duration per month 44 to 225h i.e 1668h per year,
- Average wind speed 3.3m/s,
- 58 foggy days per year, 1 to 9 par month.

2.1 Temperature sensors used

All temperature sensors are 100 ohms, platinum thread probes, class A. The 0°C error does not exceed +- 0.15°C. The margin of error is +-0.1°C. This type of sensor is used in the Météo-France network. Before field use, they are calibrated in our metrology laboratory.

2.2 Acquisition equipment

The 4 thread probes are connected to a FLUKE Helios 1 station. The RTD channels allow the setting of 3 and 4 thread probes. There are 20 channels with a ground connection common to 10 channels. A 1mA current is injected. This low current avoids any self heating problems.
For temperatures between -200°C and +150°C and for class A probes, The Helios system accuracy is 0.1°C (0.006°C resolution,0.04°C repetability). The acquisition of temperatures and other variables considered as influence factors are simultaneously done every minute.

2.3 Sensors used to analyse influence factors

Influence factor	Sensors
Wind at 2m (above ground level)	DEOLIA 92 (Degreane): cup anemometer.
Global radiation	Pyranometer CM11 (Kipp & Zonen)
Infrared radiation	Pyrgeometer (Eppley)
Précipitations	Tipping bucket rain gauge resolution 0.05mm
Visibility	FD12P,(Vaïsala) & Belfort
Sunshine duration	Optical fiber heliograph (Cimel)
Temperature at -100, -50, -20, -10, at ground, at +10, +50, +100, 150, 180cm	Pt100 probes outside screen
Humidity	Hygrometer Hmp35DE (Vaïsala)
Sun elevation	Computed
Cloud cover (Nebulosity)	Observed by the regular synoptic station

2.4 Screens tested

Ventilation	Manufacturer	Model	Legend
Natural	Socrima	Bmo1152	**GM2**
	Socrima	Bmo1161	**MRE**
	Socrima	Bmo1167	**MIN**
	Young	41002	**YOU**
	Vaïsala	Dtr13	**VAI**
	Cimel	601	**CIM**
	Précis-mécanique	Bmo1180	**MAR**
Artificial	Vaïsala	Dtr13F	**VAF**
	Young	43408	**YVN**
	Qualimétrics	8150	**QVE**
	CEN	prototype	**GRE**

Legend	materials, design, characteristics
GM2	White ABS, white painted,shutter Stevenson type
MRE	White ABS, white painted,shutter Stevenson type
MIN	blue ABS, white painted,11 cups + covers
YOU	UV resistant white thermoplastic, 12cups among which 3 plain ones on the top.
VAI	Polyester reinforced fiberglass, 12 cups piled up among which 2 plain ones on the top, white painted upperpart, black painted underpart.
CIM	white painted aluminium, 10 cups among which a plain one on the top.
MAR	White painted polyester plastic, 5 cups piled up.
VAF	The same as **VAI** with a solar panel on the top and an autonomous fan (1.8m/s).
YVN	UV resistant thermoplastic, ventilation speed 6m/s
QVE	White painted aluminium, ventilation speed 1.8m/s
GRE	White painted grey PVC, speed 1.8m/s

2.5 Screens installation

The screens are installed above grass more than 2.5m from each other and more than 50m from any building. The sensors are located at 1.5m above ground level.

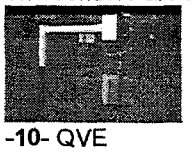
-10- QVE


-11- GRE


-12- YVN

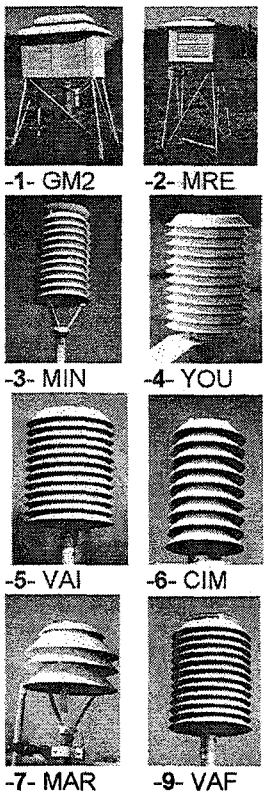

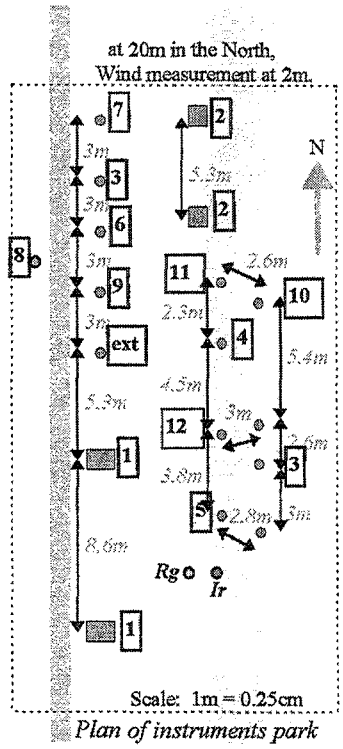

Plan of instruments park

3 CHOOSING THE REFERENCE (12)

The ventilated screen YOUNG 43408 was chosen as a relative reference for the following reasons:

- The manufacturer claims that YVN presents a minimal overheating around 0.1°C for a total radiation below or equal to 1080W/m²,
- The results show that YVN is always the coldest screen in the day as soon as the sun shines,
- We have not noticed any case of psychrometric effect even in winter,
- The constant flow of ventilation makes the comments on the behaviour of natural ventilation screens easier.

4 INFLUENCE OF SCREENS UPON T,Tmin,Tmax.

The percentage of data T,Tmin,Tmax showing a deviation from the reference within the interval (-0.2°C, +0.2°C) are displayed in the following histogram (Fig1).

9 screens out of 11 obtain more than 50% of the instantaneous data (T) within the interval (-0.2;+0.2°C) and 3 screens out of 11 obtain more than 60%.

The influence of the screen over temperature measurement is much more important in the day. Percentages are lower for the maxima (6% to 61%) than the minima (57% to 85%).

The screen must protect the sensor from sun (direct and diffused) and earth and atmospheric radiation. In the day, 3 screens (GRE,CIM,MAR) obtain less than 20% maxima meeting the above criterion. These are screens particularly sensitive to solar radiation.

Any vapour, dew or microdroplets on a probe produces a quantity of energy through condensation, at dawn in particular. This accounts for the strange behaviour of QVE regarding the minima for which several cases of psychrometric effect have been noted. The screen is sensitive to heat transfers by changing state (evaporation, condensation).

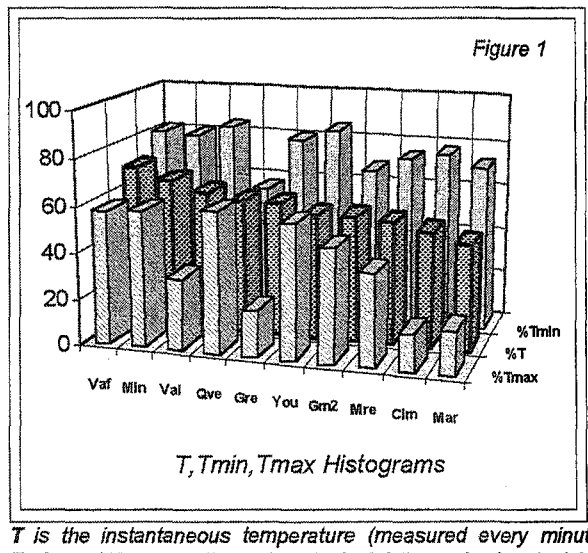

*T is the instantaneous temperature (measured every minute). **Tmin** and **Tmax** are the meteorological daily maximal and minimal temperatures calculated . The maximum (minimum) temperature is calculated from the data acquited from 6h01 (18h01) on D.day (D.day - 1) to 6h00 (18h00) on D.day + 1 (D.day) and assigned to D.day*

5 SCREENS USED BY DAY TIME

The data are processed only if the optical fiber heliograph detects a direct radiation above the 120W/m² threshold. Three wind speed intervals are considered (FF<1m/s, 2<FF<3m/s, FF>5m/s). In figures 2,3,4 the medians of the deviations from the reference (on Y-axis in °C) are compared according to global radiation classes "RG" (on X-axis in W/m²) depending on wind speed at 2m.

The deviation from the reference results from overheating due to "RG" from a quantitative point of view. The standard deviation reveals a data scattering that is to say the ability of the screen to homogenize the air temperature round the sensor by mixing the internal air either through natural or artificial convection. All sensors are influenced by the global radiation "RG". The deviation of median from the reference increases with "RG" by -0.2°C to.+1.7°C ,considering the set of screens (fig 2,3,4).

5.1 Natural ventilation screens

With a light wind, a natural ventilation screen in white thermoplastic or white painted ABS shows a standard deviation which decreases as "RG" increases. This can be explained by the fact that natural convection increases (in direction earth-sky) due to the rise in the temperature of the ground compared with that of the air on sunny days. This increase in natural convection on clear and windless day with a high "RG" can also account for the overheating limit of these screens for a RG >= 700W/m² (Fig2). The standard deviations decrease when the wind increases (from 0.46 to 0.18°C for GM2, from 0.33 to 0.13°C for VAI).

(In fig2, VAI and YOU are not shown. They are similar to MIN)
(In fig3, GRE is not shown since similar to MAR and MIN,GM2,VAI have their plotting points between MRE and VAF)
(In fig4 MIN and YOU are not shown since similar to VAI)

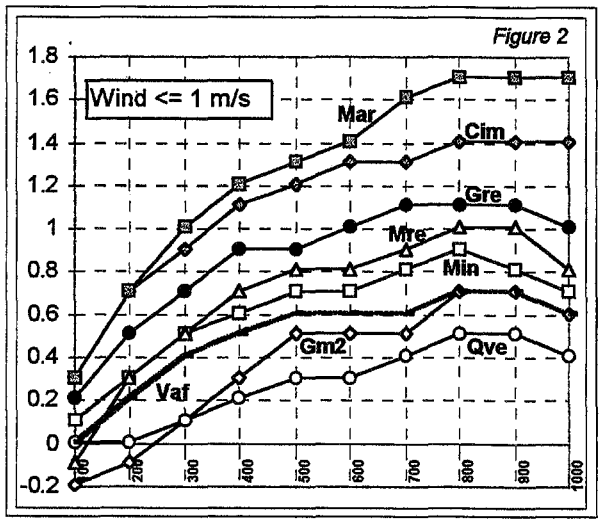

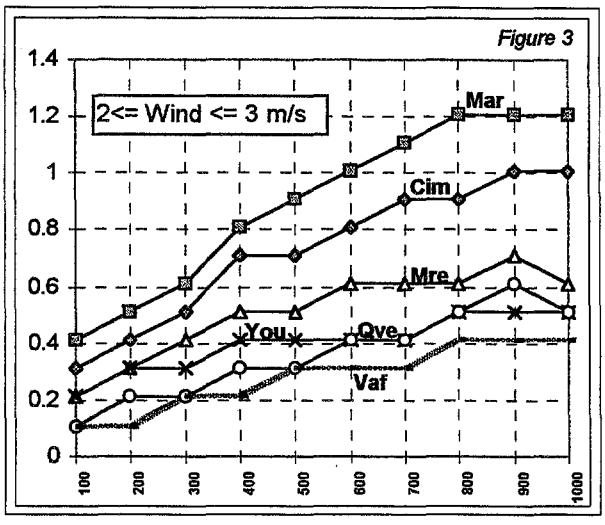

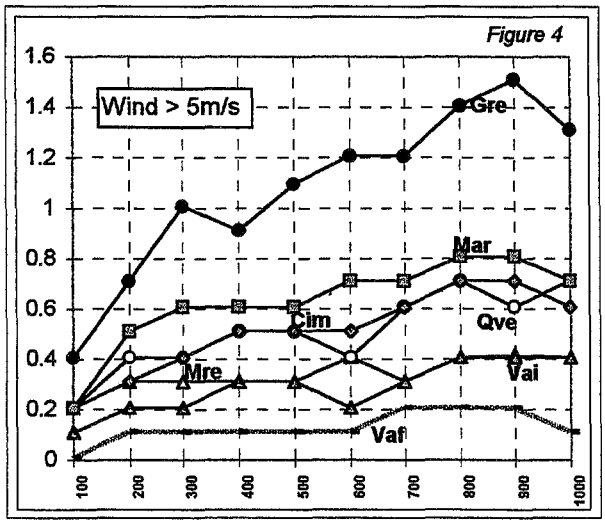

5.1.1 Stevenson type screens

These screens (GM2,MRE) are characterized by their large size and important mass (#100kg,#50Kg). They have a smoothering effect upon temperature curves due to their high thermal inertia. They react with delay to high temperature gradients. Consequently, they under-estimate the temperature at dawn (Fig2, 0<RG<400W/m²) and over-estimate it when it starts dropping at the end of the day. The clearer the day is, the more important the streaking effect is. These screens take more time to set calorific balance between structure, external and internal air. Stevenson screens overheat up to 0.7°C for GM2; up to 1°C for MRE. Their standard deviation is higher than those of the other screens due to their higher thermal inertia and their large capacity.

5.1.2 Cup screens

The VAI, YOU and MIN screens overheat up to 0.8°C in the day and show a deviation (of the medians) from the reference which increases as wind speed decreases (0 to 1°C). So it is with CIM and MAR, but these overheat much more (0 to 1.7°).

The CIM is made of aluminum. In spite of white paint albedo (0.8), this metal favours a higher flux density (F=(T1-T2)/P) compared to a thermoplastic plate (*for the temperature conditions of the 2 sides of a plate (T1-T2)*). Aluminium has a high thermal conductivity K=200 and consequently a low thermal resistance P=e/K, where e is the thickness.

5.2 Artificial ventilation screens

The GRE shows an abnormal overheating (Fig2 1.2°C for 700W/m²) which increases with wind speed (Fig4 +1°C for 300W/m², 1.5°C for 900W/m²). It has been noted that, according to wind direction, the internal flux speed changed from 1.8m/s with no wind to 1m/s with a 5m/s wind. The standard deviation increases when the wind increases (from 0.28 to 0.55°C).

The QVE tends to overheat in spite of its internal fan. Here again, the internal flux speed is problably influenced by the wind speed. This may explain radiation errors increasing with the wind speed. This may be due to the low thermal resistance of the material. The standard deviation doesn't depend on wind but it increases when "RG" increases (from 0.2 to 0.34°C).

The VAF overheats less than the ventilated VAI (+0.7°C with no wind Fig2) and shows the same behaviour towards the wind as cup screens (Fig4, 0.2°C). It is generally colder than natural ventilation screens by 0.2°C.

6 SCREENS USED BY NIGHT TIME

In the night, the screens are only submitted to earth and air radiation (IR=infrared radiation, 5 < wave length < 100µm). The effect of the screen upon temperature measurement is reduced.

In order to process night data, a filter selects any information for which the "RG" is below 2W/m². The plotting of cumulated differences (Tsens-Tref) curves concerning natural ventilation screens (MIN,VAI,CIM) allowed to select the nights for which the cumulative total is constantly increasing ((Tsens-Tref)>0), or constantly decreasing ((Tsens-Tref)<0) during the night, or both. The mixed situations show that the sign of (Tsens-Tref) is correlated with the wind. For an average wind > 1m/s, all the screens have a behaviour practically similar to that of the reference ((Tsens-Tref) around +0.1 to +0.2°C). As soon as the wind drops (or is below 0.5m/s) the natural ventilation screens get colder than the YVN reference. This cooling is immediate, as soon as the wind drops or stops.

Any object is emitting a radiation depending on its temperature and emissivity (0.9 for natural objects). If

the screen receives a "IR" radiation from colder (warmer) objects than itself, it will emit more (less) "IR" radiation than it receives. It will be then cooled (or warmed).This imbalance mainly occurs between ground and sky but also between the thermometer and the screen itself on a smaller scale. If the sensor is well protected by the screen against radiation, the effect of "IR" is reduced and the probe mainly receives a "IR" from the walls of the screen itself. The lower the temperature difference between the screen and the external air is, the lower the "IR" flux density between the probe and the screen is. The main effect of "IR" imbalance is the cooling of the screen itself leading to the cooling of the air passing through. It depends on the ventilation (natural or artificial) or on wind speed.

Processings of descriptive statistics according to wind classes allowed to quantify the effect of the wind on the deviation from the reference for each screen used by night time. When the deviation from the reference is constantly negative all night (no or very light wind , Fig 9) and when it is constantly positive all night (average wind over 1m/s, Fig8).

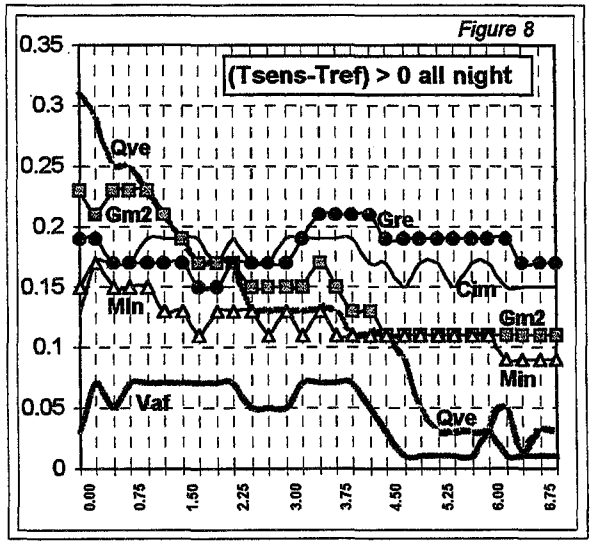

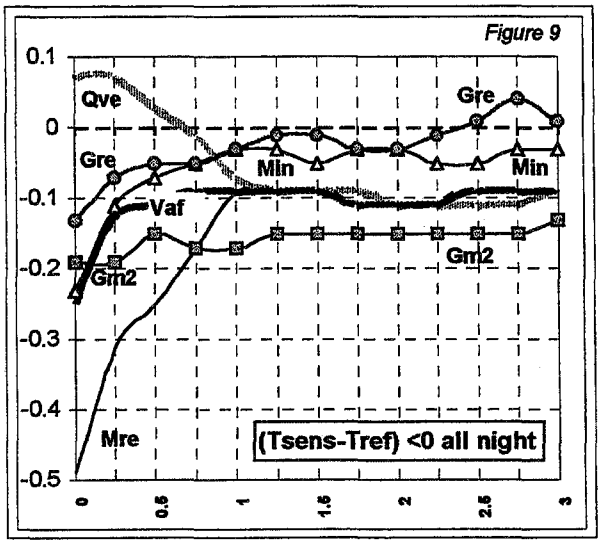

Figures 8,9 show the deviation of medians from the reference (on Y-axis in °C) according to wind classes (on X-axis in m/s).
(In fig 8, VAI and YOU curves which were quite similar to MIN curve were not plotted)
(In fig 9, VAI [CIM] {YOU} curves were not plotted because they were quite similar to YOU [VAF] {GRE}).

Average wind over 1m/s case (Fig 8):

We think that these cases occur when the screens have been heated during day time and stay warmer during night time, due to their thermal inertia. This explains the positive deviations by light wind here.

All natural ventilation screens have similar behaviours (their medians deviate from the reference by +0.1°C to 0.2°C) whatever the wind speed (Fig 8). The natural ventilation screens overheating in the day (CIM,MAR) deviate from the reference by 0.2°C instead of 0.1°C. (slightly more than for screens GM2, MRE, MIN VAI,YOU). The QVE's deviation from reference is less important (+0.3°C to #0°C) when the wind increases (0 to 6m/s).

No (or light) wind case: (Fig 9)

All natural ventilation screens are slightly colder than YVN. The MRE has a singular behaviour at night. It is colder (0.5°C under YVN reference) than other natural ventilation screens with no wind.

7 CONCLUSION

The YVN screen is the coldest. It seems to be a good reference, but this should be confirmed by other designs. The use of such screens in a meteorological surface network would generate a break in climatological data mainly based on Stevenson screens measurements. The other artificial ventilation screens have their ventilation disturbed by the wind. All the natural ventilation screens have solar radiation and night cooling effects. Some cup screens show behaviours rather similar to Stevenson screens. The change of screen type has certainly an influence over the continuity in climatic measurements (Fig 10).
If GM2 is replaced by YVN (or similar type), Tmin and Tmax are under-estimated throughout the year. If GM2 is replaced by MIN, Tmax is slightly over-estimated only in summer (no problem for Tmin).

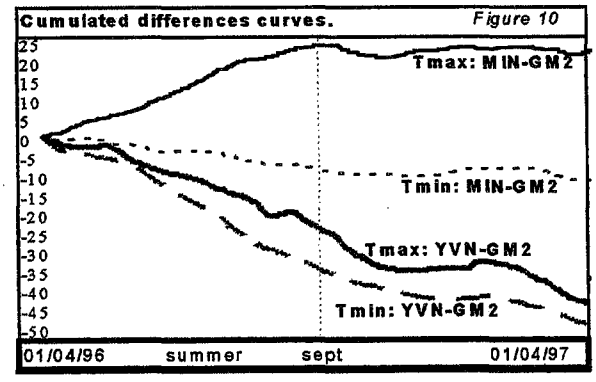

References

Anderson T. and mattison I.: A field test of thermometer screens. Swedish Meteorological and Hydrological Institute (SMHI),Norrköping,RMK n°62,1191,40p.

Leroy M.: Test methods for comparing the performance of thermometer shields/screens and definiting of important characteristics. Météo-France SETIM, Trappes,ISO/TC 146 SC5 Meteorology WG3,1997,14p.

Perrin de Brichambaut C.: Propagation de la chaleur et mesure de la température de l'air. Météo-france,SETIM,Trappes,Revue de la Météorologie,N°SMF 93-137,1993,8p.

W.R Sparks : The effect of thermometer screen design on the observed temperature.1972, 80p.

A Thermometer Screen Intercomparison

Jitze P. van der Meulen,
Royal Netherlands Meteorological Institute,
Postbus 201, 3730 AE de Bilt, Netherlands
meulenvd@knmi.nl

1. Introduction

In order to choose for an appropriate design of a radiation shield for the automatic measurements of air temperature and humidity, an intercomparison of seven different screens was organized from 1989 to 1995. At the instruments test site at KNMI in De Bilt, the Netherlands, the air temperature is measured every 15 seconds during a contiguous period of seven years. These temperatures are measured synchronously inside 7 screens of very different designs (different materials, shapes, sizes and type of ventilation)

2. Background

Although different thermometers and sensors of different shape, type and quality are in use, these devices confirm in principle to a standard. However, the design and construction of shields demonstrate significant mutual differences. In fact thermometers and sensors can be calibrated with respect to internationally approved standard procedures. Shields however are not subject to any kind of international WMO approved standardization. In the Guide to Instruments and Methods of Observation, (WMO No. 8), advises to construct these screens are presented, but a typical standard screen is not recommended. Today the size of screens is subject to charge. From the well known Stevenson screen, designed to contain a number of thermometers, today small sized screens are produced to contain the small sensor elements. Moreover, besides the natural ventilated screen also artificially ventilated screen are in practice.

In the past a limited number intercomparisons [1, 2, 3] are carried out world wide, especially between Stevenson screens. With the introduction of the new types of screens, more fundamental knowledge and experiences of these screens are essential to be able to interpret any charge in the time series. For that reason the intercomparison described in this report is carried out. After analyses of 6 years of field measurements conclusions are presented on the performance of the various types of screens.

The WMO Commission for Instruments and Methods of Observation(CIMO) has recommended to its WMO Members the following accuracy requirements:

- required accuracy for temperature measurements: 0.1 K
- best achievable operational accuracy: 0.2 K

3. Overview of causes and results by environmental affection

Temperature measurements are influenced by a number of environmental circumstances, such as:

1 direct radiation by the sun (by day) on the sensor
2 indirect radiation (after reflection by the ground, water surface, snow or the screen itself) form the sun on the sensor
3 direct and indirect infrared radiation by the screen itself and from outside the screen (ground, water surface, snow) on or from the sensor (i.e. there is no balance in IR radiation heat transfer).
4 Insufficient natural or artificial ventilation of the air inside the screen with the air outside causing typical micro-climate effects and long response times.
5 Non-natural mixing of the air around the screen caused by local artificial ventilation or wind shields.
6 Cooling of the screen and the sensor caused by:
   - precipitation (rain, showers, drizzle and snow will cool down the screen)
   - wetting by aerosols (during precipitation and fog) of the (day bulb) sensor. The sensor may act as a wet bulb sensor as a result, typically is case of strong winds, or ventilated shields.
   - snow and ice on top or around the screen
   - collection of water inside the screen (evaporation) will cool down the air inside the screen).
7 Shadowing of the site by large trees, buildings or separate screens.
8 Strong heating of the stand caused by absorbtion of the sunlight and as a result an upwards warm air current passing the screen.

A special issue is wind. In case of no wind at all the natural ventilation of the air inside the screen is limited to diffusion only. The effects stated above will be more significant than in case of strong winds in combination of precipitation the sensor inside the screen will be affects by deposition of aerosols or small droplets. However it must be stated that temperature is measured at a specific height above the ground (in The Netherlands: 150 cm above a well

maintained and flat grass cover in an open area). During day and night different vertical temperature profiles appear which will be influenced by the wind. Moreover continuous sunshine, occasionally sunshine or no sunshine by complete overcast demonstrates significant different effects on the temperature profile, especially up to 2m above the ground. Due to this issues the representativeness of the temperature measured at 150 cm for the area around the observation site will be limited, and the stated accuracies as well.

4. Quality related issues

Besides environmental effects the sensor itself might be subject to degradation causing drift or instable read-outs. As a consequence all sensors and measuring devices must be checked and calibrated within regular intervals to fulfil the stated accuracy. Essential to this requirement is the necessity of a qualified calibration facility which ensures an absolute accuracy of the sensors. This accuracy is based on appropriate reference or workings standards, well skilled personnel and appropriate procedures. Moreover the reference must be traceable to an international certified standard (e.g. certified by EAL related Member States).

Another issue is contamination and degradation of the screen itself. It is understood that dark pollution will increase the absorbtion of the sun sunlight resulting in self heating. Also the state of the ground or soil is relevant. In the Netherlands KNMI measures the air temperature at 150cm above short cut grass. In dry climates or with rocky grounds, the grass will not have the desired condition. In polar regions snow will cover the ground frequently. In such cases the interactions between (heated or cooled) ground and the air will be different then with grass and also the radiation from the ground will be significant.

5. Construction of the screen or shield

As stated above screens are used to protect the thermometer or sensor against environmental phenomena, principally sunshine. Nevertheless such a shelter inevitably introduces micro-climate effects. To learn about the performance of a specific screen is to learn about the micro-climate inside the screen. For any intercomparison of thermometer screens the largest problem will the definition of a standard screen, which may act as reference. Since such a standard is not available at this moment, one should define a specific screen for which the performance is rather well known and suitable as a reference.

The large number of screens, manufactured today may classified as follows:

I Stevenson screen - type (material: Wood or synthetic), typically with "Louvre" screens.
II Larger round-shaped screens (material: Synthetic), ~25cm diameter and 20 to 40 cm tall
III Smaller round-shaped screens (material: Synthetic), <10cm diameter and <12 cm tall
IV Specific screens, designed in combination with artificial ventilation

Traditionally the screens in class 1 to 3 are not ventilated; however ventilation is an option. The round shaped screens consist of a number of round, open plates above each other, but their designs are very different for the various types.

6. Intercomparison

In the period from 1989 to 1995 the following screens were investigated at the KNMI instruments test site in de Bilt, Netherlands (situated at WMO 06 260):

Type:	*period:*	*Class:*
- KNMI round shaped multi plate ("reference")	890109 - 950201	II
- Vaisala look-alike DTR11	890109 - 930220	II
- Young: Gill multi-plate radiation shield model 41002	890109 - 930220	III
- Socrima round 'weather station shelter' BMO 1167A	910308 - 950201	II
- Young: Gill Aspirated radiation shield model 43408	901209 - 920818	IV
- Young: The same, but newer model (smaller tubes)	920818 - 950201	IV
- KNMI Stevenson screen (PVC, unventilated)	890109 - 910306	I
- KNMI Stevenson screen (PVC, ventilated)	910307 - 950201	I
- KNMI Stevenson screen (wood, unventilated)	890109 - 930220	I

Every 15 s a temperature sample was registered. To be able to determine the effect of other meteorological elements on the temperature measurements, the following parameters were collected as well: Windspeed, radiation (global) and precipitation-intensity/detection. Typically, temperature measurements are carried out at 150 cm above well cut grass unless when snow covers the ground.

7. Results

Although the whole dataset is not analyzed in full detail, it is already possible to give some significant results

here. Since no standard screen is available as a real and scientifically well understood reference, we choose for the "KNMI round shaped multi plate" for use as a "reference". This screen looks very similar to Vaisala's DTR11. It is obvious off course that differences between both type of screens were very neglectable small. On the other hand, difference between screens give a good impression of the mutual temperature differences, caused by local natural variations. In fig. 1 a typical example is presented of these differences from a 24h cycle. In this figure the effect of the local temperature variations on the mutual difference can clearly be observed. Also the effect of sunrise and sunset on the flat vertical sides of the Stevenson screens is rather well demonstrated.

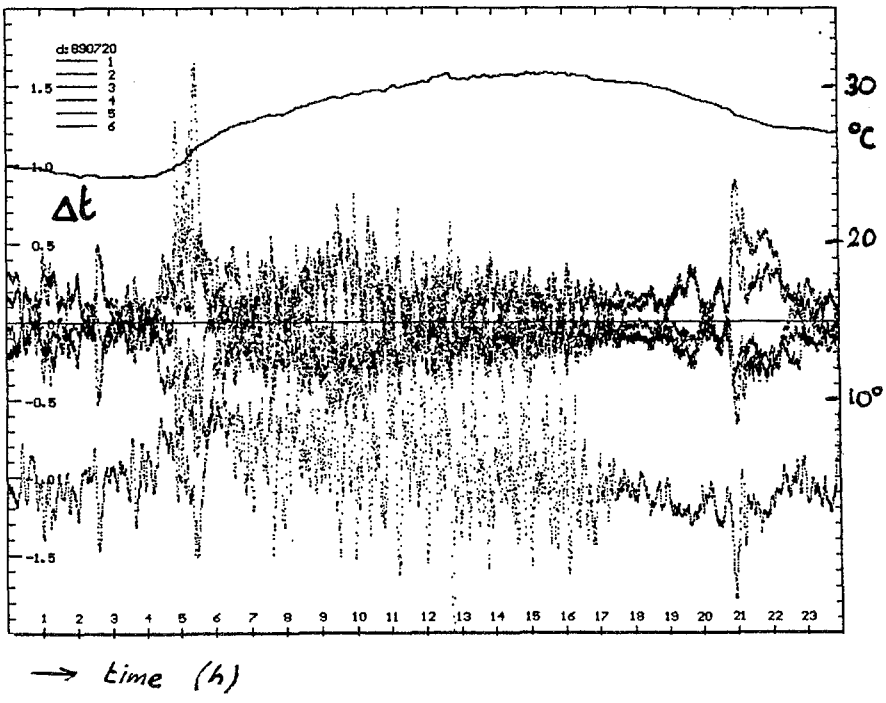

Fig. 1, Typically example of the mutual temperature differences measured during a sunny summer day in July.

Radiation impacts: A good impression of the effect of radiation on temperature measurements is given in fig. 2 where the differences of the temperatures, measured in the various screens are presented. Typically temperatures measured in synthetic (all classes) differ significantly from the old operational KNMI Stevenson screen (wood, unventilated). The first group give similar results, within 0.1 to 0.2°C. The wooden stevenson screen shows a clear difference of max. -1.7 K, which means that the air inside that screen is 1.7°C higher than that within the others. Obviously, this screen suffers significantly from self heating.
Wind impacts: In fig. 3 an example of the wind effect is shown. We have chosen for the wooden screen, which the same differences as in fig. 2: It is very clear that wind has a positive effect on temperature measurements.

Note however that there exists a strong correlation between wind, radiation and temperature, which can easily be demonstrated by figures of the daily cycle of those heth. This implies that investigation on the impact of those elements on temperature measurements should take care of this correlation.

Long term effects: Since in winter and in summer the impact of radiation, wind, etc. may expected to be different, daily results are plotted for a period of 6 months (see fig. 4). In this figure again the differences between the temperatures of the wooden screen and the reference is shown on a daily base: The average difference together with the standard deviation and the minimum and maximum values of these differences. Obviously, in summer time the differences are significant larger than in winter time.

For all other screens analyzed until today average daily differences of 0.1 to 0.2°C are normal. The daily minimum and maximum differences are about 0.5°C (in winter) to 1.0°C (in summer).

8. Conclusions

Based on the analysis of the dataset, carried out until today, it is found that the temperatures in most screens are similar within approximately 0.2°C. Some screen however show, under particular circumstances large deviations (1°C or more).

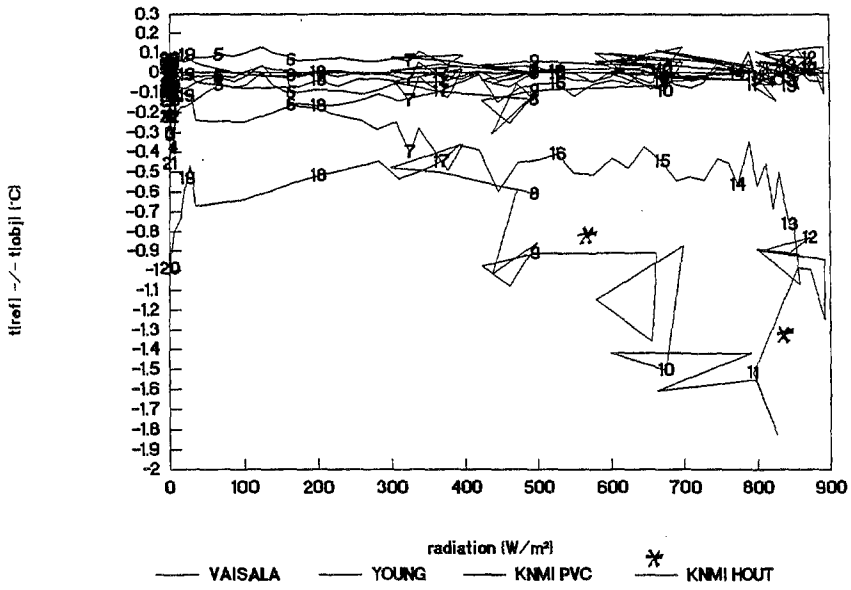

Fig. 2, An example of the impact of radiation on temperature measurements: Most of the screens give results within 0.2°C, but the wooden Stevenson screen shows a significant difference of more than 1°C.

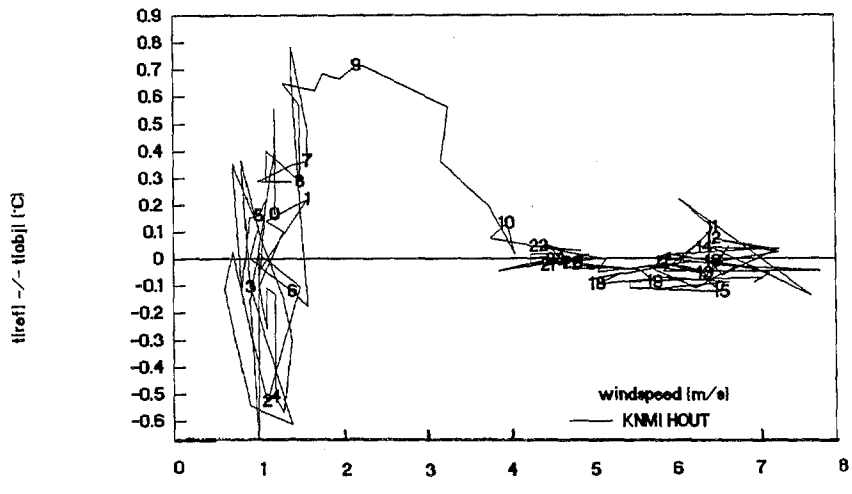

Fig. 3, A typical example of the wind impact on the wooden Stevenson screen: With low wind speed (also at night time), significant differences are observed

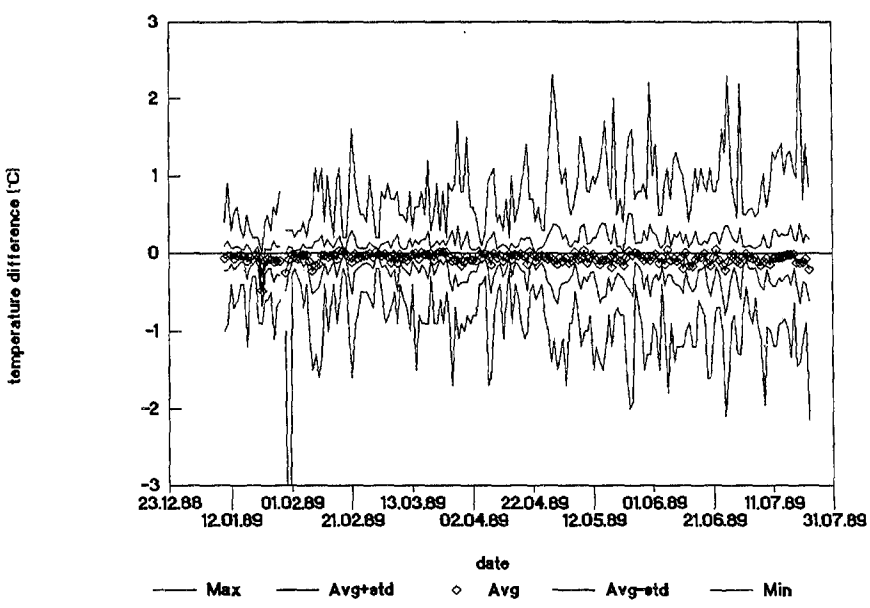

Fig. 4, A seven month's plot of the daily differences (average, min, max) between the wooden Stevenson screen and a round multiplate screen, acting as a reference.

[1] Sparks, W.R. (1972): "The Effect of Thermometer Screen Design on the Observed Temperature", WMO-No. 315

[2] Andersson, T. and I. Mattision (1992): "A Field Test of Thermometer Screens", Instr. and Obs. Meth. Rep. 49 (WMO No. 462), p. 436

[3] Warne, J. (1995): "Temperature Screen Comparison" (in draft), Australian Bureau of Meteorology Test Facility, Melbourne, Australia.

AWOS PERFORMANCE EVALUATION DATA ANALYSIS RESULTS

AUTHORS: Mike Crowe*, André Giguère, Stu McNair.
Atmospheric Environment Service, Canada

1. INTRODUCTION

In late 1994, aviation user groups expressed concern that the AWOS (Automated Weather Observation System) observation program was not meeting their needs. This resulted in a moratorium on any further commissionings of AWOS for aviation use until such time as those concerns could be addressed through a demonstration of AWOS capabilities. The resulting AWOS Performance Evaluation (APE) was carried out at seven Canadian airports during 1995/1996. The evaluation was designed and conducted by a steering committee with representation from government agencies, employee associations, and private sector airlines and associations. An AWOS was collocated with a 24-hour human observing program at each of the seven sites and data collection was handled electronically. AWOS reports have been time-synchronized with the corresponding official human observations (hourly and special) and organized in a database. Analyses have been performed comparing various elements of the two observing programs to determine the degree of agreement, and ultimately, to allow aviation users to decide if AWOS can meet their needs.

In particular, several analyses were performed comparing the AWOS ceilings and visibilities with those of the observers. This paper presents some of the results of those analyses.

2. DATA ANALYSIS METHODS

Given the aviation motivation for the APE, analysis focused on those parameters of greatest importance for that industry. The approach taken was to identify deficiencies with the AWOS performance as perceived by the aviation user groups, develop and implement software and hardware enhancements to the AWOS at the test sites that addressed those deficiencies and perform analyses that would give a clear picture of AWOS performance in those areas of interest. All identified performance deficiencies concerned the parameters of sky condition, visibility and reporting of present weather phenomenon. User satisfaction was expressed with AWOS performance in reporting wind, pressure, temperature and humidity.

When comparing two time series, one must first give consideration to how one matches the data for analysis purposes. For datasets involving meteorological observations, the approach may seem obvious - compare observations that are concurrent in time. Although useful for some purposes, a number of inherent weaknesses with this matching technique were identified:

- AWOS and the observer rarely issued special observations at the same time. Thus, much of the data would be left out of the analysis - especially data that occurred during interesting and changeable weather conditions.
- The observer's instrument compound was located anywhere from a hundred meters to a kilometer away from the AWOS sensor compound at the test sites. Temporal differences could be induced by this spatial separation of observing areas making this matching technique inappropriate and misleading.
- This type of matching leads one to compare the AWOS observation to the human observation, using the latter as the standard. It was acknowledged that the human observation could contain errors for a variety of reasons. Furthermore, from the beginning, the intent of the evaluation was not to determine whether AWOS could mimic a human observation, but rather to evaluate the extent to which AWOS could meet aviation operations requirements.

Thus, each analysis was performed on a number of datasets created using different matching techniques. In addition to analyzing observations concurrent in time, the following datasets were analyzed:

1. Closest in time ± 15 minutes; starting with the human observation, if there was no concurrent AWOS observation, the observation that was closest in time within a 30 minute time "window" around that observation was chosen as a match for analysis purposes. This had the effect of adding many of the special observations to the dataset.
2. Closest in value ± 15 minutes; in this technique, if there were a number of AWOS observation from which to choose in the 30 minute window, the AWOS observation that best agreed with the human observation was chosen as a match. This effectively gave the AWOS a time "leeway" within which to agree with the observer.

* Corresponding author's address:
Michael.Crowe@ec.gc.ca
4905 Dufferin St. Downsview, ON Canada M3H 5T4.

3. Closest in value +15/-59 minutes; this technique is entirely analogous to technique #2, but the time window has been broadened to ensure that *all* data gets included. In the worst case (a human special observation at H + 0:59) one may need to go back 59 minutes to retrieve the valid AWOS observation

As might be expected, technique #3 invariably produced the best agreement between the human and AWOS, followed by # 2, then #1. Observations concurrent in time generally showed the least agreement.

When discussing the analysis results, it was generally agreed by the steering committee that technique #2 could be used to best describe AWOS performance as compared to the observers, and it is the results using this technique that are reproduced here. For a more complete accounting of the various analyses refer to the AWOS web page at www.tor.ec.gc.ca/readac/index.html

3. CEILING ANALYSIS RESULTS

Results of ceiling analyses are reproduced in figures 1-4. The figures show that AWOS agreed best with the observer in the absence of precipitation, particularly at heights below 2000 feet. In rain or snow there was less agreement, with AWOS demonstrating a bias to report lower than the observer. This can best be explained by looking at the number of observations issued by AWOS compared with that of the observer. The number of specials issued by AWOS was found to be on the order of six times that of the observers. For any given observer ceiling, a number of AWOS ceilings would be reported surrounding that report in time. The different datasets described in Part 2 showed that those AWOS ceilings would range from very close to that of the observer to somewhat lower.

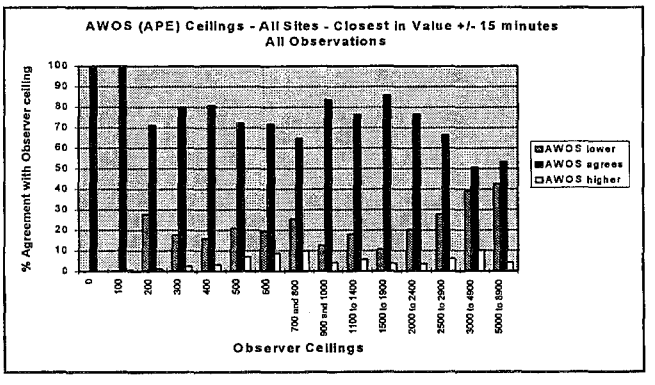

Fig. 1 - Ceiling Agreement for All Observations

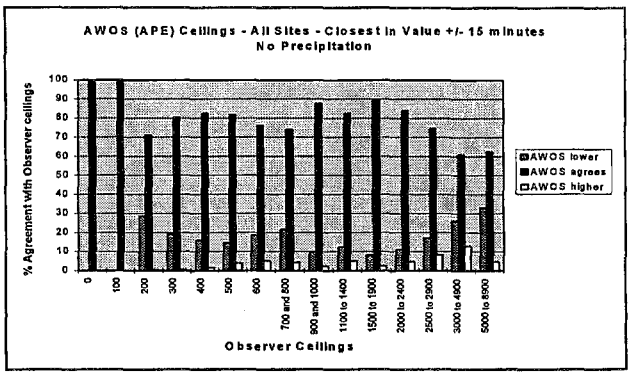

Fig. 2 - Ceiling Agreement with no precipitation occurring

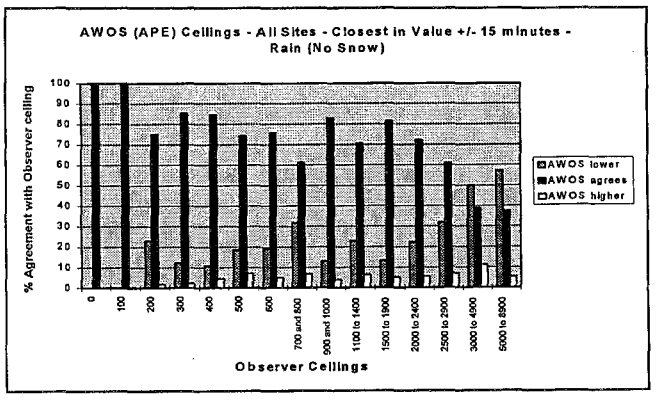

Fig. 3 - Ceiling Agreement in Rain

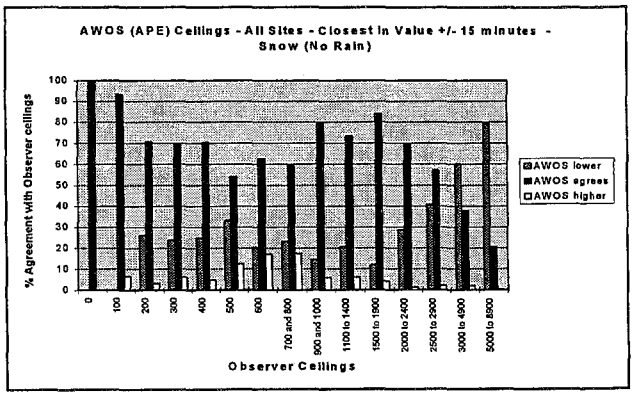

Fig. 4 - Ceiling Agreement in Snow

Other conclusions that were drawn concerning the comparability of AWOS ceilings with those of the observer are summarized below.

1. The climatology of both observing systems over the period of the study was very similar i.e. they tended to report the various reportable ceiling heights with about the same frequency.

2. The main differences observed in the climatology could be explained by two AWOS characteristics; a tendency to report a ceiling of zero during precipitation, with corresponding observer ceilings between 100 and 500 ft and reports of a ceiling below 1000 ft about 5% of the time the observer had no ceiling - usually in winter conditions with ice crystals and/or ice fog present

3. There was a perception by users that given the "point" nature of the cloud sensor (a vertically pointing laser ceilometer), AWOS may be slow to respond to rapidly changing conditions such as the onset or cessation of a ceiling below 3000 ft. A lead/lag analysis was carried out that found matched AWOS/observer observations that agreed the ceiling had fallen below or raised above 1000 or 300 ft. The analysis method then backtracked to see which observation recorded the change in ceiling first. It was found that AWOS tended to lead the observer on reporting ceiling changes through 1000 or 300 feet on the order of 2:1.

VISIBILITY ANALYSIS RESULTS

Results of visibility analyses are reproduced in figures 5-8. The figures show that AWOS agreed best with the observer in precipitation, particularly with visibilities less than three miles. In the absence of precipitation (and thus, for visibilities less than six miles, in the presence of an obstruction to vision) there was less agreement, with AWOS demonstrating a bias to report higher than the observer. As with the ceiling analysis, for any given observer visibility, a number of AWOS visibilities would be reported surrounding that report in time. The different datasets described in Part 2 showed that those AWOS visibilities would range from very close to that of the observer to somewhat higher.

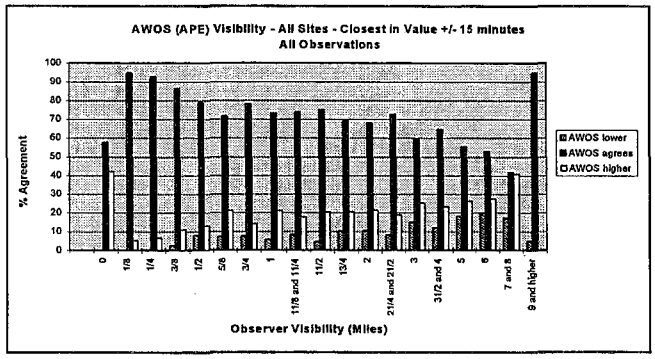

Fig. 5 - Visibility Agreement for all Observations

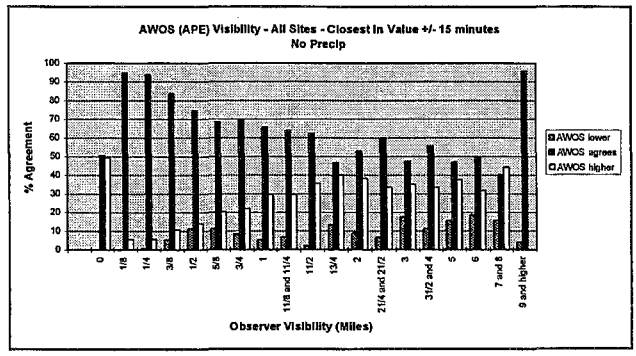

Fig. 6 - Visibility Agreement with no Precipitation Occurring

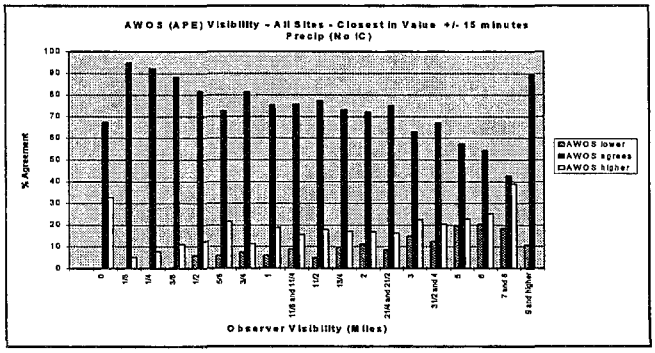

Fig. 7 - Visibility Agreement with Precip Occurring

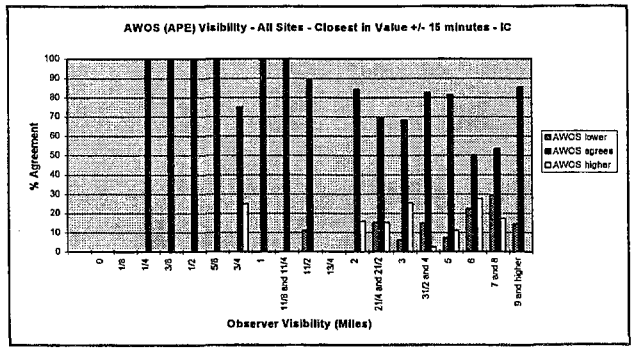

Fig. 8 - Visibility Agreement with ice crystals

Other conclusions that were drawn concerning the comparability of AWOS visibilities with those of the observer are summarized below.

1. The climatology of both observing systems over the period of the study was very similar. Visibilities below 3 miles were reported with identical frequencies by both systems - on 10.4% of the concurrent hourly reports. The results shown in the figures suggest that the systems did not always report these conditions at the same time.

2. A concern of the users was that AWOS tended to report visibilities much lower than the observers when ice crystals were present. Although the dataset was rather too small to give a good picture of characteristic performance, nothing in the data suggested that AWOS exhibited a low bias in the presence of ice crystals

3. Case studies of many particular events of the presence of an obstruction to vision suggested that in general the agreement was very good in cases where the obstruction was of a homogeneous character and reduced the visibility to below one mile. The main disagreements occurred in cases where remarks from the observer or the AWOS suggested a high degree of variability of the phenomenon (e.g. remarks of variable visibility or patchy fog, etc.)

4. There was a perception by users that given the "point" nature of the visibility sensor (a "spot" extinction coefficient sensor), AWOS may be slow to respond to rapidly changing conditions such as the onset or cessation of visibilities below 3 miles. A lead/lag analysis analogous to that for ceilings was carried out for visibility thresholds of 3, 1 and 1/2 mile. The results ~~were somewhat inconclusive and~~ did not suggest either system led or lagged the other in reporting changes through those thresholds.

OTHER ANALYSIS RESULTS

Ceiling and visibility performance were the parameters of most concern to the aviation users. There were other concerns that were identified and analyses were performed on the data to demonstrate AWOS performance in those areas as well. Some of these are summarized below

Present Weather

1. Concern was expressed that AWOS was issuing too many false reports of precipitation. Analysis of all data showed that on the order of 12% of AWOS reports of precipitation were false alarms using observer reports as the benchmark. However, when erroneous data caused by malfunctioning sensors was removed from the dataset, and other events that contained some remark from the observer that precipitation was intermittent or spotty were also removed, this false alarm rate could be shown to be less than 5%.

2. At the beginning of the APE, AWOS did not have the capacity to report freezing precipitation. As part of the evaluation, an icing sensor was deployed and integrated with the precipitation occurrence sensor to develop the capacity to report freezing drizzle and freezing rain, as well as non-precipitating icing events. Analysis of APE data showed that AWOS agreed with the observer that freezing precipitation was falling about 80% of the time. Conversely, the observer agreed with AWOS about 63% of the time.

Weather Watch Capacity

Users expressed some concern that AWOS had a tendency to issue more special reports than was operationally useful. AWOS prepares full weather reports each minute from which special reports are issued any time a particular threshold is crossed. In highly variable conditions, AWOS will relentlessly issue specials, whereas the human observer will tend to smooth conditions and minimize the number that are issued. Monitoring of specials indicated that AWOS ~~tended to~~ issue about six times the number of specials issued by the observers.

Communications Performance

Communications performance was identified as a major concern. At the time of the launching of the APE, many AWOS hourly reports were not being received and disseminated by the National Communications System, or the reports were showing up late and out of sequence. Over the last few years the integrity of the telecommunications systems has been improved, and all networks have been monitored closely. The communications performance of the AWOS network has improved to the point that it is now out-performing the human observing network in terms of availability of reports

CONCLUSIONS

The APE steering committee acknowledged that AWOS performance had markedly improved, and lifting of the moratorium has been recommended. All software and hardware enhancements to the AWOS have since been implemented on the operational network. It was also acknowledged by the group that performance deficiencies still existed. In particular, AWOS inability to report thunderstorm activity, obstructions to vision and off-site weather phenomena were cited as areas for further development. Environment Canada is installing a lightning detection grid across the country that will be integrated with the AWOS network to enable reporting of thunderstorm occurrence. Processing techniques continue to be investigated to develop the capacity to report obstructions to vision, and development of a network of remote video cameras to supplement AWOS reports is being considered.

AN INVESTIGATION OF TEMPERATURE SCREENS AND THEIR IMPACT ON TEMPERATURE MEASUREMENTS

Dr J. Warne (Ms)
Bureau of Meteorology
GPO Box 1289K Melbourne 3001
Australia

ABSTRACT

Current day concerns about enhanced greenhouse warming and the impacts of changes in climate on the economics and social fabric of the world, has given rise to questions about the accuracy of data used to identify to the small rises in temperature expected. Aside from effects such as urbanisation, the uncertainty of temperature measurements is effected by factors such as the accuracy of the temperature sensor, the time constant of the sensor, the enclosure used to house the sensor and the representativeness of the local environment.

To improve the understanding of the impact of enclosures ten different screens were installed in the Bureau of Meteorology's field test site at Broadmeadows. The screens varied from the standard wooden Stevenson screen to modern aspirated screens. One-minute data on each screen has been collected since December 1994 and has revealed some interesting results. Typically the Stevenson screen resulted in average monthly maximum temperatures in summer which were 0.7 to 0.2°C cooler than other non-aspirated screens and 0.4°C cooler than the aspirated screens. The impact on the monthly minimum temperature was significantly less with the Stevenson's screen being 0.1 to 0.3°C warmer. The magnitude of these differences means that for some screens the average daily temperature would rise by 0.25°C, masking or enhancing any greenhouse warming effect.

****

THE PRACTICAL IMPACTS OF RTD AND THERMOMETER DESIGN ON WET AND DRY BULB RELATIVE HUMIDITY MEASUREMENTS

Dr J. Warne
Bureau of Meteorology
GPO Box 1289K Melbourne 3001
Australia

ABSTRACT

Identification of differences in the wet and dry bulb temperatures in field conditions for different temperature sensor designs resulted in this study of wet bulb sensors. Analysis of laboratory tests in an environmental chamber resulted in two possible models for the psychrometer coefficient for these sensors. The first model included the "wet potential", that is a coefficient for the ratio of the wet bulb temperature divided by the wet bulb depression. The second model also included coefficients for wet, dry and the theoretical wet bulb depression. Both models explained a significant proportion, approximately 90% and 99% respectively, of the observed discrepancies.

****

COMPARISON OF MEASUREMENTS BETWEEN TRADITIONAL AND MODERN SCREENS

Mahmood Nikzad
Islamic Republic of Iran Meteorological Organization (IRIMO)
IRIMO, P.O. Box 13185-461, Iran
Fax: (+98 21) 6000 417

Abstract

For measuring the air temperature and humidity, the dry and wet bulb thermometers were formerly placed in wooden thermometer screens. The height and other dimensions of screens applied in different countries vary significantly. In Iran, modern screens were installed in 1980. As a result, the air temperature measured in the new type of screens in the morning (at 0300 GMT) is higher than that of the old one. The difference is ranging from 0 to 0.5 °C while the humidity differs by 5%. The air temperature measured at noon (0900 GMT) in the modern screen is lower than in the old one. The difference is ranging from -0.1 to -1.4 °C at 1500 GMT. Furthermore, the observed air temperature in the modern screen shows an increase in the summer season and a decrease in the other seasons, oppositely.

****

COMPARISON OF DAILY MAXIMUM AIR TEMPERATURE DATA SERIES OBSERVED BY CLASSICAL AND AUTOMATIC METEOROLOGICAL SYSTEMS

Luis Filipe A. C. Nunes
INSTITUTO DE METEOROLOGIA - PORTUGAL
Rua C do Aeroporto, 1700 Lisboa (email: Luis.Nunes@meteo.pt)

The wide use of Automatic Meteorological Stations (AMS) in the Portuguese Network is a major change in the methods of classical observation. Phase 1 of this project became operational on Jan.96 with 21 AMS [02]. Because the data in long climatological series have been recorded with those methods it's pertinent to ask if we can continue old series with new data coming from AMS. With the new automatic network there are many changes at measurement level: data aquisition frequency, data processing algoritms, instruments characteristics, instalation features, etc. The impacts produced by these changes, like inhomogenities in data series, which may appear on climatological analisys, may be serious with the lack of metadata [01].

This work is about getting some knowledge on the differences between results obtained with classical and automatic systems for the daily maxi-mum air temperature values using statistical methods for the comparison of data series. Data from 2 stations on mainland-Portugal have been used: Beja and Bragança. Both sites had good regular funcioning of classical and automatic systems for more than 1 year, producing 2 daily maximum air temperature (DMAT) series. The purpose of this work is try to reveal some of the main changes that we can expect on the new data series resulting from new methodological errors, which are mainly due to different time response and measuring frequency of the sensors, that limit the atmospheric scales to be observed.

Classical DMAT from 09 to 09UTC is measured with mercury thermometers by qualified personnel. On the other hand AMS use electrical sensors (PT100 type) to record the air temperature value every minute (sampling interval complies with WMO recomendations [03]) all day long. DMAT values of AMS were retrieved from 10' records.

The factory characteristics and instalation features of PT100 sensors results in an uncertainty of ±0.2°C [04] with a delay coeficient of 30 sec. These values, like the ones for the classical thermometers, are within the range recomended by WMO for DMAT observations. At selected sites, AMS sensors were instaled as near as possible to the corresponding classical thermometer screen, depending on local conditions and logistic

For every data series, classical and AMS, from each site, several statistical characteristics were calculated. For every climatological day (09-09UTC), the differences between pairs of DMAT values, from both systems on same site, were calculated, resulting in one time series of differences classical-AMS, for each station. For these series some other parameters were calculated, like, bias, rms error and mean error.

*The correlation between classical and AMS series were also calculated by means of linear regression. The standard error for the bias ($\sigma_{dif}/\sqrt{n}$), were also calculated, wehere **n** is the number of points. If the differences are not statisticaly independent the Bartels number **n'** can be used instead of **n** to calculate the standard error.*

Another calculation was the statistical entropy of the measured and differences data series, using the expression for the average uncer-tainty of a system with n independent ocorrences mutualy excluded. Comparing statistical entropy values from different series we can get some knowledge about their structure differences. More, the statistical entropy of the differences classical-AMS can reveal the amount of informa-tion available about the corresponding system of ocorrences [05]. So, empirical probabilities were found for each type of monthly series and then the statistical entropy values were calculated with decimal logarithms. To compare obtained values of uncertainty degrees with the theoretical limits [0, -Log n], the results are presented with no dimentions, in percentual values $\%H=100.H(Z)/H_{mdx}(Z)$, $H_{mdx}(Z) = -Log(n)$. For each series the sta-tistical entropy of the normal distribution were also calculated, with the parameters mean-m and stand.deviation-s calculated from sample series.

Regarding the characterization of the series of differences, it was seen that the distributions are nearly normal, as it could be expected for series of data with random causes. On the other hand, the values of statistical parameters for these series are within the limits of the instrumental uncertainty. The results of statistical entropy calculations for monthly series of observations taken the classical and by the AMS, for both sites, present similar values and these are very near to the entropy values calculated for the monthly normal fitted distributions. Then, differences between monthly entropy from the AMS and from the classical, on each site, aren't very significant, with only few values on the order of 10-15%, which leads to the conclusion that there won't be any significant loss (nor gain) of the amount of information about the data series, in respect to DMAT, if we replace classical data with AMS data. The results about statistical entropy calculated from the differences AMS-classical showed a high similarity between these and the entropy calculated for normal fitted distribution, which confirms that monthly series of differences are nearly normal. Looking at the standard error calculations from the series of differences it can be seen, for instance for Bragança, that we have to mantain both systems operating for more than 3 years if we want a standard error not less than 0.01°C. These results are not very distant from the initial planing of the project which pointed to a duration of at least 2 years.

1. Introduction With the new automatic network there are many changes at measurement level: data aquisition frequency, data processing algoritms, instruments characteristics, instalation features, etc. Many impacts can be produced on data series, by these changes, which may appear at post-processing level or in climatological analisys.

The purpose of this work is not to find data series inhomogenties but is a try to reveal some of the main changes that we can expect on the new data series that result from new methodological errors. These are mainly due to the different time response and measuring frequency of the sensors, which limit the atmospheric scales to be observed.

DMAT values from the automatic stations located in Beja and in Bragança were post calculated with the 10 minute records collected at the National Center. Due to the existance of data gaps in these 10' data series it was necessary to create an algoritm and to define some criteria in order to find the days with high probability of calculation error for the maximum air temperature value [02]. Maximum air temperature values retrieved from 10' records were used to produce DMAT series for the AMS. Days with high probability of calculation error were excluded from the AMS series by means of a computer program which identifies the days with too many data gaps or with long gaps during the hours of higher probability of ocorrence of the daily maximum.

Besides the differences of sensors, another great difference between classical and automatic systems lies on the radiation shield construction and design, which can represent significant differences on measurement process.

On the selected sites, the AMS sensors were instaled as near as possible to the classical thermometer screen, depending on the local conditions and logistics. At Bragança, PT100 sensor and mercury thermome-ters were ≅5m apart (inside the same instruments park), while at Beja, they were ≅80m apart, because the AMS had to be instaled inside a separate and new parque. All thermometers (classical and electrical) were instaled at 1.5m above ground.

2. Calculations For every data series, classical and AMS, for both sites, the following parameters were calculated: dimension, average, median, maximum, minimum, percentiles 25 and 75, standard deviation, variance, amplitu-de, assimetry and curtosis. For the series of differences classical-AMS for each station the following parameters were calculated: bias, rms error and mean error. The correlation between classical and AMS series were also calculated by means of linear regression and the standard error for the bias ($\sigma_{dif's}/\sqrt{n}$), were also calculated, wehere n is the number of points where Bartels number n' can be used instead of n to calculate the stand. error, if differences are not statisticaly independent. To calculate the statistical entropy of the measured and differences data series, the following expression were used for the average uncertainty of a system with n independent ocorrences mutualy excluded, with probability $p_1,p_2,...,p_n$

$$H(Z) = -\sum_{i=1}^{n} p_i \cdot \text{Log}(p_i) \quad \text{where} \quad \sum_{i=1}^{n} p_i = 1$$

highest degree of uncertainty $p_1=p_2=..=p_n=1/n$, $H=-\text{Log}(n)$; lowest degree of uncertainty (probability $p_i=1$), then $H=0$.

Comparing statistical entropy values from different series we can get some knowledge about the structure differences of the series. More, the statistical entropy of the differences classical-AMS can reveal the amount of information available about the corresponding system of ocorrences [05].

For each station, monthly statistical entropy was calculated for the following data types of series: AMS observations, classical observations, differences AMS-classical; and also for the series of differences acumulated month by month. For these calculations fixed frequency intervals were defined for each stations and for each data type, in order to avoid false changes on the entropy results, due to changes on the statistical system. So empirical probabilities were found for each case and then the statistical entropy values were calculated with decimal logarithms. To compare the obtained values of uncertainty degrees with the theoretical limits [0, -Log n], the results are presented with no dimensions, in percentual values $\%H=100.H(Z)/H_{máx}(Z)$, $H_{máx}(Z) = -\text{Log}(n)$. For each series the statistical entropy of the normal distribution were also calculated with the parameters mean-m and stand.deviation-s calculated from sample series.

3. Results (Nºs: Bragança=575, Beja=562) The results presented here are only refered to the series of "prevalidated" series, i.e. the series with no data for the days that didn't pass the validation tests on the AMS data.

The table shows that the main sampling characteristics of the DMAT series obtained with classical and with AMS have similar statistical behavior, for both sites.

Series	Avg.	Dim.	Med.	Min.	Max.	pc 25	pc 75
562 Cla	21.17	241	19.2	9.6	41.0	15.0	26.5
562 AS	20.98	241	18.8	9.5	41.1	14.6	26.2
575 Cla	18.48	310	18.2	3.1	38.8	11.2	25.5
575 AS	18.66	310	18.2	3.0	38.7	11.4	25.4

Series	St.Dev.	Varianc	Amplit.	Assim.	Kurtosi
562 Cla	7.67	58.82	31.4	0.65	0.57
562 AS	7.70	59.32	31.6	0.67	0.52
575 Cla	8.39	70.39	35.7	0.30	0.94
575 AS	8.51	72.34	35.7	0.32	0.94

Next figures shows monthly values of the average and standard deviation (SD) of DMAT in Bragança measured with both systems. As expected in Portugal the maximum values of the monthly averages ocorred in August and the minimum values in January (Febr. in Beja). For the SD the maximum ocorred in May and the minimum in Febr.

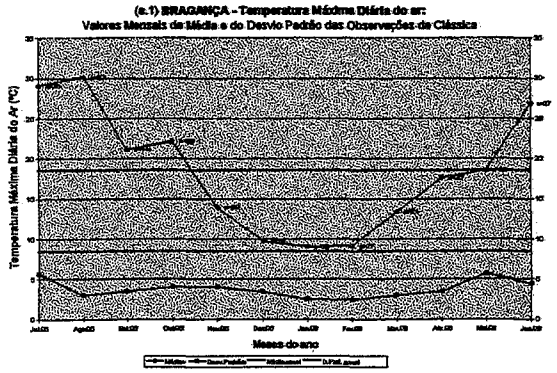

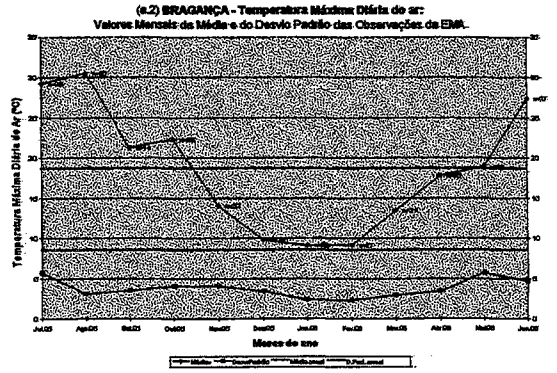

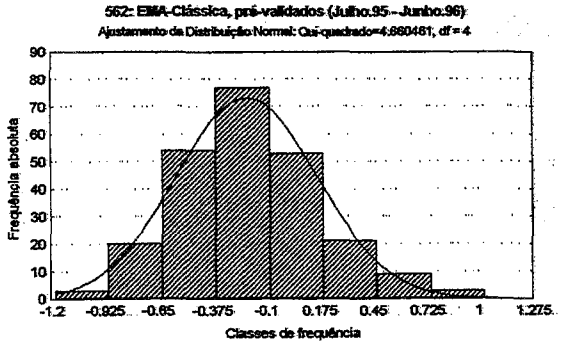

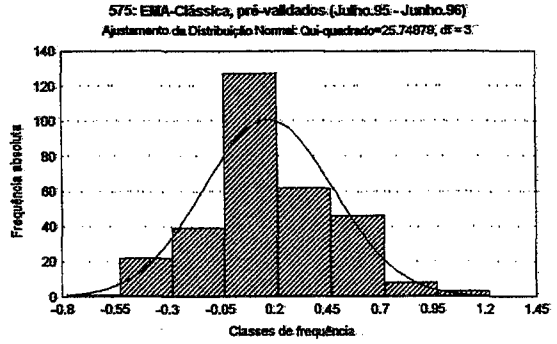

Histograms of the differences AMS-classical can be used to check the good fit of a normal distribution for **Beja** χ^2=4.66 (significance level 0.05); but not for **Bragança**, $\chi^2 = 25.7$ (out of significance level 0.05)

Next graph presents the averages and the SD of the monthly differences AMS-classical from Bragança; it can be seen that the averages have a well pronounced anual cycle with maximum values in June and minimum values in November (Jan. for Beja). The SD have maximum values in June and minimum values in December (Nov. for Beja).

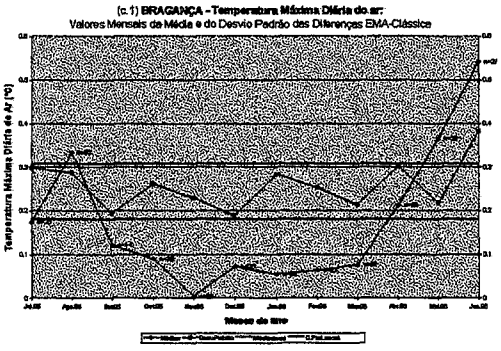

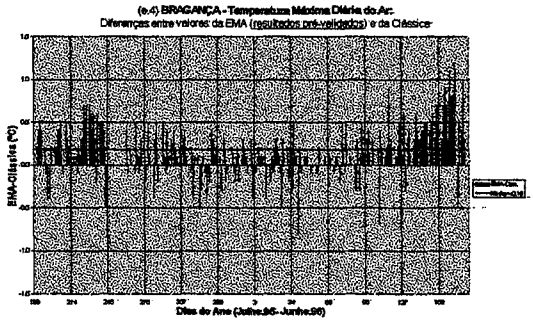

The graphic of the daily differences AMS-classical from Bragança shows that most of differences are positive, with the highest values ocorring during summer months.

In Beja there are more negative values but also during summer the differences tend to become positive.

The series of differences can be characterized by the following parameters; about the sampling characteristics it can be seen that both sites have similar dispersion values.

	Bias	R.M.S.	Av.Dev
Beja	−0.19	0.41	0.31
Brag.	+0.18	0.36	0.28

Série	Méd.	Dim.	Med.	Men.	Maior	pc.25	pc.75
562	0.19	241	0.2	1.20	1.0	0.4	0.0
575	0.18	310	0.2	0.80	1.2	0.0	0.4
Série	D.Padr.	Variânc	Amplit.	Assim.	Curtose		
562	0.36	0.13	2.2	0.09	0.53		
575	0.31	0.09	2.0	0.09	0.61		

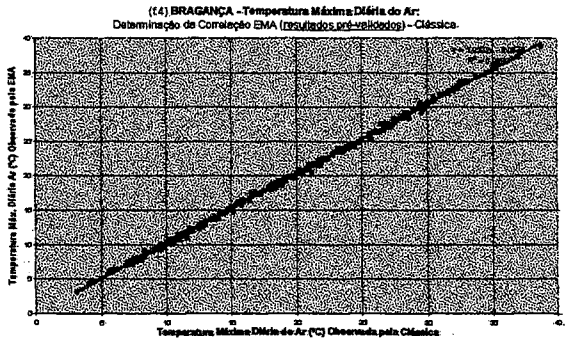

Left figure shows, linear regression results between AMS data and classical data series for Bragança, where a very strong correlation is revealed with correlation coeficient of 0.9 and trend nearly equal to 1. Similar results have been found with the data series from Beja.

Now the graphics with the percent values of the monthly statistical entropy are shown for AMS and classical observational data taken in Bragança, together with the monthly statistical entropy of the normal adjusted to the series

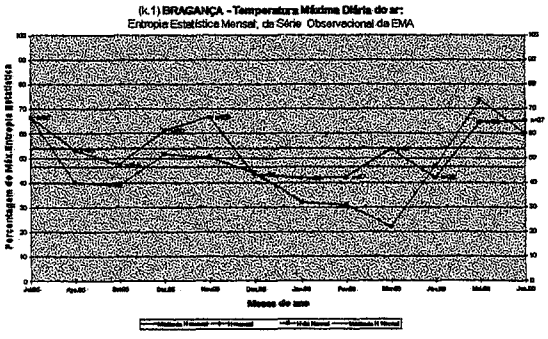

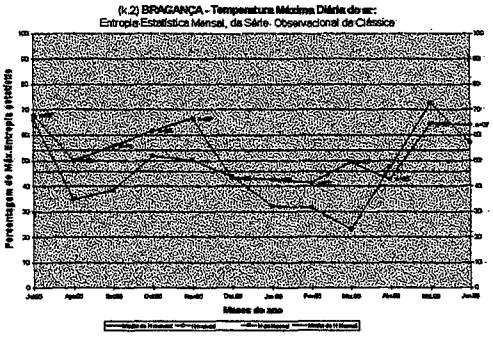

The results from Bragança, shows that the monthly entropy varies from 42 to 66% (AMS data) and from 41 to 68% (classical data), while the entropy of the normal curve from 22 to 73%. The results from Beja are a little different with the entropy of observational data varying between 10 and 66% and the entropy of normal between 2 and 80%.

Left graphic shows the diferences between monthly statistical entropy values of AMS data and classical data.

This shows that the monthly variation on the amount of information between AMS and classical data from Bragança is nearly null on almost every months, with little loss in August and March, the exception beeing September with a good gain. Same kind of results were found for Beja data.

On the right graphic, monthly entropy values of differences AMS-Classical data from Bragança are shown.

The Bragança series of differences have monthly entropy values from 46 to 73% (30 to 84 for Beja). For the normal curve adjusted the following values of entropy were found: 41 to 78% for Bragança and 34 to 85% for Beja. The lines on all these graphics are very close to each other.

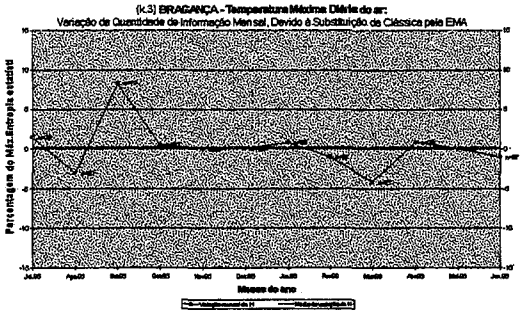

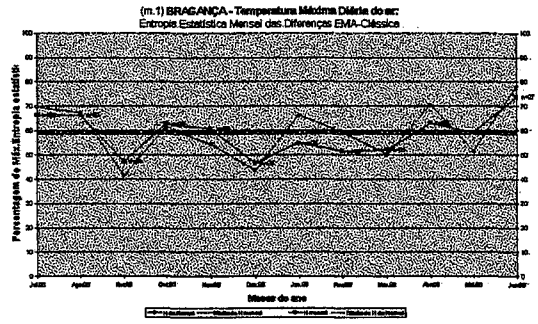

Left figure shows entropy values for the series of differences acumulated month by month together with entropy values of the corresponding normal distribution and also with monthly average and SD values for the same serie

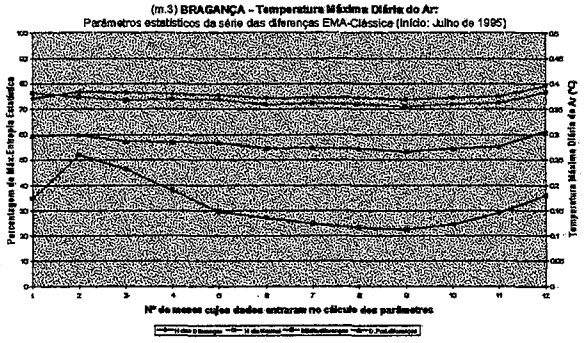

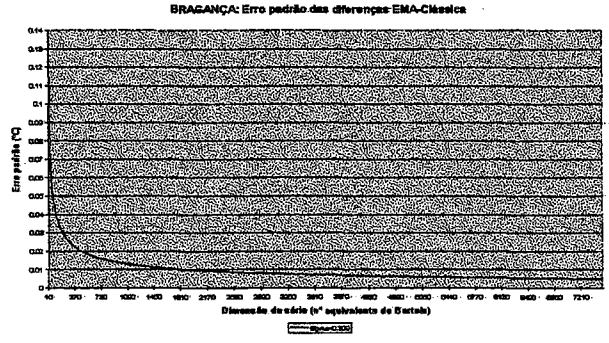

The entropy of the monthly cumulated differences from Bragança is nearly constant, varies from 74 to 79% (65 to 78% from Beja). Comparing this curve with the one of the entropy calculated for the normal fitted, a growing similarity can be seen between them. For the monthly averages of the cumulated differences extreme values found were 0.26 and 0.11 for Bragança and -0.19 and -0.5 for Beja. About the monthly SD extreme values found were 0.31 and 0.27 for Bragança and 0.37 and 0.26 for Beja. The lines of SD values follows the lines of normal distribution entropy.

The right figure shows standard error values of the bias calculated for Bragança data as function of the series dimension. This graphic permits to estimate for how long do we need to keep both systems operating in order to ensure a certain standard error. For instance, results from Bragança says that we have to mantain classical station operation for more than 3 years if we want a standard error not less than 0.01ºC.

4. Conclusions

In order to avoid the data gaps on 10'series from AMS, caused by telecomunications difficulties, the data processing and transmiting procedures should be improved in some way. The developed algorithm to make a pre-validation of DMAT values showed good results but needs more testes if we want to use it on an operational basis.

Regarding the characterization of the series of differences, it was seen that the distributions are nearly normal, as could be expected for series of data with random causes. On the other hand, the values of statistical parameters for these series are within the limits of the instrumental uncertainty.

The results of statistical entropy for the monthly series of observations from the classical and from the AMS, for both stations, have identical values, and these are near to the values obtained for the normal distribution adjusted for each month. With the small differences between the classical and AMS entropy values one can conclude that there are no significant loss nor gain in the amount of information if we use the AMS data instead of the classical ones. Regar-ding the statistical entropy for the monthly series of differences Classic-AMS it can be seen that the good fit with the monthly normal entropy is a good check for the near-normal distribution hipotesis of those series. The lines of entropy values for the differences Classic-AMS and for normal fits calculated with succesive acumulated data months, they are near and near and from the 3rd month on, the lines are almost parallel which leads to the conclusion that there are no much advantage in continuing to make the comparison of data because longer series of differences do not corresponde to a decrease on the uncertainty of our knowledge about the differences.

Regarding the standard error results for Beja, one can have similar conclusions: if we want to have a series with a value of 0.01ºC, for standard error, we must have 740 to 1300 observations (2 to 3.5 years).

5. Some References

[01] K.D.Hadeen, N.B.Guttman-"*Homogeneity of data and the climate record*", CIMO Technical Conference, WMO, Geneve, 1994.

[02] R.Carvalho, C.Gonçalves, L.Nunes, V.Prior-"*Sistema-Rede de Estações Meteorológicas Automáticas*", 2ª Conf.Int.Des.Meteor.PLOP Lisboa95

[03] WMO-Nº8 "*Guide to Meteor.Instrum. Methods of Observ.*", Geneve 83.

[04] C.P.Brichambaut- "*La mesure de la temp.de l'air*", "La Meteor.", Paris 95.

[05] R.Faria-"*Utilização do conceito de Entropia no planeamento da densidade de uma rede de udómetros.Aplicação a S.Miguel*" INMG Lisboa 81

Session XI

PRECIPITATION AND RADIATION OBSERVATIONS

CORRECTION OF WIND-CAUSED ERROR OF PRECIPITATION MEASUREMENTS USING HORIZONTAL PRECIPITATION

Li Mingqin , Zou Yaofang and Ren Zhihua

Chinese Academy of Meteorological Sciences

ABSTRACT

Based on the analysing the physical mechanism of wind-caused precipitation measurement error, it is found that horizontal precipitation and wind-caused error follow some relationship. Thirty evaluation stations with one horizontal gauge, two national gauges and one reference pit gauge were set up in 1992. The results of experiments with horizontal gauge at thirty evaluation stations of China for four years are as follows:

1. Comparing about 15000 events between pit gauge, national gauge and horizonal gauge, the exponential correlation of horizontal precipitation and absolute difference in catch between by national gauge and by pit gauge was confirmed. The relationship is built up for the different geography climate condition, so it has wide universality.

2. Adjusted error distribution is similar to distribution of random error of precipitation. Adjusted accuracy approaches pit gauge level.

3. For present observations, correction of per measurement or per day is carried out only by applying horizontal gauge which is as simple as general gauge. Correction method is simple and easy. This method is very suitable for correcting point precipitation (rain or snow) measurements of routine observations.

REFERENCE PIT RAIN GAUGE

Dominique LEGAIN, Marcel ZEPHORIS, Thierry DOUFFET, Frédéric SARTER
Météo-France/SETIM*

1. Introduction

To evaluate the performance of various precipitation measurement sensors and systems, Météo-France designed and built a reference pit rain system. The system is composed of a collecting cone of 5,000 cm^2 flush with the ground and temperature regulated just over 0°C. The quantification of precipitation is provided by a continuous weighing and automatic emptying system. This reference allows the description of precipitation at 10 s intervals, outside of the emptying period. At 60 s intervals, precipitation can be resolved in real time to within 0.004 mm and this up to an intensity of 600 mm/h.

This rain gauge was installed at the Trappes site in the middle of SETIM's rain gauge evaluation platform.

2. Description of pit rain gauge

The rain gauge, made up of a funnel with a collection area of 5,000 cm^2, 100 cm high, made of fabricated, polished and anodized aluminium alloy, is placed flush with the ground at the centre of an anti-turbulence grid. This grid consists of stainless steel blades (1 mm thick and 6 cm high) crossing to form a grating having openings with 10 cm sides. This grid limits turbulence at ground level and especially does not generate any bouncing of raindrops whatever the wind velocity (see Figure 1).

Water flows at the base of the funnel through a normally-open solenoid valve (29 mm passage diameter) to a bottle of 10 litre capacity closed by another solenoid valve. This bottle is suspended freely through two knife-edges to a strain gauge load cell. Throughout the precipitation accumulation phase, the amount of water is weighed continuously by the load cell with a resolution of 2 g (corresponding to 0.004 mm of precipitation height).

* 7, rue Teisserenc de Bort, BP 202,
78195 Trappes cedex, FRANCE
Tel. 33 1 30 13 61 69 Fax 33 1 30 13 63 21
Email dominique.legain@meteo.fr

The valves are operated by an automatic controller which manages the emptying of the bottle every 10 mm of precipitation height. This load cell is temperature-regulated at +15°C in order to neutralize strain gauge temperature drifts. The programmable controller also allows the storage of data and remote monitoring of the rain gauge.

The bottle is emptied completely in 15 minutes after the end of precipitation, even if it is only partially full, so as not to let the water stagnate in the bottle. Information on the end of precipitation is delivered by an Eigenbrodt RS 85 precipitation detector.

If there is continuous precipitation, the emptying cycle takes place as soon as 10 mm of precipitation has been sampled. The automatic controller closes the valve placed at the base of the funnel and then opens the one that empties the bottle. The bottle is emptied in 15 seconds. There is a calibration in 10 s after the closing of the valve. After this calibration phase, the funnel valve opens again and frees the water accumulating in the funnel during the 30 seconds or so required for the preceding operations. These operations are transparent to the 60 s interval on intensities lower than 600 mm/h (the system can manage, without information clipping, the collection of 5 litres of water per minute).

Considering the size of the collector (1.55 m^2 of developed area), three heating regulation systems controlled by five temperature probes placed on critical zones maintain a temperature of +2°C over the surface of the funnel [1]. The heating system is activated only during precipitation by the RS 85 precipitation detector. This heating strategy was chosen in order to prevent the sublimation of the first snowflakes at the beginning of precipitation and accumulate them during the 4 to 5 minutes required for warming up the funnel and thus cause the "gradual" melting of flakes as soon as the surface of the collector reaches 0°C.

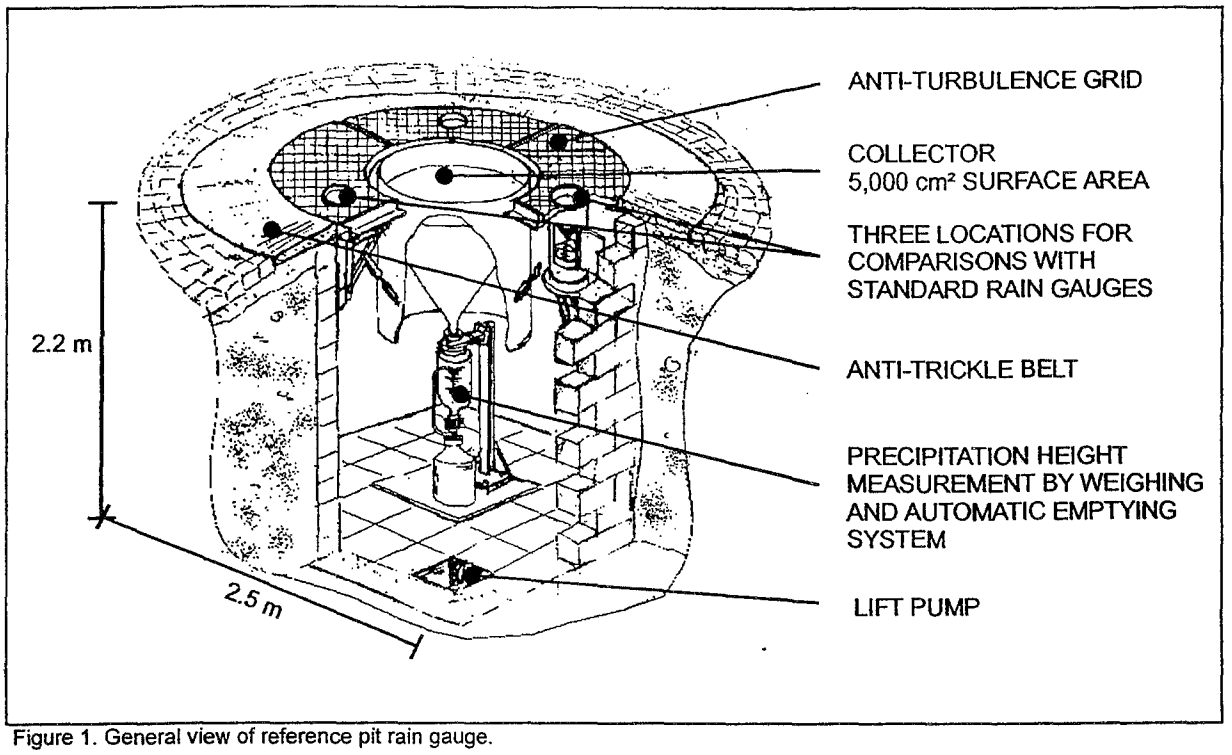

Figure 1. General view of reference pit rain gauge.

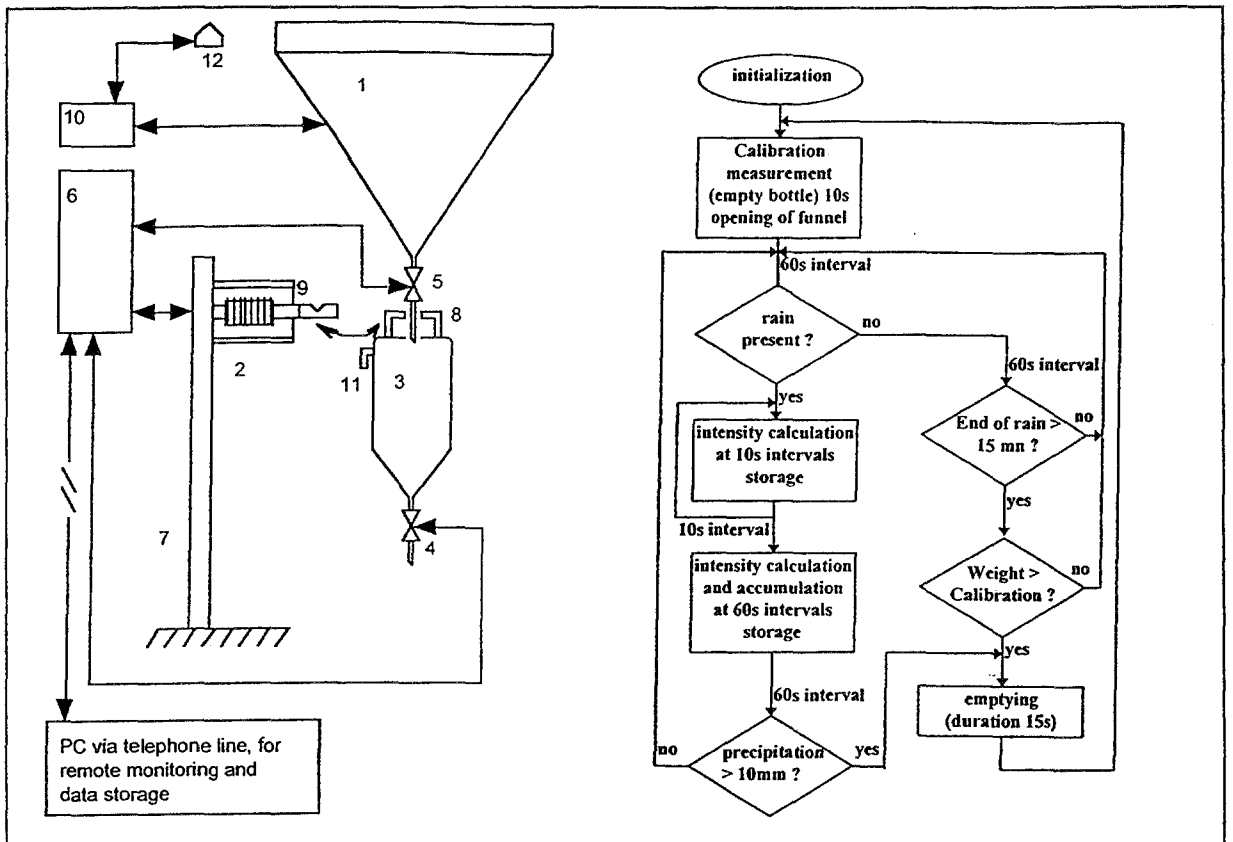

1 Collector, 5,000 cm2
2 Thermostatic strain gauge load cell
3 10-litre bottle
4 Bottle emptying valve
5 Funnel closure valve
6 Programmable controller for control and data storage
7 Leg supporting load cell/bottle assembly
8 Knifes edges
9 Brackets integral with load cell
10 Heating regulators set at +2°C
11 Safety removal
12 RS85 precipitation detector

Figure 2. Weighing system and simplified processing algorithm.

A lift pump located in pan at the bottom of the rain measurement chamber (2.5 m x 2.5 m, height 2.2 m, 5 m^2 of opening for rain), periodically removes the accumulated water.

3. Metrological Characteristics

The system is dimensioned to offer a resolution of 2 g, or 0.004 mm of precipitation.

3.1. Losses due to wettability

On a dry cone, previously rid of dust and grease, water spray tests have made it possible to show a maximum loss of 0.1 mm due to cone wettability.

Referring to an FD12 optical rain gauge installed near the reference, it is possible to estimate on real precipitation the loss due to wettability (see Paragraph 3.4).

3.2. Effect of wind

A comparison carried out for several months between the pit rain gauge and the average of nine SPIEA rain gauges, sampling one metre from the ground, showed an average deficit of 6.5% in precipitation height for the SPIEA rain gauges (see Figure 3).

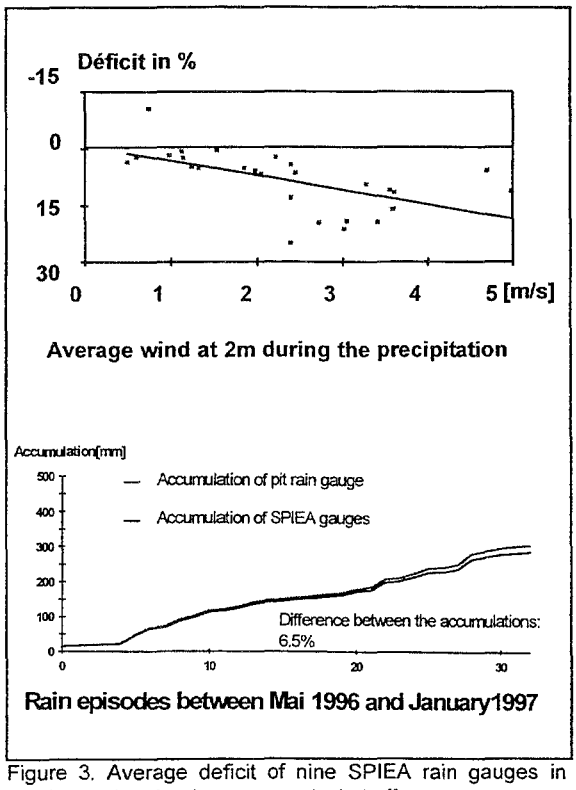

Figure 3. Average deficit of nine SPIEA rain gauges in relation to the pit rain gauge and wind effect.

On given episodes, when the average wind measured at 2 metres exceeds 3 to 4 m/s, the deficit can reach 30%.

On two snow episodes presented in Figure 4, the differences observed between the reference and conventional rain gauges, sampling at one metre, reached 78%.

Snow episode	2-dec-98 2h to 15h UTC	6 and 17-dec-98 22h40 to 7h20 UTC
Accumulation reference pit rain gauge	23.23 mm	15.92 mm
Accumulation Socrima heated (déficit)	13 mm (78%)	9.2 mm (73%)
Accumulation OTT (déficit)	16.76 mm (38%)	11.08 mm (44%)
Accumulation Géonor (déficit)	17.61 mm (32%)	11.87 mm (34%)
Average wind speed measured at 2 m (maximum)	2.7 m/s (4.8 m/s)	2.7 m/s (4 m/s)

Figure 4. Deficit of standard rain gauges in relation to the reference two snow episodes.

3.3. Heavy precipitation measurement

Between two emptying operations, the system can measure precipitation in real time at 10 s intervals up to 600 mm/s. Emptying during continuous precipitation necessarily entails the averaging of the 10 s information over a minute. At extreme intensities, this measurement system can describe precipitation of 1,800 mm/h at 10 s intervals for up to 20 s. At higher intensities, for example, 2,000 mm/h, the funnel spills over only after 20 minutes of continuous precipitation. On the other hand, the measurement of the accumulation of such a rain event lasting 20 minutes would take 40 minutes.

Figure 5 shows the first minutes of intense rain, recorded at 10 s intervals, and illustrates the capabilities of such as system for a fine description of such rain.

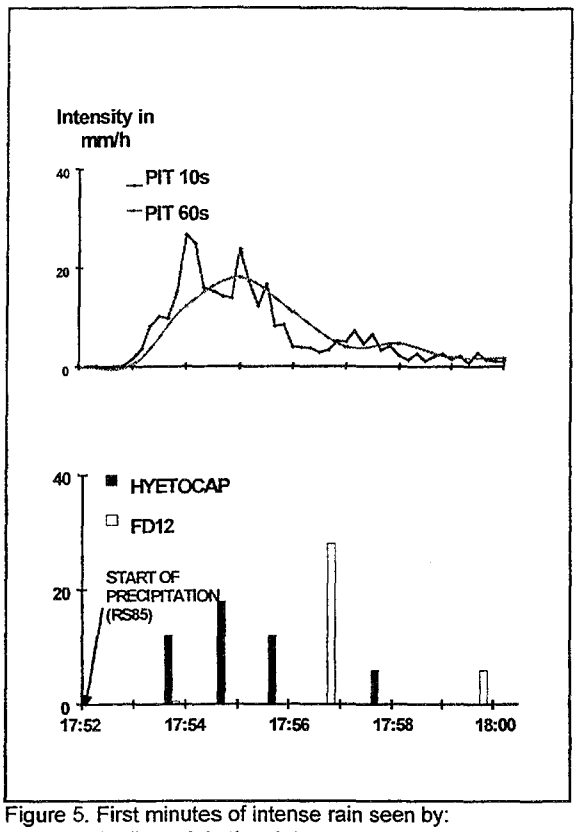

Figure 5. First minutes of intense rain seen by:
- the RS 85 precipitation detector
- the pit rain gauge
- a VAISALA FD12 optical rain gauge
- a HYETOCAP weighing rain gauge.

3.4. Light precipitation measurement

A light rain intensity made it possible to quantify the performance of the pit reference under precipitation intensities between 0.1 and 1 mm/h (Figure 6). This episode shows excellent agreement between the measurements of the FD12 optical rain gauge, the HYETOCAP rain gauge and the pit rain gauge around 1 mm/h. On the accumulations, the differences are of the order of the resolution of the measurement systems.

For intensities of around 0.1 mm/h, the differences fall within the range from 0.01 to 0.02 mm accumulated between the two weighing systems and 0.05 mm accumulated between the optical rain gauge and the pit rain gauge.

Referring to the measurements of the optical rain gauge during the start of precipitation between 8:30 and 9:00, losses by wettability may be evaluated at 0.02 mm over this episode.

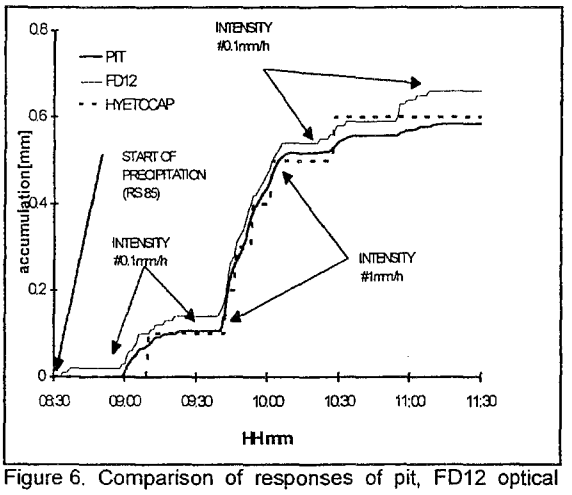

Figure 6. Comparison of responses of pit, FD12 optical sensor and HYETOCAP rain gauges to a light rain.

4. Conclusions

This rain gauge reference system, by design, really collects the precipitation reaching the ground, independent of wind effects, and constitutes an absolute precipitation reference. Measurement by weighing is a measurement principle which allows a fine description of precipitation practically in real time. The system will provide better information on the influence of wind, on the response of conventional and optical rain gauges, as well as on new microwave systems. This reference will also make it possible to establish correction functions (wind, intensity) for each type of rain gauge.

5. References

[1] Zéphoris M., D. Legain, A. Gander, 1998 *Collecteur réchauffé pour précipitations*, WMO technical conference on meteorological instruments and methods of observation, Casablanca, Maroc.

Characteristics of rain gauges used in this study:

- SPIEA rain gauge: direct reading, 400 cm^2, height 1 m (Benoit Frères, France)
- HYETOCAP rain gauge: weighing, 400 cm^2, resolution 0.1 mm, height 1 m (Centralp, France)
- GEONOR T200 rain gauge: weighing, 200 cm^2, resolution 0.016 mm, height 1.75 m (Norway)
- OTT rain gauge: weighing, 200 cm^2, resolution 0.001 mm, height 1 m (Germany)
- Present weather sensors FD12, optical, resolution 0.016 mm, height 1.80 m (Vaisala, Finland)
- SOCRIMA rain gauge: tipping troughs, 400 cm^2; resolution 0.2 mm, height 1 m (France).

COLLECTEUR RECHAUFFE POUR PRECIPITATIONS

Marcel ZEPHORIS, Dominique LEGAIN, Alain GANDER
Météo-France/SETIM*

Le réchauffage des pluviomètres a fait l'objet d'une nouvelle étude dans le cadre de la refonte et du redéploiement des réseaux de mesures de Météo-France. Des essais en laboratoire [1], suivis par des campagnes de tests en montagne, ont montré qu'un pluviomètre avait, en matière de réchauffage, trois zones critiques: la bague de collecte, le fond du cône et le système de mesure, chaque zone ayant des besoins énergétiques très différents.

Description du collecteur

Le réchauffage du collecteur est assuré par une électronique de régulation en température à trois voies indépendantes et à faible temps de réponse, qui associées à trois résistances chauffantes et trois capteurs de température permettent d'assurer les trois fonctions suivantes:

- régulation de la zone collectrice (ou bord d'attaque) ayant pour fonction principale d'éviter la formation de glace autour de la bague du collecteur ;
- régulation du fond du cône assurant la fonte de la neige (ou la grêle) à température la plus proche possible du zéro, afin de minimiser les pertes en eau par sublimation;
- régulation du système de quantification de la précipitation.

Les deux premières fonctions, associées à un cône métallique à forte inertie thermique, maintiennent la surface et le bord d'attaque du cône collecteur à la température de consigne quelles que soient les conditions de vent et de température et permettent au système d'assurer la description des évènements précipitants de toutes natures (grêle, neige, pluie..). Ce collecteur est adaptable aux divers systèmes de mesure des précipitations existants (augets basculants, pesons, ...). Le nouveau pluviomètre de 400 cm^2 de surface de collecte de Météo-France a été développé sur la base de cette idée et est en cours d'industrialisation (Figure 3).

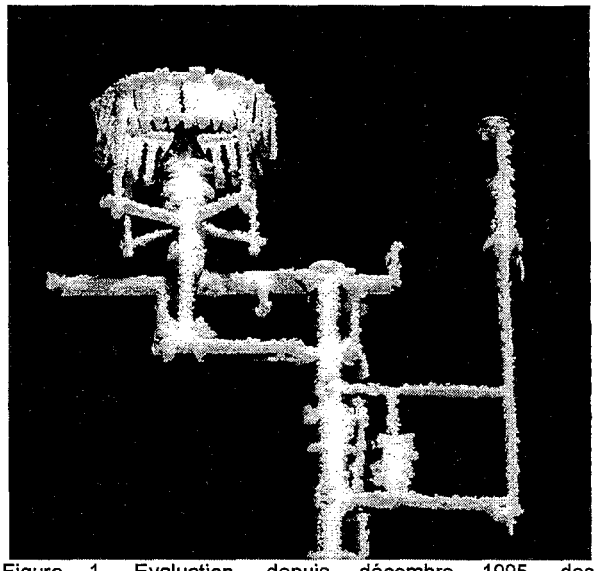

Figure 1. Evaluation, depuis décembre 1995, des performances du nouveau pluviomètre chauffant de 400 cm^2 (à droite) et comparaison avec un pluviomètre GEONOR (à gauche) dans les Alpes à 2800 m d'altitude. (Photo Météo-France/CEN).

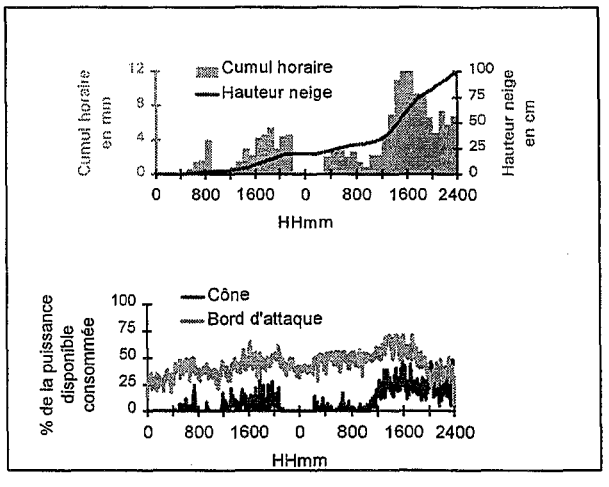

Figure 2. Episode neigeux des 27 et 28 janvier 1996, observé par le nouveau pluviomètre au Mont Aigoual (1567 m). (vent moyen de 50 km/h, rafales à 90 km/h, température de -1°C en moyenne). Il est à remarquer la forte corrélation entre l'intensité de la précipitation et la puissance consommée au fond du cône pour la fonte de la neige.

Références

[1] ABEILLÉ P.S., 1994, Optimisation du réchauffage des pluviomètres, note de travail de l'Ecole Nationale de la Météorologie n° 469.

* 7, rue Teisserenc de Bort, BP 202,
78195 Trappes cedex, FRANCE.
Tél 33 1 30 13 64 33 Fax 33 1 30 13 63 21
Email marcel.zephoris@meteo.fr

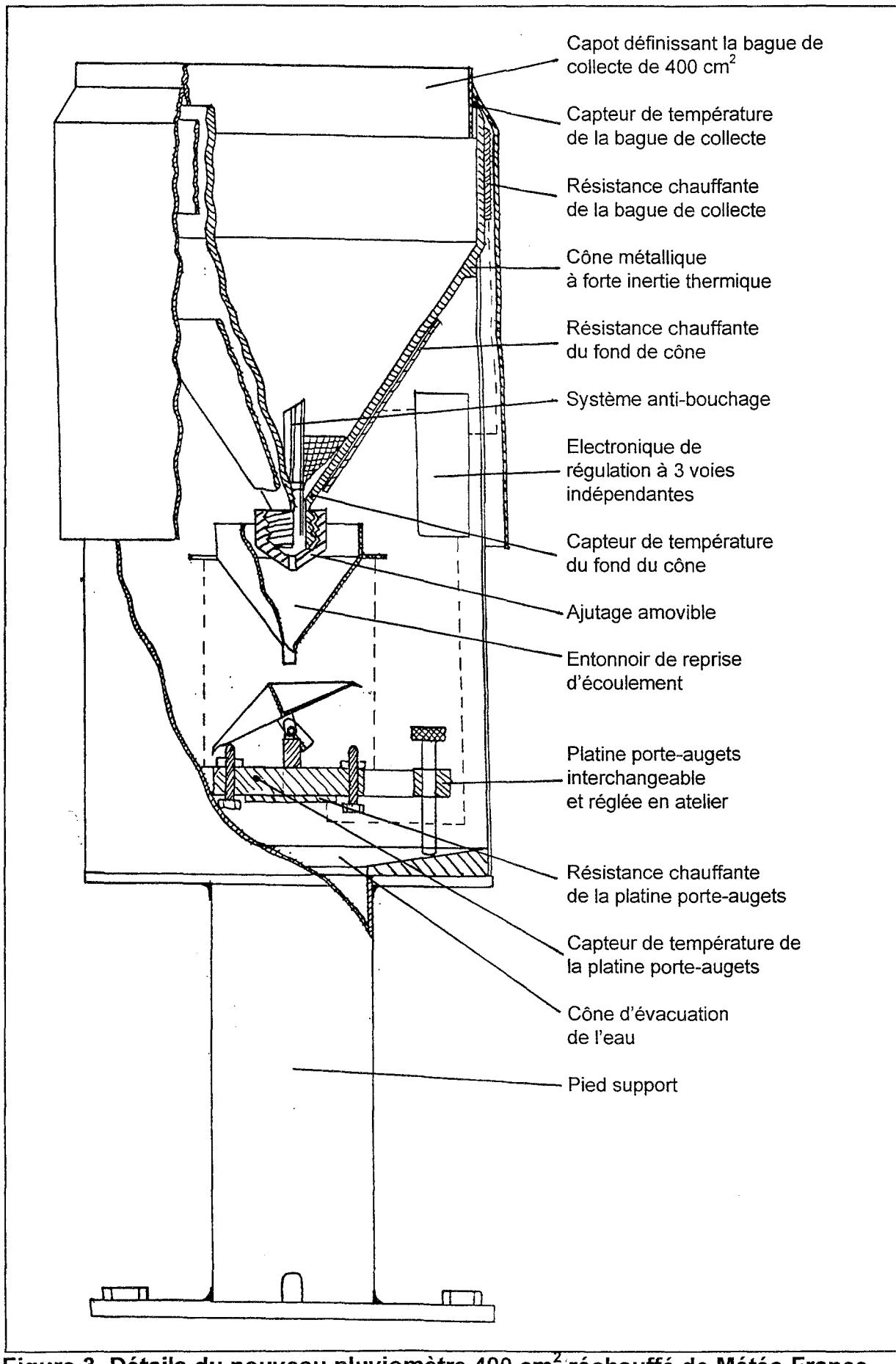

Figure 3. Détails du nouveau pluviomètre 400 cm² réchauffé de Météo-France

КОРРЕКТИРОВКА ИЗМЕРЕНИЙ ОСАДКОВ И КАЧЕСТВО ОТКОРРЕКТИРОВАННЫХ ДАННЫХ

В.С. Голубев, Д.А. Коновалов, А.Ю. Симоненко, Ю.В. Товмач,
Государственный гидрологический институт, С.-Петербург, Россия

ABSTRACT

The estimates of quality characteristics of the corrected precipitation measurement results are presented. Data of long-term observations at the precipitation polygon of the State Hydrological Institute in Valdai were used to correct. The correction has been performed by several procedures for the half-daily precipitation amounts measured by the WMO Intercomparison Reference (DFIR) and by the national Tretjakov precipitation gauge.

The evaluation of quality of the corrected data has been carried out by the method of comparing these data with the readings of the Valdai Control System for precipitation measurements. The estimates of random and unexcluded systematic errors has been obtained for solid, liquid and mixed precipitation as a whole as well as for different ranges of their half-daily amounts.

The is drawn of necessity to maintain a number of the National and Regional Intercomparison Centres for long with a view to continue the researches related to precipitation measurements and correction methods is concluded.

Более века уже известно, что данные наблюдений за атмосферными осадками содержат большие систематические ошибки. Теперь стало ясно, что эти ошибки нельзя не учитывать при выполнении воднобалансовых и теплобалансовых расчетов, а также при долгосрочном прогнозировании изменений водных ресурсов в связи с антропогенными изменениями глобального климата. Поэтому оценка погрешностей и корректировка накопленных данных об осадках в настоящее время становятся важнейшими задачами в исследованиях долгопериодных трендов современного климата и прогнозировании изменений водных ресурсов.

Всемирная метеорологическая организация неоднократно осуществляла руководство сравнениями результатов измерения осадков стандартными национальными сетевыми приборами. Однако, получить приемлемое для практики решение задачи до сих пор не удавалось. Чаще всего, результаты таких взаимосравнений носили относительный (качественный) характер, так как надежность и достоверность "истинных" величин осадков, полученных по контрольным средствам измерения, объективно не оценивались, а метод контрольных измерений (pit gauge) был применим, в основном, только для наблюдений за жидкими осадками. Выбор эталона взаимосравнения и оценка качества результатов измерения по нему имели решающее значение в успехе последнего взаимосравнения, которое было сосредоточено на измерении твердых осадков. Для этого взаимосравнения Международный организационный комитет (МОК) ВМО назначил измерения по осадкомеру Третьякова в двойной заборной защите (DFIR) в качестве эталонных. Тестирование показаний DFIR было выполнено в Валдае относительно параллельных измерений осадков по Валдайской контрольной системе (VCS).

Валдайская контрольная система позволяет надежно измерять твердые, смешанные и жидкие осадки. В отличие от методов контрольных измерений, которые применяли ранее, характеристики точности и достоверности результатов измерений по VCS были оценены. Надежность и достоверность показаний VCS проверена многолетними результатами разносторонних полевых испытаний и разработанной авторами оригинальной методикой объективной оценки характеристик точности применяемых средств измерения (Голубев и др, 1997).

Учет этих оценок позволил разработать методы корректировки показаний эталона взаимосравнений ВМО (DFIR), благодаря чему стало возможным привести результаты измерений по DFIR к ряду, однородному с показаниями VCS. В дальнейшем это позволит выполнить тестирование результатов измерения осадков национальными методами во всех пунктах взаимосравнения ВМО, где были выполнены измерения по DFIR.

В настоящее время предложено две методики корректировки показаний DFIR. В основе методики, разработанной в России (Голубев, 1973, 1991), лежит полуэмпирическая модель взаимосвязи между величиной систематической погрешности измерения, видом осадков и силой динамического воздействия турбулентного воздушного потока на осадкомерную установку. Методика, предложенная МОК ВМО (Yang, et al.,1993), опирается на эмпирические связи между величиной систематической погрешности измерения для различных видов осадков, скоростью ветра, характеристиками температуры воздуха и сопутствующими атмосферными явлениями.

Для испытаний этих методик корректировки были выбраны ряды регулярных измерений осадков по трем установкам DFIR, эксплуатировавшимся на Валдае в период с 1973 по 1984 гг. (табл. 1).

Таблица 1

Характеристики качества результатов измерения осадков по VCS и эталону взаимосравнения ВМО (DFIR)

Вид осадков	Число случаев наблюдений	Результаты измерения и оценки погрешностей						
		VCS			DFIR			
		Общая сумма, мм	Средняя сумма за одно измерение, мм	Случайная погрешность одного измерения, $\pm \sigma_p$,%	Общая сумма, мм	Средняя сумма за одно измерение, мм	Погрешность систематическая, ΔP,%	Погрешность случайная, $\pm \sigma_p$,%
Жидкие	603	1542,6	2.6	6	1425,2	2.4	-8	18
Смешанные	173	435,4	2.5	6	406,2	2.3	-7	18
Твердые	732	1133,7	1.5	8	997,3	1.4	-12	32

Из анализа исходных данных следует, что систематическая составляющая погрешности для результатов измерений по DFIR составляет от -7 до -12%, а случайная от ± 18 до ±32. Случайная погрешность измерений по VCS в 3-4 раза меньше (6-8%).

Оценка характеристик качества откорректированных результатов наблюдений по DFIR (табл. 2) выполнена для полусуточных сумм осадков. Из рассмотрения полученных результатов можно сделать вывод о том, что значения осадков эффективно корректируются с помощью обеих вышеназванных методик. Неисключенная составляющая систематической погрешности откорректированных результатов

измерений лежит в пределах от -4 до 5 %. Случайная составляющая погрешности также несколько уменьшилась. Однако, обе методики требуют уточнений для корректировки измерений смешанных осадков.

Таблица 2

Характеристики качества
откорректированных различными методиками результатов измерения по DFIR

Вид осадков	Методика МОК ВМО				Российская методика			
	Общая сумма осадков, откорректированная (мм)	Погрешность единичного измерения			Общая сумма осадков, откорректированная (мм)	погрешность единичного измерения		
		Систематическая, неисключенная (ΔP),%	Случайная $(\pm\sigma_p)$,%	$\frac{\lvert\Delta P\rvert}{\sigma_p}$		Систематическая, неисключенная (ΔP),%	Случайная, $\pm\sigma_p$,%	$\frac{\lvert\Delta P\rvert}{\sigma_p}$
Жидкие	1513,9	-2	16	0,1	1518,5	-2	16	0,1
Смешанные	440,0	1	16	0,1	458,0	5	17	0,3
Твердые	1126,4	-1	25	0.1	1110,3	-2	20	0,1

Национальные методы измерения осадков содержат заметно большую систематическую и случайную составляющие погрешности по сравнению с DFIR (Голубев, Симоненко,1992). Характеристики качества исходных данных (табл. 3) по национальному осадкомеру Третьякова, назначенного МОК ВМО в качестве рабочего эталона взаимосравнения (WNRG), приведены для двух приборов (№2 и №7). Приборы расположенны на ровной открытой площадке на расстоянии 70 м один от другого. Систематическая погрешность исходных данных составляет от -11 до -40%, а случайная - от ±17 до ± 64%.

Таблица 3

Характеристики качества результатов измерения осадков
по VCS и осадкомеру Третьякова (WNRG)

Вид осадков	Число случаев наблюдений	Результат измерения						
		VCS			WNRG			
		Общая сумма осадков, мм	Средняя сумма за одно измерение, мм	Погрешность одного измерения, $\pm\sigma_p$,%	№ осадкомера и сумма осадков, мм	Средняя сумма за одно измерение, мм	Погрешность систематическая, ΔP,%	Погрешность случайная, $\pm\sigma_p$,%
Жидкие	1000	2724	2.7	6	№2 2427	2.4	-11	17
	1390	3806	2.7	6	№7 3402	2.4	-11	18
Смешанные	270	700	2.6	6	№2 522	1.9	-25	35
	340	885	2.6	6	№7 672	2.0	-24	33
Твердые	1161	1837	1.6	8	№2 1100	0.9	-40	64
	1512	2415	1.6	8	№7 1453	1.0	-40	63

Для корректировки значений WNRG были выбраны три методики: методика МОК ВМО (Yang, et al.,1995), России (Голубев, 1973) и Скандинавских странах (Forland (ed), 1996).

Откорректированные по этим методикам результаты измерений характеризуются близкими по величине показателями качества (табл. 4). Систематическая погрешность откорректированных данных стала меньше, чем исходных. Случайная погрешность уменьшилась, в основном, при корректировке значений твердых осадков. При корректировке результатов измерений смешанных осадков методика МОК ВМО более эффективна, если применять формулу для снега с дождем (цифры в скобках).

Таблица 4

Характеристики качества откорректированных различными методиками результатов измерения осадков по осадкомеру Третьякова

Вид осадков и номер осадкомера		Число случаев измерений	Характеристики качества откорректированного результата измерения								
			Методика МОК ВМО			Методика РФ			Методика Скандинавских стран		
			ΔP,%	$\pm\sigma$,%	$\frac{\Delta P}{\sigma_p}$	ΔP, %	$\pm\sigma$,%	$\frac{\Delta P}{\sigma_p}$	ΔP, %	$\pm\sigma$,%	$\frac{\Delta P}{\sigma_p}$
Жидкие	№2	1000	-2	20	0,1	1	18	<0,1	-4	18	0,2
	№7	1390	-2	19	0,1	1	17	<0,1	-4	18	0,2
Смешанные	№2	270	-11(4)	31 (38)	0,4	2	41	<0,1	9	41	0,2
	№7	340	-9 (5)	27 (36)	0,3	4	38	0,1	11	39	0,3
Твердые	№2	1161	-7	48	0,1	-4	48	<0,1	5	50	0,1
	№7	1512	-7	41	0,2	-4	48	<0,1	4	48	0,1

Из рассмотрения характеристик качества откорректированных результатов измерения следует сделать вывод о необходимости дальнейших исследований по усовершенствованию методик корректировки. Учитывая это обстоятельство, а также необходимость исследования новых методов измерения осадков, целесообразно сохранить на ближайшее время некоторое число национальных и региональных центров взаимосравнения средств измерения осадков.

Литература

Голубев В.С. Методика корректировки срочных и месячных величин атмосферных осадков и результаты ее проверки. - Труды ГГИ, 1973, вып. 207, с.11-27.

Голубев В.С. Предварительные оценки точностных характеристик осадкомера в двойной заборной защите. - "Метеорология и гидрология", 1991, №2, с. 116-121.

Голубев В.С., Симоненко А.Ю. Результаты сравнения сетевых методов наблюдений за атмосферными осадками зимой. - "Метеорология и гидрология", 1992, №5, с. 100-107.

Голубев В.С. и др. Оценка погрешностей измерений атмосферных осадков Валдайской контрольной системой. - "Метеорология и гидрология", 1997, №7, с.108-116.

Yang, D. et al.,1993: An Evaluation of Double Fence Intercomparison Reference (DFIR) gauge. - Proc. Eastern Snow Conference, 50th Meeting, Quebec City, pp.105-111

Yang, D.et al.,1995: Accuracy of Tretyakov Precipitation Gauge: Result of WMO Intercomparison. - "Hydrological Processes", vol. 9, pp. 877-895

Forland E. J. (ed), 1996: Manual for operational correction of Nordic precipitation data. - Nordic Working Group on Precipitation, Report NR. 24/96, Oslo,- 66 p.

CORRECTION OF PRECIPITATION MEASUREMENT USING FRESH SNOW AS REFERENCE

Sevruk, B., M. Paulais* and Y.-A. Roulet
Swiss Federal Institute of Technology, ETH Zurich
Switzerland
*Meteo-France, Toulouse, France

The problem of precipitation measurement techniques is that, despite the simplicity of a common precipitation gauge, the process of precipitation measurement is loaded with a number of systematic errors, in particular wind-induced, wetting and evaporation losses (Sevruk, 1986a). The wind-induced error is caused by the blocking effect of the body of a free exposed precipitation gauge (Nespor & Sevruk, 1998). It systematically distorts the wind field, forcing the wind speed to increase over the gauge orifice. This prevents the smaller precipitation particles from entering the gauge. Instead, they are carried beyond the lee of the gauge orifice. The precipitation measurement loss amounts to 3-25% for rain and 20-80% for snow, depending on wind speed, the weight of precipitation particles, gauge construction parameters such as the thickness and shape of the gauge orifice rim, and wind protection used. The systematic error of precipitation measurements, particularly the wind-induced error, reduces the accuracy of meteorological, hydrological and climatological studies and causes the spatial and temporal inhomogeneities of precipitation time series. Correction procedures have been derived using empirical and theoretical approaches. The empirical approaches are based on field experiments using the WMO reference measurements such as the pit gauge for rain and the double fence for snow (Sevruk, 1993). These measurements are compared to the measurements of standard gauges. The difference is related to the wind speed during the precipitation period and some measure of precipitation structure (e.g. the rate of precipitation or air temperature for snow). The theoretical approach is based on the mathematical simulation of the wind-field above the precipitation gauge orifice and of precipitation particle paths. It uses commercial software of computational fluid dynamics and different terminal velocities of precipitation particles as assessed from studies of the structure of precipitation (Nespor & Sevruk, 1998).

Methods and Data

The double fence reference measurements are not easily carried out. The fence is a relatively large and costly structure, having an outer diameter of 12 meters and the inner diameter of 4 metres (WMO, 1998). This is why, in some cases, the values of the water equivalent of fresh snow, W, measured on a snow board, located a few metres from the precipitation gauge, were also used as reference measurements (Sevruk, 1986b). However, taking the depth of fresh snow, H, as a reference would represent a much easier approach. Such measurements are widely available. This would be possible only when the density of fresh snow, D, as measured on the snow board, could be indirectly derived from meteorological variables. Sevruk (1986b) showed that such a relationship exists, and that D depends on the air temperature, T, and the local wind speed, U. Using 780 daily data of D, T and U for seven Swiss locations, situated in different altitudes from 600 m up to 2540 m a.s.l., a respective diagram was derived as shown in Figure 1. A similar diagram was presented by Navarre & Rey (1990). Both diagrams are compared in Figure 1. It is shown that, in contrast to the Swiss diagram (left), the later diagram is very schematic and therefore its application is limited. The latter is based on only 190 measurements carried out at the same site in France, at an altitude of 1300 m a.s.l. By using such diagrams, particularly the Swiss one, the assessment of D values can be made. Moreover, having the H measurements, D can be assessed from the precipitation measurement, P, ($D' = P/H$). In this case, however, D' values are subject to wind-induced error which can be expressed by $k = D/D'$. Therefore, k values can be used to correct the wind-induced error. For this aim, the D/D' daily values were related to the mean wind speed during the periods of snow at the level of the precipitation gauge orifice, U, using linear regression analysis. The U values were obtained from the standard observations of wind at heights at least 10 m above the ground using the logarithmic profile and the average vertical angle of obstacles, as described by Sevruk (1988) and Sevruk and Zahlavova (1994). The above-mentioned approach was applied to derive correction procedures for the French precipitation gauges ASSOCIATION and SPIEA. The reason is that, in France, no measurements of water equivalent, W, are made at meteorological stations near the precipitation gauge. Instead, the depth, H, of fresh snow or total depth of snow-cover are measured.

A set of data consisted, all in all, of 350 events as selected by Meteo-France (1996) from nine French stations, most of them exposed (vertical angle of obstacles smaller than 7°), as follows (number of

events is in brackets): Amberieu (36); Cannes (12); Carcassonne (43); Grenoble (102); Lyon (62); Nice (11); Nimes (19); Perpignan (16) and Saint-Auban (45). In the final analysis, only 320 events have been used. The reason was that 10 events showed unrealistically high k values, (greater than 4) and consequently, have been excluded from the analysis, and 20 events were related to an another type of gauge (Transducteur). The observation period used was from 1950 to 1994. For each event, direct measurements of P were available. In some cases, H values were derived from the total snow depth, and the values of U and T have been obtained by the reduction of direct observations (at least 1 fixed-time observation per 3 hr) to snow periods (T, U), and to the height of precipitation gauge orifice (Meteo-France, 1996). To obtain more accurate correction values, P was corrected for wetting losses and evaporation. The wetting loss correction applied per snow event amounted to 0.07 mm for the Association and 0.10 mm for the SPIEA gauges, and evaporation correction was applied according to the evaporation duration and the time of day from 0 to 0.1 mm (Meteo-France, 1996).

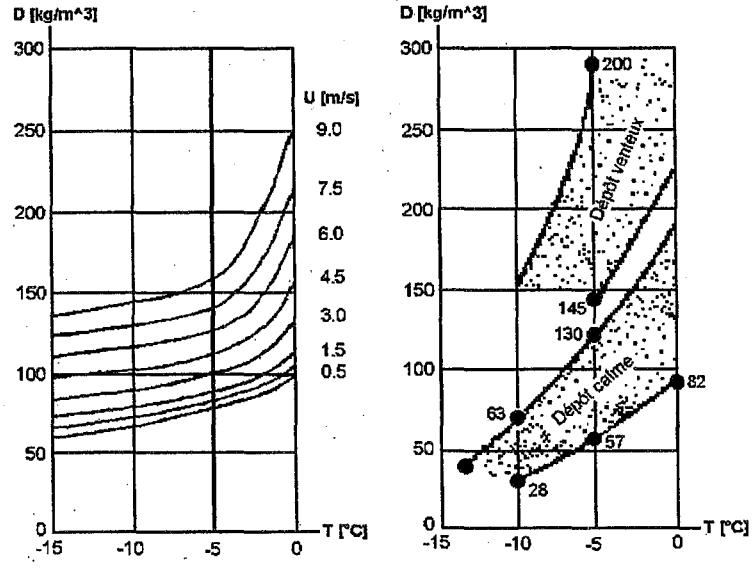

Fig. 1 The effect of temperature T and wind speed U on the density of fresh snow D according to Sevruk (1986) (left) and Navarre & Rey (1990) (right).

Results and Discussion

The correction of the wind-induced error amounted on average from 21 to 26 % at stations with U smaller than 1.5 m/s (Cannes, Amberieu, Saint-Auban, Grenoble and Lyon). The D values range from 98 to 117 kg/m^3. At stations with U greater than 1.8 m/s, the correction varied between 40 and up to 70 % for Perpignan (U equal 3.3 m/s). The respective values of D varied from 112 to 142 kg/m^3. The plots of k values against U for the ASSOCIATION and SPIEA gauges are presented in Figures 2 and 3. Despite the large scatter, the effect of U is evident. The scatter is due to random errors in P and H measurements, particularly for small values (P<3 mm, H<5 cm), and to the possible occurrence of mixed precipitation on days with T above zero. Because k values are smaller for rain than snow, the resulting k for T above zero is generally smaller than for T below zero as shown in Table 1. The effect of H values smaller or larger than 5 cm, is not very obvious, but P amounts, smaller or larger than 3 mm can significantly affect the accuracy of the assessment of k (Table 1). Further, the effect of wind speed is very significant. Zero wind speed in Table 1 does not mean complete calm due to the threshold velocity of wind measuring instruments (above 0.5 m/s) and to the reduction of wind speeds to the level of the precipitation gauge orifice. Thus, for zero wind speed, k can be larger than 1.0 as also shown in Table 1.

The scatter was reduced using the class averages. In such a case, the random errors have the tendency to balance out. The samples were subdivided, according to U intervals, as shown in Figures 2 and 3 (second diagram each from top). Nevertheless, this did not change the original results at all, but the correlation was much better for class averages (see insert in Figures 2 and 3). Thus snow measurements using the two types of French gauges show considerable wind-induced losses. For a wind speed of 2.0 m/s, this loss is up to 50 % of measured P values, whereas the SPIEA appears to have a slightly better performance than the Association. This is still considerably more than for the Hellmann gauge, as assessed during the WMO (1998) Intercomparison using the double fence as reference (Table 2). This seems to be confirmed also by the results of intercomparison measurements

carried out by Poncelet (1959) at a protected site in Uccla, Belgium with wind speeds smaller than 3 m/s. The Association gauge snow catch on average of five years was approximately 5 % smaller than that of the Hellmann gauge. In contrast, for wind speed above 3.0 m/s, the Hellmann gauge performance is worse, as showed during the WMO (1998) Intercomparison (Table 2). In any case, using the French gauges, only one-half of the snow is measured when U equals 2 m/s.

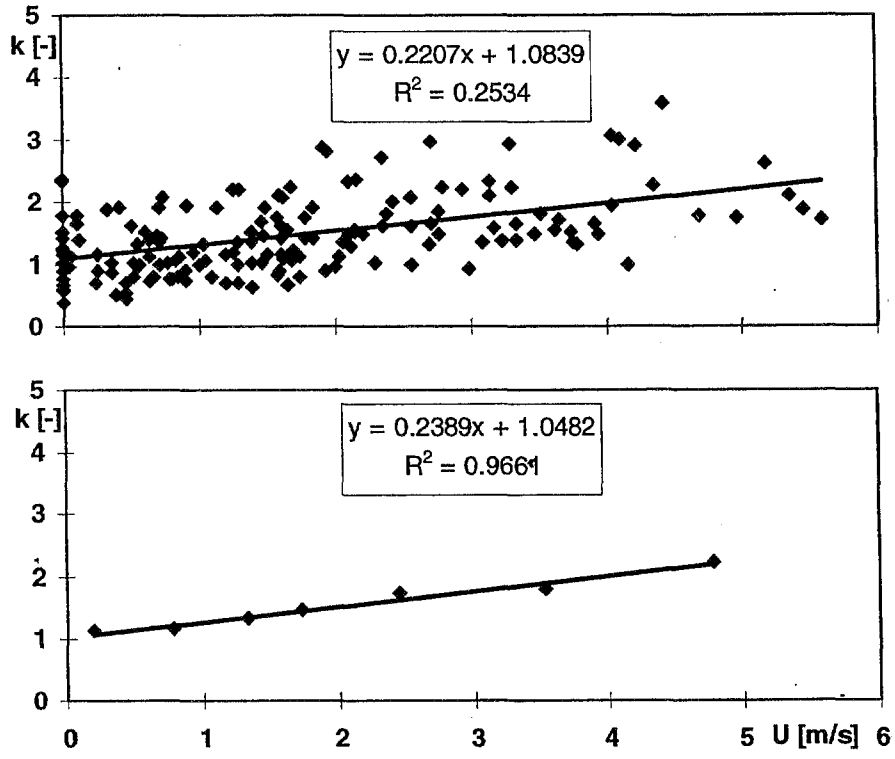

Fig. 2 Plot of correction factor, k, against wind speed, U, for the French gauge type ASSOCIATION. Above: individual events. Below: class averages according to wind speed.

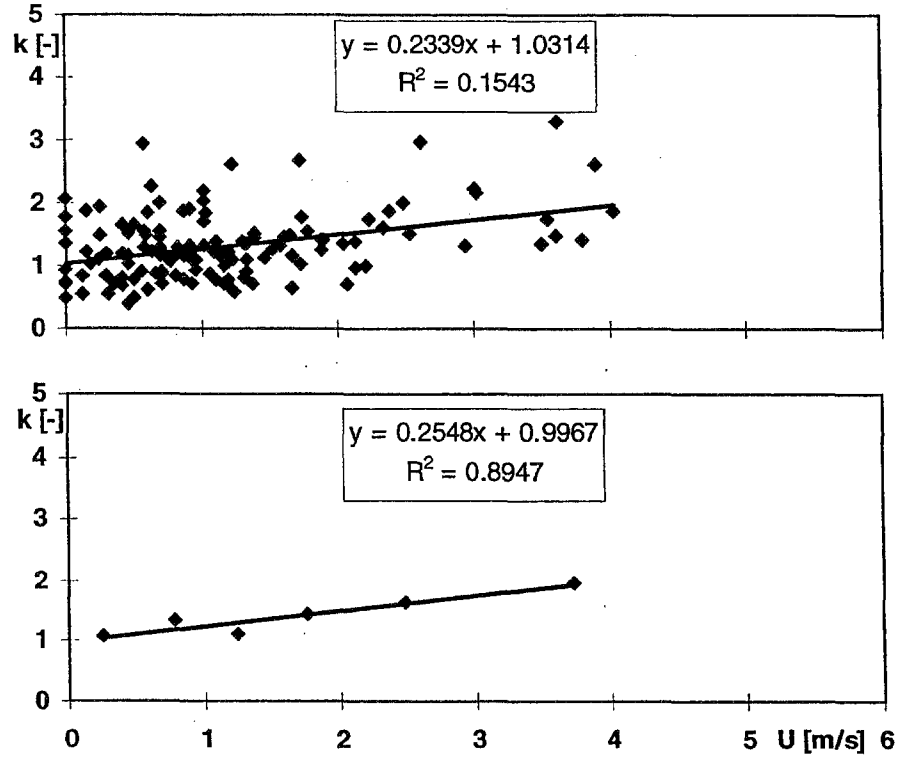

Fig. 3 Plot of correction factor, k, against wind speed, U, for the French gauge type SPIEA. Above: individual events. Below: class averages according to wind speed.

Table 1 The effect of random errors on precipitation measurements and snow depth on the accuracy of the correction factor, k, as a function of wind speed.

Wind speed [ms-1]		0	1	2	3	4
Temperature	T≥ 0°C	0.97	1.27	1.56	1.86	2.16
	T< 0°C	1.20	1.52	1.84	2.16	2.48
Snow depth	H≤5 cm	1.24	1.55	1.86	2.18	2.49
	H>5 cm	1.17	1.49	1.82	2.14	2.47
Precipitation	P>3 mm	1.07	1.34	1.60	1.87	2.14
	P≤3 mm	2.61	2.93	3.26	3.59	3.91

Table 2 Comparison of correction factor, k, of the Hellmann gauge and the French gauges ASSOTIATION and SPIEA as a function of wind speed

Wind speed [ms-1]		0	1	2	3	4
Hellmann gauge	T= 0°C	0.96	1.12	1.35	1.69	2.22
	T=-2°C	1.01	1.19	1.45	1.82	2.50
SPIEA		1.03	1.27	1.50	1.73	1.97
ASSOCIATION		1.08	1.30	1.52	1.75	1.97

Conclusions

Correction procedures of the wind-induced error of snow measurement using the French precipitation gauges, ASSOCIATION and SPIEA, were derived applying the depth of fresh snow measurements and the density of fresh snow as derived from temperature and wind speed measurements. The wind-induced loss is large. For a wind speed of 2. 0 m/s, it amounts up to 50 % of measured precipitation.

References

Meteo-France: Etude de la masse volumique de la neige fraiche pour quelques stations francaises, par M. Paulais, Meteo-France, Service central d'exploatation de la meteorologie, Toulouse, France, 24 pp., Decembre, 1996.

Navarre, J. P. et L. Rey: La neige et les constructions: Surcharges et interactions neige-construction. Cahiers du Centre Scientifique et Technique du Batiment, No. 2398, 12, 1990, Paris.

Nespor, V. and B. Sevruk: Estimation of wind-induced error of rainfall gauge measurements using a numerical simulation. J. Atmos. & Oceanic Tech., 13 pp., (in press), 1998.

Poncelet, L. : Sur le comportement des pluviomètres. Inst. Roy. Meteorol. Belg., Publ. Ser. A, Bruxelles, No. 10, 3-58, 1959.

Sevruk, B. (Editor): Correction of precipitation measurements. Proc. Workshop on the Correction of Precipitation Measurements. Zürcher Geographische Schriften, Swiss Federal Institute of Technology, ETH Zürich, Switzerland, No. 23, 289 pp., 1986a.

Sevruk, B. : Conversion of snowfall depths to water equivalents in the Swiss Alps. In: B. Sevruk (Ed.) Proc. Workshop on the Correction of Precipitation Measurements. Zürcher Geographische Schriften, ETH Zürich, No. 23, p. 81-88, 1986b.

Sevruk, B.: Wind speed estimation at the precipitation gauge orifice level. In: WMO Technical Conference on Instruments and Methods of Observation (TECO-1988). Instruments and Observing Methods Rep., No. 33, 317-320, 1988, World Meteorol. Org., Geneva.

Sevruk, B.: WMO precipitation measurement intercomparisons. In: B. Sevruk and M. Lapin, (editors) Precipitation Measurement and Quality Control. Proc. Symposium on Precipitation and Evaporation, Vol. 1, 120-121, 1993. Slovak Hydrometeorological Institute, Bratislava and Swiss Federal Institute of Technology, Department of Geography, Zurich, 1993.

Sevruk, B. and L. Zahlavova: Classification system of precipitation gauge site exposure: Evaluation and application. Internat. J. Climatol., 14(6), 681-689, 1994.

WMO: International Organizing Committee for the WMO Solid Precipitation Measurement Intercomparison, Final Report. Instruments and Observing Methods Rep., World Meteorol. Org., Geneva. (in press), 1998.

Détermination de la nébulosité par radiométrie infrarouge.

Jean-Louis GAUMET, Willy MORSCHEIDT
Météo-France, Service des Equipements et des Techniques instrumentales
Trappes, FRANCE.

1. Introduction

La description de l'état du ciel fait partie du message d'observation synoptique défini par l'Organisation Météorologique Mondiale. Ce message est utile pour la prévision générale, les opérations aéronautiques et la climatologie. Actuellement, la couverture nuageuse est décrite par des observateurs spécialement formés à ce type de relevés. Cependant, l'observation humaine peut parfois conduire à des erreurs d'appréciation importante, notamment la nuit.

L'automatisation de la description du ciel a été l'objet d'études faisant appel à deux techniques différentes : La radiométrie infrarouge et l'interprétation d'images délivrées par des caméras numériques.

Les progrès technologiques des caméras numériques ont permis d'atteindre une qualité d'image remarquable. La numérisation et les méthodes modernes d'analyse permettent de décrire relativement facilement la couverture nuageuse; par contre, la reconnaissance du type de nuage est beaucoup plus délicate et nécessite le développement d'algorithmes complexes. Malgré ces progrès, le coût de ces caméras numériques reste élevé et limite tout déploiement de ces systèmes dans un réseau opérationnel.

D'autres technologies utilisant des capteurs radiométriques infrarouges (I.R). ont été étudiées. Werner (1973) expérimente un balayage de la voûte céleste au moyen d'un miroir tournant et à inclinaison variable. Coombes et Harrison (1981, 1984) ont également utilisé le déplacement d'un miroir pour balayer le ciel. Leurs résultats ont conduit à la réalisation industrielle d'un tel système par VALCOM Inc. au Canada.

Cette communication a pour but de présenter un prototype de laboratoire dont le principe est fondé sur la thermographie I.R., et capable de décrire l'état du ciel en un temps de l'ordre de 1 à 3 minutes. Dans une première étape, il s'agit de déterminer le taux de couverture nuageuse ou nébulosité. Pour cela, un capteur I.R. effectue une séquence de mesures de température en différents points de la voûte céleste au moyen d'un dispositif de balayage site/azimut (Figure 1). Dans une deuxième étape, un objectif plus difficile sera d'identifier certains nuages dangereux comme les cumulonimbus.

Adresse de correspondance :J.L Gaumet.
Météo-France,SETIM, 7, rue Teisserenc de Bort
BP 202, F78195 Trappes, Cedex, France.

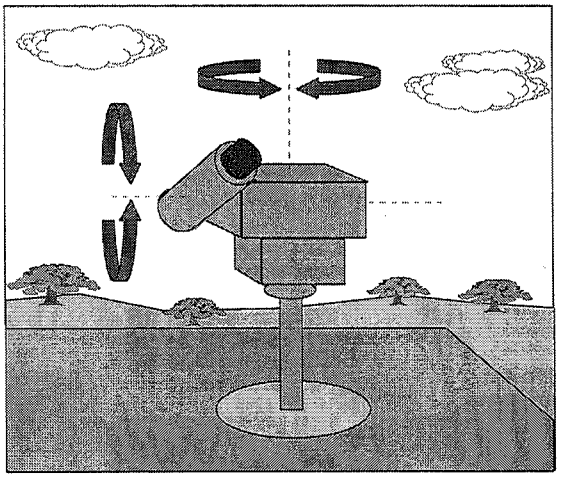

Figure 1. Représentation schématique du système de détermination de la nébulosité.

Ce document décrit la méthodologie, la technologie et les principaux résultats obtenus par situations de plafond nuageux en période hivernale. Des comparaisons systématiques du taux de couverture nuageuse déduit de mesures radiométriques avec des observations humaines ou des photographies sont présentées.

2. Méthodologie

2.1 Principe des mesures physiques

La méthode repose sur le principe de la thermographie I.R. En pratique, il s'agit de mesurer le flux I.R. provenant de différents éléments de la voûte céleste au moyen d'un pyromètre optique. La température est alors le paramètre discriminant entre la présence de nuages et le ciel clair. Dans le cas d'un corps noir à la température T, l'émittance sur tout le spectre de longueur d'onde λ est obtenue par l'intégration de la loi de Planck :

$$R = \int_0^\infty \frac{2hc^2\lambda^{-5}}{\exp\left(\frac{hc}{k\lambda T}\right) - 1} \qquad (1)$$

où h, k, et c sont respectivement les constantes de Planck et Boltzmann et la vitesse de la lumière.

L'émittance du corps noir ($W.m^{-2}$) est alors donnée par la loi de Stefan-Boltzmann :

$$R = \sigma T^4 \qquad (2)$$

où σ est la constante de Stefan exprimée en $W.m^{-2}K^{-4}$

Comme l'émittance est mesurée par un détecteur de bande passante (λ_1,λ_2), il faut effectuer l'intégration numérique de la fonction de Planck (1). La fonction

résultante F(T) est donnée par l'ajustement polynomial d'ordre 4 présenté à la Figure 2. Elle permet de calculer l'émittance par la relation :

$$R = F(T) \quad (3)$$

Les objets communs n'étant généralement pas des corps noirs, les précédentes lois nécessitent une correction. On introduit alors le terme d'émissivité ε qui est le rapport entre l'émittance réelle et celle du corps noir. La relation (3) devient:

$$R = \varepsilon F(T) \quad (4)$$

Malheureusement, l'émissivité des nuages est très variable, surtout pour les nuages moyens et élevés tels que les cirrus pour lesquels ε peut prendre toutes les valeurs. Par contre, ε est voisin de 1 pour les nuages bas (Stratus, stratocumulus, cumulus).

Il en résulte qu'en pratique, la température radiative mesurée ne correspond pas à la température thermodynamique; mais ceci n'est pas essentiel puisqu'il s'agit surtout de trouver une valeur limite en dessous de laquelle les régions les plus froides correspondent à un ciel clair. C'est ce qui a été fait avec la valeur ε = 1 pour laquelle ont été obtenus les résultats présentés ci-après.

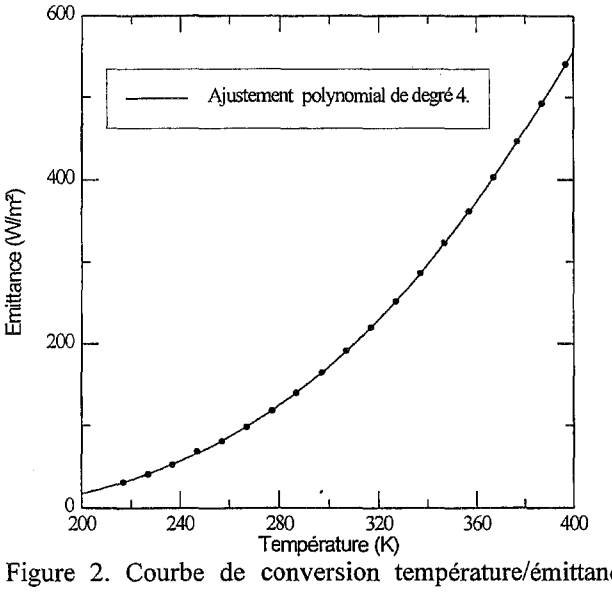

Figure 2. Courbe de conversion température/émittance par intégration numérique de la fonction de Planck.

2.2 Balayage de la voûte céleste

La description du ciel, actuellement faite par observation humaine, est renouvelée seulement toute les heures. En effet, cette information n'est pas de première importance; et on accepte volontiers des erreurs allant jusqu'à ± 2 octas. Elle évolue en général lentement; cependant, dans certains cas, les nuages peuvent se déplacer rapidement sous l'influence de vents violents. Il en résulte que pour saisir une scène de nuages et si possible sans prendre en compte deux fois le même amas, il est alors nécessaire de balayer la voûte céleste en un temps suffisamment court, par exemple de l'ordre de la minute. Ainsi, le nombre de points de mesure doit être limité au strict nécessaire. Une mosaïque de 187 points centrée sur le zénith a été retenue (Figure 3).

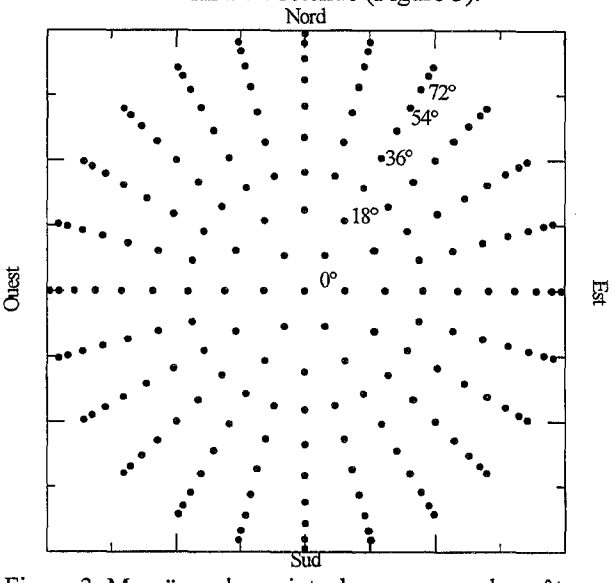

Figure 3. Mosaïque des points de mesure sur la voûte céleste (187 points, 1 capteur sur tourelle)

Le pyromètre I.R. est installé sur une tourelle orientable en site et en azimut. Un programme de commande permet de sélectionner une séquence prenant en compte les 187 points. Le balayage effectue une rotation en azimut par pas de 15° et pour chacune de ces positions, 10 mesures sont faites entre la verticale et une direction sous un angle zénithal de 81°. (site de 9°).

Une succession particulière des points a été adoptée pour obtenir une distribution des mesures sur la voûte céleste la plus uniforme possible. La densité des points près du zénith ne doit pas être très supérieure à celle près de l'horizon. La distance entre 2 points varie néanmoins de 150 m près du zénith, à environ 3 km pour les directions à 81° d'angle zénithal.

Actuellement, la séquence de balayage de la voûte céleste s'effectue en un temps de l'ordre de 3 minutes. Ce temps pourra être ramené à environ 1 minute avec l'installation d'une nouvelle tourelle orientable site-azimut. Le système de balayage du ciel par tourelle n'est probablement pas une solution exempte de risques de panne. Aussi, un nouvel instrument équipé de 5 capteurs OMEGA installés sur 1/4 de cercle depuis le zénith jusqu'à un angle zénithal de 80° et balayant le ciel par une simple rotation, est en cours de réalisation. La mosaïque de points correspondante est différente. Les 322 points de mesure possibles sont moins bien répartis qu'avec le système actuel; il sera nécessaire de valider les observations correspondantes de nébulosité.

2.3 Discrimination nuage-ciel clair

Les données radiométriques obtenues par l'instrument ne sont pas directement exploitables dans la mesure où la température de l'air ainsi que l'angle zénithal jouent un rôle important. Ceci est particulièrement le cas pour les directions proches de l'horizon où la colonne d'air traversée devient importante. La température mesurée tend alors vers la

température de l'air des basses couches . Pour corriger les mesures et obtenir un paramètre normalisé et indépendant de l'angle zénithal d'une part et de la température de l'air d'autre part, on utilise la formule suivante:

$$C_d = \frac{L_a - L_b}{L_a - L_0} L_c(\theta) \qquad (5)$$

où C_d est le coefficient discriminant nuage-ciel clair, L_b la donnée radiométrique de mesure sur le ciel, L_a la luminance calculée de l'air, L_0 le seuil de détection du capteur et $L_c(\theta)$ un coefficient de correction fonction de l'angle zénithal θ.

Les coefficients $L_c(\theta)$ ont été obtenus expérimentalement sur des cas de ciel clair.

Le paramètre C_d ainsi obtenu est normalisé (variations entre 0 et 1). Il est alors possible de fixer des seuils pour déterminer présence de nuage de nuages. Une mesure par ciel clair donne typiquement des valeurs de C_d proches de l'unité, un ciel couvert donne C_d de l'ordre de 0.5. Enfin une valeur de C_d inférieur à 0.1 est indicatrice d'un cas de brouillard.

3. Instrumentation

Le capteur I.R. est un pyromètre OMEGA OS 65-BB sensible dans la bande passante 8-13µ. Cette réponse spectrale correspond à une fenêtre atmosphérique de l'absorption de la vapeur d'eau et du gaz carbonique. Le champ de réception de ce capteur est plutôt étroit (3,8 degrés en demi-angle). Par conséquent, la surface observée sur le plafond nuageux à 1 km est réduite à un cercle de rayon 60 m. L'émissivité est réglable sur l'instrument sur tout le domaine de 0,1 à 0,99. Les principales caractéristiques techniques de ce capteur sont rassemblées dans le tableau 1.

OMEGA OS 65-BB	SPECIFICATIONS
Réponse spectrale	8 à 13 µm
Domaine de température	-57 à + 500°C
Précision sur la température	± 1°C
Temps de réponse	300 ms
Champ de réception (demi-angle)	3,8°
Emissivité réglable	0,1 à 0,99

Tableau 1. Caractéristiques techniques du capteur I.R.

Malgré un bon isolement vis à vis des échanges thermiques et radiatifs, il est probable que les températures extérieures extrêmes contribuent à des erreurs dans la détermination de la température radiative du ciel. Une étude est actuellement en cours pour évaluer l'impact de cette influence dans l'estimation du taux de couverture nuageuse. Si une influence significative est démontrée, il sera envisagé de disposer le capteur dans une enceinte thermostatée malgré le surcoût engendré par cette opération.

4. Résultats

A la fin de chaque série de 187 points de mesure, il est facile de déterminer le taux de couverture nuageuse ou nébulosité exprimée en 1/8^e ou en octa. Les estimations de nébulosité délivrées par l'instrument (448 relevés) ont été systématiquement comparées au relevés effectués par observation humaine sur le même site. Une comparaison entre les deux types d'observation peut être faite au moyen de l'histogramme présenté à la Figure 4. On peut y voir le nombre de cas observés pour les lesquels les différences de nébulosité déterminées par les deux méthodes sont : ±1, ±2,...octas.

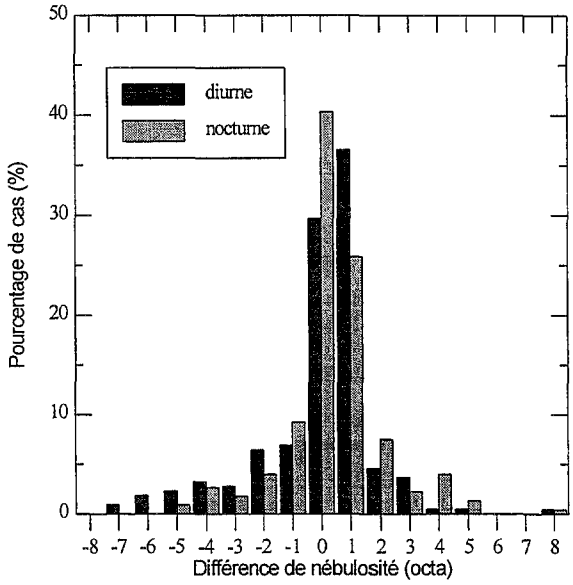

Figure 4. Histogramme de comparaison Instrument - Observation humaine (séparation jour/nuit)

Les données sont en fait très voisines puisqu'une majorité de cas (>70%) se situe à ±1 octa. Il faut noter deux points; d'une part, une assez bonne symétrie de l'histogramme, malgré une surestimation systématique de l'instrument de 1 octa et d'autre part, l'absence de différence significative entre le jour et la nuit.

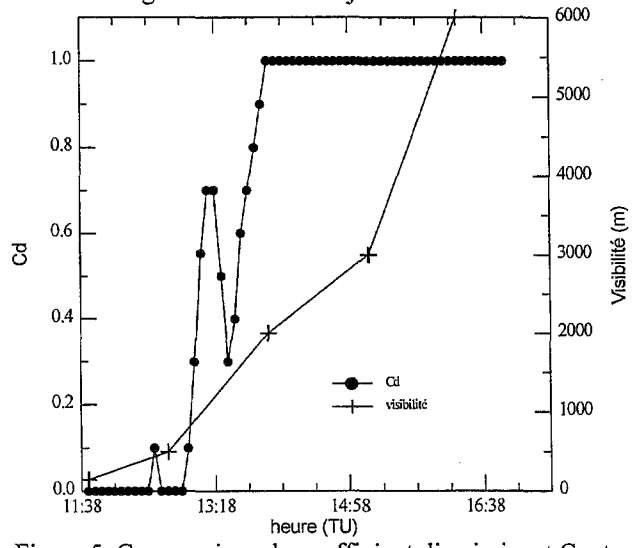

Figure 5. Comparaison du coefficient discriminant C_d et de la visibilité lors d'un épisode de brouillard (5/2/98).

La Figure 5 montre un exemple d'enregistrement de nébulosité déterminée par infrarouge et de visibilité au cours d'un épisode de brouillard. Lorsque le brouillard est dense, le coefficient de discrimination C_d est inférieur à 0.2. Puis il augmente au moment de la dissipation pour

atteindre 1.0 par ciel clair. Ce résultat illustre l'aptitude à identifier le brouillard.

Les données obtenues à partir des 187 points de mesures sont interpolées au moyen d'un logiciel graphique (SURFER de Golden Software Inc). Une représentation du coefficient discriminant sous forme de courbe de niveau est ainsi obtenue. Un exemple de cartographie IR du ciel près du zénith est comparé à une photographie simultanée de la même portion de ciel avec un objectif « fish-eye » (Figure 6). Un excellent accord entre les deux représentations est observable.

5. Conclusion

Les comparaisons de relevés automatiques de nébulosité avec des observations humaines et des photographies « fish-eye » montrent que l'instrument fonctionne très bien dans une grande majorité des cas.

La délimitation ciel clair / couvert est déterminée empiriquement. Aussi est-il encore nécessaire de faire des observations pour atteindre les valeurs optimales d'emissivité et des facteurs de correction.

La caractérisation de la nature des nuages est une observation difficile qui a été seulement abordée dans le cas spécifique du brouillard. Celui-ci a été identifié dans les exemples rencontrés. Cependant, cette identification qui est très utile pour les applications aéronautiques doit être vérifiée sur un plus grand nombre de cas.

Pour les applications opérationnelles, le système devra être très fiable. Aussi pour éviter l'usage d'une tourelle site-azimut sujette à des pannes, un nouveau prototype avec 5 capteurs installés sur un dispositif à rotation simple est actuellement à l'étude.

6. Références

Coombes C. A. and Harrison A., 1982 : An Automatic All Sky Scanning Radiometer. *Can. J. Phys.*,**60**, 919-925.

Coombes C. A. and A. W Harrison., 1985 : Radiometric Estimation of Cloud Cover. *J. Atmos.Oceanic Technol*, **2**, 482-490.

Davis, J. B. ; D. Griggs, and J. D. Sullivan, 1992 : Automatic Estimation of Cloud Amount Using Computer Vision. *J. Atmos. Oceanic Technol*, **9**, 81-85.

Gaumet J.L.and N.Renoux, 1998 : Cloud Cover Observations Using An I.R. Sensor. Preprints 10th Symp. on Meteorological Observations and Instrumentation, Phoenix, AZ, *Amer .Meteor. Soc.*, 161-164.

Werner C., 1973 : Automatic Cloud Cover Indicator System. *J. Appl. Meteor.*, **12**, 1394-1400.

Observation d'état du ciel dans un exemple « broken »

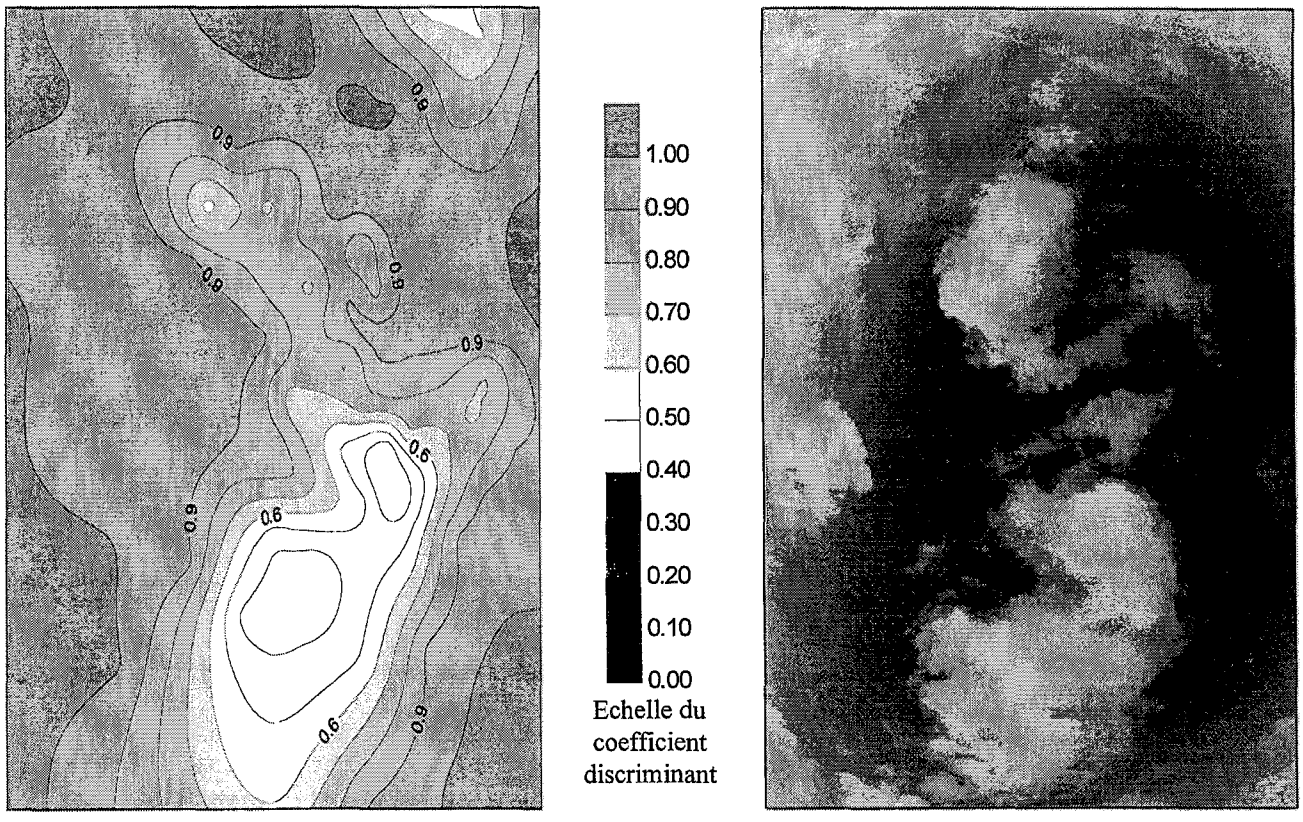

Figure 6. Exemple de comparaison d'une représentation infrarouge avec la photographie « fish-eye » correspondante.

SUNSHINE DURATION MEASUREMENT USING A PYRANOMETER

Jean C. Oliviéri *
Radiometric Center, Carpentras.

1. INTRODUCTION

It is well known that sunshine duration ***SD*** and Global exposure are strongly correlated. A Ångström then J. A. Prescott and others proposed very simple formulae to estimate Global exposure from the number of bright sunshine hours and vice versa. Nevertheless such formulae are valid only if we consider sunshine hours totalled during one month or at least 10 days. Our intention is different. We think that it is possible to use the Pyranometer as a sunshine recorder. This presents a double advantage : sunshine duration ***and*** Global Irradiance (which is a more interesting datum) are measured at the same time for a very reasonable price.

2. THE METHOD

The measured Global Irradiance is compared every one minute (for example) to the value of the product :

Fc×Mod,

- **Mod** represents the Global Irradiance obtained from a **cloudless** day model,
- **Fc** represents a factor the empirical value of which is close to 0.7.

We consider that if the measured Global Irradiance is superior to the product above mentioned, the Direct Irradiance of the Sun is superior to 120 W/m². If the Direct Irradiance reaches or exceeds this threshold level the number of minutes of bright sunshine is increased of one unit.

The model **Mod** that is presently tested is:

$$G = 1080\left[\sin(h+\alpha)\right]^{\beta}$$

where : h represents the elevation of the Sun,
α represents a parameter close to 0 to 0.15 (these values of α are given in degrees of angle),
β represents an exponent close to 1.22.

This model (with $\alpha = 0$) is given for a clear sky and a mean value of the turbidity. In fact the influence of the turbidity is relatively low on the Global Irradiance.

The method was tested using 3 estimations of the factor **Fc** :

- Fc_1 = 0.7 (or a fixed value close to 0.7),
- Fc_2 varies according the date of the day,
- Fc_3 varies according the date ***and*** the hour of the day.

A fixed value of Fc tested during several years, showed that it was necessary to correct Fc according to the season; after which a correction of Fc was also evident according the time of the day, or more correctly the elevation of the Sun. This last improvement is also essential in order to reduce sunshine duration errors when the sky is more or less overcast in the middle of a day.

The annual sunshine durations are correct, they are within ± 1% of the Pyrheliometric Reference with the second and the third Models. Of course daily and hourly errors may be larger : they can reach one hour and sometimes more than one hour. But usually the sunshine profile of the day is acceptable.

Figure 1 that follows, represents the daily variations of the Global and Direct Irradiances, and the product $\mathbf{Fc_3}$**×Mod** on May 19, 1995 in Carpentras. During this day the sky was overcastted with very thick Cirrus before noon. The result of the comparison between the Global irradiance measured and the model is automatically put equal to 0 if the elevation of the sun is inferior to 3 degrees. The effect of this threshold on the accuracy of the SD may be corrected.

Table 1 that follows, represents the results of the sunshine durations obtained using the model and the 3 values of **Fc** above mentioned on May 19, 1995. This day gave us trouble. The results are given in minutes.

The global irradiance measured is compared to the function:

$$\left[A + B\cos\left(\frac{2\pi}{365}d\right)\right] \times \left[a\,h + b\right] \times 1080\left[\sin(h+\alpha)\right]^{\beta}$$

with $A = 0.74$, $B = 0.04$
$a = -0.0028$, $b = 1$
h represents the Sun elevation
d represents the number of the day.

Figure 2 represents the variations of the difference ($SD_{estimated}$ - $Sd_{reference}$) added all-over the years 1994 and 1996.

* *Corresponding author address:* Jean C. Oliviéri
Météo-France, Centre radiométrique
Chemin de l'Hermitage
F - 84200 Carpentras (France)

FIGURE 1

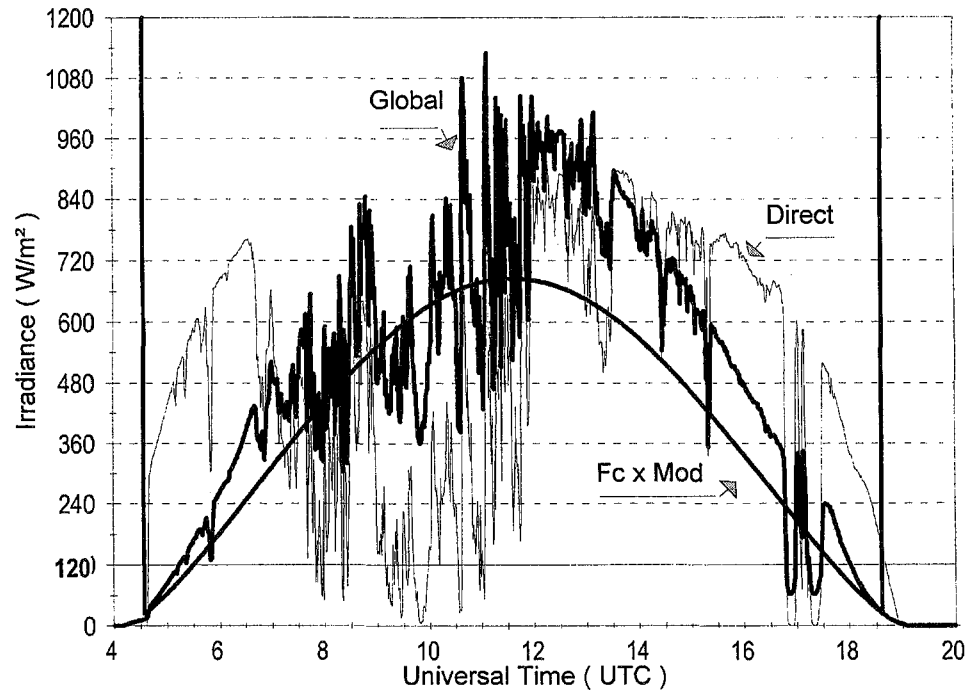

Diurnal variations of Global and Direct Irradiances, and Fc x Mod on a very cloudy day.

TABLE 1

Sunshine durations (SD) are given in minutes.

UTC	SD Reference (1)	SD Fc1=0.7 (2)	Error (2-1)	SD Fc2 (3)	Error (3-1)	SD Fc3 (4)	Error (4-1)
5	16	20	4	20	4	20	4
6	60	57	-3	57	-3	57	-3
7	60	60	0	60	0	60	0
8	55	50	-5	50	-5	55	0
9	57	44	-13	43	-14	52	-5
10	22	9	-13	9	-13	25	3
11	54	36	-18	34	-20	52	-2
12	57	39	-18	38	-19	50	-7
13	60	60	0	60	0	60	0
14	60	60	0	60	0	60	0
15	60	60	0	60	0	60	0
16	60	59	-1	59	-1	59	-1
17	50	48	-2	48	-2	48	-2
18	44	40	-4	40	-4	42	-2
19	42	38	-4	38	-4	38	-4
SD Day	757	680	-77	676	-81	762	-19
Error		-77		-81		0	

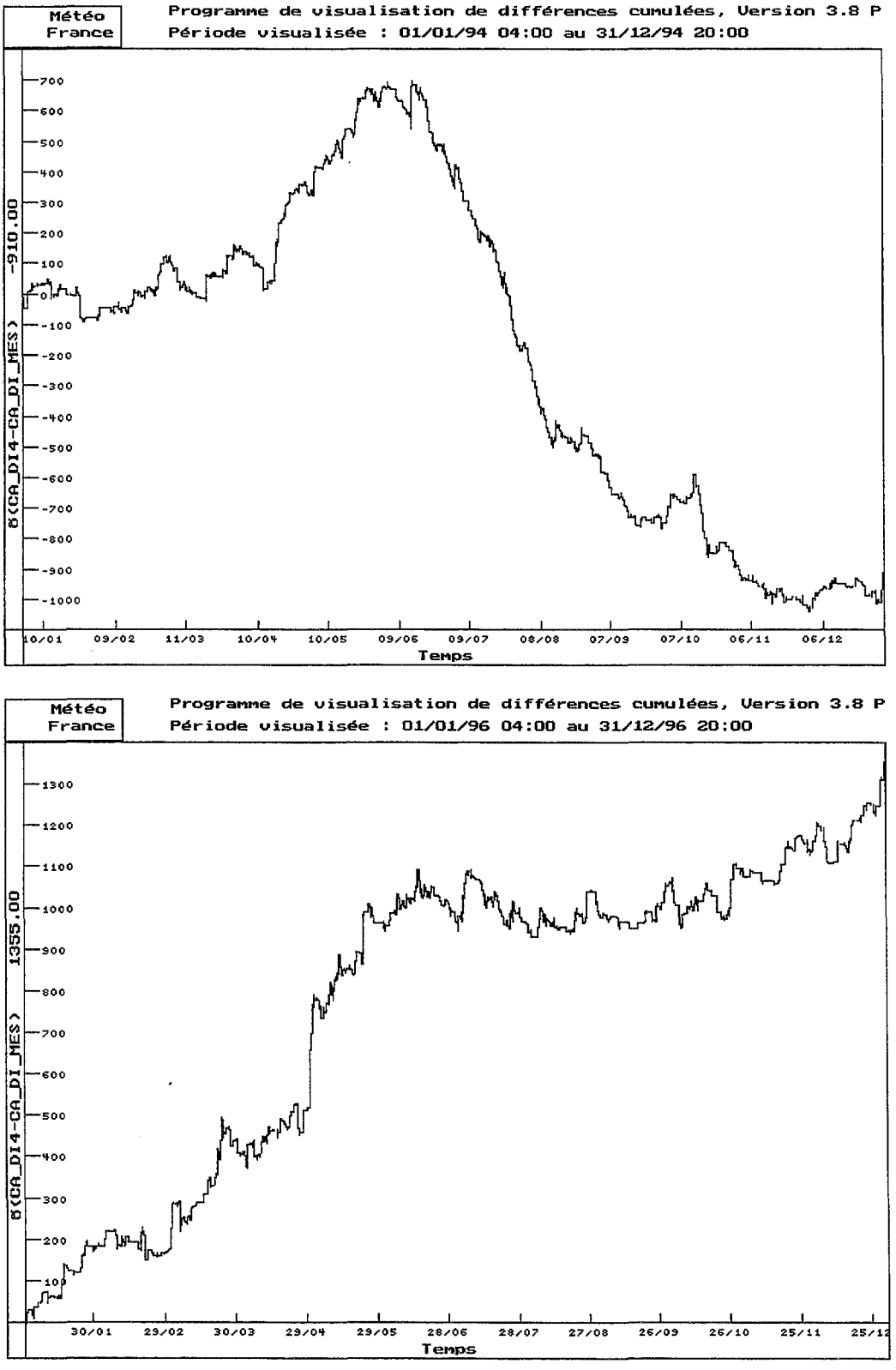

FIGURE 2 Variation of the difference added all-over the year between the sunshine duration estimated using a pyranometer and the reference sunshine duration measured using a pyrheliometer.
For the year 1994 the result is –910 minutes, and for the year 1996 the result is +1355 minutes.
SD for 1994 is equal to 165523 minutes (2759 hr) , SD for 1996 is equal to 153640 minutes (2561 hr).
The errors are respectively – 0.55% and + 0.88%.

A LABORATORY TEST FACILITY FOR SOLAR RADIATION INSTRUMENTS AND ITS APPLICATIONS

Lu Wenhua and Mo Yueqin

Chinese Academy of Meteorological sciences, Beijing 100081, *china*

I. INTRODUCTION

For evaluation of the solar radiation measurement data and instrument specifications, the new laboratory facility for solar radiation instruments has been developed. It consists of a commercially available solar simulator and a rotating mechanism with an instrument mount The spectral distribution is in accordance with Air Mass 1.5 global spectral conditions. The range of irradiance is 250-1250 Wm^{-2}. The effective irradiance area is 100×100 mm. A personal computer takes control over the operation states of the rotating mechanism, so the error of rotation angle is less than $\pm0.05°$. In our measurements we used a personal computer in conjunction with a Keithley 181 nanovoltmeter with IEEE-488 interface and output of instruments can be measured and processed automatically. Directionality, tilt and nonlinearity tests of pyranometers can be made by using this facility. Satisfactory results have been obtained, according to calibration measurements of pyranometers, it is shown that the difference values of the sensitivity are within the range of $\pm0.60\%$ measured in the outdoor exposure.

II. STRUCTURE OF THE FACILITY

1. *Optical System*

Optical system of the facility is based on the commercially available solar simulator (Fig. 1). A 500W spherical xenon lamp is surrounded by a high efficiency ellipsoidal reflector which focuses the radiation onto an optical integrator, passed through a mirror and a spectral correction filrer. A uniform secondary source is formed by the optical integrator and the radiation passes through the collimating lens and the projection mirror to irradiate the target area. Therefore the solar simulator produes a uniform collimated output beam with a close spectral match to sunlight.

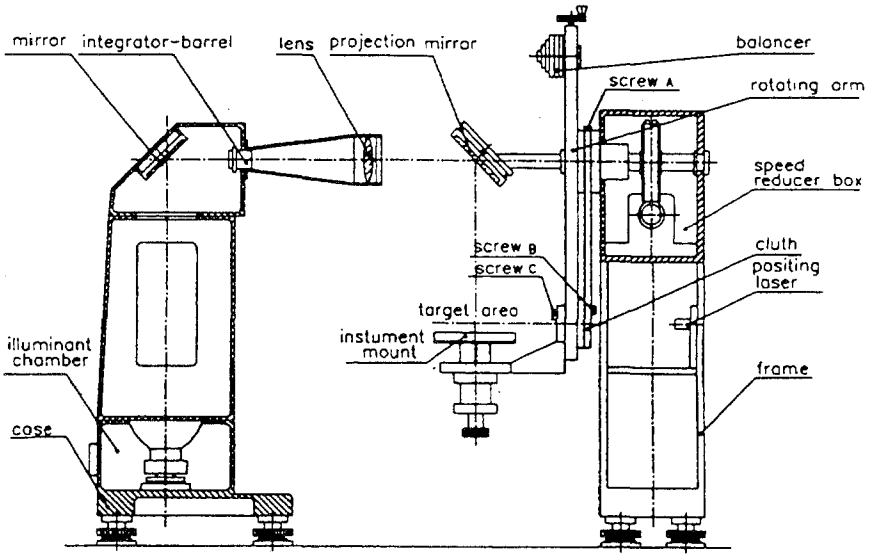

Fig. 1. Structure for the lab test facility

2. *Mechanism Structure*

The mechanism structure of the facility includes solar simulator mechanism and the rotating mecha-

nism (Fig. 1). The solar simulator mechanism comprises an adjustable stand of the xenon lamp, lens-mounts, the optical integrator barrel and the case of solar simulator. A precision adjustable stand can adjust six freedoms for xenon lamp. Other mechanism on solar simulator is used for fixing optical parts. There is an axial-flow fan for cooling the optical parts in the solar simulator.

The rotating mechanism consists of a projection mirror, instrument mount, balancer, rotating arm, speed reducer box with stepping motor, clutch, position laser and frame. A projection mirror is mounted on the front of the rotating arm axis. It can reflect the collimated beam onto the instrument mount which includes a rotating disc and up-and-down movement device. In the projection plane the instrument mount allows the instrument to be turned around the center of the radiation beam and to be moved up-and-down in the range of 0-40 mm. At the rear of rotating arm axis there is a 360° graduated ring for indicating the angle of rotation. The mainshaft of rotating arm is connected with the shaft of the speed reducer driven by stepping motor. The cluth consists of an upper whell, lower wheel and belt. When the screw A of upper wheel and the screw B of lower wheel are scrwed down and the screw C of lower wheel is screwed out, the rotating arm can rotate in the range of $\pm 90°$ and the instrument mount is in level position (see Fig. 2c). The cosine, azimuth response and sensitivity for pyranometers can be tested. When the screw A of upper wheel is screwed out and the screw B. C of lower wheel is screwed down, the rotating arm can rotate in the range of 360° and the instrument mount plane is perpendicular to the radiation beam (see Fig. 2b). The tilt effect for solar radiation instruments can be tested in this case.

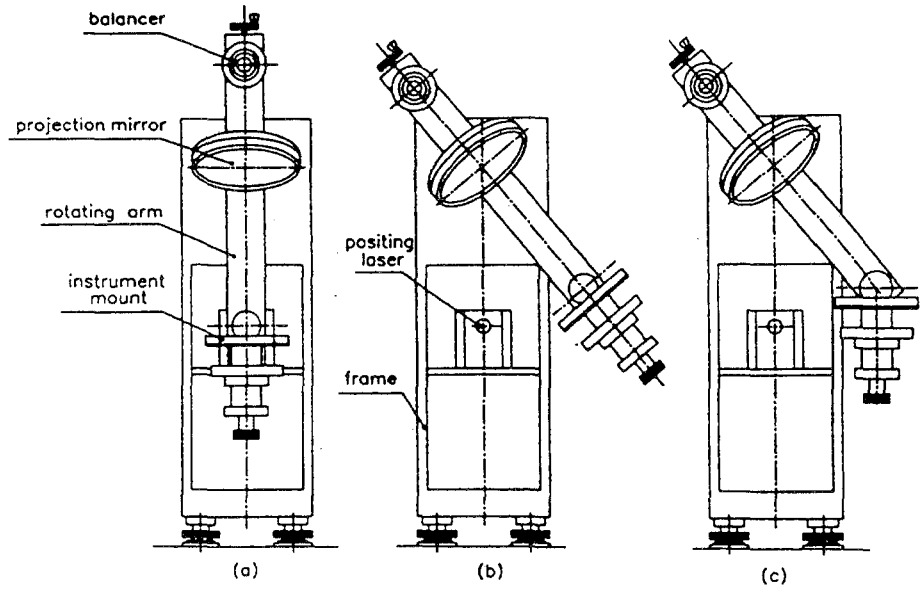

Fig. 2. Schematic diagram for operating state

3. *The Facility Characteristics*

According to China General Specification for Solar Simulator GB/T 12637-90, we have tested the radiation beam in the target area with solar cell. The irradiance nonuniformity is less than $\pm 0.4\%$ within a radius of 40 mm. The irradiance instability is less than $\pm 0.08\%/h$. The facility system error, which is caused by image turned, nonuniformity, instability, diverging beam and mechanism error in the case of making a turn for rotating arm, is less than $\pm 0.3\%$.

Maximum irradiance in the target area is 1250 Wm^{-2}, of which measurement is made with Eppley PSP No. 20461 pyranometer when the xenon lamp power is about 410W.

Ⅲ. APPLICATIONS

In the process of making the China Verification Regulation of Pyranometer, this facility is used for testing performances of pyranometers. Instruments tested are the DFY4, TBQ-2 and TBQ-2-B pyranome-

ters made in China.

1. *Calibration of Pyranometers*

In the lab calibration the Eppley PSP No. 20461 pyranometer is used as a reference instrument. Measurements are based on a comparison of the signal of the test instrument with the irradiance measured with the reference pyranometer. During our test measurements the instruments are exposed to irradiance values of 1000 Wm^{-2}, the angle between the radiation beam and the receiver surface is 90°(see Fig. 2a). Then the rotating arm is turned to 70°. The two instruments are put on the instrument mount alternately and the instrument level is adjusted, respectively. The cable of pyranometer is pointing to north similar to the field position. The instrument is irradiated after five minutes and the signal of instrument is collected. Then turn the instrument mount to 180° and take another group of measurements automatically. Table 1 shows that the results of the laboratory measurements are highly consistent with the outdoor calibrations. The relative errors of sensitivity values are within ±0.6% for six pyranometers. This result demonstrates reliability for calibration pyranometers with the lab test facility.

Table 1. The relative error of sensitivity values between indoor and outdoor calibrations

No.	Type	Outdoor	Indoor	Error(%)
0002	DFY4	8.18	8.14	0.5
0060	DFY4	7.97	7.94	0.4
0058	DFY4	8.35	8.40	0.6
9313	TBQ-2	8.56	8.54	0.3
9303	TBQ-2	8.21	8.21	0.0
9317	TBQ-2	8.59	8.62	0.4

2. *Directional Test*

Directionality includes the cosine responses and azimuth responses. The cosine response test is made at the angle between the radiation beam and the normal of the receiver surface ranged from 10° to 80°. The results are listed in Table 2. From the results we know the fact that cosine error of the TBQ-2-B pyranometer which is as reference instrument in our calibration net is less than other types of pyranometers. The azimuth response test is made at the angle of 10° to the radiation beam and the receiver surface and the azimuth angles ranged in 0—360°. The results are listed in Table 3.

Table 2. The relative error for cosine responses

No.	Type	10°	20°	30°	40°	50°	60°	70°	80°
9201	TBQ-2-B	0.1	0.1	0.3	0.5	0.6	0.8	1.5	2.4
9202	TBQ-2-B	0.4	0.3	0.3	0.1	0.2	0.3	0.8	2.5
9203	TBQ-2-B	0.3	0.2	0.1	0.6	0.5	1.0	1.9	3.1
0058	DFY4	0.2	0.4	0.5	0.7	0.7	0.6	1.3	−3.8
0053	DFY4	−0.1	−0.2	−0.3	−0.2	−0.1	−0.1	−0.2	−0.5
0011	DFY4	−0.1	0.3	0.7	1.4	2.6	3.7	5.5	10.7
9313	TBQ-2	−0.4	−0.9	−1.6	−2.4	−3.1	−4.0	−6.2	−13.4
9303	TBQ-2	−4.8	−0.1	−0.2	−0.1	−0.2	−0.2	−0.6	−2.4
9312	TBQ-2	−0.3	−0.3	−0.3	0.0	0.9	1.7	2.1	1.3

3. *Tilt Effect Test*

The tilt effect of pyranometers is tested by using this lab test facility. The tilt angles for pyranometer are selected as follows: 0°,45°,90°,135°,180°. During the lab experiments, the receiver surface

for pyranometer is always perpendicular to the radiation beam. The results (see Table 4) from the Eppley PSP No. 20462 and No. 20463 show that this measurement is correct.

Table 3. The relative error for azimuth responses

No.	Type	0°	30°	60°	90°	120°	150°	180°	210°	240°	270°	300°	330°
0058	DFY4	0.2	0.3	0.3	−2.1	0.7	4.0	3.7	1.5	−2.7	−1.7	−3.0	−1.2
0053	DFY4	−4.6	−3.7	−2.3	−0.7	1.8	2.2	0.8	4.2	5.3	3.9	−1.3	−5.5
0011	DFY4	−3.8	−4.6	−7.1	−8.6	−4.7	0.0	2.6	8.3	7.0	4.8	4.5	1.5
9313	TBQ-2	−6.7	−5.0	−4.3	0.3	4.4	6.5	7.3	6.4	2.6	−0.3	−4.6	−6.8
9303	TBQ-2	0.5	0.0	−0.2	−0.7	−0.2	−0.5	−0.1	−0.7	1.0	0.5	0.2	0.1
9312	TBQ-2	0.3	0.3	0.7	0.5	−0.3	0.0	0.7	0.3	0.1	−1.0	−1.0	−0.8

Table 4. The relative error of tilt responses

No.	Type	45°	90°	135°	180°
20463	PSP	−0.3	−0.3	−0.4	−0.5
20462	PSP	−0.5	−0.4	−0.4	−0.5
9313	TBQ-2	0.7	1.2	2.0	2.8
9303	TBQ-2	1.1	1.8	2.7	3.1
9312	TBQ-2	0.7	1.0	1.8	2.8
0058	DFY4	−0.2	−0.4	−0.1	−0.1
0053	DFY4	0.7	0.3	0.3	0.3
0011	DFY4	−0.2	−0.3	−0.1	0.3

Nonlinearity, response time, and zero shift tests for solar radiation instruments can also be made with this lab facility. Further, the facility can be used with a temperature test chamber to measure the temperature characteristics in the stable and well-characterized radiation beam.

Ⅳ. CONCLUSIONS

The new laboratory test facility for solar radiation instruments has been developed and used in characterizing pyranometers. Very satisfactory reslts have been obtained on calibration measurements of pyranometers and the difference value of sensitivity is with ±0.6% between indoor and outdoor measurements. Through the experimental investigation. irradiance of the facility ranges in 250-1250 Wm^{-2}, nonuniformity is less than ±0.4% within a radius of 40 mm, instability is less than ±0.08%/h. and system error is less than ±0.3% when the rotating arm turns in 0—360°.

This facility is also suitable for a variety of other experiments testing solar radiation instruments or other meteorological instruments on which solar radiation exposure may interfere with their measurement. It is of great importance to evaluate solar radiation measurement and improve instrument specifications for manufacture with this new lab test facility.

REFERENCES

Philipona, R., Heimo, A. and Hoegger, B. (1993), Investigations of solar radiation detectors using a laboratory test facility for solar radiation meteorological instruments, *Solar Energy*, **51**:159—163.

Measuring rain and rain drop distribution at sea

Lutz Hasse, Martin Grossklaus, and Klaus Uhlig
Institut fuer Meereskunde, D-24105 Kiel, Germany

1. Introduction

Determination of rain at sea is a prime requirement for operational weather and climate forecasts and research. Unfortunately, satellite estimates by microwave and IR methods differ by a factor of two and are not well suited to calibrate numerical models. Rain measurements at ships are often deemed unreliable too, e.g. referring to flow distortion by ships. However this difficulty can be alleviated by positioning the instrument above the superstructure of the ship where the flow is nearly level. The high wind speeds at sea and additional the speed of ships result in flow distortion at the instrument itself, that would make measurements with standard cylindrical instruments useless. A special ship rain gage has been developed that is able to work at high speeds. Additionally, an optical disdrometer has been built for use at high wind speeds too. This instrument measures dropsize distributions and is thus able to give an independent determination of the rain fall rate. Ship rain gage and optical disdrometer have been reported on at TECO 90 and TECO 94 (Hasse et al, 1992, 1994), detailed descriptions are given by Hasse et al. (1998) and Grossklaus et al (1998).

2. Technical realisation of ship rain gage

The ship rain gage (fig. 1) is based on the idea that under high wind speeds the rain is carried almost horizontally over the ship, leading to severe undercatch. However, measuring the liquid water content of the air at a lateral collector, determination of rain rate is possible even at high wind speeds. The upper collector is used for lower wind speeds, the lateral at higher speeds, with a transition near 10 m/s. The relevant speed here is the local relative wind at the site of the rain gage, that results from the addition of speed of ship and wind and from local accelerations.The efficiency of catch for both collecting surfaces has been determined by comparison against independent measurements by disdrometer.

The water amount from both sides is measured separately by drop forming devices, called dropper. The droppers form drops of 0.1 g each. By counting the number of drops that pass through a light barrier, flow rates can be determined. It showed that the calibration curve for droppers is sufficiently linear up to a flow rate that corresponds to 60 mm/h at the standard 200 mm^2 area used at the upper collector. At the side, with its smaller cross-sectional area, rain rates

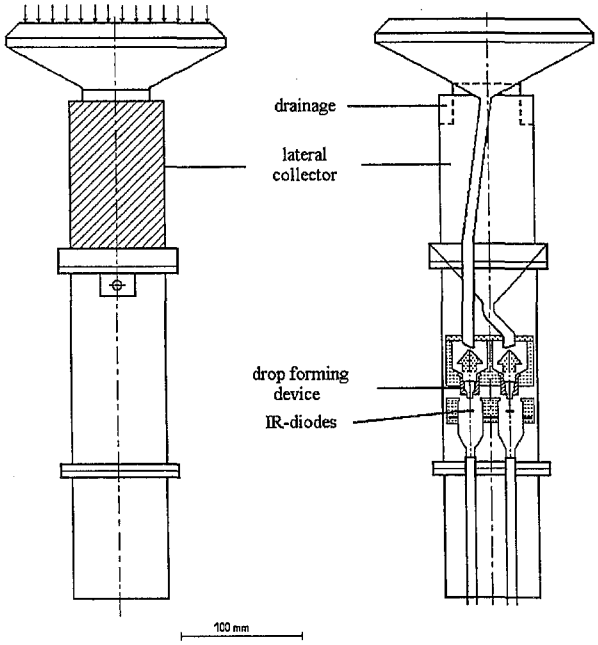

Figure 1: Side view and vertical cross-section of ship rain gage. Water is collected at the upper orifice (arrows) and the lateral collector (shaded). There are 5 vertical T-bars at the lateral collector that hinder rain water to wander around the cylinder and be blown off in lee (not shown in the diagram).

of 140 mm/h were measured successfully. Rain rates of 80 or 90 mm/h can be evaluated using individual calibration curves (fig. 2a).

Tropical rainfalls may show even higher instantaneous rain rates. Then the flow through the dropper takes the form of elongated drops. In this case it is possible to measure the length of time that the light in the infrared light barrier is interrupted by each elongated drop and determine the rain rate from summation of these times, an example is shown in figure2b.

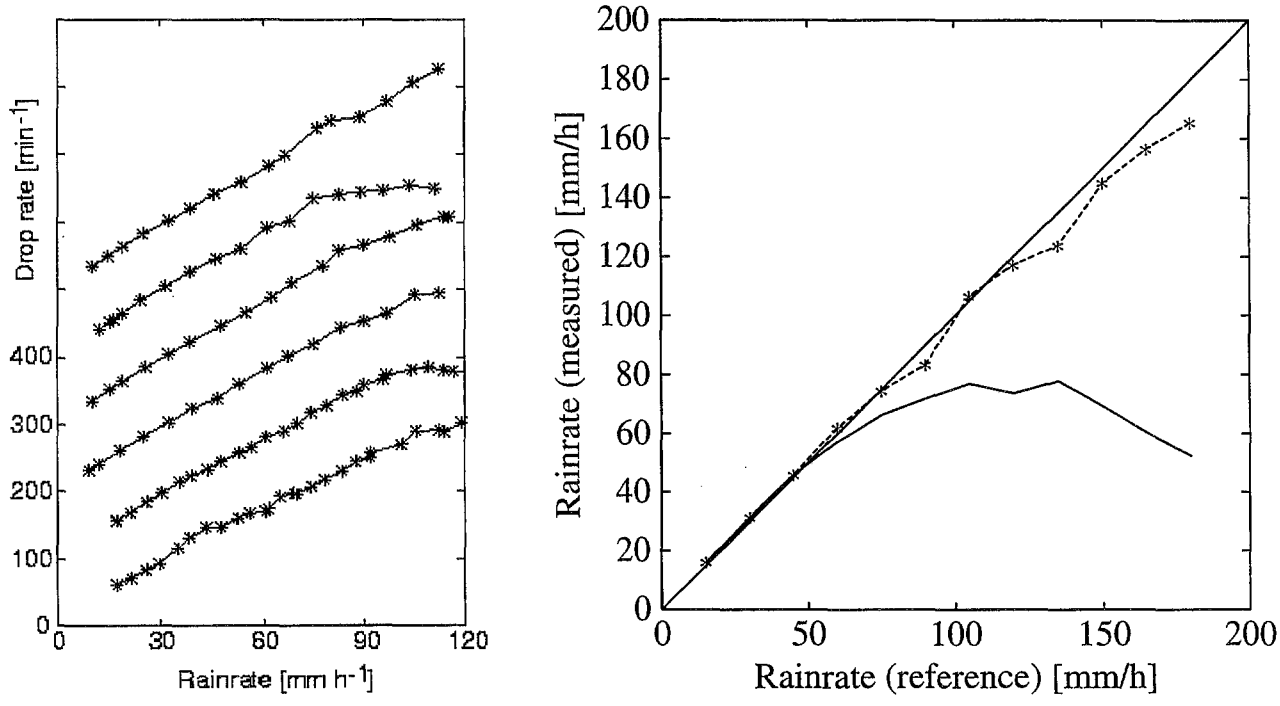

Figure 2. Calibration of dropper. a) drop count rate per minute versus rain rate for 6 individual doppers. Curves are shifted by 100 counts each for clarity.
b) calibration curve for high flow rates. Abszissa is reference rain rate, ordinate measured by ship rain gage. Full line, rain rate determined by counting drops of dropper, broken line determined using length of drop time signal. Also indicated is the 1:1 line.

3. Technical realisation of optical disdrometer.
The disdrometer has been built to measure drop size distribution. Knowing the number of drops in a given volume, and inferring their fall velocity as function of radius, the rain rate can be determined. A cross-section of the instrument is shown in fig. 3. The principle of measurement is light extinction of individual rain drops that pass through the optical active volume. The depth of a pulse is proportional to the vertical cross-section of the drop. The signal to noise ratio allows to measure drops of 0.35 mm, typical resolution is 0.05 mm.
For groundbased disdrometers there is a need for compromise: In order to obtain a good sample in a short time, a large optically active volume is required. However, with a larger volume the probability coincidences , i.e. situations where two or more drops are simultaneously in the active volume, increases. Since we use light extinction, the instrument sees coincidences of two (or more) drops as the shadow of a larger one. This effect is relevant, since rain drop size distribution typically have an exponential distribution with many small drops and few large drops. Hence, coincidences of the frequent small drops are likely. Taking drop size distribution as probability functions, the coincidences can be seen as convolution of drop size spectra with itself.

A program to invert the measured spectra to obtain the true spectra has been developed by Grossklaus et al (1993, 1998). This procedure has been verified inter alia by Monte Carlo calculations.

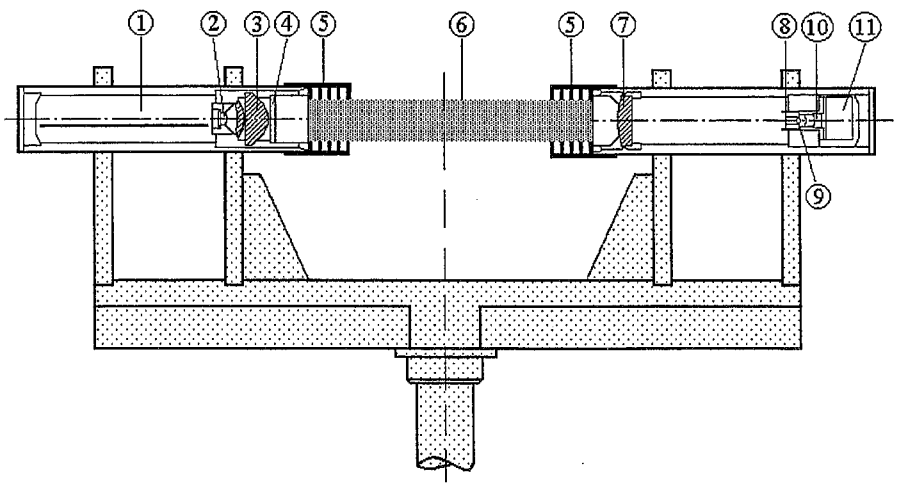

Figure 3. Cross-section of optical disdrometer. From left to right: 1 electronics, 2 light emitting diode, 3 lens system, 4 windows, 5 baffles, 6 sensitive volume, 7 collector lens, 8 optical blend, 9 ocular, 10 photo diode, 11 electronics

While the instrument originally has been developed to calibrate ship rain gages for their wind speed dependence it is evident that drop size distributions have a much wider application in meteorology: The scatter of microwave signals at rain drops is size dependent, hence a knowledge of size distributions in tropical rains would be of interest for example to resolve the differences of rain estimates from satellite remote sensing.

Another interesting application of the disdrometer is for solid precipitation. It is understood that the ship rain gage is not built to measure solid precipitation. The disdrometer, however, can also measue the light extinction by solid precipitation up to a size limit of 2.2 cm, the limit being imposed by the size of the optical active volume. While the relation between snow flake size and rain rate is not unique, at least a good estimate of snowfall intensity and its water content can be obtained. First studies in the wintertime Labrador Sea gave good agreement between different methods to estimate solid precipitation rates.

Table 1. Intercomparison at the test site of Deutscher Wetterdienst at Harzgerode, 1992/1996

wind speed	< 5 m/s	> 5 m/s
Hellmann rain gage in pit	2370 mm	142 mm
ship rain gage	98.3%	100.4%
standing Hellmann rain gage	92.0%	84.7%

4. Results

The windspeed dependence of collection efficieny of ship rain gages has been obtained originally by simultaneously operating ship rain gage and disdrometer on moving ship at a distance of few meters. An independent intercomparison was obtained at the test site of the Deutscher Wetter-Dienst at Harzgerode. A Hellmann type recording rain gage in a pit, orifice level with the ground, is taken for comparison, because it can be assumed that the instrument in the pit will not have wind induced errors. The ship rain gage was mounted with the orifice of the upper collector at 1.15 m above ground, the same height as the orifice of a second Hellmann rain gage at a few meters

distance. Several years of intercomparison are available now, a shown in table 1. Note that calibration of the ship rain gage for collection efficiency was obtained independently of this test.

An example for application of rain measurements obtained at the ocean is available from the eastern Pacific. The NOAA RV "Ron Brown" was station keeping in the ITCZ. During a 20 day period in August 1997, the ship rain gage measured 214 mm of rainfall. The operational global model of the Deutscher Wetterdienst gave 236 mm for the same area and time span (Courtesy DWD).

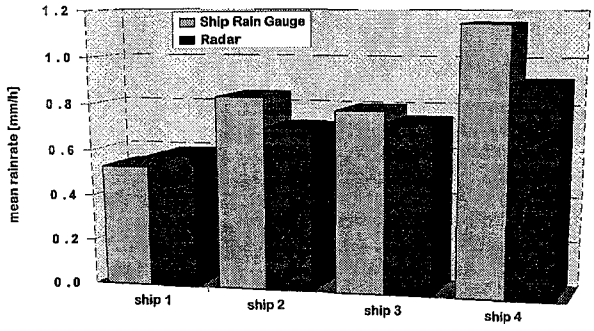

Figure 4: Intercomparison between precipitation measurements at ships and radar estimates which have been interpolated to the ship's position. Results are given for the period Aug, 13th to Oct, 31st 1995.

Another example was obtained at the Balltic Sea (fig.4, where in fall 1995 precipitation was estimated by radar (courtesy of SMHI) and rain gages mounted on ferry boats that pass through the area (Franke et al. 1998). While there is some scatter in the individual results - unevitable comparing point and areal measurements - rather good agreement was found in the mean: radar 190 mm, ship rain gages 194 mm.

The ship rain gage has now been operated for several years at different parts of the world oceans with good success, and has proven to be a reliable instrument. Its accuracy in the field is estimated to 2% -3% percent for hourly estimates (Hasse et al., 1998) which includes some of the notorious variability of rain.

Acknowlegdement is made to BMBF for funding this research, to Station Manger Rönsch of the test site Harzgerode for collecting the data, to Swedish Meteorological and Hydrological Institute for the radar data, and Deutsche Wetterdienst for model results.

References

Franke A., M. Grossklaus, L. Hasse and D. Michelson, 1998; Comparison of ship rain gauge and radar precipitation measurements over the Baltic Sea. Int. BALTEX Sec.*Publ. 10 (submitted).*

Grossklaus M., K. Uhlig and L. Hasse, 1998: An optical disdrometer for use in high wind speeds. J Atmos Oceanic Techn., (in press).

Grossklaus M., L. Hasse and K. Uhlig, 1993: Correction of in-situ rainrate measurements at high wind speeds (extended abstract). In: B. Sevruk and M. Lapin (eds.): Precipitation measurement and quality control. Slovak Hydromet. Inst., Bratislava, and ETH, Zürich, 157-158.

Hasse L., M. Grossklaus, K. Uhlig and P. Timm, 1998: A ship rain gauge for use in high wind speeds. J Atmos Oceanic Techn., (in press).

Hasse L., M. Grossklaus and K. Uhlig, 1994: New ship rain gage. In: Instruments and Observing Methods, report No **57**. World Meteorological Organisation, Geneva, WMO/TD No **588**, 97–101.

Hasse L., M. Grossklaus, H.-J. Isemer and K. Uhlig, 1992: New instrumentation for measurement of precipitation at sea. In Instruments and observing methods, Report No. **49**. World Meteorological Organisation, Geneva. WMO/TD No. **462**, 195–198.

A Simple Audio Technique to Determine the Characteristics of Precipitation.

Kirk, V. L., Hatton, D. B. and Jones, D. W.
The Meteorological Office, United Kingdom.

1. Introduction.

The acoustic domain is a relatively unexplored sensing modality for the detection and identification of precipitation. Most documented research seems to have concentrated on the analysis of noise created during the impact of rain and hail with a body of water [1,2,3]. Although the mechanisms are different, recent research does not seem to have been extended to consider impacts with a solid surface for use with land based observations. However the noise made by rain or hail impacting on a solid surface is often, (assuming one is not outside,) one of the first indicators that precipitation has begun.

As a human can easily notice the differences between sound created through impacts of rain and hail it is hoped that, through the characterisation of precipitation impacts, a simple but effective solution to distinguish between rain and hail can be implemented. It is the purpose of this paper to describe the work being done in an effort to achieve this.

2. Data Acquisition.

Microphones were placed within a range of plastic containers that were then left in an exposed position. Audio data was then acquired for a number of rainfall events and for simulated solid and liquid precipitation. The signal from the microphones was recorded direct to a PC via two audio capture cards. Each of these cards allow for sampling on four channels simultaneously at rates up to 48kHz at a resolution of 32bits, a practical capability that has only relatively recently been available at reasonable cost through the rapid developments in PC technology

The set-up used sampled the microphone signals from up to 8 channels simultaneously at 44.1kHz with a resolution of 32 bits.

Unfortunately, since the start of this project, local weather conditions have not been suited to a full range of trials; some of the initial experiments were therefore performed using simulated precipitation. Rain was simulated using a sprinkler system, while hail was simulated using ice pellets.

3. Results.

Figures 1 and 2 show the spectral composition of the noise made by the impact of precipitation with the containers for two of the recorded events, and are typical of other events. Both of these plots were obtained using a 1024 point FFT with a Hamming window. The data in figures 1 and 2 were acquired using the same container and condenser boundary layer microphone.

From figures 1 and 2 it can be seen that the signal from simulated hail is much greater than that for rain. Another obvious difference is in the frequency components of the signals. The signal from rain consists predominantly of low frequencies, up to approximately 8kHz, while that for ice pellets has a broader spectral content covering the whole range up to 22kHz.

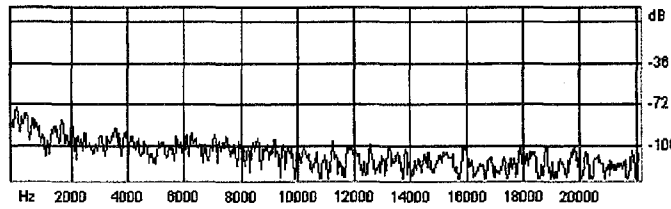

Figure 1; Spectra for a real moderate rain event.

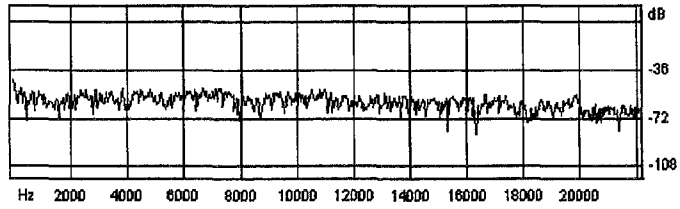

Figure 2; Spectra for simulated hail.

4. Conclusion and Future Work.

Rudimentary analysis on these initial experiments suggests that the technique may prove useful in precipitation detection. However there is still a considerable amount of research to be undertaken to fully characterise the noise generated by different precipitation impacts.

This data seems to indicate that an instrument could distinguish between rain and hail through simple analysis using low and high pass filters, and the level of the signal.

Future work will involve investigating a number of areas, but is likely to initially concentrate on two; effects of the configuration of microphone and container set-up, and spectral analysis of precipitation impacts.

It is necessary to study the characteristics of different microphones, housings and impact surfaces in order to identify an optimum set-up to ensure repeatable high quality data.

It is hoped, that through characterisation of impact noise through spectral analysis, an instrument can be developed that can provide a low cost method of distinguishing between hail and rain.

5. References.

1. Scrimger, J. A. Underwater noise caused by precipitation. *Nature* **318**, 647-649 (1985).

2. Prosperetti, A., Oguz, H. N. The impact of drops on liquid surfaces and the underwater noise of rain. *Annu. Rev. Fluid Mech.* **25**, 577-602 (1993).

3. Nystuen, J. A., Acoustic rainfall analysis: rainfall drop size distribution using the underwater sound field. *J. Atmos. Oceanic Technol.*, **13**, 74-84 (1995).

A COMPARISON BETWEEN A PROPOSED ASOS SUNSHINE SENSOR AND A PYRHELIOMETER

Joseph V. Fiore Jr. *
Robert Wnek
Lynn Wynans
Hughes STX Corporation, Sterling, Virginia

Meka E. Laster
ASOS Surface Observation Modernization Office
Silver Spring, Maryland

1. INTRODUCTION

The Automated Surface Observing System (ASOS) Surface Observation Modernization Office (SOMO) started the test and evaluation of candidate sunshine sensors in 1992 for future use in a limited number of ASOS sites (~100 sites). An extensive field test at four ASOS sites comparing an EKO MS-91 Sunshine Sensor and the Eppley Pyrheliometer has been conducted and monitored by Hughes STX for the ASOS SOMO since March 1996. One of the main reasons for adding a sunshine sensor to ASOS is to replace the Foster-Foskett sunshine switches which have been the National Weather Service (NWS) standard sunshine sensor since the 1950's. The Foster-Foskett sensors cannot be easily automated, and they are no longer maintainable due to constant potentiometer adjustments that need to be made almost daily. The EKO MS-91 Sunshine Sensor evaluated in this study can be automated for ASOS, and it has performed well within the ASOS Specification for a sunshine sensor.

This paper summarizes the results of the study between an EKO MS-91 Sunshine Sensor and the Eppley Normal Incidence Pyrheliometer (NIP). The paper also answers several questions about sensor performance including: 1.) What percent of the time does the EKO MS-91 Sunshine Sensor report daily total minutes of sunshine within 10% of the Eppley NIP? 2.) What percent of the time does the EKO MS-91 Sunshine Sensor report "sun" when the Eppley NIP is reporting less than 108 Watt/m^2? (120 - 10%), and 3.) What percent of the time does the EKO MS-91 Sunshine Sensor **not** report "sun" when the Eppley NIP is reporting greater than 132 Watt/m^2? (120 + 10%).

2. BACKGROUND

2.1 Candidate Sensors for an ASOS Sunshine Sensor

The NWS Office of Meteorology requirement for a sunshine sensor is that the sensor indicate "sunshine" at a solar flux density greater than or equal 120 Watt/m^2, with an accuracy of + or - 10% total minutes of "sunshine" as measured by an Eppley NIP. The sunshine sensors' "sunrise" is determined when the amount of direct solar insolation (exclusive of the effects of diffuse radiation) as received by the sensor (voltage) exceeds a solar flux density threshold of 120 Watt/m^2 (World Meteorological Organization (WMO) standard).

*Corresponding author address: Joseph V. Fiore Jr., 43872 Weather Service Road, Sterling, VA 20166
e-mail: Joseph.Fiore@noaa.gov

The ASOS SOMO began testing candidate ASOS sunshine sensors in the spring of 1992. Several sensors were evaluated, including the Foster-Foskett sunshine switch which has been used by the NWS since 1952.

The Foster-Foskett sunshine switch was eliminated from the evaluation due to poor performance and frequent maintenance (potentiometer adjustments). All other candidate sunshine sensors except the EKO MS-91 sunshine sensor were eliminated due to relatively poor comparability to the reference sensor (Eppley NIP). The EKO MS-91 sunshine sensor was the only sensor that performed with an accuracy of + or - 10% of the Eppley NIP.

2.2 EKO Sunshine Sensor

The EKO MS-91 sunshine sensor consists of a special reflective mirror rotating within a glass tube, with a pyroelectric sensor mounted on the end of the glass tube. As the reflective mirror rotates, it catches and directs sunlight to the sensor. The pyroelectric sensor outputs an electric signal (voltage) proportional to the direct solar radiation intensity. The sensor's reflective mirror is driven by a pulse motor that revolves once every 30 seconds. The EKO sensor raw voltage values are converted to flux values once a minute in a Data Acquisition System (DAS) developed by Hughes STX to collect and analyze the sunshine data.

2.3 Eppley NIP

The Eppley NIP consists of a wirewound thermopile at the base of a tube, the aperture of which has a ratio of 1 to 10 to its length. This design limits the solar radiation received by the thermopile to only direct solar radiation. The Eppley NIP measures the direct solar radiation at normal incidence. The Eppley NIP is mounted on an Eppley Model SMT-3 Automatic Solar Tracker, which keeps the pyrheliometer pointing directly at the sun. The Eppley NIP takes a five minute average of flux values reported every minute.

3. TEST RESULTS

3.1 Test Sites

Four test sites, representing both high and low latitude sites, were chosen for the study. These sites were Albuquerque, NM (ABQ); Tallahassee, FL (TLH); Bismark, ND (BIS); and Sterling, VA (SRD).

Each test site is a level 1 station in the NOAA Integrated Surface Irradiance Study (ISIS) (Hicks, Deluisi, and Matt, 1995). The EKO sensor and Eppley NIP at each site was connected to the shared Campbell data logger, which is also

part of the ISIS level 1 test sites. The Eppley NIP's are all calibrated to national standards, and thus are acceptable as reference sensors to the EKOs'. The one minute stored data from each site was sent to Sterling, VA each week for analysis.

3.2 Data Analysis

This paper summarizes test results during the period from June 1996-June 1997.

3.2.1 Daily Total Minutes of Sunshine

The main objective of the analysis of the daily total minutes of sunshine was to answer the following question. What percent of the time does the EKO sensor report daily total minutes of sunshine within 10% of the Eppley NIP?

Test results show that the daily total minutes of sunshine from the EKO's were 3.8% higher than the Eppley's daily total minutes of sunshine, which is well within the ASOS specification for percent difference of +/- 10%.

Table 1 below, summarizes the test results for each test site for the period of June 1996-June 1997. Table 1 shows the number of minutes when the Eppley NIP and the EKO were reporting "sun".

Table 1: Total Minutes of Sunshine EKO vs. Eppley

TOTAL MINUTES OF SUNSHINE			
SITE	Eppley >120 Watt/m^2	EKO >120 Watts/m^2	Percent Difference EKO-Eppley
ABQ	125033	128796	3.0
TLH	134478	140586	4.5
BIS	117638	123108	4.6
SRD	135096	139298	3.1
ALL	512245	531788	3.8

The EKO MS-91 generally reported slightly more daily total minutes of sunshine than the Eppley NIP. The vast majority of these minutes occurred when the Eppley NIP was just below the 120 Watt/m^2 threshold. Only a very small percentage occurred when the Eppley NIP was below 108 Watt/m^2 (over reporting threshold). One reason why the EKO sensor tends to report slightly more daily total minutes of sunshine than the Eppley NIP may be due the fact that the EKO sensor collects raw voltage readings twice a minute (which then must be converted to flux values reported every minute in the DAS), while the Eppley NIP takes a five minute average of flux values reported every minute. Thus, the EKO sensor may have a faster response time than the Eppley NIP.

3.2.2 Over-Reporting Sunshine Minutes

The main objective of the analysis of the over-reporting of daily total minutes of sunshine was to answer the following question. What percent of the time does the EKO report "sun" when the Eppley NIP is reporting less than 108 Watt/m^2?

Test results have shown that the EKO's over-report daily total minutes of sunshine by only 1.8% or less when compared to the Eppleys daily total minutes of sunshine.

Table 2: Over-Reported Minutes of Sunshine EKO vs. Eppley

	EKO OVER-REPORTED MINUTES OF SUNSHINE		
SITE	Eppley <108 Watt/m^2	EKO >120 Watt/m^2	% Diff EKO-Eppley
ABQ	180229	3415	**1.8**
TLH	336689	5802	**1.7**
BIS	281107	5070	**1.8**
SRD	347412	4331	**1.2**
ALL	1145437	86618	**1.6**

Only a very small percentage of the EKO Daily Total Minutes of Sunshine occurred when the Eppley NIP was below 108 Watt/m^2.

3.2.3 Under-Reporting Sunshine Minutes

The main objective of the analysis of the under-reporting of daily total minutes of sunshine was to answer the following question. What percent of the time does the EKO **not** report "sun" when the Eppley NIP is reporting greater than 132 Watt/m^2?.

Test results have shown that the EKO's under-report daily total minutes of sunshine by only 0.6% or less when compared to the Eppley's daily total minutes of sunshine.

Table 3: Under-Reported Minutes of Sunshine EKO vs. Eppley

	EKO UNDER-REPORTED MINUTES OF SUNSHINE		
SITE	Eppley >132 Watt/m^2	EKO <120 Watt/m^2	% Diff EKO-Eppley
ABQ	124284	147	**0.1**
TLH	129820	879	**0.7**
BIS	116866	498	**0.4**
SRD	133218	1326	**1.0**
ALL	504118	2850	**0.6**

3.3 ASOS Algorithm

The current requirements for an ASOS sunshine algorithm include calculating the Daily Total Minutes of Sunshine, Monthly Hours of Sunshine, Monthly Percent Possible Sunshine (for Monthly Summary Message), and Daily Percent Possible Sunshine. The requirements do not include the use or storage of raw flux values at this time.

The ASOS algorithm would convert raw voltage values received from the EKO twice a minute, and convert the voltage to flux values. The algorithm would use the higher of the two flux values each minute and count each minute as "sun" if the highest EKO flux value was above 120 Watt/m^2 threshold, or

"no sun" if the highest EKO flux value was at or below the 120 Watt/m^2 threshold. The algorithm would then add the number of minutes of "sun" for the day, and use that number as the Daily Total Minutes of Sunshine.

To meet climatological requirements for sunshine, the ASOS Sunshine Algorithm must calculate percent possible sunshine (a function of latitude) at each site. Maximum possible daily sunshine tables are currently available for each ASOS station. These sunshine tables can be found on the ASOS site normals page. These sunshine tables will be modified based on obstructions such as buildings or mountains at each site. The sunshine tables will be designed so they can be edited if corrections are needed in the future.

An independent test was conducted at Sterling, VA (SRD) to determine if the station's latitude had any effect on the daily total minutes of sunshine calculated from the EKO sensors. To simulate latitudinal variation, several EKO sensor were tilted at 5^0 increments from angles simulating low latitudes (5^0) to angles simulating high latitudes (60^0). The results showed that latitude variation did not change the daily total minutes of sunshine calculated by the algorithm.

A separate study was conducted by Hughes STX for the ASOS SOMO to determine the standard solar elevation angle at which the EKO sensor exceeds the threshold of 120 Watt/m^2. The results of the study conclude that under clear atmospheric conditions the solar elevation angle when the EKO exceeded 120 Watt/m^2 would be near 0^0. Therefore, the ASOS sunshine algorithm will calculate the possible minutes of sunshine between 0^0 elevation angle in the morning, and 0^0 elevation angle in the evening.

The daily total minutes of sunshine with the EKO sensor (or any sunshine sensor) will decrease when compared to the historical human observed daily total minutes of sunshine. This is due to the fact that humans add "correction minutes" to the total daily minutes of sunshine to account for obstructions from trees, buildings, hills, etc. The ASOS sunshine sensor algorithm will NOT add "correction minutes" to the Daily Total Minutes of Sunshine. Thus the Daily Total Minutes of Sunshine measured by a sunshine sensor will decrease when compared to climatological daily total minutes of sunshine. However, the daily percent possible sunshine will not change.

4. CONCLUSIONS

Test results from the 1996-1997 field test have shown that the EKO MS-91 Sunshine Sensor is well within the specifications (+/-10%) for sunshine duration, sunshine duration over-reporting, and sunshine duration under-reporting. The EKO MS-91 is a good candidate sensor for ASOS because it fully meets these ASOS sunshine algorithm requirements.

The ASOS SOMO will continue to test the EKO MS-91 Sunshine Sensor at the four field sites chosen for this study at least until the summer of 1998. Decisions about implementation of the EKO MS-91 Sunshine Sensor into operational ASOS sites will not be made until the study is concluded, and all meteorological, engineering, and software concerns about integrating the EKO sunshine sensor into operational ASOS sites are addressed.

ACKNOWLEDGMENT

This work was sponsored by the National Weather Service ASOS Program Office under Contract Number 50-DGNW-2-00054. Opinions expressed in this paper are solely those of the authors, and do not represent an official position or endorsement by the United States Government. This work was also conducted in cooperation with the NOAA Integrated Surface Irradiance Study (ISIS) (Hicks, Deluisi, and Matt, 1995)

REFERENCES

Hicks, B. B., Deluisi, J. J., and D. R. Matt, 1995: The NOAA Integrated Surface Irradiance Study (ISIS) - a New Surface Radiation Monitoring Program, *Bulletin of the American Meteorological Society*, vol. 77, no. 12, Dec 1996, 2857-2873, American Meteorological Society.

****

THE SHADED PICHE EVAPORIMETER AS AN ANCILLARY ISOTHERMAL ANEMOMETER

C.J. STIGTER[1], R.M.R. KAINKWA[2], S.B.B. OTENG'I[3], AHMED A. IBRAHIM[4], AHMED E. MOHAMMED[5] AND L.O.Z. ONYEWOTU[6]

[1] TTMI-Project, Department of Environmental Sciences, C.T. de Wit Graduate School for Production Ecology, Wageningen Agricultural University, Wageningen, Netherlands

[2] TTMI-Project, Agricultural Physics Research Group, Department of Physics, University of Dar es Salaam, Dar es Salaam, Tanzania

[3] TTMI-Project, Department of Meteorology, University of Nairobi, Nairobi, Kenya

[4] TTMI-Project, Hydraulics Research Station, Wad Medani, Sudan

[5] TTMI-Project, Department of Environmental Sciences and Natural Resources, University of Gezira, Wad Medani, Sudan

[6] TTMI-Project, Shelterbelt Research Station, Forestry Research Institute of Nigeria, Kano, Nigeria

Introduction

In the late seventies and early eighties Stigter and his local collaborators intensively researched in Tanzania the physics of the Piche evaporimeter (or atmometer), to understand how values obtained with its shaded version could be used for two purposes: in replacement of the aerodynamic term in the Penman equation and as an ancillary isothermal anemometer. The fifteen references of a paper presented at TECIMO-IV in Brussles (Ibrahim et al., 1989) review the early work in Tanzania and that paper reports on the results of validation experiments in the Sudan.

Ibrahim et al. (1989) proved the suitability of the use of a round 25 cm diameter shade in the open, developed to overcome the problems of using Piches within a Steevenson screen (Stigter et al., 1995). They also showed the seasonal variation of the relationship between shaded Piche evaporation and the aerodynamic term of the Penman equation, exemplified with data from Sudan.

The shaded Piche evaporimeter as an ancillary anemometer

Results obtained by Kainkwa and Stigter in two rather different agroforestry systems (unpublished, data in Kainkwa, 1992) confirm that shaded Piche evaporimeters can be used in interpolating or extrapolating wind speeds measured with cup anemometers, using the simple square root of mean wind dependence model

$$E_p = b * \sqrt{u} + \underline{a}$$

as long as e_s/T_s - e_a/T_a is conservative (Stigter and Uiso, 1981). This means in practice that spatial temperature gradients (T_a, averaged air temperture; T_s, averaged blotting paper surface temperature, both in K) and spatial water vapour pressure gradients (e_a, averaged partial water vapour pressure in air; e_s, averaged saturated partial water vapour pressure at the evaporating surface, both in hPa) should be small for high accuracy of the correlation between $\sqrt{u}$ and E_p. Here E_p (mm/h) is Piche evaporation averaged over an experimental run, varying from half a day to several days when wind speeds are relatively low (order between 0.5 and 2 m/s), or of at least several hours (for higher wind speeds).

The values of the empirical constant a were found to be close to zero, particularly when the (0,0) point was added as a measuring point. The values of empirical constant b were found to vary, run by run and height by height, particularly due to inequalities in temperatures, in humidities and in turbulence. However, this does not negatively influence the use of the Piche as an ancillary anemometer in such agroforestry systems for quantifying wind speed gradients. In a coffee system with huge umbrella shade trees, in Lyamungu, Tanzania, on the slopes of the Kilimanjaro, correlations between cup anemometers and Piches were ≥ 0.90 for the low wind speeds experienced, while for the conditions at a savanna woodland edge, at Setchet, Hanang, Tanzania, with high wind speeds, these correlations were ≥ 0.95, after separating the data at 1 m and 2.5 m height (Table 1, Kainkwa, 1992).

In Sudan, Mohammed et al. (1996; 1998) reported that wind speed reduction within the windward edge of a eucalyptus shelterbelt keeping sand out of an irrigated area at Sihaimab, north-western Gezira, was in the order of 15%, 25%, 40% and 65% for 2.5 m, 7.5 m, 12.5 m and 17.5 m inwards into the shelterbelt, compared to the wind speed 2.5 m in front of the belt, as obtained from roughly temperature corrected evaporation reduction of shaded Piches at a height of 1 m. Piche evaporation had also here been calibrated against cup anemometry.

Oteng'i et al. (unpublished, data in Oteng'i, 1996), in a complex agroforestry system, with hedges around and dispersed fruit trees within a traditional maize/bean intercrop, in semi-arid Matanya, Laikipia region, Kenya, tested Piche evaporimeters for wind speed interpolations and extrapolations. They correlated wind reductions obtained from cup anemometers with those obtained from the squares of Piche evaporation, with the reference cup outside the agroforestry system as well as with the reference cup within the system. The latter case gave high correlations ($r \geq 0.99$) under all conditions while for the former case the correlation was only that high when the (0,0) point was included (Oteng'i, 1996).

Between multiple shelterbelts at Yambawa, northern Nigeria, Onyewotu et al. (unpublished, data in Onyewotu, 1996) confirmed that highly changing conditions near the start and end of the rainy season, rainfall itself, low wind speeds and low wind speed ranges negatively influence the correlations between shaded Piche evaporation and the square root of weekly mean wind speed. These data were taken weekly for two growing seasons. Data were not corrected for changes in humidity and temperature. The Piche could also be used to check on variation in shelterbelt permeability (Onyewotu, 1996).

Concluding remarks

The five examples reviewed here show that within agroforestry systems, woodlands, shelterbelts and other relatively dense plantings, where spatial gradients of temperature and humidity are small, the shaded Piche may be used for wind speed interpolations and extrapolations, if the range of wind speeds is considerable and wind speeds are not too small (below 0.5 m/s) for too long a period. Taking a reference from within these systems considerably improves the correlations in comparison to a reference outside the system, such as in front of an edge or shelterbelt or in a clearing or just in the open (Oteng'i, 1996; Mohammed et al., 1996; 1998).

Special applications, such as in quantifying variations in shelterbelt permeability (Onyewotu, 1996), in detecting tunnelling effects (Kainkwa and Stigter, 1994) and differences in turbulence with height (Kainkwa, 1992), as well as in separating horizontal and vertical air movement (Kainkwa, 1992; Oteng'i, 1996), show the value of multi-point observations under highly inhomogeneous conditions. Cheap interpolation and extrapolation possibilities such as with the shaded Piche in wind observations yield substantial advantages in such cases.

References

Ibrahim, A.A., Stigter, C.J., Adeeb, A.M., Adam, H.S. and Jansen, A.E, 1989. Development and validation of shaded Piche evaporimeters for the tropics to replace humidity and wind speed data in the aerodynamic term of the Penman equation. Proceedings of TECIMO-IV, Instruments and Observing Methods Report No. 35, WMO/TD - No. 303, WMO, Geneva, 147 - 152.

Kainkwa, R.M.R., 1992. Shelter efficiency of some traditional wind breaks in Tanzania. Ph.D.-thesis, Department of Physics, University of Dar es Salaam, Dar es Salaam, Tanzania, 300 pp.

Kainkwa, R.M.R. and Stigter, C.J., 1994. Wind reduction downwind from a savanna woodland edge. Neth. J. Agric. Sc. 42: 145 - 157.

Mohammed, A.E., Stigter, C.J. and Adam, H.S., 1996. On shelterbelt design for combating sand invasion. Agric. Ecosyst. Environm. 57: 81 - 90.

Mohammed, A.E., Stigter, C.J. and Adam, H.S., 1998. Wind regimes windward of a shelterbelt protecting gravity irrigated crop land from moving sand in the Gezira scheme (Sudan). Submitted for publication to Theor. Appl. Meteorol.

Onyewotu, L.O.Z., 1996. Effects of multiple shelterbelts on microclimate and agricultural use of a desertified semi-arid environment at Yambawa, near Kano, Nigeria. Ph.D.-thesis, Department of Geography, Ahmadu Bello University, Zaria, Nigeria, 467 pp.

Oteng'i, S.B.B., 1996. An investigation of the influence of mulching and agroforestry systems on the microclimatic conditions affecting soil moisture and a maize/bean intercrop in semi-arid areas of Laikipia district, Kenya. Ph.D.-thesis, Department of Meteorology, University of Nairobi, Nairobi, Kenya, 676 pp.

Stigter, C.J. and Uiso, C.B.S., 1981. Understanding the Piche evaporimeter as a simple integrating mass transfer meter. Appl. Sc. Res. 37: 213 - 223.

Stigter, C.J., Rashidi, A.M.G.M., Uiso, C.B.S. and Ibrahim, A.A., 1995. Precautions in using Piche evaporimeters. Internal Report IR9502, Department of Meteorology, Wageningen Agricultural University, Wageningen, Netherlands, 10 pp.

Table 1: Example of correlations between square root of average wind speed and average Piche evaporation. a is the Y intercept, b is the slope of the line, r is the correlation coefficient, h is the run period in hours, Uo and Ux are respectively maximum and minimum wind speed records in m/s for an average of h hours, Ep(av) is average Piche evaporation in mm/h, n is the number of data points, EY is the standard error of Y estimate and EX is the standard error of X coefficient. Bold values are regression coefficients where the point (0,0) was added as a measuring point.

Groups of 6 data points for 2.5 m height.

Case	a	EY	Uo	Ux	Ep(av)	r	h	n	b	EX
P12	0.25	0.12	6.29	5.40	7.44	0.90	16	6	2.95	0.73
	0.00	**0.11**				**1.00**			**3.05**	**0.05**
P22	-13.90	0.43	9.20	8.33	9.57	0.76	3.5	6	7.88	3.34
	-0.03	**0.47**				**0.99**			**3.22**	**0.17**
P32	-0.29	0.84	7.38	4.60	13.27	0.85	5	6	5.39	1.64
	-0.01	**0.76**				**0.99**			**5.28**	**0.32**
P42	0.23	0.46	6.93	2.38	3.21	0.81	13.5	6	1.36	0.49
	0.04	**0.41**				**0.96**			**1.45**	**0.18**
P52	-0.93	0.36	6.22	2.90	12.46	0.99	8	4	6.26	0.53
	-0.08	**0.34**				**1.00**			**5.87**	**0.16**
P62	-1.13	0.19	5.96	2.51	4.20	0.98	13.5	6	2.57	0.24
	-0.14	**0.24**				**0.99**			**2.11**	**0.12**
P72	0.98	0.37	7.76	3.85	11.60	0.98	5	6	4.46	0.49
	0.09	**0.36**				**1.00**			**4.83**	**0.15**
P82	2.96	0.38	7.59	4.43	13.08	0.96	6.5	6	4.22	0.63
	0.18	**0.47**				**1.00**			**5.36**	**0.20**

THE DEVELOPMENT OF CHINESE METEOROLOGICAL EQUIPMENT TOWARDS THEIR MODERNIZATION

Ji Qiwu
China Meteorological Administration
Department of Corporate and Facility Development
46, Baishiqiaolu No. 46, Western Suburb, Beijing 100081, China
E-mail: cyfz@rays.cma.gov.cn

Currently, almost all the instruments used by the Chinese meteorological service are designed and manufactured at home. A dozen primary manufacturers are involved in the production of surface observation, upper-air sounding, weather radars, profilers and satellite image receiving/processing system. The products manufactured have satisfied the basic equipment needs of meteorological observatories and stations. At the same time, through ever-growing worldwide exchanges and cooperation, these products' performances have been improved steadily, and been adaptive to the modernization of the Chinese meteorological service.

Chinese surface observing stations are equipped with various instruments used for routine observations such as glass thermometers, mercury barometers, thermohygrometers, aneroid barometers, auto-anemoscopes, rain gauges, telemetering precipitation gauges , sun detectors, radiometers, radiation auto-recorders, etc. These instruments have been manufactured in great quantity for several decades and are automatizing and telemetering their single or multi-elements. In recent years, 3 types of telemering weather stations have passed the service qualification test and a few of them have been installed at weather stations on pilot operation. In addition, 114 sets of domestically produced Four-Element Automatic Weather Stations and 52 sets of telemetering precipitation stations have been installed in four local hazardous weather observation networks and rainfall observation networks, in order to acquire high-density observing data.

In China, 120 stations have been set up for upper-air detection, using the upper-air sounding systems composed of Model 701 secondary wind-finding radar and Model 59 code sounder (400 MHz). Five of them have been equipped with newly developed C-band primary wind-finding radar/electronic upper-air sounding system (400 MHz). At the same time, the development of an L-band secondary wind-finding radar/electronic sounding systems is being undertaken, and is expected to replace the current secondary wind-finding radar/code sounding systems currently in use. All the systems mentioned have microcomputer processing terminals for the automatic processes of detection data.

Two domestic factories provide sounding balloons made of natural latex, ranging in weight from 10 grams to 1500 grams, whose good performance satisfy the need of sounding operation.

In China, almost half of the sounding stations are equipped with hydrogen producing canisters, creating hydrogen by chemical means. The other half are equipped with electrolysis equipments where hydrogen is obtained by electrolyzing water. There are two types of equipments: high voltage and normal voltage with production rates of 3 stere/hour and 2 stere/hour respectively. These can fully meet the needs of 2-4 soundings each day.

With the increased needs for remote sensing technology to be used in severe weather detection, the China Meteorological Administration has focused on the development of weather radars and wind profilers.
Currently, there are 7 types of weather radar and digital signal processing equipments, manufactured by 4 factories, including those working on S, C, and X band and two systems which are Doppler Weather Radars. 17 S-band, 42 C-band and 175 X-band weather radars have been installed nationwide, ten of which are Doppler Radars. In 1995, the Chinese Huayun Corp. and Lockheed Martin Corp., which is the manufacturer of the WSR-88D Radar, set up a joint venture to develop S-band Doppler Radar (called CINRAD) on the basis of WSR-88D. CINRAD's performance will be as good as WSR-88D and its selling price will be far lower than WSR-88D. The product will be the new generation radar installed and interconnected in a weather radar net of China in the 21st century. The first one will be installed in Hefei city for Anhui Provincial Meteorological Bureau.

In 1995, we began the production of wind profilers operating at 900 Hz for temperature measurement, whose highest detection altitude is 2000 meters. Three systems have been installed in China to date in order to provide wind and temperature profiles up to 2000m for meso- and small-scale weather detection.

Since 1988, China has launched three meteorological satellites of the series FY-1 and FY-2. The former is polar orbiting and the latter is geo-stationary. FY-2 was just launched and put into operation in 1997. The weather data obtained has found wide application in stations at different levels. In addition to the data obtained from Chinese satellites, information from NOAA (U.S.A) and GMS (Japanese) are also received and processed. China has manufactured a dozen different types of satellite data receiving and processing equipments with adequate software supports. The following five are widely used:

HY-1A, CMAPPS and WF are used to process satellite images, which are received from geo-stationary satellites S-VISSR and LR-FAX, and can also process S-band phototelemetry (synoptic charts and satellite images) from the Chinese FY-2. The CMAPPS mentioned above is an expansible integrated microcomputer.

There are two kinds of multi-purpose meteorological satellite information receiving & processing systems, each with all the functions in processing nephograms from polar orbit satellite HRPT and geo-stationary satellites S-VISSR and LR-FAX.

To ensure the steady and reliable operation of meteorological instruments used in all the meteorology departments, CMA has built an instrument and technology support system including supply, maintenance, quality supervision and measurement verification. License regulation is applied in the quality supervision. Only those instruments with an authentication license issued by CMA can be used in the Weather Service.

Besides satisfying the domestic needs, through the VCP program of WMO and various bi-lateral cooperation programs and trade, a certain number of equipments are exported every year, including kits of instrument of surface observation , upper air detection and satellitic data receiving processor system. So far, almost 60 developing countries have received the donated meteorological instruments or equipments from China, and the AFDOS system, a system for data collecting, processing and analyzing and for forecasting is used in many countries. After all, China is a developing country, the development of meteorological instruments are based on application low cost purpose, at the same time, with the technical advancement, the performances are promoted steadily. China would like to cooperate with other member countries in the development of meteorological instruments, and is ready to provide equipments or experts on that respect to any country in need. As one of the two regional instrument centers of RAII, China would continue to commit to its duties, and make contribution to technical exchange, personnel training, and instrument comparison, and so on.

APPENDICES

LIST OF MEMBERS OF THE INTERNATIONAL ORGANIZING COMMITTEE FOR PREPARATION OF THE WMO TECHNICAL CONFERENCE ON INSTRUMENTS AND METHODS OF OBSERVATION

TECO-98

A. Van Gysegem	Scientific Director	Belgium
A. Belhouji		Morocco
E. Ekuwem		Nigeria
J. Kruus		Canada
M. Rochas		France
K. Schulze	Co-ordinator	WMO Secretariat

LIST OF PUBLICATIONS
in the
INSTRUMENTS AND OBSERVING METHODS REPORTS SERIES

No. 1 Automated Meteorological Systems.
Papers presented at the Technical Conference on Evolution and Standardization of Observing Techniques in Light of Automation
(Norrköping, Sweden, 1980)

No. 2 Instrument Development Inquiry (Third Edition), 1980

No. 3 Lower Tropospheric Data Compatibility. Low-level Intercomparison Experiment (USA, 1979)

No. 4 WMO Equipment Survey - Meteorological Satellite Ground-based Receiving Equipment, 1980

No. 5 WMO Catalogue of Radiosondes in Use by Members, 1981
(out of print)

No. 6 Preliminary Analysis of a Questionnaire on Aerodrome Meteorological Measurements
By M. M. Etienne (Belgium), 1981

No. 7 The Meteorological Use of Navaid Systems - A brief technical assessment
By A. Lange (Finland), 1981

No. 8 Report on Meteorological Radars
By G. A. Clift, 1981

No. 9 Papers presented at the Second WMO Technical Conference on Instruments and Methods of Observation (TECIMO-II)
(Mexico City, 1981)

No. 10 Radiation Effects on the WMO Reference Psychrometer in the Field
By R. G. Wylie and T. Lalas (Australia), 1981

No. 11 WMO Catalogue of Radiosondes in Use by Members, 1982

No. 12 Meteorological Observations by Laser Indirect Sensing Techniques
By A. O. van Gysegem (Belgium), 1982

No. 13 The Use of Hydrogen for Inflation of Meteorological Balloons, 1982

No. 14 Summary Results of a 1978 Survey of Calibration Facilities and of Tests and Evaluation of Instruments
(out of print)

No. 15 Papers presented at the WMO Technical Conference on Instruments and Cost-Effective Meteorological Observations (TECEMO)
(Noordwijkerhout, Netherlands, 1984)

No. 16 Comparison of Pyranometers and Electronic Sunshine Duration Recorders of RA VI
(TD 146) (Budapest, Hungary, 1984)
By G. Major (Hungary), 1986

No. 17 International Comparison of National Precipitation Gauges with a Reference Pit Gauge
(TD 38) By B. Sevruk and W. R. Hamon, 1984

No. 18 Guidance Material on Meteorological Instruments Suitable for Use in Developing Countries
(TD 112) By E. S. Engawi (Saudi Arabia), 1986

No. 19 Some General Considerations and Specific Examples in the Design of Algorithms for Synoptic
(TD 230) Automatic Weather Stations
By D. T. Acheson (USA), 1987

No. 20 Stations Automatiques à Faible Coût
(TD 177) By P. Viton (France), 1986

No. 21 Algorithms for Automatic Aerological Soundings
(TD 175) By A. H. Hooper (United Kingdom), 1986

No. 22 Papers presented at the WMO Technical Conference on Instruments and Methods of
(TD 50) Observation (TECIMO-III) (Ottawa, 1985)

No. 23 Keynote papers presented at the Third WMO Technical Conference on Instruments and Methods
(TD 51) of Observation (TECIMO-III) (Ottawa, 1985)

No. 24 Instruments Development Inquiry (Fourth Edition)
(TD 231) By E. Prokhorov (USSR), 1987

No. 25 Papers presented at the Workshop on the Correction of Precipitation Measurements
(TD 104) (Zürich, Switzerland, 1985)

No. 26 Lectures presented at the Workshop for Instrument Specialists, (Buenos Aires 1984)(in Spanish)
(out of print)

No. 27 WMO Catalogue of Radiosondes and Upper-Air Wind Systems in Use by Members
(TD 176) (1986)

No. 28 WMO International Radiosonde Comparison, Phase I (Beaufort Park, UK, 1984)
(TD 174) By A. H. Hooper (United Kingdom), 1986

No. 29 WMO International Radiosonde Intercomparison, Phase II (Wallops Island, USA, 1985)
(TD 312) By F. Schmidlin (USA)

No. 30 WMO International Radiosonde Comparison (UK, 1984 / USA, 1985)
(TD 195) By J. Nash (United Kingdom) and F. Schmidlin (USA), 1987
(out of print)

No. 31 The Measurement of Gustiness at Routine Wind Stations - A Review
By A. C. M. Beljaars (Netherlands), 1987

No. 32 WMO International Ceilometer Intercomparison (UK, 1986)
(TD 217) By D. W. Jones, M. Ouldridge and D. J. Painting (all United Kingdom), 1988

No. 33 Papers presented at the WMO Technical Conference on Instruments and Methods of
(TD 222) Observation (TECO-1988) (Leipzig, German Democratic Republic, 1988)
(out of print)

No. 34 WMO Assmann Aspiration Psychrometer Intercomparison
(TD 289) (Potsdam, German Democratic Republic, 1987)
By D. Sonntag (Germany), 1989

No. 35 Papers presented at the Fourth WMO Technical Conference on Instruments and Methods of
(TD 303) Observation (TECIMO-IV) (Brussels, 1989)
(out of print)

No. 36 Compatibility of Radiosonde Geopotential Measurements
(TD 344) By M. Kitchen (United Kingdom), 1988

No. 37 Information on Weather Radars used by WMO Members
(TD 309) By M. Gilet (France), 1989

No. 38 WMO International Hygrometer Intercomparison (Oslo, Norway, 1989)
(TD 316) By J. Skaar, K. Hegg, T. Moe, K. Smedstud (all Norway)
(out of print)

No. 39 Catalogue of National Standard Precipitation Gauges
(TD 313) By B. Sevruk (Switzerland) and S. Klemm (Germany), 1989

No. 40 WMO International Radiosonde Comparison, Phase III (Dzhambul, USSR, 1989)
(TD 451) By A. Ivanov, A. Kats, S. Kurnosenko, J. Nash, and N. Zaitseva (all Russian Federation)

No. 41 First WMO International Intercomparison of Visibility Measurements (UK, 1989)
(TD 401) By D. J. Griggs, D. W. Jones, M. Ouldridge, W. R. Sparks (all United Kingdom)
(out of print)

No. 42 WMO Automatic Sunshine Duration Measurement Comparison (Hamburg, Germany, 1989)
(in preparation)

No. 43 First WMO Regional Pyrheliometer Comparison of RA II/RA V
(TD 308) (Tokyo, Japan, 1989)

No. 44 First WMO Regional Pyrheliometer Comparison of RA IV (Ensenada, Mexico, 1989)
(TD 345) By I. Galindo (Mexico)

No. 45 Analysis of Instrument Calibration Methods used by Members
(TD 310) By H. Döring (Germany), 1989

No. 46 The WMO Automatic Digital Barometer Intercomparison (De Bilt, Netherlands, 1989)
(TD 474) By J.P. van der Meulen (Netherlands), 1992

No. 47 Reports of the CIMO Working Group on Surface Measurements
(TD 452) Guidance on the Establishment of Algorithms for Use in Synoptic Automatic Weather Stations - Processing of Surface Wind Data
By D. Painting (United Kingdom), 1991

No. 48 International Workshop on Precipitation Measurements
(TD 328) (St. Moritz, Switzerland, 1989)

No. 49 Papers presented at the WMO Technical Conference on Instruments and Methods of
(TD 462) Observation (TECO-92), (Vienna, Austria, 1992)
(out of print)

No. 50 Historical Changes in Radiosonde Instruments and Practices
(TD 541) By D. J. Gaffen (USA), 1993

No. 51 Overview of Real-time Lightning Detection Systems for use by Meteorological Services
(TD 570) By R.L. Holle and R.E. López (both USA), 1993

No. 52 Results of the Working Group on Weather Radars
(TD 571) Part I: Severe Weather Recognition, By G. G. Shchukin (Russian Federation)
Part II: Utilization of Doppler Radars for Monitoring Tropical Cyclones as one Element of the Global Monitoring System, By Hisao Ohno (Japan), 1993

No. 53 Segunda Compariación de la OMM de Pirheliómetros Patrones Nacionales AR III
(TD 572) (Buenos Aires, 1991)
By M. Ginzburg (Argentina), 1992
(out of print)

No. 54 Instruments Development Inquiry (fifth edition)
(TD 578) By J.P. van der Meulen (Netherlands), 1993
(out of print)

No. 55 Siting and Exposure of Meteorological Instruments
(TD 589) L'emplacement des sites et l'exposition des instruments météorologiques
By J. Ehinger (Switzerland), 1993

No. 56 Report by the Rapporteur on Radiosonde Compatibility Monitoring
(TD 587) Part A - WMO Catalogue of Radiosondes and Upper-air Wind Systems in Use by Members
Part B - Compatibility of Radiosonde Geopotential Measurements 1990, 1991 and 1992
By T. Oakley (United Kingdom), 1993

No. 57 Papers presented at the WMO Technical Conference on Instruments and Methods of
(TD 588) Observation (TECO-94), (Geneva, Switzerland, 1994)
(out of print)

No. 58 Papers presented at the International Workshop on Experiences with Automatic Weather Stations
(TD 670) on Operational Use within National Weather Services (Vienna, Austria, 1995)
(out of print)

No. 59 WMO International Radiosonde Comparison - Phase IV; Final Report (Tsukuba, Japan, 1993)
(TD 742) By S. Yagi, A. Mita and N. Inoue (all Japan), 1996

No. 60 Description and User Guide for the Radiosonde Comparison and Evaluation Software Package
(TD 771) *(RSKOMP - Version 3/Version 4)*
By S. Kurnosenko (Russian Federation) and T. Oakley (United Kingdom), 1996

No. 61 Road Meteorological Observations
(TD 842) By R.E.W. Pettifer (United Kingdom) and J. Terpstra (The Netherlands), 1997

No. 62 WMO Wind Instrument Intercomparison
(TD 859) By P. Gregoire and G. Oualid (both France), 1997

No. 63 Operational Use of Ground-based Remote Sensors: A Review
(TD 860) By D.W. Beran (USA), 1997

No. 64 Tercera Comparación Regional de la OMM de Pirheliómetros Patrones Nacionales De la AR III
(TD 861) Informe Final, Centro Regional de Radiación, Santiago de Chile, 24 de Febrero al 7 Marzo de 1997
Preparado por Manuel Vargas Muñoz (Chile), 1997

No. 65 Guidance on Automatic Weather Systems and their Implementation
(TD 862) Part I: Guidance Specifications (Functional) for a General Purpose Automatic Weather Station
Part II: Implementation and User Training Considerations
By Observation & Engineering Branch, Australian Bureau of Meteorology, 1997

No. 66 Recent Changes in Thermometer Design and their Impact
(TD 871) By A. Barnett, D.B. Hatton and D.W. Jones (all United Kingdom),1998

No. 67 WMO Solid Precipitation Measurement Intercomparison - Final Report
(TD 872) By B.E. Goodison, P.Y.T. Louie (both Canada) and D. Yang, (China), 1998

No. 68 Guidance Material on the Choice of Meteorological Instruments for Surface Observations Suitable for Use
(TD 873) in Developing Countries
By J.B. Odero (Kenya), 1998

No. 69 Weather Radars used by Members
(TD 874) By T. Mammen, Germany (1998)

****